Violent Wave Action at Seawalls and Breakwaters

Tom Bruce

A thesis submitted for the degree of Doctor of Philosophy by Research Publication.
The University of Edinburgh.
June 2006

Abstract

This submission comprises critiques of 24 of the author's papers published in journals or the proceedings of refereed international conferences. The subject is vertical seawalls and breakwaters, focussing on wave kinematics in front of these structures; loadings on them and wave overtopping. Further responses, including overtopping velocities; extent and direct hazard due to this overtopping are also investigated. The thesis is that improved prediction methods for the structure responses – *e.g.* loadings; overtopping; hazard – must be much more firmly based upon the physical form of the wave-structure interaction than the methods in standard use at the outset of the research.

The author began research in this specific field with a study on kinematics of breaking waves in front of vertical breakwaters (Oumeraci *et al.*, 1995). The 1995 study was revisited by a study to measure kinematics of breaking waves at a breakwater in irregular seas (Bruce & Vicinanza, 1998). These velocity data formed the basis of a detailed numerical comparison (Wood *et al.*, 2000).

Under the EC *PROVERBS* project, a tool was developed to identify wave-structure combinations susceptible to impulsive / breaking wave loads and for the prediction of these loads. Contributing to this synthesis was a review of sources of scatter in data and of engineering approaches to the problem (Walkden & Bruce, 2000). During *PROVERBS* an example of a seaward-acting impulsive wave load on a breakwater was observed. The mechanisms for such an effect were explored (Walkden *et al.*, 2001).

Key consequences of wave overtopping include flooding; wave transmission (into the sheltered area); and direct hazard. Thus there is a need for well-supported design tools for the prediction of overtopping discharge for common coastal structures. A new UK guidance manual on wave overtopping published in 1999 included a crucial distinction between overtopping as a result of non-breaking waves and as a result of waves actually breaking onto the wall.

This new guidance has been critically examined and extended to a wider range of realistic structures (Bruce *et al.*, 2001a; Allsop *et al.*, 2005a). For the first time, the new tool was validated against laboratory scale effects (Pearson *et al.*, 2002) and advice offered on other uncertainties (Pearson *et al.*, 2001). No guidance was offered on the (3-d) effect of oblique wave attack under impulsive conditions – a gap closed by a major programme of tests at HR Wallingford

resulting in new guidance (Napp *et al.*, 2002; 2003 & 2004). A major comparison with field measurements formed part of the EC *CLASH* project (Pullen *et al.*, 2003 & 2004).

Many seawalls employ recurves / wave return walls as an overtopping reduction measure. New studies were carried out to synthesise new guidance on their design (Kortenhaus *et al.*, 2003; Pearson *et al.*, 2004). Historically out of necessity and still, out of economics, seawalls tend to be built at or close to the lowest tide level. Existing guidance formulae break down when the water depth in front of the wall is zero. Novel studies were carried out to extend guidance into these regimes (Bruce *et al.*, 2003).

The first steps towards the linking of existing predictive tools, individual wave overtopping events and direct hazard were reported in Bruce *et al.* (2001b), including the first data and guidance on overtopping "throw" velocities, and also for the first time, data and guidance on pressures generated on the crown deck of a structure due to downfalling overtopped discharge - a topic expanded upon greatly in Wolters *et al.* (2005). The work on velocities and hazard was elaborated by Bruce *et al.* (2002), including data from large-scale tests. Further consideration of direct hazard and public and professional response to this hazard appeared in Allsop *et al.* 2003; 2004 & 2005b), with new data and guidance on the zone of hazard appearing in Bruce *et al.* (2005).

Declaration of originality

I hereby declare that this critical review was composed and originated entirely by myself in the School of Engineering and Electronics at The University of Edinburgh. I further declare that the work has not been submitted for any other degree or professional qualification.

In accordance with the regulations governing "PhD by Research Publication", a "Declaration of Contribution" is included alongside each published paper submitted as part of this critical review. These may be found in the Appendices A to X.

Tom Bruce

Acknowledgements

It will be clear from reading the papers forming the basis of this critical review that an enormous degree of academic and professional cooperation has gone into them. These cooperations have made this journey not only academically rich, but also personally rewarding, with many warm friendships arising out of these professional collaborations. To list these is hard - I do so with trepidation at missing anyone out. But here is a list of friends who have helped along the way;

Jon Pearson and Mike Walkden; thoughtful, skilful, careful and hugely trusted post-docs. - Jon on *VOWS*, *Big-VOWS* and *CLASH*; Mike before him on *PROVERBS*.

Nicolas Napp; All the adjectives applied to Jon and Mike apply equally to Nic. Nic was the author's first PhD student, so we learned about PhD supervision together!

Leo Franco; Jentsje van der Meer; for some great ideas and telling interventions along the way.

VOWS friends at Manchester Metropolitan University – Derek Causon, Dave Ingram and Clive Mingham. Being thrown together with you by EPSRC was a stroke of great fortune.

All the team at UPC Barcelona - Xavi Gironella, Quim Sospedra, Javier Pineda and Oscar. You facilitated an absolute high point in this author's research career. And Stephen Richardson and Giovanni Cuomo for invaluable assistance during testing - much more than extra pairs of hands.

My local supervisor, Frank Mill; your advice on this review has been of huge value.

William Allsop; listed last on the professional roll-call – for emphasis (and to keep him guessing). The person who led the author into the world of breakwaters and has since guided, encouraged and cajoled the author through good times and hard. Contribution incalculable. Gratitude immense.

The financial support of UK EPSRC and the EC for *PROVERBS* (EC DG XII, MAS3-CT95-0041); *VOWS* (UK EPSRC GR/M42312); *Big-VOWS* (UK EPSRC GR/R42306/01); *CLASH* (EC FP5, EVK3-CT-2001-00058) and *Safe at the Seaside* (UK EPSRC GR/S23827/01) projects is also gratefully acknowledged.

Shifting to the personal supporters; gratitude to William and Jane for giving me a study in which to hide away for two weeks to break the back of the task of writing this review. Thank you for having no junk food in the house; for living as close to the middle of nowhere as one can in Oxfordshire; for leaving early for work and coming back late, and for having no decent internet connection!.

Finally and most importantly, heartfelt gratitude to my wife Claire and to wee Catherine (aged 20 months) for emotional support of the greatest kind, and too, for the practical support of allowing me time to prepare this review. I love you both more than words can say.

Notation

β	angle of wave attack [°]; $\beta = 0°$ for perpendicular wave attack
γ_b	reduction factor for influence of a berm
γ_h	reduction factor for influence of a shallow foreshore
γ_f	reduction factor for influence of slope roughness
γ_β	reduction factor for influence of oblique wave attack
μ_s	coefficient of static friction
c_D	drag coefficient
d	diameter (of cylinder representing a person) [m]
F	"Ahrens-type" notation for crest freeboard ($= R_c$) [m]
F'	"Ahrens-type" dimensionless crest freeboard $= \frac{F}{(H_{m0}^2 L_p)^{1/3}}$
F_D	drag force [N]
G	position of centre of mass
h	(local) water depth [m]
h_G	height to centre of overtopping flow [m]
h_o	thickness of overtopping flow [m]
h_p	height of person [m]
h_s	water depth at toe of structure [m]
h_*	wave breaking parameter $= \frac{h_s}{H_{si}} \frac{2\pi h_s}{g T_m^2}$
$H_{1/10}$	statistical wave height defined as mean of largest $\frac{1}{10}$th of individual waves in irregular sea [m]
$H_{1/3}$	statistical wave height defined as mean of largest $\frac{1}{3}$rd of individual waves in irregular sea [m]
H_{m0}	(preferred) spectral measure of wave height based upon energy spectrum [m]
H_o'	Goda's "equivalent offshore wave height" [m]
H_s	significant wave height (term in ambiguous use; = $H_{1/3}$ or H_{m0} [m]
H_{si}	significant wave height of incident waves at the location of structure [m]
k	multiplier accounting for overtopping reduction due to parapet / recurve / wave return wall
ℓ_G	lever arm length (for tumbling person) [m]
L_m	wavelength based upon mean period [m]
L_{op}	wavelength in deep water, based upon peak period [m]
$P_{1/250}$	pressure defined as mean of largest $\frac{1}{250}$th of measured (event) pressures [Pa]

q	(dimensional) mean overtopping discharge [m^3/s/m]
Q'	"Ahrens-type" notation for dimensionless mean overtopping discharge $= \frac{q}{\sqrt{gH_{m0}^3}}$
Q_b	dimensionless mean overtopping discharge for plunging waves $= \frac{q}{\sqrt{gH_s^3}}\sqrt{\frac{s_{op}}{\tan\alpha}}$
Q_h	dimensionless mean overtopping discharge for impulsive conditions $= \frac{q}{h_*^2\sqrt{gh_s^3}}$
Q_n	dimensionless mean overtopping discharge for surging waves $= \frac{q}{\sqrt{gH_s^3}}$
Q_*	"Burcharth-type" dimensionless mean overtopping discharge $= \frac{qT_m}{L_m^2}$
R_b	dimensionless crest freeboard for sloping structures $= \frac{R_c}{H_s}\frac{s_{op}}{\sqrt{\tan\alpha}}\frac{1}{\gamma_b\gamma_h\gamma_f\gamma_\beta}$
R_{ba}	dimensionless crest freeboard for vertical walls with emergent toe ($h_s < 0$) $= R_b s_{op}^{0.17}$
R_c	crest freeboard [m]
R_h	dimensionless crest freeboard for impulsive conditions $= h_*\frac{R_c}{H_s}$
R_*	'Burcharth-type" dimensionless crest freeboard $= \frac{H_s}{R_c}$
s_{op}	wave steepness based upon offshore peak period
S	location of centre of rotation
$T_{m-1,0}$	spectral wave period (weighted to account for bi-modal spectra) [s]
T_p	spectral peak wave period [s]
T_z	statistical "zero-crossing" wave period [s]
u	flow speed [m/s]
u_{crit}	critical flow speed [m/s]
W	effective weight (of person in overtopping flow) [N]

Contents

List of figures

List of tables

Part 1: Critical Review

Chapter 1
Introduction

1.1 Introduction to critical review

This thesis comprises critiques of 24 papers published in journals or the proceedings of established, refereed international conferences. The subject matter falls broadly into three overlapping areas covering a range of structures including breakwaters and seawalls, with plain, composite and / or steeply sloped (battered) geometries.

- Wave kinematics in front of vertical breakwaters, and loadings (forces / pressures) on such structures.
- Wave overtopping of vertical breakwaters / seawalls under breaking wave conditions, and
- Post-overtopping processes and responses, including overtopping velocities, extent and direct hazard due to this overtopping.

These areas are inextricably linked. Without the progress made on kinematics and on wave loadings at vertical breakwaters made in the 90s, there would have been neither the understanding of the physical processes nor the prediction tools required for the design and analysis of test programmes into impulsive overtopping and its consequences. The critiques will emphasise these links whenever appropriate. The work presented has almost all emerged from collaborative projects – indeed only one of the 24 papers has an authorship which is only from the University of Edinburgh. This is a positive thing – progress in the fields reported on has been very great over the last 10 years, and this must be due in large measure to the success of collaborative projects such as *PROVERBS* (Section 2.1), *VOWS* (Section 3.3) and *CLASH* (Section 3.10.1) in bringing together the best researchers in Europe. Co-authors include Jentsje van der Meer, Leopoldo Franco, William Allsop, Hocine Oumeraci, Andreas Kortenhaus and Howell Peregrine. As such, there are no papers for which the author can (or indeed would wish to) claim sole credit, but he can claim significant input *via*, in the case of some of the earlier work, carrying out tests and analysis and, for much of the body of work, *via* (*e.g.*) direction of

testing / analysis; detailed discussion of results and formulation of conclusions, in addition to work in preparation of text, figures and graphs.

1.2 Introduction to technical context of work

The publications forming this submission and the accompanying critique tell a story of the technical development in the field of impulsive wave loadings and overtopping at vertical breakwaters and seawalls from the mid-90s to date, but it is instructive to begin by looking back rather further to identify the factors and drivers which led to the identification of the particular problem and treatment of impulsive waves at these structures. This is not intended to mirror the technical introductions given in each of the published works, but rather to paint the historical context only.

- In the Unites States, the standard guidance manual – the Shore Protection Manual (SPM, 1984) – was revised in its final version. It attempted to incorporate Japanese and European understanding / methods based upon irregular / random waves, but did not do so in an entirely satisfactory manner. An example of this is the use of Ahrens' methods for overtopping of sloping structures (based upon the $H_{1/10}$ wave height) instead of van der Meer's (then) new methods based upon H_{m0} which were better supported. Additionally, the SPM devoted only little attention to vertical walls giving ill-supported methods. Goda's method for loading prediction was offered but without key explanations of strengths or limitations, with principal recommendations based upon Minikin's (1950) method. This method has been shown (*e.g.* Goda, 2000) to produce unrealistically large design pressures, and also has fundamental short-comings in terms of its qualitative predictive behaviour.

- In Europe, building on the identification by Battjes (1974) of the role of the surf-similarity parameter in determining the *form* of wave breaking on slopes, van der Meer (in his PhD thesis) and coauthors from 1987 onwards, were the first to identify that loading and overtopping responses of structures did not necessarily follow a single physical form over the full range of wave and freeboard conditions, but that switches could occur between regimes.

- 1990 saw the publication of the *Handbook of Coastal and Ocean Engineering*, edited by Herbich (1990). Volume 1 of this manual contained summaries of current methods for

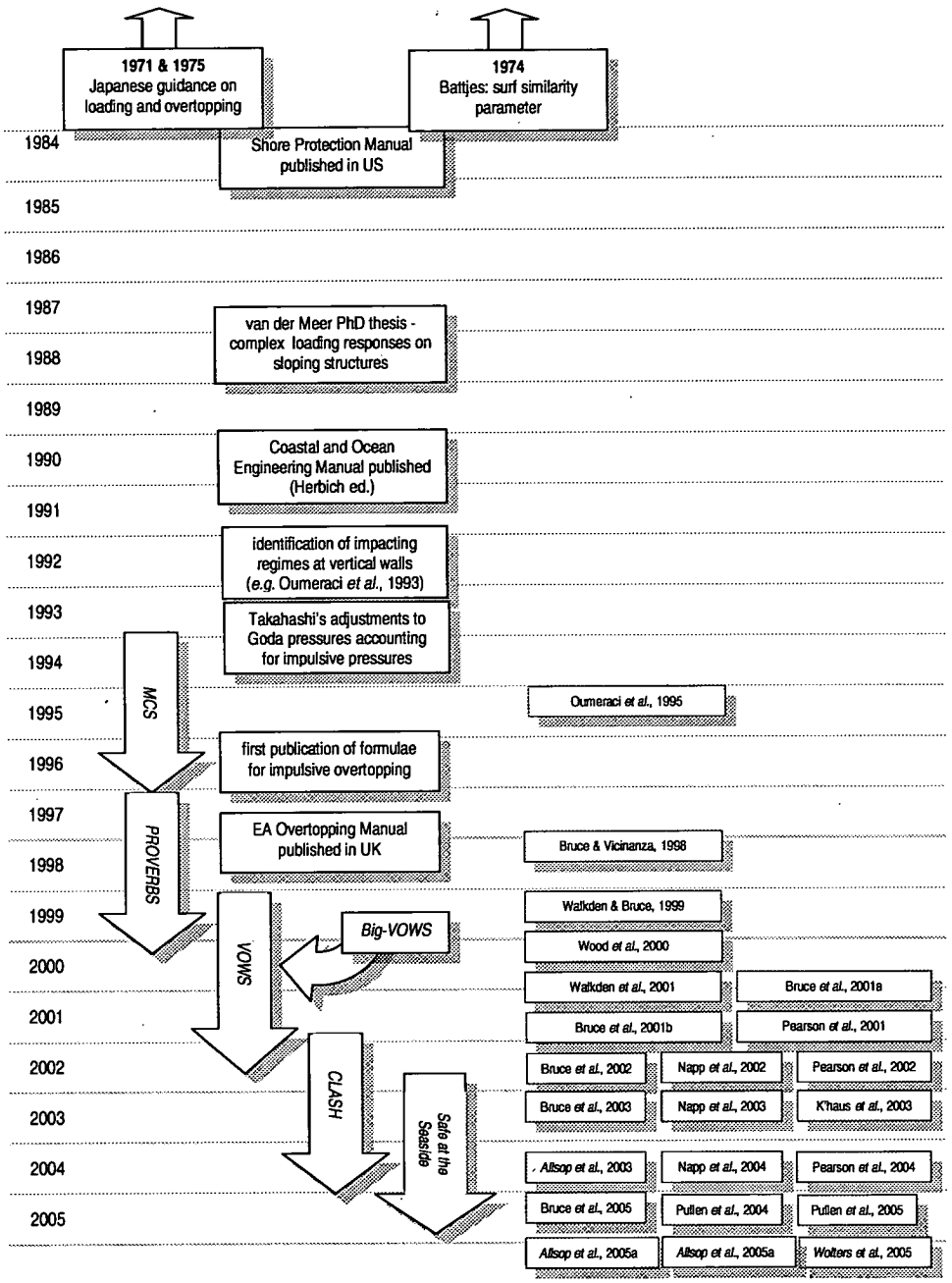

Figure 1.1: *Time-line diagram showing evolution of the field and contributed publications*

predictions of pressures, forces and overtopping at vertical structures, including Goda's method for loadings and Goda's design diagrams for overtopping.

- In the UK in the 1990s, the publication of new guidance in the form of the CIRIA / CUR Manual on the use of Rock at the Coastline (CIRIA / CUR, 1991) saw inclusion of Goda's

method to predict wave forces and advice on the occurrence of impact loads at vertical structures under some shallow water conditions (though this was a very minor aspect of a very large guidance document focussed almost exclusively on rock structures). The use of Goda's wave pressure predictions was also suggested in BS 6349 (1991).

- In Japan, Takahashi *et al.* (1993) published coefficients which allowed the allowed the adjustment of existing (Goda) pressure formulae to for conditions in which wave breaking at the structure was significant.

- From 1991 to 1994, the Monolithic Coastal Structures (MCS) project (led by Oumeraci, then at Franzius Institut, University of Hanover) made tremendous advances in the analysis of the responses of caisson breakwaters to wave action. In particular, different regimes of wave / structure interaction at vertical walls were properly identified for the first time (*e.g.* Oumeraci *et al.*. 1993). Conditions were observed to move from reflecting / pulsating, to breaking and ultimately to the cases where the waves are already broken before reaching the wall. Reflecting waves are characterised by waves simply running up the wall and back down again, with pressures / loads on the structure varying slowly (on timescales of the same order as the wave period). Breaking waves are observed to trap a pocket of air between the overturning wave crest front and the wall. The impact of the crest and the entrapped air give very high, short-duration pressure / force peaks, followed by a more slowly-varying quasi-static loading similar to that observed for reflecting conditions. Further, the compression of the trapped air pocket can give rise to a rapidly oscillating pressure. As the incident wave gets larger (or the depth in front of the structure becomes shallower), there comes a point when the wave no longer breaks onto the wall, but breaks before reaching the wall. What then reaches the wall is a broken wave characterised by a turbulent mass of water with a great deal of entrained air. Additionally, at the transition between pulsating and breaking conditions, a condition in which the incident wave almost, almost breaks onto the wall is identified. These flip-through conditions give very large, short-duration pressures (as per breaking conditions) but without any air being trapped (as so without any subsequent oscillatory pressures).

1.3 Structure of critical review

This critical review is broken down into three major technical sections; one dealing with issues relating to wave kinematics and loadings at vertical structures (Chapter 2), one with wave overtopping (Chapter 3) and the third with post-overtopping responses (Chapter 4). These sections begin with introductions which aim to show how the papers presented for critique form a coherent contribution to the development of that particular field. Paper critiques are then presented, either singly or where it makes more logical sense, as groups of two or more closely related papers. Each such sub-section begins with a short summary of the paper's (or papers') technical context, objectives, methodologies and conclusions. A critique is then given. In some cases, this may be quite short, whereas in others, it may be quite lengthy and include new material (*e.g.* graphs) following up on issues raised.

Chapter 5 follows through some issues identified by the critical review as gaps, presenting new comparisons of overtopping prediction methods, and visiting a previously neglected analytical framework for the assessment of direct overtopping hazard. Chapter 6 looks at some wider issues raised by the body of work. Finally, Chapter 7 gives overall conclusions and some vision of the next challenges.

The papers forming the subjects of this critical review are collected and presented in Appendices A to X.

The work is presented as two parts. Part 1 is the critical review; Part 2 contains the published papers.

Chapter 2
Wave forces and kinematics at breakwaters and seawalls

2.1 Introduction

The critiques presented in this Chapter relate to investigations focussed on loadings and wave kinematics at vertical breakwaters and related structures. These papers mark the author's entry into the field of hydrodynamics relating to breakwaters and seawalls. The importance of distinguishing between different physical forms of wave action at a vertical breakwater had begun to emerge clearly in the early 1990s (*e.g.* Oumeraci *et al.*. 1993). At that time, the author was involved primarily with the development and application of the Particle Image Velocimetry (PIV) flow measurement technique. While in Franzius Institute (FI) Hannover on a exchange visit funded by the British Council, he met Oumeraci, from which a collaborative study emerged, looking for the first time at the kinematics of breaking waves in front of vertical breakwaters linking to FI's main interest in loadings on caisson breakwaters under the EC *Monolithic Coastal Structures (MCS)* project (Oumeraci *et al.*, 1995). The Oumeraci *et al.* (1995) PIV study was revisited some years later in a collaborative project between Edinburgh and the University of Naples, which extended the study to measure kinematics of breaking waves at a breakwater in irregular seas (Bruce & Vicinanza, 1998). These velocity data formed the basis of a detailed comparison with a numerical method (Wood *et al.*, 2000).

The field was moved forward very significantly by the EC *PROVERBS* project (*Probabilistic Design Tools for Vertical Breakwaters*, see Oumeraci *et al.*, 2001). *PROVERBS* was a particularly large project, with 21 partners from 9 European nations. It was divided into four tasks;

1. Task 1: Hydrodynamic Aspects, led by Allsop, HR Wallingford;
2. Task 2: Geotechnical Aspects; led by de Groot, Delft Geotechnics;
3. Task 3: Structural Aspects; led by Crouch, University of Sheffield; and
4. Task 4: Probabilistic Design Tools; led by Vrijling, TU Delft.

Under Task 1, significant progress was made in developing a tool to identify wave-structure combinations susceptible to impulsive / breaking wave loads – the *PROVERBS* parameter map, and in developing methodologies for the prediction of the impulsive loads and their force *vs.* time histories. Contributing to this synthesis was a review of sources of scatter in data and of engineering approaches to the problem (Walkden & Bruce, 1999). During *PROVERBS* an example of a seaward-acting impulsive wave load on a breakwater was observed. The mechanisms for such an effect were explored and an investigation carried out to determine what classes of breakwater under what conditions might be susceptible to such impulsive seaward loads (Walkden *et al.*, 2001), supported by numerical comparisons carried out to confirm the physical mechanisms.

2.2 Wave kinematics in front of a vertical breakwater – measurements

Oumeraci, H., Bruce, T., Klammer, P. & Easson, W.J. (1995), *PIV measurement of breaking wave kinematics and impact loading of caisson breakwaters*, Proc. 4th Int. Conf. Coastal and Port Eng. in Developing Countries (COPEDEC IV), pp2394–2410, COPEDEC, Colombo (see Appendix A)

Bruce, T. & Vicinanza, D. (1998), *Wave kinematics in front of caisson breakwaters*, Proc 8th Int. Polar and Offshore Eng Conf (ISOPE'98), Montreal, 3, pp658–664 (see Appendix B)

2.2.1 Context, aims, methodology and contribution

The principal motivation of the 1995 work was to elaborate explanation of different wave loading regimes recently identified by Oumeraci *et al.* (1993). Previous studies were based upon measurements of loadings (*via* pressure measurements) and upon observations of the wave form at the structure. This work aimed to provide quantitative evidence in support (or otherwise) of the qualitative observations. The objectives were to measure simultaneously the velocity field under the wave through its impact with the wall, and the resulting pressure distributions up the wall. Four wave-structure regimes were studied;

- Non-breaking wave (but very near breaking – close to the *flip through* condition as described by *e.g.* Oumeraci *et al.* (1993).

- Breaking wave with small trapped air pocket
- Breaking wave with large trapped air pocket
- Broken wave

Velocity measurements were made using Particle Image Velocimetry (PIV). The measurement area was illuminated by a continuous wave (CW) laser and scanning beam system – the very best approach then available. PIV flow records were recorded on a Hasselblad large-format (50mm × 50mm) camera. The flow records were analysed using an Optical Flow Systems optical / digital PIV processor – a system in whose design the author had taken a leading role, and one which was again a "state-of-the-art" method at the time.

The 1995 study had been very successful in achieving its objective of elaborating the physical mechanisms / processes at work in the different wave-wall regimes *e.g.* non-breaking, breaking and broken wave conditions. The study used short wave groups rather than long tests with irregular seas. The wave groups were based upon those used in a study in deep water without a structure or beach in place (Skyner, 1992 & 1996). Skyner generated deep water breaking events using linear theory to bring into phase at a particular breaking point a large number of smaller waves of different periods, *i.e.* the wave breaking was induced by constructive interference of waves. For this study, Skyner's parameters were adjusted in an iterative manner to compensate for the effects of reflection from the wall until the required wave form at the wall was obtained.

Work under the *PROVERBS* project (Oumeraci *et al.*, 2001) gave methods to identify the dominant wave loading regime for a given wave-structure combination – the so-called *parameter map* first developed by Allsop *et al.* (1996) and presented in revised / expanded form in Oumeraci *et al.* (2001). Allsop *et al.*'s work gave a tool which enabled the 1995 PIV work to be revisited and moved on into "conventional" irregular sea states – the principal aim of the 1998 paper. The methodology was broadly similar to that employed in the 1995 study, with simultaneous PIV and pressure measurements. The hardware available for PIV image capture and analysis had moved on, with images now recorded using a 1024 × 1024 pixel Kodak MegaPlus monochrome digital camera (which cost *c.* £25k in 1994!). Images were analysed entirely digitally using Optical Flow Systems *VidPIV* software.

The 1995 paper presented, for the first time, detailed velocity fields extending into wave crests. The successor (1998) study yielded the first measurements of kinematics of largest events in

irregular seas.

2.2.2 Critique

Critical appraisal of worth

Due to the particular nature of the waves used in the 1995 study, it is difficult to ascribe to these wave height and wave period parameters. For the 1998 study with irregular seas, there were no previous comparable studies upon which to base a methodology, so this had to be considered and designed from scratch. The methodology adopted was to run a particular test (wave-structure combination) initially with only pressure measurements. These pressure data were then analysed to identify the four largest loading events within the (approximately) 1000-wave series. The nominally identical sea state was then re-run, with PIV measurement triggered to coincide with these previously identified large events. In addition to the PIV maps, this methodology gave some useful early insights into repeatability of nominally identical irregular seas. While in no case did the largest event as first measured reappear as the largest event again, it was always the case that the event did reappear in the top ten of events in subsequent runs. This added to the body of evidence on the sensitivity of pressure maxima under breaking wave events to small changes in the incoming wave profile.

The paper included a comparison with Calabrese's (1998) formulae for the prediction of the onset of breaking conditions at a wall. Calabrese's method was shown to work well. It perhaps deserves to be more widely recognised and used as an additional tool when testing for the possibility of impulsive conditions at vertical or steep plain or composite walls.

The data lent itself well to a comparison with an analytical approach – the pressure impulse model (*e.g.* Cooker & Peregrine, 1995) – Wood *et al.*, 2000). Comparison with numerical approaches would have been (and might remain) an interesting study, though it is only quite recently that numerical models capable of going past the *flip through* condition into regimes in which the wave crest front becomes concave have become more readily available.

Subsequent work / publications(s) arising

The numerical model comparison (Wood *et al.*, 2000 – Section 2.3) was built directly upon data from the kinematics measured in the 1995 and 1998 studies.

The Walkden & Bruce (1999) study on scatter in wave loading measurements reinforced and took forward the conclusions of this study on repeatability of loading events in irregular seas.

Other comments

Modern PIV equipment based upon specialist cameras and the cross-correlation method would have enormously simplified this work. At the time, it was a real achievement to obtain the data of the quality that was obtained. The quality of this data stands up well even today. Although analysis took a very long time, the resolution achieved using the 55mm photographic format is significantly higher than that achieved by most of the specialist digital PIV cross-correlation cameras in use today.

The velocity and pressure data obtained in this study might well be worth revisiting in context of new approaches which are emerging for the modelling of large / extreme events, *e.g. NewWave* (Tromans *et al.*, 1991, see Section 7.3.3). These methods are becoming established as a methodology for physical modelling of wave-structure interactions in deep water (*e.g.* ship and semi-submersible responses to extreme waves) but their modification / extension for shallow water conditions remains a major challenge. Given the sensitivity / variability of the wave processes occurring in front of a vertical wall, it may be that such "average extreme wave" approaches cannot be applied in these regimes. Any attempt to apply such methods will certainly need detailed verification in terms of comparison with what is learned from the 'conventional' (irregular sea state) approach. Such a comparison will certainly involve measurements of pressures and loadings, but will also include qualitative observations of wave shapes in front of the wall.

Overall assessment

The 1995 paper was a most novel piece of work which resulted from a good collaboration between teams with complimentary skills. It provided detailed supporting evidence for the emerging consensus about the various wave-structure interaction regimes observed at vertical breakwaters. The 1998 paper was a ground-breaking application of the PIV method. In terms of the contribution to the field, the contribution was only modest as the velocity data, though interesting, made no generic contribution to guidance.

2.3 Wave kinematics in front of a vertical breakwater – numerical comparison

Wood, D.J., Peregrine, D.H. & Bruce. T. (2000), *Wave impact on a wall using pressure-impulse theory. I : Trapped air*, J. Waterway, Port, Coastal and Offshore Eng. 126, 4, pp182–190, ASCE, New York (see Appendix C)

2.3.1 Context, aims, methodology and contribution

The data sets of Oumeraci *et al.* (1995) and Bruce & Vicinanza (1998) (Section 2.2) formed the basis of the detailed numerical comparison carried out with the University of Bristol team, which in turn led to this publication.

This detailed comparison demonstrated the physical mechanism for very high, short duration impulsive part of 'classic' church roof force-time history for impulsive wave loads on a wall. It also illuminated the role of air in modifying the form of the impact in terms of magnitude and duration – a role which remains an important component of the argument on scale correction of impact pressures.

2.3.2 Critique

Critical appraisal of worth

This publication stands as the basic verified explanation for force-time histories measured for very-nearly-breaking and just-breaking waves at a vertical wall. Detailed, truly like-for-like comparisons of numerical and physical models are not easily obtained and certainly not common. This comparison has particular value for its detail.

In common with all analytical and numerical models of wave-wall interaction, the key restriction upon worth remains the fact that they model only a single wave, or a short series of (usually regular, possibly irregular) waves. This means that while the comparison provides good verification for the model, it is under quite restrictive conditions which are not straightforwardly expanded to conditions understood by designers of such structures, *i.e.* irregular sea states. It is possible that methods based upon "average extreme conditions" (see Section 7.3.3) may build this missing bridge. As noted in the critique of the papers on measured kinematics (Section 2.2),

though these methods are becoming established for deep-water problems, there remain many issues to be resolved before they could be applied to the breaking wave conditions studied here.

Subsequent work / publications(s) arising

The numerical model team (at Bristol) extended work to include a study into the effect of a porous berm in front of the reflective wall. The pressure impulse model was also used as the basis for a further physical / numerical model comparative study - on impulsive seaward loadings (Walkden *et al.*, 2001, Section 2.5).

Other comments

Recent tests at the Forschungszentrum Kuste (FZK) in the Grosser Wellenkanal (GWK) under the EPSRC *BWIMCOST* project in partnership with EC *HYDRALAB II* have recorded not only even larger pressures that recorded before (at GWK, or any other large flume, or indeed in the field), but also local pressure-time traces with unusual shapes (Obhrai *et al.*, 2004). Of particular interest are traces that show the impulsive part of the church roof, but without the quasi-static part. Interestingly, these observations tie in with other very recent observations reported by Allsop & Clarke (2004) during hydraulic model testing at HR Wallingford of the proposed Turner Centre at Margate, Kent.

Overall assessment

This paper has lasting value in providing a strong physical rationalisation of the basis of wave impact mechanism.

2.4 Impulsive wave loadings at vertical breakwaters – uncertainties and inherent scatter

Walkden, M. & Bruce, T. (1999), *Scatter in wave impulse load maxima: a review*, Proc Int. Conf. Coastal Structures '99, Santander, 1, pp 439–444, A A Balkema, ISBN 90 5809 092 2 (see Appendix D)

2.4.1 Context, aims, methodology and contribution

The *PROVERBS* "parameter map" (Oumeraci *et al.*, 2001, after Allsop *et al.*, 1996) gives likely extreme loading regimes as function of wave and structure geometry combinations. Although apparently a deterministic tool, in reality it tells us about the probability of occurrence of wave loading regime for a particular case, though this is not explicit. Further, only Calabrese (1998) gives a predictor of this probability, and this is not yet strongly validated. *PROVERBS* (Oumeraci *et al.*, 2001) also gives formulae to predict forces under impacting conditions, but the data that these are based upon show considerable scatter. The thesis of this paper was that this scatter could be reduced only by resort to a tool more firmly founded on a physical basis – in this case, that impulse should be a conserved quantity in wave-structure loading events. The paper is based upon a review of existing datasets of wave impact pressures and forces and the scatter therein. Possible origins of the measured scatter are then considered in turn. A survey of *Engineering Solutions* to the problem that have evolved leads finally to some recommendations on the most likely fruitful way forward. Perhaps the most useful contribution of the paper is its a review of sources of variability in wave loading measurements and the engineering methods that have been established to overcome these uncertainties.

2.4.2 Critique

Critical appraisal of worth

This was a timely review of the state of the art in loading prediction. At a time when the *PROVERBS* project was making significant headway in analysis / understanding of the detail of impulsive loads on vertical breakwaters, the paper attempted to build a bridge between these (then) new data and existing methodologies.

Other comments

This works stands as a useful caution against two facts that are occasionally overlooked by enthusiastic experimenters:

1. The exciting chase for the highest impact pressures may have little importance in terms of changing guidance on the design of practical maritime structures. The variability of such events / measurements and their very small spatial footprint means that engineering

approaches have evolved, been verified and have become established which are founded upon more general, stable physical mechanisms, particularly impulse.

2. Repeatability: scatter is absolutely inherent in measurements of processes surrounding wave breaking at structures. Experimenters must be aware of this when establishing their methodology and in drawing conclusions from their data. This may indeed even drive the type of data sought, *e.g.*, the *CLASH* project chose to use mean overtopping as the key parameter in its assessment of laboratory, model and scale effects after difficulties experienced in a predecessor project (*OptiCrest*; see *e.g.* van de Walle *et al.*, 2002) which used wave run-up.

Overall assessment

This was a helpful and timely review and cautionary reminder. To some extent, it served its purpose and may not have lasting value as a stand-alone contribution

2.5 Impulsive seaward loads

Walkden, M., Wood, D.J., Bruce, T. & Peregrine, D.H. (2001), *Impulsive seaward loads induced by wave overtopping on caisson breakwaters*, Coastal Engineering, 42, 3, pp257–276, Elsevier (see Appendix E)

2.5.1 Context, aims, methodology and contribution

Van der Meer presented to a *PROVERBS* project Task 1 workshop (Edinburgh, 1997) an example wave loading case in which an impulsive seaward load had been measured on a low-crest breakwater (van der Meer, 1997, private communication). His thesis was that this could be due to air trapped on the rear face of the structure during a large overtopping event with a substantial plume of green water overtopping and re-entering behind the breakwater.

The principal objective of the work leading to this paper was to validate (or otherwise) the possibility of such a loading / failure mechanism being important for real structures. The methodology employed was an initial design study on most susceptible classes of real (at least designable) structures. This was followed by a 2-d physical model study using a Hansholm-type

low-crest breakwater. The model breakwater section was instrumented with pressure transducers on front, slant, top and rear faces, enabling all forces and moments to be estimated. This work established the clear possibility that the mechanism proposed (air entrapment at rear face of breakwater) could give rise to impulsive seaward loads. Importantly, it was also established that conditions giving rise to such events could occur on structures that would indeed be designable (*i.e.* not just behind structures which would never be built in reality).

2.5.2 Critique

Critical appraisal of worth

This paper was helpful in demonstrating a newly-identified loading mechanism that should be considered in the design of *Hansholm-type* breakwaters. The generic impact of the work was weakened by focus on single "freak" wave events. Results thus do not comfortably fit into a conventional design framework based upon irregular seas characterised by the usual parameters (significant wave height, peak period or similar). It may be that current developments in the characterisations of large / extreme / freak events in irregular seas may enable a reappraisal of the data with the possibility of making this missing link in the future.

Other comments

The principal likely causes of seaward loading on vertical breakwaters are those described by McConnell *et al.* (1999). For monolithic vertical structures, there may exist combinations of structure and sea state for which the seaward forces due to the run-down at the wave trough exceed the landward forces at the crest. This has been evident from Goda's design diagrams (*e.g.* Goda, 1974, 1985, 2000) for very many years, but may be overlooked in the design / analysis of a breakwater. McConnell *et al.* (1999) present new data on negative pulsating loads suggesting that the Goda approach may underestimate these quasi-static seaward loads, and they present revised guidance.

Overall assessment

A useful piece of work which gave important pointers to issues of negative loads and scaling. The findings may yet feed into design for a specialist class of structure. This paper remains the

only published study on such a physical process.

Chapter 3
Wave overtopping at breakwaters and seawalls

3.1 Rationale for study of wave overtopping

Wave overtopping occurs when water passes over the crest of a coastal defence – a breakwater or seawall. The consequences of wave overtopping can be divided into four broad areas;

- Flooding: If waves overtop a seawall, the water must go somewhere. Modest overtopping discharge may simply flow back over the defence and back into the sea, but under extreme conditions, flooding may occur. This is a particular concern when valuable infrastructure / properties lie close in behind the defence (as is very often the case - coastal sites are popular!)

- Wave transmission: Waves overtopping a breakwater will land in the area of water supposedly sheltered by the defence. The result of this will be enhanced wave activity in the protected area. For a commercial port, this may mean difficulties in loading / unloading operations, or even their suspension. For a yacht marina, this may cause risk of collisions between vessels and pontoons, or even the risk of vessels breaking free of moorings and causing further damage (see *e.g.* Franco & Bellotti, 2005).

- Direct hazard: Overtopping water carries with it potentially quite some momentum (not to mention sand, shingle, stones or larger matter). Thus it may present a direct hazard to people, vehicles or buildings in its path. The consequence can vary over the spectrum from minor damage, structural deterioration and interruption of normal operations or communications, through to personal injury or death. These effects are revisited in Chapter 4.

- Damage to the defence structure itself. A violent overtopping event may throw a large volume of water to some height, and the subsequently falling water mass is capable of exerting very significant pressures / forces on the crown deck of the defence (see

Chapter 4). Green water overtopping flowing over the crest can initiate damage too, with this effect perhaps being most pronounced (and studied) for flow over sloping dikes (*e.g.* Möller *et al.*, 2004; Schüttrumpf *et al.*, 2004).

It is clear that coastal defences must be appropriately designed against overtopping or rather, given that the target of zero overtopping is unrealistic and unnecessary, they must be designed to an appropriate admissible level of overtopping. Thus there is a need for robust and verified generic design tools for the prediction of overtopping discharge for commonly occurring / commonly designed coastal structures.

The economic case for research into improvements to design tools is not hard to make. Coastal defences are costly. The replacement cost of sea defences around England alone has been estimated as about £6000M. UK government spends approximately £100M per annum on new coastal defences, although damage from winter 1989/90 alone was estimated at £40M. A substantial proportion of the cost of a sea defence scheme is related directly to the design crest height, itself a direct consequence of the overtopping discharge predicted, and of the limit set. An uncertainty of just 0.5m in setting defence crest levels has been estimated to cost £830 per metre length. Over a scheme of 2km, such an uncertainty might be worth £1.7M out of a total budget of perhaps £10M.

3.2 Studies of wave overtopping presented in this critical review

So where were the gaps in the knowledge at the outset of this series of investigations in 1999? And how has the story progressed since then? 1999 saw the publication in the UK of a new guidance manual on wave overtopping (EA / Besley, 1999). This manual presented methods for predicting wave overtopping over both sloping / rubble mound and vertical / near-vertical structures. Much of the guidance reiterated methods for the prediction of mean and wave-by-wave overtopping discharges / volumes. For sloping structures, this was Owen (1980); for vertical structures Allsop *et al.* (1995). What was really new was that for vertical structures, a distinction was made between those cases where the wave overtopping was as a result of non-breaking waves (*pulsating* conditions / *green water* overtopping) and cases which could see waves actually breaking onto the wall (*impulsive* conditions / *violent* overtopping).

The new formulation was based upon what was then recent work by Allsop *et al.* (1995) and

Besley *et al.* (1998), which itself arose after it was observed that existing methods for vertical walls gave some very poor and unsafe predictions when extrapolated beyond the immediate, supported limits of their stated validity. In addition to the the HR Wallingford test set, these authors drew upon other test sets containing strongly impulsive conditions in the development and verification of the new formulae; these included small-scale tests at Delft Hydraulics (de Waal *et al.*, 1994)and field data (Herbert, 1996). By way of example, Figure 3.1 (based upon a similar graph in Besley *et al.*, 1998) shows small-scale data (HR Wallingford and Delft Hydraulics) and field data plotted on the "conventional" axes, together with the extrapolation of the prediction line for non-impulsive overtopping conditions.

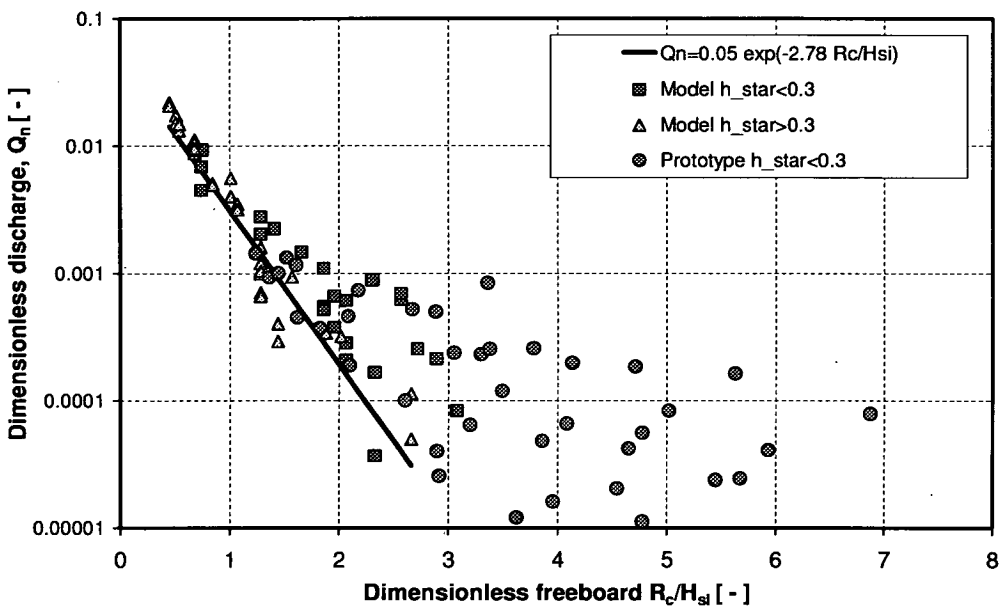

Figure 3.1: *Graph of dimensionless mean overtopping (Q_n)* vs. *dimensionless freeboard ($\frac{R_c}{H_{si}}$) showing problems encountered in extrapolation of guidance existing in 1996 beyond its supported limits. Graph based upon graph in Besley* et al. *(1998).*

This was the starting point for the author's involvement in studies of overtopping. Work is still very much on-going, and no claim to a complete solution is made, though very significant progress is reported. Prediction tools for overtopping under strongly impulsive conditions have been critically examined and extended to a wider range of realistic structures (Bruce *et al.*, 2001a; Allsop *et al.*, 2005a). For the first time, the new tool was validated against laboratory scale effects (Pearson *et al.*, 2002). No guidance was then available on the (3-d) effect of oblique wave attack under impulsive conditions. This gap was addressed by a major programme of tests in a wave basin at HR Wallingford (Napp *et al.*, 2002, 2003) resulting in new

Besley *et al.* (1998), which itself arose after it was observed that existing methods for vertical walls gave some very poor and unsafe predictions when extrapolated beyond the immediate, supported limits of their stated validity. In addition to the the HR Wallingford test set, these authors drew upon other test sets containing strongly impulsive conditions in the development and verification of the new formulae; these included small-scale tests at Delft Hydraulics (de Waal *et al.*, 1994)and field data (Herbert, 1996). By way of example, Figure 3.1 (based upon a similar graph in Besley *et al.*, 1998) shows small-scale data (HR Wallingford and Delft Hydraulics) and field data plotted on the "conventional" axes, together with the extrapolation of the prediction line for non-impulsive overtopping conditions.

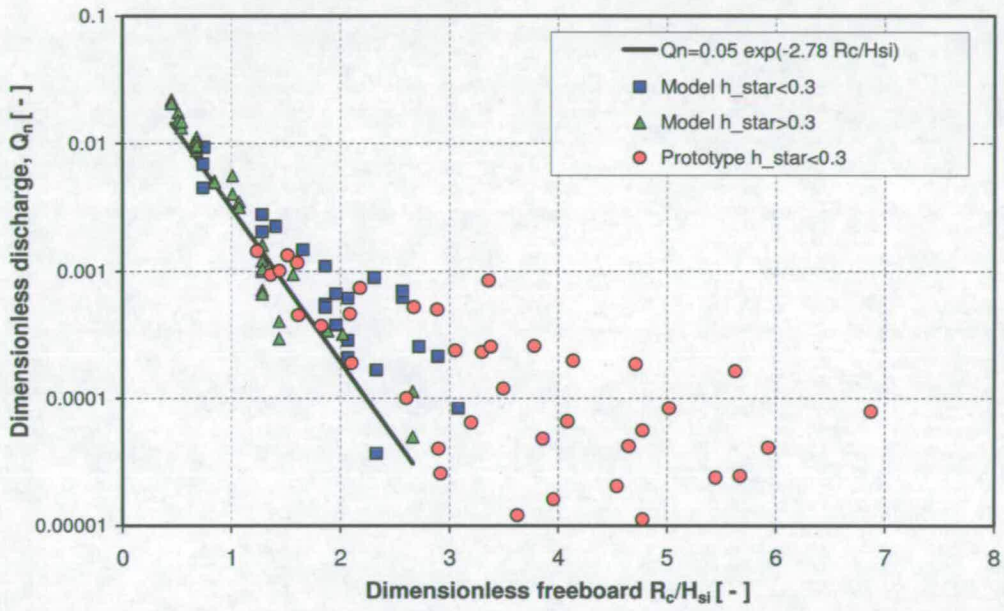

Figure 3.1: *Graph of dimensionless mean overtopping (Q_n)* vs. *dimensionless freeboard ($\frac{R_c}{H_{si}}$) showing problems encountered in extrapolation of guidance existing in 1996 beyond its supported limits. Graph based upon graph in Besley* et al. *(1998).*

This was the starting point for the author's involvement in studies of overtopping. Work is still very much on-going, and no claim to a complete solution is made, though very significant progress is reported. Prediction tools for overtopping under strongly impulsive conditions have been critically examined and extended to a wider range of realistic structures (Bruce *et al.*, 2001a; Allsop *et al.*, 2005a). For the first time, the new tool was validated against laboratory scale effects (Pearson *et al.*, 2002). No guidance was then available on the (3-d) effect of oblique wave attack under impulsive conditions. This gap was addressed by a major programme of tests in a wave basin at HR Wallingford (Napp *et al.*, 2002, 2003) resulting in new

guidance filling the gap (Napp *et al.*, 2004). Having examined possible scale effects by way of a comparison between small- and large-scale laboratory tests, the next logical step and major investigation was a comparison with field measurements. This was accomplished as part of the EC *CLASH* project (Pullen *et al.*, 2004). During this progression from small-scale 2-d tests to field comparisons *via* 3-d small-scale tests and large-scale 2-d tests, diversions were made to extend guidance to other commonly-occurring configurations not covered by the EA / Besley manual.

- Many seawalls employ overhanging parapets / recurves / wave return walls as an overtopping reduction measure. Despite their familiarity in the field, remarkably there existed little systematic guidance on their design and performance. Studies were thus carried out to synthesise more wide-ranging guidance (Kortenhaus *et al.*, 2003; Pearson *et al.*, 2004).

- Historically out of necessity and still, out of safety and economics, seawalls tend to be built with their toes at or just below the lowest tide level. Examination of the existing guidance reveals that key formulae will break down when the water depth in front of the wall is zero, and a designer would probably lose confidence in their predictions even before that, as waves move from a breaking regime to one in which all waves have already broken before reaching the wall. Studies were carried out to extend guidance into these regimes (Bruce *et al.*, 2003).

This subject progression *via* the major projects cited is shown graphically in Figure 3.2

3.3 An introduction to the *VOWS* project

While *PROVERBS* focussed on wave loadings on vertical structures, it did not consider overtopping. (In fact, the original proposal had included overtopping as an issue, but this had been removed in a subsequent scaling-back of what was still a giant project). In parallel with the run of *PROVERBS*, work was going on principally in the UK on extending to vertical breakwaters and seawalls established methods for the prediction of wave overtopping. It became evident that the distinction between breaking and non-breaking, or impulsive / non-impulsive conditions first described by Oumeraci *et al.* (1993) and greatly illuminated in terms of consequence for loading by the *PROVERBS* "parameter map" (Oumeraci *et al.*, 2001, after Allsop *et al.*,

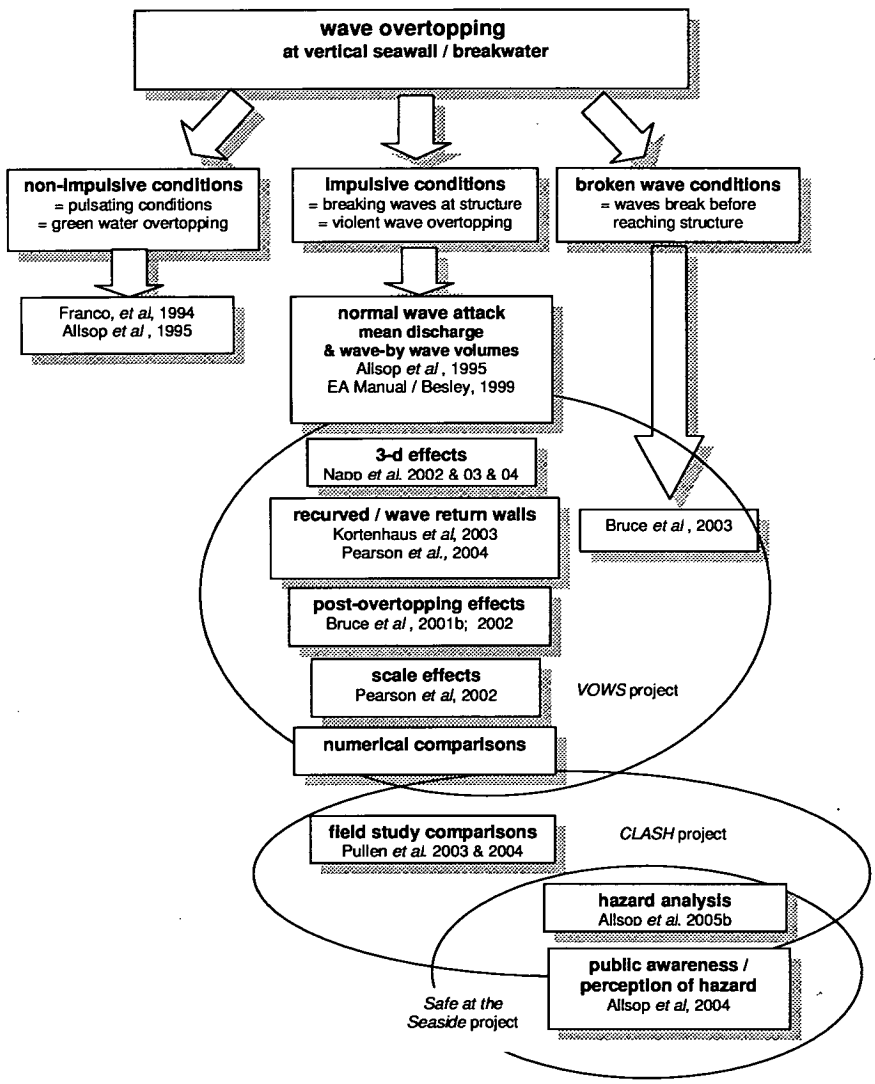

Figure 3.2: *Summary of elements of overtopping research covered by papers in this critique.*

1996) was similarly important for the description and quantification of overtopping processes. In the large body of work which followed, a key is the distinction made between green water overtopping arising from non-breaking / non-impulsive / pulsating wave conditions at the wall, and violent / impulsive overtopping arising from impulsive / breaking conditions.

Besley synthesised new UK guidance (EA / Besley, 1999) on wave overtopping under impulsive conditions based on Allsop *et al.*'s (1995) work. Bruce and Allsop then secured EPSRC funding for a three-year programme of more detailed investigation into such violent overtopping processes. The project which became known as *VOWS* (Violent Overtopping by Waves at Seawalls) sought to expand the basis of the new guidance, with extension into a wider range of impulsive conditions. *VOWS* was initially two projects – the physical model study led by Bruce and Allsop (which was the basis for many of the papers whose critiques are presented in this thesis) and a sister numerical model study led by Causon and his team at Manchester Metropolitan University. At the time of the proposal, EPSRC suggested that the physical and numerical model teams make a joint or linked proposal; a suggestion which was enacted despite no prior connection with the MMU team. This partnership turned out to be a most fruitful and rewarding one, and one which has endured well past the funded period of the *VOWS* project and into subsequently funded projects *CLASH* (see Section 3.10.1) and *Safe at the Seaside* (see Section 4.3.1). The numerical models serve not only as a basis for possible future design, but as a here-and-now tool for rationalising / verifying physical mechanisms as part of the analysis and explanation of physical model results.

The physical modelling strand of the *VOWS* project was later expanded to include large-scale tests (*Big-VOWS*) taking advantage of an opportunity to access the large wave channel at UPC Barcelona under the EC *HYDRALAB* project. This work is introduced and described in Section 3.9.

3.4 Impulsive wave overtopping – simple vertical walls

Bruce, T, Allsop, N.W.H. & Pearson, J. (2001a), *Violent overtopping of seawalls – extended prediction methods*, Proc. "Breakwaters, coastal structures and coastlines", pp 245–256, Thomas Telford, London, ISBN 0 7277 3042 8 (see Appendix F)

Allsop, N.W.H., Bruce, T., Pearson, J., Alderson, J. & Pullen, T. (2003), *Violent overtopping at the coast - when are we safe?* International Conf. on Coastal Man-

agement 2003, pp54–69, ICE London, Thomas Telford, ISBN 0-7277-3255-2 (see Appendix G)

Allsop, N.W.H., Bruce, T., Pearson, J. & Besley, P. (2005a), *Wave overtopping at vertical and steep seawalls*, Proc. ICE, Maritime Engineering, 158, 3, pp103–114, ISSN 1741 7597 (see Appendix H)

3.4.1 Context, aims, methodology and contribution

The context of / motivation for this study is set out in Section 3.3 above.

The aim of the 2001 paper was to place into the public domain the first major set of data validating (or otherwise) the then newly published UK guidance on overtopping (EA / Besley, 1999). The four intervening years of study and experience, together with the extended journal article format allowed the 2005 paper to be a more thorough review of the technical background. The 2005 paper also offered revised guidance which will appear in a new overtopping assessment manual currently in preparation.

The methodology was a detailed 2-d physical model study, designed to focus for the first time on wave / structure combinations likely to give impulsive / breaking wave conditions. Such a study could not have been designed before new analysis tools became available from the *PROVERBS* project (Oumeraci *et al.*, 2001). The overtopping detection and measurement system used in these first series of Edinburgh overtopping tests was developed from scratch. Overtopping discharge was channelled *via* a chute from the model wall crest into a collection tank suspended from a load cell. The load cell trace was analysed not only to give mean discharge, but also to allow individual increments of collected water mass to be identified and measured to give wave by wave overtopping volumes. A siphon arrangement emptied the collection tank as necessary during tests, with software being written to correct for this emptying and allow individual overtopping volumes to be measured even during periods of tank emptying.

The principal contribution of the 2001 work was to further support the (then new) EA / Besley (1999) guidance as a benchmark tool for prediction of mean overtopping under "violent" conditions.

The 2003 paper showed for the first time how different methods might be applied to a real structure, thereby illustrating the dramatic consequences of the switch between pulsating and impulsive regimes at the structure.

The 2005 paper offers some small improvements based upon further tests and reappraisal of earlier data, but principally set out the collection of new and improved methods. This paper will form the basis of the chapter on steep and vertical structures in the new "European Wave Overtopping Assessment Manual (*EurOtop*)" currently in preparation.

3.4.2 Critique

Critical appraisal of worth

The 2001 contribution was an early part of a major process of making the case for use of distinct predictors for breaking and non-breaking cases, in distinction from all other national / international guidance (though it should be acknowledged that in certain parts of the world, most notably Japan, this class of problem is not nearly as commonly occurring as around UK / European coasts). The presentation of the paper at a conference popular with senior practitioners from private and government / agency sectors from UK and abroad gave a most appropriate audience group. The paper was well-received and interesting and helpful discussion followed, including comments from Goda (see Section 3.6).

The 2003 paper's intent was to present to a very practical audience the key consequences that arise out of the (then) new understandings of the different overtopping regimes at seawalls. Its lasting contribution was the identification of the *consequence* in terms of *actual* overtopping discharge of the switch between pulsating and impulsive conditions. Because the formulations for these two regimes are so different (one an exponential relationship based upon the simple relative freeboard R_c/H_{m_0}; the other a power-law relationship including water depth and wave period parameters too) they cannot readily be plotted in a general way on the same graph. This paper took the approach of looking at this switch between formulae for a particular structure, and showed a striking result - that the overtopping response was not necessarily a monotonic function of the freeboard. Under certain conditions, as the tide recedes (and thus R_c increases), the overtopping can actually *increase* due to the switch from pulsating into impulsive mode.

To some extent, the 2003 paper can also be considered as leading the way in making the essential link from overtopping discharges to direct hazard (to people, vehicles and structures) in the zone immediately behind the defence. This topic is explored in more depth by papers presented and critically reviewed in Chapter 4.

Although the firm conclusion offered in the 2001 paper on the agreement of the data with EA

/ Besley (1999) was justified, it was offered without any (minor) adjustment based upon the *VOWS* dataset, nor with any quantification of the spread in the data. The 2005 paper proposed a revised fit;

$$Q_h = 1.92 \times 10^{-4} R_h^{-2.92} \tag{3.1}$$

valid over $0.05 \leq R_h \leq 1.0$

Returning to the data, the author has now drawn upper and lower bounding lines to include approximately 95% of the data (Figure 3.3).

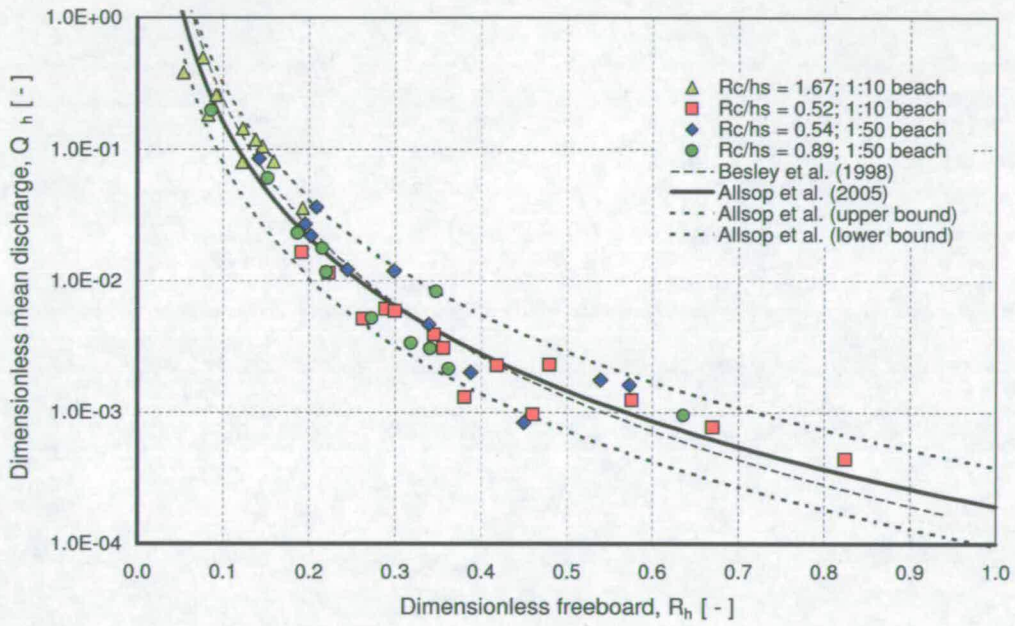

Figure 3.3: *Graph of dimensionless mean overtopping (Q_h) vs. dimensionless freeboard (R_h), showing 95% confidence limits.*

It can be seen that the minor adjustment being proposed makes almost no difference over a wide range of conditions but provides an improved fit with the data for highest R_h values ($R_h > 4$). The upper and lower bounds include 46 of the 48 data, and are (simply) a factor of two greater and less than the mean prediction line (Equation 3.1) respectively. This paper contained a great deal of new data and did a thorough job of validating EA / Besley (1999) guidance over a substantial parametric range. Although reference was made to earlier tests and prediction methods, quantitative comparisons were not carried out at the time. Some further analysis and

reflection therefore seems appropriate here.

The *VOWS* data are plotted in the same manner as that adopted by Franco & Franco (1999) together with their predictor and its 95% confidence limits (Figure 3.4). Over their stated range of validity ($1.2 \leq \frac{R_c}{H_s} \leq 1.7$), the agreement is good, with 19 of the 21 *VOWS* data over that $\frac{R_c}{H_s}$ range falling within the 95% confidence bounds. As expected and as seen by Allsop, Besley and other investigators in studies which drove first investigations of new prediction tools for impulsive conditions, (incautious, unsupported) extrapolation gives predictions which are very much less good as $\frac{R_c}{H_s}$ increases above about 1.8.

While revisiting the early *VOWS* data, a brief new study into whether the fit with EA / Besley (1999) was better or poorer in any particular parameter ranges is presented here. In the graphs that follow, the variate is the ratio of measured to predicted mean overtopping discharge. Thus a value of 1.0 represents perfect agreement between measurement and predictor. The variate is plotted on a logarithmic axis in order that a difference of a given factor away from 1.0 appears as the same distance above (under-prediction) or below (over-prediction) the line. *E.g.* a point which is a factor of two over-predicted appears as far from the line as one under-predicted by the same factor.

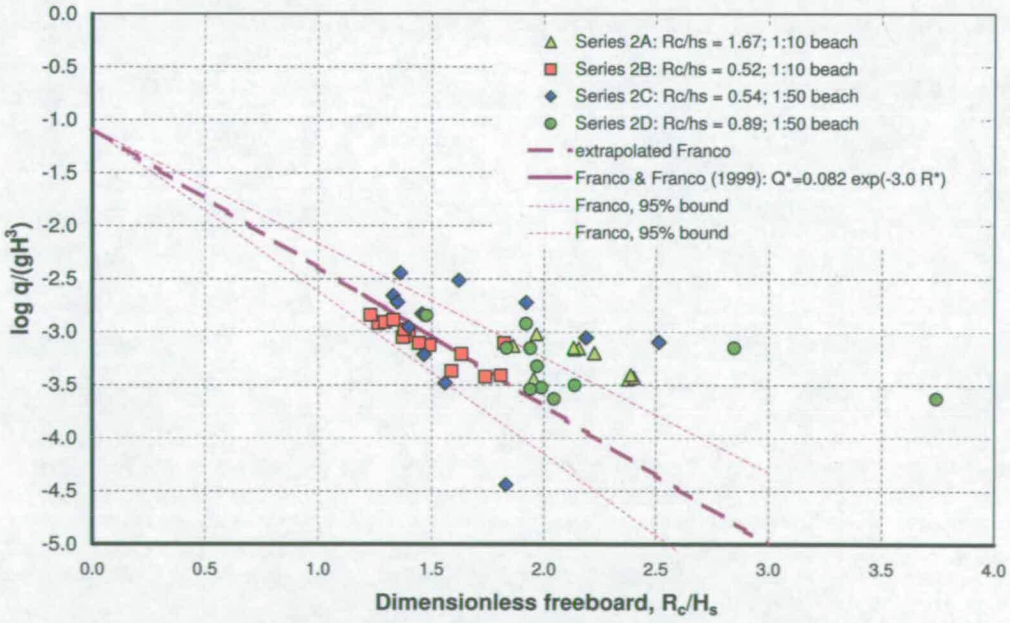

Figure 3.4: *Graph of dimensionless mean overtopping* vs. *dimensionless freeboard* ($\frac{R_c}{H_s}$), *showing Franco & Franco (1999) predictor (in part extrapolated) and 95% confidence limits.*

Plotting the ratio of measured:predicted mean overtopping against the h_* parameter (Figure 3.5), it is seen that with the exception of two data lying at very lowest h_* ($h_* < 0.03$), all data for expected impulsive conditions according to EA / Besley (1999) ($h_* < 0.3$) are in agreement with the predictor to within a factor of 2.5 or better. As expected, agreement with Franco & Franco (1999) is very good under non-impulsive conditions ($h_* > 0.3$) and much less good for lower h_* values.

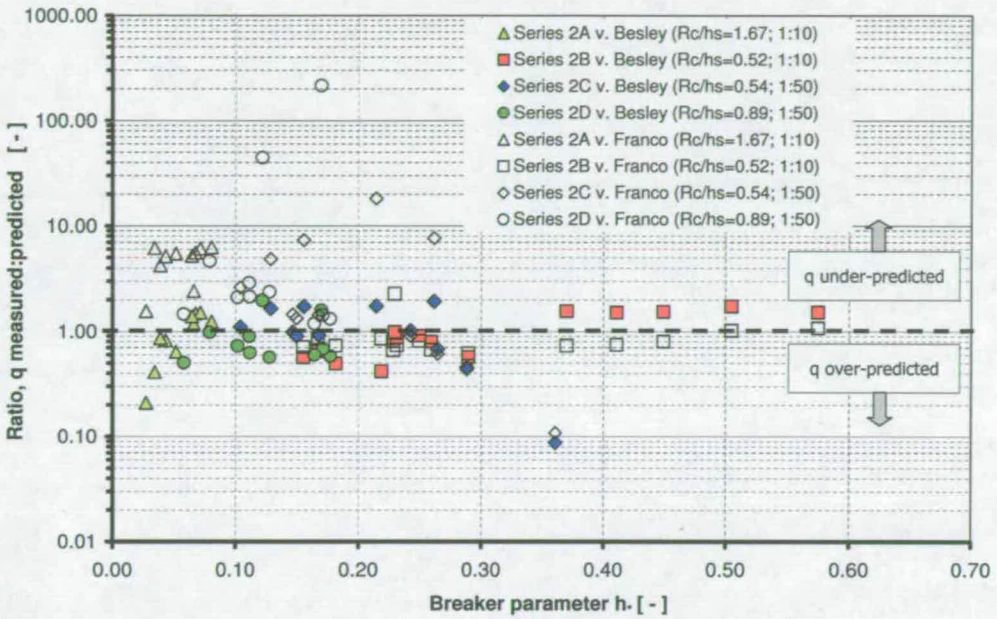

Figure 3.5: *Graph of ratio of measured : predicted mean overtopping* vs. h_*. *Filled symbols are for EA / Besley (1999) predictor; unfilled symbols for Franco & Franco (1999) (in many cases extrapolated outside its stated range of validity).*

It is interesting to get a sense of whether the greatest scatter away from the prediction line might be associated with the smallest measured volumes which will have the largest associated measurement error (Figure 3.6). There is indeed some indication of a somewhat greater spreading about the ratio = 1 line for lowest q, with the point at $q = 1.14 \times 10^{-6} m^3/s/m$ notable for being more than a factor of 10 smaller than predicted (but is infact a pulsating condition with $h_* > 0.3$). In terms of volume actually collected, 469 ml was collected during the 1024s test with only 15 of the *c.*1100 waves overtopping.

A further issue that has emerged over the years since publication of this paper is the strong shift away from statistical to spectral measures of wave / sea-state characteristics. While the original work used statistical measures $H_{1/3}$ and T_z, the original wave elevation-time histories

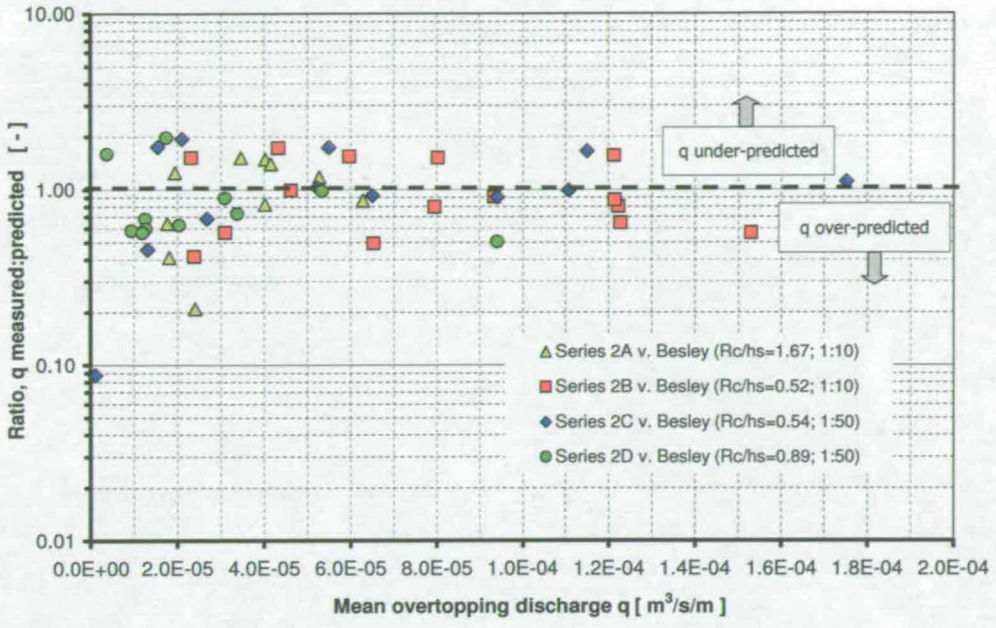

Figure 3.6: *Graph of ratio of measured : predicted (EA / Besley, 1999) mean overtopping* vs. *mean overtopping discharge q.*

were kept and subsequently reprocessed for the *CLASH* overtopping database (*e.g.* Steendam *et al.*, 2004). The author thought it timely to compare the picture using the preferred spectral measures H_{m0} and $T_{m-1,0}$ to that published using $H_{1/3}$ and T_z. The result (Figure 3.7, comparing with Figure 3.3) is reassuring in that the differences observed are slight and largely within the inherent data scatter. There is some evidence of under-prediction for lowest R_h values, but discussion of this is abbreviated in the light of the result of a similar cross-check for the large-scale laboratory data reported in Section 3.9, which shows almost zero effect when the transition between sets of measures is made.

Finally, the benefit of hindsight reveals that the exceptionally good agreement found with the methods given in EA / Besley (1999), after Allsop *et al.* (1996) and Besley *et al.* (1998) may have resulted in the *VOWS* team paying less attention to comparisons with other existing formulations than they might have done. Having made this observation, the author has attempted to redress this omission as part of this critical review – see Section 5.2

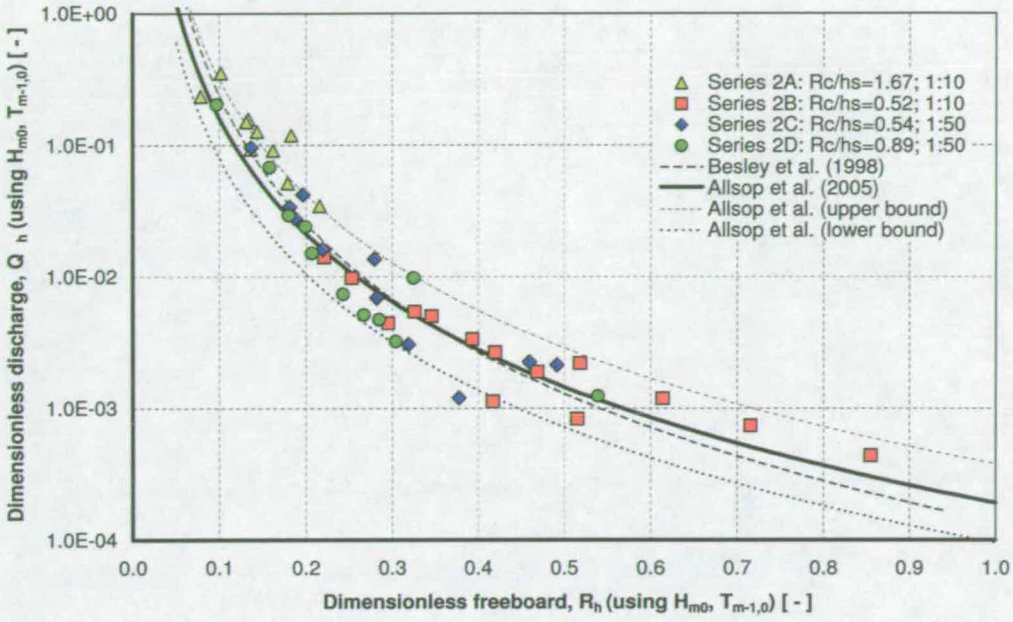

Figure 3.7: *Graph of dimensionless mean overtopping (Q_h) vs. dimensionless freeboard (R_h), with data evaluated using spectral measures H_{m0} and $T_{m-1,0}$. The lines correspond to EA / Besley (1999) mean and 95% confidence bounds which have already been established in comparison to data using statistical measures $H_{1/3}$ and T_z.*

Subsequent work / publications(s) arising

The work provided the basis for a successful bid for access to a large wave channel to expand *VOWS* to include a detailed investigation of scale effects (Pearson *et al.*, 2002). The *VOWS* 2-d work also provided a secure basis for the detailed design of the programme of wave basin tests at HR Wallingford to determine corrections for oblique wave attack. (Napp *et al.*, 2002; 2003; 2004; Section 3.8). The 2-d method was extended to two further situations common in engineering practice for which no generic guidance existed;

- wave / structure regimes under which incident waves break before reaching the wall; Bruce *et al.*, 2003 (Section 3.6);
- reduction of mean discharges by *recurves / wave return walls / parapets*; Kortenhaus *et al.*, 2003; Pearson *et al.*, 2004 (Section 3.7).

Other comments

The Besley / EA (1999) guidance turned out to be particularly robust in engineering terms, and thus the 2001 paper offered no new guidance for vertical wall overtopping, but rather a carefully planned and fairly wide-ranging validation. New coefficients were proposed to account for off-vertical (*battered*) walls at 10:1 and 5:1 which are very common in the field.

After the presentation, van der Meer asked after the physical basis of the h_* parameter used to discriminate between impulsive and non-impulsive conditions. Besley (also in the audience) noted that originally, the parameter had been arrived at by analysis of the overtopping data set. While some physical rationale can be seen by inspection – h_* gets less (conditions become more impulsive) as relative depth at structure ($\frac{h}{H_s}$) reduces, and / or as wavelength (relative to depth) increases – it is not clear why this particular dimensionless combination should be critical. This comment led to a short, subsequent investigation, also reported in the conference proceedings (Allsop, 2002). The argument was made as follows:

> Owen (1980) developed a simple-method to give a first-estimate of the permissible upper limit of the significant wave height. Digitised limits for three beach slopes are shown in Figure 3.8, together with three lines for values of h_* = 0.30; 0.15; 0.10. To explain the h_* parameter, consider the following simplified example: consider a wave of small significant height approaching the shore with a significant period of $7s$, and the water depth at the toe of the structure is $5m$, hence $\frac{h_s}{gT^2} \sim 0.01$. Thus adopting the somewhat simplified assumption that the wave height changes and that all the parameters remain the same, the wall undergoes the following changes due to the wave climate; for $H_{si} < 1m$ ($\frac{H_{si}}{h_s} < 0.20$), $h_* > 0.30$, hence the wall is subject to pulsating waves. As the wave height increases, $1m < H_{si} < 2m$ ($0.2 < \frac{H_{si}}{h_s} < 0.4$), a corresponding decrease in h_* is observed ($0.15 < h_* < 0.30$), hence the wall is subject to waves in the transition region from pulsating to impacting waves. As the wave height increases further $2m < H_{si} < 3.25m$ ($0.4 < \frac{H_{si}}{h_s} < 0.65$), the wall is subject to impacting waves. Finally, the approaching waves reach their depth limited values, hence although it's not possible for the wave height to increase the waves have broken hence the wall is subject to broken waves.

Van der Meer also asked

> Do the data points in the figures all relate to violent overtopping? Or are there situations which still are according to 'deeper' water and do they match with overtopping formulae without h_*?.

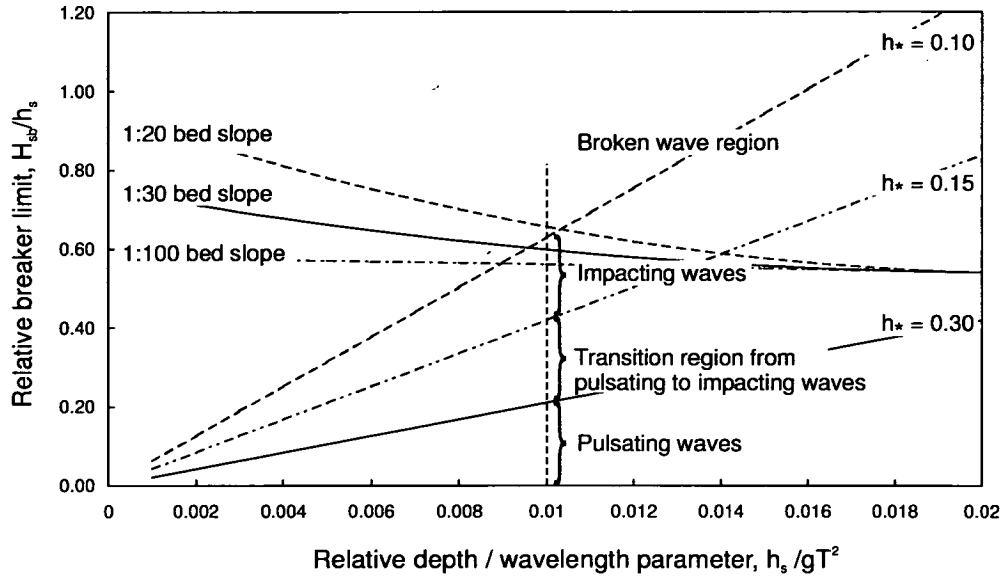

Figure 3.8: *Shoaling – permissible shallow-water significant wave heights (after CIRIA / CUR, 1991).*

Our response (published in the proceedings – Allsop, 2002) was as follows:

> As demonstrated in the paper, we need to distinguish whether the waves approaching the shore are of an impulsive or pulsating nature. For pulsating waves, we have adopted Franco & Franco (1999) deeper water formula, and for impulsive waves we have adopted EA / Besley (1999) impulsive formula. The aim of the study was to investigate violent overtopping processes at coastal structures, hence the test matrix was designed to ensure impacting events were predominant. Nevertheless, we can look at how the two prediction tools perform as we increase h_*; *i.e.*, as we move from highly impulsive ($h_* < 0.15$) towards pulsating conditions ($h_* > 0.3$). The ratio of measured (dimensional) mean discharge to that predicted by the two formulae are plotted against h_* in Figure 3.5. A value of 1 indicates agreement between predicted and measured discharge, with larger values indicating under-prediction. Clearly as the experiments were designed for impulsive conditions, the EA / Besley (1999) prediction method gives more accurate results when $h_* < 0.15$. It should also be pointed out that the Franco & Franco (1999) formula *has been applied outside the suggested permissible limits for most test conditions.* Using Franco and Franco (1999) within its permissible limits demonstrates that when $h_* > 0.3$ good agreement exists between predicted and measured discharges.

A further comment was made by Goda:

> It is nice to see your data fit quite well in dimensionless expressions. However, the data does not cover the range of shallow water where $\frac{h}{H_s} < 1.0$, where your dimensionless parameters may not function well. Practising engineers would like to have the data in this range also. Do the authors plan to extend their laboratory study to cover the shallow water zone in the near future?

This comment led directly to such a study, appearing as Bruce *et al.* (2003) – Section 3.6.

Overall assessment of publication

The 2001 paper was of immediate worth to end user community in

1. providing further strong support in what was then quite new guidance for wave overtopping under impulsive conditions, and
2. in providing helpful correction factors for battered walls.

The worth of the 2001 and 2003 papers have been overtaken by the 2005 journal article, which should have lasting worth. The 2005 paper (together with parts of Wolters *et al.*, 2005) forms the basis of a major chapter in the "European Wave Overtopping Assessment Manual (*EurOtop*)" currently in preparation.

3.5 Impulsive wave overtopping – measurement scatter

> Pearson, J., Bruce, T. & Allsop, N.W.H. (2001), *Prediction of wave overtopping at steep seawalls – variabilities and uncertainties*, Proc. Ocean Wave Measurement and Analysis ('Waves 2001'), 2, pp1797–1808, ASCE, New York, ISBN 0-7844-0604-9 (see Appendix I)

3.5.1 Context, aims, methodology and contribution

The need to make extensive and detailed quantitative comparisons of model test data with prediction tools makes a knowledge of uncertainties associated with measurements a necessity. Key questions which often arise following a series of experiments are

- what is inherent scatter in nominally identical tests?
- what is the effect of wave spectrum generation method?
- is the conventional / "accepted" 1000-wave sequence an appropriate length and based upon a well-supported argument?

Walkden & Bruce (1999) gave a review of uncertainties in wave loading processes; this paper addressed key sources of uncertainty with respect to overtopping measurement. The methodology was strongly based on a small-scale physical model study in the flume at Edinburgh, supported by flume data from HR Wallingford. The Edinburgh tests were for a vertical structure, with the HRW tests on a sloping embankment. The paper delivered some quantitative advice on the variabilities inherent in nominally identical overtopping tests, and on the (small) effect of using (as is typical in laboratory wave generation) nominally identical realisations of a spectrally-defined sea state (*i.e.* with all component phase angles the same for each run).

3.5.2 Critique

Critical appraisal of worth

The paper was very well-intentioned and addressed a neglected but very important issue. We were however disappointed with what general advice we were able to distil from what was quite an extensive series of tests. With hindsight is seems that we allowed ourselves to focus to closely on a particular albeit important part of the process of modelling when a broader view of modelling uncertainties and laboratory and scale effects more generally might have yielded outcome of more generic value.

The *CLASH* project returned to these issues in 2002 – 2004, with an excellent summary given by Kortenhaus *et al.* (2004a). One of the most useful outcomes of the *CLASH* project was a thorough survey of sources of uncertainty in laboratory experiments (Kortenhaus *et al.*, 2005)]. Uncertainties were divided into three categories;

- measurement errors; uncertainties introduced by virtue of the limitations of the measurement system employed, *e.g.*, uncertainty in measurement of overtopping volume collected. In principle, these errors could be reduced by improvements to the measurement systems.

- model effects; uncertainties due to the methodology of representing a real situation in the laboratory. Examples of model effects include the selection of a (probably standard) wave spectrum; the length of test run used; the simplifications made to the structure / foreshore geometry / bathymetry. The effect of wind on wave overtopping is identified as a key model effect.

- scale effects; inaccuracies introduced by virtue of the model being at a different (usually smaller) scale then the prototype. Scale effects will arise from the scaling of processes which will not scale according to Froude scaling. Examples for rubble mound breakwaters are in the wave run up around an armour layer on a rubble mound breakwater and the flow in the core of the breakwater. For impermeable vertical structures, scale effects could relate to processes in the wave-structure interaction where entrapped or entrained air plays a role, *i.e.* especially under impulsive conditions.

It has thus become clear that the field has moved on significantly since this paper was presented in 2001, and is now characterised by a broader perspective placing errors and uncertainties in the context of the whole process of modelling a real situation.

Overall assessment

Ultimately a modest contribution, but the issue highlighted was an important one, and one to which much more effort was given by others as part of the *CLASH* project (Kortenhaus *et al.*, 2004a & 2005).

3.6 Wave overtopping under broken wave attack

Bruce, T., Pearson, J. & Allsop, N.W.H. (2003), *Violent wave overtopping – extension of prediction method to broken waves*, Proc "Coastal Structures 2003", pp619–630, ASCE, Reston, Virginia, ISBN 0-7844-0733-9 (see Appendix J)

3.6.1 Context, aims, methodology and contribution

As noted in the comments on Bruce *et al.* (2001a) above, this work was largely inspired by comments made by Professor Yoshimi Goda after the presentation of that paper.

> It is nice to see your data fit quite well in dimensionless expressions. However, the data does not cover the range of shallow water where $\frac{h}{H_s} < 1.0$, where your dimensionless parameters may not function well. Practising engineers would like to have the data in this range also. Do the authors plan to extend their laboratory study to cover the shallow water zone in the near future?

His remarks were timely. *VOWS* work had firmly supported EA / Besley tool over its stated range of validity characterised by $h_* < 0.3$ and $0.05 < R_h < 1.0$ (Bruce *et al.*, 2001a; Section 3.4). It can be seen from the definition of h_* that it continues to decrease as the water depth decreases, a decrease which must ultimately lead to conditions under which all waves reaching the structure will already have broken due to limited water depth. This is a widespread and thus important design case. As noted in the introductory remarks (Section 3.2), most seawalls have their toe at or only a little below the water level at lowest tides. Broken wave attack may represent the design case for loading and perhaps also for overtopping.

Investigations into wave-structure problems under broken wave attack have been severely limited by grave concerns over scaling of small-scale hydraulic model test data to prototype. It is long-established that (quasi-static) wave loadings scale well under green water conditions. *PROVERBS* (Oumeraci *et al.*, 2001) gives some useful guidance on scaling of impulsive loads due to breaking waves, but its section on broken wave loads on plain vertical walls (Section 2.6.1, pp 120–121) demonstrates in the clearest terms that little progress had been made for scaling of broken wave loadings. Guidance remained that based upon Blackmore & Hewson's (1984) tests, though with alternatives given without detail. The reason for this difficulty is clear – the heavy entrained air content can and does have a very strong influence upon the loading, and this air entrainment does not scale according to the rest of the model (*i.e.* by Froude) but rather by Mach / Cauchy (and possibly also Weber).

The *Big-VOWS* tests (Pearson *et al.*, 2002; Section 3.9) showed such strong evidence that overtopping volumes and discharges scaled very robustly even under quite severe wave breaking gave the team new confidence that there could be worth in pursuing small-scale overtopping measurements under breaking conditions, and discussions with *CLASH* partners backed this up. While it was considered possible, indeed likely that the EA / Besley (1999) method could be adjusted for shallower water conditions, it is apparent that a simple adjustment is no longer possible when the water depth at the structure, $h_s = 0$, as the h_* parameter goes to zero, which in turn results in the collapse of the prediction formulae. The paper was able to present, for the first time, clear guidance on how to predict mean overtopping under broken wave conditions

1. for small positive h_s (*via* an adjustment to EA / Besley, 1999) and
2. for small negative h_s ie still water lying just below the toe of the wall (*via* an adjustment to van der Meer & Janssen's (1995) formula for sloping structures).

The methodology was a small-scale physical model study in the flume at Edinburgh. Overtopping measurements were made over a range of structure configurations straddling the case where the wall's toe is at still water level ($h_s = 0$). The dataset was split into those with small positive h_s and small negative h_s. The separated datasets were then explored to establish a prediction tool. The research was able to identify suitable predictors for both $h_s > 0$ and $h_s < 0$ situations, with the former being based upon an adjustment to Besley (1999) and the latter an adjustment to van der Meer & Janssen (1995). At the very end of the work, additional data was taken to check the performance of the new $h_s < 0$ tool, which seemed to work well.

3.6.2 Critique

Critical appraisal of worth

The paper presented clear results and conclusions from careful and fairly wide ranging small-scale study. It is emphasised in the paper and again here that direct validation of robustness of scaling / applicability to prototype case remains to be carried out. That said, recourse to the complete lack of scale effect measured under strongly breaking conditions demonstrated by Pearson *et al.* (2002) (Section 3.9) gives some confidence that the effect may not be as great on overtopping as on loadings and (especially) on localised pressures.

Further, if there exists a significant scaling effect affecting the regimes studies by this paper, it is highly likely that the result would be lower than predicted overtopping. Studies of broken wave loads (*e.g.* Blackmore & Hewson, 1984) point to model tests underestimating the amount of energy dissipation which takes place during the breaking process and during the subsequent propagation of the highly aerated, turbulent residual wave front or bore. Even if arguments about the robustness against scale effects of the data remain somewhat open, this data gives a clear lower bound on the applicability of EA / Besley guidance into the shallow water / low h_* / broken wave regime.

Interestingly (especially given Professor Goda's encouraging comments, above), the only existing guidance comes from Goda's (1975, 1985, 2000) design charts, which extend down to

water levels $0.5 \times H_s$ below the wall toe – a point made in the paper. The comparison done for this paper (Figure 10 in the paper) showed that Goda's chart gave safe predictions in these regimes.

Other comments

A possible source of supporting evidence for scalability might be the large-scale data set from the *VOWS* tests at UPC, Barcelona (Pearson *et al.*, 2002; Section 3.9). Although the test matrix did not include any broken wave conditions – with hindsight, an unfortunate omission – some conditions may have been quite near to this. If these could be identified, a review of the data might give some insight into whether there was any sign of a shift in the way in which the results seemed to scale extremely well from small- to large-scale. The author is not aware of any field data set which would be (even remotely) comparable to the $h_s < 0$ cases presented in this paper.

Wave loading under broken wave attack received scant attention owing to known difficulties with scaling. The result is that guidance remains uncertain. This is a concern, given that many seawalls have sufficiently shallow water conditions in front of them to make broken wave loads the likely dominant loading case. It seemed to the authors (and Goda – see above) that the broken wave regime should not be overlooked for overtopping, and that guidance with caveats about scaling was a worthwhile and useful objective.

Overall assessment

Further tests at large / prototype scale will be the ultimate judge of the worth of these tests. If there is further supporting evidence of scale-ability, then this paper will provide immediate, useful guidance to end-users and as such would be a valuable contribution.

3.7 Overtopping reduction by recurve walls / parapets

Kortenhaus, A., Pearson, J., Bruce, T., Allsop, N.W.H. & van der Meer, J.W. (2003), *Influence of parapets and recurves on wave overtopping and wave loading of complex vertical walls*, Proc "Coastal Structures 2003", pp 369–381, ASCE, Reston, Virginia, ISBN 0-7844-0733-9 (see Appendix K)

Pearson, J., Bruce, T., Allsop, N.W.H., Kortenhaus, A. & van der Meer, J.W. (2004), *Effectiveness of recurve wave walls in reducing wave overtopping on seawalls and breakwaters*, Proc. 29th Int. Conf. Coastal Engineering, 4, pp 4404–4416, ASCE / World Scientific, Singapore, ISBN 981-256-298-2 (see Appendix L)

3.7.1 Context, aims, methodology and contribution

Wave return walls / recurves / parapets are widely used in real coastal defence schemes, particularly on urban sea walls. Given their commonplace occurrence in practice, it comes as a surprise to learn that there is almost no detailed and / or generic guidance on their design and their effect upon overtopping discharge. Owen & Steele (1991) tested recurved walls on the crest of 1:4 and 1:2 sloping structures, with the effect of oblique wave attack being investigated by Banyard & Herbert (1995). The conclusions of these studies form the basis of guidance given in EA / Besley (1999). No guidance was then available for recurves on steep or vertical walls.

Such a study is considered to be particularly timely, as these modifications / design features tend to be installed in conditions of shallow water and possibly impulsive overtopping. In times when there is a very strong suspicion of increased storminess and medium-term predictions of sea level rise, these structures also represent a convenient modification / retro-fit to bring overtopping discharges back down to their original design / admissible levels. These papers set out with the aim of filling this knowledge gap and providing some form of generic guidance.

The methodology employed was a gathering together of data from four laboratories; Edinburgh, Leichtweiß-Institut (Technical University of Braunsweig, Germany), HR Wallingford and Delft Hydraulics (The Netherlands). For the 2003 paper, a method was evolved which determined whether the recurve was operating in one of three regimes, and gave discharge factors k. While the method gave quite good results in the 'little or no reduction' and 'some reduction' regimes, there remained very poor modelling of the 'large reduction' regime ($k < 0.05$). It was speculated that this was due to the method not distinguishing between impulsive and non-impulsive conditions. Although there must be a caution about whether it is possible to design for $k < 0.05$ without site-specific physical model tests given the uncertainties involved, the 2004 study focussed upon whether impulsive conditions would throw interesting and useful light upon the physical mechanism(s) at work in determining the recurve / parapet effectiveness for lowest k factors.

The 2003 paper presented, for the first time, a generic method for predicting the reduction in overtopping achieved by the addition of a simply-shaped recurved / parapet. The 2004 paper gave a method to adjust the method presented by the 2003 paper to give better predictions for cases of large reduction in overtopping (k factors < 0.05). Three k factor regimes were identified, and equations given for each

3.7.2 Critique

Critical appraisal of worth

The 2003 paper's main short-coming is that the method is based upon a one-size-fits-all approach. This approach is a sensible and defensible initial methodology which gave a method which is conservative and generic thus matching the aspirations of its client users, but it masks the detail of the mechanisms driving the overtopping reduction behaviour of the recurves / parapets. On a linear scale, the fit between the new prediction method and the data is good. Plotting on a logarithmic scale, however, reveals that the fit is much less good for conditions under which the parapet gives very large reductions, *i.e.* conditions for very small recurved k factor < 0.05 – see Figure 5 in the paper. Thus the method will not give reductions of more than a factor of 20 for any reasonable-sized parapet, although conditions under which reduction by a factor of 100 or more for modest-sized parapets have been recorded and are in the data set. In engineering use, this is a prudent precaution.

Perhaps the principal reason for the scatter at lowest k is that the method does not differentiate between impulsive and non-impulsive events / conditions. Observations suggest that the processes at work for overtopping reduction under impulsive conditions are significantly more complex, with there being some evidence of something akin to a switch at work; the parapet is highly effective at deflecting an uprushing jet back out to sea, but there comes a point when the gap under the parapet fills with water during the wave impacting process, at which point the effectiveness of the parapet is almost 'switched off' and water flows over this filled volume and overtops much more readily.

This speculation is yet to be backed up by further experiments which should focus on the switching mechanism and the location of such a switch in parameter space.

In any case, it is important to consider whether $k < 0.05$ is realisable in design, given the possible sensitivity of k to precise incoming wave conditions and uncertainties associated with

design wave conditions and overtopping prediction.

The original idea for the 2004 work was to revisit the data set which drove the 2003 paper and distinguish between impulsive and non-impulsive conditions. Then, for the impulsive conditions, it was hoped that a means of identifying the 'switch' between highly effective and less effective recurved / parapet performance could be identified. Attempts to proceed with a new, detailed method more firmly based upon physical processes were stalled by the scatter in the data set. New data were not available as originally planned (see below), and what resulted was then a reworking of the existing data set.

This reworking was not entirely unsatisfactory, as the data did show some 'switch' behaviour (see Figure 6 in the paper) between regimes giving modest reductions (of the order of a factor of 20) and a regime in which reductions could be much larger (smaller k factors). Nevertheless, it remains an outstanding problem to properly found a method (this one or another one) on the physical processes at work. Only then might there be sufficient information to design for $k < 0.02$ or so anyway. The above critique may paint a picture of a piece of work which did not fulfil all of its original (and multi-client) objectives. To some extent, this is the case, but it is worth noting that both papers were received with interest and led to substantial improvements in engineering guidance, even if not in the science.

Subsequent work / publications(s) arising

Other comments

This problem might lend itself to a neural-network-based approach, with a sufficiently diverse data set within which are hidden (perhaps) a relatively small number of physical processes.

A large set of further experiments were carried in advance of the 2004 presentation to expand the data set available (*c.* 80 further tests). The tests were carried out by an honours student. On subsequent review, a small number (one or two) inconsistencies were identified in this new data set. Although it is likely that it was for the most part a valid set, the author decided that he had insufficient confidence in it for any of the data to be used. The entire data set was therefore discarded. It would be useful to revisit this issue and repeat these experiments.

Overall assessment

This is a practical contribution to the literature addressing a commonly occurring design feature for which there existed no previous generic guidance (although note Cornett *et al.*, 1999, for landward-sloping parapets). Problems with a new data set led the 2004 paper to be only an increment to Kortenhaus *et al.* (2003).

3.8 Impulsive wave overtopping – three-dimensional effects

Napp, N., Allsop, N.W.H., Bruce, T. & Pullen, T. (2002), *Overtopping of seawalls under oblique and 3-d wave conditions*, Proc. 28th Int. Conf. Coastal Engineering, 2, pp 2178–2190, ASCE / World Scientific, Singapore, ISBN 981 238 238 0 (see Appendix M)

Napp, N., Pearson, J., Bruce, T. & Allsop, N.W.H. (2003), *Overtopping of seawalls under oblique wave attack and at corners*, Proc. "Coastal Structures 2003", pp 528–541, ASCE, Reston, Virginia, ISBN 0-7844-0733-9 (see Appendix N)

Napp, N., Bruce, T., Pearson, J. & Allsop, N.W.H. (2004), *Violent overtopping of vertical seawalls under oblique wave conditions*, Proc. 29th Int. Conf. Coastal Engineering, 4, pp 4482–4493, ASCE / World Scientific, Singapore, ISBN 981-256-298-2 (see Appendix O)

3.8.1 Context, aims, methodology and contribution

A major component of the VOWS project was a programme of wave basin tests designed to deliver adjustments to 2-d tools for conditions of oblique wave attack. There existed a limited body of work on 3-d overtopping effects, but it was strongly focussed upon sloping structures. Where vertical structures were considered, the few papers (*e.g.* Franco & Franco, 1999) were focussed on conditions which were predominantly non-impulsive.

Earlier studies (on overtopping and on wave loadings / pressures) also present somewhat contradictory evidence, with some suggesting small increases for small obliquities (up to *c.* 15°) while others show only monotonic, decreasing behaviour.

These three papers tell the story of this investigation, from the reporting of data 'hot off the press' – Napp *et al.* (2002) was presented during the period of testing at HR Wallingford – through to the final guidance presented in Napp *et al.* (2004).

The papers were all founded upon an extensive series of 3-d physical model tests carried out in a wave basin at HR Wallingford. The experimental set up was designed to replicate as closely as reasonably possible that used for the *VOWS* 2-d tests at Edinburgh. Overtopping was collected at four locations along the model seawall. Each collection station consisted (as in the Edinburgh tests) of a chute and collection tank, suspended from a load cell. Mean and wave-by-wave overtopping measurements were determined from analysis of load cell time histories. A submersible pump was placed in each tank, enabling the tanks to be emptied during testing under heavy overtopping conditions (*c.f.* the syphon arrangement used in the Edinburgh tests).

Napp *et al.*(2002) concluded that no increase in mean overtopping discharge was observable for small obliquities. Only decreases in overtopping with obliquity were measured.

The paper also gave, for the first time, evidence that overtopping behaviour moved away from a functional form typical of impulsive conditions (power law for Q_h *vs.* R_h) for large obliquities (up to 60^0). It was subsequently demonstrated (Napp *et al.*, 2004) that it shifted to an exponential relationship between dimensionless discharge and dimensionless freeboard in agreement with the predictions for non-impulsive conditions.

The physical insights into transition from impulsive behaviour to non-impulsive were completely novel. In particular, the identification of an *impact-like* regime intermediate between impulsive and non-impulsive regimes specific for 3-d conditions was new and exciting. This wave–structure regime (more fully described in Napp, 2004, p71) does not exist in 2-d experiments, or under normal wave attack. It is an intermediate condition between impulsive and non-impulsive regimes for vertical walls under oblique wave attack. The wave breaks, but along rather than onto the wall. The resulting overtopping response has the characteristics of impulsive conditions, following an adjusted form of the EA / Besley (1999) method.

This set of papers draw a number of important conclusions;

- Guidance was given for mean overtopping discharge for oblique wave attack at angles of up to 60°. This guidance took the form of adjustments to the EA / Besley guidance for $\beta = 0°$ for obliquities of up to $\beta = 30°$, and advice on switching to a modified form of the pulsating (*i.e.* non-impulsive) for higher obliquities.

- Guidance was given on prediction of the distribution of individual, wave by wave overtopping volumes. In a manner similar to that for mean discharges, suggested formulae

given for wave by wave volumes are adjusted forms of EA / Besley (1999) ($\beta = 0°$ case applies for $\beta = 15°$ and $\beta = 30°$, and then a switch to the non-impulsive method given in EA / Besley).

- Excitingly, a new wave-structure interaction regime dubbed *impact like* by the authors was identified and described. This regime, lying intermediate between impulsive and non-impulsive conditions is peculiar to conditions of oblique wave attack. In *impact-like* conditions, the loadings are no longer impulsive, but the overtopping response continues to follow the physical form associated with impulsive / violent overtopping (clearly demonstrated by *e.g.* Figure 3 in the paper).

3.8.2 Critique

Critical appraisal of worth

Napp *et al.* (2002) was absolutely 'hot off the press' with wave basin tests still in progress. This was a helpful contribution, placing some exciting new results before end users at a top conference within days of data collection. More detailed analysis, appraisal of results and new, quantitative guidance appeared in the subsequent publications (Napp *et al.*, 2003 and 2004).

Napp *et al.* (2004) summarised key outcomes of a major research project investigating a difficult and important problem. Many supporting charts and arguments were not included because of the imposed page limit. Indeed, it was with this knowledge that it was decided to write this paper as a summary of key results and new guidance. The full supporting material has since been set out in Napp's PhD thesis (Napp, 2004) and will appear in journal articles currently in preparation. It was not a comfortable decision to minimise supporting argument to such an extent – some of the evidence for the switches of regime of overtopping from impulsive to *impact-like* to pulsating with increasing angle of incidence is exciting, striking and compelling.

Napp *et al.* (2004) was the third in the line of papers arising from the VOWS 3-d wave basin tests carried out in 2002. It was a confident contribution based upon data which had been thoroughly and painstakingly explored. The final guidance offered was extensively discussed among the author team, which included a potential end-user (Allsop).

The original test programme had included tests to examine the effect on overtopping of non-uniform plan geometry, specifically breakwaters with sharp corners or smaller angle elbows

along their length. While these tests were included in the model design phase and indeed some tests were carried out, it became clear that a proper parametric, generic description of the problem and the overtopping response could not be achieved within the time available for the project in the wave basin. This was a pity, but with 10 days or so of remaining time, the decision was made to concentrate on further basin calibration tests whose need had been identified during initial data analysis. Hindsight confirms that this was the right decision, but it would be most interesting and potentially valuable to revisit the issue of corners / elbows.

The issue of spatial variability of overtopping along even a straight wall could be revisited too. This paper touches on this effect and makes conservative allowance for it in the guidance offered. Napp expands upon his observations and explanations in his PhD thesis (Napp, 2004).

The fitting to the data of the adjusted prediction curves for $\beta = 15°$ and $\beta = 30°$ was done using a simple regression (via *MS Excel*). While this gave a fit to each dataset which was in itself satisfactory, it overlooked the overall picture. As pointed out by Pullen (2006, private communication), although the fitted lines (Figure 3.9) give physically sensible behaviour for $R_h > 0.2$, as R_h decreases below 0.2, the lines cross the $\beta = 0°$ prediction (the $\beta = 15°$ line crossing first at $R_h = 0.2$ and the $\beta = 30°$ line following suit at $R_h = 0.09$. Some adjustment to the lines would be in order, though a simple immediate adjustment to the guidance to correct for this would be to suggest the use of the $\beta = 0°$ formula for all $R_h \leq 0.2$.

Subsequent work / publications(s) arising

Twin journal articles are at an advanced stage of preparation for submission to the ASCE Journal of Waterway, Port, Coastal and Offshore Engineering which will contain a great deal of supporting evidence (graphs *etc*) which could not be included in these papers. Napp's PhD thesis (Napp, 2004) gives a great deal of detail about the test set up and data gathering / analysis methodologies.

Other comments

The amount of thought and careful effort that went into transforming the initial raw data set into a useable form was enormous, amounting to some months. The wave paddles used at HR Wallingford were brand new and suffered from inevitable teething problems. In particular, their calibration and reflection absorption performance was uncertain and being constantly adjusted.

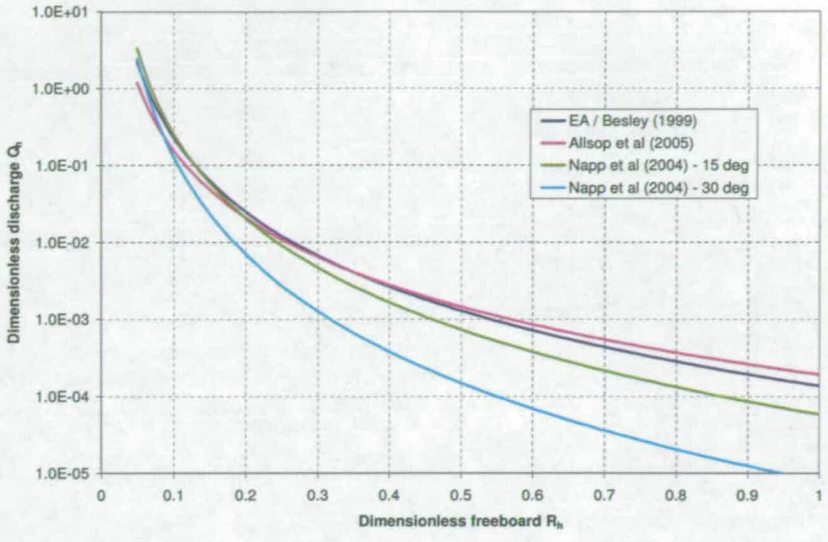

Figure 3.9: *Graph showing the prediction lines as given by Napp* et al. *(2004).*

The result were very many lengthy discussions to explore and establish a route to confident and supportable calibration of the measured seas, remembering all the time that further tests were completely out of the question.

The challenges associated with wave basin testing cannot be underestimated, particularly when operating in a laboratory 600 km from Edinburgh. That the tests have resulted in such firmly-based and useful conclusions is particularly satisfying for all concerned.

Napp's PhD thesis was examined and passed by van der Meer, who commented favourably on the worth of the investigation and outcomes.

Overall assessment

The 2004 paper was an important contribution based upon a piece of work that had reached maturity. This has been a strong contribution offering detailed guidance on a topic of genuine practical worth to end-users. The range of guidance spans mean and wave-by-wave overtopping. The conclusions of Napp *et al.* (2004) were suitable for immediate end-user uptake.

3.9 Scale effects in impulsive wave overtopping tests

Pearson, J., Bruce, T., Allsop, N.W.H. & Gironella, X. (2002), *Violent wave overtopping – measurements at large and small scale*, Proc. 28th Int. Conf. Coastal Engineering, 2, pp 2227–2238, ASCE / World Scientific, Singapore, ISBN 981 238 238 0 (see Appendix P)

3.9.1 Context, aims, methodology and contribution

The EPSRC *VOWS* project comprised small-scale 2-d wave flume tests (at Edinburgh) and small-scale 3-d wave basin tests (at HR Wallingford) to assess 3-d corrections. During the course of *VOWS*, an opportunity arose to bid for access to a large wave channel under the EC *HYDRALAB II* project (itself under the EC Transnational Access to Major Research Infrastructure – *TAMRI* – programme). It was recognised that this presented a most timely opportunity to extend *VOWS* (into a project which became known as *Big-VOWS*) to include a study on scale effects. The bid was successful, and was followed up by a successful proposal to EPSRC for 6 months of additional funding for the project RA (Dr Jon Pearson). Finally, a six-month extension to the original *VOWS* project put all of the pieces in place for this exciting new opportunity.

The methodology was designed to replicate as closely as possible the methodology of the *VOWS* small-scale test programme at Edinburgh so that uncertainties associated with comparing the two datasets could be minimised.

This work delivered a conclusion of substantial generic worth – that laboratory scale effects are not significant for overtopping of vertical / near-vertical structures under violent / impulsive wave attack. This conclusion was unexpected given the strong indicators of scale effects identified in the EU *OptiCrest* project on run-up on armoured, sloping structures (*e.g.* van de Walle *et al.*, 2002). The study included measurement of individual wave-by-wave overtopping volumes, and the conclusion of no scale effect was demonstrated for the maximum individual overtopping volume too.

3.9.2 Critique

Critical appraisal of worth

This piece of work was very strongly focussed and carefully bounded, and led to a very useful result of some fundamental importance.

Many large-scale test programmes lead to inconclusive findings, often due to the limited access time at the facility, and to the inevitable difficulties of working in a strange laboratory remote from home. One of the factors in the success of the project was its focus on being an investigation into scale effects alone. Every attempt was made to recreate a representative subset of the small-scale Edinburgh tests as closely as possible, and temptation to divert and explore new questions was resisted (with the exception of an investigation into the trajectories followed by violent overtopping discharge jets – see Bruce *et al.*, 2002 (Section 4.2).

Other factors in the success were the overall level of cooperation within the *VOWS* team and of course the skills of the project RA (Dr Jon Pearson) and of the local support team – see below.

Even with hindsight, it remains interesting to speculate whether the lack of scale effects could have been anticipated. It should be acknowledged that there are fewer parameters to scale for a study of a plain, impermeable, (near-) vertical wall than in tests on rubble mound structures, for which armour units, filter layer and core materials must all be scaled according to practice based upon experience and compromises rather than exact analysis. Nevertheless, the project's focus on violent overtopping meant that the majority of conditions were characterised by waves breaking at / onto the wall. It is well-known (*e.g.* summary in *PROVERBS*, Oumeraci *et al.*, 2001) that wave loading under breaking conditions is strongly influenced by the characteristics of any trapped or entrained air in the wave front. Thus, it was certainly not clear that overtopping volumes would not be affected to a similar, significant degree.

Returning to scaling of wave loadings; under impulsive conditions, it is the impulsive 'spike' part of the pressure *vs.* time (or force *vs.* time) history of the event which does not scale straightforwardly or reliably. The quasi-static part of the event can be scaled much more confidently. The explanation of the absence of scale effects in the impulsive overtopping may point to the bulk of the overtopping process being driven by (or at least linked more to) the quasi-static part of the wave event, despite the visual impression of a very sudden, impulsive overtopping event. Taking this argument a step further, it might be speculated that at least for the higher overtop-

ping conditions, the majority of the overtopping volume passes over the crest of the wall in a mass of water in a state approaching green water, with only a smaller fraction forming the visually striking uprushing jet.

From the critique of Pearson *et al.* (2003), and in particular, the attention drawn to concerns over scale effects in the assessment of overtopping under broken wave conditions, it is apparent that the omission of broken wave conditions from the test matrix for these large-scale tests was regrettable but understandable given that, at the time, it was not expected that the breaking wave conditions would scale well, let alone broken wave conditions. The flume time available for the tests was of course restricted, so other tests would have to have been dropped – perhaps the tests with the parapet contributed less of lasting worth than would have tests under broken wave attack.

One minor aspect of the test set up that might have been designed differently was the choice of a 10:1 battered wall as the core case, though with some tests done with a vertical wall. The decision to use the 10:1 wall did not diminish the level of confidence in the small- to large-scale comparison – equivalent tests had been carried out in Edinburgh – but it simply made the set up appear less generic. The reason that 10:1 was chosen over vertical was with the numerical modellers in mind. Our numerical model partners preferred the prospect of modelling a steeply sloping wall to a fully vertical one, though with hindsight (and with only admiration for what they achieved) that level of detail in the comparator set ups was not justified.

Subsequent work / publications(s) arising

The conclusions of this work fed neatly into the EC *CLASH* project. *CLASH* studied overtopping on both rubble mound and vertical structures. For the latter type, field measurements were carried out by a team from HR Wallingford, and comparisons made with small-scale laboratory tests at Edinburgh. The results of this paper were important in these *CLASH* studies in that they bridged the gap between the small-scale tests and field measurements.

Other comments

The results in this paper were also presented to the EC *HYDRALAB II* final workshop (Budapest, May 2003). The presentation was very well-received. Indeed, the project was notable among a number of large wave flume projects in its success in drawing a very firm conclusion

about scale effects.

The support received from the local team at UPC Barcelona was of the highest possible quality. They worked long hours and with remarkable commitment to ensure the ultimate success of the project. The co-authorship of this paper reflects the depth of that support. In addition to Xavi Gironella, the team have placed on record their appreciation of the great efforts and technical support of Quim Sospedra and Oscar. Further, Jon Pearson was assisted most ably during the first phase of testing by Stephen Richardson (then Manchester Metropolitan University, now HR Wallingford) and during the second phase by Nicolas Napp (University of Edinburgh) and Giovanni Cuomo (University of Roma Tre).

The progress of *Big-VOWS* was not without its problems. After suffering some weeks of delay due to problems with the wave paddle at UPC Barcelona, when the first violent breaking / overtopping waves were generated, they dislodged the wall from its mount (within the first three breakers)! This did however confirm that the test design had correctly generated substantial impact pressures. Once the wall had been re-installed, tests progressed remarkably smoothly and efficiently.

It has been said that the flume at UPC Barcelona is not truly a large-scale facility, but really operates at some intermediate scale. While it is true that the wave heights H_{m0} achievable are smaller than those achievable in either the Delta Flume operated by Delft Hydraulics (The Netherlands) or the Grosserwellenkanal (GWK) operated by the Forschungszentrum Kuste (FZK) (Hannover, Germany), it gave wave conditions approximately six times larger than the small scale tests. As such, these tests were truly large-scale, taking place at a scale much larger than a 'normal' laboratory scale but somewhat less than prototype scale. Additionally, the wave paddle at UPC Barcelona has fairly good reflection absorption performance – an important facet for tests with a highly reflective structure.

Pressures on the front face of the structure were measured throughout the test programme, but were not analysed by the *VOWS* team. These data were revisited by Cuomo (University of Roma Tre) and initial analysis presented in Cuomo & Allsop (2004). Interestingly, pressures were under-predicted by the *PROVERBS* method (Oumeraci *et al.*, 2001). A journal article on this study is in preparation at the time of writing.

During the project negotiation phase, *HYDRALAB* managers 'piggy-backed' onto the *Big-VOWS* a proposal from a team from the Bulgarian Academy of Sciences, led by Dr Jordan

Marinski. Marinski sought to investigate some of the details of the physical processes associated with wave impacts. While this collaboration was characterised by warmth and enthusiasm, little technical progress has yet emerged from it (though lines of communication remain active).

Overall assessment

This was a contribution of which the author was particularly proud. The paper draws a firm conclusion on scale effects in models of this class of structure which has wide-ranging implications. This conclusion resulted from a project which was notably self-contained and focussed. The project was strongly supported by a wide range of partners with whom the author had built genuine levels of cooperation.

3.10 Field study comparisons

Pullen, T., Allsop, N.W.H., Bruce, T. & Geeraerts, J. (2003), *Violent wave overtopping: CLASH field measurements at Samphire Hoe*, Proc "Coastal Structures 2003", pp 469–480, ASCE, Reston, Virginia, ISBN 0-7844-0733-9 (see Appendix Q)

Pullen, T., Allsop, N.W.H., Bruce, T., Pearson, J. & Geeraerts, J. (2004), *Violent wave overtopping at Samphire Hoe: field and laboratory measurements*, Proc. 29th Int. Conf. Coastal Engineering, 4, pp 4379–4390, ASCE / World Scientific, Singapore, ISBN 981-256-298-2 (see Appendix R)

3.10.1 An Introduction to the *CLASH* Project

In studies of hydraulic problems, the route to engineering guidance (Figure 3.10) will usually begin with an investigation into the problem carried out at small-scale and in 2-d. The rationale for this starting point is clear – small scale tests are (relatively) cheap and (relatively) easy to run, and so offer the best opportunity to explore physical dependencies and mechanisms, and to draw initial conclusions. In addition to cost considerations, it usually makes sense to start with a 2-d representation of the problem, as this reduces somewhat the complexity of the processes which need to be investigated and understood.

Only once the 2-d case has been analysed, understood and tentative conclusions drawn can a programme of 3-d tests be appropriately and efficiently designed. These tests should be

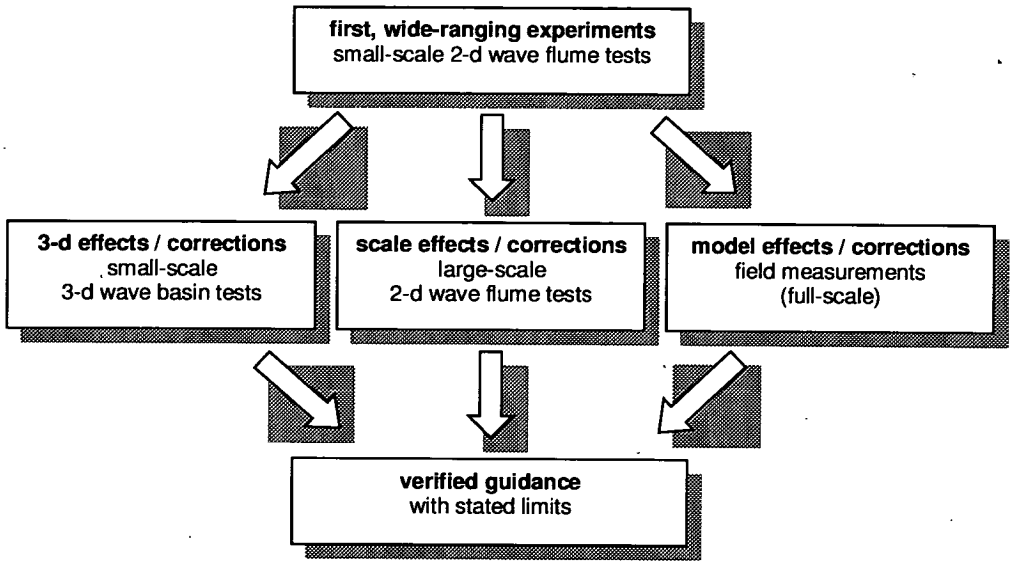

Figure 3.10: *The route from initial experimental exploration to guidance – a* composite modelling *approach.*

designed to focus upon 3-d effects only, leading to adjustments / corrections to the formulae synthesised from the 2-d tests (*e.g.* Napp *et al.*, 2004; Section 3.8). Similarly, for scale effects, tests should be considered as a perturbation of the basic small-scale, 2-d case, and corrections sought for these (scale) perturbations only (*e.g.* Pearson *et al.*, 2002; Section 3.9)

The ideal final stage in the process of synthesis of verified design guidance is a comparison with measurements in the field. For the case of impulsive wave overtopping, the opportunity for such a comparison arose at just the right stage in the process. In 2000, the *CLASH* project began, led by De Rouck of University of Gent (Belgium).

The basic philosophy of *CLASH* was to carry out comparisons between measurements at three field sites with different structures, each modelled by two separate laboratories.

- a concrete (Antifer cube) armoured rubble mound breakwater at Zeebrugge, Belgium; relatively low overtopping; modelled at TU Braunsweig (Germany) and UP Valencia (Spain);
- a rock armoured rubble mound at Ostia, by Rome, Italy; relatively high overtopping; modelled in 3-d by Flanders Hydraulics, Belgium, and in 2-d by University of Gent,

Belgium.

- a vertical seawall with small rock berm at Samphire Hoe, UK; relatively high, impulsive overtopping; modelled at Edinburgh (in 2-d) and at HR Wallingford (in 3-d).

3.10.2 Context, aims, methodology and contribution

See 'Introduction to *CLASH* project', Section 3.10.1, above.

The *CLASH* Samphire Hoe field / model comparison was the basis for these papers, which presents results from a detailed comparison of measurements of mean overtopping from a field site with those from small-scale models of the site in 2- and 3-d. The main conclusion is that model and scale effects are not significant and that overtopping measured at small-scale was in very good agreement with the field data.

3.10.3 Critique

Critical appraisal of worth

The papers present results from a well-focussed, particularly direct field / laboratory comparative study (in keeping with the philosophy of *CLASH*).

Given the conclusion of the large-scale laboratory study (the *Big-VOWS* project; Pearson *et al.*, 2002; Section 3.9) that there were not significant scale effects in going from small-scale to large-scale laboratory tests, there were some grounds for an expectation that the field measurements would be in line with the small-scale laboratory studies.

The large tidal range at the Samphire Hoe site led to an issue of suitable averaging times for measurement of mean overtopping discharges. While longer averaging times would have been expected to give the most stable measure of the overtopping, the changing water level in front of the wall and thus changing crest freeboard meant that a compromise of 30 minutes had to be arrived at – a compromise between scatter introduced by too short an averaging period and scatter introduced by changing physical conditions (changing h_s and R_c).

A criticism that can reasonably be made of the comparative study is that only standard wave spectra were reproduced and used in the laboratory investigations. It would certainly have been the ideal to have had locally measured wave conditions at the field site (*e.g. via* a wave-rider

buoy) to enable exact wave heights and periods to be determined, and to enable a check on the spectral shape to be made. This was simply not possible within the budget constraints imposed by *CLASH* (dedicated wave measurement would have required at least a 50% increase in project budget), and so the best possible work-around was discussed and agreed.

The modelling of the rock berm for the small-scale tests was done in an approximate manner as detailed field data on its composition was not available. In the light of this, a short series of tests (not reported in the paper) were carried out to investigate the sensitivity of the overtopping to the way in which the rock berm was constructed. The results indicated that the overtopping was insensitive to the choice of rock size over a range encompassing sizes thought to be somewhat too large and too small.

The effect of wind during some of the field measurements is not properly explained within the confines of the page limit imposed on this paper. The incorporation of field data under windy conditions required some careful guesstimates to be made by the field investigator (Pullen, HR Wallingford) of the proportion of discharge that was blown away from the collection tanks. His *guesstimate* (for the storm of the 2nd May only) was that two-thirds of the discharge was blown away and was not collected in the tanks. This appears to have been a good guesstimate: data gathered under calm conditions is in close agreement with the adjusted data from the windy day.

Subsequent work / publications(s) arising

This work fed directly into *CLASH* Workpackage 7 'Scale Effects' in demonstrating minimal scale effects for vertical structures, including those subject to impulsive conditions (see de Rouck *et al.*, 2005). The small-scale 3-d tests reported in this paper were extended to include tests with a large wind effect added (by way of a large fan blowing air over the model wall). These tests were not reported in this paper – see instead Bruce *et al.*, 2005 (Section 4.2 but the results formed an important contribution to the synthesised *CLASH* guidance on how to deal with the model effect of absence of wind.

Other comments

While it would have been desirable to have more field data for comparison, the difficulty of obtaining such data cannot be underestimated. In the Samphire Hoe case, the usual difficulties

were compounded by (reasonable) constraints placed upon the field measurement team by the operators of the site (Eurotunnel) which meant that the field measurement apparatus had to be deployable immediately in advance of a storm and demountable immediately after. Despite efforts to use detailed weather forecasts to identify best opportunities for deployment, many planned deployments were aborted at the last minute as weather changed course.

Overall assessment

These two papers are valuable contributions, establishing as they do the final link in the direct chain of evidence connecting small-scale tests on impulsive overtopping at vertical walls with the reality of the prototype case. These papers (and supporting reports) also reopen the window to more fundamental work on wind and spray processes and effects.

Chapter 4
Post-overtopping processes and effects

4.1 Introduction

With the most important gaps in the guidance on mean overtopping discharges closed, attention turned more towards the most direct consequences of overtopping – direct hazards to people, property and to elements of the defence structure itself. The first steps towards the linking of existing predictive tools, individual wave overtopping events and hazard were reported in Bruce *et al.* (2001b), including the first data and tentative guidance on overtopping *throw* velocities, and also for the first time, data and tentative guidance on pressures generated on the crown deck of a structure due to downfalling overtopped discharge. The work on velocities and hazard was elaborated by Bruce *et al.* (2002), including data from large-scale tests. Downfall pressures were revisited in collaboration with colleagues from Queen's University Belfast who had made similar measurements during a programme of measurements at large-scale (Wolters *et al.*, 2005). Further consideration of direct hazard and public and professional response to this hazard appeared in Allsop *et al.* (2004 & 2005b), with new data and tentative guidance on the zone of hazard appearing in Bruce *et al.* (2005).

4.2 Post overtopping effects - throw velocities, spatial extent and downfall pressures

Bruce, T., Franco, L., Alberti, P., Pearson, J. & Allsop, N.W.H. (2001b), *Violent wave overtopping: discharge throw velocities, trajectories and resulting crown deck loading*, Proc. Ocean Wave Measurement and Analysis ('Waves 2001'), 2, pp 1783–1796, ASCE, New York, ISBN 0-7844-0604-9 (see Appendix S)

Bruce, T., Allsop, N.W.H., & Pearson, J. (2002), *Hazards at coast and harbour seawalls – velocities and trajectories of violent overtopping jets*, Proc. 28th Int. Conf. Coastal Engineering, 2, pp 2216–2226, ASCE, World Scientific, Singapore, ISBN 981 238 238 0 (see Appendix T)

Bruce, T., Pullen, T., Allsop, N.W.H. & Pearson, J. (2005), *How far back from a seawall is safe? Spatial distributions of wave overtopping*, Proc. Coastlines,

Structures & Breakwaters 2005, pp166–176, ICE London, Thomas Telford, ISBN 0 7277 3455 5 (see Appendix U)

Wolters, G., Müller, G., Bruce, T. & Obhrai, C. (2005), *Large scale experiments on wave downfall pressures on vertical and steep coastal structures*, Proc. ICE, Maritime Engineering, 158, pp137–145 (see Appendix V)

4.2.1 Context, aims, methodology and contribution

This work evolved from the *VOWS* project. It became clear during *VOWS*, particularly in discussions with the end-user community, that what happened after the water had overtopped mattered not simply in terms of discharged volumes, but also in terms of the form of that discharge;

- How fast is it moving?
- Where does it go?
- What is the direct hazard to people who might be struck by the overtopped discharge?
- What loadings could it cause on structures shoreward of the structure's seaward crest?

It can be seen that these questions are very strongly linked to each other. It has turned out that seeking answers has led to a number of quite major further investigations.

Leading on from the study reported in Bruce *et al.* (2001b), Bruce *et al.* (2002) aimed to bring direct hazard arising from wave overtopping to the fore. The importance of the topic had already been acknowledged by the inclusion of a key task on 'Hazard Assessment' within the *CLASH* project (Workpackage 6).

The 2001 paper saw two important 'firsts'

- The first published data on downfall pressures resulting from the impact of overtopped discharge falling back onto the crown deck of a breakwater. A tentative prediction formula was also given.
- The first published data on velocities of thrown discharge was given, leading to approximate guidance. These measurements further reinforced the need to make distinction between impulsive and non-impulsive overtopping conditions.

The 2002 paper strengthened guidance on likely scale of throw velocities given in Bruce *et al.* (2001b), now based upon large- and small-scale tests.

Additionally, this was the first paper to really rehearse the case for the linking of overtopping to hazard, reinforcing that knowledge of overtopping discharges, even wave-by-wave volumes, is not sufficient, and that the next stages of the process must be identified, understood and quantified if a full description of hazard and response is to be given.

The starting point for Bruce *et al.* (2005) lay in the *CLASH* project, with an agreed need for some quantitative guidance on how far back (in a landward direction) overtopping discharge might travel. The rationale was to get closer to an answer to the question posed in the title of the paper.

Early tests were carried out as an undergraduate Masters project at Edinburgh by Stephen Masterton (now at Imperial College London). Masterton's study focussed upon impulsive overtopping at a vertical wall, and delivered the first quantitative rule of thumb[1] – that in the absence of strong wind, 95% of discharge lands within the first quarter of a wavelength behind the structure crest. Interestingly, the effect of a very strong onshore wind is simply to modify this rule of thumb from 95% to 90% of discharge falling within the first $0.25 \times L_{op}$, where L_{op} is the wavelength in deep water associated with the peak period.

This paper was successful in the synthesis of a simple generic predictor for landward distribution of overtopping discharge behind a vertical wall subject to impulsive overtopping conditions.

The journal paper (Wolters *et al.*, 2005) arose from work carried out by the first two authors at the Large Wave Channel (GWK) in Hannover, Germany, under the EPSRC *BWIMCOST* project. Bruce was invited to join the author team in order to provide a link to the small-scale tests on downfall pressures reported in Bruce *et al.* (2001b). The *BWIMCOST* GWK tests had two main strands; a study on wave loads on the front face of the structure (led by Bullock, University of Plymouth) and a study of the propagation of impacting-wave-induced pressures in cracks (led by Muller, then Queen's University, Belfast, now University of Southampton). The team seized the opportunity to deploy further pressure transducers on the top of the structure. This paper's aim was to synthesise results from the new GWK tests (large-scale, regular waves)

[1] In the question session following the presentation of Allsop *et al.* (2004) in Lisbon, a senior figure asked a question about landward extent of hazard. We responded that we had Masterton's tentative guidance. Then asked why we did not present this to conference, we could only respond that the abstract had been rejected!

with the earlier Edinburgh tests (small-scale, irregular waves) to produce some guidance for the assessment of likely loadings from this mechanism.

4.2.2 Critique

Critical appraisal of worth

The work on downfall pressures delivered new quantitative data and tentative guidance. This work would have been further strengthened had it been possible to measure loadings more directly. There remains a concern that localised pressure measurements may lead to over-estimates of total loads, as the extent of high pressures may be quite small. Also, because of the likely high spatial variability, the pressure data may not provide the most stable basis for a statistical prediction method – see *e.g.* Walkden & Bruce (1999), Section 2.4.

There also remains some question over possible scale effects in the small-scale downfall pressure experiments reported in the 2001 paper. Some of the highest pressures recorded were impulsive in nature resulting from a slam of a 'globule' of water directly onto the transducer. This raises two scaling concerns: first, the scaling of impulsive pressures / forces already referred to, and secondly, the question of whether the physical form / make-up of the descending water mass is similar in small-scale tests and in the field. In fact, it would be expected that it would not be – the break up of a mass of water into successively smaller globules and then droplets is driven strongly by drag and surface tension forces, neither of which will scale according to Froude (but rather, according to Reynolds and Weber scaling respectively). Nevertheless, it would be expected that scale corrections for both these effects would result in smaller loadings in prototype and a conservative predictor. Further, a comparison between small- and large-scale downfall pressure data presented in Wolters *et al.* (2005) show excellent agreement, though the comparison is weakened by the need to make assumptions in relating regular wave data from the large scale tests to a predictor based upon irregular waves (at small-scale).

Throw velocity estimators have proved useful to specialist consultants *e.g.* Scott Wilson and HR Wallingford, and have been further validated by subsequent large scale and field measurements.

The data from the throw trajectory device deployed in the large-scale tests at UPC Barcelona had not been properly examined when this paper was written. Subsequent examination and analysis proved not to be especially fruitful and was cut short – a comment which also applies to Bruce *et al.* (2002) (Section 3.9). Although the device itself functioned reasonably well, it

was designed without the insight that we now have into impulsive overtopping. As it turned out, overtopping 'throw' trajectories in the absence of wind were very much straight up-and-down in nature and most of the array, lying shoreward of the crest of the seaward crest of the wall, was never reached by spray and was redundant. Further, it became evident that alternative approaches to extracting the key data on velocities and shoreward distribution remained simpler and more robust;

- Analysis of video records continued as the basis for estimation of throw velocities;
- Multiply-chambered collection tanks offered the chance to gather data on the shoreward extent to overtopping and could also give quantitative distributions in terms of volumes.

Throw velocity data from the large-scale tests appeared to suggest slightly larger velocities than those measured at small scale. This is perhaps a little surprising, given that the large-scale uprushing jet should have more time to break up into smaller filaments, globules and drops than its small-scale equivalent. It then might be reasoned that these smaller water masses would be more affected by drag leading to a lower velocity. What may explain the difference (which is not large in any case – taking estimates up from a factor of six or seven times the inshore wave celerity to nine or ten times) is that the uprushing jets in the large-scale experiments exhibit greater cross-flume variation than those on the video records from the small-scale tests. This larger cross-flume variation may be real or may be due to the different angles from which the events were recorded (almost head-on at UPC Barcelona, side-on in Edinburgh – see Figure 4.1) but whether real or an artefact of the video records, it is likely that the data sets would be in close agreement were the throw velocity to be taken as the cross-flume average in the large-scale tests,

Since this publication, the importance of velocities in post-overtopping has begun to take root (not solely but in part due to this work). For example, it is now more common for measurements of overtopping velocity to be made on experiments on dike stability and damage initiation.

The idea of a simple on/off water detector has been taken up elsewhere, being used at one of the *CLASH* field sites (Zeebrugge, Geeraerts *et al.*, 2003).

The final rule offered for landward extent is believed to be conservative. It is based largely upon small-scale tests, some of which included a model wind. With any inclusion of wind in a small-scale model, some alarm bells rightly ring loud. How should this wind effect be scaled? Does

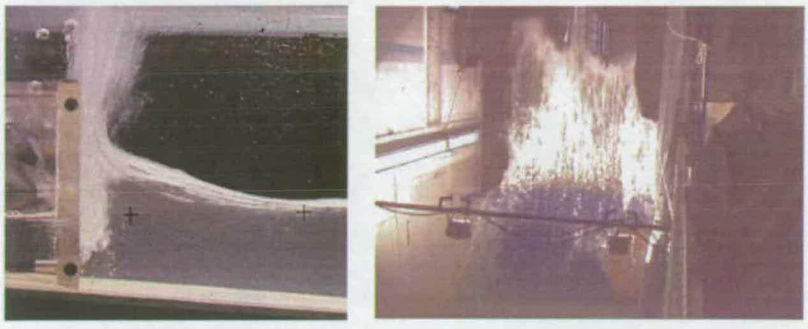

Figure 4.1: *Viewing angle for throw velocity measurements at small-scale in Edinburgh (left) and for the large-scale measurements at Barcelona (right).*

it relate at all to the real effect of wind in prototype conditions (including transformation of incident wave shapes near the structure)? These concerns are entirely valid and very important ones. In these tests, the model wind was increased to up to 28 ms^{-1} in the laboratory over the 1:20 scale model. 28 ms^{-1} is Force 10 in reality, so whatever the undefined model equivalent speed is, it will be a very high speed corresponding to storm force. This is not at all an elegant approach to the problem, but it is defended as an approach in line with the need to arrive at a conservative quantitative predictor for a problem where none existed.

Subsequent work / publications(s) arising

This group of papers provide a link between studies which focussed broadly on overtopping discharges (mean and wave by wave), and studies in which the focus shifted to hazard. As such, they led to the EPSRC 'Partnership for Public Awareness' project *Safe at the Seaside* (see Section 4.3.1).

The throw velocity data also provides some supportable quantitative input data for a simple analytical model for the assessment of direct personnel hazard under wave overtopping (Endoh & Takahashi, 1994) – revisited and reappraised in Section 5.3 of this critical review.

Other comments

The 2002 paper was particularly well-received, perhaps in part to some striking images (still and video – particularly the clip of violent overtopping at Newbiggin-on-Sea) being presented!

The 2005 "How far back is safe ...?" paper offered the first practical guidance on the extent of the affected zone of hazard due to violent wave overtopping. Bruce presented the paper to the conference, whose audience included very many members of the potential end-user community.

The 2005 journal paper reinforced the engineering significant of pressures / loadings associated with the downfalling, overtopped water mass.

Overall assessment

This paper was an important one – for the first time, 'post-overtopping' was considered specifically, and the importance of it identified and promulgated. The approximate guidance on throw velocities has stood the test of time and end-user application.

The 2002 paper was a helpful contribution made to an influential audience.

4.3 Public perception of hazards from wave overtopping

Allsop, N.W.H, Bruce, T., Pearson, J., Franco, L., Burgon, J. & Ecob, C., (2004), *Safety under wave overtopping: how overtopping processes and hazards are viewed by the public*, Proc. 29th Int. Conf. Coastal Engineering, 4, pp 4263–4274, ASCE / World Scientific, Singapore, ISBN 981-256-298-2 (see Appendix W)

4.3.1 An introduction to the 'Safe at the Seaside' project

By 2003, quite some progress had been made in modelling, understanding and predicting the physical aspects of violent wave overtopping volumes, velocities and spatial distributions, and while there remained (and still remain) technical challenges, it was becoming clear that the next major challenges lay in making the link to direct hazard to people from overtopping (the subject of *CLASH* Workpackage 6 'Hazard Analysis' – see *e.g.* Allsop *et al.* (2005b) – and crucially, in distilling and conveying this message to the wider public.

An *ad hoc* investigation by the author in 2002 had revealed approximately 2–4 deaths per year around the UK coast which could be at least in part attributed to wave overtopping. A similar study for Italian coasts (Franco & Lotito, 2004) led to very similar findings. A recent (2005) revisiting of the investigation suggested that the winter of 04/05 had taken a particularly high

toll of 11 deaths, including the tragedy of the family of five in their car swept off a causeway off North Uist (Western Isles). While this number is small compared to the death toll due to (*e.g.*) smoking or traffic accidents, for those responsible for public safety at coastal sites, *e.g.* local authorities, the National Trust, any measure to reduce the risk of a death is of great value. Furthermore, for every fatal accident that reaches the news, there are very many near-misses, often requiring the emergency services (principally the Coastguard) to risk personnel in rescue operations.

Funding was sought and obtained *via* the EPSRC *Partnership for Public Awareness (PPA)* programme. PPAs span science and engineering topics, but usually address the public directly, *e.g. via* school education packages, community projects. For the case of wave overtopping hazard awareness, the proposers (Bruce & Allsop) decided that attempting to interface with the public directly was not an appropriate strategy. Rather, the project proposed to interface with those with experience in and responsibility for public safety issues at the coastline, and with engineers who will need to consider hazard in future designs. The team of supporters was

- The Environment Agency (Christine Ecob – responsible for annual flood awareness campaigns etc)
- The National Trust (Jo Burgon – Head, Access and Recreation)
- The Maritime and Coastguard Agency (Peter Brown)
- The Civil Engineering Contractors Association (Duncan Glen)
- The Einstein Network – producers of specialist videos, including "Civil Engineer's TV", a series of Continuing Professional Development (CPD) programmes.

Additionally, the project is supported by a specialist consultant with strong links into DEFRA and EPSRC (Michael Owen) and by the *VOWS* numerical team partners (led by David Ingram, Manchester Metropolitan University).

4.3.2 Context, aims, methodology and contribution

The paper rehearses the rationale for the PPA project (summarised above) by way of a number of examples of hazards, incidents and possible responses to these. It describes existing approaches to public awareness, and considers the way forward.

Also presented are revised, more detailed guidance on admissible overtopping discharges, for people (with a distinction made, for the first time, between those unaware of the potential hazard, those aware, and those trained to be in the line of hazard) and for vehicles. This new guidance was the result of the synthesis of a great deal of evidence, old and new, on incidents, carried out under *CLASH* Workpackage 6 'Hazard Analysis' (Allsop, 2004).

4.3.3 Critique

Critical appraisal of worth

The paper makes a helpful contribution, rehearsing important arguments about direct hazard and appropriate responses, both from the public and crucially from the profession.

New guidance synthesised within *CLASH* Workpackage 6 is included as this was an opportunity to accelerate its dissemination into the professional, end-user community. In fact, the new guidance was not fully evolved at the time of the presentation, only being finalised shortly before the paper deadline. As such, it is presented in rather raw form, with little space to give attention to the supporting evidence and arguments. This is done in Allsop *et al.* (2005b) (Section 4.4).

An interesting and important piece of evidence from the Samphire Hoe field site could have been usefully included in this paper, although it had been touched upon in Allsop *et al.* (2003). The Samphire Hoe site is a countryside park, access to which is closed off when hazard due to wave overtopping is perceived to be present. Records have been kept of these closures over some three years. If a plot was to be made of wave height *vs.* water depth at the wall (which varies greatly due to a large tidal range of *c.* 7m), we would expect to see a distribution of hazardous conditions as in the sketch in Figure 4.2. Only the very largest waves would be expected to give an overtopping hazard when the tide was low (*i.e.* the crest freeboard R_c was highest, and overtopping discharges would be expected to be lowest), whereas hazardous conditions would be expected to be more common and occur at lower wave heights when the tide was highest (effectively lowest R_c, right side of graph)

In fact what is seen is the data in Figure 4.3, in which hazardous conditions are marked by the squares. This is quite different from the distribution expected intuitively. The explanation of this is quite subtle, and quite profound. As the tide falls, the freeboard increases and so overtopping reduced. But there may come a point as the tide recedes at which the water depth becomes

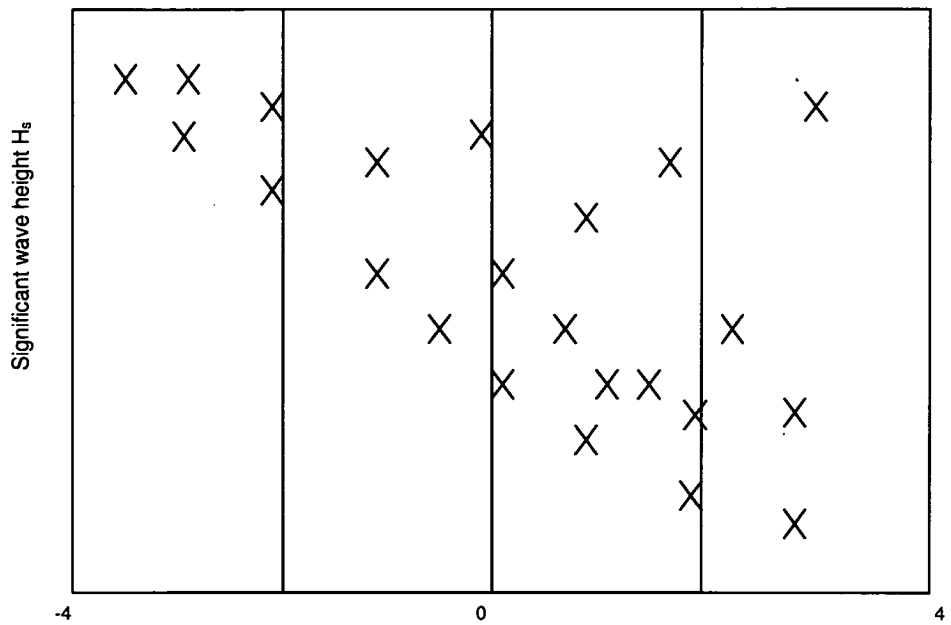

Figure 4.2: *A sketch of the expected distribution of hazardous conditions in wave height / water level space.*

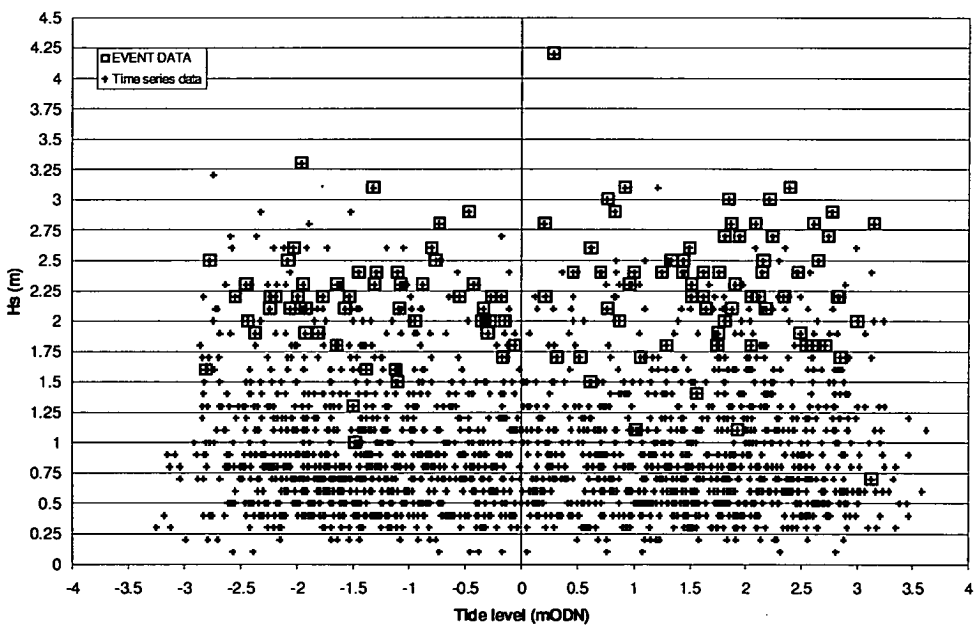

Figure 4.3: *The actual distribution of hazardous events at Samphire Hoe.*

shallow enough to trip the waves from non-breaking into a breaking, impulsive condition. If this trip, this switch of regime happens, the overtopping could increase sharply again. This

transition is also quite sensitive to wave period.

In summary, hazardous overtopping can be seen even at low tide levels because the reduction in overtopping due to increased freeboard can be more than cancelled out by the switch to impulsive overtopping (which can give much higher overtopping than non-impulsive conditions for a given wave height and freeboard). A consequence of these observations and this joining together of the outcomes of two quite different overtopping formulae to reveal possible non-monotonic behaviour of discharge with freeboard reinforces the hazard message that overtopping hazard can occur suddenly and without any obvious warning.

Subsequent work / publications(s) arising

As noted above, the material on new / revised admissible overtopping was a late addition to this paper. It is fully described with supporting evidence and arguments in Allsop *et al.* (2005b), Section 4.4.

Overall assessment

This paper put down a marker about the important issues relating to direct hazard and as such, played its part in the general campaign of awareness-raising among the professional community.

4.4 Admissible overtopping and direct hazard

Allsop, N.W.H, Franco, L., Bellotti, G., Bruce, T. & Geeraerts, J. (2005b), *Hazards to people and property from wave overtopping at coastal structures*, Proc. Coastlines, Structures & Breakwaters 2005, pp153–165, ICE London, Thomas Telford, ISBN 0 7277 3455 5 (see Appendix X)

4.4.1 Context, aims, methodology and contribution

This paper is broadly a summary of the findings of the recently-completed *CLASH* project, and specifically those of Workpackage 6 on Hazard Analysis. To some extent, it led on from Allsop *et al.* (2004), taking forward lessons learned about public perception of hazard and marrying

these up with a fresh look at evidence supporting quantitative limits on admissible overtopping under various conditions.

This paper presented new / adjusted / extended guidance on admissible overtopping discharges, giving the supporting evidence and arguments from which is was synthesised. (The raw guidance was published without rationale / explanation / justification as a late addition to Allsop *et al.*, 2004 in order that the earliest opportunity be taken to place it in the public domain.

The paper also presented quantitative evidence relating to forces that can be experienced by structures / buildings which are exposed to overtopped discharge.

4.4.2 Critique

Critical appraisal of worth

This paper's main contribution was the first fully referenced presentation of the new guidance of admissible overtopping discharges. This was a timely piece of work – the established guidance had not been reviewed in many years. Despite very many advances in the understanding and prediction of overtopping, the limits were based primarily on work by Fukuda *et al.* (1974) and Goda *et al.* (1975). A unified set of thresholds based on these mean overtopping discharges was tabulated by Owen (1980), with modifications suggested by Franco *et al.* (1994). Design advice by Besley (1999) suggested that Franco's modifications may have been biased towards users aware of possible overtopping hazards rather than members of the public.

Beyond this, it presented useful data, though it might be open to the criticism that the data presented on safe velocity of flow and on building loading is somewhat anecdotal in nature, and perhaps not sitting at ease with the generic conclusions on admissible volumes. In defence, it is the publication of such individual pieces of evidence that eventually enables later gathering of the pieces together and new synthesis from what were an apparently disparate set of observations.

Another area which could be strengthened is the data from force measurements on *dummies*. Life-sized dummies were deployed at the Zeebrugge field site under the *CLASH* project (Geeraerts *et al.*, 2003; Geeraerts & Boone, 2004), but the overtopping experienced at the location of the dummies was not large ($q < 6 \times 10^{-4} m^3/s/m$). Model dummies were also deployed in the comparable small-scale tests on the Zeebrugge model at Leichtweiß-Institut, TU Braun-

schweig (Kortenhaus *et al.*, 2004b). The author has some concern that if these model dummies were exposed to impulsive loads, the direct peak force measurements recorded by means of a load cell (*i.e.* a strain gauge-based method) would not be reliable as a quantitative measure.

Subsequent work / publications(s) arising

While this paper presented a state-of-the-art review of hazardous overtopping discharges with much reference to direct personnel hazard, the approach is 'black box' in nature – overtopping discharge in; hazard / consequence out. What is missing is an insight into / understanding of the physical mechanisms and processes at work in transforming the overtopping discharge into that hazard. This understanding will require improved knowledge / characterisation of the physical properties of overtopping discharges (air content, solid matter transported *etc*) and the response of the individual being struck (stability; effect of shoe / ground friction; effect of age / size / level of surprise). These issues are intricate and complex. A 'composite modelling' approach has recently been the subject of a funding proposal (to the UK EPSRC, co-led by Bruce, Müller and Causon), comprising extensive small-scale physical model tests supported by field studies (involving instrumented dummies at Samphire Hoe) and numerical modelling.

It is worth noting that an analytical model of direct overtopping hazard has been proposed by Endoh & Takahashi (1994). This model is revisited and reappraised in Section 5.3, with the conclusion that it provides a useful framework as the basis for a more sophisticated and supportable model, but that it dangerously overestimates safe levels of overtopping under some conditions.

Other comments

Some outstanding work by Professor Franco and his team at University of Roma Tre studying public perception of overtopping hazard was originally going to the included in this paper, but became a separate presentation to the same conference – see Bellotti *et al.* (2005). Video records of overtopping at the Ostia field site were analysed, and 50 individual overtopping events were selected, and the actual volume of the overtopping associated with that wave estimated (from the video itself, with suitable assumptions). These 50 clips were then collated and shown to two different audiences

- a group of *c.* 50 delegates at the 29th International Conference on Coastal Engineering,

and

- a group of *c.* 50 undergraduate students at the University of Roma Tre.

The audience members were asked to imagine themselves placed directly in line with the location of the spatial peak of the discharge, and to rate the level of hazard on a scale of 1 to 5, where

1. "spray"
2. "unpleasant"
3. "loss of equilibrium"
4. "violent fall"
5. "risk of death"

The results were most interesting.

- Each of the 50 events attracted hazard scores across at least three hazard categories.
- The results from the "expert" group were much more scattered than the results from the "Italian student" group, probably due to the much greater inhomogeneity of the former group.
- Hazard began to be *perceived* for overtopping of 0.16 litres/s/m (mean); 34 litres/m (individual wave event). This mean discharge is five times greater than the (then) standard UK guidance.
- The smallest overtopping event *perceived* as a "risk of death" event had a discharge of approximately 0.24 litres/s/m (mean); 64 litres/m (individual wave event) – less than double the *perceived* threshold for onset of any hazard.

The over-riding conclusion is that people's perception of hazard is at dangerous odds with the actual hazards posed.

Overall assessment

The primary importance of this paper lies with the timely placement into the public domain of the enhanced guidance resulting from studies under *CLASH* Workpackage 6. It also flags up the issue of loads on structures immediately shoreward of the seawall. The revised guidance on admissible levels should have lasting value, at least until a comprehensive methodology based more closely on the physical processes giving rise to hazard is fully developed.

Chapter 5
Further analysis

5.1 Introduction

New analysis does not form a required part of the critical review. It seems a pity, however, to have identified gaps, weaknesses and open questions in earlier Chapters and not follow up at least some of the issues. This short Chapter therefore discusses new / updated analysis on comparisons with other methods and formulations – Goda's design charts (Section 5.2.2; Ahrens-type formulae (Section 5.2.3; Burcharth-type formulae (Section 5.2.4; and the *CLASH* neural network (Section 5.2.6). The Chapter then revisits, critically appraises and extends an analytical approach to direct personnel hazard from wave overtopping (Endoh & Takahashi, 1994 - Section 5.3).

5.2 Comparisons with other formulations

5.2.1 Introduction

The *VOWS* project tested the new UK (EA / Besley, 1999) guidance over a wide range of conditions, including large-scale tests and 3-d wave basin tests. It was demonstrated to be a robust method which is now very well-supported by extensive experimental data. Because the EA / Besley (1999) formulations worked so well, a careful comparison with other available approaches was not made at the time. This was an omission which this section aims to rectify. The principal alternative methods available are Goda's (1971 / 1975 / 1981 / 2000) design charts, and empirical approaches that could be termed Ahrens-type (*e.g.* Ahrens & Heimbaugh, 1988) and Burcharth-type (*e.g.* Pedersen & Burcharth, 1992). These original papers were not for vertical structures, but it seemed worthwhile to explore whether their methods, particularly, their different ways of non-dimensionalising the problem – could have formed the basis of a method which could have competed with EA / Besley (1999). Additionally, results of tests at the Large Wave Channel (GWK) under impacting conditions have been reported recently, and a comparison with these is also made here.

5.2.2 Comparison with Goda design charts

Nearing the conclusion of this review and critique, it is perhaps appropriate to compare what has been learned in terms of the new / better supported guidance based upon the identification of the overtopping regime with Goda's ground-breaking work in Japan in the 1960s and 70s.

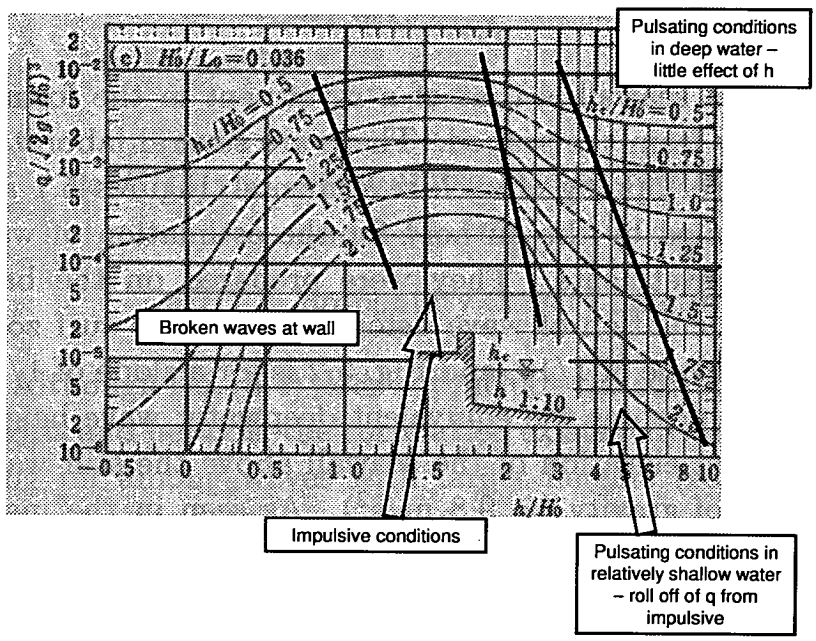

Figure 5.1: *Goda's design chart (from Goda, 2000) for wave steepness* $s_{op} = 0.036$ *showing different wave regimes.*

An example of Goda's (1971 / 1975 / 1985 / 2000) design charts for overtopping is shown in Figure 5.1 (here, for steepness $s_{op} = 0.036$). The annotations (added for this critical review) show regime shifts implicit in these charts (regime shifts described in Allsop *et al.*, 1995). It is clear why Goda's design charts have stood the test of time so well. His test matrix was sufficiently wide (and his insight sufficiently great) that he was able to cover all the regions of parameter space that we now identify as the regimes of pulsating, impulsive and broken wave (both for submerged and emergent toes).

One short-coming of Goda's charts for UK application has always been that they extend only up to wave steepnesses $s_{op} = 0.036$ – rather on the low side for many UK coasts. This short-coming was partially addressed by the work of Herbert (1993), who drew a "Goda-type" chart for wave steepness of 0.045, based upon a large series of tests at HR Wallingford (Figure 5.2).

Another is Goda's use of an "equivalent offshore wave height" which results in shallow water transformations and wave overtopping effects being convolved together. This is particularly troublesome for complex bathymetries, when the designer must consider how best to work with predictions based upon only three discrete, plain foreshore slopes.

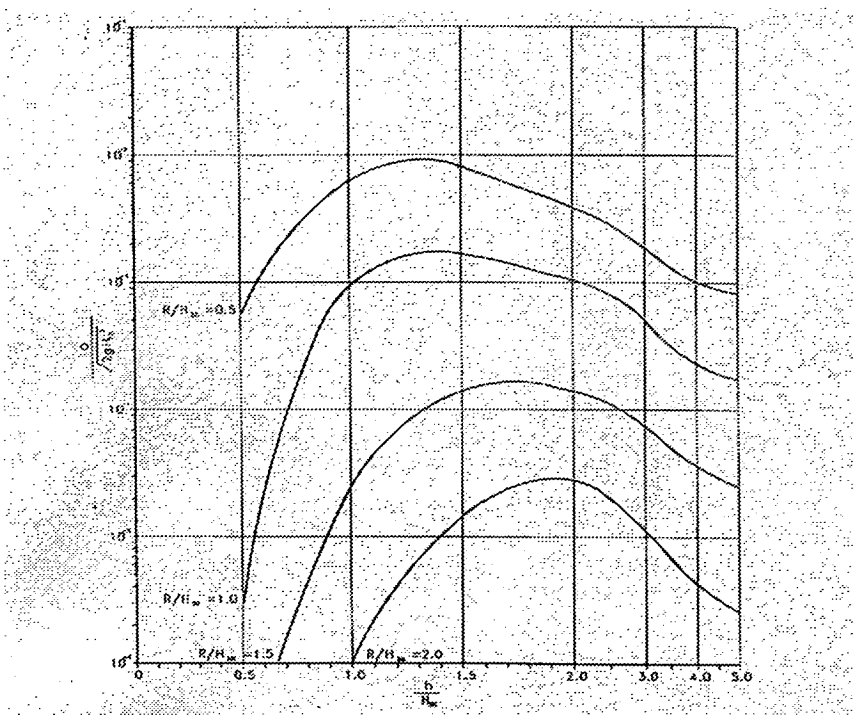

Figure 5.2: *Herbert's "Goda-type" design chart (from Allsop* et al., *1995, after Herbert, 1993) for wave steepness* $s_{op} = 0.045$.

The final step (that cannot be resisted by the author!) therefore must be to plot the predictions of the new framework of tools in approximately the same style as the Goda design charts but based upon inshore wave conditions – firstly the chart for $s_{op} = 0.036$ (Goda's highest steepness; Figure 5.3; *c.f.* Figure 5.1), and then what would be a logical "next chart" for $s_{op} = 0.055$ (Figure 5.4).

Despite the difference in the definition of the wave height parameter (Goda's "equivalent offshore wave height" (H'_o) and the H_{m_0} measured at the toe of the wall used in the new analysis) the broad similarity in the behaviour of the curves is striking, reinforcing the point that these curves are well-founded on the key physical processes.

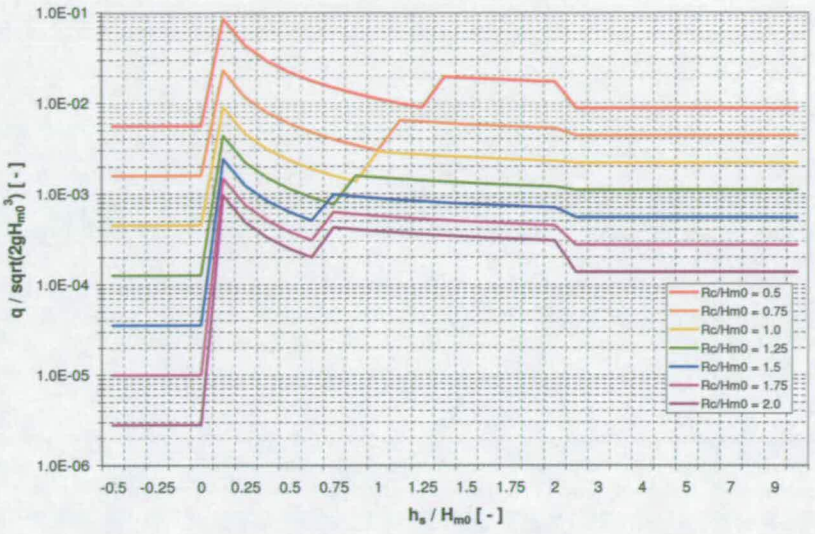

Figure 5.3: *Predictions of current guidance presented in the style of Goda's design charts;* $s_{op} = 0.036$. *Note that ordinate (x) axis is neither linear nor logarithmic, but drawn to approximately recreate Goda's choice.*

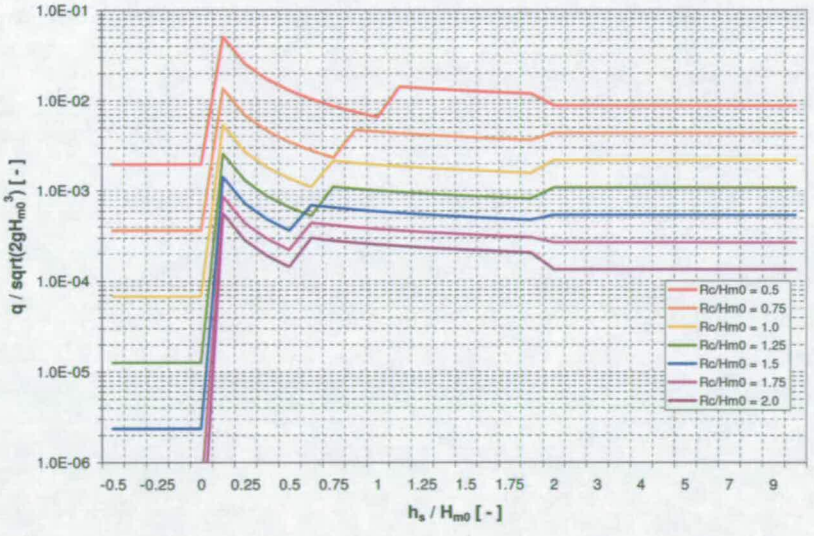

Figure 5.4: *Predictions of current guidance presented in the style of Goda's design charts;* $s_{op} = 0.055$. *Note that ordinate (x) axis is neither linear nor logarithmic, but drawn to approximately recreate Goda's choice.*

5.2.3 Comparison with "Ahrens-type" approach

Ahrens & Heimbaugh (1988) give a method for overtopping discharges at a variety of sloping structures. While vertical or steep walls are not included in their dataset, it seems worth-

while to examine whether their formulation of the problem (and in particular, their choice of non-dimensional freeboard parameter) might have merit as the basis of a method for vertical structures.

The Ahrens & Heimbaugh (1988) dimensionless discharge is the familiar one (though labelled Q' by these authors);

$$Q' = \frac{q}{\sqrt{gH_{m0}^3}} \tag{5.1}$$

Unlike the most familiar dimensionless freeboard $\frac{R_c}{H_s}$, but in common with Owen's (1980) R_* and Allsop *et al.*'s (1995) R_h, their dimensionless freeboard (labelled F') includes an influence of wave period (via the wavelength L_p):

$$F' = \frac{F}{(H_{m0}^2 L_p)^{1/3}} \tag{5.2}$$

where $F \equiv R_c$ is the crest freeboard. The spectral wave height is that measured at the toe of the structure. The wavelength L_p is that based upon the peak period also at the toe of the structure. The overtopping is then given by a relation of the form

$$Q' = A \exp\left[-BF'\right] \tag{5.3}$$

The small-scale data from the Edinburgh *VOWS* tests are recast according to the Ahrens & Heimbaugh method and plotted in Figure 5.5. The best fit Ahrens-type line for the *VOWS* data is

$$Q' = 3.5 \times 10^{-3} \exp\left[-2.22F'\right] \tag{5.4}$$

Plotting the ratio of measured:predicted discharges *vs.* the measured discharge using this new "Ahrens-type" fit (Figure 5.6 confirms that it gives a predictor for the impulsive *VOWS* measurements which works as well as the EA / Besley (1999) approach. It would be worth trying this predictor on future datasets to assess whether it really is as effective as the EA / Besley method.

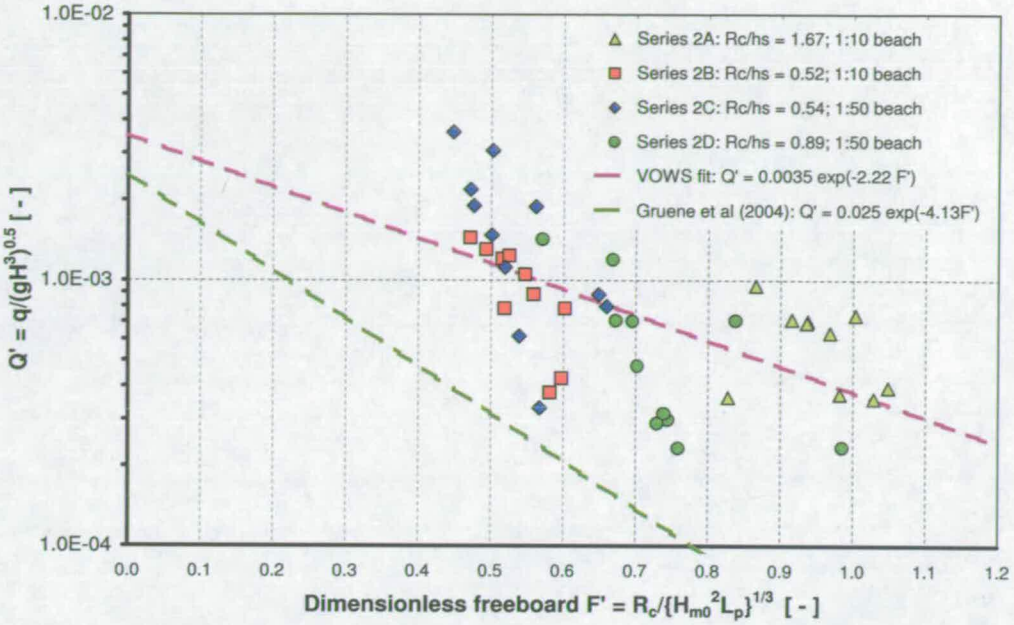

Figure 5.5: VOWS *data plotted on an "Ahrens-type" graph using the non-dimensionalisations of Ahrens & Heimbaugh (1988). Also plotted is Grüne* et al.*'s (2004) best "Ahrens-type" fit to their recent GWK data.*

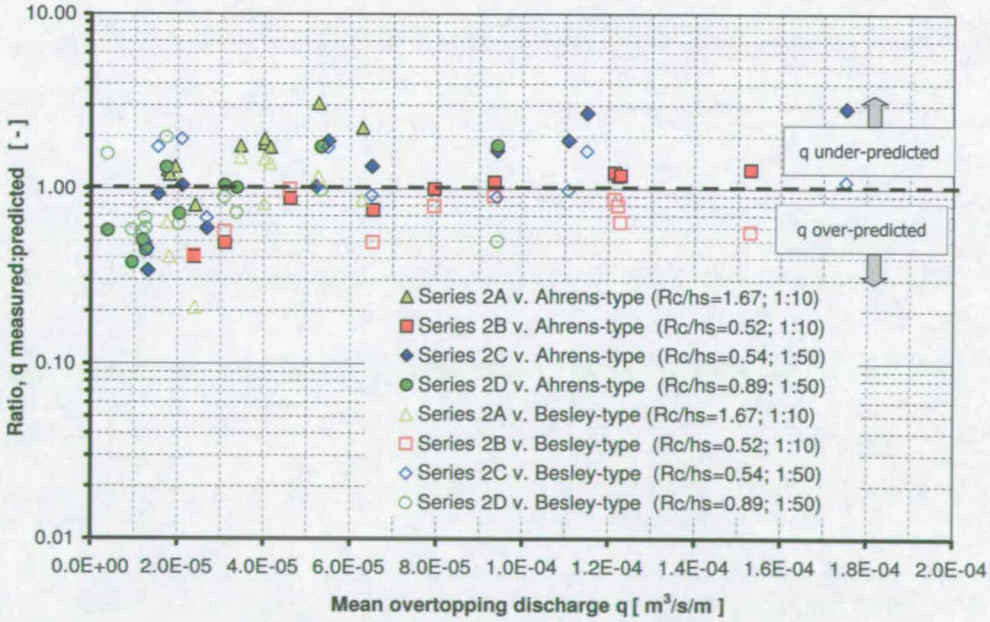

Figure 5.6: *Graph showing ratio, measured:predicted, of mean overtopping discharges* vs. *measured mean discharge q. Prediction according the "Ahrens-type" fit prepared for this critical review.*

5.2.4 Comparison with "Burcharth-type" approach

Pedersen & Burcharth (1992) present a method for the assessment of loading and overtopping of rubble mound structures with a crown wall. As per the comparison with the "Ahrens-type" approach, no predictor for vertical steep walls is given, so the comparison is really a study of whether the different non-dimensional formulation (again including influence of wave period) is a useful one for strongly impulsive conditions.

The Pedersen & Burcharth (1992) dimensionless discharge is reciprocal of the familiar one, $R_* = \frac{H_s}{R_c}$.

The influence of wave period (directly and *via* wavelength) is included in the non-dimensional overtopping discharge;

$$Q_* = \frac{qT_m}{L_m^2} \tag{5.5}$$

The overtopping is then given by a relation of the form

$$Q_* = \alpha(\frac{H_s}{R_c})^\beta \tag{5.6}$$

Note that Pedersen & Burcharth (1992) do not explicitly give location of measurement of T_z and therefore inferred L_p. For the purpose of fitting this type of formulation to the current data, $T_{m-1,0}$ at the toe of the structure is used, with the corresponding wavelength $L_{m-1,0}$ estimated by the Fenton & McKee's (1990) approximation. The best fit line for the *VOWS* data on a Burcharth-type plot is

$$Q_* = 6.98 \times 10^{-5}(\frac{H_s}{R_c})^{1.59} \tag{5.7}$$

This formulation appears to give a predictor which works almost as well as the EA / Besley-type predictors for impulsive conditions, with all data fitted to within a factor of approximately 7. The scatter however is noticeably greater than for the EA / Besley-type formulation and therefore offers no obvious advantage over it.

It is noted that Grüne *et al.* (2004 - see Section 5.2.5) also use a Pedersen & Burcharth for-

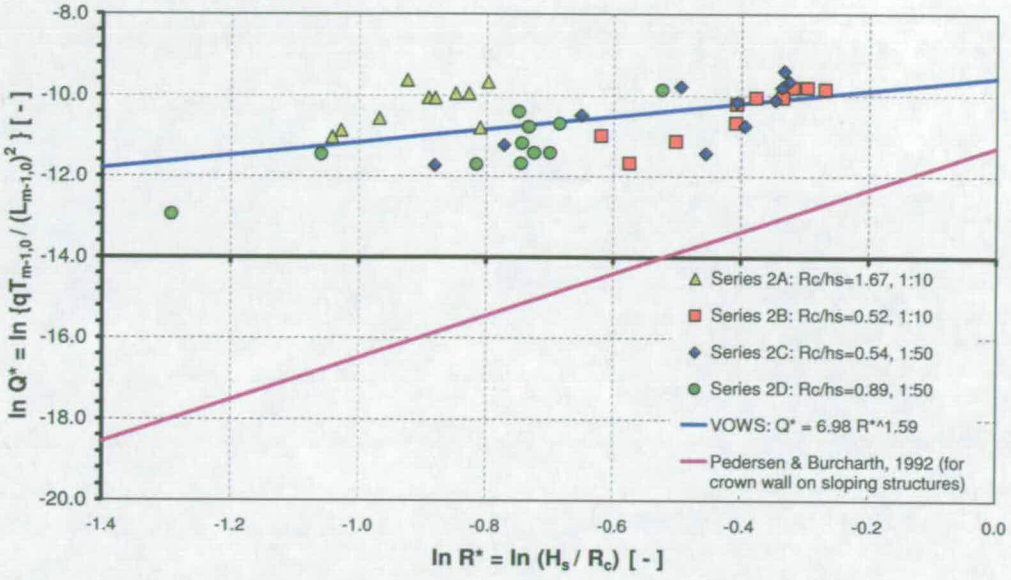

Figure 5.7: VOWS *data plotted on an "Burcharth-type" graph using the non-dimensionalisations of Pedersen & Burcharth (1992).*

mulation to fit their GWK vertical wall data. It is unclear however, whether this has been done correctly as the graph they present (Figure 13 in their paper) has simply $\frac{R_c}{H_s}$ as ordinate, rather than ln $\frac{H_s}{R_c}$ as would have been expected.

Plotting the ratio of measured:predicted discharges *vs.* the measured discharge using this new "Burcharth-type" fit (Figure 5.8 confirms that it gives a predictor for the *VOWS* measurements almost as good as the EA / Besley (1999) approach.

5.2.5 Comparison with recent GWK data (Grüne *et al.*, 2004)

Grüne *et al.* (2004) present data from large-scale tests carried out at the Large Wave Channel (GWK) in Hanover, Germany. Test data was in range $1 \leq \frac{R_c}{H_s} \leq 3.5$. Fitting this data to the conventional Franco- / Allsop-type formulation, Grüne *et al.* (2004) give, for a vertical wall subject to "violent" overtopping

$$\frac{q}{\sqrt{gH_{m0}^3}} = 0.014 \exp\left[-1.65 \frac{R_c}{H_s}\right] \tag{5.8}$$

This predictor, together with the small-scale *VOWS* data are plotted in Figure 5.9. Also plotted

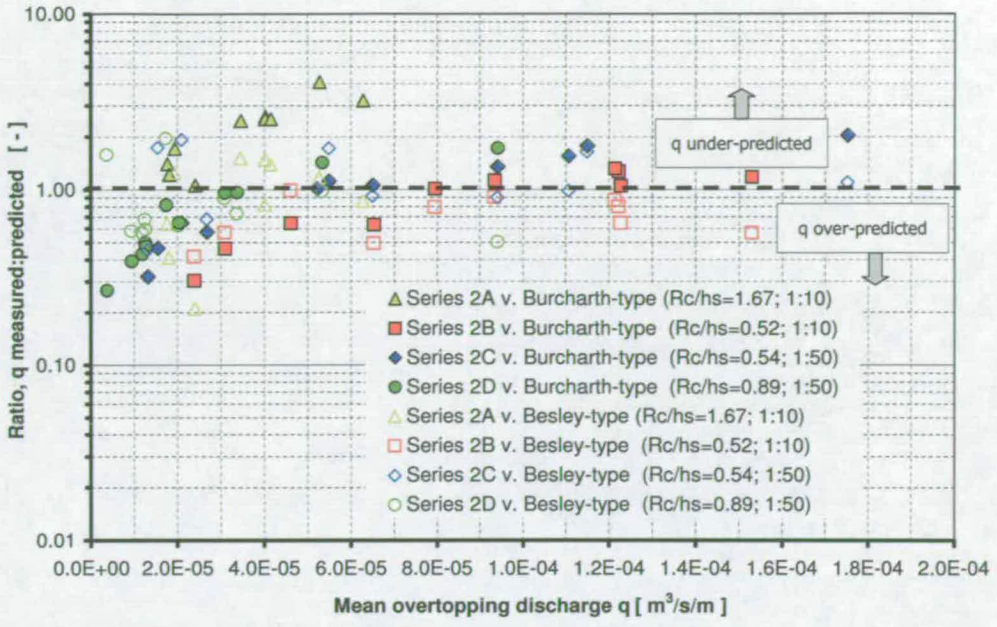

Figure 5.8: *Graph showing ratio, measured:predicted, of mean overtopping discharges* vs. *measured mean discharge q. Prediction according the "Burcharth-type" fit prepared for this critical review.*

are the predictions of Franco *et al.* (1994) and Allsop *et al.* (1995) – both methods explicitly for non-impulsive conditions. It is immediately notable that the Grüne *et al.* (2004) line lies somewhere between the lines for non-impulsive conditions (Franco *et al.* and Allsop *et al.*) and the *VOWS* data. There must therefore be some question as to whether the conditions tested were genuinely impulsive-dominated, or were infact basically non-impulsive with one or two impacts occurring, but not sufficient to shift the overtopping response away from the familiar exponential relationship (*e.g.* Equation 5.8).

Plotting the ratio of measured:predicted discharges *vs.* the measured discharge using Grüne *et al.* (2004) (Figure 5.10 confirms that this predictor gives significantly greater scatter for the *VOWS* data than any of the others – EA / Besley (1999); Allsop *et al.* (2005); Ahrens-type (Section 5.2.3); Burcharth-type (Section 5.2.4).

5.2.6 Comparison with *CLASH* neural network

One of the major deliverable of the *CLASH* project was a new "generic prediction method". This method is a neural network (NN) based upon the *CLASH* overtopping database (see *e.g.*

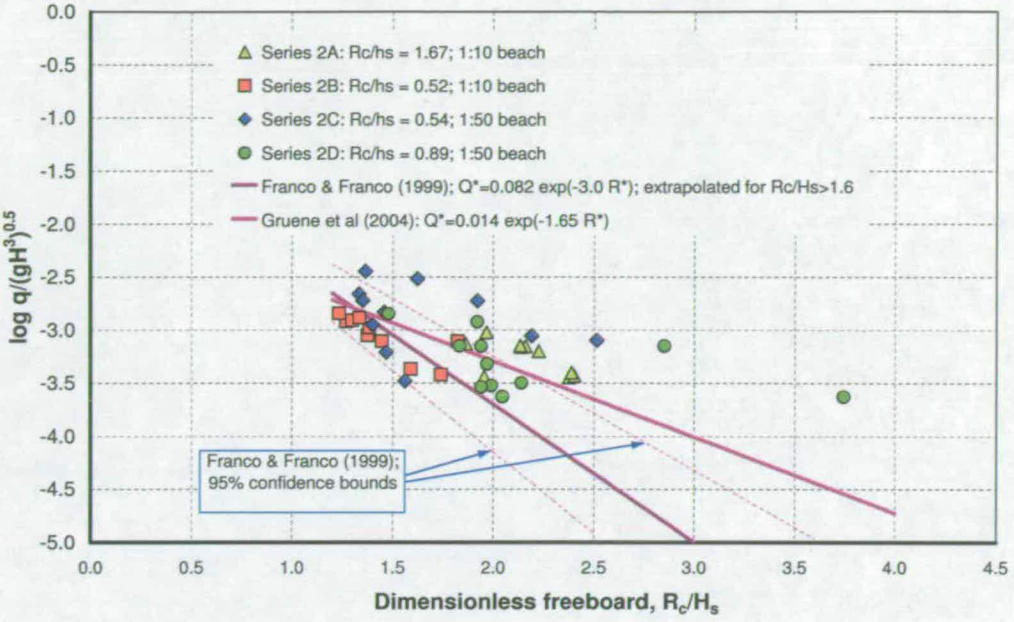

Figure 5.9: VOWS *data plotted with predictions lines of Grüne* et al. *(2004); Franco* et al. *(1999) and Allsop* et al. *(1995).*

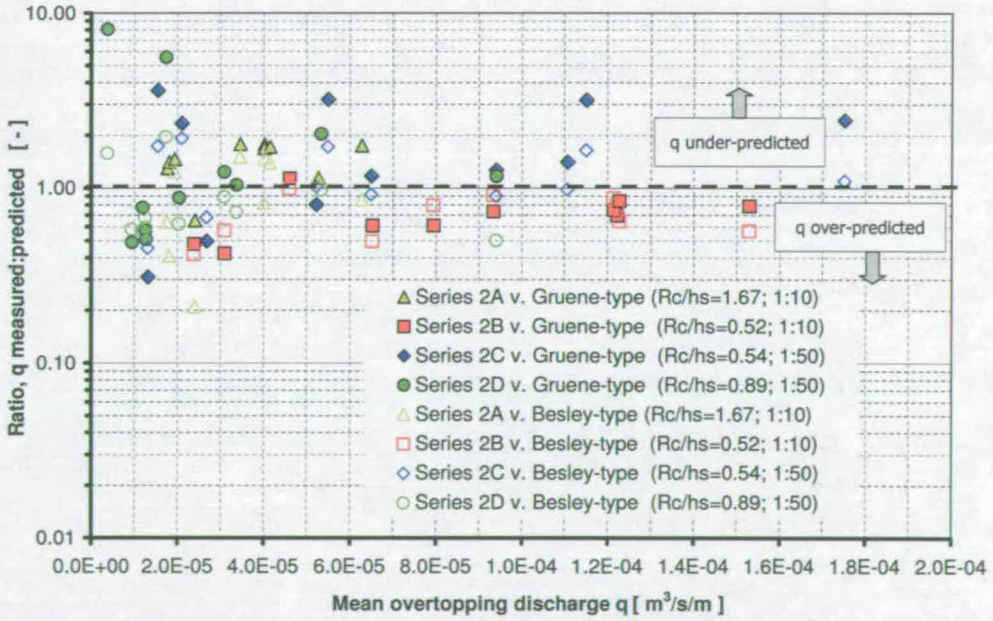

Figure 5.10: *Graph showing ratio, measured:predicted, of mean overtopping discharges* vs. *measured mean discharge q. Prediction according Grüne* et al. *(2004).* et al. *(1994) and EA / Besley (1999).*

Steendam *et al.*, 2004). The neural network is described in detail in van der Meer *et al.* (2005).

The success of the neural network for plain vertical walls can be gauged from the graph in Figure 5.11. It is instructive to compare this result with that in Figure 3.6 showing the success of the EA / Besley (1999) prediction formulae for the same dataset. While it is clear that the neural network performs reasonably well for these cases - the worst (unsafe) under-prediction is by less than a factor of 10, and most data are predicted to within a factor of 3, as expected, the fit is not as tight as that given by the formulae.

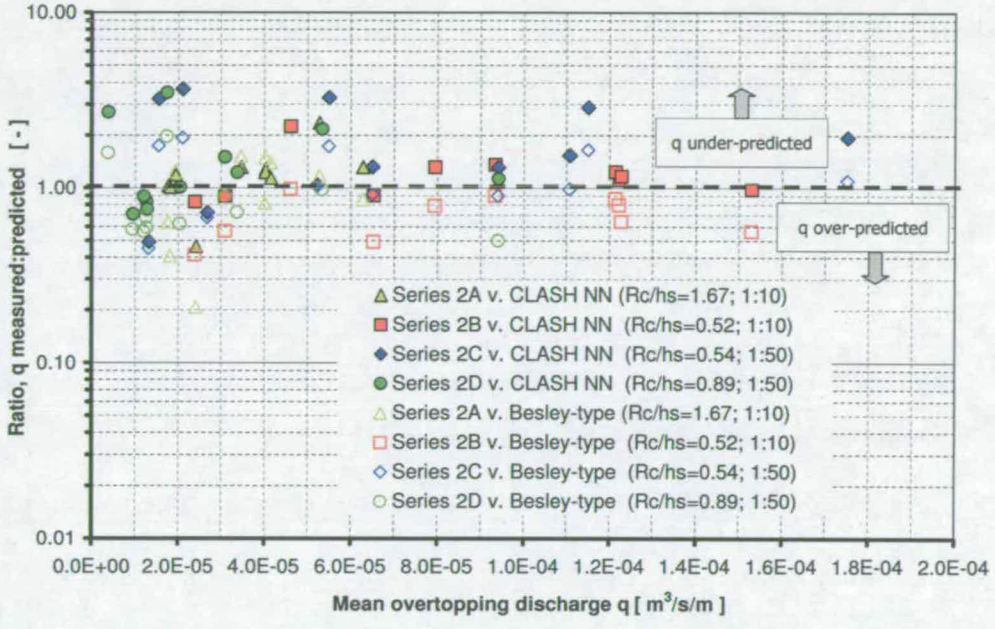

Figure 5.11: *Graph comparing* VOWS *measured overtopping with that predicted by the* CLASH *Neural Network* – VOWS *plain wall tests only.*

5.2.7 Conclusions from comparisons

There is not a simple, single measure which embodies in it the success of any of the prediction tools examined in matching the *VOWS* measured data. One measure could be the root mean square (r.m.s.) error. This however may not be the most appropriate measure for overtopping problems in which we may be just as interested in getting the smallest mean discharges well-predicted as the largest. A large relative error in a low-overtopping case will contribute very little to the r.m.s. error, which will be dominated by errors in the high-overtopping cases. For

	$\overline{\epsilon}$	σ_ϵ	$\epsilon_{r.m.s.}$
EA / Besley (1999)	-0.073	0.211	0.221
Allsop *et al.* (2005a)	-0.014	0.203	0.201
Grüne *et al.* (2004)	0.063	0.308	0.310
"Ahrens-type"	0.036	0.248	0.247
"Burcharth-type"	0.003	0.291	0.287
CLASH Neural Network	0.113	0.218	0.243

Table 5.1: *A comparison of the performance of various predictions tools for the prediction of impulsive* VOWS *data. See text for explanation of error measures.*

this sort of problem, some error measure which accounts for the fact that the parameter varies over many orders of magnitude (all of which range is of interest) is required. An *ad hoc* measure is given here – the "log distance error", $\epsilon_{logq-ratio}$ where

$$\epsilon_{logq-ratio} = \log \frac{q_{measured}}{q_{predicted}} \tag{5.9}$$

Thus a perfect match gives $\epsilon_{logq-ratio} = 0$ and factor of (*e.g.*) 3 over-prediction contributes the same to the summed error as a factor of 3 under-prediction. Using this measure, the various prediction methods are compared in Table 5.1. Also included in this Table is a note of the r.m.s. value of $\epsilon_{logq-ratio}$

The numbers bear out the impressions given by the graphs presented in the preceding subsections. For the impulsive *VOWS* data, (discriminated by $h_* \leq 0.3$), the EA / Besley (1999) method is only bettered by the adjusted form of the same basic method given in Allsop *et al.* 2005a (first column of Table 5.1).

The author's attempt to use "Ahrens-type" and "Burcharth-type" formulations have given reasonable predictions though with significantly more scatter than Allsop *et al.* (2005a) or EA / Besley (1999). It is to be expected that $\overline{\epsilon}$ for these methods is close to ideal as the methods have been based solely on a fit to this dataset. The σ_ϵ measure (second column of Table 5.1) is more telling.

The predictor of Grüne *et al.* (2004) gives noticeably greater scatter (second column) and a tendency to under-predict (first column > 0). This supports the concern expressed earlier that this method is not based upon data in truly impulsive regimes.

The *CLASH* neural network also shows a tendency to under-predict (first column > 0), which might be expected given that its training set of data is dominated by non-impulsive conditions.

The performance (on this limited dataset) of all models is nevertheless quite reasonable - with the exception of Grüne *et al.* (2004), all data under impulsive conditions is predicted to with a factor of 4.

5.3 Analytical model for direct personnel hazard under wave overtopping

5.3.1 Introduction

Chapter 4 reviewed publications dealing with post-overtopping processes, and noted that quite some progress has been made in characterising these processes (throw velocities; spatial extents; downfall pressures ...). It was also noted, however, that quite some further research will be required to produce a detailed, robust and flexible model linking the wave / structure condition to direct personnel hazard. The work of Endoh & Takahashi (1994) may provide a basis for such a model, though to the author's knowledge, it has not been extended or revisited in the light of progress in understanding and quantification of post-overtopping processes. This short Section revisits, extends and critically appraises Endoh & Takahashi's work.

5.3.2 The models

Endoh & Takahashi (1994) propose two analytical models – one for conditions leading to a person *slipping* due to the passage of an overtopped flow, and a second for conditions leading to a person *tumbling*. A definition sketch is given in Figure 5.12.

The *slipping* model considers the force required to push the person's feet away from under him / her. A critical condition for slipping is therefore reached when the drag force exerted upon the person standing in an overtopping-induced flow exceeds the largest force that can be resisted *via* the friction between their feet and the surface upon which they are standing. Basically the condition is

$$F_D > \mu_s W \tag{5.10}$$

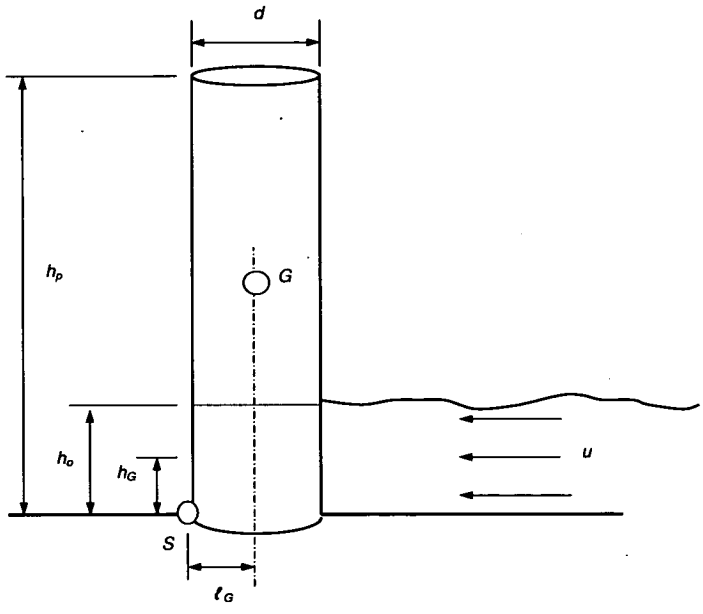

Figure 5.12: *Definition sketch for analytical formulation of direct overtopping hazard (after Endoh & Takahashi (1994).*

where F_D is the drag force; μ_s is the coefficient of static friction and W is the person's effective weight W when standing partially submerged. The drag force F_D experienced due to the overtopping flow moving at a speed u is given by the familiar

$$F_D = \frac{1}{2} c_D \rho A u^2 \tag{5.11}$$

Endoh & Takahashi consider the flow past a person's legs, and offer expressions giving c_D varying depending upon whether the person is standing head-on or side-on into the flow. For the purposes of this short revisit to their work, the simplest model of a person as a single cylinder (Figure 5.12) is used, with $c_D = 1.1$. Given the other uncertainties in the model, and mechanisms not considered, it is believed that this is an appropriate simplification.

Thus, for slipping, the critical condition might be described by

$$\tfrac{1}{2}c_D\rho A u^2 > \mu_s W \tag{5.12}$$

$$\Rightarrow \quad \tfrac{1}{2}c_D\rho h_o d u^2 > \mu_s(1-\tfrac{h_o}{h_p})mg \tag{5.13}$$

$$\Rightarrow \quad u_{crit} \simeq \sqrt{\frac{2\mu_s(1-\frac{h_o}{h_p})mg}{c_D\rho h_o d}} \tag{5.14}$$

For tumbling, the model is similar, but the overturning moment (about the centre of rotation S (Figure 5.12) of the drag force is now considered. A critical condition is reached when this overturning moment exceeds the righting moment supplied by the person's effective weight W, *i.e.*

$$F_D h_G > W\ell_G \tag{5.15}$$

In the simple model, the lever arm for the righting moment is simply $\ell_G = \frac{1}{2}d$. In reality, it is this lever arm which may be most affected by whether the person is taken by surprise, perhaps already unbalanced, or whether the person sees the flow approaching and is braced against it, even leaning into it. In the former case, ℓ_G might be zero or close to zero. In the latter, ℓ_G could be at least $2d$.

Assuming $h_G \sim 0.5h_o$, the critical condition for tumbling is;

$$\tfrac{1}{2}c_D\rho h_o d u^2 h_G > (1-\tfrac{h_o}{h_p})mg\ell_G \tag{5.16}$$

$$\Rightarrow \quad \tfrac{1}{4}c_D\rho {h_o}^2 d u^2 > (1-\tfrac{h_o}{h_p})mg\ell_G \tag{5.17}$$

$$\Rightarrow \quad u_{crit} \simeq \sqrt{\frac{4(1-\frac{h_o}{h_p})mg\ell_G}{c_D\rho h_o d}} \tag{5.18}$$

Both *slipping* and *tumbling* conditions as described by Endoh & Takahashi are for cases where the person is initially standing in a stream of flowing water from their feet up. There is clearly a third and possibly most critical condition – that where the person is struck higher up their body by an airborne jet (*c.f.* Bellotti *et al.*'s (2005) conditions at Ostia) (Figure 5.13). It is clear that the impact of the overtopped flow further up the person's body will result in a greater

overturning moment, but furthermore, these conditions may occur behind crown walls which obstruct the person's view of the sea conditions while at the same time perhaps enhance the person's sense of security. The author will now develop a short analysis of this condition (which might be termed *toppling*).

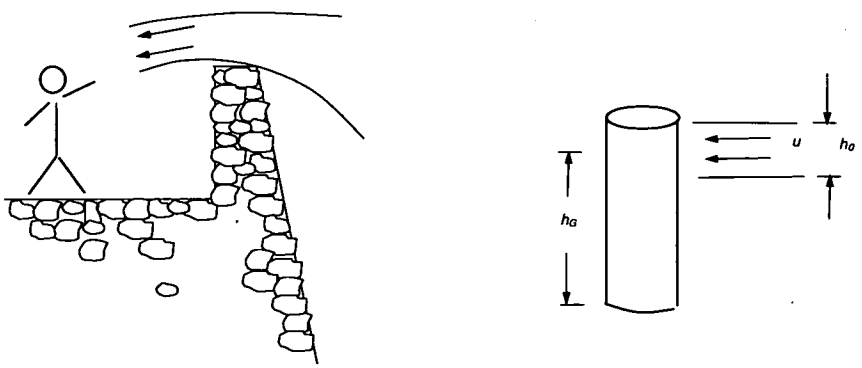

Figure 5.13: *Person being struck by airborne jet of overtopped water – here, termed the* toppling *condition.*

The brief analysis that follows assumes that the jet is airborne; has a thickness h_o with its centre striking person at a height of h_G. As for *tumbling*, the critical condition is reached when the overturning moment of this jet exceeds the righting moment supplied by the person's effective weight W, *i.e.*

$$F_D h_G > W \ell_G \tag{5.19}$$

$$\tfrac{1}{2} c_D \rho h_o d u^2 h_G > (1 - \tfrac{h_o}{h_p}) mg\ell_G \tag{5.20}$$

$$\Rightarrow \qquad u_{crit} \simeq \sqrt{\frac{2(1-\frac{h_o}{h_p})mg\ell_G}{c_D \rho h_o d h_G}} \tag{5.21}$$

	height (m)	mass (kg)
adult (taller)	1.8	75
adult (smaller)	1.5	50
7 year-old boy	1.22	24
3 year-old boy	0.95	16

Table 5.2: *Heights and masses of representative human sizes*

5.3.3 Results on critical overtopping parameters

Four representative human sizes are used here to examine the critical conditions given by these models – these are shown in Table 5.2.

Three graphs are presented showing the results for *slipping*, *tumbling* and *toppling* – Figures 5.14, 5.15 and 5.16 respectively.

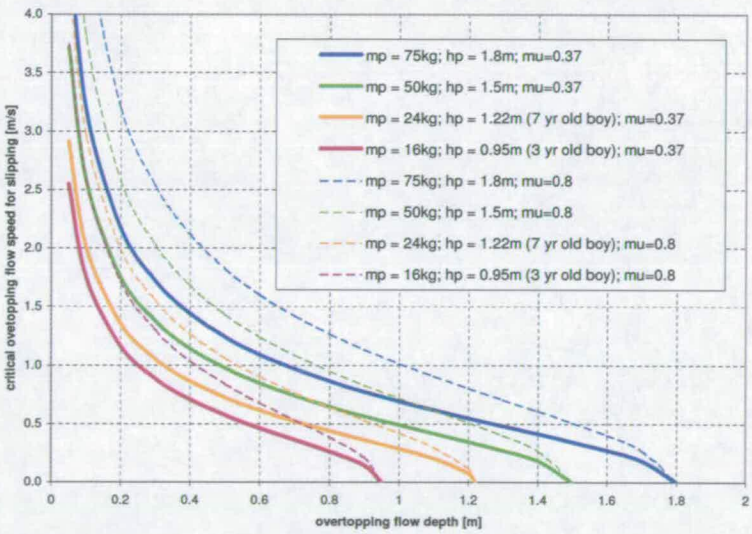

Figure 5.14: *Graph showing critical overtopping velocity for the* slipping *condition. The heavy, unbroken lines are for the least safe conditions assuming a friction coefficient of $\mu_s = 0.37$. The lighter, dashed lines are for $\mu_s = 0.8$ and are included to give a sense of the sensitivity of the result to μ_s.*

When examining these graphs, it should be remembered that for overtopping at steep and vertical walls, the *throw* speed – the speed of the overtopped discharge jet – may be estimated at *c.* twice the inshore wave celerity for non-breaking conditions, and at up to eight times the inshore wave celerity for violent overtopping under breaking conditions. A water depth of as little as 2m in front of the seawall would give *throw* speeds of over $4ms^{-1}$ – the *maximum* value shown

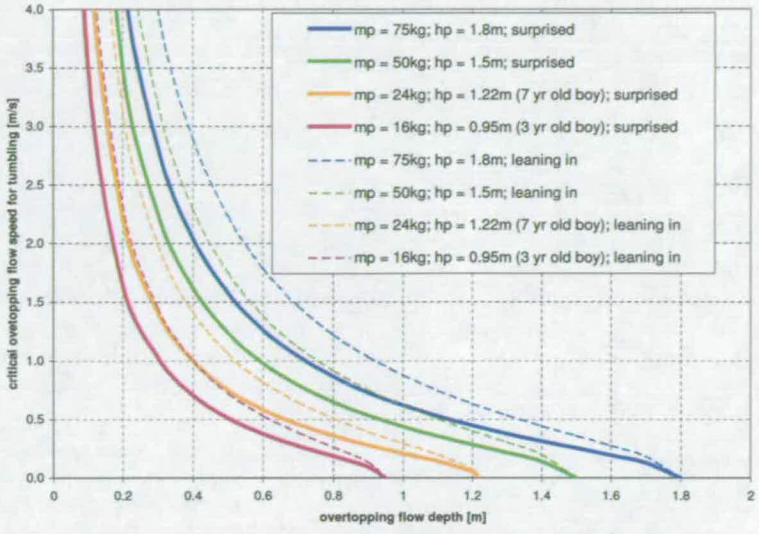

Figure 5.15: *Graph showing critical overtopping velocity for the* tumbling *condition. The heavy, unbroken lines are for the least safe conditions assuming that the person is surprised and nor leaning into the flow in any way. The lighter, dashed lines assume that the person is able to lean into the flow to some extent and are included to give a sense of the sensitivity of the result to this response.*

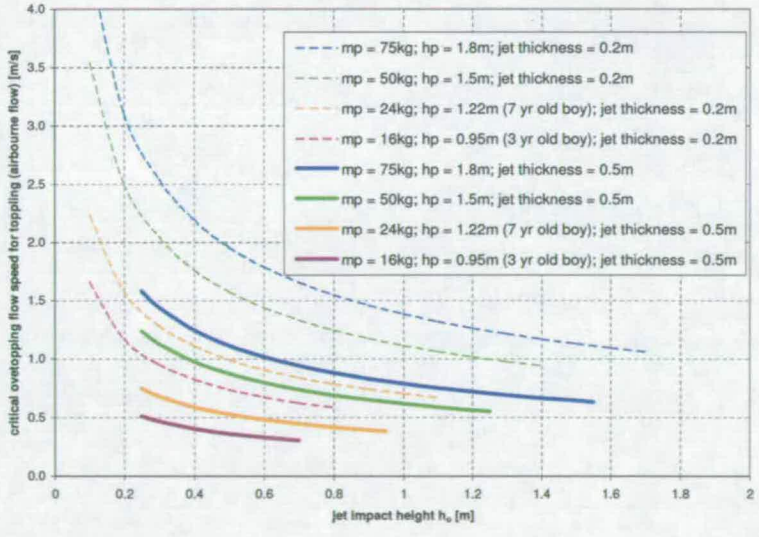

Figure 5.16: *Graph showing critical overtopping velocity for the* toppling *condition. The heavy, unbroken lines are for the least safe conditions assuming a jet thickness of 0.5m. The lighter, dashed lines are for a jet of thickness 0.2m and are included to give a sense of the sensitivity of the result to this parameter.*

on the graphs. Even with some significant reservations (see below) about these models, it is clear that conditions for hazard due to slipping could easily occur, requiring overflowing depths of as little as a few centimetres for a small child, and still only *c.* 10–15cm for an adult. If the overflowing discharge was significantly slowed to (*e.g.*) $1ms^{-1}$ then the depths required to cause an adult to slip increases to quite a substantial 0.65m, and to about 0.25m for a small child. The effect of footwear and ground conditions is shown by the lines for good shoe tread on clean, rough concrete ($\mu_s = 0.8$) and for smoother-soled shoes on a seaweed-covered surface ($\mu_s = 0.37$). Going from the former condition to the latter approximately halves the critical overflow depth.

Superposing the graphs for slipping and tumbling (Figures 5.14 and 5.15) slipping conditions are more critical (*i.e.* occur at lower flow speeds / flow depths) when the surface is slippery (friction coefficient $\mu_s = 0.37$). For better friction, a person may be more likely to tumble than slip for larger flow depths. These observations are in line with intuitive expectations.

Again as expected, the toppling case offers the greatest concern, with even quite slow overtopping jets impacting the person quite low down offering significant hazard.

To place these critical velocities into the more familiar overtopping hazard context of overtopping volumes, a rather sweeping assumption about the event duration must be made. Making such an assumption (while being conscious of its dubious nature) allows the three critical speed graphs to be transformed into three graphs showing critical individual overtopping volumes, assuming each flow is sustained for 1 second – Figures 5.17 (for slipping), 5.18 (for tumbling) and 5.19 (for toppling).

Perhaps the most interesting parts of the critical volume graphs are the areas in their lower lefts where the overtopping flows are still of modest depth. For slipping (Figure 5.17) the model suggests that volumes of *c.* 120 litres/m are required to cause a small child to slip, rising to over 200 lites/m for larger adults. Critical volumes for tumbling (Figure 5.18) tend to be larger than for sliding until the person is submerged to a depth of around half his/her height, after which tumbling becomes the more critical condition by volume. As expected for toppling under the impact of an airborne jet (Figure 5.19, the smallest critical volumes are under conditions when the jet strikes the person high up his/her body (lower right of graph). Here, the model suggests critical volumes down to *c.*120 litres/m for a small child, rising to over 200 lites/m for an adult.

These figures can be compared with those given in Franco *et al.* (1994) based upon tests

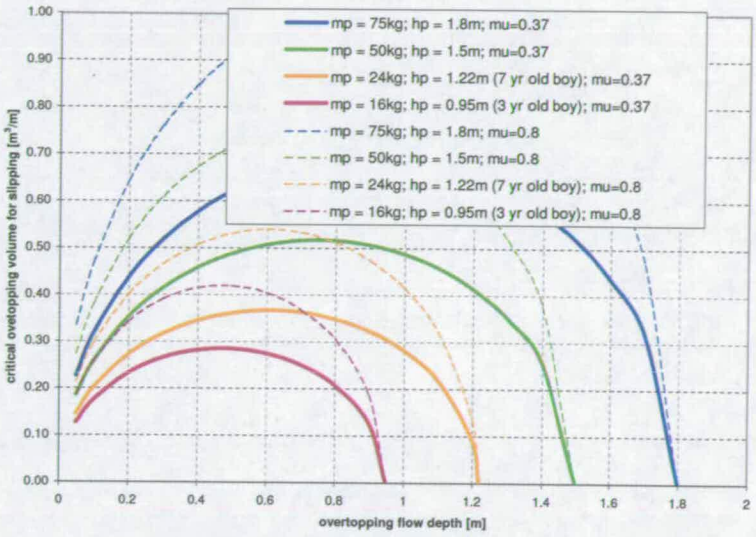

Figure 5.17: *Graph showing critical individual overtopping volume for the* slipping *condition (assuming an event duration of 1s). The heavy, unbroken lines are for the least safe conditions assuming a friction coefficient of $\mu_s = 0.37$. The lighter, dashed lines are for $\mu_s = 0.8$ and are included to give a sense of the sensitivity of the result to μ_s.*

with volunteers and manikins. Franco *et al.* suggest that critical volumes for pedestrians *"lie between 0.2 and 2.0 m^3/m (but a concentrated jet of 0.05 m^3/m on the upper body can be enough to make a person fall down...)"*. Even Franco *et al.*'s 50 litres/m is considered in the UK to be quite a high threshold, with recent guidance (Allsop *et al.*, 2005b) suggesting 2–5 litres/m for an unaware pedestrian, and 20–50 litres/m for an aware pedestrian with a clear view of the sea and on a wide walkway.

While the model of Endoh & Takahashi (1994) (and its extension by the author here to include toppling conditions) provides a physical rationalisation of the problem of direct personnel hazard due to wave overtopping, it is too simple to give safe, supportable guidance. In particular, the model is a static one, whereas it is clear that the sudden nature of a person being hit by a jet of water is key to the hazard posed. As such, a dynamic model is required to consider the initial "loss of equilibrium" phase, after which the person's ability to exert a righting moment may be diminished or have gone altogether. Until such time as these additional components are incorporated, this framework appears to give generally *unsafe* estimates of critical overtopping quantities and should not be used in design and assessment.

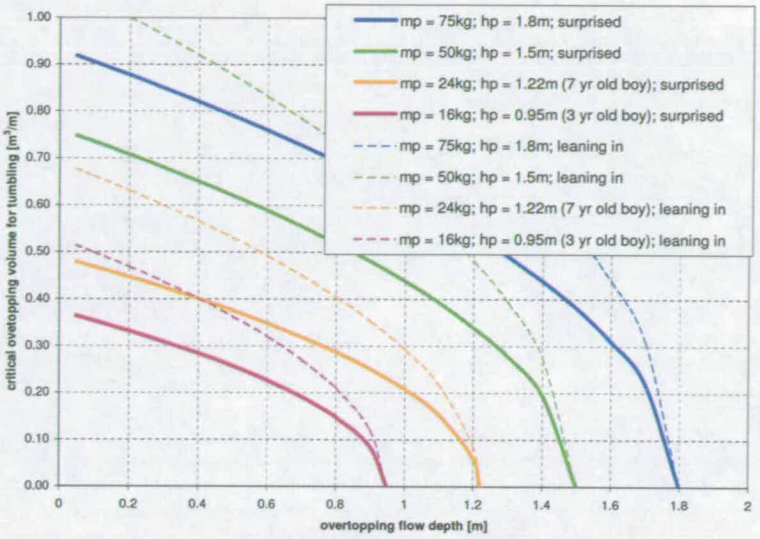

Figure 5.18: *Graph showing critical individual overtopping volume for the* tumbling *condition (assuming an event duration of 1s). The heavy, unbroken lines are for the least safe conditions assuming that the person is surprised and nor leaning into the flow in any way. The lighter, dashed lines assume that the person is able to lean into the flow to some extent and are included to give a sense of the sensitivity of the result to this response.*

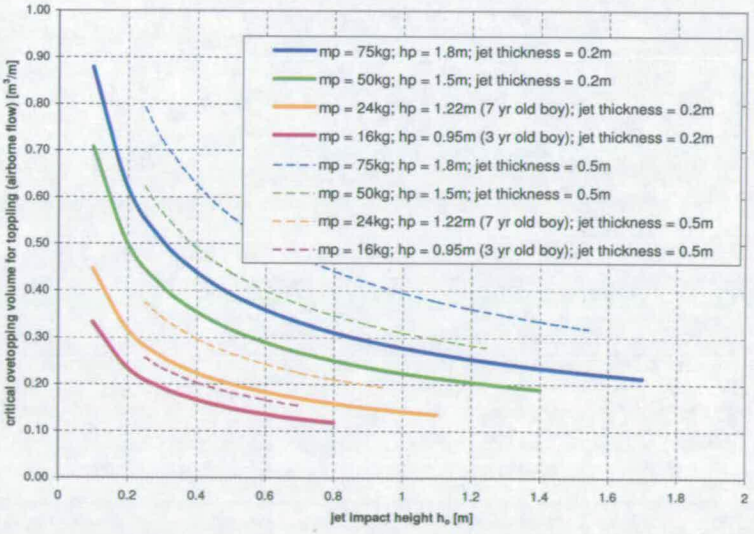

Figure 5.19: *Graph showing critical individual overtopping volume for the* toppling *condition (assuming an event duration of 1s). The heavy, unbroken lines are for the least safe conditions assuming a jet thickness of 0.5m. The lighter, dashed lines are for a jet of thickness 0.2m and are included to give a sense of the sensitivity of the result to this parameter.*

Chapter 6
Discussion

6.1 General observations and discussion

It appears that the field of hydraulic aspects of vertical breakwaters and seawalls has moved ahead in a remarkably organised way over the last ten years. New understandings about wave impact mechanisms and conditions for their occurrence enabled problems with impulsive overtopping prediction to be studied and resolved. This in turn opened the way for more detailed studies to increase the scope and reliability of overtopping prediction tools.

At each stage, an opportunity for seeking support for the new research was identified and proposals successful. The *VOWS* project proposal was made in response to a 1998 EPSRC call under the then *Coastal, Estuarine and Water Engineering (CEWE)* programme. At an appropriate stage in *VOWS*, the opportunity to extend the scope of *VOWS* to include the large-scale test programme at Barcelona was identified and seized upon. After *VOWS* and *Big-VOWS*, the remaining piece of the jigsaw - field study comparisons - emerged as a possibility via the *CLASH* project.

During the period covered by the papers discussed in this thesis, there has been very great convergence in practices among contributors to the field. Where once there were very many competing methods for wave measurement and sea state characterisation, and associated, often ambiguous terminology and notation, now there are some levels of harmony.

The work discussed in this thesis has generally been intended to be generic in nature, with the obvious exception of the direct field / model comparisons for the Samphire Hoe site. While it is entirely understandable and rational for generic prediction tools to be based upon simple structures and wave conditions, inevitably real structures do not always fall neatly into one of the standard geometries. How to offer guidance applicable to the widely possible range of structures has always been an issue. Two routes forward can be identified: numerical methods, and a "generic prediction method" which has emerged from the *CLASH* project (*e.g.* van der Meer *et al.*, 2005).

The attraction of a numerical prediction tool is that, in principle, it could deal with an arbitrary combination of structure, foreshore / bathymetry and wave conditions. While it is clear that numerical models have taken quite some strides forward over the last ten years, they remain some way off offering a direct alternative to physical models. Increasingly however, this gap is due to sheer processing power (and time) required for increasingly sophisticated models, rather than due to fundamental short-comings inherent in the model.

The *CLASH* "generic prediction method" is a neural-network-based tool. The neural network is based upon a database of overtopping measurements collected over a three-year period under the *CLASH* project. It currently comprises over 10000 overtopping tests (Steendam *et al.*, 2004) from laboratories worldwide (many times as big as its compilers originally expected). Importantly, the tool's creators and the wider *CLASH* team emphasise that the tool is not a complete design tool; it simply provides another (albeit buried and very complex) set of formulae whose output should be evaluated alongside the predictions of conventional methods, with engineering critical judgement exercised as always.

The work gathered and critically reviewed in this thesis has been focussed almost exclusively on responses to impulsive wave conditions at simple, vertical or steep-fronted walls, there remain however some important issues to be resolved for non-impulsive conditions. In particular, a number of prediction formulae are in current use, *e.g.* the UK guidance (EA / Besley, 1999) uses Allsop *et al.* (1995), while the U.S. *Coastal Engineering Manual* (Burcharth & Hughes, 2002) uses Franco & Franco (1999). While these predictors give very similar results over the most-often used range of relative crest free-boards, they diverge significantly for $R_c/H_s < 1$ and for $R_c/H_s > 3.5$. These formulae should be revisited together with the datasets from which they were derived and the issue resolved. Some recourse to the *CLASH* neural network (see Section 5.2.6) might prove helpful.

Looking at developments in the field of vertical breakwaters and seawalls, and in particular, physical modelling of wave loadings and overtopping at these structures, it clear that the vast majority of world activity and progress has taken place through the European / UK projects which have been the underpinning of the work whose critiques have been given here. Why this should be so is an interesting question on which to speculate. Certainly Europe is home to one of the biggest concentrations of breakwaters and coastal defences in the world. It may also be home to the greatest variety of such defences, with the whole gamut in evidence – old blockwork seawalls and breakwaters; smooth sloping dikes and block revetments; rock and

concrete armoured rubble mound breakwaters, reshaping berm breakwaters, and monolithic, vertical breakwaters and seawalls. The pre-eminence of European research may also be in part due to the extent to which senior figures and their teams communicate and cooperate (at least in part stimulated by the EC!).

With so much progress on hydraulic aspects of vertical seawalls and breakwaters, it is timely to speculate on whether there exist further major gaps in the knowledge which will require in response conventional research projects of the nature of *VOWS* or *CLASH*. While of course there are very many detailed aspects of the physical processes and hydraulic design which remain unresolved, it may well be that the field has reached the phase of diminishing returns. Indeed, the fact that the current focus is on direct hazard from overtopping and the public / professional / societal response to these hazards in itself says a great deal about the advanced state of the technical knowledge of the physical (hydraulic / structural) processes themselves.

6.2 Impact of work

At this stage, it is perhaps valuable to reflect on the impact of the body of work reviewed here as a whole. The principal contributions have focussed upon impulsive violent conditions, both for wave loadings and for overtopping. These conditions present a whole set of challenging and fascinating problems to the researcher, but just how important are they to the designer; to the end-user? Are the beneficiaries so often cited actually deriving benefit? A comment to this effect was made by van der Meer after presentation of Bruce *et al.* (2001) at the Breakwaters, Coastal Structures and Coastlines conference (Allsop, 2002). He said

> Your work concentrates on violent wave overtopping. Test conditions were created to create this violent wave overtopping, by a steep foreshore slope, *etc.* It would be good to mention to designers of maritime structures, or even warn them, that in design situations you should really try to avoid such conditions. In that sense your work is maybe more academic than that readers should use your work for design.

Of course van der Meer is correct that "prevention is better than cure" - far far better (and cheaper and safer too). And prevention is possible for most new schemes at most sites. But can violent overtopping be prevented by design at all locations at all times? Certainly not, and probably not even at all new schemes. There is an immense existing infrastructure in seawalls and breakwaters. Although most sites are not subject to violent overtopping, many are, and

with apparent increased storminess, such conditions may occur with increasing frequency and at locations previously unaffected. Taking an even wider view, violent wave overtopping takes place also at natural steep shorelines with consequent hazard in line with hazards at seawalls and breakwaters. Many such sites are places of exceptional natural beauty popular for recreation, with coastal paths which could be defended neither economically nor with regard to the impact on the natural environment. Thus the author and his many collaborators believe that there is a genuine, end-user need for the new design tools, not simply for identification of "at risk" wave / structure combinations which should be avoided, but also to give quantitative predictions of what will happen under impulsive conditions. Only armed with such predictions can a coastal engineer then design an appropriate response, be that response structural or "soft", *e.g.* changes to access / operating rules.

Further evidence for the worth of the deliverables to the end-user community comes from private specialist consultancy work carried out by HR Wallingford, which has seen modelling and analysis of recent problems and new schemes draw upon many of these findings. Notably, the physical model study for the proposed Turner Centre outside the breakwater at Margate, Kent (Allsop *et al.*, 2005c) showed impact-like behaviour under large, oblique wave attack a type of behaviour only identified and explained some months previously (Napp *et al.*, 2003 & 2004).

More generally, the author and his colleagues have, from the outset of the *VOWS* project, tried at every opportunity to drive home the message of the importance of distinguishing between impulsive and non-impulsive conditions when analysing overtopping at vertical and steep structures. What was then a new concept has become established practice. While the author and colleagues cannot begin to claim sole responsibility for this advance in the core operating wisdom, it is nevertheless gratifying that this distinction and its tremendous importance in analysis of a problem is now so widely appreciated.

Chapter 7
Key conclusions and recommendations

7.1 Key technical conclusions from the published work

7.1.1 Key conclusions relating to wave impact processes

The distribution of pressures on the front face and berm of a vertical breakwater subject to wave impacts may be predicted using pressure–impulse theory. When entrapped air plays a significant role, *e.g.* on the front face under breaking wave attack, the inclusion of "bounce back" in the model improves predictions significantly (though not when the trapped air pocket extends over more than half of the impact area). Where air plays a lesser role, *e.g.* on the berm, or in a "flip through" condition, the simple version of the model is preferred. (Wood *et al.*, 2000)

Waves overtopping breakwaters can produce transient seaward forces that are large relative to landward loads when they plunge into the harbour-side water. Air trapped by the plunging wave plays an important role – the pressure impulse it causes could be as much as 80% of the contribution by the plume impact. The risk of seaward failure is probably greatest for low-crest structures specifically designed to admit large overtopping to reduce landward force maxima. These structures should be assessed carefully for seaward stability. (Walkden *et al.*, 2001).

Wave impact pressures on the crown deck of a breakwater have been measured in small- and large-scale tests. These impacts are the result of an impacting wave at the front wall of the breakwater generating an upwards jet which in turn falls back onto the crown deck of the structure. Small-scale tests suggest that local impact pressure maxima on the crown deck are smaller than *but of the same order of magnitude as* local wave impact pressure maxima on the seaward, vertical face of the structuredone. For high-crested structures ($R_c/H_{si} > 0.5$), pressure maxima were observed to occur within a distance of $\sim 1.5H_{si}$ behind the seaward crest. For lower-crested structures ($R_c/H_{si} < 0.5$) this distance was observed to increase to $\sim 2H_{si}$. Over all small-scale tests, pressure maxima were measured over the range

$$2 < \frac{p_{1/250}}{\rho g H_{si}} < 17$$

with a mean value of 8. (Bruce *et al.*, 2001b).

The largest downfall impact pressure measured in large-scale tests was 220kPa (with a duration of 0.5ms). Largest downfall pressures were observed to result from overtopping jets thrown upwards by very-nearly breaking waves (the "flip through" condition). (Wolters *et al.*, 2005).

7.1.2 Key conclusions relating to overtopping processes

The switch between non-impulsive and impulsive wave regimes at a seawall or vertical breakwater can result in a non-monotonically varying overtopping response. For particular combinations of structure and wave parameters, this switch can result in the overtopping discharge reducing as the tide falls (as expected) but *then increasing again* as the reducing water depth switches the overtopping mode into violent / impulsive conditions. It is possible that this unexpected increase in discharge could be hazardous especially as under particular conditions, the switch could occur quite suddenly. (Allsop *et al.*, 2003)

Scale effects are absent in comparisons between small- and large-scale laboratory experiments for impulsive overtopping conditions at steep and vertical seawalls and breakwaters. This conclusion applies to both mean and wave-by-wave overtopping measures. (Pearson *et al.*, 2002).

Field measurements of impulsive wave overtopping show good agreement with the prediction of EA / Besley, 1999 (and in its adjusted form as given by Allsop *et al.*, 2005a). (Pullen *et al.*, 2004)

Under oblique wave attack, wave-wall interaction becomes less impulsive with increasing wave obliquity. The transition of the wave process at the wall is not from impulsive to non-impulsive as for normal wave attack, but instead *via* an intermediate regime dubbed "impact-like". When in this regime, waves break along rather than against the structure, so loadings resemble more the non-impulsive forms, while overtopping response continues to follow a trend according to the physical dependencies seen for impulsive conditions. (Napp *et al.*, 2004)

7.1.3 Key conclusions giving new guidance

The guidance offered by EA / Besley (1999) for the assessment of wave overtopping discharge at vertical breakwaters and seawalls has been demonstrated to be robust in the impulsive regime. (Bruce *et al.*, 2001a)

On the basis of small- and large-scale laboratory studies under *VOWS* and *Big-VOWS* projects, a slightly adjusted / improved formula is now suggested:

$$Q_h = 1.92 \times 10^{-4} R_h^{-2.92} \tag{7.1}$$

applicable for $h_* < 0.2$ (Allsop *et al.*, 2005a)

For breakwaters / seawalls with steeply battered front faces under impulsive conditions, the following corrections may be applied to the predictions for vertical walls given by EA / Besley (1999): For 10:1 batter;

$$Q_h = 1.89 \times 10^{-4} R_h^{-3.15} \tag{7.2}$$

and for 5:1 batter;

$$Q_h = 2.81 \times 10^{-4} R_h^{-3.09} \tag{7.3}$$

(Allsop *et al.*, 2005a)

For vertical seawalls / breakwaters subject to broken wave attack, two assessment formulae are offered; one for the case of a positive water depth h_s at the toe of the wall, the other for cases where the toe is emergent ($h_s \leq 0$). For $h_s > 0$, an adjusted form of EA / Besley (1999) formula is suggested:

$$Q_h = 0.27 \times 10^{-4} R_h^{-3.24} \tag{7.4}$$

For $h_s \leq 0$, an adjusted form of van der Meer & Janssen (1995) formula is suggested:

$$Q_b = 0.06 \exp\left[-4.7 R_{ba}\right] \tag{7.5}$$

where

$$R_{ba} = R_b \times s_{op}^{0.17} \tag{7.6}$$

(Bruce *et al.*, 2003; Allsop *et al.*, 2005a)

For vertical seawalls / breakwaters subject to oblique wave attack (angle β measured from normal), the following formulae should be used to estimate mean discharge:

For $\beta = 15°$

$$Q_h = 5.8 \times 10^{-5} R_h^{-3.66} \tag{7.7}$$

For $\beta = 30°$

$$Q_h = 8 \times 10^{-6} R_h^{-4.22} \tag{7.8}$$

For $\beta = 60°$, the use of the EA / Besley method for oblique wave attack ($\beta = 60°$) under pulsating conditions is recommended. (Napp *et al.*, 2004)

The vertical "throw" velocity of overtopping discharge at a vertical wall may be estimated as 2 to 3 times the inshore wave celerity for non-impulsive conditions ($h_* > 0.2$), and as 5 to 7 times the inshore wave celerity for impulsive conditions ($h_* < 0.2$). (Bruce *et al.*, 2001a & 2002)

The reduction in mean overtopping discharge due to the provision of a wave return wall / parapet / recurve may be estimated from the "decision chart" in Figure 7.1. Multiplying the overtopping discharge in the absence of the parapet / recurve by the factor k gives the new, reduced discharge. (Pearson *et al.*, 2004)

Under impulsive overtopping conditions at a vertical seawall, the landward distribution of discharge can be described by an exponential decay. The distribution is affected by the presence

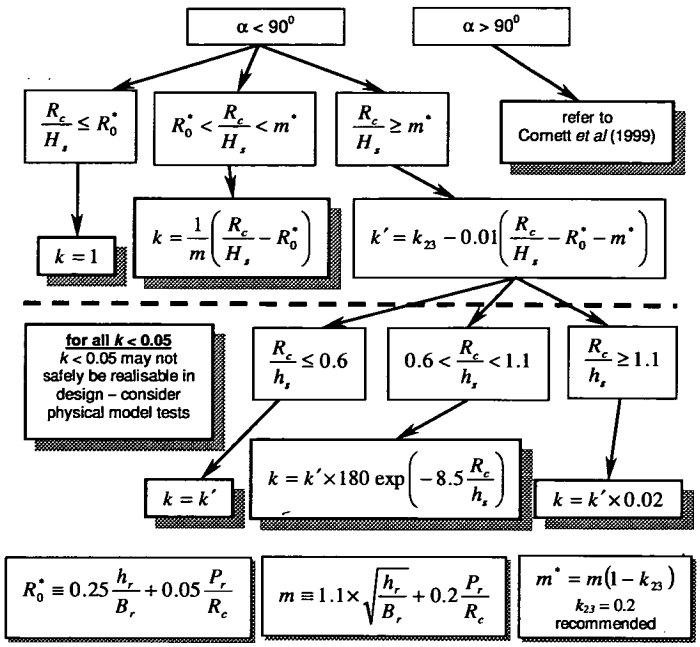

Figure 7.1: *"Decision chart" summarising methodology for prediction of k-factor.*

of wind. Under worst-case conditions (storm-force onshore wind), 90% of the discharge falls within a distance of $\sim 0.25 \times L_{op}$ shoreward of the seaward crest. (Bruce *et al.*, 2005)

7.2 Key conclusions of the critical review

The work on wave kinematics led to an important comparison with velocity and pressure-impulse predictions of an analytical model. The analytical model (pressure-impulse) is based directly on the physics of wave impacts, and enabled the key role of entrapped air in determining the characteristic of the resulting wave loads to the confirmed. (Oumeraci *et al.*, 1995; Bruce & Vicinanza, 1998; Wood *et al.*, 2000)

The research on impulsive seaward loads on low-crest breakwaters remains the only study of its kind. The study highlighted a potentially important design issue for low-crest (Hansholm-type) breakwaters. The study's use of focussed wave groups giving single events made interpretation of the results in a conventional design context more difficult, though conclusions should assist a designer in identifying 'at risk' cases and an enhanced need for physical model testing.

(Walkden *et al.*, 2001)

Early overtopping papers (arising from the small-scale, 2-d *VOWS* tests) provided strong support for the (then) new EA / Besley (1999) guidance and gave the opportunity for a key audience to be reminded of its distinctiveness from earlier guidance – the crucial importance of distinguishing the regime of overtopping. They also provided helpful extensions to include battered (near-vertical) walls – a very common structure configuration around the UK coastline. More comparisons could have been made at the time with alternative models and formulations. (Bruce *et al.*, 2001a)

The *VOWS* 3-d wave basin tests did an effective job of filling the gap in the EA / Besley (1999) guidance on the effect of oblique wave attack on wave overtopping under impulsive conditions. This was a challenging test programme which delivered well-supported and detailed guidance. Though all key objectives were met, it would have been most interesting to pursue the study with a more detailed investigation into spatial variation of overtopping along the oblique wall, and to look at the local effects due to changes in breakwater / seawall plan geometry, (*i.e.* at corners / elbows. (Napp *et al.*, 2004)

The large-scale tests carried out at UPC Barcelona under the *Big-VOWS* project were a professional high-point for the author. The detailed experimental design and planning carried out led to a highly focussed test programme, which in turn led to a very clear conclusion which could not have been fully anticipated, and which was of significant generic worth. It is speculated that the observation that the impulsive overtopping (both mean and wave-by-wave quantities) scale so well suggest that the volumes associated with the visually highly-striking part of the impulsive events are less important than might have been guessed, with a large water mass overtopping in an almost *green water* manner. This was a piece of work of which the author is particularly proud. (Pearson *et al.*, 2002)

The work on overtopping under broken wave attack stands as the only guidance available on this important but neglected problem in overtopping assessment. It is accepted that its worth is tempered by concerns about the difficulty / uncertainty of the scaling of broken wave loadings, but results from breaking wave conditions (Pearson *et al.* 2002, above) lead to a greater degree of confidence in the findings of the study. (Pearson *et al.*, 2003)

The study of overtopping reduction by recurves / wave-return walls / parapets provided, for the first time, some generic, quantitative guidance. For this alone, the work has significant worth,

though the fact that attempts to more firmly base prediction methods on the underlying physical mechanisms were not successful remains a short-coming. (Kortenhaus *et al.*, 2003; Pearson *et al.*, 2004)

The extension of research emphasis from overtopping volumes into post-overtopping process and the consequences of these processes was an important one. Though the work of other researchers had identified elements of the key processes, the author's contributions have assisted in the synthesis of a more holistic approach linking 'traditional' overtopping assessment methods predicting volumes to direct hazard *via* considerations of the velocity, trajectory and resulting landward spatial extent of the overtopping discharge. Only with further research, however, will a model linking hazard truly to the detailed physical processes be realised. (Bruce *et al.*, 2001b; Bruce *et al.* 2002; Bruce *et al.*, 2005)

Another aspect of research into post-overtopping effects has been the identification of impulsive loads on the crown deck of a structure as a possibly important loading case. Tentative guidance was offered on the basis of novel, small-scale tests (in collaboration with University of Roma Tre). Some years later, a return to the topic by the *BWIMCOST* project team during large-scale tests at the GWK allowed the author to revisit the earlier tests and further support conclusions drawn. (Bruce *et al.*, 2001b; Wolters *et al.*, 2005)

New comparisons carried out for this critical review have better supported the assertion that the EA / Besley formulation was the best available one for the assessment of overtopping under impulsive conditions. (Section 5.2 of this critical review)

A revisiting of an analytical model for wave overtopping hazard to personnel (Endoh & Takahashi, 1994) showed that while the model continues to offer a promising basis for a rational model of overtopping hazard based upon the physical processes at work, its predictions (and those of an extension of the model by the author) appear to be unsafe. (Section 5.3 of this critical review)

Looking back over the 10 years spanned by papers in this critical review, the overall sense is of a subject area that has moved forward very substantially and in quite an organised and rational manner, with key projects dove-tailing remarkably neatly into their successor projects. There may be many reasons for this, but foremost must be the level of interaction, genuine professional cooperation and indeed friendship that has arisen among many of the key players. The author has been privileged to be (a small) part of this process.

7.3 Thoughts for future work

7.3.1 Processes causing direct hazard from wave overtopping

Established guidance on admissible levels of (mean) wave overtopping have very recently been revisited and revised. This new guidance was synthesised from a large number of separate (and disparate) observations and tests under Workpackage 6 of the *CLASH* project. While the "headline" level for personnel safety has been reaffirmed at 0.03 $m^3 s^{-1} m^{-1}$, guidance has been refined to distinguish between discharge striking a person unaware of its approach, someone who is aware of the hazard, and for those trained and equipped to work in a hazardous location.

The time is now right for research into the physical processes that take place between the overtopping event and the interaction of the overtopped volume with people and objects (vehicles / structures) in its path. Only by this route can this guidance to be more firmly based upon the driving physical processes and become less "black box" in nature.

Such research into hazard should comprise linked laboratory and field measurements of loadings on carefully instrumented dummies –measurements which should be capable of giving in addition to the total force, some indication of the force *vs.* time history and its spatial extent / distribution on the person, so that an assessment of disruption to stability could be made. Access to a large wave channel might even enable experiments using volunteers, with all appropriate safety precautions taken, of course!

There might also be quite some interesting work to be carried out examining the way in which solid matter – sand, shingle or even larger rocks *etc* – is picked up and entrained with overtopping discharge. This is well-known to happen, and affects significantly the hazard posed to people and infrastructure struck directly by the overtopping water.

7.3.2 Spray

The process of the break up of a plume of violently overtopped discharge is not well-characterised. The physical form of the plume is however of quite some importance in that it determines the characteristics of any resulting loadings. Further, it is this breakup which ultimately leads to seawater being carried many 100s of metres into the back-shore area with consequent implications for the ecology of the affected area. This process is thus an important link between the

domain of the coastal engineer and those with an interest in the complex and fragile ecology of the coastal margin.

While there exist some detailed models of how individual drops / droplets break up in accelerating flow (*e.g.* Pilch & Erdman, 1987), establishing a link between these models and the complex processes taking place during a violent wave overtopping event presents a significant challenge. With so many physical mechanisms playing potentially important roles over a wide range of scales (*e.g.* surface tension, two-phase flow, form drag ...), a numerical simulation could prove prohibitively difficult, and some form of large-scale, controlled, physical model study would appear to be the best route forward.

7.3.3 Improved statistically-based approaches for the estimation of extreme values in hydraulic model studies

A problem that the hydraulic modeller is often confronted with is that the greatest interest / importance lies with the rarest, hardest to measure events. In the case of wave overtopping, the investigator may wish to design to a particularly low admissible discharge; from a typical test of approximately 1000 irregular waves being run at the structure, zero or only one or two overtopping events may result. We would therefore have little confidence in this giving a stable, repeatable, reliable measure of this very low overtopping rate.

Importance sampling methods exist which use knowledge of statistical distributions of a parameter to extrapolate more securely into the range of highly unlikely events, but these have never been applied to hydraulic model testing. It would be a most interesting and potentially valuable exercise to pursue such a methodology. Early findings of such an study will be reported in Davey *et al.* (2006).

For deep water (offshore conditions), there exists a methodology which enables an "average extreme wave group" to be identified simply from spectral wave parameters. The method is called *NewWave* and was first proposed by Tromans (1992). *NewWave* is firmly founded only for linear, deep water waves. A means of identifying shapes of extreme wave groups presents a significantly greater challenge in inshore conditions (if indeed it is possible to do in any way which could allow predictions to be made).

Chapter 8
References

Ahrens, J.P. & Heimbaugh, M.S. (1988), *Seawall overtopping model*, Proc. 21st Intl. Conf. on Coastal Eng., pp795–806, ASCE, New York, ISBN 0-87262-687-3

Allsop, N.W.H., Bruce, T., Pearson, J. & Besley, P. (2005a), *Wave overtopping at vertical and steep seawalls*, Proc. ICE, Maritime Engineering, 158, 3, pp103–114, ISSN 1741 7597

Allsop, N.W.H, Franco, L., Bellotti, G., Bruce, T. & Geeraerts, J. (2005b), *Hazards to people and property from wave overtopping at coastal structures*, Proc. Coastlines, Structures & Breakwaters 2005, pp153–165, ICE London, Thomas Telford, ISBN 0 7277 3455 5

Allsop, N.W.H., Ulrick, C. & Alderson, J. (2005c), *Wave effects on a building in the sea: the Turner Contemporary gallery*, Proc. Coastlines, Structures & Breakwaters 2005, pp535–545, ICE London, Thomas Telford, ISBN 0 7277 3455 5

Allsop, N.W.H. (2004), *Report an hazard analysis, CLASH* internal project report D38 *Workpackage 6*, University of Gent (www.clash-eu.org)

Allsop, N.W.H, Bruce, T., Pearson, J., Franco, L., Burgon, J. & Ecob, C., (2004), *Safety under wave overtopping: how overtopping processes and hazards are viewed by the public*, Proc. 29th Int. Conf. Coastal Engineering, 4, pp 4263–4274, ASCE / World Scientific, Singapore, ISBN 981-256-298-2

Allsop, N.W.H. & Clarke, J. (2004), *Pulsating and impulsive loads on seawalls and buildings – some recent experience and practice*, presentation to Coastal Structures Network workshop on 'Design Methods for Wave Impact Pressures & Forces', Edinburgh (http://cozone.org.uk/impacts/jcl.pdf)

Allsop, N.W.H., Bruce, T., Pearson, J., Alderson, J. & Pullen, T. (2003), *Violent overtopping at the coast - when are we safe?* International Conf. on Coastal Management 2003, pp54–69, ICE London, Thomas Telford, ISBN 0-7277-3255-2

Allsop, N.W.H. (ed.) (2002), *Breakwaters, coastal structures and coastlines* – conference proceedings, ICE London, Thomas Telford, ISBN 0 7277 3042 8

Allsop, N.W.H., McKenna, J.E., Vicinanza, D. & Whittaker, T.T.J. (1996), *New design methods for wave impact loadings on vertical breakwaters and seawalls*, Proc. 25th Intl. Conf. on Coastal Eng., 2, pp2508–2521, ASCE, New York

Allsop, N.W.H., Besley, P. & Madurini, L. (1995), *Overtopping performance of vertical and composite breakwaters, seawalls and low reflection alternatives*, Paper 4.7 in MCS Project Final Report, University of Hannover

Banyard, L. & Herbert, D.M. (1995), *The effect of wave angle on the overtopping of seawalls*, Report SR396, HR Wallingford, Wallingford, UK

Battjes, J.A. (1974), *Surf similarity*, Proc. 14th Intl. Conf. on Coastal Eng., 1, pp466–480, ASCE, New York

Bellotti, G., Brigante, R. & Franco, L. (2005), *Analysis of perceived hazard from wave overtopping at the Ostia harbour rubble mound breakwater: a pilot test*, Proc. Coastlines, Structures & Breakwaters 2005, pp231–239, ICE London, Thomas Telford

Besley, P., Stewart, T. & Allsop, N.W.H. (1998), *Overtopping of vertical structures: new prediction methods to account for shallow water conditions*, Proc. Conf. Coastlines, Structures and Breakwaters, ICE, London, Thomas Telford, ISBN 0 7277 3455 5

Blackmore, P.A. & Hewson, P. (1984), *Experiments on full scale impact pressures*, Coastal Engineering, 8, pp331–346, Elsevier

Bruce, T., Pullen, T., Allsop, N.W.H. & Pearson, J. (2005), *How far back from a seawall is safe? Spatial distributions of wave overtopping*, Proc. Coastlines, Structures & Breakwaters 2005, pp166–176, ICE London, Thomas Telford, ISBN 0 7277 3455 5

Bruce, T., Pearson, J. & Allsop, N.W.H. (2003), *Violent wave overtopping – extension of prediction method to broken waves*, Proc "Coastal Structures 2003", pp619–630, ASCE, Reston, Virginia, ISBN 0-7844-0733-9

Bruce, T., Allsop, N.W.H., & Pearson, J. (2002), *Hazards at coast and harbour seawalls – velocities and trajectories of violent overtopping jets*, Proc. 28th Int. Conf. Coastal Engineering, 2, pp 2216–2226, ASCE, World Scientific, Singapore, ISBN 981 238 238 0

Bruce, T, Allsop, N.W.H. & Pearson, J. (2001a), *Violent overtopping of seawalls – extended prediction methods*, Proc. "Breakwaters, coastal structures and coastlines", pp 245–256, ICE,

London, Thomas Telford, ISBN 0 7277 3042 8

Bruce, T., Franco, L., Alberti, P., Pearson, J. & Allsop, N.W.H. (2001b), *Violent wave overtopping: discharge throw velocities, trajectories and resulting crown deck loading*, Proc. Ocean Wave Measurement and Analysis ('Waves 2001'), 2, pp 1783–1796, ASCE, New York, ISBN 0-7844-0604-9

Bruce, T. & Vicinanza, D. (1998), *Wave kinematics in front of caisson breakwaters*, Proc 8th Int. Polar and Offshore Eng Conf ("ISOPE'98"), Montreal, 3, pp658–664, ISOPE, Golden, Colorado, ISBN 1-880653-34-6

BS 6349 (1991), *British Standard - Maritime Structures. Part 7: Guide to the Design and Construction of Breakwaters*, British Standards Institution, London

Burcharth, H.F. & Hughes, S.A. (2002), *Fundamentals of Design* in *Coastal Engineering Manual, Part VI, Design of Coastal Project Elements*, eds. Vincent, L. & Demirbilek, Z., US Army Corps of Engineers, Washington D.C., chapter VI-5-2, Engineer Manual 1110-2-1100

Calabrese, M. (1998), *Onset of breaking in front of vertical and composite breakwaters*, Proc 8th Int. Polar and Offshore Eng Conf ("ISOPE'98"), Montreal, 3, pp590–595, ISOPE, Golden, Colorado, ISBN 1-880653-34-6

CIRIA / CUR (1991), *Manual on the use of rock in hydraulic engineering*, Construction Industry Research and Information Association (CIRIA, United Kingdom), Centre for civil engineering research codes and specifications (CUR, The Netherlands)

Cooker, M.J. & Peregrine, D.H. (1995), *Pressure-impulse theory for liquid impact problems*, J. Fluid Mechanics, 297, pp193–214

Cornett, A., Li, Y. & Budvietas, A. (1999), *Wave overtopping at chamfered and overhanging vertical structures*, Proceedings International Workshop on Natural Disasters by Storm Waves and Their Reproduction in Experimental Basins, Kyoto, Japan

Cuomo, G. & Allsop, N.W.H. (2004), *Wave impacts at sea walls*, Proc. 29th Intl. Conf. on Coastal Eng., 4, pp4050–4062, ASCE / World Scientific, Singapore, ISBN 981-256-298-2

Davey, T.A.D., Bruce, T., Allsop, N.W.H. & Wolfram, J. (2006), *Use of importance sampling methods in the derivation of extreme responses on coastal structures*, to appear in Proc. 30th Intl. Conf. on Coastal Engineering, ASCE / World Scientific, Singapore.

De Rouck , J., Geeraerts, J., Troch, P., Kortenhaus, A., Pullen, T. & Franco, L. (2005), *New results on scale effects for wave overtopping at coastal structures*, Proc. Coastlines, Structures & Breakwaters 2005, pp29–43, ICE London, Thomas Telford, ISBN 0 7277 3455 5

de Waal, J.P. (1994), *Wave overtopping of vertical coastal structures: influence of wave breaking and wind*, paper to 2nd workshop of *Monolithic Coastal Structures (MCS)* project, Milan, University of Hannover

EA / Besley, P. (1999), *Overtopping of seawalls – design and assessment manual*, R & D Technical Report W 178, Environment Agency, Bristol, ISBN 1 85705 069 X

Endoh, K. & Takahashi, S. (1994), *Numerically modelling personnel danger on a promenade breakwater due to overtopping waves*, Proc. 24th Intl. Conf. on Coastal Engineering, 1, pp1016–1029, ASCE, New York, ISBN 0-7844-0089-X

Fenton, J.D. & McKee, W.D. (1990), *On calculating the lengths of water waves*, Coastal Engineering, 14, 6, pp499–513, Elsevier

Franco, C. & Franco, L. (1999), *Overtopping formulas for caisson breakwaters with non-breaking 3d waves*, J. Waterway, Port, Coastal and Offshore Eng., 125, 2, pp98–107, ASCE, New York

Franco, L. & Bellotti, G. (2004), *Overtopping damage in Italian marinas*, Appendix E to *CLASH* internal project report D38 *Workpackage 6: Analysis of overtopping hazards*, University of Gent (www.clash-eu.org)

Franco, L. & Lotito, A. (2004), *Overtopping accidents along the Italian coastline (Oct 1983 – Nov 2002)*, Appendix D to *CLASH* internal project report D38 *Workpackage 6: Analysis of overtopping hazards*, University of Gent (www.clash-eu.org)

Franco, L., de Gerloni, M. & van der Meer, J.W. (1994), *Wave overtopping on vertical and composite breakwaters*, Proc. 24th Intl. Conf. on Coastal Engineering, pp1030–1044, ASCE, New York, ISBN 0-7844-0089-X

Fukuda, N., Uno, T. & Irie, I. (1974), *Field observations of wave overtopping of wave absorbing revetment*, Coastal Engineering in Japan, 17, pp117–128, JSCE, Tokyo

Geeraerts, J. & Boone, C. (2004), *Report of full-scale measurements: Zeebrugge: 2nd full winter season*, *CLASH* internal project report D31, University of Gent (www.clash-eu.org)

Geeraerts, J., Troch, P., de Rouck, J., van Damme, L. & Pullen, T. (2003), *Hazards resulting from wave overtopping – full scale measurements*, Proc "Coastal Structures 2003", pp 481–493, ASCE, Reston, Virginia, ISBN 0-7844-0733-9

Goda, Y. (2000), *Random seas and design of maritime structures (2nd edition)*, World Scientific Publishing, Singapore, ISBN 981-02-3256-X

Goda, Y. (1985), *Random seas and design of maritime structures*, Univ. Tokyo Press

Goda, Y. (1974), *New wave pressure formulae for composite breakwaters*, Proc. 14th Intl. Conf. on Coastal Engineering, 3, pp1702-1720, ASCE, New York

Grüne, J., Wang, Z., Bullock, G. & Obhrai, C. (2004), *Violent wave overtopping on vertical and inclined walls: large scale model tests*, Proc. 29th Intl. Conf. on Coastal Eng., 4, pp4469–4481, World Scientific, Singapore, ISBN 981-256-298-2

Herbert, D.M. (1996), *The overtopping of seawalls, a comparison between prototype and physical model data*, Report TR 22, HR Wallingford, Wallingford

Herbert, D.M. (1993), *Wave overtopping of vertical walls*, Report SR 316, HR Wallingford, Wallingford

Herbich, J.B. (ed.) (1990), *Handbook of Coastal and Ocean Engineering; Volume 1 – Wave Phenomena and Coastal Structures*, Gulf, ISBN 0-87201-461-4

Kortenhaus, A., van der Meer, J.W., Burcharth, H.F., Geeraerts, J., Pullen, T., Ingram, D.M. & Troch, P. (2005), *Quantification of measurement errors, model and scale effects related to wave overtopping*, *CLASH* internal project report D40 *Workpackage 7*, University of Gent (www.clash-eu.org)

Kortenhaus, A., Oumeraci, H., Geeraerts, J., de Rouck, J., Medina, J.R. & González-Escrivá, J. (2004a), *Laboratory effects and further uncertainties associated with wave overtopping measurements*, Proc. 29th Intl. Conf. on Coastal Eng., 4, pp4456–4468, ASCE / World Scientific, Singapore, ISBN 981-256-298-2

Kortenhaus, A., Medina, J.R., González-Escrivá, J. & Garrido, J. (2004b), *Laboratory measurements on the Zeebrugge breakwater*, *CLASH* internal project report D34 *Workpackage 4*, University of Gent (www.clash-eu.org)

Kortenhaus, A., Pearson, J., Bruce, T., Allsop, N.W.H. & van der Meer, J.W. (2003), *Influence of parapets and recurves on wave overtopping and wave loading of complex vertical walls*, Proc "Coastal Structures 2003", pp 369–381, ASCE, Reston, Virginia, ISBN 0-7844-0733-9

McConnell, K.J., Allsop, N.W.H. & Flohr, H. (1999), *Seaward wave loading on vertical coastal structures*, Proc Int. Conf. Coastal Structures '99, Santander, 1, pp 447–454, A A Balkema, Rotterdam, ISBN 90 5809 092 2

Minikin, R.C.R. (1950), *Winds, waves and maritime structures*, Griffin, London

Möller, J., Weissmann, R., Schüttrumpf, H., Grüne, J., Oumeraci, H., Richwien, W. & Kudella, M. (2004), *Interaction of wave overtopping and clay properties for seadikes*, Proc. 28th Int. Conf. Coastal Engineering, 2, pp 2105–2115, ASCE / World Scientific, Singapore, ISBN 981 238 238 0

Napp, N. (2004), *Impulsive overtopping of vertical seawalls under oblique wave conditions*, PhD Thesis, University of Edinburgh

Napp, N., Bruce, T., Pearson, J. & Allsop, N.W.H. (2004), *Violent overtopping of vertical seawalls under oblique wave conditions*, Proc. 29th Int. Conf. Coastal Engineering, 4, pp 4482–4493, ASCE / World Scientific, Singapore, ISBN 981-256-298-2

Napp, N., Pearson, J., Bruce, T. & Allsop, N.W.H. (2003), *Overtopping of seawalls under oblique wave attack and at corners*, Proc. "Coastal Structures 2003", pp 528–541, ASCE, Reston, Virginia, ISBN 0-7844-0733-9

Napp, N., Allsop, N.W.H., Bruce, T. & Pullen, T. (2002), *Overtopping of seawalls under oblique and 3-d wave conditions*, Proc. 28th Int. Conf. Coastal Engineering, 2, pp 2178–2190, ASCE / World Scientific, Singapore, ISBN 981 238 238 0

Obhrai, C., Bullock, G., Wolters, G., Müller, G., Peregrine, D.H., Bredmose, H. & Grüne, J. (2004), *Violent wave impacts on vertical and inclined walls: large scale model tests*, Proc. 29th Intl. Conf. on Coastal Eng., 4, pp4075–4086, ASCE / World Scientific, Singapore, ISBN 981-256-298-2

Oumeraci, H., Kortenhaus, A., Allsop, N.W.H., de Groot, M.B., Crouch, R.S., Vrijling, J.K. & Voortman, H.G. (2001), *Probabilistic design tools for vertical breakwaters*, A A Balkema, Rotterdam, ISBN 90 580 248 8

Oumeraci, H., Bruce, T., Klammer, P. & Easson, W.J. (1995), *PIV measurement of breaking wave kinematics and impact loading of caisson breakwaters*, Proc. 4th Int. Conf. Coastal and Port Eng. in Developing Countries (COPEDEC IV), pp2394–2410, COPEDEC, Colombo

Oumeraci, H., Klammer, P. & Partenscky, H.W. (1993), *Classification of breaking wave loads on vertical structures*, J. Waterway, Port, Coastal and Offshore Eng. 119, 4, pp381–397, ASCE, New York

Owen, M.W. & Steele, A.A.J. (1991), *Effectiveness of recurved wave return walls*, Report SR261, HR Wallingford, Wallingford, UK.

Owen, M.W. (1980), *Design of seawalls allowing for overtopping*, Report EX924, HR Wallingford, Wallingford, UK

Pearson, J., Bruce, T., Allsop, N.W.H., Kortenhaus, A. & van der Meer, J.W. (2004), *Effectiveness of recurve wave walls in reducing wave overtopping on seawalls and breakwaters*, Proc. 29th Int. Conf. Coastal Engineering, 4, pp 4404–4416, ASCE / World Scientific, Singapore, ISBN 981-256-298-2

Pearson, J., Bruce, T., Allsop, N.W.H. & Gironella, X. (2002), *Violent wave overtopping – measurements at large and small scale*, Proc. 28th Int. Conf. Coastal Engineering, 2, pp 2227–2238, ASCE / World Scientific, Singapore, ISBN 981 238 238 0

Pearson, J., Bruce, T. & Allsop, N.W.H. (2001), *Prediction of wave overtopping at steep seawalls – variabilities and uncertainties*, Proc. Ocean Wave Measurement and Analysis ('Waves 2001'), 2, pp1797–1808, ASCE, New York, ISBN 0-7844-0604-9

Pedersen, J. & Burcharth, H.F. (1992), *Wave forces on crown walls*, Proc. 23rd Intl. Conf. on Coastal Eng., 2, pp1489–1502, ASCE, New York, ISBN 0-87262-933-3

Pilch, M. & Erdman, C.A. (1987), *Use of breakup time data and velocity history data to predict the maximum size of stable fragments for acceleration-induced breakup of a liquid drop*, Intl. J. Multiphase Flow, 13, 6, pp741–757, Elsevier

Pullen, T. (2006) *private communication*

Pullen, T., Allsop, N.W.H., Bruce, T., Pearson, J. & Geeraerts, J. (2004), *Violent wave overtopping at Samphire Hoe: field and laboratory measurements*, Proc. 29th Int. Conf. Coastal Engineering, 4, pp 4379–4390, ASCE / World Scientific, Singapore, ISBN 981-256-298-2

Pullen, T., Allsop, N.W.H., Bruce, T. & Geeraerts, J. (2003), *Violent wave overtopping: CLASH field measurements at Samphire Hoe*, Proc "Coastal Structures 2003", pp 469–480, ASCE, Reston, Virginia, ISBN 0-7844-0733-9

Schüttrumpf, H., Möller, J. & Oumeraci, H. (2004), *Overtopping flow parameters on the inner slope of seadikes*, Proc. 28th Int. Conf. Coastal Engineering, 2, pp 2116–2127, ASCE / World Scientific, Singapore, ISBN 981 238 238 0

Skyner, D.J. (1996), *A comparison of numerical predictions and experimental measurements of the internal kinematics of a deep-water plunging wave*, J. Fluid Mechanics, 315, pp51–64

Skyner, D.J. (1992), *The Mechanics of Breaking Waves*, PhD thesis, University of Edinburgh

SPM (1984), *The Shore Protection Manual*, US Army Coastal Engineering Research Center,

Steendam, G-J., van der Meer, J.W., Verhaeghe, H., Besley, P., Franco, L. & van Gent, M.R.A. (2004), *The international database on wave overtopping*, Proc. 29th Intl. Conf. on Coastal Eng., 4, pp4301–4313, ASCE / World Scientific, Singapore, ISBN 981-256-298-2

Takahashi, S., Tanimoto, K. & Simosako, K. (1993) *Experimental study of impulsive pressures on composite breakwaters – Fundamental feature of impulsive pressure and impulsive pressure coefficient*, Rept. Port and Harbour Res. Inst., 31, 5, pp 33–72

Tromans, P.S., Anaturk, A.R. & Hagemeijer, P. (1991) *A new model for the kinematic of large ocean waves – application as a design wave*, Proc. 1st Int. Offshore and Polar Eng. Conf. ("ISOPE'91"), 3, pp64–71, ISOPE, Golden, Colorado

Van de Walle, B., De Rouck, J., Van Damme, L., Frigaard, P. & Willems, M. (2002), *Parameters influencing wave run-up on a rubble mound breakwater*, Proc. 28th Int. Conf. Coastal Engineering, 2, pp 2008–2018, ASCE / World Scientific, Singapore, ISBN 981 238 238 0

Van der Meer, J.W., van Gent, M.R.A., Pozueta, B., Verhaeghe, H., Steendam, G-J. & Medina, J.R. (2005), *Applications of a neural network to predict wave overtopping at coastal structures*, Proc. Coastlines, Structures & Breakwaters 2005, pp259–268, ICE London, Thomas Telford, ISBN 0 7277 3455 5

Van der Meer, J.W. (1997) *private communication to* PROVERBS *Task 1 workshop, Edinburgh*

Van der Meer, J.W. & Janssen J.P.F.M. (1995), *Wave run-up and wave overtopping at dikes*,

Chapter 1 in "Wave Forces on Inclined and Vertical Wall Structures", pp 1–26, ed. Kobayashi, N. & Demirbilek, Z., ASCE, New York, ISBN 0-7844-0080-6

Walkden, M., Wood, D.J., Bruce, T. & Peregrine, D.H. (2001), *Impulsive seaward loads induced by wave overtopping on caisson breakwaters*, Coastal Engineering, 42, 3, pp257–276, Elsevier

Walkden, M. & Bruce, T. (1999), *Scatter in wave impulse load maxima: a review*, Proc Int. Conf. Coastal Structures '99, Santander, 1, pp 439–444, A A Balkema, Rotterdam, ISBN 90 5809 092 2

Wolters, G., Müller, G., Bruce, T. & Obhrai, C. (2005), *Large scale experiments on wave downfall pressures on vertical and steep coastal structures*, Proc. ICE, Maritime Engineering, 158, pp137–145

Wood, D.J., Peregrine, D.H. & Bruce. T. (2000), *Wave impact on a wall using pressure-impulse theory. I : Trapped air*, J. Waterway, Port, Coastal and Offshore Eng. 126, 4, pp182–190, ASCE, New York

Part 2: Collected Papers

appendix	paper
A	Oumeraci, H., Bruce, T., Klammer, P. & Easson, W.J. (1995)
B	Bruce, T. & Vicinanza, D. (1998)
C	Wood, D.J., Peregrine, D.H. & Bruce. T. (2000)
D	Walkden, M. & Bruce, T. (1999)
E	Walkden, M., Wood, D.J., Bruce, T. & Peregrine, D.H. (2001)
F	Bruce, T, Allsop, N.W.H. & Pearson, J. (2001a)
G	Allsop, N.W.H., Bruce, T., Pearson, J., Alderson, J. & Pullen, T. (2003)
H	Allsop, N.W.H., Bruce, T., Pearson, J. & Besley, P. (2005a)
I	Pearson, J., Bruce, T. & Allsop, N.W.H. (2001)
J	Bruce, T., Pearson, J. & Allsop, N.W.H. (2003)
K	Kortenhaus, A., Pearson, J., Bruce, T., Allsop, N.W.H. & van der Meer, J.W. (2003)
L	Pearson, J., Bruce, T., Allsop, N.W.H., Kortenhaus, A. & van der Meer, J.W. (2004)
M	Napp, N., Allsop, N.W.H., Bruce, T. & Pullen, T. (2002)
N	Napp, N., Pearson, J., Bruce, T. & Allsop, N.W.H. (2003)
O	Napp, N., Bruce, T., Pearson, J. & Allsop, N.W.H. (2004)
P	Pearson, J., Bruce, T., Allsop, N.W.H. & Gironella, X. (2002)
Q	Pullen, T., Allsop, N.W.H., Bruce, T. & Geeraerts, J. (2003)
R	Pullen, T., Allsop, N.W.H., Bruce, T., Pearson, J. & Geeraerts, J. (2004)
S	Bruce, T., Franco, L., Alberti, P., Pearson, J. & Allsop, N.W.H. (2001b)
T	Bruce, T., Allsop, N.W.H., & Pearson, J. (2002)
U	Bruce, T., Pullen, T., Allsop, N.W.H. & Pearson, J. (2005)
V	Wolters, G., Müller, G., Bruce, T. & Obhrai, C. (2005)
W	Allsop, N.W.H, Bruce, T., Pearson, J., Franco, L., Burgon, J. & Ecob, C., (2004)
X	Allsop, N.W.H, Franco, L., Bellotti, G., Bruce, T. & Geeraerts, J. (2005b)

Appendix A: Oumeraci *et al.*, 1995

Oumeraci, H., Bruce, T., Klammer, P. & Easson, W.J. (1995), *PIV measurement of breaking wave kinematics and impact loading of caisson breakwaters*, Proc. 4th Int. Conf. Coastal and Port Eng. in Developing Countries (COPEDEC IV), pp2394–2410, COPEDEC, Colombo

Appendix A
Oumeraci *et al.*, 1995

Oumeraci, H., Bruce, T., Klammer, P. & Easson, W.J. (1995), *PIV measurement of breaking wave kinematics and impact loading of caisson breakwaters*, Proc. 4th Int. Conf. Coastal and Port Eng. in Developing Countries (COPEDEC IV), pp2394–2410, COPEDEC, Colombo

A.1 Declaration of contribution

The collaborative project reported in this paper arose from informal discussions (initially during a chance meeting in the staff coffee room!) between the author and Oumeraci during the author's visit to Franzius Institut, University of Hannover in 1991.

The author carried out the laboratory work together with Klammer (Franzius Institut). The author set up and ran the flume, which involved adjusting wave groups which gave deep water breakers such that the required wave breaking shapes occurred at the seawall. The author carried out all PIV measurements and subsequent velocity data analysis. Franzius Institut supplied the pressure sensors and carried out the analysis of the loading data. The author was closely involved in discussion of the results (both in Edinburgh and subsequently in Hannover). He wrote the text on the kinematics part of the study and was involved at all stages in the subsequent editing of the paper.

A.2 Published paper

overleaf

Proc. 4th Int. Conf. Coastal and Port Eng. in Developing Countries
"COPEDEC IV" 1995

PIV-Measurement of Breaking Wave Kinematics and Impact Loading of Caisson Breakwaters

Oumeraci, H.[1]; Bruce, T.[2]; Klammer, P.[3]; Easson, W. J.[4]

1. Introduction

The phenomena associated with wave breaking are undoubtedly among the most complicated non-linear aspects of wave dynamics. It is therefore not surprising that one of the most persisting problem in offshore, coastal and harbour engineering is the hydrodynamic loading induced by breaking waves on structures in their natural environment.

The importance of breaking waves and the destructive impact loads they may induce on coastal structures are illustrated by the results of a review of vertical breakwater failures (Oumeraci, 1994). One of the major lessons drawn from these failures is that dynamic stability analysis must necessarily be adopted to supplement the present static design approach. For this purpose, the design impact loads must be specified and rational prediction methods must be developed.

A previous study (Oumeraci et al, 1993) has shown that the characteristics of the impact loads are essentially governed by the type of breaking and the kinematics of the breaker just as it impinges on the wall. A rational method for the prediction of impact loads should therefore necessarily account for the breaker type and the related kinematics. The main difficulty encountered in the past in trying to get information on breaker kinematics experimentally lies in the difficulty to obtain reliable velocity profiles from point measurement procedures (e. g. Laser Doppler Anemometry). Particle Image Velocimetry (PIV) which has been developed for over a decade allows now a complete 2D-flow field to be captured at a single instant (Quinn et al, 1993; Bruce et al, 1993). It is the main objective of this paper to demonstrate the capability of this new technique to help in the development of rational methods for the prediction of breaking wave impact loads on caisson breakwaters.

[1] Prof. Dr.-Ing., Techn. University of Braunschweig, Braunschweig, Germany
[2] Lecturer, University of Edinburgh, Edinburgh, U.K.
[3] Research Engineer, University of Braunschweig, Braunschweig, Germany
[4] Dr.-Ing., Senior Lecturer, University of Edinburgh, Edinburgh, U.K.

2. Theoretical Considerations - Position of the Problem

A breaking wave impinging on a vertical wall induces impulsive pressures on the wall which are difficult to predict in terms of their magnitude, spatial and temporal distribution.

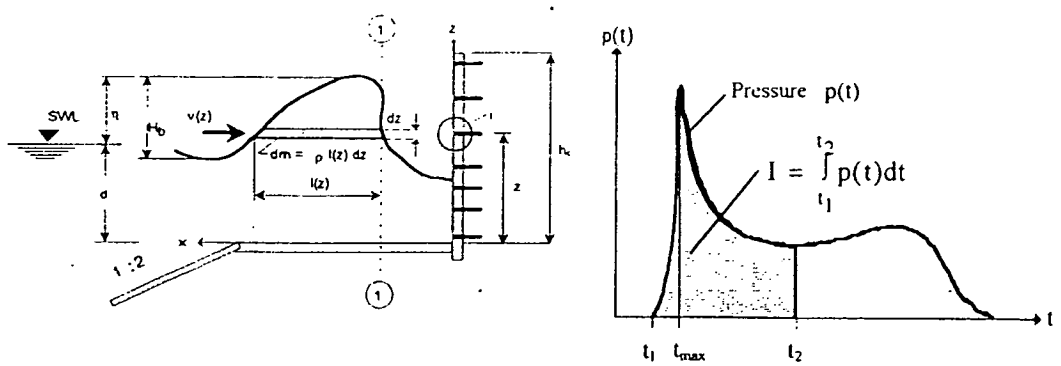

a) Breaking wave on a wall

b) Pressure history recorded at point i

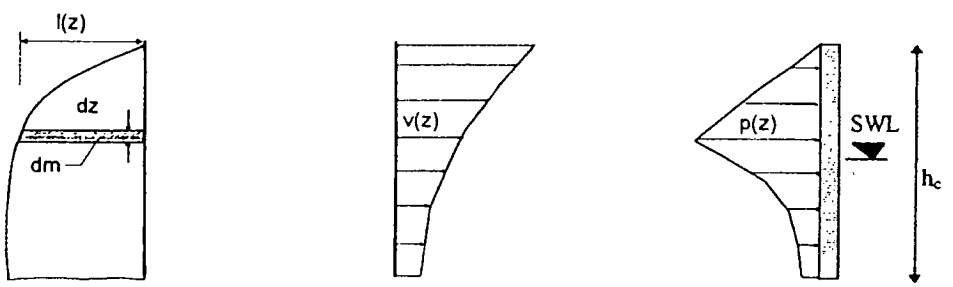

c) Mass distribution

d) Velocity distribution

e) Pressure distribution

Fig. 1- Principle sketches for the calculation of breaking wave impact loads

The forward momentum of water mass $dm(z) = \rho \cdot l(z) \cdot dz$ advancing with a horizontal velocity v(z) at an elevation z is:

$$v(z) \cdot dm(z) = v(z) \cdot \left[\rho \cdot l(z) \cdot dz\right] \tag{1}$$

This momentum must be equal to the pressure impulse between time t_1 and t_2 (Fig. 1b) on the wall $dI(z) = p(z) \cdot dt$ at the same elevations:

$$p(z) \cdot dt = \rho \cdot l(z) \cdot dz \cdot v(z) \tag{2}$$

This means that each instant t, the velocity distribution v(z) (Fig. 1d) and the mass distribution expressed by $\rho \cdot l(z) \cdot dz$ (Fig 1c) must be known in order to compute the pressure distribution p(z) (Fig 1e) which would result.

(Fig. 1e) which would result. The spatial integration over the height h_c of the wall will then provide the total impact force per unit length of the wall at the instant t:

$$F = \int_{z=0}^{hc} p(z) \cdot dz \qquad (3)$$

Hydraulic model tests were conducted at the University of Edinburgh for the simultaneous measurement of the temporal variation of the velocity and pressure distribution for three of the four breaker types which were previously identified by Oumeraci et al (1993). The mass distribution is determined according to Eq. (2). Knowledge of the mass, velocity and pressure distribution at each time step will allow the derivation of rational formulae applicable for each breaker type for the prediction of total force and pressure histories at each wall elevation. The former are generally needed for the dynamic analysis of the overall stability of the structure and its foundation while the latter are needed for the analysis of the structural strength of the caisson wall and further structure members.

3. Experimental Set-up and Test Procedure

The facility used for this study was a 10 m wave flume at the University of Edinburgh. The flume has a width of 0.4 m, a water depth of 0.75 m, and is equipped with an electrically driven, absorbing wave paddle. The flume was purpose-built for PIV studies with a glass bottom and glass walls. The model caisson was constructed from perspex (plexiglass) to allow the laser illumination to pass through the berm and slope, and to enable the wave impacts to be photographed from the side. The caisson model was positioned at the end of a 1:20 plane beach. A general view of the experimental set-up in the wave flume at the University of Edinburgh is given in Fig. 2, showing the bottom slopes, the position of the wave gauges, the vertical model structure and the position of the PIV-System with an illuminated plane sheet.

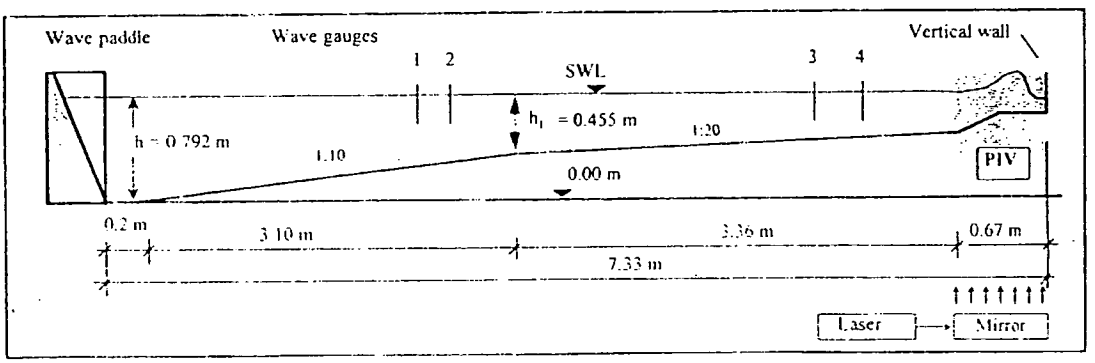

Fig. 2 - Experimental set-up in the wave flume at the University of Edinburgh

The cross-section of the model with the position of the pressure transducers installed at different wall elevations and on the toe berm is shown in Fig. 3.

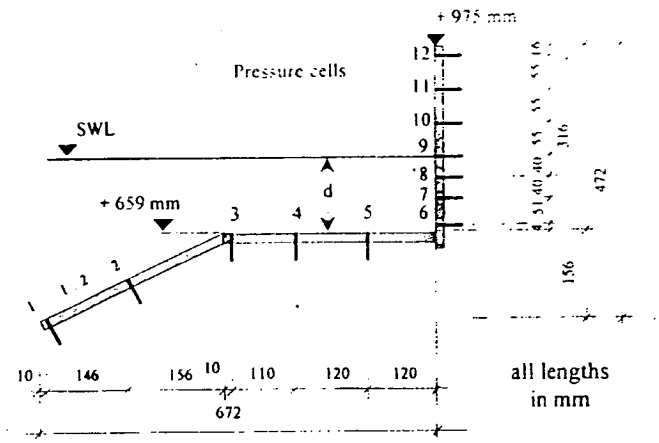

Fig. 3 - Position of pressure transducers

PIV is a relatively new technique which gives a quantitative map of instantaneous flow velocities over a large area. Additionally, the velocities obtained are of high accuracy and high resolution. The basis of PIV is to stroboscopically illuminate a two-dimensional plane through the flow, which has been seeded with tiny reflective particles following the flow accurately. The illuminated plane is then photographed, the shutter being held open long enough to record at least two illuminations. Thus each seeding particle gives rise to at least two particle images. Fig. 4 shows the measurement zone schematically.

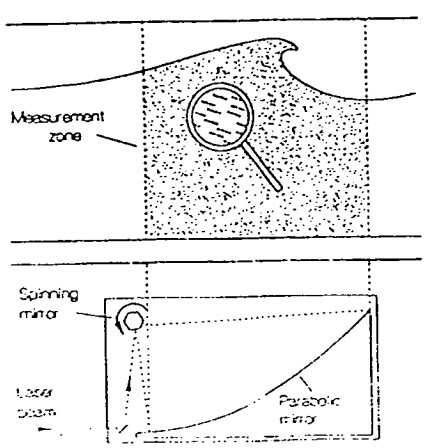

Fig. 4 - Measurement zone of PIV (schematically)

A two-dimensional plane in the flow is illuminated stroboscopically through the glass bottom of the flume by a 15 W Argon Ion continuous wave laser and a scanning beam system (Greated et al, 1992, Gray et al, 1991). Typical illumination frequencies for this study were 1000 Hz. The flow is seeded with conifer pollen and photographed using a Hasselblad medium (55mm) format camera. For these experiments, the camera was triggered electronically from the wave generation system, so that precise phases of the breaking could be captured to form a sequence of velocity maps.

The local flow velocity can then be determined from the separation of the image pairs at any given point in the photographed area. A fully automated system is used to "interrogate" the photograph over an array of points to build up a flow velocity map. A detailed description and appraisal of PIV can be found in Greated et al. (1992).

Frequency modulated waves with heights up to about 15 cm were used for this study. Simultaneous measurements of the pressure (at the wall and on the berm) and velocity field in the breaker just before impinging on the wall were performed. The wave motion was also recorded by video through the glass wall of the flume.

4. Experimental Results

Three of the most common breaker types were investigated: plunging breaker with a large entrapped air pocket, plunging breaker with a small entrapped air pocket and a 'flip-through' (Fig. 5). For each of these breaker types, the two-dimensional velocity field in the breaker at the wall and its temporal development have been investigated.

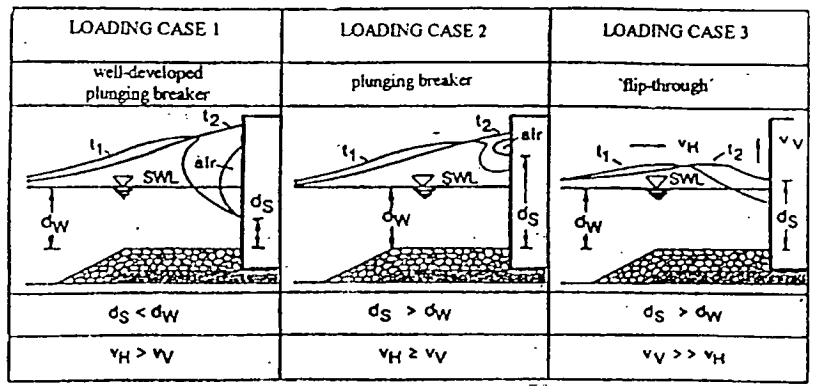

d_s = water elevation at the wall; d_w = water depth at the wall (SWL)
v_h = horizontal velocity ; v_v = uprush velocity at the wall

Fig. 5 - Investigated breaker types and loading cases

a) Loading Case 1: Plunging Breaker with Large Air Pocket

Photo 1 shows the plunging breaker with large air pocket at three single instants t_1, t_2 and t_3 just before breaking at the vertical wall. The breaker has a height of H_B= 0.15 m and a period of T= 1.1 s. The breaker crest curls over the front face as it advances. It reaches the caisson front just before collapsing, so that it strikes the wall and enclosed a large cushion of air and air-water mixture. This cushion is then highly compressed by the following impinging water mass.

The velocity field of these three single instants t_1, t_2 and t_3 in Fig. 6a-c shows that the velocity of the breaker crest increases rapidly towards the wall. The air pocket is to be expected at still water level.

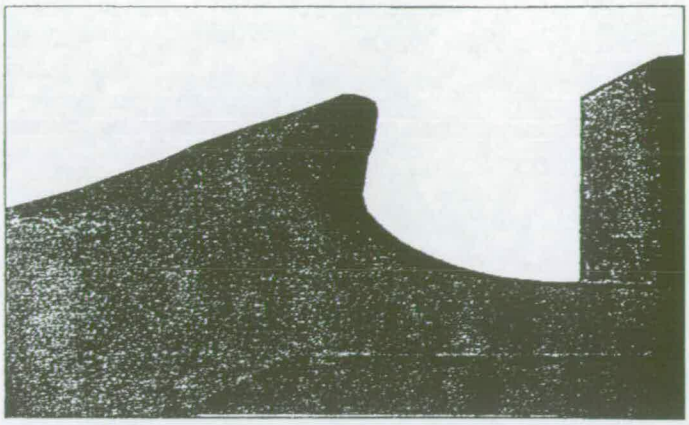

a) At time $t_1 = 0.00$ s

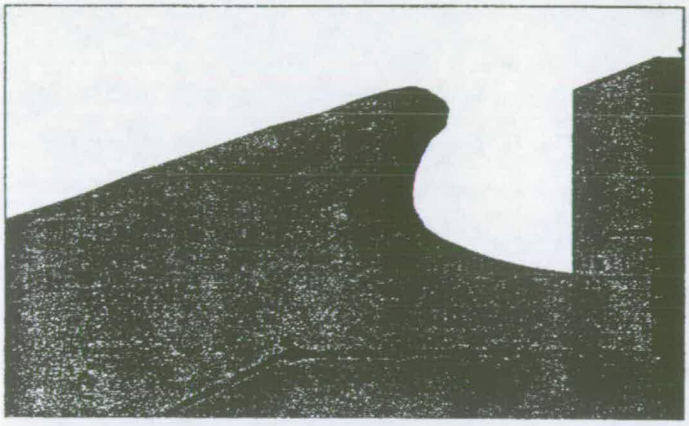

b) At time $t_2 = 0.05$ s

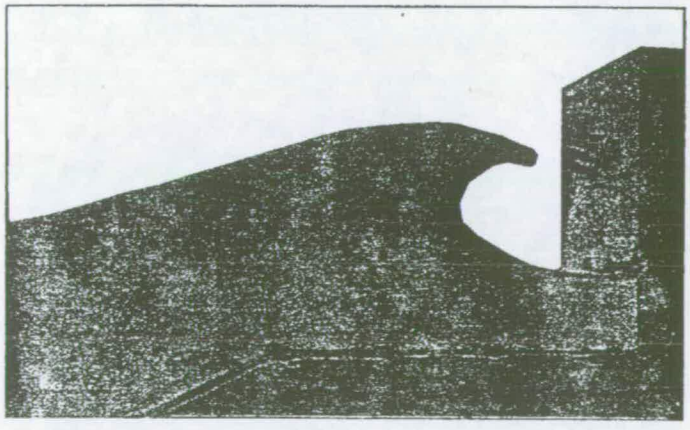

c) At time $t_3 = 0.10$ s

Photo 1: Plunging breaker with large air pocket

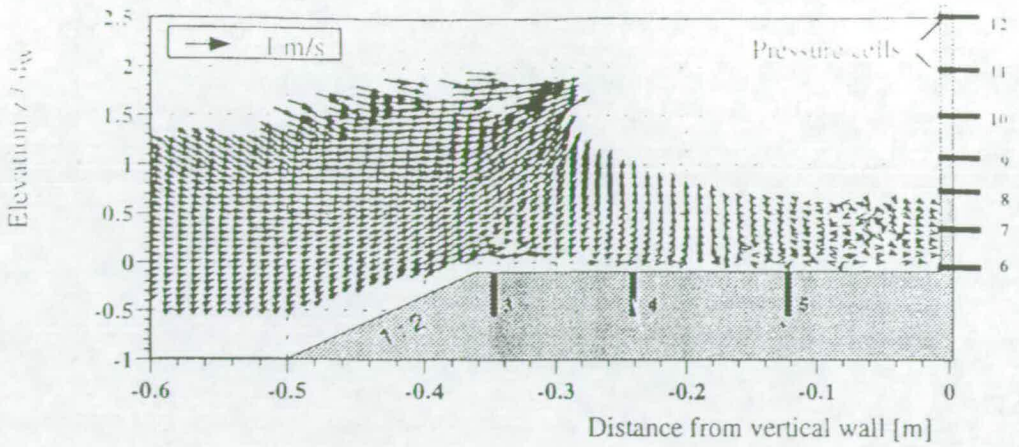

a) Velocity field at time t_1 = 0.00 s

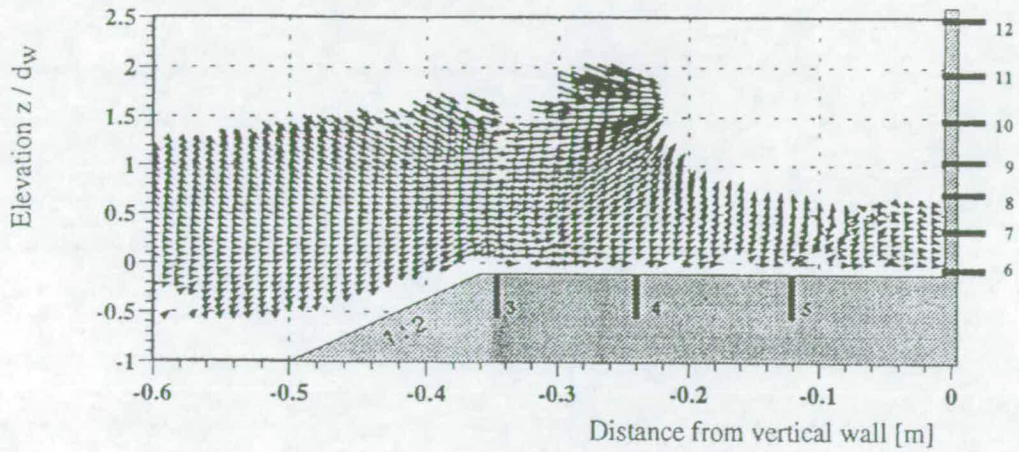

b) Velocity field at time t_2 = 0.05 s

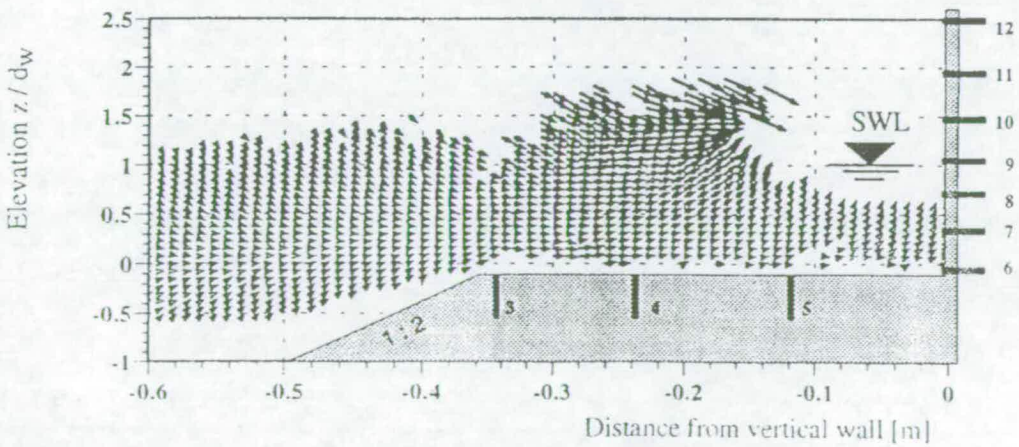

c) Velocity field at time t_3 = 0.10 s

Fig. 6 - Velocity field in the plunging breaker with large air pocket

The vertical distributions of the horizontal velocity components in non-dimensional form $u / \sqrt{gH_B}$ at t_1, t_2 and t_3 corresponding to relative distances from the wall $x_1/b = 0.86$, $x_2/b = 0.69$ and $x_3/b = 0.44$ (b = berm width = 0.35 m) with the crest level s of the breaker are shown in Fig. 7a. The impact zone to be expected is not limited but extends over a relatively large height (in order of H_B).

The velocity profile at t_3 together with the impact pressure distribution at occurrence of peak force in Fig. 8a was used to determine the mass distribution dm (Fig. 7b) at different elevations dz according to Eq. (2). It is seen, that for this breaker type the water mass is more concentrated around the still water level.

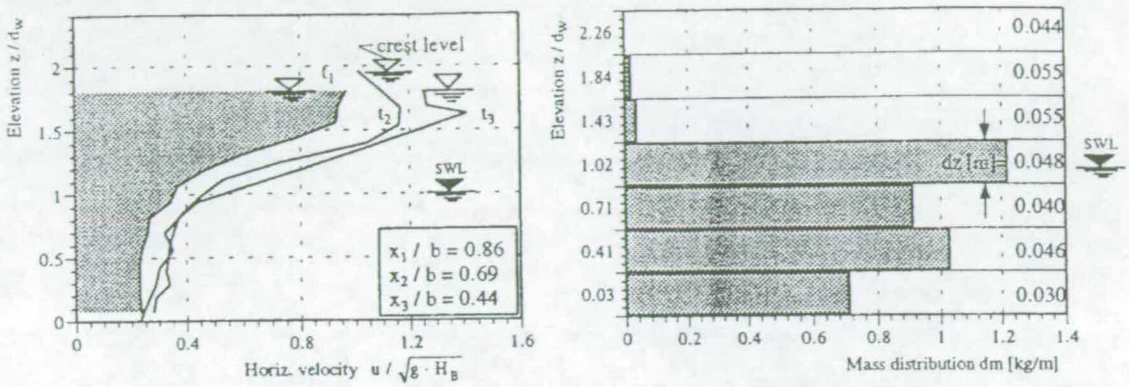

a) Velocity profiles

b) Water mass

Fig. 7 - Velocity distribution and water mass in the plunging breaker with large air pocket

The corresponding vertical distribution of the impact pressure at occurrence of force peak is shown in Fig. 8a while the whole time history of the impact force is illustrated by Fig. 8b.

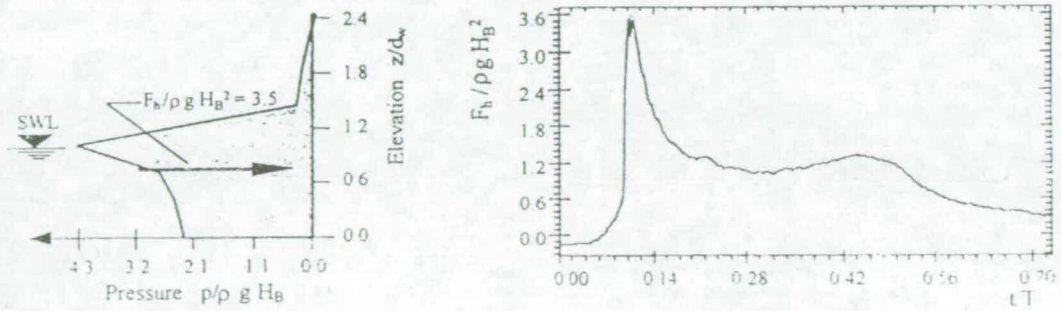

a) Impact pressure distribution at occurrence of peak force

b) Impact force history

Fig. 8 - Impact force induced by breaker in Photo 1

The most striking feature in this case is the occurrence of two distinct pressure distributions the first one develops at higher elevations and exhibits very high impact pressures with shorter durations and smaller impact areas, whereas the second one which develops immediately under the first impact zone acts on a larger area and depicts smaller impact pressures with longer durations. These different distributions are induced by the impinging breaker tongue and the compression of the large air pocket. These appear in the force traces as two distinct peaks (Fig. 8b).

b) Loading Case 2: Plunging Breaker with Small Air Pocket

Photo 2 shows the plunging breaker with small air pocket at three single instants t_1, t_2 and t_3 under study. The breaker has a height of H_B= 0.13 m and a period of T= 0.9 s. In Photo 2b and c the very small air cushion near the breaker crest can be seen.

The velocity field of these three single instants t_1, t_2 and t_3 in Fig.9a-c shows the very short time interval between overturning and the impact of the breaker crest on the wall. The crest level of the breaker is much lower than in loading case 1.

The vertical distributions of the horizontal velocity components in non-dimensional form $u / \sqrt{gH_B}$ at t_1, t_2 and t_3 corresponding to relative distances from the wall x_1/b= 0.86, x_2/b= 0.69 and x_3/b= 0.44 (b= berm width= 0.35 m) are shown in Fig. 10a.

Like for loading case 1 the mass distribution was calculated at time t_3 (Fig. 10b). A comparison between the vertical distributions of the horizontal velocity components and the mass distributions in Figs. 7 and 10 shows that:

- the relative breaker velocities $u / \sqrt{gH_B}$ are larger in loading case 2 than in loading case 1;
- the velocity increase at a larger rate towards the wall in loading case 2, resulting in higher accelerations;
- the maximum of hydrodynamic mass is larger and at a higher elevation in loading case 1.

The corresponding impact pressure distribution at the time of the occurrence of the force peak and the whole impact force history induced by the breaker in Photo 2 are shown in Fig. 11.

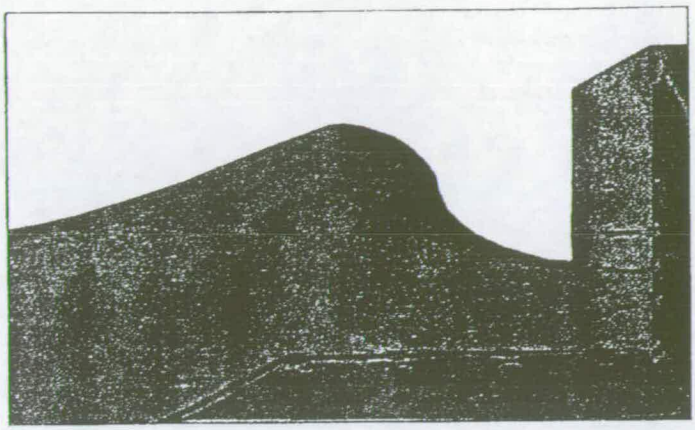

a) At time $t_1 = 0.00$ s

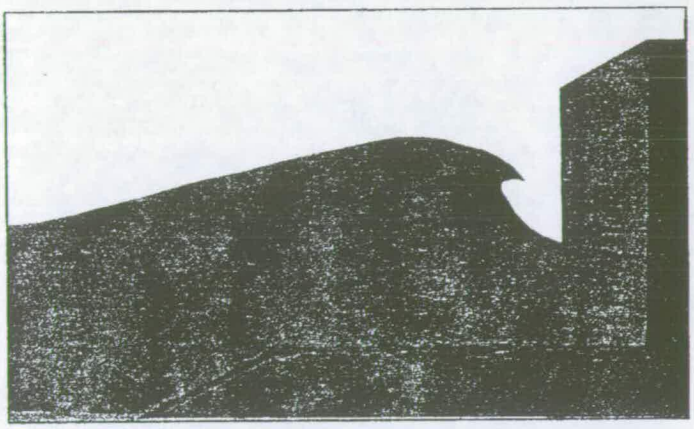

b) At time $t_2 = 0.05$ s

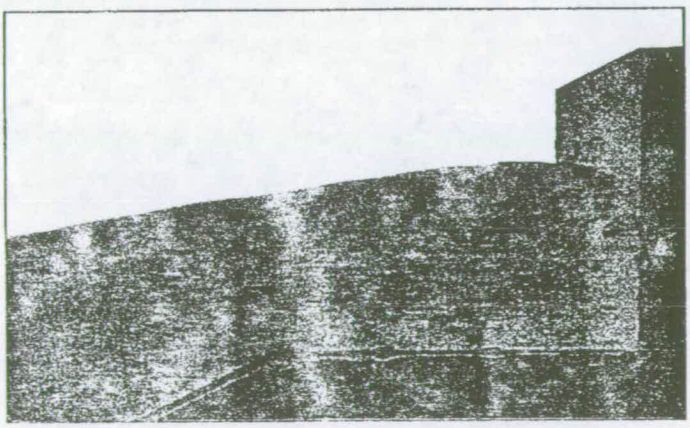

c) At time $t_3 = 0.10$ s

Photo 2: Plunging breaker with small air pocket

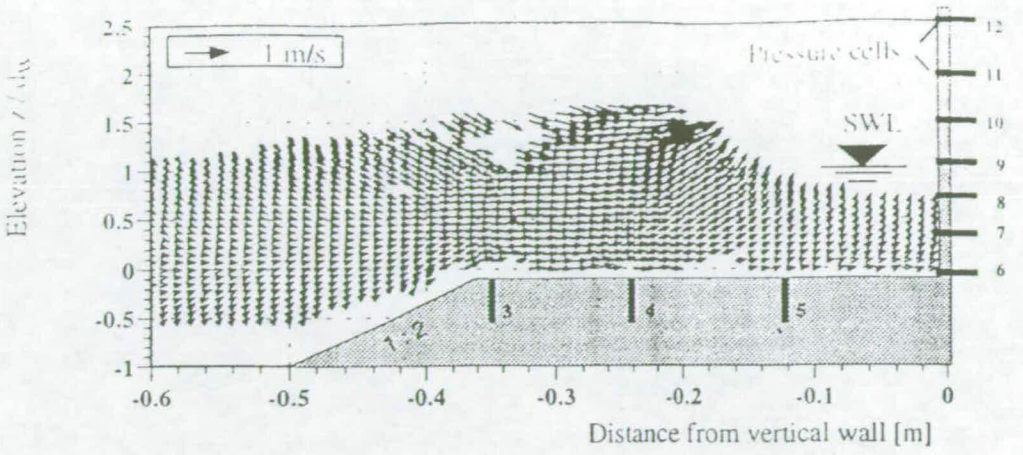

a) Velocity field at time $t_1 = 0.00$ s

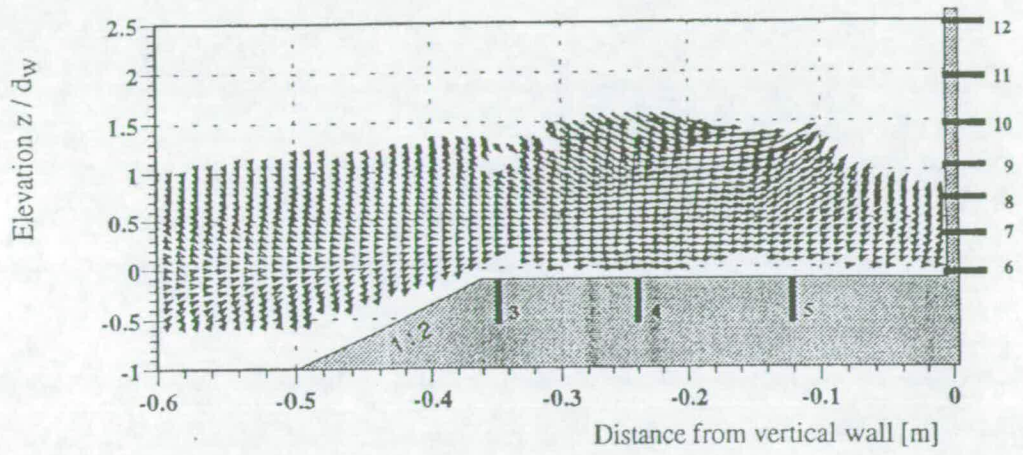

b) Velocity field at time $t_2 = 0.05$ s

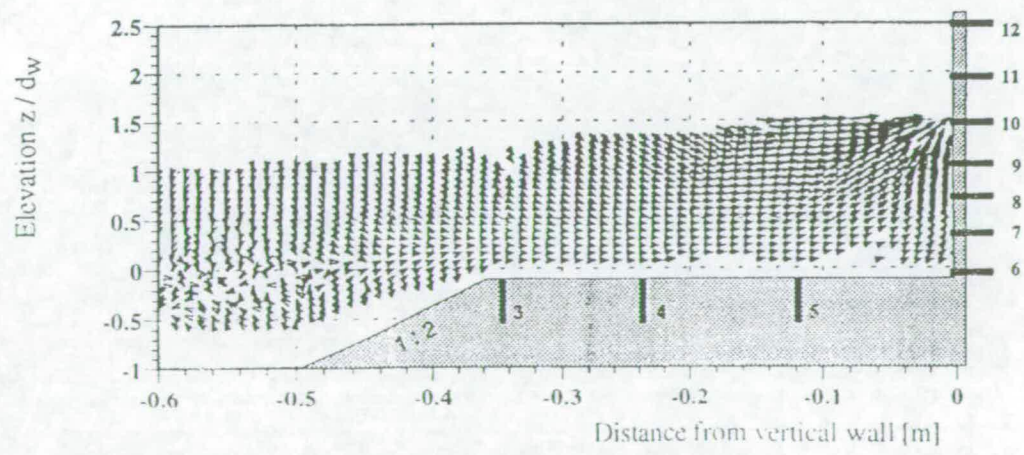

c) Velocity field at time $t_3 = 0.10$ s

Fig. 9 - Velocity field in plunging breaker with small air pocket

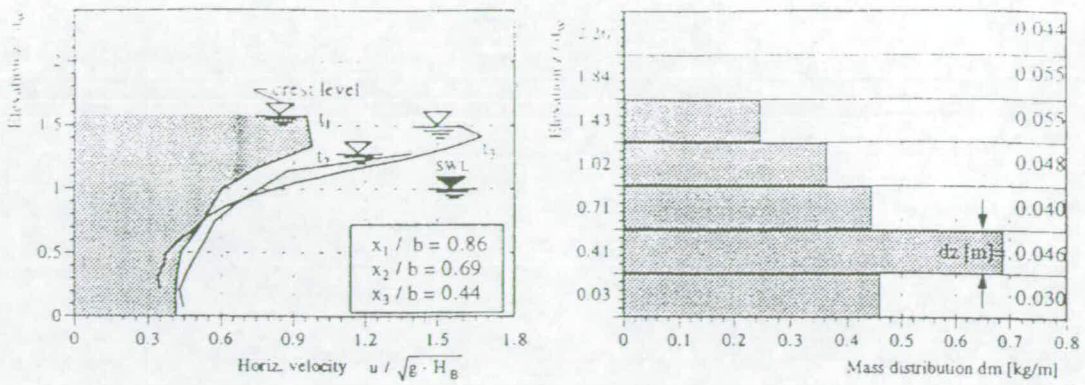

a) Velocity profiles

b) Water mass

Fig. 10 - Velocity distribution and water mass in plunging breaker with small air pocket

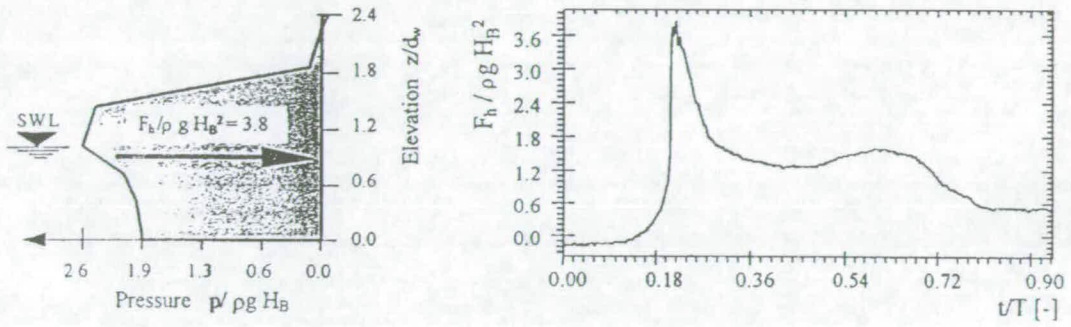

a) Impact pressure distribution at occurrence of peak force

b) Impact force history

Fig. 11 - Impact force induced by breaker in Photo 2

The most typical are the relatively high impact pressures which occur almost simultaneously over a large area and at different elevations of the wall. This may explain why in this case the larger force results. The force history is generally characterised by a very sharp peak (Fig. 11b).

c) Loading Case 3: 'Flip-Through'

For the 'flip-through' case in Photo 3, the uprush velocity at the wall is large as compared to the horizontal velocity. The waterline at the wall generally reaches the anticipated 'impact point' just before the wave crest overturns and hits the wall. Thus, no air is entrapped and the wave develops into a sudden upward sloshing-motion.

In a similar manner to both loading cases 1 and 2, the velocity fields, the corresponding velocity distributions and the mass distribution at time t_2 are shown in Figs. 12 and 13. A comparison with the other two loading cases in Photos 1 and 2 shows that much larger accelerations are expected for the 'flip-through' case.

The corresponding impact pressure distribution at the time of the occurrence of the force peak as well as the whole impact force history induced by the 'flip-through' are shown in Fig. 14.

The characteristics of the pressure distributions are almost the same as for loading case 2, with the exception that loading case 3 does not display any sharp force peak and any high impact pressure. These relatively low loads result from incomplete breaking, due to the presence of the wall. This loading case represents a transition between loading case 2 and a standing wave loading situation.

A comparison with Figs. 7 and 8 and Figs. 10 and 11 shows that:

- the largest acceleration occurs in loading case 3;
- the mass distribution is similar to that in loading case 2, that exhibits slicely smaller values.

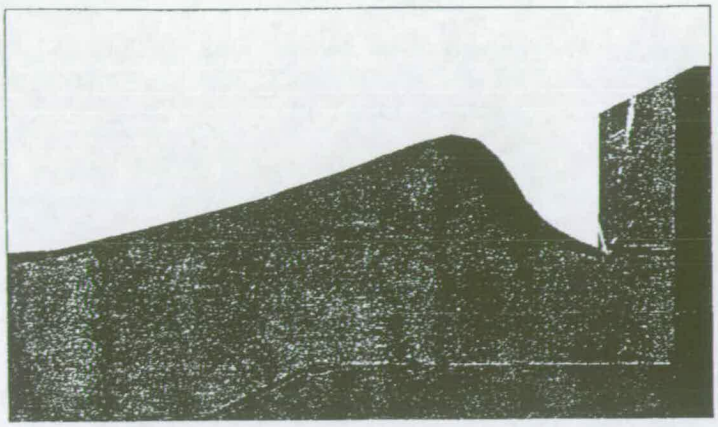

a) At time $t_1 = 0.00$ s

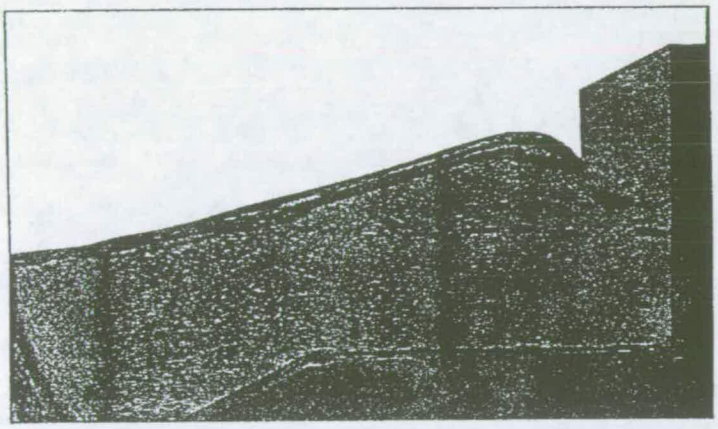

b) At time $t_2 = 0.05$ s

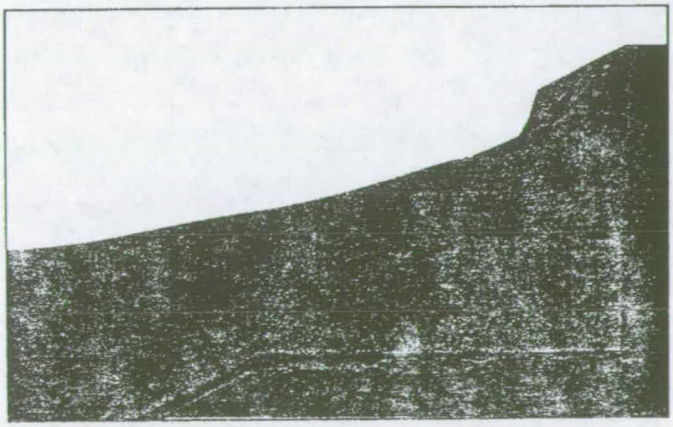

c) At time $t_3 = 0.10$ s

Photo 3: 'Flip-through' case

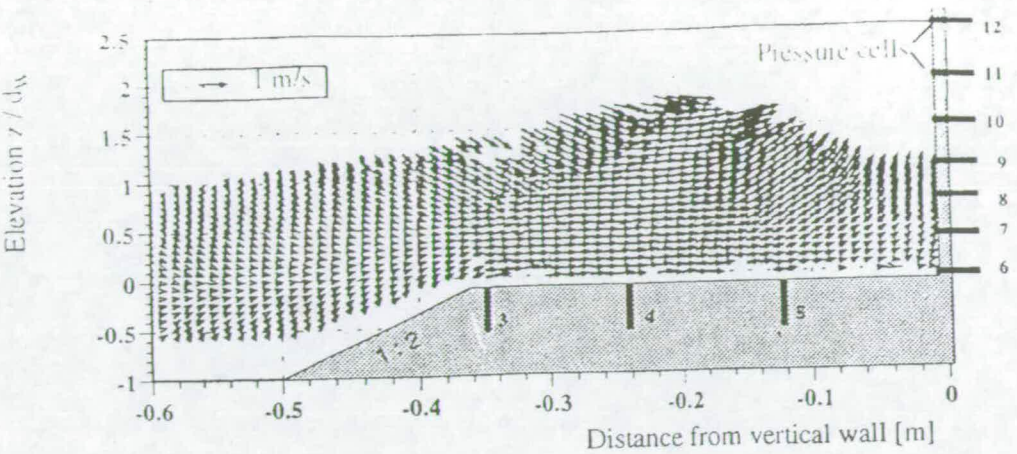

a) Velocity field at time t_1 = 0.00 s

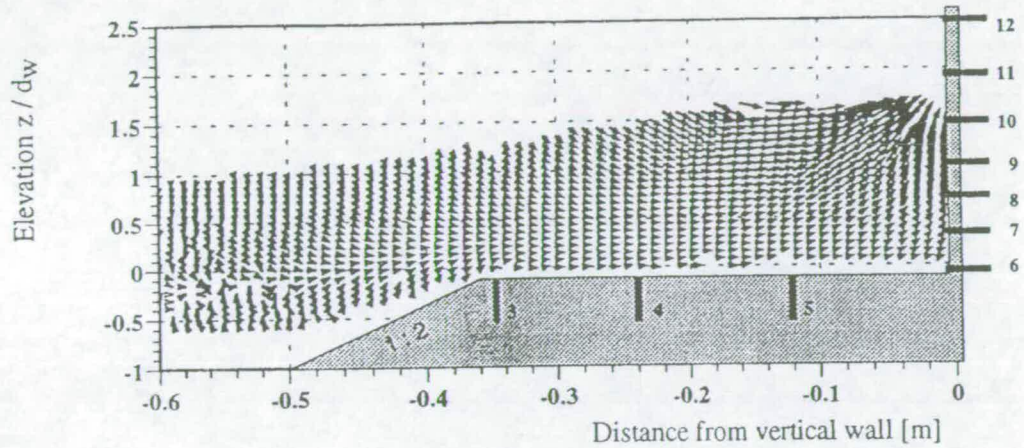

b) Velocity field at time t_2 = 0.05 s

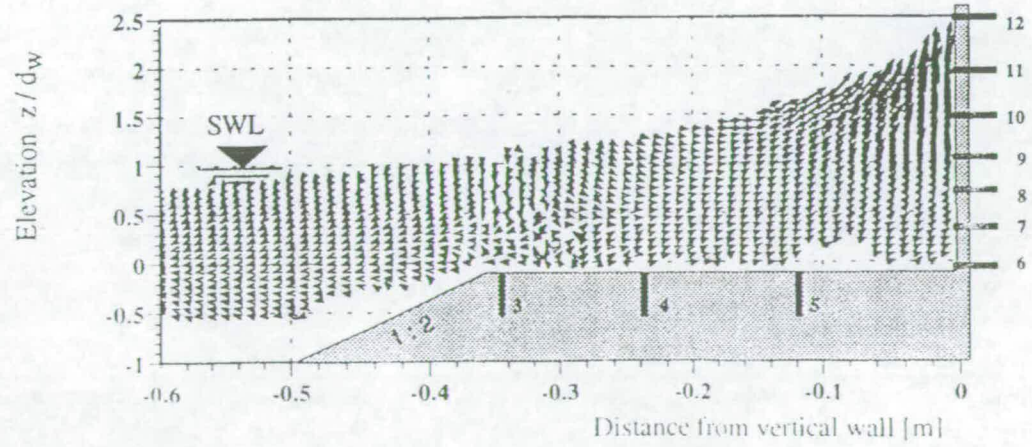

c) Velocity field at time t_3 = 0.10 s

Fig. 12 - Velocity field for the 'flip-through' case

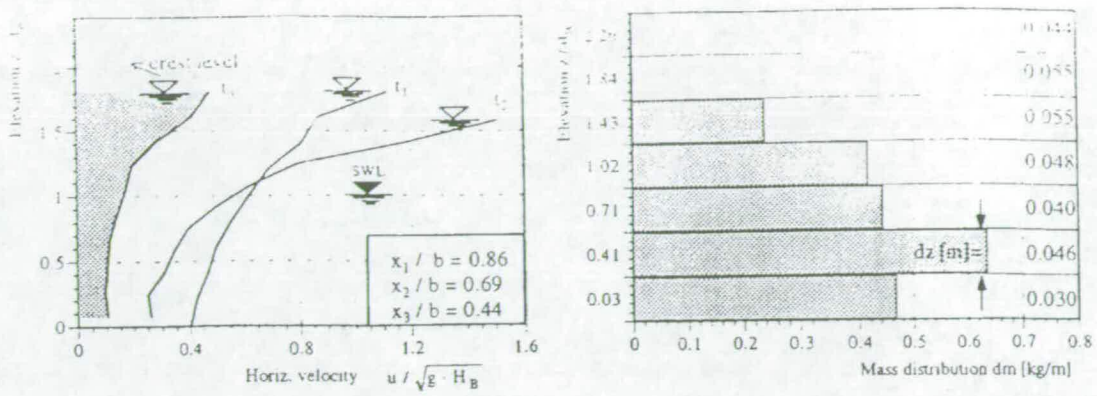

a) Velocity profiles

b) Water mass

Fig. 13 - Velocity distribution and water mass for the `flip-through´case

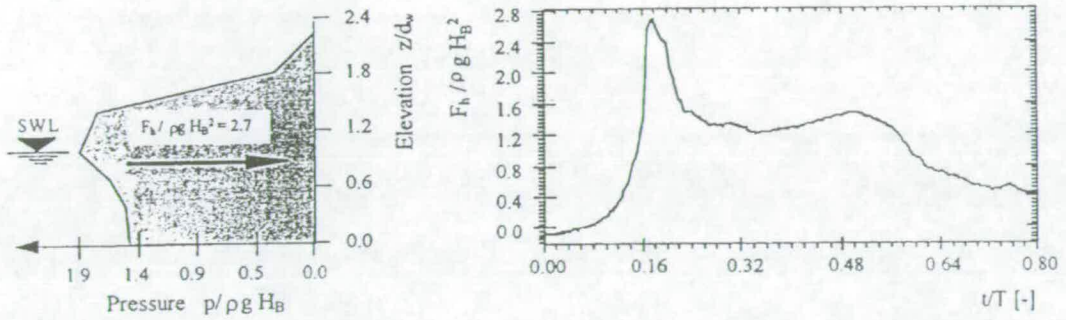

a) Impact pressure distribution at occurrence of peak force

b) Impact force history

Fig. 14 - Impact force for `flip-through´case

The typical set of the experimental results illustrated by Figs 6-14 for three different loading cases, together with similar results, are being analysed in order to develop an impact force prediction formula for each of the investigated loading cases by using the procedure presented under Section 2 above.

5. Concluding Remarks

The capability of Particle Image Velocimetry (PIV) in obtaining reliable velocity profiles was demonstrated.

The most common breaker types were investigated: plunging breaker with a large entrapped air pocket, plunging breaker with a small entrapped air pocket as well as the 'flip-through' case.

The results of the analysis are being used to develop formulae for the prediction of breaking wave impact loads on caisson breakwaters.

6. Acknowledgements

The work described in this paper was carried out in the wave tank of the University of Edinburgh. The first and the third author would to acknowledge the support of the Deutsche Forschungsgemeinschaft within SFB 205 and the very nice co-operation with Tom Bruce and Bill Easson from the University of Edinburgh.

7. References

Bruce, T.; Easson, W. J. (1993): Kinematics of wave-induced flow around seabed pipelines, ASCE, 23rd ICCE '92, Venice/Italy, Vol. 3, pp 2990-2998.

Gray, C.; Greated, C.A.; McCluskey, D.R. & Easson, W.J. (1991). An Analysis of the Scanning Beam PIV Illumination System, Journal of Physics (Measurement Science and Technology), Vol. 2, pp717-724.

Greated, C.A.; Skyner, D.J. & Bruce, T. (1992): Particle Image Velocimetry (PIV) in the Coastal Engineering Laboratory, Proc. 23rd Int. Conf. on Coastal Engineering, Vol. 1, pp 212-225.

Oumeraci, H. (1994): Review and analysis of vertical breakwater failures - lesson learned. Special issue on vertical breakwaters, Ed. Oumeraci, H.; Van der Meer, J.; Franco, L.; Coastal Engineering, Elsevier/Amsterdam, Vol. 22, pp 3-29.

Oumeraci, H.; Klammer, P.; Partenscky, H. W. (1993): Classification of breaking wave loads on vertical structures, ASCE, Journal of Waterway Port Coastal and Ocean Engineering, Vol 119, No. WW 4, pp 381-397.

Quinn, P. A.; Skyner, D. J.; Gray, C.; Easson, W. J. (1993) A critical analysis of the Particle Image Velocimetry Technique as applied to water waves, in Flow Visualisation and Image Analysis; Kluwer Academic Publ., Dordrech/Netherlands

Appendix B: Bruce & Vicinanza, 1998

Bruce, T. & Vicinanza, D. (1998), *Wave kinematics in front of caisson breakwaters*, Proc 8th Int. Polar and Offshore Eng Conf ("ISOPE'98"), Montreal, 3, pp658–664, ISOPE, Golden, Colorado, ISBN 1-880653-34-6

Appendix B
Bruce & Vicinanza, 1998

Bruce, T. & Vicinanza, D. (1998), *Wave kinematics in front of caisson breakwaters*, Proc 8th Int. Polar and Offshore Eng Conf ("ISOPE'98"), Montreal, 3, pp658–664, ISOPE, Golden, Colorado, ISBN 1-880653-34-6

B.1 Declaration of contribution

The author drove (or co-drove with Vicinanza) all stages of this project, from assisting in securing the funding for Vicinanza's stay in Edinburgh through to the preparation of the final paper. This was the first series of tests using Edinburgh's own pressure transducers. The author designed and built the necessary power supplies and signal amplifiers for the pressure transducers. He and Vicinanza together designed and carried out all tests; discussed and carried out subsequent analysis, and co-wrote the text.

B.2 Published paper

overleaf

WAVE KINEMATICS IN FRONT OF CAISSON BREAKWATERS

T. Bruce[1] & D. Vicinanza[2]
Department of Mechanical Engineering
The University of Edinburgh
Scotland

ABSTRACT

The interaction of breaking waves with vertical and composite breakwaters is a complex problem in which there are strong correlations between breaking wave shapes and the magnitude, duration and distribution of the impact forces and pressures. This paper presents results from a series of laboratory experiments to measure wave kinematics and pressures in front of composite breakwaters in random wave conditions.

KEY WORDS: Breakwaters, wave breaking, wave impact, wave kinematics, random waves, Particle Image Velocimetry, PIV

1. INTRODUCTION

Vertical wall structures are frequently employed for the protection of harbours. Although these systems are widely used, considerable damage, some of which is recent, has led to further studies of the design features involved. Takahashi *et al* (1994), Oumeraci *et al* (1995) and Allsop *et al* (1996a) have pointed out that, in a storm, particular combinations of wave conditions and of mound geometry can generate a large number of *impact* loads of such force as to cause cumulative sliding and eventually bring about the failure of the structure.

A co-ordinated programme of research on caisson structures was initiated in 1990 under EC MAST I. The current programme under EC DG XII MAST III, "PROVERBS" (Probabilistic Design Tools for Vertical Breakwaters) aims to develop and implement probability based tools for an integrated design of vertical breakwaters and further classes of monolithic structures where wave effects dominate design considerations. These tools will be developed by integrating various aspects associated with hydrodynamic, geotechnical and structural processes into a Probability based Integrated Design Approach (PIDA).

Under PROVERBS, the breakwater is treated explicitly as a dynamic structure: conventional design methods predict a pressure distribution on the structure's faces, but if the response of the structure is to be predicted, then the force variation with time is also required. Under quasi-static *pulsating* loading, this relatively straightforward, but the problem of the impulsive loadings generated by breaking wave impacts is complex.

Two methods for the prediction of force impulse maxima and duration have been tentatively suggested. One (Walkden *et al*, 1996) is intended for use when designing a structure based upon physical model tests. The other (Oumeraci & Kortenhaus, 1997) uses knowledge of site conditions as its starting point. As part of their approach, Oumeraci & Kortenhaus use the solitary wave theory of Munk (1949) to predict the maximum velocity under the crest of an incident wave from its height and the water depth in front of the structure. However, the kinematics of a solitary wave differ from those occurring in a random sea, and the suitability of Munk's predictions should be checked.

The kinematics of breaking waves can be studied using Particle Image Velocimetry (PIV), *eg* Skyner (1996) describes the measurement of the kinematics of the breaking of a deep-water focussed wave. The authors know of only two studies of the internal kinematics of waves breaking at a breakwater carried out to date: Oumeraci *et al* (1995) involved focussed, additive waves; Walkden *et al* (1998) use short sets of regular waves. This paper presents loading and velocity measurements of breaking waves in random seas.

This paper will describe a series of physical model tests to measure wave kinematics in front of composite breakwaters. Firstly, for each wave / geometry combination, loading measurements are made to determine the type of event responsible for extreme loadings. Next, PIV velocity data is obtained for these representative large events. The characteristics of the pressure measurements for each event type are described with reference to video records showing the form of wave breaking. The first results of measured kinematics are compared with the prediction of Munk (1949).

---

[1] Lecturer, Department of Mechanical Engineering, The University of Edinburgh, King's Buildings, Edinburgh, EH9 3JL, Scotland; tel: +44 131 650 8701, fax: +44 131 667 3677, email: Tom.Bruce@ed.ac.uk
[2] PhD Researcher, Dipartimento di Ingegneria Idraulica e Ambientale "G. Ippolito", Università di Napoli Federico II, Via Claudio, 21 - 80125 Napoli, Italy, tel.+39 81 768 34 26, fax +39 81 5938936, email: diegovic@cds.unina.it

2. BREAKER TYPES AND BREAKING CRITERIA

The loading experienced by a breakwater depends strongly upon the form of the largest waves reaching the structure. The structure may experience either *pulsating* or *impact* loads. Within the impact loading regime, it is now well established that the form of the breaker at the wall is of crucial influence on the form of the pressure and force impulse at the structure. Thus the designer needs to know whether impact loads may occur, and if so, the form of the wave responsible.

Oumeraci *et al* (1993) describes a classification of wave impact events which are poorly modelled by a quasi-static model. These classifications are *flip-through*, *plunging breaker* and *broken wave*. These event types will be described and illustrated in the results presented (Section 5).

The form of breaking wave loading that is likely to occur is dependent upon a multitude of factors relating to the structure geometry and the prevailing sea state. These dependencies have been synthesised into a simplified *parameter response map* (Allsop *et al*. 1996a,b, Vicinanza, 1997) which shows, for a given combination of sea state and structure geometry, whether non-pulsating loadings will be experienced, and if so, of what type.

An even more recent approach to determine whether non-pulsating loads may be experienced under a given set of conditions is that of Calabrese (1998) who presents an empirical criterion to predict, as a function of water depth at the structure toe and the berm width, whether breaking wave loading events will occur. Figure 1 shows the definitions of the parameters which define the structure geometry. The wave height for the onset of breaking events is given by

$$H_{99.6b} = \left(0.1025 + 0.0217C^*\right) L_{pi} \tanh\left(2\pi\xi h_s / L_{pi}\right) \qquad [1]$$

where L_{pi} is the local wavelength corresponding to the peak frequency, h_s is the water depth at the toe of the mound and C^* is a wave reflection parameter given by

$$C^* = \left(1 - k_r\right) / \left(1 + k_r\right)$$

where k_r is the coefficient of reflection from the model. The formula includes a *mound parameter* ξ which depends upon the relative length of the mound in front of the structure expressed by B_{eq}/d:

$$\xi = f_1\left(B_{eq} / d\right)$$

where $B_{eq} = B_h + (h_b / 2 \tan \alpha)$ is the *equivalent berm width*, a parameter which includes the influence of the berm width B_h and the front slope angle α. h_b is the berm height and d is the water depth over the berm. In the range of relative depths covered by Calabrese's (1998) tests, $0.075 \le h_s / L_p \le 0.225$, the mound parameter is given by

$$\xi = 0.0076\left(B_{eq} / d\right)^2 - 0.1402\left(B_{eq} / d\right) + 1 \qquad \text{for } 0 \le B_{eq}/d \le 10$$

It is worth noting that it is possible that, for relative depths shallower than those covered by Calabrese's study, a different relationship for ξ may exist, including a dependency upon the bed slope in front of the structure, m, *ie*

$$\xi = f_2\left(m, B_{eq} / d\right)$$

The present work aims to investigate kinematics under the full range of impulsive loading conditions, from *flip-through* to a broken wave, and for both *low mound* ($0.3 < h_b/h_s < 0.6$) and *high mound* ($0.6 < h_b/h_s < 0.9$) composite structures.

3. EXPERIMENTAL SETUP

The tests were carried out in the wave channel at Edinburgh. The channel is 20m long, 0.4m wide and has a working water depth of 0.7m. The wavemaker is of a flap design, and is reflection-absorbing using force feedback. The channel walls and bed are all constructed from 25mm glass to allow full optical access for PIV.

PIV is capable of measuring the instantaneous two-dimensional velocity field under a wave. The basis of the method is simple: tiny tracer particles are introduced into the flow, and a two-dimensional plane through the flow is illuminated stroboscopically. The flow is photographed, with the camera shutter held open long enough to record at least two illuminations of the particles. The resulting *flow record* can then be divided into a grid of small cells, and the flow velocity in each cell determined from the distance moved by the tracer particles in the interval between pulses of illumination. Details of the method can be found in *eg* Gray & Bruce (1995).

For the tests described in this paper, the flow field extending 0.5m in front of the face of the caisson was illuminated by a Spectra Physics 15W Argon Ion continuous wave (CW) laser. The laser light was formed into a sheet by a scanning beam system (Gray & Bruce, 1995). Conifer pollen was used as the tracer particle: it has a diameter of c.50 - 70 μm and, once immersed and allowed to absorb water, it is neutrally buoyant. The flow record was recorded on a Kodak *MegaPlus* still-image CCD camera of resolution 2k x 2k pixels. The PIV flow records were stored as bitmaps and analysed using Optical Flow Systems *VidPIV* software.

In addition to measurements of the kinematics, pressures on the front face of the caisson were measured. Seven Druck PDCR 8310 transducers were mounted flush with the front face of the model as shown in Figure 1. The transducer signals were sampled and digitised at 2 kHz using a Data Translation DT21-EZ card and DT-VEE software.

An existing model (Figure 1) with $h_b = 0.160$ m, $B_{eq} = 0.520$ m was available for the tests. It was decided to mount the model in low and high mound configurations as follows:

low mound: $h_s = 0.310$ m, $d = 0.150$ m $\Rightarrow h_b/h_s = 0.52$
high mound: $h_s = 0.250$ m, $d = 0.090$ m $\Rightarrow h_b/h_s = 0.64$

The beach slope in front of the model was fixed at 1:20.

4. EXPERIMENTAL PROCEEDURE

Tables 1 and 2 show the JONSWAP seas selected for the tests for the low and high mound structure respectively. H_{si} is the significant wave height measured at the location of the structure but without the structure in place. Also shown is the breaker type subsequently most frequently observed for each test set, determined from a video analyses

Each test comprised approximately 1000 waves and was run at least twice. On the first run, only pressure measurements were made and video recorded. These pressure v. time histories were analysed according to a standard algorithm developed under PROVERBS (McConnell & Kortenhaus, 1997) to determine $F_{h99.6}$, the 0.4% exceedence level of the horizontal force, and locate the four largest events in the sequence. The test was then rerun, again with pressure and video measurements, but also taking PIV measurements at the times of the four largest events. Yet further repeat tests were run until the investigators were satisfied that the timing of the triggering of the camera taking the PIV flow records was giving measurements as close to the impact events as possible.

The multiple tests permitted the level of repeatability of the events within the tests to be verified: the four largest events identified from

the pressure measurements for the first run were observed in subsequent runs as the same type of breaker at the same instant. The actual wave impact pressures are somewhat variable as expected (*eg* Chan 1994, Kirkgoz, 1991), varying over 2 or 3 kNm^{-2} for pressure maxima ~10 kNm^{-2}. The shape of the spatial pressure distribution on the front face and the temporal variation of this distribution through the event showed very good repeatability. Thus, for each combination of geometry and wave height, a typical pressure distribution history could be associated with the representative breaker type for the extreme events and the corresponding PIV kinematic data.

H_{so} (m)	H_{si} (m)	T_m (s)	breaker type
0.081	0.058	1.2	flip-through
0.095	0.068	1.2	plunging
0.103	0.075	1.2	plunging
0.116	0.088	1.2	plunging
0.121	0.094	1.2	plunging

Table 1: Wave parameters for low mound tests.

H_{so} (m)	H_{si} (m)	T_m (s)	breaker type
0.056	0.044	1.2	plunging
0.066	0.051	1.2	plunging
0.081	0.056	1.2	plunging
0.095	0.070	1.2	plunging
0.116	0.087	1.2	broken

Table 2: Wave parameters for high mound tests.

5. RESULTS

5.1 Comparison with Breaking Criterion

Figure 2 shows equation 1 (Calabrese, 1998) plotted for the low mound ($B_{eq}/d = 4$) and the high mound ($B_{eq}/d = 6$) structures. On the graphs, the 0.4% exceedance wave height for the onset of breaking predicted by equation 1, $H_{99.6b}$, is plotted against the water depth at the toe of the mound, h_s, with both axes non-dimensionalised by L_{pi}. The points corresponding to each test set are also plotted. The lines should delimit, for each structure, the region within which only pulsating loads occur from the region in which breaking wave impact loads occur.

For the low mound structure, the observed loading types are in good agreement with the prediction: for the test corresponding to the only point falling below the line, the representative extreme event was a *flip through* event in which the wave *just* does not break. The other cases all lie clearly above the line and for each the representative loading case was observed to be an impacting breaking wave.

For the high mound tests, agreement with Calabrese's breaking curve was also good. In these cases, all tests lay in the impact region above the line. In each case, the representative extreme loading was observed to be due to an impacting breaking wave or, in the case of the largest H_s test, a broken wave.

The results show how an increase in $H_{99.6}/L_{pi}$ modifies the extreme wave shape in a sequence starting from the *pulsating* regime, moving to *flip through* events, then to plunging breaking wave impacts, and finally, for the largest $H_{99.6}/L_{pi}$, to the situation where the wave is broken before impact with the structure. The following sections look at flip through, breaking wave and broken wave events in more detail.

5.2 Flip-through ($H_{99.6}/H_{99.6b} < 1$)

The sequence of video frames in Figure 3 illustrates a flip through event. The shape of the flip-through breaker is due to the quick rise of the water level up the wall. This case constitutes a transition between a total clapotis and a plunging breaker. For a given relative depth and wave steepness the pressure shows a symmetrical double hump. As the wave steepness increases and the wave moves closer to breaking condition the double peak becomes asymmetrical and the first peak is sharper and higher than the second - the pressure v. time graph in Figure 4 is typical of a flip through event. In this case the pressure values measured were up to five times greater than those of the standing wave.

5.3 Plunging ($1 < H_{99.6}/H_{99.6b} < 2$)

Plunging wave breaking occurs when the front of the wave is almost vertical at the moment of impact. From among all the tests, the highest loads on the structure were measured in these conditions. The pressure signal (*eg* Figure 5) shows a typical impulsive progression characterised by extremely high values at the pressure peak and very short rise times(Δt). When a pocket of air is trapped between the wall and the front of the wave crest at the moment of impact, the pressure signal shows, immediately after the peak, oscillations due to the compression of the air. Figure 6 shows a video sequence illustrating the steepening of the impacting wave and the entrapment of an air pocket at impact with the wall.

As $H_{99.6}/H_{99.6b}$ increases, the pocket of air entrapped by the breaker at the wall becomes larger. The air has a cushioning effect upon the impact and a reduction in the maximum pressures is observed for larger amounts of entrapped air, coupled with an increase in the rise time of the pressure peak. The overall impulse, however, remains largely unaffected by changes in the size of the trapped air pocket. During the experiments maximum pressures up to fifty times greater than those occurring in the presence of a standing wave were measured. Rise times are of the order of Δt = 0.005-0.02s.

5.4 Broken ($H_{99.6}/H_{99.6b} > 2$)

The final type of event considered is one in which the onset of breaking occurs so early that the breaker collapse occurs before reaching the caisson front. A PIV flow record for a broken wave is shown in Figure 7. The large foamy mass of water preceding the impact is clearly visible. Figure 8 is a pressure v. time graph for a broken wave event, showing that the impact is considerably damped by the preceding foamy mass.

5.5 Wave Kinematics

Examples of PIV velocity maps for a flip through event, a plunging breaker and a broken wave are shown in Figures 9, 10 and 11. Comparison of measured horizontal velocity maxima with the predictions of Munk (1949) for solitary waves is of interest for the reason noted in Section 1. Munk leads to

$$u = \sqrt{g(d + H_b)} \qquad [2]$$

where H_b is the breaking wave height. Oumeraci & Kortenhaus (1997) use the breaking limit $H_b/d = 0.78$ to estimate H_b.

H_{si} (m)	H_b (m) from video	u_{max} (ms^{-1}) from PIV	breaker type
0.058	0.11	0.9	flip through
0.068	0.11	0.9	plunging
0.075	0.12	0.85	plunging
0.088	0.11	0.85	plunging
0.094	0.12	1.1	plunging

Table 3: Measured wave height at structure and maximum measured horizontal velocities (low mound tests).

For the low mound tests, d = 0.15 m; thus H_b = 0.12 m and Munk gives u_{max} = 1.6 ms^{-1}. Table 3 shows the values of H_b estimated from the

video record of the same wave event as for the measured kinematics, and the maximum measured horizontal velocity.

For the high mound tests, Oumeraci & Kortenhaus would use $H_b \approx 0.07$ m and $u_{max} \approx 1.25$ ms^{-1}. The measured results are shown in Table 4.

H_{si} (m)	H_b (m) from video	u_{max} (ms^{-1}) from PIV	breaker type
0.044	0.06	0.75	plunging
0.051	0.06	0.7	plunging
0.056	0.06	0.7	plunging
0.070	0.07	0.75	plunging
0.087	0.07	0.80	broken

Table 4: Measured wave height at structure and maximum measured horizontal velocities (high mound tests).

The results summarised in Tables 3 and 4 appear to indicate that the use of Munk will lead to a conservative design loading as the velocities measured are ~30% and ~40% less than predicted for low and high mound cases respectively. However, analysis of further PIV data is yet required as the measured maxima may depend to some extent upon the precise moment of the trigger for the flow record as the wave shape and therefore kinematics change rapidly immediately before impact. Nevertheless, the uniformity of the measured velocity maxima suggests that these values are indicative of the speed of approach of the water mass involved in the impact.

6. CONCLUSIONS

1. Wave loading measurements were made for a low mound and a high mound composite breakwater over a range of significant wave heights. For each case, a representative extreme loading case was identified. All cases in which wave impact loading was observed fell correctly within the *impact loading* region predicted by Calabrese (1998).

2. For each test condition, a representative extreme loading event was taken to be at the 0.4% exceedance level. The physical process of this event varied as expected (Oumeraci, 1993) from flip through to plunging breaker and then to broken wave as the wave steepness increased.

3. The repeatability of the form of the temporal and spatial pressure distributions measured for the extreme events was satisfactory. Although pressure maxima varied by up to 30%, the shape of the pressure v. time graphs was consistent at all elevations on the front face of the structure.

4. Particle Image Velocimetry was successfully applied to measure wave kinematics immediately prior to impact events in random sea tests. The velocities predicted by Munk (1949) for solitary waves are significantly greater than those observed in the random sea tests: measured velocity maxima were less than predicted by ~30% and ~40% for low and high mound tests respectively. The use of Munk's predictions in new design formulae (*eg* Oumeraci & Kortenhaus, 1997) may be conservative. A fuller sequence of velocity data up to impact is required to confirm this preliminary finding.

ACKNOWLEDGEMENTS

The authors gratefully acknowledge the financial support of the EC DG XII via the MAST III PROVERBS project (MAS3-CT95-0041) and the Italian Research Council (CNR). The input of Michael Walkden (University of Edinburgh) is also gratefully acknowledged.

REFERENCES

Allsop, N.W.H., Vicinanza, D. & McKenna, J.E. (1996a): "Forces on vertical breakwaters and related structures", *Report SR 443 - HR Wallingford*, March 1995, revised March 1996.

Allsop, N.W.H., Vicinanza, D., Calabrese, M. & Centurioni, L. (1996b), "Breaking wave impact loads on vertical faces", *Proc. 6th Int. Offshore and Polar Eng. Conf. (ISOPE'96)*, 3, pp185-191.

Calabrese, M. (1998). "Onset of breaking in front of vertical and composite breakwaters", *Proc.8th Int. Offshore and Polar Eng. Conf. (ISOPE'98)*.

Chan, E.S. (1994), "Mechanism of deep water plunging wave impacts on vertical structures", *Coastal Engineering, Special Issue on Vertical Breakwaters*, 22, pp.115-134, Elsevier Science BV, Amsterdam.

Gray, C. & Bruce, T. (1995), "The application of particle image velocimetry (PIV) to offshore engineering", *Proc. 5th Int. Offshore and Polar Eng. Conf. (ISOPE'95)*, 3, pp701-708.

Kirkgoz, M.S. (1991), "Impact pressure of breaking waves on vertical and sloping walls", *Ocean Engineering*, 18, 1, pp.45-49.

McConnell, K.J. & Kortenhaus, A. (1997), "Analysis of pressure measurements from hydraulic model tests and prototype measurements", *Proc. 1st overall project workshop, MAST III / PROVERBS*, Las Palmas, Annex C3.

Munk, W.H. (1949), "The solitary wave theory and its application to surf problems", *Annals of the New York Academy of Science*, pp.378-424.

Oumeraci ,H. & Kortenhaus, A. (1997), "Wave impact loading: tentative formulae and suggestions for the development of final formulae", Discussion note *to the 2nd Task 1 MAST III Workshop (PROVERBS)*, Edinburgh, July 1997.

Oumeraci, H., Kortenhaus, A. & Klammer, P. (1995a), "Displacement of caisson breakwaters induced by breaking wave impacts", *Proc. Conf. on Coastal Structures and Breakwaters '95*, Institution of Civil Engineers, London.

Oumeraci, H., Bruce, T., Klammer, P. & Easson, W.J. (1995b), "PIV measurements of breaking wave kinematics and impact loading of caisson breakwaters", *Proc. 4th Int. Conf. Coastal and Port Eng. in Developing Countries ("COPEDEC IV")*, 4, 3, pp2394-2410.

Oumeraci, H., Klammer, P. & Partenscky, H.W. (1993), "Classification of breaking wave loads on vertical structures", *Journal of Waterway, Port, Coastal and Ocean Eng.* (ASCE), 119, 4, pp. 381-397.

Skyner, D.J. (1996), "Comparison of numerical predictions and experimental measurements of the internal kinematics of a deep-water plunging wave", *J. Fluid Mechanics*, 315, pp.51-64.

Takahashi, S. Tanimoto, K. & Shimosako, K. (1994), "Dynamic response and sliding of breakwater caissons against impulsive breaking wave forces" *Proc. Workshop on Wave Barriers in Deep Waters*, Port and Harbour Research Institute, Yokosuka.

Vicinanza, D. (1997), "Pressioni e forze di impatto di onde frangenti su dighe a paramento verticale e composte", PhD. thesis, University of Naples.

Walkden, M.J.A., Hewson, P.J. & Bullock, G.N. (1996), "Wave impulse prediction for caisson design", *Proc. 25th Int. Conf. On Coastal Engineering, (ASCE)*, 3, pp2584-2597.

Walkden, M., Müller, G. & Bruce, T. (1998), "Low-cost particle image velocimetry: system and application", *Proc.8th Int. Offshore and Polar Eng. Conf. (ISOPE'98)*, Montreal.

FIGURES

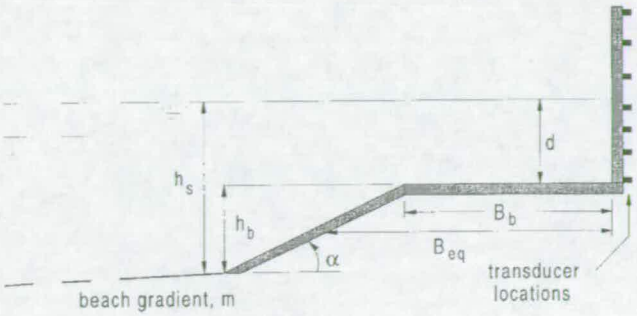

Figure 1: Parameter definition sketch. Also shown are the locations of the pressure transducers for the tests reported.

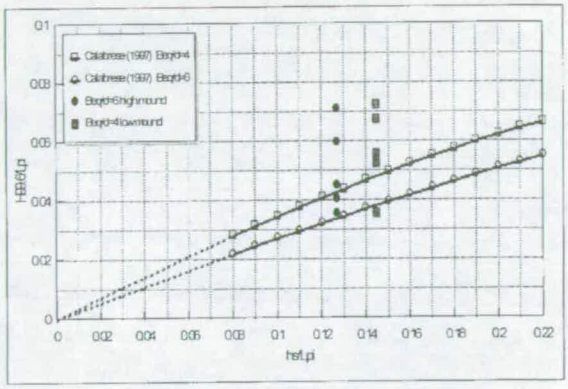

Figure 2: Observed loading types compared to the breaking prediction of Calabrese (1998).

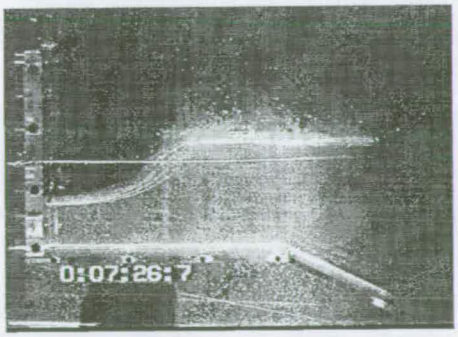

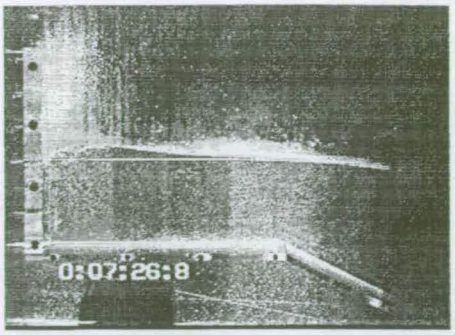

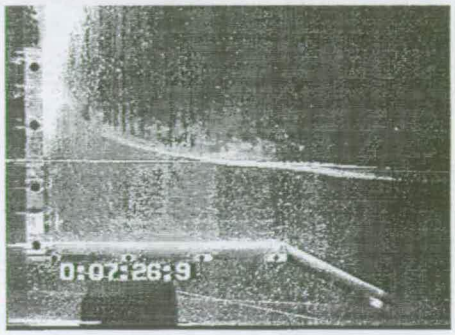

Figure 3: Sequence of video frames showing a flip-through event.

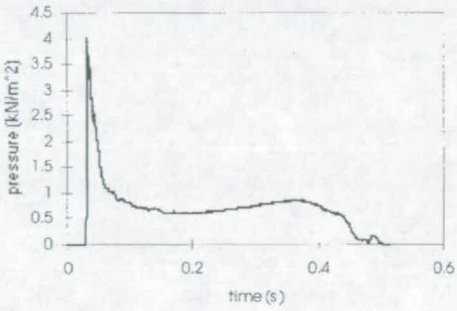

Figure 4: A characteristic pressure history for a flip-through event for the transducer closest to still water level.

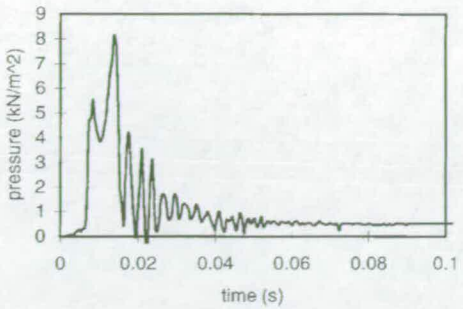

Figure 5: A characteristic pressure history for a plunging event for the transducer closest to still water level.

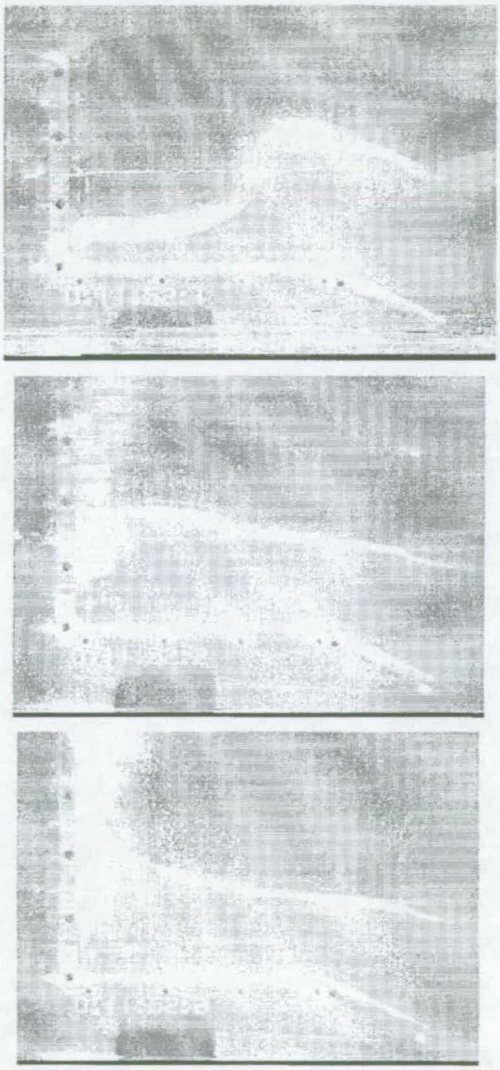

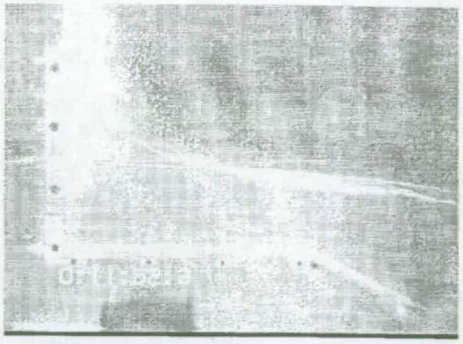

Figure 6: Sequence of video frames showing a plunging event.

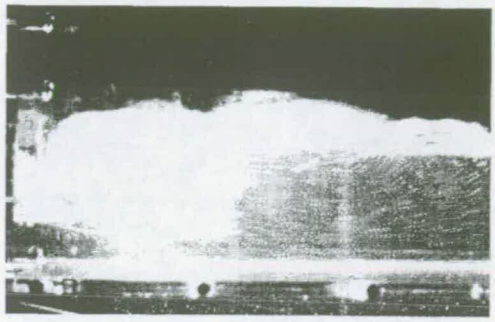

Figure 7: PIV flow record for a broken wave event.

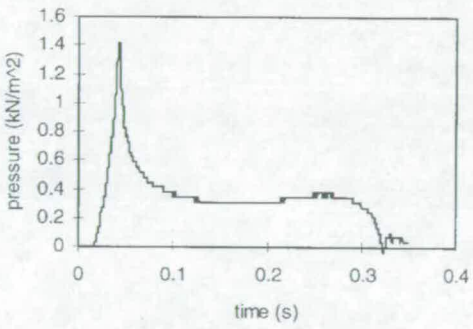

Figure 8: A characteristic pressure history for a broken wave event for the transducer closest to still water level.

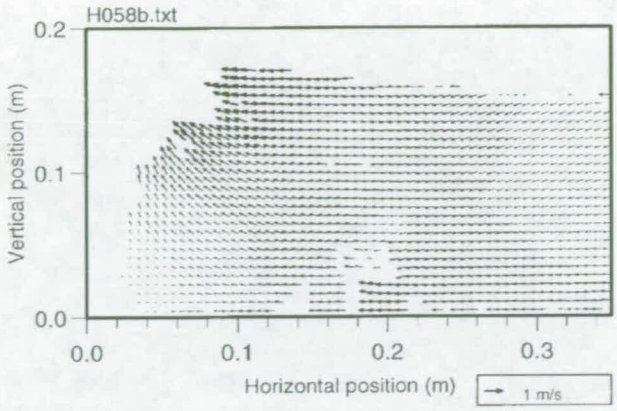

Figure 9: PIV velocity map for a flip-through event

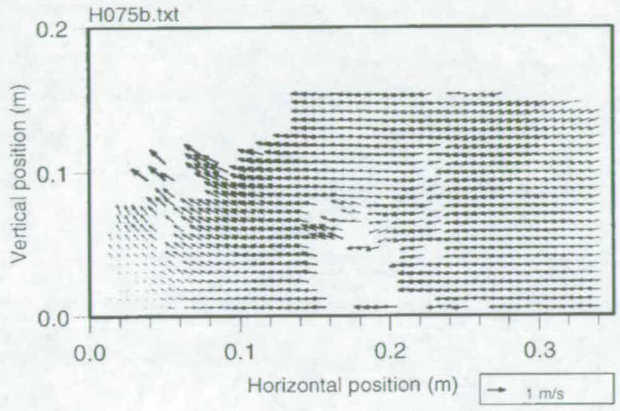

Figure 10: PIV velocity map for a plunging event.

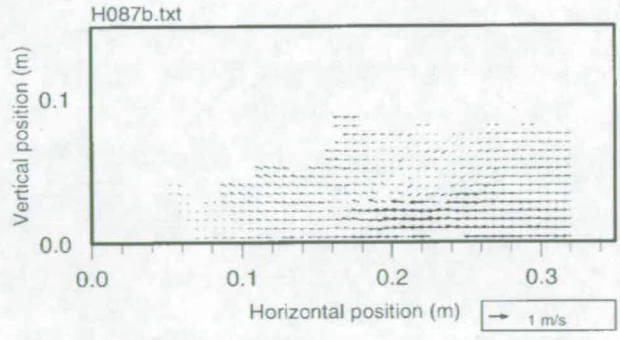

Figure 11: PIV velocity map for a broken wave event.

93-WSC-04 BRUCE 7 of 7

Appendix C: Wood *et al.*, 2000

Wood, D.J., Peregrine, D.H. & Bruce. T. (2000), *Wave impact on a wall using pressure-impulse theory. I : Trapped air*, J. Waterway, Port, Coastal and Offshore Eng. 126, 4, pp182–190 (ASCE)

Appendix C
Wood *et al.*, 2000

Wood, D.J., Peregrine, D.H. & Bruce. T. (2000), *Wave impact on a wall using pressure-impulse theory. I : Trapped air*, J. Waterway, Port, Coastal and Offshore Eng. 126, 4, pp182–190 (ASCE)

C.1 Declaration of contribution

The author's principal contribution was to cover the physical model side of the comparison. This involved identification and abstraction of appropriate PIV kinematic data from the tests at Edinburgh (Oumeraci *et al.*, 1995), and subsequent liaison with the analytical modellers (principally with Wood) to ensure genuine comparability. The author wrote the sections on the physical model part of the study and was involved in subsequent editing and later revision of the paper.

C.2 Published paper

overleaf

WAVE IMPACT ON A WALL USING PRESSURE-IMPULSE THEORY. I: TRAPPED AIR

By Deborah J. Wood,[1] D. Howell Peregrine,[2] and Tom Bruce[3]

ABSTRACT: Often when a plunging breaker impacts on a wall, an air pocket is trapped at the wall. This paper extends a pressure-impulse model for wave impact on a wall to include a simple model of a trapped air pocket. The inclusion of an air pocket leads to a higher impulse at impact for a given wave as there is some rebound of the water. The model is shown to compare satisfactorily with small-scale experimental data performed on a caisson breakwater with an impermeable berm. The effect of a porous berm on pressure impulse is investigated theoretically in a companion paper.

INTRODUCTION

Waves interacting with a near-vertical structure can be roughly grouped into three types: standing waves, broken waves, and waves in the process of breaking. The first two produce smoothly varying loads, whereas the latter often produces impulsive loads on a structure. Fig. 1 is a pressure-time plot for such an impulsive wave from tests conducted at the University of Edinburgh in 1994 (described later in the fourth section). This particular plot illustrates a large air pocket becoming trapped at the wall, and it is from a pressure-transducer close to the foot of the vertical wall (see the fourth section for more details of the experiments). We can see that the curve has two peaks: a high peak of short duration (impact pressure) followed by a more slowly varying peak (reflective pressure). It is the impact pressure that is the topic of this paper. Furthermore, smaller oscillations may sometimes be present due to trapped air. In addition, a second high peak in pressure close to the first may occur (Schmidt et al. 1992), but this seems to happen rarely and only near still water level. The high impulsive pressure peak, though too short in duration to disturb large monolithic caisson structures, may be significant in damage to smaller elements such as crown walls or blocks within blockwork seawalls or breakwaters. However, prediction of the magnitude of this peak is difficult as, even with nominally identical waves impacting on a structure, the variance in the peak pressure can be quite large. However, Bagnold (1939) noted that the pressure impulse, given by the integral of pressure over the duration of the impact, is a much more reproducible quantity.

In experiments of waves impacting on a vertical wall, the effect of dispersed bubbles or trapped air is important. If a wave is breaking, or near breaking, when it hits a wall, a large amount of air often becomes trapped. The air can be present in one of two forms: as a trapped bubble or as dispersed air (aeration of the water), or most likely as a combination of both. In particular, Topliss (1994) looked at a theoretical model of a trapped air pocket. In that study the trapped air was taken to be an oscillating circular air bubble. The oscillations of the radius of the bubble were taken to be small, and hence an equation for the complex potential of the flow could be calculated. Topliss (1994) also developed a model for the bubbly mixture in the fluid that a plunging wave leaves behind after it has impacted on a structure. Peregrine (1994) gave a review of some of the methods used to model air entrainment trapping during impact. Peregrine and Thais (1996) modeled scaling for entrained air in violent water wave impacts by using a "filling flow" model (where a region is rapidly filled with liquid), following the study of Peregrine and Kalliadasis (1996). This model has many similarities to the "flip through" impact flow. Peregrine and Thais (1996) gave an estimate of the reduction in pressure caused by the presence of dispersed air in a related problem.

When a plunging breaker impacts on a vertical wall and an air pocket is trapped, the bubble first contracts in size under pressure from the oncoming water and then expands. Hence, at the surface of the bubble during impact, the velocity of the body of water reverses direction. This is as if the bubble causes water to "bounce" back. Cooker and Peregrine (1990, 1992, 1995) used pressure impulse to develop a model for the pressure impulse caused by more direct wave impact on a vertical wall, effectively assuming an inelastic impact on the wall. In particular, their model is used for the cases of flip through impact, where just before impact the wave face is nearly parallel to the wall. Chan (1994) and Losada et al. (1995) showed good agreement of this model with experiments for wave impact on a wall. We extend the pressure-impulse model to allow for a "bounce back" effect due to trapped air. In addition, we make a comparison with experiments carried out at the University of Edinburgh in 1994 and 1997 (Oumeraci et

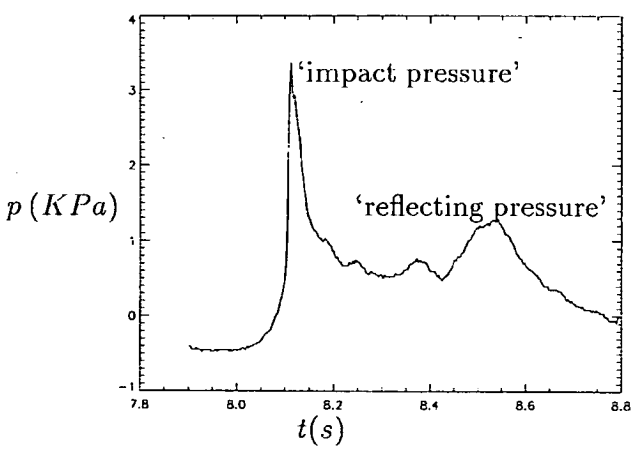

FIG. 1. Typical Pressure-Time Curve for Impact on Wall [Edinburgh 1994 Data; Large Air Bubble; Transducer Close to Foot of Vertical Wall (See Fig. 7)]

[1]Dept. of Mathematics, Univ. of Oslo, Mech. Div., P.O. Box 1053, Blindern, N-0316 Oslo, Norway; formerly, Res. Asst., School of Mathematics, Univ. of Bristol, University Walk, Bristol BS8 1TW, U.K. E-mail: deborah@math.uio.no

[2]Prof. of Appl. Mathematics, School of Mathematics, Univ. of Bristol, University Walk, Bristol BS8 1TW, U.K. E-mail: D.H.Peregrine@bristol.ac.uk

[3]Lect., School of Mech. Engrg., Univ. of Edinburgh, Sanderson Build., King's Build., Edinburgh EH9 3JL, U.K. E-mail: Tom.Bruce@ed.ac.uk

Note. Discussion open until January 1, 2001. Separate discussions should be submitted for the individual papers in this symposium. To extend the closing date one month, a written request must be filed with the ASCE Manager of Journals. The manuscript for this paper was submitted for review and possible publication on February 2, 1999. This paper is part of the *Journal of Waterway, Port, Coastal, and Ocean Engineering*, Vol. 126, No. 4, July/August, 2000. ©ASCE, ISSN 0733-950X/00/0004-0182–0190/$8.00 + $.50 per page. Paper No. 20188.

al. 1995, 1997; Bruce and Vicinanza 1998), which gave particle image velocimetry (PIV) and video and pressure data. The theoretical model is used to predict pressure impulse, from the impact part of the pressure, down the wall and along the berm. The procedure for a comparison with the experimental data is not entirely straightforward, because for these waves the impact pressure does not have as short a duration and as high a magnitude as strictly theoretically required by the model (see the fourth section). Nevertheless, the comparison with the experiment is satisfactory.

Little research has been done to model the effect of impact with a trapped air bubble, with the exceptions of Bagnold (1939), Mitsuyasu (1966), Ramkema (1978), Oumeraci and Partenscky (1991), and Topliss (1994). The model in this paper, though very crude, goes some way to predict the pressure-impulse distribution, usually to within 40%, both up the wall and along the bed in front of the wall.

The effect of a porous berm on pressure impulse is investigated theoretically in a companion paper (Wood and Peregrine 2000).

PRESSURE IMPULSE

Pressure impulse is defined as

$$P^D = \int_{t_b}^{t_a} p \, dt \tag{1}$$

where p = pressure measured relative to atmospheric pressure; and t_b and t_a = times before and after impact, respectively (Batchelor 1967; Lamb 1995). We begin by considering the dimensional pressure impulse P^D, but will later change to nondimensional pressure impulse P. A brief outline of the Cooker and Peregrine modeling approach is given below.

Let $\mathbf{u}(x^D, y^D, t)$ be the velocity of the liquid (x^D and y^D are dimensional coordinates, where D is used to distinguish from the nondimensional units used later), and $t_a - t_b = \Delta t$. We assume that the liquid is inviscid, and the motion is 2D. Let the wave have a velocity scale U, and a length scale H, with ρ the density of the fluid. We follow Cooker and Peregrine (1990, 1992, 1995) and assume that the impact occurs over such a short period of time that gravity and the nonlinear terms involving a spatial derivative of $\mathbf{u}$ [whose ratio with $\partial\mathbf{u}/\partial t$ is $O(U\Delta t/H)$] can be neglected if $\Delta t << H/U$, as they are small compared to the pressure gradient and $\partial\mathbf{u}/\partial t$. The equation of motion is then approximated by

$$\frac{\partial \mathbf{u}}{\partial t} = -\frac{1}{\rho}\nabla p \tag{2}$$

Integration with respect to time over the duration of the impact gives

$$\mathbf{u}_a - \mathbf{u}_b = -\frac{1}{\rho}\nabla P^D \tag{3}$$

where $\mathbf{u}_a$ and $\mathbf{u}_b$ = velocity fields just after and just before impact, respectively. Now we assume the water is incompressible, and so we have $\nabla\cdot\mathbf{u}_a = \nabla\cdot\mathbf{u}_b = 0$. Therefore, the pressure impulse $P^D(x, y, t)$ satisfies

$$\nabla^2 P^D = 0 \tag{4}$$

in the fluid domain, subject to appropriate boundary conditions.

We use the component of (3) in the direction $\mathbf{n}$ normal to the solid boundaries (with direction out of the fluid) to derive the boundary conditions. We assume flow into the solid boundaries is zero so $\mathbf{n}\cdot\mathbf{u}_a = 0$. Where no impact occurs, along part of the wall and on the bed, $\mathbf{n}\cdot\mathbf{u}_b$ is also zero; thus the boundary condition is (Fig. 2)

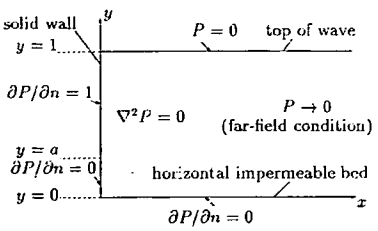

FIG. 2. Dimensionless Boundary Conditions on Pressure Impulse for Impact on Wall with No Bounce Back (Cooker and Peregrine 1990, 1992, 1995)

$$\partial P^D/\partial n = 0 \tag{5}$$

At the solid boundary where impact occurs, the horizontal velocity goes to zero on impact and so from (3)

$$\partial P^D/\partial n = \rho U \tag{6}$$

where U = velocity of water impact and is a function of position along the part of the wall on which impact occurs. However, because we have little information on its variation we take it to be a constant for simplicity. The velocity of the wave is directed toward the wall, and we choose U as our velocity unit, so that the boundary condition (in nondimensional units) becomes (Fig. 2)

$$\partial P/\partial n = 1 \tag{7}$$

Along the upper free surface the pressure is atmospheric, and because atmospheric pressure is used as the reference pressure (Fig. 2)

$$P = 0 \tag{8}$$

The appropriate far-field condition at large distances away from the impact region is $P \to 0$. Hence, to find the pressure impulse for an impact problem, we must solve Laplace's equation [(4)] subject to these boundary conditions.

As a starting point, and for comparison, we give the Cooker and Peregrine (1990) example shown here in Fig. 2 in terms of nondimensional units. The free surface is taken to be horizontal ($y = 1$); that is, the wave is of great length, height, $(1 - a)$, and rectangular shape. Here a is the nondimensional height of the bottom of the bubble (the corresponding dimensional value given by a^D). Cooker and Peregrine (1995) showed that the pressure impulse is little affected by the shape of the wave away from the impact region. In addition, this problem is linear so that any pressure-impulse contour can be taken to be an alternative free surface at a later stage, by subtracting the constant value of P along that contour. This can give more realistic wave profiles. We have taken the length scale H to be the height of the wave at the wall at impact, and the velocity scale U to be the velocity of the water that hits the wall, so P^D may be nondimensionalized by ρUH and x^D and y^D by H (dimensional values of x and y are given by x^D and y^D, respectively). Impact is on the left-hand wall between $y = a$ and $y = 1$. Laplace's equation [(4)] is solved using separation of variables to get a Fourier series solution

$$P = \sum_m A_m e^{-\alpha_m x}\cos(\alpha_m y) \tag{9}$$

where

$$A_m = \frac{2}{\left(m + \frac{1}{2}\right)^2 \pi^2}\left[(-1)^m - \sin(\alpha_m a)\right] \tag{10}$$

and $\alpha_m = [m + (1/2)]\pi$. In this and the following sums, m is summed from 0 to ∞. In practice, the series must be truncated,

and for this study summing m from 0 to 100 was found to be sufficient.

THEORY FOR WAVE BOUNCE BACK

We consider first a large air bubble trapped at the wall, which produces oscillatory pressures. Later we examine cases where the air bubble is not so well defined. The impulse over the first oscillation instead of just bringing the water to rest may bounce the water backward, and so the velocity of the part of the impacting water may reverse in sign. Cooker and Peregrine (1990) introduced the pressure-impulse model for the flip through conditions that corresponds to water motion normal to the wall ceasing on impact. If the compressed air pocket causes the water to be pushed back, then boundary conditions corresponding to a reversal of the normal component of velocity may be more appropriate. Hence the boundary conditions for a wave with a trapped air bubble that bounces back are the same as for the Cooker and Peregrine example, except at the position on the vertical wall where the bubble is present.

We make a considerable simplification here by neglecting the shape of the bubble, and some aspects of the pressure changes within the bubble. Although the shape of a bubble trapped at the wall by impact of a plunging breaker may be roughly that of a half-circular cylinder (Oumeraci and Partenscky 1991) and we use one aspect of that shape below, we simplify the region in which we solve Laplace's equation [(4)] by taking the bubble to have zero thickness (i.e., the boundary condition at the bubble is imposed on the vertical wall and not on the actual bubble surface), thus leaving the domain of solution as the simple rectangular shape for which Fourier series provide an easy solution method. We feel a more complex solution is not justified by the available data and the large variation of impact properties that occurs even in regular experimental waves. As may be seen below, most other aspects of the bubble's influence on the impact pressures are ignored.

When the bubble pushes back the water that is behind it, we assume that the velocity is normal to the semicircular profile of a bubble with the same magnitude as the incoming velocity. Hence, a reasonable assumption for the horizontal component of the nondimensional velocity after impact is a cosine distribution. Let a and b be the nondimensional position of the bottom and top of the air bubble, respectively (the corresponding dimensional values given by a^D and b^D). From (3), the boundary condition on the middle section of the left-hand wall ($a < y < b$), representing the bubble (Fig. 3), is then

$$\frac{\partial P}{\partial n} = 1 + \cos(C(y - D)) \tag{11}$$

with $C = \pi/(b - a)$ and $D = (b + a)/2$. Fig. 3 shows a summary of the boundary conditions. More complicated distributions of $(\mathbf{u}_a - \mathbf{u}_b)\cdot\mathbf{n}$ are not really justified as detailed velocity profiles of the wave are not available at impact. The simpler constant value was also investigated but gave less good results.

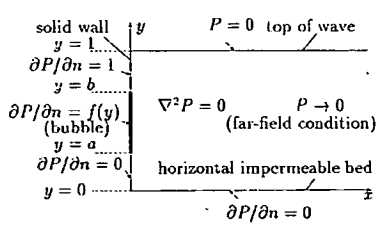

FIG. 3. Dimensionless Boundary Conditions on Pressure Impulse Required for Wave Impact with Bounce Back (Vertical Section), Where $f(y) = 1 + \cos(C(y - D))$ with $C = \pi/(b - a)$ and $D = (b + a)/2$

The Fourier series solution is

$$P = \sum_m A_m e^{-\alpha_m x} \cos(\alpha_m y) \tag{12}$$

where $\alpha_m = [m + (1/2)]\pi$ and

$$A_m = \frac{1}{\alpha_m}\left[\frac{\sin(C(b - D) + \alpha_m b)}{\alpha_m + C} + \frac{\sin(C(b - D) - \alpha_m b)}{C - \alpha_m}\right] - \frac{1}{\alpha_m}\left[\frac{\sin(C(a - D) + \alpha_m a)}{\alpha_m + C} + \frac{\sin(C(a - D) - \alpha_m a)}{C - \alpha_m}\right] + \frac{2}{\alpha_m^2}[\sin(\alpha_m) - \sin(\alpha_m a)] \tag{13}$$

We note that to get back to dimensional pressure impulse we simply multiply (12) by ρUH and y and x by H.

Figs. 4 and 5 show the pressure-impulse contours for no bounce back and bounce back, respectively. The thick line at the wall shows the position of the middle bounce-back region. Clearly, a much bigger impulse arises from bounce back. If we examine Fig. 6, which is a plot for pressure impulse down the wall, we can see that the peak P is about 1.5 times as big for the bounce back situation as for the no bounce back case.

Pressure-impulse contours give a fair approximation to maximum pressure contours if a good estimate of impact duration is available. However, in the case of bounce back, the timescale is dependent on the compression of the air and hence is longer. Because bounce back gives a longer duration, the estimated maximum pressures are generally smaller. However, if the duration is too long (i.e., $\Delta t > H/U$), the pressure-impulse approximation becomes inappropriate.

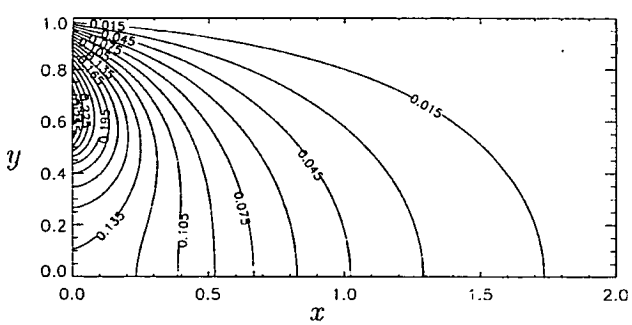

FIG. 4. Nondimensional Pressure-Impulse P Contours without Bounce Back ($a = 0.5$)

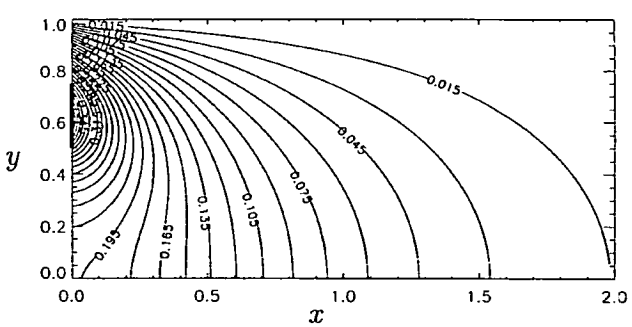

FIG. 5. Nondimensional Pressure-Impulse P Contours with Bounce Back; Bubble Position Is Shown by Dark Line ($a = 0.5$; $b = 0.75$)

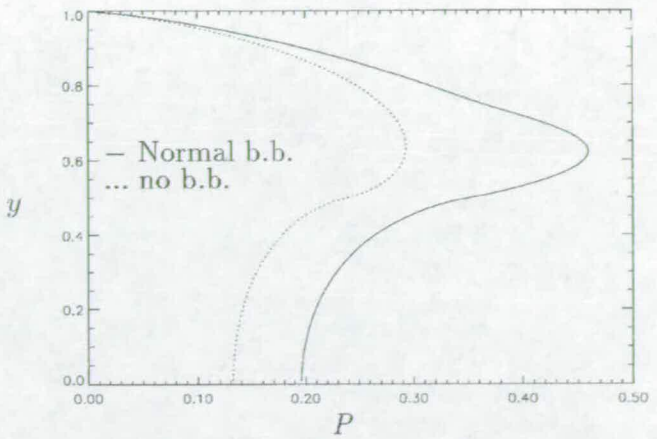

FIG. 6. Vertical Distribution of Nondimensional Pressure Impulse P at Wall ($a = 0.5$, $b = 0.75$) (b.b. Denotes Bounce Back)

COMPARISON WITH EDINBURGH EXPERIMENTS

One of the major problems with comparing experimental data with theoretical models is that often the information required for the theoretical model is difficult to measure experimentally. In these theoretical models we need not only an estimate of the breaking height of the wave at the wall, and position of the air pocket at impact, but also a measure of velocity at impact. Most experiments concentrate on the measurement of pressures, but no measurements of velocity are made. However, it is sometimes possible to make estimates of the velocity of the wave if high speed video is available. Another problem is that the definition of pressure impulse is not straightforward. We must make a choice of interval of integration and which pressures we class as impulsive pressures. This is discussed in detail later.

A relatively new method of experimentally obtaining a velocity profile for an impact is PIV. Oumeraci et al. (1995, 1997) describe PIV measurements made at the University of Edinburgh in 1994. The measurements in these papers together with further data and an analysis program (A. Kortenhaus, private communication, 1997) are used in this section to compare the bounce back and no bounce back models with experimental data. Both of these tests and the ones described in the fifth section used the same model structure—a vertical-walled composite breakwater (shown in Fig. 7). The difference in the test runs was the difference in water level. In the 1994 tests, the depth of water above the berm was 0.13 m (classed as a low mound), whereas in the 1997 tests the depths of water over the berm were 0.090 and 0.150 m representing composite structures with "low" and "high" mounds, respectively.

PIV is capable of measuring an instantaneous 2D velocity field. The method involves the introduction of tiny seeding tracer particles into the flow and the stroboscopic illumination of a 2D plane through the flow. The flow is photographed, with the camera shutter speed held open long enough to record at least two illuminations of the particles. The resulting flow record then can be divided into a grid of small cells, and the flow velocity in each cell can be determined from the distance moved by the tracer particles in the interval between pulses of illumination. Details of this method can be found in, for example, Gray and Bruce (1995).

We examine first the data from a test where an impacting plunging breaker is well developed and traps a large pocket of air and an air-water mixture. Fig. 8 shows such a wave. Note that the berm and positioning of the pressure transducers (numbered 1–12) can also be seen in the picture. From a plot of horizontal force against time, as in Fig. 9, we make a choice of the period of integration for the calculation of the pressure impulse. We notice that there is not only a high impulsive peak in the curve, but in addition a much broader and lower peak (hump) some time after. This hump is caused by the water being accelerated to slow down at the wall as it falls back. In a similar manner, if the wave had not impacted, then where the high impulsive force is present there would have been a similar broad peak when water accelerated up the wall. These pressures, which occur in ordinary wave reflection, are primarily due to water motions influenced by gravity. However, we do not want to include these pressures of wave reflection in our evaluation of pressure impulse because this theory neglects gravity for the short duration of the impact. For more violent impacts, this process would not be necessary. We can justify pressure-impulse calculations only if both $u_t >> uu_{x0}$ and $u_t >> g$, where u is the dimensional velocity. That is the ratio of the nonlinear term to the $\partial u/\partial t$ term, $[O(\Delta t U/H)]$, is

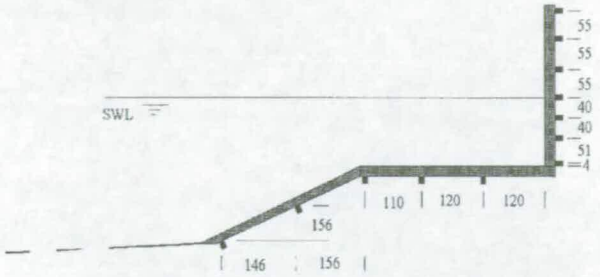

FIG. 7. Model Test Setup Showing Position of Transducers (in mm)

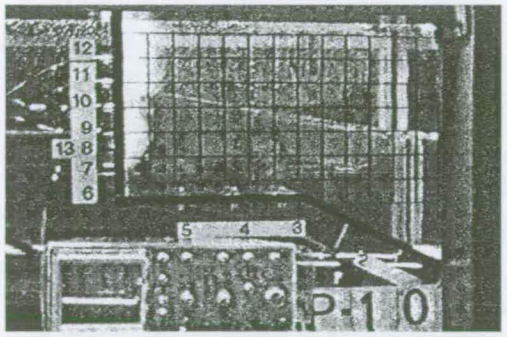

FIG. 8. Video Frame of Wave Used in Edinburgh 1994 Tests, after Trapping Large Air Bubble (Test No. P10) Approximately 0.12 s (Three Video Frames) after Initial Impact

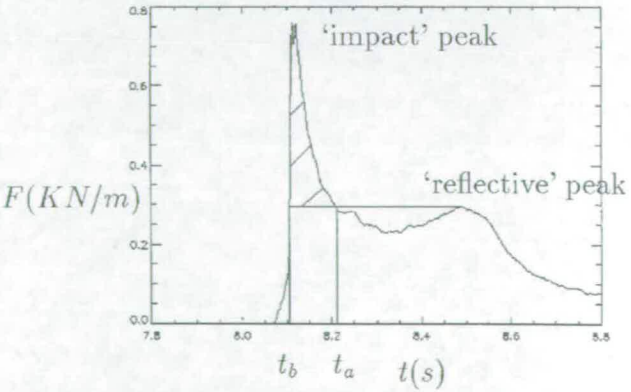

FIG. 9. Horizontal Force F on Wall for Impact of Plunging Breaker Trapping Large Air Pocket from Edinburgh Data; from Figure B-5 of Oumeraci et al. (1997), Plotted Using Analysis Program (A. Kortenhaus, Private Communication, 1997); Shaded Area Is Impulsive Force

small, and accelerations are much greater than gravity. We require $\Delta t << H/U$. In this particular experiment we have a horizontal velocity U of 1.3 m/s (see later), and a length (height of the water at the wall at impact H) of 0.22 m; hence the timescale must be much <0.17 s. For this particular case, Δt = 0.105 s (see later). This duration is about as large as it can be for our assumptions to apply, and so we need to determine carefully which part of the pressure is the "impulsive pressure." Accelerations are clearly >10g.

An almost exact removal of these reflective pressures would be to reflect the secondary hump about the local minimum between the high peak and the secondary hump and then to subtract it to remove the reflective pressures from the pressure impulse. However, this is an unrealistic process for analysis of a lot of data. Walkden et al. (1997) suggested that the removal of reflective pressures could be approximated by the removal of a triangular portion of the area under the pressure-time graph. A similar approach is one in which a triangle or trapezoidal shape of area $(t_a - t_b)(p_a + p_b)/2$, where p_a and p_b are the pressure at time t_a and t_b, respectively, is removed. However, this approach was found to be unsatisfactory for these comparisons as it leads to an underestimate of the pressure impulse when compared with the exact removal suggested above. Instead, we see that in our example the second maximum is at t = 8.490 s; we draw a horizontal line through this and choose our period of integration to be between the two places where the horizontal line cuts the force-time curve at t = 8.105 and 8.210 s (Fig. 9). When we examine the individual pressure-time series we take the pressure at t = 8.210 s as our base pressure and remove a rectangle of height equal to this base pressure and width equal to the period of integration. The shaded area shows the "impulsive" force. In a similar manner we calculate the impulsive pressure, keeping t_a and t_b (chosen from the force-time graph) to be the same for all curves. Thus, the impulsive pressure is the integration of pressure between t_b and t_a, with the rectangle $(t_a - t_b)p_a$ subtracted, where p_a is the pressure at t_a. This is approximately equivalent to subtracting the reflective pressures. We calculate the experimental pressure impulse using a trapezoidal method of integration over the data points that are sampled at 400 Hz.

Although the method based on Walkden et al. (1997) was found to work satisfactorily for the large air bubble case, for impacts where the air bubble is not so well defined and the impact not so great, the removal of the triangular/trapezoidal shape led to underestimates of the pressure impulse. One reason for this is that the individual pressure profiles normally rise more steeply than their triangle slope (predicted by the force graph) at the start of the pressure-time profile, so that the triangle/trapezoid subtracts pressures that simply did not exist in the first place.

We must make an estimate of the wave height at the structure and the position of the bubble at impact. Estimates from the PIV measurements are not feasible as PIV images are not taken close enough to the time of impact due to air entrainment. The video of the tests shows a cathode ray oscilloscope and a pressure trace on the oscilloscope, from which we determine that the initial violent impact has occurred by the third video frame after the frame where we consider the impact to begin. The video was taken at 25 Hz; thus this is approximately 0.12 s after the initial impact, which is in agreement with our impact duration from the force-time graph (Figs. 8 and 9). At this point we measure h = 0.22 m, a^D = 0.08 m, and b^D = 0.17 m (Table 1). When the wave is in the early stages of impact, the water depth at the wall increases. The choice of period of integration (0.105 s) implies that we should take account of the pressures caused by this. If we had taken the water depth and position of the trapped air pocket from a profile earlier in the event, the theoretical model would predict zero impulse above the earlier, lower water level, which would clearly be in error.

We also need an estimate of the horizontal velocity of the wave. Using Figs. 6 and 7 from Oumeraci et al. (1995), which use the PIV data, we see that the ratio of wave height to water depth at the wall for the underside of the jet from the plunging breaker is approximately 1.4. Here the horizontal velocity does not change much in time and hence, even though the PIV is not taken at impact, we can still estimate the velocity as 1.3 m/s. A similar value for velocity is obtained from the video record, although with a larger error bound than the PIV data. Feeding these into the bounce back and no bounce back models, we obtain the plots of pressure impulse on the wall shown in Fig. 10.

The distribution prediction is far from perfect, but adequate (within 20%). The pressures on the berm in front of the wall were also measured and are reasonably predicted using this model, as shown in Fig. 11. Note that the experimental values for the two transducers farthest away from the wall give a higher value than the predicted pressure impulse. In addition, the measurements for these two transducers would not lie on an extrapolated line through the other pressure transducer measurements (Fig. 11). These two transducers were on the sloping part of the berm farthest from the wall, where the impulsive pressure is significantly smaller than other pressure components, and so it is not surprising the model prediction is less accurate at these points.

Next, we make a similar comparison for a wave from the same set of experiments, but this time with a small (thinner) trapped air pocket. Fig. 12 shows the wave profile. For this wave h = 0.28 m, a^D = 0.16 m, b^D = 0.28 m, U = 1.35 m/s^{-1}, t_b = 6.975 s, and t_b = 7.068 s (Table 1). We note that Δt is

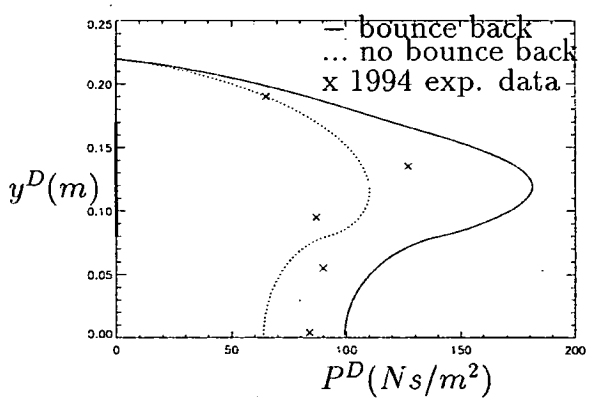

FIG. 10. Pressure Impulse on Wall for Impact of Plunging Breaker Trapping Large Air Pocket; No Bounce Back Uses Eqs. (9) and (10) and Bounce Back Uses Eqs. (12) and (13); Dark Line Shows Position of Bubble

TABLE 1. Values of Variables from Edinburgh 1994 Tests for Use in Theoretical Model

Thickness of bubble (1)	Mound (2)	U (m/s) (3)	a^D (m) (4)	b^D (m) (5)	h (m) (6)	t_b (s) (7)	t_a (s) (8)	Δt (s) (9)
Small	Low	1.30	0.08	0.17	0.22	8.105	8.210	0.105
Large	Low	1.35	0.16	0.28	0.28	6.975	7.068	0.093

only slightly smaller than when the large air bubble is present. Figs. 13 and 14 show the pressure-impulse plots along the wall and berm, respectively.

We note that for this impact the wave profile is very steep close to the wall. Our assumption that the free surface approximates a horizontal line becomes questionable. Instead we could choose another contour of pressure impulse that better approximates the free surface. We would then need to subtract the value of that constant from our predicted pressure impulse showing that, for this wave, the theory overpredicts.

In addition, air leakage, which is not modeled in this theory, will cause the effect of bounce back to be reduced. This can be seen clearly happening in Fig. 8 and may account for some of the overestimate of the bounce back model.

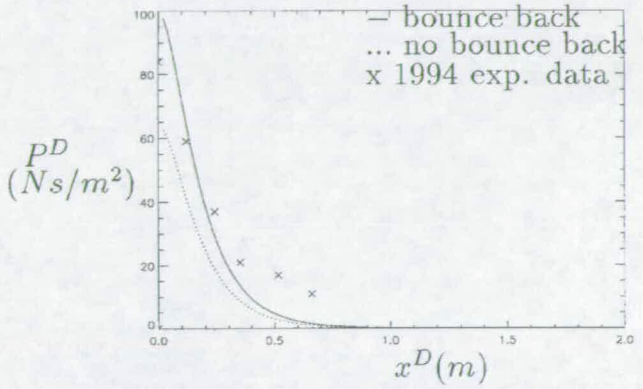

FIG. 11. Pressure Impulse along Berm for Impact of Plunging Breaker Trapping Large Air Pocket; No Bounce Back Uses Eqs. (9) and (10) and Bounce Back Uses Eqs. (12) and (13)

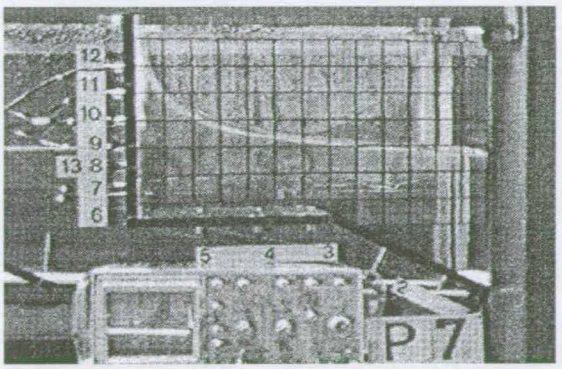

FIG. 12. Profile of Wave Used in Edinburgh 1994 Tests after Trapping Small (Thin) Air Bubble (Test No. P7) Approximately 0.12 s (Three Video Frames) after Initial Impact

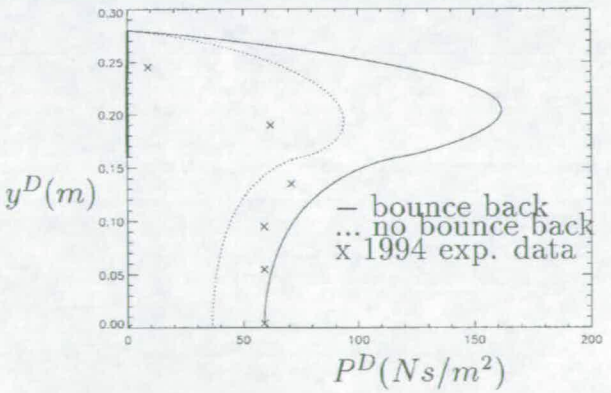

FIG. 13. Pressure Impulse on Wall for Impact of Plunging Breaker Trapping Small (Thin) Air Pocket; No Bounce Back Uses Eqs. (9) and (10) and Bounce Back Uses Eqs. (12) and (13); Dark Line Shows Position of Bubble

FURTHER EXPERIMENTAL DATA

A second series of tests were run at the University of Edinburgh over the summer 1997. Bruce and Vicinanza (1998) described these tests and included estimates of a maximum value of velocity that we have used for our velocity in the

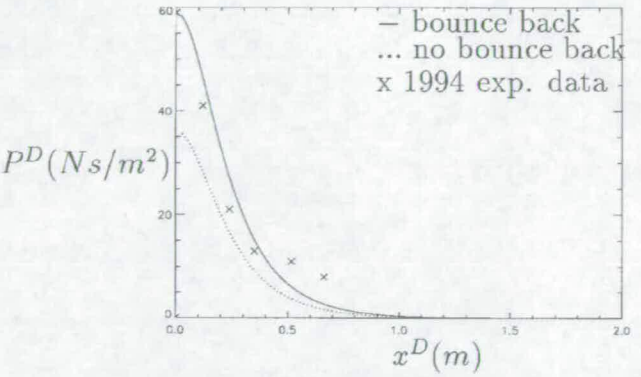

FIG. 14. Pressure Impulse along Berm for Impact of Plunging Breaker Trapping Small (Thin) Air Pocket; No Bounce Back Uses Eqs. (9) and (10) and Bounce Back Uses Eqs. (12) and (13)

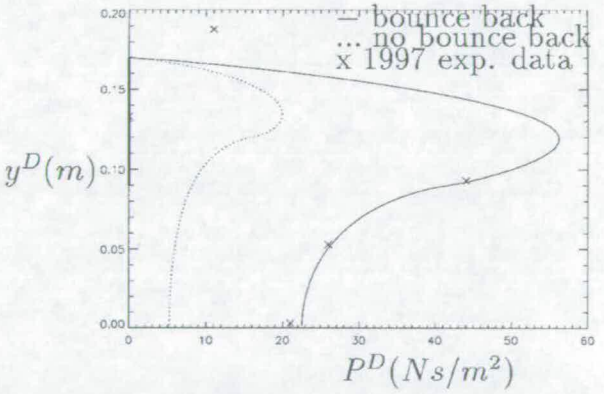

FIG. 15. Pressure Impulse up the Wall for Test H056 of Edinburgh 1997 Tests; No Bounce Back Uses Eqs. (9) and (10) and Bounce Back Uses Eqs. (12) and (13); Dark Line Shows Position of Bubble

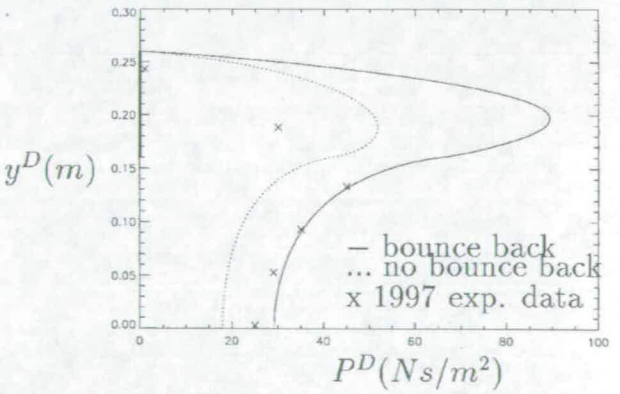

FIG. 16. Pressure Impulse up the Wall for Test H058 of Edinburgh 1997 Tests; No Bounce Back Uses Eqs. (9) and (10) and Bounce Back Uses Eqs. (12) and (13); Dark Line Shows Position of Bubble

model. These estimates were taken from the wave a short time before impact. However, Bruce and Vicinanza (1998) concluded that, although more investigation is needed, the maximum velocities measured are reasonable approximations of the speed of water at impact.

Wave profile measurements were again taken at three video frames after the beginning of the impact frame. In these tests the air appears to be present in an air/liquid layer all the way to the free surface. A clearly defined air pocket is not present even though it is not possible to see all the way through the air bubbles near the sidewall. However, the model predictions are still quite good. Figs. 15–20 show pressure impulse comparisons for tests H056, H058, H068, H075, H088, and H094, whose parameters are given in Table 2. The pressure data were sampled at a frequency of 1,984 Hz. For the cases where the air pocket is less than half the height of water at impact, the agreement is reasonably good with the bounce back method and slightly less so with the no bounce back example. However, H075 has an air bubble that is just over half the depth of water, and the agreement is better without bounce back than with bounce back. H094 has an air pocket that goes almost all the way down the depth of water, and from the video we see a large amount of entrained air, rather than a well defined air pocket. For this test there is no agreement between experimental and theoretical predictions as there appears to be no impulsive pressure. Breaking of the wave is the most developed in H094; thus the air pocket is the most fragmented, and cushioning by air leakage is more likely.

For our assumptions about the violence of the impact to hold, we require $\Delta t << H/U$. For the 1997 data $U\Delta t/H$ for all tests is between 0.14 and 0.4. Therefore, comparisons are close to the limits within which we should use this theory. We expect better agreement with more violent examples.

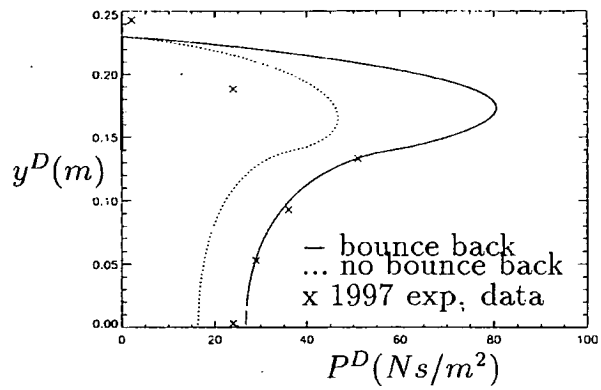

FIG. 17. Pressure Impulse up the Wall for Test H068 of Edinburgh 1997 Tests; No Bounce Back Uses Eqs. (9) and (10) and Bounce Back Uses Eqs. (12) and (13); Dark Line Shows Position of Bubble

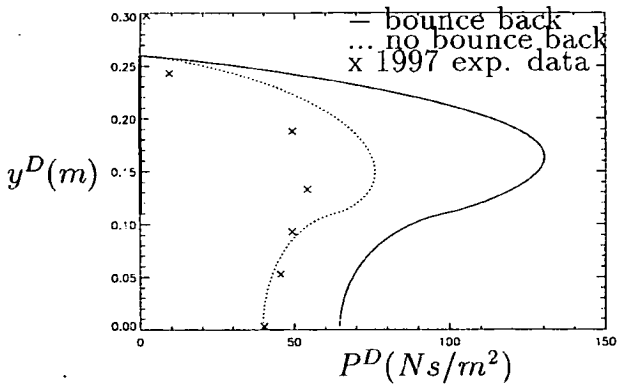

FIG. 18. Pressure Impulse up the Wall for Test H075 of Edinburgh 1997 Tests; No Bounce Back Uses Eqs. (9) and (10) and Bounce Back Uses Eqs. (12) and (13); Dark Line Shows Position of Bubble

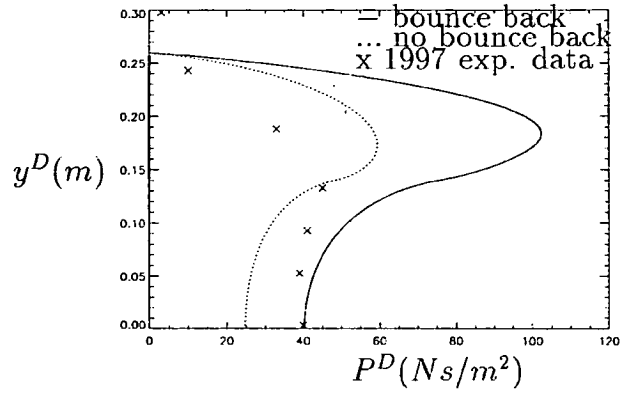

FIG. 19. Pressure Impulse up the Wall for Test H088 of Edinburgh 1997 Tests; No Bounce Back Uses Eqs. (9) and (10) and Bounce Back Uses Eqs. (12) and (13); Dark Line Shows Position of Bubble

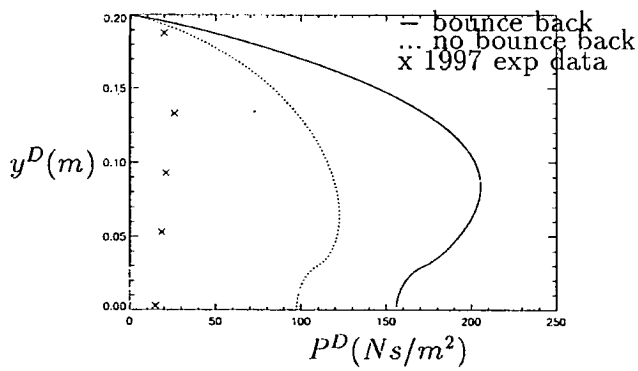

FIG. 20. Pressure Impulse up the Wall for Test H094 of Edinburgh 1997 Tests; No Bounce Back Uses Eqs. (9) and (10) and Bounce Back Uses Eqs. (12) and (13); Dark Line Shows Position of Bubble

TABLE 2. Values of Variables from Edinburgh 1997 Tests for Use in Theoretical Model

Test (1)	Mound (2)	U (m/s) (3)	a^D (m) (4)	b^D (m) (5)	h (m) (6)	t_b (s) (7)	t_a (s) (8)	Δt (s) (9)
H056	High	0.7	0.09	0.17	0.17	0.1426	0.1794	0.0368
H058	Low	0.9	0.16	0.26	0.26	0.2283	0.3004	0.0721
H068	Low	0.9	0.14	0.23	0.23	0.4491	0.5176	0.0685
H075	Low	0.85	0.11	0.26	0.26	0.3009	0.3821	0.0812
H088	Low	0.85	0.14	0.26	0.26	0.0827	0.1759	0.0932
H094	Low	1.1	0.03	0.20	0.20	0.1663	0.2374	0.0711

CONCLUSIONS

A theoretical pressure-impulse model has been compared with experimental pressure measurements for breaking waves impacting on a vertical wall and trapping an air pocket. The novel aspect of the theory is the idea of bounce back, which makes a simple model of the effect of air compressibility through the duration of the impact. The shape of the trapped air is also simplified (i.e., a cosine distribution of bounce back velocity is taken to represent a hemispherical bubble). This simplification could also be taken to represent a distribution of smaller bubbles.

In addition to the simplifications of the air bubble, we must consider other factors that cause inaccuracies in our model. The estimation of parameters such as the velocity, wave height, and bubble position are also a source of error. This is because PIV analysis is difficult at the time of impact due to the air entrainment that occurs. Ideally, such data would come from predictions of the incident wave. In all of the available examples, the duration of impact was only marginally short enough for the pressure impulse concept to be valid. Thus, some care was needed in assessing the pressure measurements; in particular, that part of the pressure due to nonimpact pressures such as reflective pressures was subtracted.

The Edinburgh 1994 data compared relatively well with both the unmodified Cooker and Peregrine model and the bounce back model for prediction of pressure impulse up the wall. However, the bounce back model predicted the distribution of pressure impulse along the berm better than the Cooker and Peregrine model. Comparisons with the Edinburgh 1997 data showed that for the tests where the air pocket depth was less than half the wave depth (Figs. 15–17 and 19) the bounce back method gave the best prediction. These waves were the most violent and hence the best to compare. For the case where the air pocket is about half the depth of the wave (Fig. 18) the model without bounce back gave the better prediction. The case where the air pocket extended down most of the depth of the wave (Fig. 20) the pressure-impulse approach fails to predict even the magnitude of the pressure impulses involved. It is thought that air leakage may have caused a large amount of cushioning in this particular case and that the pressure-impulse model is not suitable. However, in such cases pressure-impulse theory overpredicts, thus giving conservative upper values on pressures.

It must be noted that scaling to prototype of this model must be done with care considering some of the theory's limitations. The model is compared with 2D wave tank tests. In the field the air bubble may not be so well defined and, sideways 3D leakage of the trapped air may also occur reducing the effect of the bounce back. On the other hand a suitably conservative estimate is obtained by neglecting air leakage. Models for detailed aspects of air bubble breakup, such as those including air leakage, are unlikely to be of much relevance to field conditions where incident waves are not ideal.

A prediction of the peak impulsive pressure p_i may also be needed. It is reasonable to assume that the variation of pressure with time through the impact is triangular, and hence $p_i = 2P/\Delta t$. In practice, it is difficult to estimate Δt, and further work continues in this area.

Pressure-impulse theory has the advantage of providing simple Fourier series solutions to complex situations. These solutions are quick to evaluate, and from this study it is shown they can be reasonably accurate. In particular, if the air bubble is well confined, with little air leakage, and $U\Delta t/H << 1$, the comparisons with laboratory experiments are good.

ACKNOWLEDGMENTS

Support of the U.K. EPSRC and the European Commission, Directorate General XII, Science, Research, and Development, Contract No. MAS3-CT95-0041 (PROVERBS), is gratefully acknowledged. The writers also would like to thank A. Kortenhaus, H. Oumeraci, and D. Vicinanza for the provision of the experimental data in this paper.

APPENDIX I. REFERENCES

Bagnold, R. A. (1939). "Interim report on wave-pressure research." *J. Inst. Civ. Engrgs.*, 12, 202–226.

Batchelor, G. K. (1967). *An introduction to fluid dynamics*, Cambridge University Press, Cambridge, U.K.

Bruce, T., and Vicinanza, D. (1998). "Wave kinematics in front of caisson breakwaters." *Proc., 8th Int. Polar and Offshore Engrg. Conf. (ISOPE '98)*, Vol. 3, ISOPE, Golden, Colo., 658–664.

Chan, E. S. (1994). "Mechanics of deep water plunging-wave impacts on vertical structures." *Coast. Engrg.*, 22, 115–133.

Cooker, M. J., and Peregrine, D. H. (1990). "A model for breaking wave impact pressures." *Proc., 22nd Int. Conf. Coast. Engrg.*, Vol. 1, ASCE, New York, 1473–1486.

Cooker, M. J., and Peregrine, D. H. (1992). "Wave impact pressure and its effect upon bodies lying on the sea bed." *Coast. Engrg.*, 18, 205–229.

Cooker, M. J., and Peregrine, D. H. (1995). "Pressure-impulse theory for liquid impact problems." *J. Fluid Mech.*, Cambridge, U.K., 297, 193–214.

Gray, C., and Bruce, T. (1995). "The application of particle image velocimetry (PIV) to offshore engineering." *Proc., 5th Int. Offshore and Polar Engrg. Conf. (ISOPE '95)*, Vol. 3, ISOPE, Golden, Colo., 701–708.

Lamb, H. (1995). *Hydrodynamics*, 6th Ed., Cambridge University Press, New York.

Losada, M. A., Martin, F. L., and Medina, R. (1995). "Wave kinematics and dynamics in front of reflective structures." *Wave forces on inclined and vertical wall structures*, N. Kobayashi and Z. Demirbilek, eds., ASCE, New York, 282–310.

Mitsuyasu, H. (1966). "Shock pressures of breaking wave." *Proc., 10th Int. Conf. Coast. Engrg.*, Vol. 1, ASCE, New York, 268–283.

Oumeraci, H., Bruce, T., Klammer, P., and Easson, W. J. (1995). "Breaking wave kinematics and impact loading of caisson breakwaters." *Proc., Int. Conf. on Coast. and Port Engrg. in Developing Countries (COPEDEC)*, Vol. 4, Part 3, Rio de Janeiro, Brazil, 2394–2410.

Oumeraci, H., and Partenscky, H.-W. (1991). "Breaking wave impact loading of caisson breakwaters—Effect of entrapped air on structural response." *Proc., 1st Workshop on Wave Impact Loading of Vertical Struct.*, Contract 0032-M(JR), Hannover, Mass.

Oumeraci, H., Partenscky, H.-W., Klammer, P., and Kortenhaus, A. (1997). "Entwicklung von Bemessungsgrundlagen für Monolithische Wellenbrecher." *Abschlussbericht zum forschungsvorhaben*, Braunschweig, Germany (in German).

Peregrine, D. H. (1994). "Pressure on breakwaters: A forward look." *Proc., Int. Workshop on Wave Barriers in Deep Waters*, T. Takayama, ed., Port and Harbour Research Institute, Tokosuka, Japan, 553–573.

Peregrine, D. H., and Kalliadasis, S. (1996). "Filling flows, coastal erosion and cleaning flows." *J. Fluid Mech.*, Cambridge, U.K., 310, 365–374.

Peregrine, D. H., and Thais, L. (1996). "The effect of entrained air in violent water wave impacts." *J. Fluid Mech.*, Cambridge, U.K., 325, 377–397.

Ramkema, C. (1978). "A model law for wave impacts on coastal structures." *Proc., 16th Int. Conf. Coast. Engrg.*, Vol. 3, ASCE, New York, 2308–2327.

Schmidt, R., Oumeraci, H., and Partenscky, H.-W. (1992). "Impact loads induced by plunging breakers on vertical structures." *Proc., 23rd Int. Conf. Coast. Engrg.*, ASCE, New York, 1545–1558.

Topliss, M. E. (1994). "Water wave impact on structures." PhD dissertation, University of Bristol, Bristol, U.K.

Walkden, M. J. A., Hewson, P. J., and Bullock, G. N. (1997). "Scaling." *Proc., Task 1 Tech. Workshop on Probabilistic Des. Tools for Vertical Breakwaters*, Edinburgh, Scotland.

Wood, D. J., and Peregrine, D. H. (2000). "Wave impact on a wall using pressure-impulse theory. II: Porous berm." *J. Wtrwy., Port, Coast., and Oc. Engrg.*, ASCE, 126(4), 191–195.

APPENDIX II. NOTATION

The following symbols are used in this paper:

A_m = constant in Fourier series;

a^D, a = dimensional and nondimensional heights of bottom of bubble, respectively;

b^D, b = dimensional and nondimensional heights of top of bubble, respectively;

C = constant;
D = constant;
F = force;
g = gravity;
H = length scale;
h = height of wave at wall, when first stages of impact are complete;
m = number of term in Fourier series;
$\mathbf{n}$, n = normal direction and direction out of fluid, respectively;
P^D, P = dimensional and nondimensional pressure impulses, respectively;
p = pressure above atmospheric;
p_a = pressure at time t_a;
p_b = pressure at time t_b;
p_i = peak impulsive pressure;
t = time;
t_a = time after impact;
t_b = time before impact;
U = velocity of wave impact;
$\mathbf{u}$ = dimensional velocity of fluid;
$\mathbf{u}_a$ = dimensional velocity after impact;
$\mathbf{u}_b$ = dimensional velocity before impact;
x^D, x = dimensional and nondimensional horizontal axes, respectively;
y^D, y = dimensional and nondimensional vertical axes, respectively;
α_m = $[m + (1/2)]\pi$;
Δt = $t_a - t_b$; and
ρ = density of fluid.

Appendix D: Walkden & Bruce, 1999

Walkden, M. & Bruce, T. (1999), *Scatter in wave impulse load maxima: a review*, Proc Int. Conf. Coastal Structures '99, Santander, 1, pp 439–444, A A Balkema, Rotterdam, ISBN 90 5809 092 2

Appendix D
Walkden & Bruce, 1999

Walkden, M. & Bruce, T. (1999), *Scatter in wave impulse load maxima: a review*, Proc Int. Conf. Coastal Structures '99, Santander, 1, pp 439–444, A A Balkema, Rotterdam, ISBN 90 5809 092 2

D.1 Declaration of contribution

At the time of preparation of this paper Walkden was a post-doctoral Research Engineer working at Edinburgh under the author's guidance. The author worked closely with Walkden at all stages of this study, from initial test design, through test set up and day to day discussion of data gathered, to the synthesis of conclusions. The tests were carried out most ably by Walkden, who also prepared the first draft the paper text. The author worked closely with Walkden in subsequent editing.

D.2 Published paper

overleaf

Scatter in wave impulse load maxima: a review

M.J.A.Walkden
Department of Civil Engineering, University of Bristol, Bristol, UK
T.Bruce
Department of Mechanical Engineering, University of Edinburgh, Edinburgh, UK

ABSTRACT: Examples are given of wave impact loads measured in laboratory and marine tests that show considerable scatter. The causes of variation between impact load maxima are considered in general and specifically for nominally identical monochromatic laboratory waves. Several alternative models are described but, it is argued, none of them provide a complete description. Examples are then shown of engineering methods that overcome the inherent uncertainty to provide design loads for vertical breakwaters. These methods are shown to be based on the same basic approach. It is concluded that this approach provides a valuable example for the development of design methods for other structure types.

1 INTRODUCTION

For many vertical or near vertical breakwaters and seawalls a proper assessment of the impact loads generated by breaking waves is critical to ensure structure stability and integrity. This is largely beyond current theoretical models so is usually achieved using methods, such as that given by Goda (1974), which are partly based on physical model tests. Alternatively a potential design might be based directly on investigations made by means of physical models. Although such tests are very useful their results can be difficult to interpret. One of the main reasons for this is the large scatter found in the impact load maxima.

When we observe marine waves the water surface that we see is normally an interference pattern formed by many waves of different period, height and direction. When such waves break they can assume a wide variety of forms. Although these may be classified into general types (see for example Battjes 1974, Galvin 1968, Oumeraci et al. 1993, Walkden et al. 1995, Allsop et al. 1996) the great number of frequencies which may compose a wave and the variety in the way in which they may be combined means that the range of breaker forms is potentially infinite. Though this fact may be easily recognized there is a tendency to assume that it is not significant since differences may appear minor. In fact even small fluctuation can introduce significant stochastic variation into wave impact loads. This was recognized by Hayashi & Hattori (1958) who stated:

"The initial shock pressure varies so enormously from wave to wave that it seems to have nothing to do with our theoretical considerations."

It is important to consider why minor variation have such a strong effect, whether we can model the involved processes and how we can overcome uncertainty to design safe marine structures.

2 IMPULSE LOAD MAXIMA

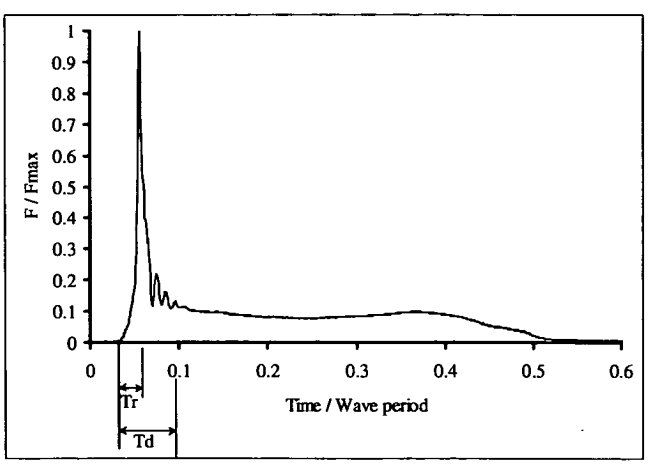

Figure 1. Laboratory impact load time history.

Figure 1 shows the force time history produced by a laboratory flume wave breaking onto on a vertical wall. Two principal regions can be seen, a short duration 'impulse' in which the forces can be characterized as being of relatively high magnitude and rapidly changing and a 'quasi-hydrostatic' part in

which the forces are lower and more constant. The impulse is associated with the rapid change in momentum experienced by the steep wave front as it arrives at the wall. The quasi-hydrostatic region is formed during the reflection of the remainder of the wave. Figure 1 also indicates the maximum impact force (F_{max}), the rise time to that force (T_r) and an estimation of the impulse duration (T_d).

When such wave impacts are measured in a marine environment the load maxima are found to be highly variable. A good example of a marine data set is provided by Blackmore & Hewson (1984). Their values for maximum impact pressure (P_{max}) range from 5 to approximately 27 kN/m^2. Other studies show values ranging up to 690 kN/m^2 (Rouville et al. 1938). This range of values, around two orders of magnitude, can simply be attributed to differences in wave heights, periods and angles of approach. Also different foreshores disturb waves in different ways and tidal variation affects the location of wave breaking.

One of the principal methods used to avoid the natural variability of marine phenomena is to conduct physical model tests. Typically experiments will be repeated a number of times and a single variable incrementally changed. Once the effect of this variable on the output of the system in question is established it is fixed and another variable is investigated in the same way. It is clearly fundamentally important that the experiment be repeatable, similar conditions should bring about a similar result. It is therefore a serious complication to the investigation of wave impacts that laboratory wave loads are highly variable. Figure 1 shows a histogram of pressure maxima normalized by ρgH, where ρ is the density of the water, g is the acceleration due to gravity and H is the wave height. The data were obtained using monochromatic, and therefore nominally identical, quasi-two-dimensional waves.

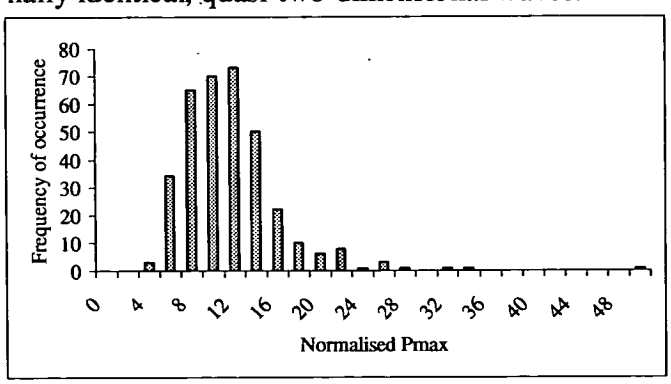

Figure 2. Histogram of pressure maxima resulting from the impacts of 330 monochromatic waves (from Walkden 1999).

The waves were generated with an energy absorbing paddle in a tank that was narrow and rigid (see Walkden 1999). Despite these controlled conditions the range of the pressure maxima is greater than an order of magnitude. Impact force maxima tend to show slightly less scatter due to the averaging effect of spatial integration. Figure 2 shows force data from that same test, which is normalized by ρgH^2. The range is reduced but is still substantial.

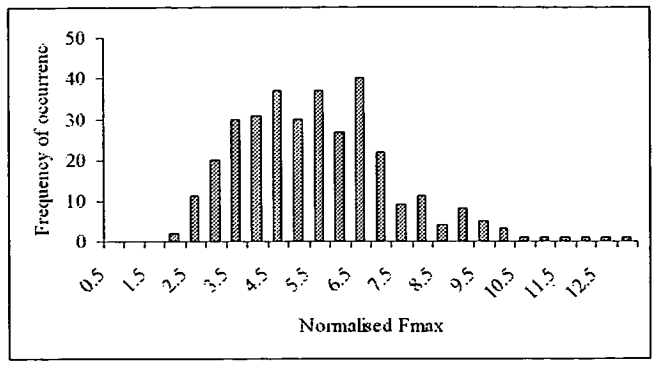

Figure 3. Histogram of force maxima resulting from impacts of 330 monochromatic waves (from Walkden 1999).

The implication of variation on the way in which physical model tests are interpreted will be discussed below. Firstly potential causes of this scatter will be considered.

2.1 *Causes of variation in impact load maxima*

Many factors are known to affect the maximum load measured from an impacting wave, these include:

1 Physical boundary conditions; topography, permeability and roughness.
2 Wave conditions; height, period, direction and water depth.
3 Measurement apparatus
4 Wave type
5 Model motion
6 Aeration
7 'Noise'
8 Others

Causes (1), (2) and (3) refer to all wave impacts, whether naturally occurring or artificially produced in the laboratory. The wave and physical boundary conditions are associated with the general shape of the wave as it breaks, which clearly influences impact loads (see for example Oumeraci et al. 1993). The measurement apparatus is included to recognize that the measurements are not of reality, but nature exposed to a method of questioning. Transducer size, location, sample rate and frequency response all influence recorded loads. (4) and (5) tend to be specific to laboratory conditions. 'Wave type' refers here to the variety of waves that may be generated including long-monochromatic (see Walkden et al. 1995) short-monochromatic (see Richert 1968), solitary (see Bagnold 1939), single (see Hull et al. 1999), convergent frequency packet (see Chan & Melville 1988) and pseudo-random (see Allsop et al. 1996). Differences in wave type can make load maxima recorded during different studies difficult to compare. Model motion will also have some effect, although this is apparently usually kept to a mini-

mum through rigid mounting. Aeration is thought by most observers to be the cause of scatter in laboratory results, so will be discussed in more depth in the next section. 'Noise' refers to the high frequency, low amplitude stochastic waves that disturb water surfaces. This occurs naturally on open waters and is generated during wave breaking in the flume. The effects of noise are closely related to those of air, but will be considered here separately. (8) is included to recognize the fact that the above list is not likely to be exhaustive.

2.2 *Aeration*

The significance of aeration is not universally agreed. Ross (1955) and Lundgren (1968) believed that aeration prevents the occurrence of water hammer pressures. Kirkgoz (1982) believed that the highest pressures occurred in the absence of air whilst Bagnold (1939) suggested that impact pressures could only occur in the presence of an air pocket. Walkden (1999) argued that there are three principal forms in which air affects wave impacts, which were termed entrained, entrapped and expelled. Entrained air is mixed into the water as a bubbly mixture, entrapped air is sealed against the wall as a compressible boundary (often called an air 'pocket') and expelled air is forced from between the wave and wall at closure

2.2.1 *Entrapped air*

Bagnold (1939) suggested that differences in the thickness of entrapped air (D) caused the scatter he observed in impact pressure maxima and developed the following expression:

$$P_{max} - P_0 = 2.7(\rho U^2 K/D) \quad (1)$$

Where P_0 = atmospheric pressure, ρ = water density, K = 'effective length', which is equal to $0.2H$ and U = velocity of the approaching wave.

Although Bagnold had experimental data he was not able to measure air pocket thickness, so could not prove this model.

It was later developed by both Mitsuyasu (1966) who refined the solution for P_{max}, Lundgren (1968) who applied it to the problem of scaling wave loads and Ramkema (1978) who worked on the problem of air trapped under an overhanging deck. Oumeraci & Partenscky (1991) Topliss et al. (1992) and Hattori et al. (1994) have also modeled the frequencies of oscillation of entrapped air. The most successful of these appears to be Topliss et al. 1992 (see Hattori et al. 1994).

Validation of entrapped air models has been hampered by a need for accurate physical measurements. Such data has only recently begun to emerge. Hattori et al. (1994) used high-speed video images of impacting waves to differentiate between those with no air and those with thin or thick pockets. It was shown that impact pressures were highest with small amounts of entrapped air.

Walkden (1999) made direct measurements of entrapped air using purpose built probes. It was found that high pressures were associated with small air pockets. The relationship between air and wave load was expressed using an 'aeration flux', which was the time integral of measured air. For small air pocket impacts the load maxima increased with increasing aeration flux, for larger pockets the relationship tended to be ambiguous. This relationship appears to be counter-intuitive since aeration increases wave compressibility so is usually thought to reduce loads, as in the case of the Bagnold-Mitsuyasu model. An explanation might be found in Wood et al. (1999) in which the behavior of a compressed pocket is considered theoretically. It is shown that during the early stages of the impact the trapped air may 'bounce-back' into the flow, increasing the wave impulse as it does so. If the associated rise in T_{pr} is relatively small then this might result in an increase in load maxima.

2.2.2 *Expelled air*

The role of expelled air was modeled by Lundgren (1968). His approach was to assume that the impulse magnitude was a function of the breaking wave height (H_b) and velocity:

$$I = 0.5\, U\, \rho\, H_b^2 \quad (2)$$

The shape of the impulse was then assumed to be a simple cosine function;

$$P = P_{max}(0.5(1 - cos(T\, \pi / T_{pr}) \quad (3)$$

Where T = time.

The rise time, and therefore duration were defined as:

$$T_{pr} = A / (H_b U) \quad (4)$$

Where A is the volume of expelled air. The maximum impact load therefore depends upon the volume of expelled air and small changes in A result in large variation in P_{max}. This model has not, apparently, been tested experimentally.

2.2.3 *Entrained air*

The water hammer expression of Von Karman (1928, Equation 5) provides the first estimate of the role of entrained air in wave impact loads.

$$P = \rho\, C\, V \quad (5)$$

Where C = speed of sound, which is a strong function of the entrained air content.

No observers have recorded wave impact pressures as high as those predicted by water hammer theory. Kamel (1970) recognized this and developed an expression that accounted for the compressibility of the material of the structure:

$$P = \rho_s C_s (\rho_l C_l V/(\rho_l C_l + \rho_s C_s)) \quad (6)$$

Where ρ_s and ρ_l are the densities of the solid and liquid respectively, and C_s and C_l are their sound speeds.

Kamel compared predictions of impact loads with laboratory data from both wave impacts and drop tests. It was found that the maximum measured wave impact pressure from approximately 3700 events was eight times smaller than the predicted value. The maximum drop test pressure was 50 % of the predicted value with an average of only 3 %.

Fuhrboter (1969) studied the impacts of high speed water jets and derived an expression for the pressure maxima as a function of the elasticity of both air and water. This was intended to be analogous to a wave jet. Fuhrboter (1986) later showed that the expression failed to predict wave impact pressures during measurements on a sloping revetment in a large wave flume.

2.3 *Noise*

Denny (1951) provided insight into the significance of water surface disturbance on impact loads. Two groups of waves were tested, 450 in water that had been left to calm for 15-20 minutes between tests and 1500 others that were formed in the disturbed water left by the previous impact. It was found that the increased noise affected the second group, causing a 50 % reduction in the average impact pressure maxima.

The waves probably contained little entrained air due to their small size, the use of fresh water and the time between impacts. Most of the variation seen might be attributed to difference in entrapped air and in the shape of the wave as it closed.

2.4 *Summary*

There are several models that have been proposed which might explain the scatter of impact load maxima. Aeration is generally acknowledged to be important either in the form of entrapped pockets, expelled air or entrained bubbles. Validation of these models has suffered from a lack of experimental data, although this is now starting to become available.

It seems unlikely that any one of the currently available models will be shown to completely describe wave impact loads since expelled, entrapped and entrained air may all affect the same event. Even if a model were to be validated it is likely that it would rely on a property, such as air pocket thickness or expelled air volume, which would be unknown to an engineer designing a marine structure. It is therefore unlikely that such a model could contribute directly to the design process.

It may be pragmatic for engineering purposes to accept the large variability of impact loads as simply a property of 'noisy' waves and to consider how it can be dealt with. The next section of this paper will consider how engineers have coped with the uncertainty to develop design methods for vertical breakwaters.

3 ENGINEERING SOLUTIONS

When the stability of a structure that experiences wave impact loads is considered attention is drawn away from the load maxima to the whole of the impulse (see for example Marinski & Oumeraci 1992). Goda (1992) describes how Hiroi developed a design method in 1919 that deliberately underpredicted wave loads because he believed that they were too transient to motivate a structure with high inertia. In other words Hiroi recognized that the effect of the impulse is less than is implied by the high measured loads. As knowledge of the involved processes has increased, the manner in which they have been described has become more refined. A property of impact loads that has often been used is a relationship between load maxima and load duration of the form:

$$P_{max} = K_1 T_{pr}^{-c} \quad (7)$$

Where T_{pr} is the pressure rise time and K_1 is a constant. Such relationships have been shown by Weggel & Maxwell (1970), Blackmore and Hewson (1984), Kirkgoz (1990), Hattori et al. (1994) and Walkden (1999). The value of K_1 was different in each case and the index C varied from 0.5 to 1. The equation of Bagnold (Equation 1) is a variation of this basic form since the rise time varies with the airpocket thickness. Bagnolds model was developed by Minikin (1950) into a design method, which was then adopted in the Shore Protection Manual (1984).

Walkden 1999 argued that equation 7 represents a more fundamental relationship between impulse duration (T_d) and force maxima of the form:

$$F_{max} = 2I / T_d \quad (8)$$

Where I = the integral of the impulse forces with respect to time.

Goda (1974, 1985) used the same relationship in the development of his breakwater design method, as described by Goda (1994).

3.1 *Goda*

Goda assumed that the impulse was triangular with a rise time equal its duration ($T_r = T_d$). Working with forces rather than pressures he assumed;

$$F = 2I T_r^{-1} \quad (9)$$

A further assumption was made that the portion of the wave that contributes to the impulse load can be represented by a half cylinder of water of height H_b moving with the same velocity of the wave and therefore:

$$I = 0.4\rho U H_b^2 \quad (10)$$

Per unit run. So;

$$F = 0.8\rho U H_b^2 T_r^{-1} \quad (11)$$

A relationship was therefore defined between F_{max} and T_r as a function of the breaker height and velocity. By making a further assumption regarding the minimum possible impulse duration:

$$T_{d(min)} = \pi V/60g \quad (12)$$

It was possible to establish a single value for F_{max}.

In this way both the magnitude and form of the force impulse was defined. Goda then went on to model caisson dynamic behavior so that the hydrodynamic load could be converted into an 'effective' static load. This property could then be used by designers to represent both hydrodynamic and structural dynamic effects.

3.2 *MAST-PROVERBS*

A similar approach was developed during the European Union Marine Science and Technology Programme's 'Probabilistic Design Tools for Vertical Breakwaters', MAST PROVERBS. This was first described by Klammer et al. (1996). The relationship between the normalized impulse maxima and duration was expressed as:

$$F_{max}/(\rho g H_b^2) = 2.24(T_r/(d_b/g)^{1/2})^{-1} \quad (13)$$

Where d_b = breaker depth.

Equation 13 can be re-arranged to provide:

$$F_{max} = 2.24\rho(gd_b)^{1/2} H_b^2 T_r^{-1} \quad (14)$$

Klammer et al assumed:

$$U = 1.33(gd_b)^{1/2} \quad (15)$$

Therefore:

$$F_{max} = 1.68\rho U H_b^2 T_r^{-1} \quad (16)$$

So, using equation 9, the magnitude of the impulse integrated over the rise time is:

$$I = 0.84\rho U H_b^2 \quad (17)$$

Which is very similar to the impulse magnitude assumed by Goda, although it should be noted that equation 17 only defines the impulse up to the load maxima so that the total impulse is larger.

F_{max} is determined from an extreme value probability distribution and then used in equation 13 to provide the rise time. Having defined both the form and magnitude of the force impulse they are used to make a prediction of effective static load using a numerical model.

3.3 *Model tests*

Walkden et al. (1996) and Walkden (1999) developed a similar approach for interpreting the results of model wave impact loads. Measured force records were processed to provide values for F_{max}, T_d and I. The forces and durations were then reduced to account for the typically concave impulse shape using equation 9. Finally they were used with dynamic amplification factors to provide effective static loads. This method has the advantage that because model test results are used no assumptions need to be made about the impulse magnitude.

4 DISCUSSION AND CONCLUSIONS

A large degree of scatter is observed in wave impact load maxima, even for nominally identical laboratory waves. The scatter seems to be associated with variations in aeration and several models have been proposed to describe the relationships. None of these has been proven and recent results indicate that the role of entrapped air may not be as simple as previously believed. Increased compressibility can, apparently, increase wave loads under certain conditions.

Such variability hinders research since it makes it difficult to establish the importance of all the affecting variables. It also has important implications for the way in which potential breakwaters are modeled in the laboratory. Such tests tend to involve long pseudo-random wave tests from which a few events are selected for breakwater stability analysis. If the selection criteria is the largest impact pressure or impact force, then there is a risk that significant events will be missed. Examination of design methods shows the importance of the force impulse. It may be more appropriate for important events to be selected on the basis of their impulse magnitude rather than force maxima.

In the context of research into breakwater design methods it may be unrealistic to try and develop the means of making a deterministic prediction of impact load maxima. This is a conclusion that can simply be drawn from the fact that the pressure maxima of a controlled laboratory wave is largely unpredictable even if the same wave condition has already been tested.

Engineers have developed meaningful design methods without complete physical descriptions of the involved processes. This has been achieved partly by recognizing the importance of structural dynamic response. This changes the focus of attention from the load maxima to the impulse magnitude and form. An identifiable framework has emerged in design methods, which is to assume an impulse magnitude as a function of wave height and velocity, then combine this with a functional relationship between force maxima and impulse duration or rise time. Some pragmatic estimate is then made of F_{max} or T_d, which then determines the impulse form. Having established impulse magnitude and form it is then possible to make an estimation of structural response.

Although the design methods that have been examined here are all intended for use with large caisson structures the way in which the hydrodynamic

loads are quantified is transferable to other structure types.

REFERENCES

Allsop, N.W.H., McKenna, J.E., Vicinanza, D., & Whittaker, T.T.J. 1996. New Design Formulae for Wave Loadings on Vertical Breakwaters and Seawalls. *Proc. 25th Int. Conf. on Coastal Engineering*, Orlando.

Bagnold, R.A. 1939. Interim report of wave pressure research, *J. Inst. Civ. Eng.*, London, 12, 202-226.

Battjes, J.A. 1974. Surf Similarity. *Proc. 14th Int. Conf. on Coastal Engineering*, 257-293.

Blackmore, P.A. & Hewson, P.J. 1984. Experiments on Full Scale Wave Impact Pressures. *Coastal Engineering*, 8, pp. 331-346.

CERC, 1984. *Shore Protection Manual, 4th ed.* U.S. Army Waterways Experimental Station, U.S. Government Printing Office, Washington D.C.

Chan, E.S. & Melville, W.K. 1988. Deep water plunging wave pressures on a vertical plane wall. *Proc. Royal Soc. London.* A 417, 95-131.

Denny, D.F. 1951. Further experiments on wave pressures. *J. Inst. Civ. Eng., London*, 35, 330-344.

Fuhrboter, A. 1969. Laboratory investigation of impact forces. *Proc. Symp. Res. on Wave Action*, Delft Hydr. Lab. II.

Fuhrboter, A. 1986. Model and prototype tests for wave impact and run-up on a uniform 1:4 slope. *Coastal Engineering*, 10, 49-85

Galvin C.J. 1968. Breaker type classification on three laboratory beaches". *J. Geophysical Res.* 72, 3651-3659.

Goda, Y. 1974. New wave pressure formulae for composite breakwaters. *Proc. 14th Int. Conf. on Coastal Engineering*, Ch. 100, 1702-1720.

Goda, Y. 1992. The design of upright breakwaters. Proc. of the Short Course on Design and Reliability of Coastal Structures, *23rd Int. Conf. Coastal Engineering*, 547-568.

Goda, Y., 1994. Dynamic response of upright breakwaters to impulsive breaking wave forces. *Coastal Engineering* 22, 135-158.

Goda, Y. 1985. *Random seas and the design of maritime structures.* University of Tokyo press.

Hattori, M., Arami, A., & Yui, T. 1994. Wave impact pressure on vertical walls under breaking waves of various types. *Coastal Engineering*, 22, 79-114.

Hayashi, T., & Hattori, M. 1958. Pressure of the breaker against a vertical wall. *Coastal Eng. in Japan*, 1, 25-37.

Hull, P., Muller, G. & Allsop, N.W. 1999. Laboratory study of wave impact pressure propagation into cracks and voids in blockwork structures. *Proc. Coastal Structures*, Santander, Spain.

Kamel, M.A. 1970. Shock pressures on coastal structures. *Proc. ASCE, Waterways, Harbours and Coastal Engineering Division*, Vol. 96, 689-699.

Karman, T.v., 1928. The impact of seaplane floats during landing. *NACA Tech. Note* 321, Washington D.C.

Kirkgoz, S. 1982. Shock pressure of breaking waves on vertical walls. *J. Waterway, Port Coastal and Ocean Engineering*, ASCE, 108, 81-95.

Kirkgoz, S.M. 1990. An experimental investigation of a vertical wall response to breaking wave impact. *Ocean Engineering*, 14, 379-391.

Klammer, P., Kortenhaus, A. & Oumeraci, H. 1996. Wave impact loading of vertical face structures for dynamic stability analysis – prediction formulae. *Proc. 25th Int. Conf. on Coastal Eng.* 2(196), 2534-2547

Lundgren, H. 1968. Shock forces: an analysis of deformations and forces in the wave and in the foundation. *Proc. Symp. on Wave Action*, Delft Hydro Lab, 14.

Marinski, J.G. and Oumeraci, H. 1992. Dynamic response of vertical structures to breaking wave forces, -review of the CIS design experience-. *Proc. Int. Conf. Coastal Engineering*, 1357-1370.

Minikin, R.R. 1950. *Wind, Waves and Maritime Structures.* London: Charles Griffen,.

Mitsuyasu, H. 1966. Shock pressures of breaking wave". *Proc. 10th Int. Conf. on Coastal Eng.* 268-283.

Oumeraci, H. & Partenscky, H.W. 1991. Breaking wave impact loading of vertical structures, -effect of entrapped air on structure response-. *Proc. MAST G6 project 2 Workshop*, Hannover, Germany.

Oumeraci H., Klammer P. & Partenscky H. W., 1993. Classification of breaking wave loads on vertical structures. *J. Waterways, Port, Coastal, and Ocean Engineering*, ASCE 119(4).

Ramkema C. 1978. A model law for wave impacts on coastal structures. *Proc. 16th Int. Conf. Coastal Eng.* 2308-2327.

Richert, G. 1968. Experimental investigation of shock pressures against breakwaters. *Proc. 11th Int. Conf. Coastal Engineering*, 954-973.

Ross, C.W. 1955. Laboratory study of shock pressures of breaking waves. *Beach Erosion Board, Tech. Memo* 59.

Rouville, A., Besson, P. & Petry, P. 1938. Etudes internationales sur les efforts dus aux lames. *Annales des Ponts et Chassees*, 108 5-113.

Topliss, M.E., Cooker, M.J., & Peregrine, D.H. 1992. Pressure oscillations during wave impact on vertical walls. *Proc. 23rd Int. Conf. on Coastal Engineering.*

Walkden, M.J.A., Crawford, A.R., Hewson, P.J., Bullock, G.N., & Bird, P.A.D. 1995. Wave impact loading on vertical structures. *Proc. Coastal Structures and Breakwaters '95*, London.

Walkden, M.J., Hewson, P.J. & Bullock, G.N. 1996. Wave impulse prediction for caisson design". *Proc. 25th Int. Conf. on Coastal Engineering* 3(200) 2584-2597.

Walkden 1999. Model wave impulse loads on caisson breakwaters: aeration, scale and structural response. *Ph.D. Thesis*, University of Plymouth, UK.

Weggel, J.R. & Maxwell, W.H. 1970. Experimental study of breaking wave pressures. *Offshore Tech. Conf.* Texas, USA 623-642.

Wood, D.J., Peregrine, D.H. & Bruce, T.B. 1999. Study of wave impact against a wall with pressure-impulse theory. Part 1: trapped air. *Paper in press, Journal of Fluid Mechanics.*

Appendix E: Walkden *et al.*, 2001

Walkden, M., Wood, D.J., Bruce, T. & Peregrine, D.H. (2001), *Impulsive seaward loads induced by wave overtopping on caisson breakwaters*, Coastal Engineering, 42, 3, pp257–276, Elsevier

Appendix E
Walkden *et al.*, 2001

Walkden, M., Wood, D.J., Bruce, T. & Peregrine, D.H. (2001), *Impulsive seaward loads induced by wave overtopping on caisson breakwaters*, Coastal Engineering, 42, 3, pp257–276, Elsevier

E.1 Declaration of contribution

At the time of preparation of this paper Walkden was a post-doctoral Research Engineer working at Edinburgh under the author's guidance. Very much as per Walkden & Bruce (1999), the author worked closely with Walkden at all stages of this study, from the initial design / stability study, through model design, test set up, day to day discussion of data as it was gathered, to the synthesis of conclusions. The tests were carried out most ably by Walkden, who also prepared the first draft the paper text. The author worked closely with Walkden in subsequent editing.

E.2 Published paper

overleaf

ELSEVIER

Coastal Engineering 42 (2001) 257–276

Coastal Engineering
An International Journal for Coastal, Harbour and Offshore Engineers

www.elsevier.com/locate/coastaleng

Impulsive seaward loads induced by wave overtopping on caisson breakwaters

M.J. Walkden [a,*], D.J. Wood [b], T. Bruce [c], D.H. Peregrine [d]

[a] *Department of Civil Engineering, University of Bristol, University Walk, Queens Building, Bristol BS8 1TR, UK*
[b] *Department of Mathematics, University of Oslo, Oslo N-0316, Norway*
[c] *Division of Engineering, University of Edinburgh, Edinburgh EH9 3JL, UK*
[d] *School of Mathematics, University of Bristol, Bristol BS8 1TW, UK*

Received 12 March 1999; accepted 11 October 2000

Abstract

An investigation of seaward impulse loads on caisson breakwaters caused by wave overtopping is described. Attention is focused on mechanisms that may cause such loads, and consideration given to implications for the design of vertical breakwaters. A review of literature shows that there have been several reported cases of seaward tilting of breakwater caissons. A description of the seaward failure of a prototype structure, apparently resulting from overtopping, was also found. The measurements of seaward impulsive loads reported in the literature do not show any case in which they are higher than associated landward forces. Physical model tests that are described show overtopping of a low crest breakwater in which the maximum seaward force is greater than the maximum force acting towards the land. A theoretical model for the pressure impulse generated by the re-entry of the overtopping plume is given. Comparison with physical model data shows that, for these experiments, pressure in the air pocket trapped during overtopping contributes significantly to the impulse. When this effect is included, good agreement is obtained between experiment and theory. It is concluded that seaward overturning should be considered as a failure mode of caisson breakwater designs that allow overtopping, particularly for structures of relatively low mass. © 2001 Elsevier Science B.V. All rights reserved.

Keywords: Seaward wave loads; Wave overtopping; Vertical breakwaters; Physical model; Theoretical model; Impulse loads; Pressure-impulse theory

1. Introduction

Caisson breakwaters experience static and dynamic loads on both sides but it is usually the forces generated by wave action on the seaward side that are critical for stability (see for example Goda, 1967). As a result, design methods have developed to provide tools for the prediction of landward loads (e.g. Minikin, 1950; Goda, 1974). Recent research under the MAST III PROVERBS (PRObabilistic design tools for VERtical BreakwaterS) project included a review of the different failure modes of vertical breakwaters (see Oumeraci et al., 1999). This highlighted a case in which a model caisson was ob-

* Corresponding author. Fax: +44-117-928-7783.
E-mail addresses: Mike.Walkden@bristol.ac.uk (M.J. Walkden), Deborah@math.uio.no (D.J. Wood), Tom@srv1.mech.ed.ac.uk (T. Bruce), D.H.Peregrine@bristol.ac.uk (D.H. Peregrine).

0378-3839/01/$ - see front matter © 2001 Elsevier Science B.V. All rights reserved.
PII: S0378-3839(00)00063-6

served to displace in a seaward direction immediately after it had been overtopped by a large wave (van der Meer, personal communication). The resulting discussion revealed that relatively little was known about such a failure mechanism, but results from pressure-impulse theory indicated a likely cause. It was decided to make a special study, the results of which are described in this paper.

The aims of the study were to investigate high seaward forces resulting from large wave overtopping and the possibility that this might cause seaward failure. Specific objectives were to:

- Establish whether there were any examples of such failure of prototype structures.
- Measure seaward acting pressures during physical model experiments.
- Observe the processes causing these pressures.
- Develop a theoretical model capable of predicting the measured loads.
- Use the theoretical model to gain a deeper understanding of the processes involved.
- Draw practical conclusions to assist in the process of designing reliable vertical structures.

Experience with pressure-impulse theory calculations, especially Wood and Peregrine's (1996) study of wave impact beneath a deck, had revealed how pressure due to an impact can be enhanced if it is in a relatively confined region. The impact of overtopping water on water behind a breakwater is one such situation. During wave impact on a vertical wall, the pressure is noticeably reduced by the presence of air at the top of the wall. In contrast, impact on the surface of water close to a vertical wall can have its effect almost doubled because there is no pressure relief at the wall. The study reported here supports the initial interpretation of high pressures at the rear of a breakwater, and in addition, reveals that air trapped under overtopping water can acquire sufficient pressure to significantly enhance the seaward forces.

Section 2 describes a review of related literature that finds evidence of seaward movement of prototype breakwaters associated, in at least one case, with wave overtopping. No measurements of the associated loads could be found. Section 3 describes physical model measurements of large impulsive seaward loads occurring as a result of overtopping. In Section 4, a theoretical model is developed using the concept of pressure-impulse (Cooker and Peregrine, 1992, 1995; Wood and Peregrine, 1996; Wood et al., 2000). The model is valuable in interpreting the pressure distribution, and gives good results for some overtopping events. In Section 5 the results of the theoretical model are shown to compare well to the physical measurements and used to describe the processes involved in more detail. Finally, in Sections 6 and 7, the practical implications of the study are considered and conclusions are drawn.

2. Review of literature

Oumeraci (1994) reviewed 22 cases of vertical breakwater failure and noted several examples of seaward tilt. He reports that:

> ... most of the damaged structures had a low crest and were hence heavily overtopped. In this respect, a number of failures also occurred during construction while the superstructure was not completed. As a result, heavy wave overtopping and breaking on the structure took place which generally lead to differential settlements, thus resulting in the seaward tilt of the breakwater, irrespective of the type of structure ... Although these failure mechanisms have often been attributed to seabed scour ... and to liquefaction ... the actual reason for this 'abnormal' behaviour and the 'abnormal' forces which prevailed are still not understood.

Minikin (1950) provides a description of the seaward collapse of the Mustapha breakwater in Algeria in 1934. This structure was designed to withstand waves of 5 m height and 80 m wavelength. Within 3 years of its completion, it was subjected to a severe storm, the waves of which were estimated to be over 9 m high and 180 m in length. This caused approximately 400 m of the breakwater to collapse in a seaward direction. Minikin reports that:

> Photographs taken at the height of the storm showed waves passing over the parapet in an unbroken crest. ... The wall collapsed just after the crest of an unbroken wave passed over the

parapet: it went suddenly into the following trough.

He goes on to suggest that this failure occurred due to a combination of 'suction' forces caused by the wave trough and structural dynamic effects.

It is well known that the horizontal quasi-hydrostatic load acting on a vertical breakwater varies with fluctuations of water surface. The applied force is thus landward in the presence of a wave crest and seaward with a trough (see, for example, Fig. 9 of Oumeraci et al., 1993). The seaward force exceeds the landward force when the ratio of water depth to wave length exceeds approximately 0.25 (Goda, 1967, see also McConnell et al., 1996). Calculations made using simplified equations of Sainflou have shown that structures designed using the method of Goda (1974, 1992) have high factors of safety against failure in the seaward direction (Walkden et al., 1998). This implies that if a modern structure is to fail in this way, then it will probably be caused, at least in part, by forces caused by some other process than a low trough.

Transient negative pressures are known to occur on spillways and in stilling basins and are capable of causing great damage (see for example Hager, 1994). These are associated with high velocity flows, the presence of hydraulic jumps and turbulent flow induced to dissipate energy. Related negative pressures have been observed on the faces of breakwaters. Hattori et al. (1994) show seaward pressures caused by high velocity flow up a structure face immediately prior to impact (their Figs. 19, 21 and 23). They also show seaward pressures caused by oscillations in entrapped air (their Figs. 15, 19, 21, 23 and 25). Both phenomena had previously been noted by Chan and Melville (1988). In addition, recent marine measurements have shown that water cascading down the face of a near vertical breakwater can cause short, localised seaward impulses (Bullock et al., 1999). These authors have not suggested that such loads might represent a risk of monolithic seaward failure for prototype structures, presumably because of their transient and localised nature. However, it has been noted that they may be a cause of local block displacement in masonry structures (Müller, 1997). In addition, Oumeraci and Kortenhaus (1994) observed that fluctuation in entrapped air pocket size and the resulting pressure changes might cause dynamic amplification of structural motion and so cause overall failure. A theoretical model for entrapped air oscillation was developed by Topliss et al. (1992), and shown to agree with experimental data (Hattori et al., 1994, see their Fig. 29a).

Some evidence has been cited of seaward tilting of vertical breakwaters. In the case of the Mustapha breakwater, this displacement was so great that the structure failed. Goda (1967) showed that the force maxima in the seaward direction become larger than those in the landward direction when the water depth is a quarter or more of the wavelength. This does not explain the Mustapha failure since the depth of the water was only approximately one tenth of the wavelength (see Minikin, 1950, p. 55). Minikin describes the failure as being 'sudden', which might suggest that the structure responded to a seaward impulsive load, probably in conjunction with the seaward forces associated with the presence of the wave trough. The seaward impulsive loads described in the literature are all quite small and accompanied with landward loads of greater magnitude. In order to explain the failure of the Mustapha breakwater, it is therefore necessary to identify a mechanism capable of generating significant seaward impulsive forces. Guidance can be found in the observations of Minikin and van der Meer that seaward motion followed the plunge of an overtopping wave behind the structure. In fact, the model structure of van der Meer was designed with a low crest and sloping roof to allow overtopping in order to reduce landward loads. It was therefore decided to conduct a physical model study to investigate the loads generated during the re-entry of an overtopping wave.

3. Physical model tests

3.1. Experimentation

It was decided to base the design of the physical model on a 'Hanstholm' type of breakwater (see for example Juhl, 1994). This is because the Hanstholm breakwater was designed with a sloping superstructure which allowed overtopping and reduced landward loads. A maximum wave height of 10 m and a

spectral peak period of 12 s were assumed and the model built at a length scale of 1:52.5 (see Fig. 1). The model caisson was 200 mm wide and 286 mm high. The superstructure had a slope of 35°, joined the front face at the still water level and had a freeboard of 95 mm. The caisson and superstructure were constructed from clear acrylic of 25-mm thickness, and the base of the same material of 10-mm thickness.

The model was rigidly clamped to the tank walls and founded on a rubble mound constructed from a core of 12-mm stones with 31-mm armour. The top of the berm extended 190 mm in front and behind the caisson. There were 15 locations for pressure transducers in the caisson as shown in Fig. 1. Eight Druck PDCR 800 pressure transducers that were used had a natural frequency in air of 28 kHz and these were sampled at 2 kHz. Video images were recorded during each test to obtain the dimensions and velocities of the overtopping waves and plunging jets. Short test runs of focused waves were used to generate a wave 170 mm high with a period of 1 s. This was equivalent to a prototype wave 8.9 m high with a period of 7.2 s, and was therefore smaller than the design condition. A water level time history of this wave, which was recorded at the location of the structure face (with the structure removed), can be seen in Fig. 2.

Due to the limited number of transducers it was not possible to measure pressures at all locations simultaneously. Each test was therefore repeated a second time so that the transducers could be moved from the front and top of the model to the rear and base. One transducer in the front face was left in place so that the phase relationship between the front and rear loads could be found.

This approach was not ideal since the loads on the front face were recorded during a different event than those on the caisson rear. It was decided that this procedure did not introduce any significant problems to the study because the waves arrived at the structure without breaking. This meant that the pressures on the front of the structure were very repeatable so that, although they were not measured at the same time as the loads on the rear, it was possible to be quite confident of their magnitude and to represent them with a previously measured force time history. Two example pressure time histories that were recorded on the front face during different events are shown in Fig. 3. The one transducer that was not moved between tests allowed the loads on the front to be set to the correct phase relative to those on the rear. It should be noted that this linking of front and rear loads was only done to establish their relative magnitudes. The comparison between the physical and theoretical models described in Section 5 only required the pressure measurements from the rear of the structure.

Force records were calculated by spacewise integration of the measured pressures. It was assumed

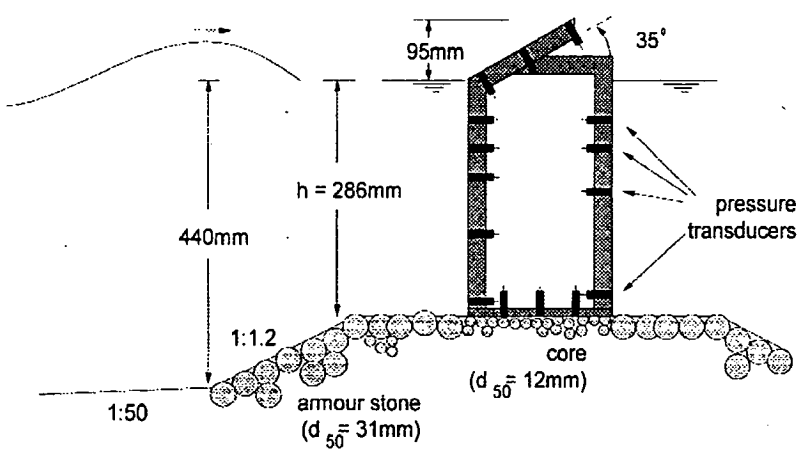

Fig. 1. Experimental model arrangement.

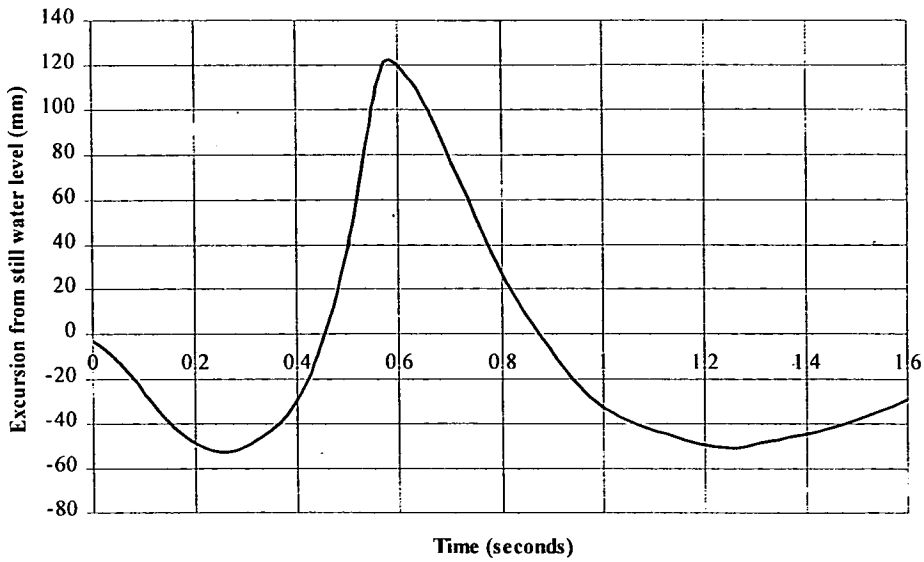

Fig. 2. Water surface time history recorded in the location of the structure face, in the absence of the structure.

that pressures varied linearly between the measurement points and were constant within regions of entrapped air. Landward forces were defined to be positive. Pressures on the sloping superstructure were resolved into horizontal and vertical components. Moments were calculated about the heel and toe of the structure using the same assumptions. A positive moment was defined as one that tends to overturn.

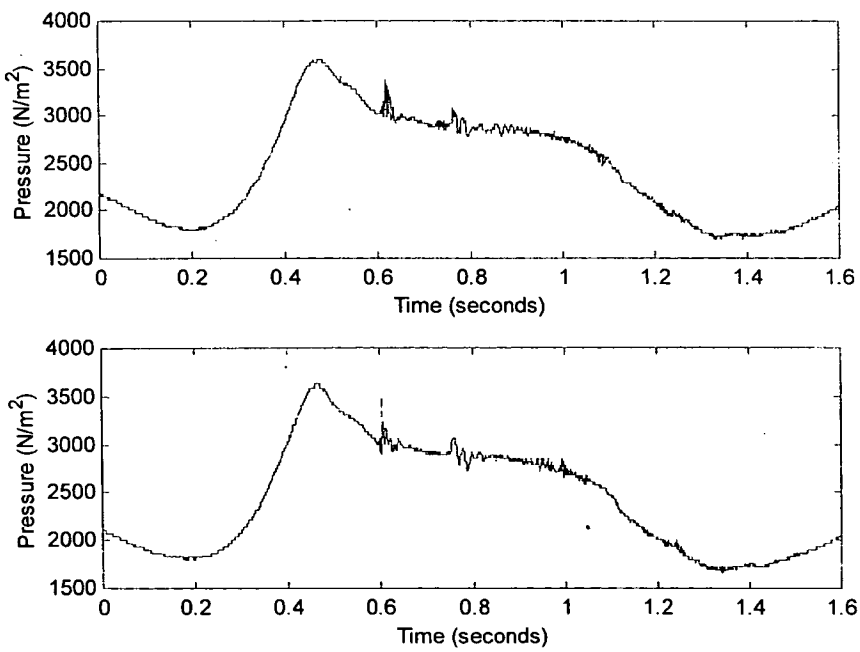

Fig. 3. Two pressure time histories recorded 266 mm below still water level on the front face of the model caisson during different events.

Thus, a positive moment about the heel tends to cause tilting towards the land, whilst a positive moment about the toe tends to cause tilting towards the sea, as illustrated in Fig. 4.

3.2. Observations

Different stages of a typical overtopping event are illustrated in Fig. 5, approximate time references are provided, so that they can be related to the pressure time histories, in Fig. 6, and the associated force time history in Fig. 7.

The physical processes that generated these forces are interpreted as follows:

0.2–0.4 s—Trough at the front face, still water at the rear.
0.5 s—Wave begins to pass over the superstructure.
0.58 s—Wave slams down onto the superstructure trapping air and producing the maximum landward horizontal force (approximately 350-N/m run).

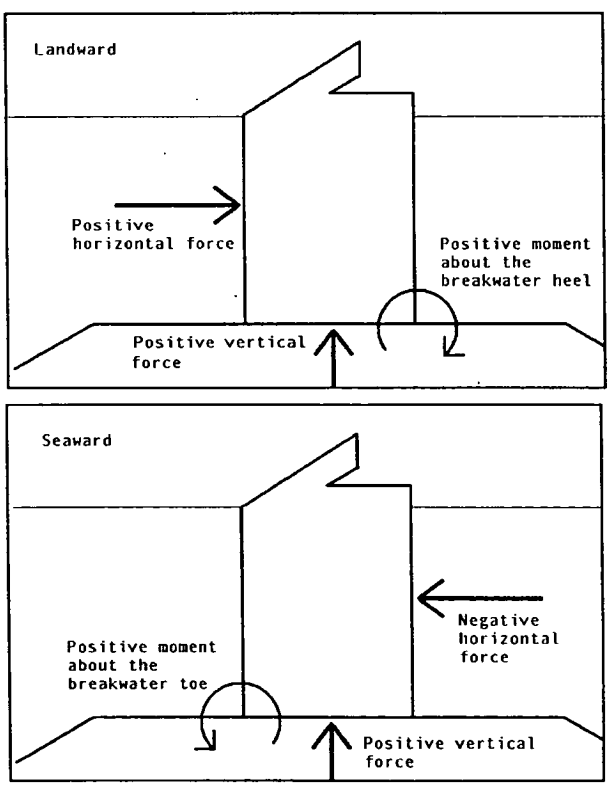

Fig. 4. Forces and moments around the model caisson.

0.825 s—Crest plunges into the harbour entrapping air pocket producing the maximum seaward horizontal force (approximately 540-N/m run, see also Fig. 8).
0.875 s—Plunging wave collapses and the overall force becomes landward again (approximately 160-N/m run).
0.9 s—Increase in water level at the rear face whilst water drains seaward off the superstructure and away from the caisson causing a seaward force.

The horizontal and vertical forces that occurred during the plunge of the wave into the harbour are shown in greater detail in Fig. 8, together with the overturning moments.

The largest overall moment of 178-Nm/m run is seaward about the toe. This is significantly larger than the maximum landward overturning moment about the heel of 112-Nm/m run, which occurred as the wave impacted on the roof (at approximately 0.58 s).

The physical model tests showed that large seaward forces could occur during the plunge of an overtopping wave. It is not clear whether the observed loads in this example would have been large enough to cause failure in the prototype structure. The seaward loads were large but they were also transient and it is also not clear what the effects of scale might be. In addition, the experiment was essentially two-dimensional, and this may limit its relationship with prototype waves. The importance of these aspects of the phenomena is discussed further in Section 6.

In order to gain a deeper insight into the physics of the plunging wave in general, and the role of entrapped air in particular, a theoretical model was developed and validated against the physical model results.

4. Theoretical model

4.1. Background

Pressure impulse is the integral through an impact, with respect to time, of the pressure. It is a

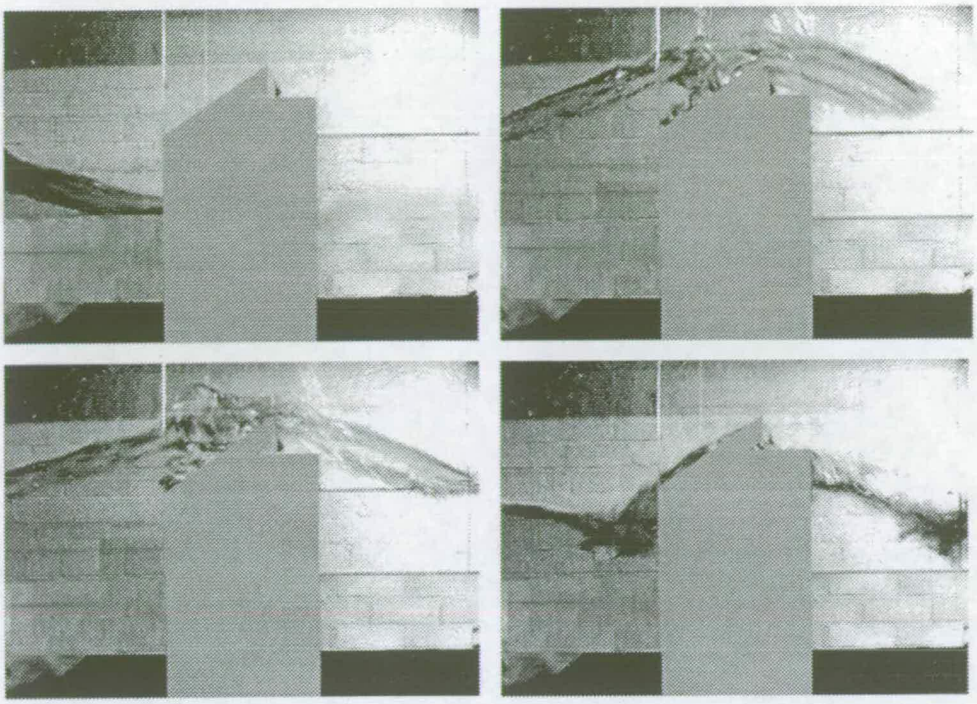

Fig. 5. (a) Trough arriving at the front face (0.2 s). (b) Jet passes over the superstructure causing a high landward load (0.75 s). (c) The jet plunges into the harbour, trapping a pocket of air (0.82 s). (d) Water level rises at the rear face and lowers at the front (0.95 s).

more robust measure of an impact than maximum pressure, since it shows less fluctuation between nominally identical wave impacts. Cooker and Peregrine (1992) discuss its use for wave impact on a vertical wall and Cooker and Peregrine (1995) give a more general discussion, illustrating that in many cases the distribution of pressure impulse on a wall does not show much dependence on the precise shape of the water surface: thus very simplified shapes give a good impression of the pressure impulse distribution. Using the approximation that impacts are very brief, pressure impulse can be evaluated without any need to account for viscosity or vorticity in the water, and satisfies Laplace's equation with relatively simple boundary conditions.

Here we consider water falling onto still water. Ideally, the pressure-impulse equation would be solved in both the previously undisturbed water and in the impacting water simultaneously, e.g. Cooker and Peregrine (1995). However, the complexity of determining such a solution does not appear to be justified given the uncertainties in estimating overtopping for prototype cases. Thus, the problem is considered in two parts: firstly, the pressure impulse due to the falling water is estimated (Section 4.2). This pressure impulse is then applied to the surface of the previously undisturbed water behind the breakwater (Section 4.3). This leads to a relatively simple mathematical problem. It is found that the solution is very sensitive to the presence of a trapped air pocket behind the breakwater. Satisfactory agreement with experiment is found when an estimate of the effect of impulsive pressure in the air pocket is incorporated in the solution.

4.2. Impulse due to overtopping water

A simple model of overtopping would be to represent the water as a two-dimensional rectangular block of width a and height b (see Fig. 9), with downward velocity W due to falling through a height D, i.e. $W = (2gD)^{1/2}$ (throughout this section D is defined as the distance from the top of the model caisson to the still water level, here 95 mm).

This assumes that $D = h_c$, which means that the velocity of impact of the water jet is somewhat

underestimated since, for some of the water, $D > h_c$. However, the general level of approximation of the model does not warrant a more detailed description of the jet impact. If this water were brought entirely to rest by the impact, it would give an impulse of:

$$I = \rho abW$$

per unit length of run. However, the impact does not bring such a block of water to rest since water is free to move sideways. For impact on a rigid surface the solution given by Cooker and Peregrine (1995) in their Eq. (3.1) with the fraction of the impacting wave (μ) equal to 1, when reflected in the x-axis and rotated through 90° (and rescaled), gives the appropriate solution. When put into the co-ordinates illustrated in Fig. 9, the pressure impulse P is given by:

$$P(x,y) = -\frac{4\rho W}{a}\sum_{n=1}^{\infty} A_n \cos(\lambda_n x)\frac{\sinh[\lambda_n(y-b)]}{\cosh(\lambda_n b)} \quad (1)$$

where:

$$A_n = [\sin(\lambda_n a/2)]/\lambda_n^2 \text{ and } \lambda_n = 2\left(n-\frac{1}{2}\right)\pi/a.$$

Fig. 10 shows a graph of total impulse against b/a (note that the equivalent figure in Cooker and Peregrine (1995, Fig. 6), is slightly distorted and

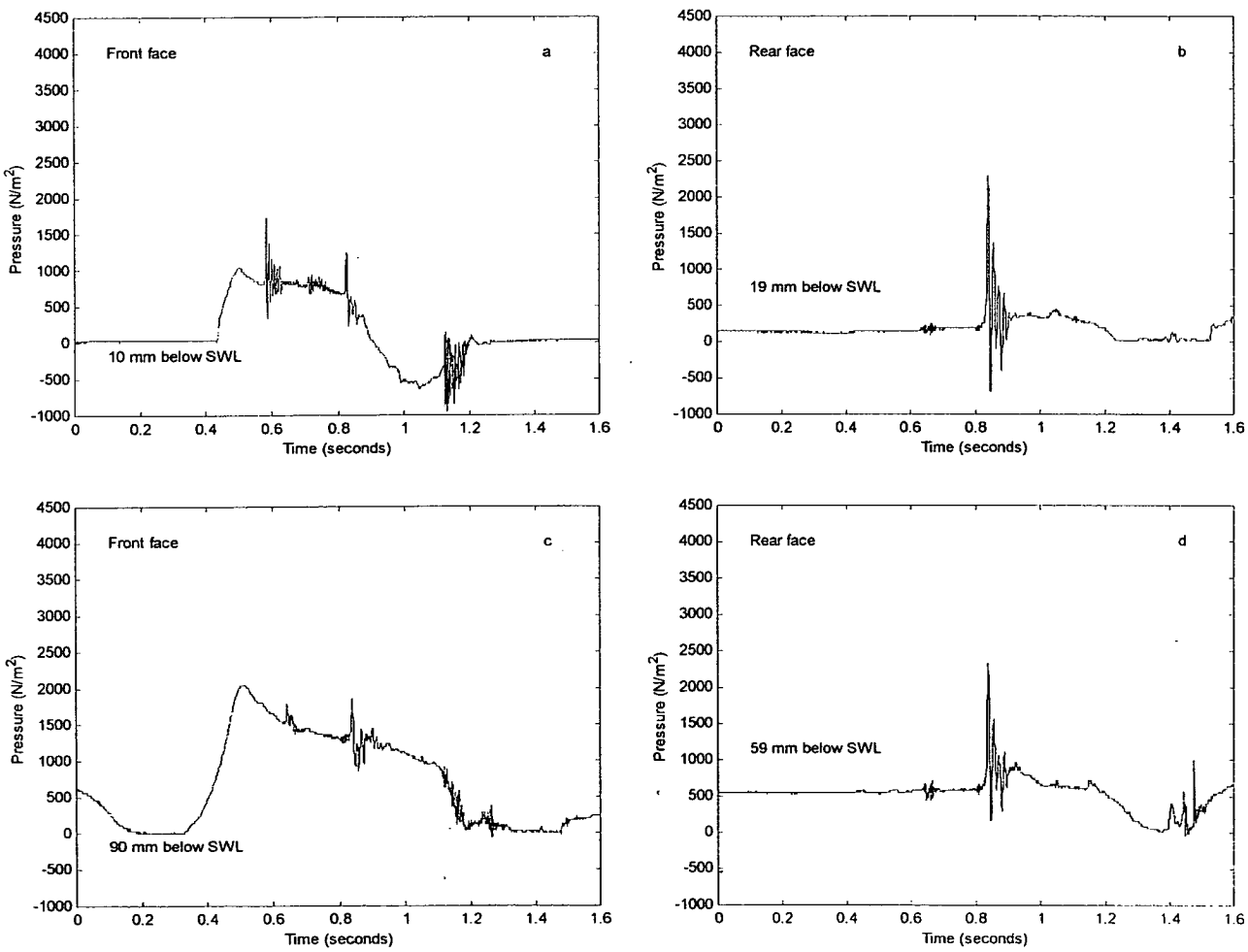

Fig. 6. Eight of the 15 pressure time histories used to calculate the force and moment time histories shown in Figs. 7 and 8.

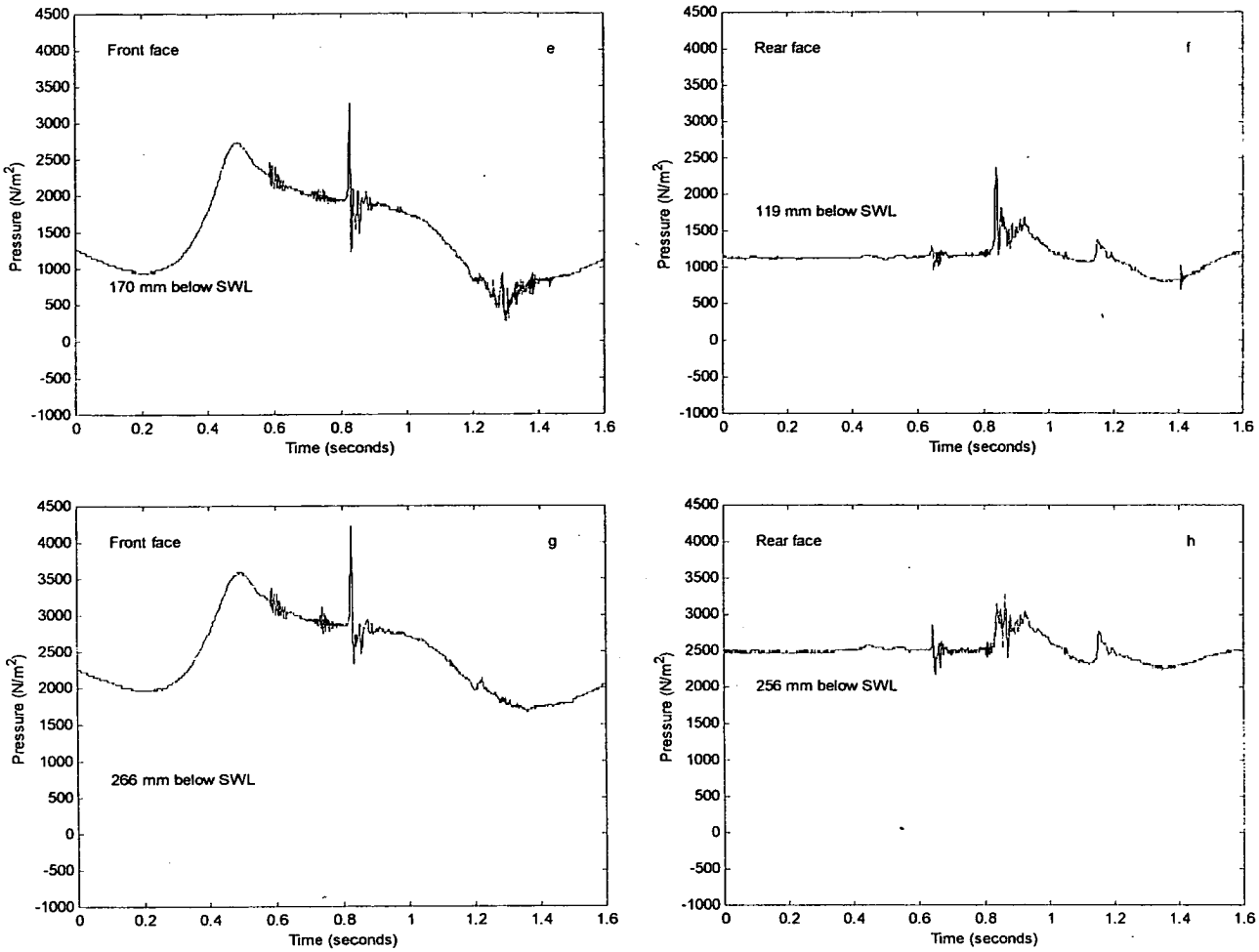

Fig. 6 (*continued*).

gives misleading results). The maximum value of the dimensional total impulse, I, for $b/a \to \infty$ is only $0.27\rho a^2 W$ (from Fig. 9). This impulse only drops noticeably when $b < 0.5a$ and is approximately ρabW only for $b < 0.1a$, and hence it is shown that the use of $0.27\rho a^2 W$ is a much better approximation than assuming the water is just brought to rest, giving ρabW as previously stated. For simplicity, in the following it is supposed that a value of I has been chosen and is then applied uniformly over the impact area, i.e. a pressure impulse I/a per unit area. There is no intrinsic difficulty in using the more appropriate expression (1), but both the presentation and results are simpler when using this approximation.

Model parameters, which are shown in Table 1, were estimated from the physical model and video records of the experiments. Measurements were taken, with a ruler, from appropriate frozen video images. Values of b were estimated by considering the vertical depth of the overtopping above the point of impact nearest the wall. These are greater than $0.5a$ so for the value I we use the $b > 0.5a$ case, i.e. $I/a = 0.27\rho aW$. For comparison with experiment, an allowance must be made for the fact that this is a liquid–liquid impact rather than a solid–liquid impact. The result for impact on water in Cooker and Peregrine (1995, Section 3.6) suggests that a multiplication of 0.58 should be applied, this being the ratio of pressure impulse due to jet impact on a

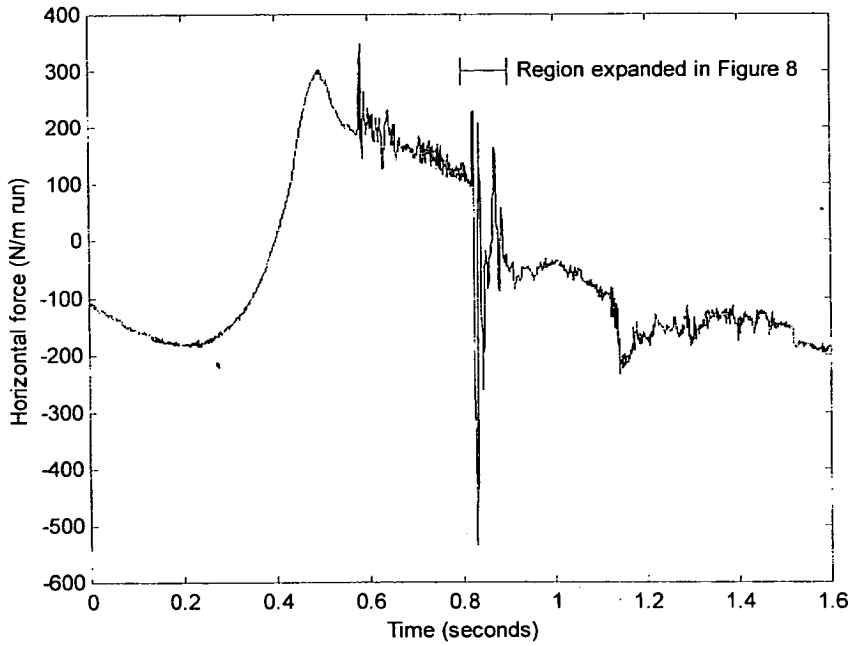

Fig. 7. Horizontal force measured during the overtopping event shown in Fig. 4, positive forces are landward.

liquid to that due to jet impact on a rigid surface (note that the figure in the text in Cooker and Peregrine (1995) for liquid–liquid impact should read 0.427 and not 0.247).

In addition, the fact that the impact under consideration is between two liquids means that the thickness of the lower liquid relative to the horizontal extent of the impact area (h/a) is important. The figures quoted above are for infinitely deep water whereas no such correction is needed for zero depth of water. Other works, in particular Wood and Peregrine's (1996) study of upward impact on a deck, suggest that if the depth is greater than $0.5a$ the result for deep water is a good approximation. Wood and Peregrine show that if we consider the impact of a plate on a finite depth of water, where the depth of water to length of plate ratio is greater than half, then inaccuracies in estimation of total impulse on the plate are at most 20%, and by the ratio of depth to plate of 0.75 the inaccuracies are only 10%.

4.3. Pressure impulse in the water behind the breakwater

If a new co-ordinate system is introduced aligned with the back of the breakwater, as shown in Fig. 11, the problem of the applied impulse can be described as follows. On the still water surface, $y = 0$, the reduced pressure impulse is $I/a\ (= 0.16\ \rho a W)$ over the impact area, extending from $x = d$ to $x = d + a$. For the portions of the still water surface beyond this area, i.e., $x > d + a$, $P = 0$. Over the area given by $0 < x < d$, where there is a trapped air pocket if $d > 0$, the appropriate boundary condition is not known. Some excess pressure might be expected, but initially we assume atmospheric pressure, i.e. $P = 0$.

The water depth is h, so in the strip $0 > y > -h$, $0 < x < \infty$, pressure impulse satisfies Laplace's equation:

$$\nabla^2 P = 0$$

with boundary conditions on the wall:

$$x = 0, \quad \frac{\partial P}{\partial x} = 0, \tag{2}$$

and on the bed:

$$y = -h, \quad \frac{\partial P}{\partial y} = 0. \tag{3}$$

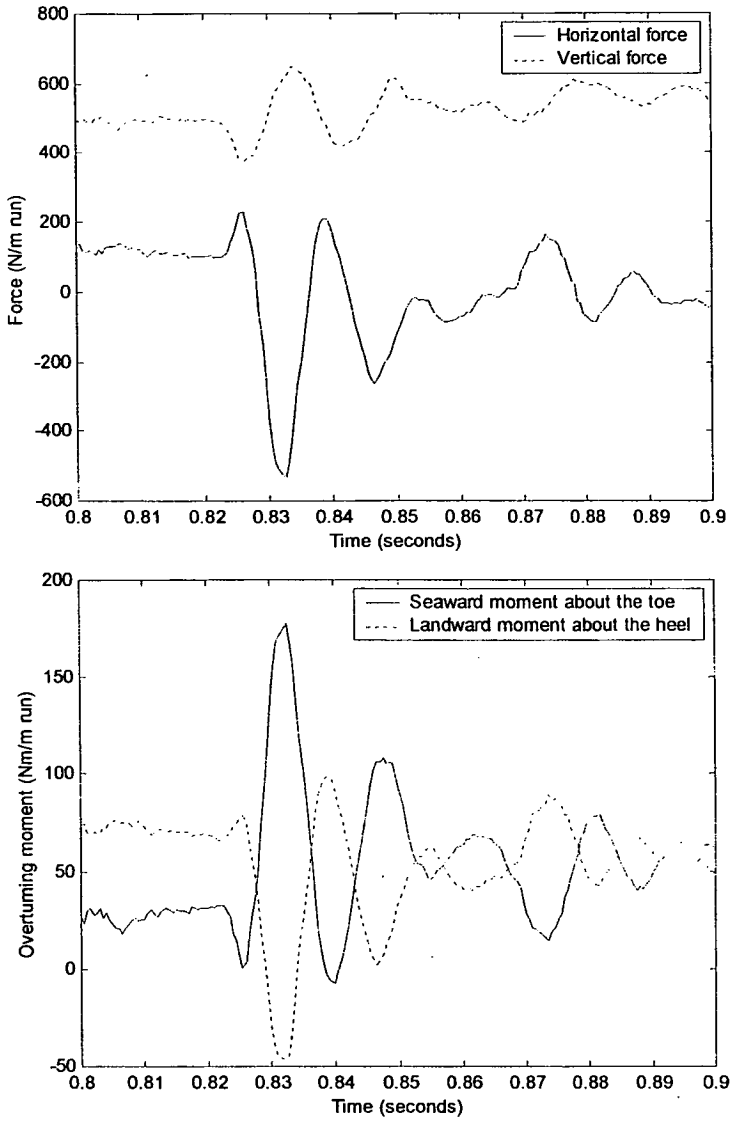

Fig. 8. Forces and moments measured during the plunge of the wave crest shown in Fig. 4.

Now by applying the Fourier cosine transform to this problem, writing:

$$\overline{P}(k,y) = \int_0^\infty P(x,y)\cos kx\,\mathrm{d}x.$$

Application of the transform to Laplace's equation and use of the boundary condition (2) gives:

$$\frac{\partial^2 \overline{P}}{\partial y^2} - k^2\overline{P} = 0.$$

Boundary condition (3) then gives:

$$\overline{P}(k,y) = A(k)\cosh k(y+h)$$

where $A(k)$ is found by imposing the still water boundary condition as follows: the Fourier transform of the still water level boundary condition gives:

$$\overline{P}(k,0) = \frac{I}{a}\int_d^{d+a}\cos kx\,\mathrm{d}x$$

$$= \frac{I}{ak}[\sin k(d+a) - \sin kd],$$

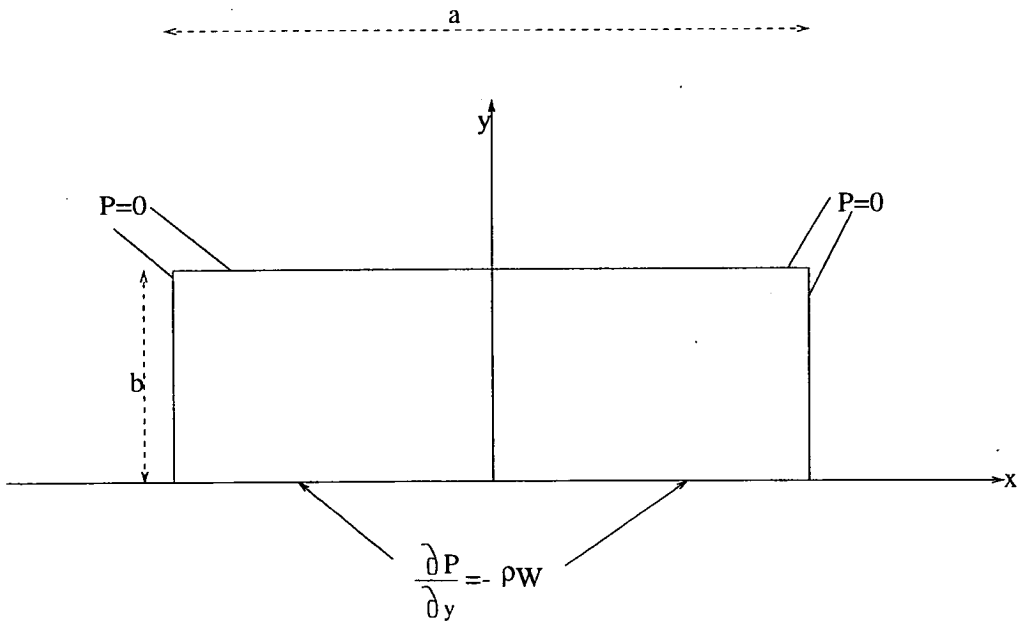

Fig. 9. Body of water impacting on a solid boundary.

which leads to:

$$\bar{P}(k,y) = \frac{I}{ak}\frac{[\sin k(d+a) - \sin kd]}{\cosh kh} \times \cosh k(y+h),$$

with the inversion:

$$P(x,y) = \frac{2}{\pi}\int_0^\infty \bar{P}(k,y)\cos kx\,dk.$$

Hence, the pressure impulse on the wall is:

$$P(0,y) = \frac{2I}{\pi a}\int_0^\infty \frac{[\sin k(d+a) - \sin kd]}{k\cosh kh} \times \cosh k(y+h)\,dk. \quad (4)$$

5. Comparison of theoretical and experimental results

Experimental data from three individual waves (labelled A, B and C) were compared with predictions made using this model. The pressure impulses shown in Table 1 are calculated from I/a given by $0.16\ \rho aW$. The initial depth of the water behind the caisson in every case was 276 mm, 10 mm less than the depth at the front, because of the projection of the base.

In order to compare the solution in Eq. (4) with the measurements, the pressure-impulse had to be evaluated by integrating the recorded pressure with respect to time over the pressure peak. For consistency between different pressure records, the time duration of the pressure peak was chosen from the force time series. The use of only four transducers to generate the force time series will not have much effect on the evaluation of the pressure impulse. As an illustration, the time series for seaward force from wave A is shown in Fig. 12. The temporal integration began at the first significant rise toward the peak and ended when the force dropped below the original hydrostatic value. The resulting values of pressure impulse from each of the four pressure transducers on the rear face of the model are shown for waves A, B and C in Fig. 13. The corresponding pressure impulse on the wall predicted by Eq. (4) is also shown in these figures with a broken line.

For the pressure impulse approach to be appropriate, the pressure peak must be considerably bigger than any related pressure due to the gravity wave, e.g. ρgh. The pressure peaks of impacts A, B and C were 3150, 1690, and 2170 N/m^2, respectively. As

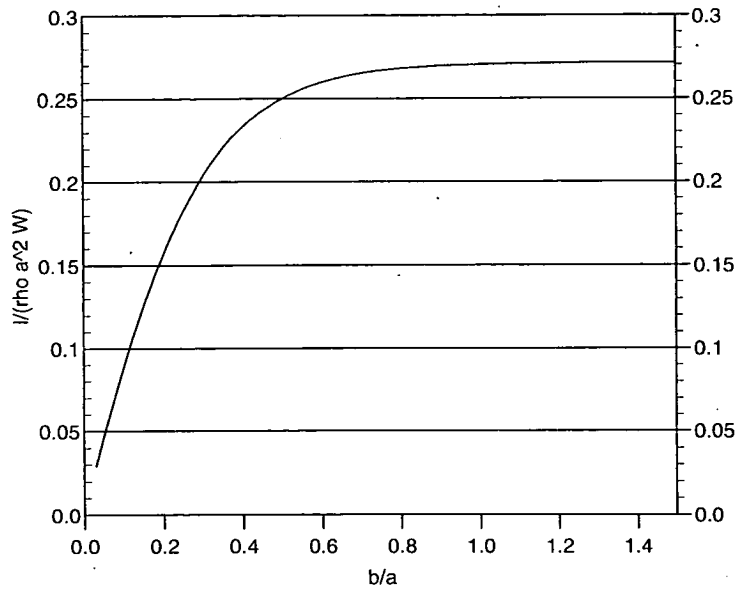

Fig. 10. Total non-dimensional impulse ($I/\rho a^2 W$) against b/a, for impact on a solid body by a rectangular block of water.

can be seen, impact B has a lower pressure maximum, so pressure impulse theory can be expected to work less well for this event than for A and C.

For all the waves A, B, and C, the broken line derived from Eq. (4) shows qualitatively different behaviour to the experimental points which increase rather than decrease as the still water level is approached. It is clear from this that the assumption in Section 4.3 that the pressures in the air pocket at the top of the wall are atmospheric is an underestimate.

Since (i) the pressure-impulse model satisfies linear equations, (ii) we can see that the effect of the water impact is near zero at the top transducer and (iii) the top transducer is close to the still water level, we deduce that it gives a good representation of the pressure in the overlying air pocket. Fig. 6b shows its record for impact A. The oscillations are typical of trapped air. Using this as a guide and comparison with the pressure impulse due to water impact, we choose to model the pressure impulse in the trapped air as $P(x) = 0.8I/a$ over the interval $0 < x < d$ (see Fig. 10). The resulting pressure impulse on the wall given by Eq. (4) is then adjusted to account for overpressure in the air pocket:

$$P(0,y) = \frac{2I}{\pi a}\int_0^\infty \frac{[\sin k(d+a) - 0.2\sin kd]}{k\cosh kh} \times \cosh k(y+h)\,dk. \quad (5)$$

The solid lines in Fig. 13 show the pressure impulse predicted using Eq. (5) for impacts A, B and C, respectively. This correction for the pressures in the air pocket provides a much closer comparison with the measurements. Fig. 14 shows the pressure impulse contours below the impacting jet for wave C. From the pressure impulse contours touching the left-hand wall, we can see that the effect of having a non-zero pressure impulse imposed in the bubble (on the free surface to the left of the solid black line which represents the jet impact) is to cause relatively high pressure impulse up the wall. This is in agreement with the experimental data.

Table 1
Parameters derived from the physical model for the theoretical model

Wave	Height of overtopping D (mm)	Air pocket length d (mm)	a (mm)	b (mm)	Estimated pressure impulse (N s/m^2)
A	95	84	144	91	32
B	95	52	91	57	20
C	95	78	84	52	17

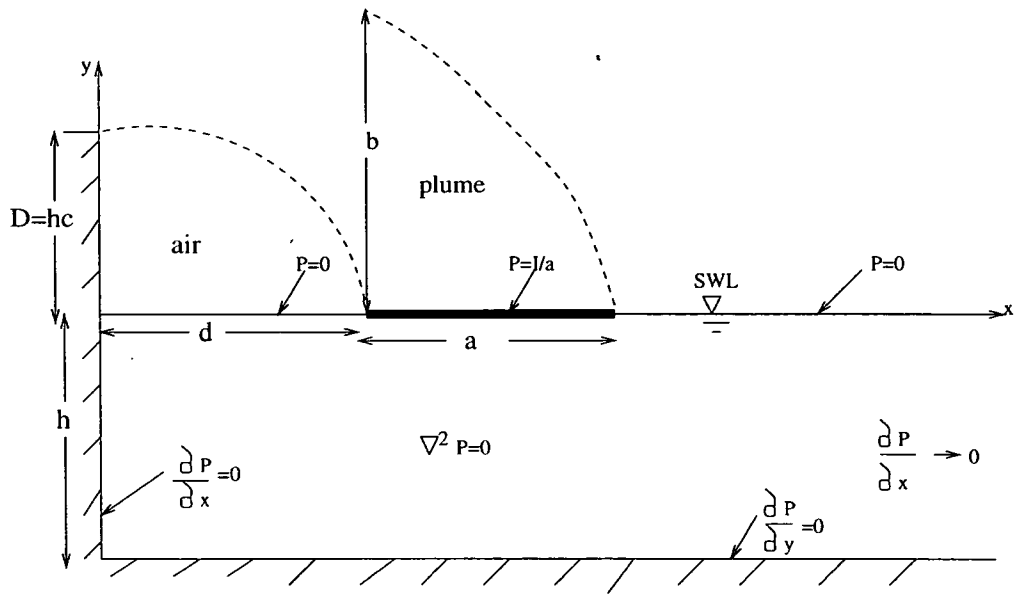

Fig. 11. Pressure impulse problem behind the breakwater.

The strength of the pressure impulse due to the trapped air, as illustrated, seems to be a surprisingly large fraction of that due to water impact. However, in studies of the effect of trapped air as a wave hits a wall directly, it has been found that the pressure-impulse model needs to take account of rebound due to

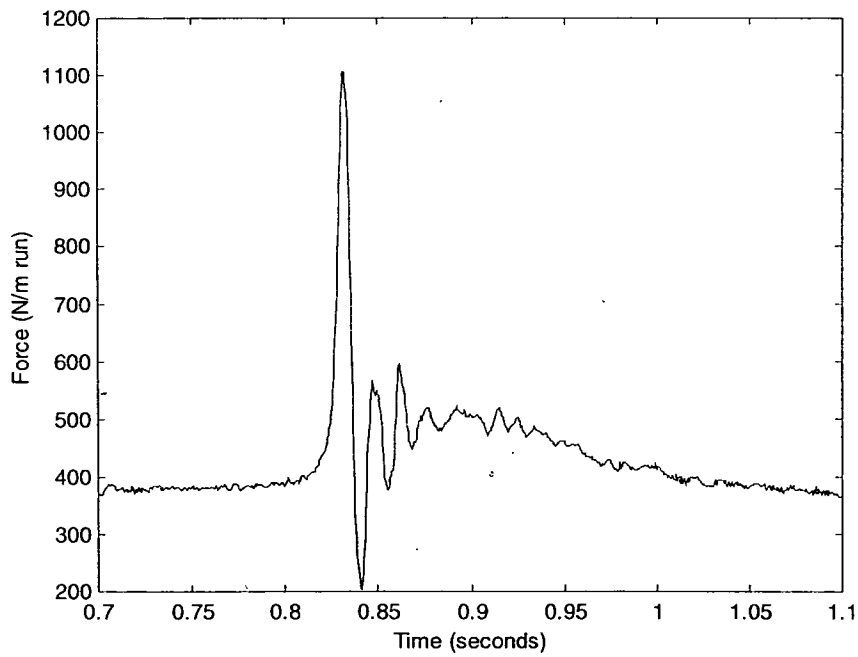

Fig. 12. Time series of force on the back of the breakwater for wave A.

air compression. Thus, in this case the choice of 80% of the water impact pressure-impulse could be interpreted as being only 40–50% of the pressure impulse if the effect of rebound is accounted for. In a practical three-dimensional situation, air can escape. However, there will still be an enhanced pressure since a positive pressure is required to accelerate the air away. Three-dimensional seas present the additional risk that may be water motion convergent towards one part of the wall.

6. Practical implications of the results

The physical model tests showed that large impulse loads can be generated on the harbour side of a low crest caisson when it is overtopped by a wave. For the events studied the seaward forces and overturning moments were larger than those acting towards the land. The loads were caused by the plunge of a wave crest into the harbour. Their characteristics appeared to be due to both the impact of the plume on the still water and the entrapment of a pocket of air underneath the plume and behind the structure. These observations were confirmed by the theoretical model, which highlighted the importance of the contribution of the trapped air pocket to the seaward impulse. In fact, for these particular experiments it appears that the pressure impulse per unit length of the water surface due to the air pocket could be as much as 80% of the contribution by the plume impact.

Forces caused by the plunge of a wave overtopping a breakwater might explain, at least in part, the seaward tilting observed in several prototype cases, and the failure of the Mustapha breakwater. Although the forces observed in the experimental model were large, it is not possible to establish whether they would be adequate to cause the structure to displace in a seaward direction. This is because the loads were transient, changed direction and depended upon the entrapment of air. This last point means that they are likely to be sensitive to three-dimensional effects and may be affected by scale. In order to understand the significance of the observations, it is necessary to consider each of these points.

6.1. Air entrapment in three-dimensional seas

Both the physical and theoretical models involved two-dimensional events. Typical marine events are three-dimensional and this will affect the form of the impacting plume. For example, if the impact of a two-dimensional block is compared with that of a circular column of the same diameter, the maximum pressure impulse for the cylinder is $0.13\rho a^3 W$ (Cooker and Peregrine, 1995), whereas for a block it is $0.27\ \rho a^2 W$. In addition, and perhaps more importantly, three-dimensionality will affect the likelihood of air pocket entrapment. The rough "80% rule" applied in the theoretical model provided a good result for the waves tested but is likely to be conservative for most marine events.

However, even if the results are conservative for the majority of overtopping events, judging by the description given by Minikin (1950), the failure of the Mustapha breakwater resulted from wave overtopping that was essentially two-dimensional. The wave fronts were long, undisturbed by wind or wave breaking, and approached with crests parallel to the line of the breakwater.

In the physical and theoretical models, the ends of the air pocket were sealed. This is not a pre-requisite for a build up of pressure in a volume of air trapped by a wave behind the structure. In order for air to be vented, it must be accelerated. The ends of a pocket may, however, become sealed either by a wave front that arrives as an arc, or because of the plan shape of the breakwater. Air entrapment may be more likely for curved breakwaters, which have the disadvantage because they face in an arc of directions; they are more likely to experience waves attacking directly, i.e. with the wave crest forming a tangent to the curve. An overtopping wave may then enclose an air pocket behind a segment of the breakwater.

6.2. Dynamic effects

Minikin (1950) suggested that structural dynamic effects might have contributed to the failure of the Mustapha breakwater. The importance of dynamic effects in problems of breakwater stability is becoming more widely accepted (see for example Goda, 1994; Oumeraci and Kortenhaus, 1994; Takahashi et

al., 1994). It is therefore appropriate to consider whether the loads measured during the physical model might induce dynamic behaviour. The force time histories of the model exhibited oscillations. Under resonance conditions these can be effective in moving a structure (Oumeraci and Kortenhaus, 1994). It is therefore important to consider whether the prototype period of force oscillation might be similar to the natural period of the structure.

Wave loading tests are usually conducted, and their results interpreted, using the Froude law, according to which;

$$\frac{T_m}{T_p} = \sqrt{\frac{L_m}{L_p}}$$

where T and L are a typical time and length, and the subscripts m and p refer to model and prototype, respectively. The period of oscillation of the force measurements shown in Section 3.2 was approximately 15 ms. The length scale of the experiment was 52.5 so, following Froude, the prototype period of oscillation may be estimated as 0.11 s. This is short compared to the natural period of a typical caisson. However, the Froude relationship does not account for the compressibility of the air, which is clearly a strong determinant of the period at which it oscillates. The relative importance of the elastic forces within the entrapped air is described by the Cauchy number (Ca);

$$\mathrm{Ca} = \frac{\rho V^2}{E}$$

where E is the modulus of elasticity. This is also the Mach number squared once the value of E for air is inserted. In order to produce similarity of elastic forces the Cauchy number must be the same at both scales;

$$\left(\frac{\rho V^2}{E}\right)_m = \left(\frac{\rho V^2}{E}\right)_p$$

or

$$\left(\frac{\rho L^2}{ET^2}\right)_m = \left(\frac{\rho L^2}{ET^2}\right)_p$$

where V and ρ are velocity and density, respectively. Since the density and modulus of elasticity of

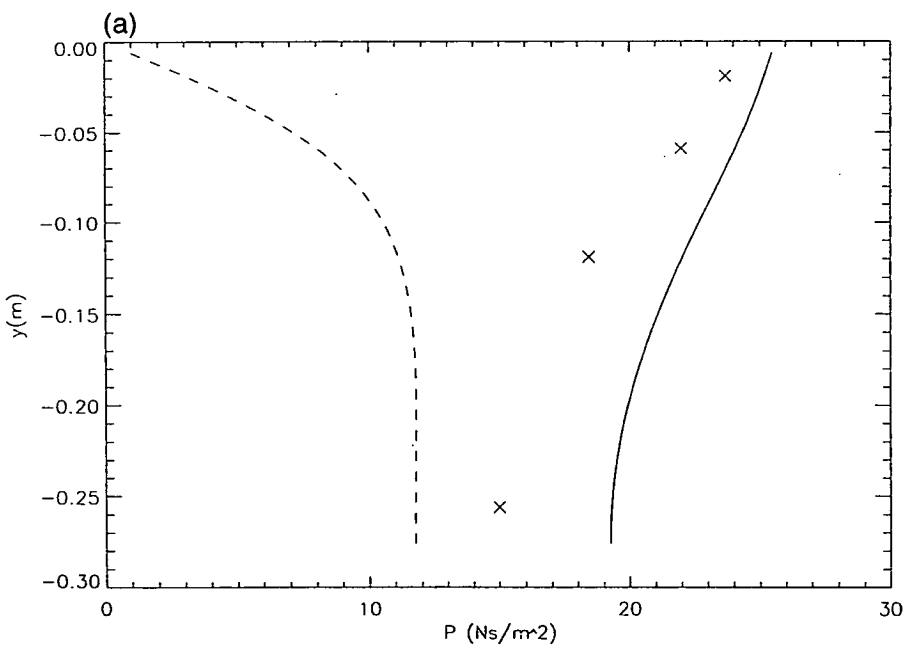

Fig. 13. (a, b and c) Pressure impulse on the back of the caisson for waves A, B and C, respectively. Crosses denote values measured with the rear face transducers, the broken lines represent the pressure impulse on the wall as predicted by Eq. (4), and the solid lines the predictions corrected for the presence of the air pocket (Eq. (5)).

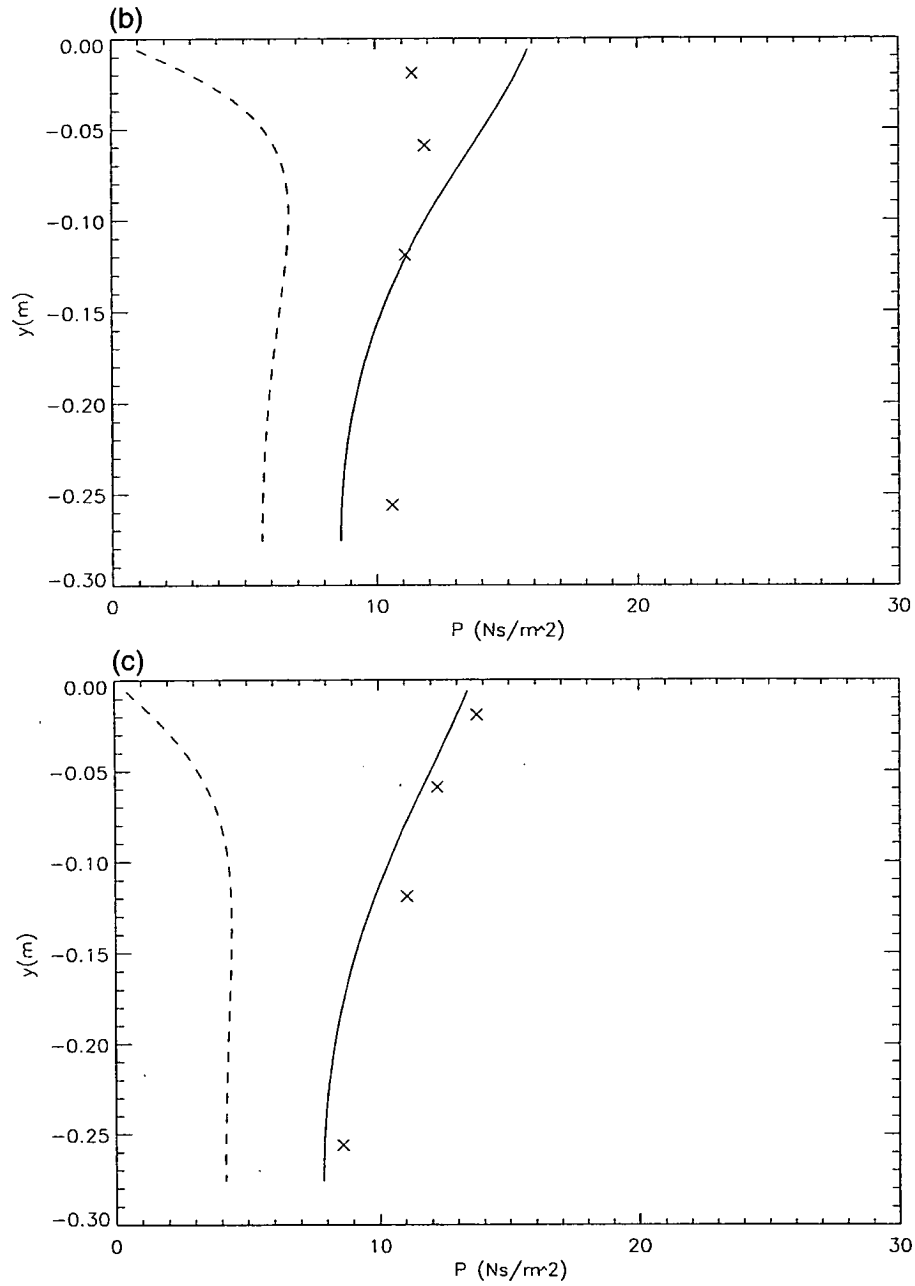

Fig. 13 (*continued*).

the air is equal at both scales, the expression reduces to:

$$\frac{T_m}{T_p} = \frac{L_m}{L_p}$$

so that the time and length scales are equal. The case of air entrapped by an overtopping crest is complicated by the added mass of the water surrounding it. The theoretical model which describes a situation most similar to the one in question was provided by Topliss et al. (1992), and tested against laboratory results by Hattori et al. (1994). This describes the entrapment and compression of a pocket of air in front of a vertical structure and shows, in that case,

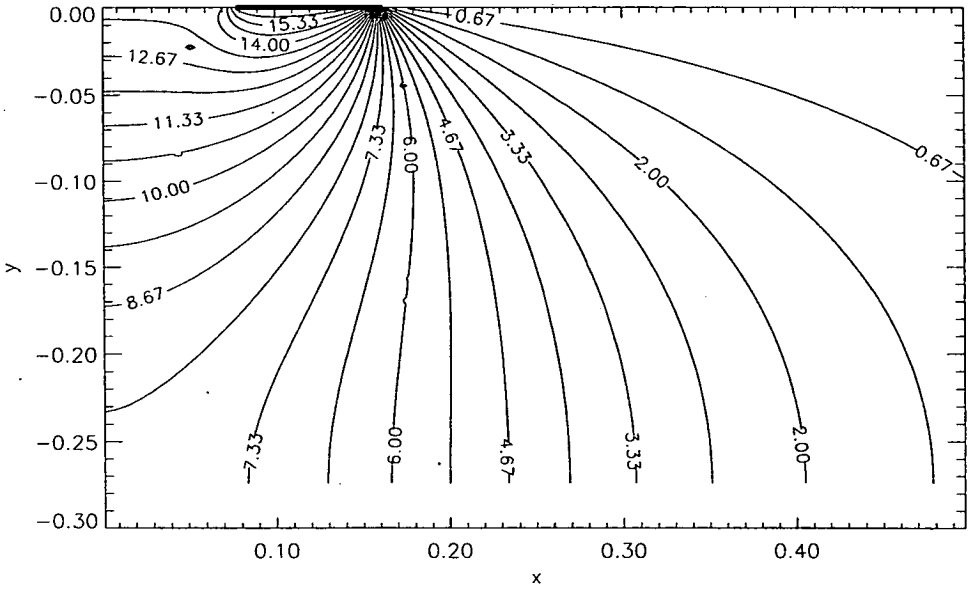

Fig. 14. Pressure impulse under the impacting jet for wave C.

that the time scale was somewhat larger than the length scale. There is therefore evidence that scaling the period of oscillation by the length scale provides a reasonable estimate of the prototype period. Following the Cauchy relationship, the prototype period of oscillation of the model results may be estimated as 0.8 s. This is very close to some of the natural periods of oscillation of prototype breakwaters measured by Lamberti and Martinelli (1998). It is therefore possible that the effectiveness of the seaward loads and moments that occur during the plunge of a prototype wave may be increased by dynamic response of the structure. However, it should be noted that the relative magnitude of the air pressure oscillations will be reduced at prototype scale. Consequently, their influence on the structure may be small, even under resonant conditions.

6.3. Other scale effects

It is generally accepted that wave impact phenomena are affected by scale because of compressibility effects caused by aeration. Higher percentages of entrained air have been measured with marine waves than laboratory waves due to the effects of both wave size and water chemistry (see Walkden, 1999; Crawford, 1999). For the reasons already discussed, this leads to an extension of the time scale in the prototype, relative to the model. This may reduce load maxima and affect the applicability of pressure impulse theory at the large scale. Another scale effect may result from the more significant air drag at the larger scale that may tend to reduce the impact velocity and increase the impact duration.

6.4. Effectiveness of the theoretical model

Formula (5) gives a good estimate of the impulses that occurred with the experimental breakwater. However, the restrictions on the application of pressure-impulse theory must be noted. The impact must be "violent" as defined with two conditions:

- The maximum pressure should be significantly higher than associated hydrostatic pressures.
- $\Delta t \ll L/U$, where Δt is the time scale of the impact (in this case the period of integration), and L and U are the length and velocity scales, respectively. In this case the length scale $(L) = a$, the length of the jet impact on the free surface (see Fig. 11) and the velocity scale $(U) = W$.

Further, for the laboratory experiments, the extent and velocity of the falling jet could be estimated

from video, whereas there is as yet no good estimate of these quantities for overtopping jets whether in prototype or laboratory scale.

7. Concluding remarks

Seaward failure should be recognised as a significant failure mode of vertical breakwaters: there has been an example of a prototype structure failing in this way, and other cases of lesser seaward tilting. In some cases, failure is not wholly attributable to better-documented failure modes such as foundation failure. Waves overtopping breakwaters can produce transient seaward forces that are large relative to landward loads when they plunge into the harbour water. This may explain, at least in part, the observed seaward motion. Air trapped by the plunging wave plays an important role, the pressure impulse it causes could be as much as 80% of the contribution by the plume impact. In addition, oscillations in the size of the pocket lead to force fluctuations that may cause dynamic amplification of structural motion. The risk of seaward failure is probably greatest for structures that are specially designed to allow overtopping in order to reduce landward loads, so that the structure size can be decreased. Such structures would be more likely to experience plunging wave induced seaward loads and have less mass to resist them, and should therefore be assessed for seaward stability.

8. Further work

Further research into dynamic effects, aeration and scale effects, extreme wave events and marine measurements are needed to develop understanding of breakwater failures whether towards the sea or the land. However, a great deal has already been achieved under the PROVERBS project (Oumeraci et al, 1999).

To investigate this failure mode further, more consideration is required of the dynamic behaviour of the structure and its response, for which the phase relationships between the different seaward and landward loads is required. It is expected that three-dimensional tests would provide data on the effect on the overtopping plume and the entrapped air for a breakwater with a curved front wall. Also, random wave tests would help to identify the frequency of occurrence of overtopping events and the proportion that generate significant seaward impulses.

In order to develop the theoretical model further, comparisons should be made with other experiments and in particular with those at prototype scale. In addition, little is known about the mechanism of wave overtopping. Tests are needed to predict the form of the overtopping plume for a given wave and structure.

Further work is required to investigate how to convert the pressure impulse predicted with Eq. (5) into pressure–time and force–time histories. It may be a fair approximation to assume that these will be triangular (see for example Goda, 1994; Takahashi et al., 1994; Oumeraci and Kortenhaus, 1994; Walkden et al., 1996) in which case the problem may be principally one of predicting the duration. The results indicate that this may be determined, for the most significant events, by the compression characteristics of the air pocket. At the present time, there is no good model for the effect of air pockets on impacts, especially for a complex situation such as this, although Wood (1997) and Wood et al. (2000) were reasonably successful in modelling a direct impact on a wall with an air pocket. Ultimately, more results are required, particularly from measurements conducted at larger or prototype scale.

Acknowledgements

Support of the European Commission, Directorate General XII, Science, Research and Development, contract number MAS3-CT95-0041 PROVERBS, is gratefully acknowledged. The authors would also like to thank Jentsje van der Meer for originally suggesting this line of research and Bill Easson for his advice and guidance at Edinburgh.

References

Bullock, G.N., Crawford, A.R., Hewson, P.J., Bird, P., 1999. Characteristics of wave impacts on a steep fronted breakwater. Proc. Coastal Structures '99. Santander, Spain. pp. 455–463.

Chan, E., Melville, W., 1988. Deep-water plunging wave pressures on a vertical wall. Proceedings of the Royal Society of London 417, 95–131.

Cooker, M.J., Peregrine, D.H., 1992. Wave impact pressure and its effect upon bodies lying on the sea bed. Coastal Engineering 18, 205–229.

Cooker, M.J., Peregrine, D.H., 1995. Pressure-impulse theory for liquid impact problems. J. Fluid Mechanics 297, 193–214.

Crawford, A.R., 1999. Measurement and analysis of wave loading on a full scale coastal structure. PhD Thesis, University of Plymouth, UK.

Goda, Y., 1967. The fourth order approximation to the pressure of standing waves. Coastal Engineering in Japan 10, 1–11.

Goda, Y., 1974. New wave pressure formulae for composite breakwaters. Proc. 14th Int. Conf. on Coastal Engineering. ASCE, pp. 1702–1720.

Goda, Y., 1992. The design of upright breakwaters. Proc. of the Short Course on the Design and Reliability of Coastal Structures, attached to the 23rd Int. Conf. on Coastal Engineering. ASCE, pp. 547–568.

Goda, Y., 1994. Dynamic response of upright breakwaters to impulsive breaking wave forces. Coastal Engineering 22, 135–158.

Hager, W., 1994. Energy Dissipaters and Hydraulic Jump. Kluwer Academic Publishers, Dordrecht, The Netherlands.

Hattori, M., Arami, A., Yui, T., 1994. Wave impact pressure on vertical walls under breaking waves of various types. Coastal Engineering 22, 79–114.

Juhl, J., 1994. Danish experience and recent research on vertical breakwaters. Proc. Conf. On Wave Barriers in Deep Waters. Yokosuka. pp. 154–171.

Lamberti, A., Martinelli, 1998. Prototype measurements of the dynamic response of caisson breakwaters. Proc. 26nd Int. Conf. on Coastal Engineering. ASCE, pp. 1972–1985.

McConnell, K., Flohr, H., Allsop, N.W., 1996. Seaward wave loading on vertical coastal structures. Proc. Coastal Structures '99. Santander, Spain. pp. 447–454.

Minikin, R.R., 1950. Winds, Waves and Maritime Structures. Charles Griffin, London.

Müller, G., 1997. Propagation of wave impact pressures into water filled cracks. Institute of Civil Engineers, Water and Maritime 124 (2), 79–85.

Oumeraci, H., 1994. Review and analysis of vertical breakwater failures—lessons learned. Coastal Engineering 22, 3–29.

Oumeraci, H., Kortenhaus, A., 1994. Analysis of the dynamic response of caisson breakwaters. Coastal Engineering 22, 159–183.

Oumeraci, H., Klammer, P., Partenscky, H.W., 1993. Classification of breaking wave loads on vertical structures. Journal of Waterways, Port, Coastal and Ocean Engineering, ASCE 119 (4), 381–397.

Oumeraci, H., Allsop, N.W., Groot, M., Crouch, R., Vrijling, J., Kortenhaus, A., Voortman, H., 1999. Probabilistic design tools of vertical breakwaters. Forthcoming book, ca. 300 pp. Balkema.

Takahashi, S., Tanimoto, K., Shimosako, K., 1994. Dynamic response and sliding of breakwater caisson against impulsive breaking wave forces. Proc. Conf. on Wave Barriers in Deep Waters. Yokosuka. pp. 362–401.

Topliss, M., Cooker, M., Peregrine, D.H., 1992. Pressure oscillations during wave impact on vertical walls. Proc. 23rd Int. Conf. on Coastal Engineering. ASCE, pp. 1639–1650.

Walkden, M.J., 1999. Model wave impulse loads on caisson breakwaters: aeration, scale and structural response. PhD Thesis, University of Plymouth, UK.

Walkden, M.J., Hewson, P.J., Bullock, G.N., 1996. Wave impulse prediction for caisson design. Proc. 25th Int. Conf. on Coastal Engineering. ASCE, Orlando, USA. pp. 2584–2597.

Walkden, M.J., Bruce, T.B, Easson, W, 1998. Seaward loads on caisson breakwaters. Proc. MAST III PROVEBS Workshop. Naples, Italy, 9 pages.

Wood, D.J., 1997. Pressure impulse impact problems and plunging wave jet impact. PhD Thesis, University of Bristol, UK.

Wood, D.J., Peregrine, D.H., 1996. Wave impact beneath a horizontal surface. Proc. 25th Int. Conf. on Coastal Engineering. Orlando, USA, ASCE, pp. 2573–2583.

Wood, D.J., Peregrine, D.H., Bruce, T.B., 2000. Study of wave impact against a wall with pressure-impulse theory: part 1, trapped air. Journal of Waterways, Port Coastal and Ocean Engineering, ASCE 126, 182–190.

Appendix F: Bruce *et al.*, 2001a

Bruce, T, Allsop, N.W.H. & Pearson, J. (2001a), *Violent overtopping of seawalls – extended prediction methods*, Proc. "Breakwaters, coastal structures and coastlines", pp 245–256, ICE, London, Thomas Telford, ISBN 0 7277 3042 8

Appendix F
Bruce *et al.*, 2001a

Bruce, T, Allsop, N.W.H. & Pearson, J. (2001a), *Violent overtopping of seawalls – extended prediction methods*, Proc. "Breakwaters, coastal structures and coastlines", pp 245–256, ICE, London, Thomas Telford, ISBN 0 7277 3042 8

F.1 Declaration of contribution

At the time of preparation of this paper Pearson was a post-doctoral Research Engineer working at Edinburgh under the author's guidance. The author led the physical model part of the EPSRC *VOWS* project (Section 3.3 was closely involved in all stages of the research leading to the paper, from preparation of the funding application through to the final drafting and editing of the paper. This involvement included a great deal of time spent on a day-to-day basis with Pearson in the design, setting up and commissioning of what was then a new test arrangement at Edinburgh. The tests themselves were carried out most ably by Pearson. The author then spent many hours together with Pearson (and later also in discussion with Allsop) pouring over the new data, and in synthesis of conclusions.

The subsequent, published discussion relating to the h_* parameter (see Section 3.4.2 was led by the author after discussion with van der Meer.

F.2 Published paper

overleaf

Violent overtopping of seawalls – extended prediction methods

TOM BRUCE [1], WILLIAM ALLSOP [2], JONATHAN PEARSON [1]
[1] Division of Engineering, University of Edinburgh, Edinburgh, EH9 3JL
[2] University of Sheffield, c/o HR Wallingford, Wallingford, OX10 8BA UK

SUMMARY
This paper reports results of a collaborative project to develop new and/or improved prediction formulae for overtopping discharges at steep or vertical walls where impulsive wave breaking is significant or dominant. It is found that methods described for largely non-impulsive conditions by Besley *et al* (1998) remain good predictors (typically within a factor of two) even under highly impulsive wave attack. Over the tested conditions, near-vertical walls of steep batter (10:1 or 5:1) show discharges in excess of those predicted by Besley *et al* (1998). Initial analysis suggests that an amplification factor based on the predicted mean dimensionless discharge for the vertical case should be applied. For the 10:1 battered wall, the average increase is by a factor of 1.3, and for the 5:1 battered wall, the factor is 1.4.

For the first time, systematic measurements have been made of overtopping discharge "throw" velocities to advance predictions of overtopping velocities / trajectories for safety assessments. For non-impacting waves at a vertical wall, the largest velocities of the discharge "throw" are found to be roughly constant at 2.5 times the inshore wave celerity. For highly impulsive wave / structure combinations, throw velocities of up to 6.5 times the inshore wave celerity have been measured.

1. INTRODUCTION
Steep, vertical and/or composite seawalls protect many kilometres of road, rail and port-related infrastructure around the UK against wave overtopping. Such walls are also widely used for cliff protection, *eg*, sections of the southern Italian coast, and port installations world-wide.

The crest levels of many of these walls were originally designed to a nominal run-up limit, usually based upon relatively simple tests with regular waves. Later analysis for overtopping, if performed at all, will generally have predicted a mean overtopping discharge over the peak of a "design" storm event. For analysis of acceptability of this overtopping performance, the predicted mean discharges will have been compared with suggested limits for safety of the structure, or for use of the zone behind, *eg* Owen (1980), Simm (1991). With wider appreciation of the safety offered to society and infrastructure by these defences, it is now clear that this approach suffers from two important short-comings.

Firstly, nearly all predictions of mean overtopping discharge rates are based on general empirical formulae fitted to laboratory measurements, see for example Goda *et al* (1975), Owen (1982), De Waal *et al* (1996), Hedges & Reis (1998), Van der Meer *et al* (1998). These

formulae mainly cover pulsating wave conditions, yet some types of seawall (particularly composite vertical walls) can suffer sudden and violent overtopping for conditions where waves break impulsively against the wall. Studies on overtopping by Besley *et al* (1998), and on wave forces by Allsop *et al* (1996), indicate configurations of vertical / composite walls for which impulsive breaking may occur. Those findings demonstrated the need to determine whether design methods based upon largely pulsating conditions may be safely used or require adjustment under strongly impulsive conditions.

Secondly, analysis by Besley *et al* (1998) extended research by Allsop *et al* (1995), and previously Franco *et al* (1994) to develop new methods to predict peak overtopping volumes. These showed that peak volumes and flow velocities are strongly influenced by the form of wave breaking, but that for a significant range of structures, reliable design methods were not yet available. Allsop *et al* (1996) showed that impulsive breaking is particularly severe for steep or vertical walls with steep beaches or rock mounds. Analysis by Besley *et al*, (1998) developed guidance on peak overtopping discharges or volumes, but showed that present methods may significantly under-estimate volumes under impulsive wave breaking. The new data and empirical methods from this study substantially extend the earlier work on vertical walls to derive prediction methods for:

- Overtopping discharge under strongly impulsive conditions
- Battered (near vertical) walls
- Composite walls

This paper reports early results of the EPSRC-funded collaborative VOWS (Violent Overtopping of Waves at Seawalls) project to develop new / improved prediction formulae for mean and peak overtopping discharges where wave breaking at the structure is significant. Also, for the first time, systematic measurements have been made of throw velocities to develop predictive methods for velocities / trajectories for safety assessments, and the first results of these tests are reported here. Physical model tests in VOWS at Edinburgh / Sheffield Universities are complemented by numerical modelling by project partners Manchester Metropolitan University, early results of which are reported by Causon & Ingram (2000).

2. EXPERIMENTAL DESIGN

The physical modelling under VOWS was initially intended to be in two stages:

- Two-dimensional wave flume testing at Edinburgh to study impulsive processes in detail, and to derive data on overtopping processes under impulsive events;
- Three-dimensional wave basin testing at Wallingford to quantify the effects of oblique attack, and study overtopping at junctions or elbows.

During the first year of the VOWS project, the physical modelling team won access under the EC "HYDRALAB" project to a large wave flume at Barcelona for testing at a much larger scale, so the VOWS project will extend to include:

- Large scale 2-d tests to quantify overtopping process at scales closer to prototype.

The 2-d tests at small-scale were all completed in the wave channel in the Division of Engineering at University of Edinburgh. The channel is 20 m long, 0.4 m wide and has an operating water depth of 0.7 m. The channel is equipped with an absorbing flap-type wavemaker. The model structures were made out of perspex.

Overtopping discharges were directed via a chute into a measuring container suspended from a load cell. Individual overtopping events were detected by two parallel strips of metal tape

run along the structure crest which acted as a switch closed by the water. Wave-by-wave overtopping volumes were measured by determining the increment in the mass of water in the collection tank after each overtopping event following the general approach first used by Franco *et al* (1994), and subsequently applied at other laboratories in UK / Europe. All tests at Edinburgh were videotaped for measurements of throw velocities. Wave pressures on the front face of the structure were also recorded.

The principal objective of these 2-d tests was to extend existing prediction methods into regimes in which wave breaking at or onto the structure is significant. The core set of tests was carried out for a simple vertical wall with approach uniform bathymetries of 1:10 and 1:50. The matrix of conditions [significant wave height at the toe of the structure (H_s), peak period (T_p), water depth at structure (h) and crest freeboard (R_c)] is shown in Appendix 1, Table 1. Each test consisted of a sequence of approximately 1000 irregular waves of a JONSWAP spectrum with $\gamma = 3.3$. Selected tests were multiply repeated, while others were re-run with longer and shorter test lengths. Conclusions from these tests relating to scatter and statistical uncertainties are outwith the scope of this paper, and are presented in Pearson *et al* (2001).

After the core tests on the vertical wall, three further sets of tests were then completed to:

- Explore the influence of moving from vertical walls to walls with small batters, 10:1 and 5:1, which are widespread in practice;
- Determine the effect of moving from vertical to composite structures;

Allsop *et al* (1995) demonstrated that overtopping processes are strongly influenced by the form of the incident waves. When waves are small compared to water depth, the waves impinging on a vertical / composite wall are generally reflected back. If the waves are large relative to water depth, then they can break onto the structure, leading to significantly more abrupt overtopping characteristics. These observations led to formulation of a wave breaking parameter, h_*., given by:

$$h_* = \frac{h}{H_s}\left(\frac{2\pi h}{gT^2}\right) \qquad (1)$$

Allsop *et al* (1995) noted that reflecting or pulsating waves predominate when $h_* > 0.3$, and that impacting waves where more likely to occur when $h_* < 0.3$. New dimensionless discharge (Q_h) and freeboard parameters (R_h), incorporating h_* were established, and were given by:

$$Q_h = Q/(gh^3)^{0.5}/h_*^2 \qquad (2)$$

$$R_h = (R_c/H_s)\,h_* \qquad (3)$$

where Q is the mean overtopping discharge per metre run.

3. OVERTOPPING CHARACTERISTICS

3.1 Vertical Walls

Measurements of mean overtopping discharge (Q_h) for the simple vertical wall show agreement with Besley *et al*'s (1998) method over the full range of test conditions studied, typically to within a factor of two, see Figure 1. The largest proportion of impulsive events was recorded under test conditions "2A", see Appendix 1, Table 1. It is of note that, even under these most impulsive conditions, the results from this present study exhibit similar characteristics to the predictive method of Besley (1998). It may be concluded that the transition between pulsating and impulsive conditions appears not to influence Q_h.

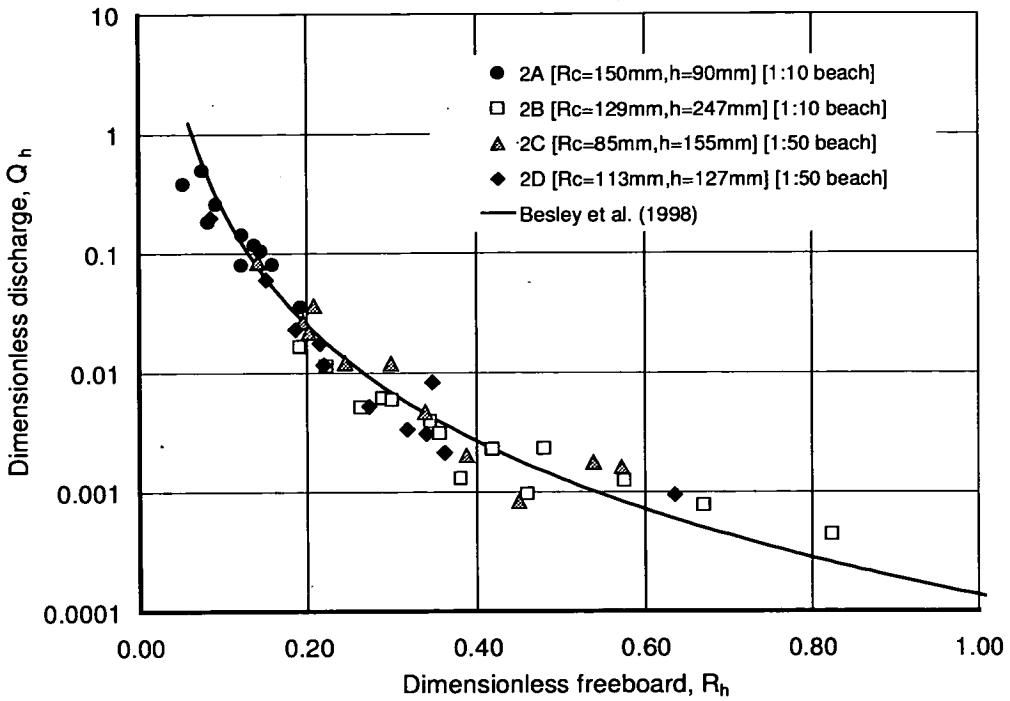

Figure 1: Overtopping discharge on a plain vertical wall, compared to the prediction of Besley *et al* (1998).

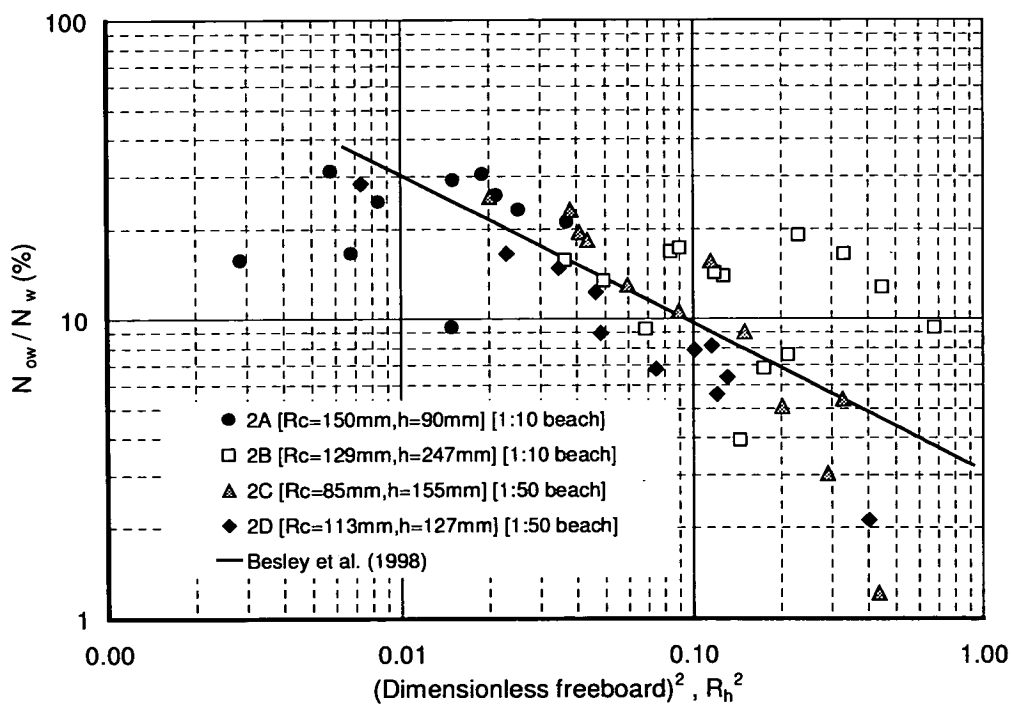

Figure 2: Percentage of waves overtopping a vertical wall, compared to Besley *et al* (1998)..

A parameter which is vital in predicting peak overtopping volumes and statistics of wave-by-wave overtopping volumes is the number or proportion of overtopping waves (N_{ow}). The variation of N_{ow} with freeboard for vertical wall, as quantified from these tests, is shown in Figure 2. It is noticeable that the results of N_{ow} deviate significantly from the prediction, which leads to uncertainty in adopting previous prediction methods for individual maxima. As for Q_h, the transition between pulsating and impulsive conditions is not apparent in the behaviour of N_{ow} within the range of conditions / configurations tested.

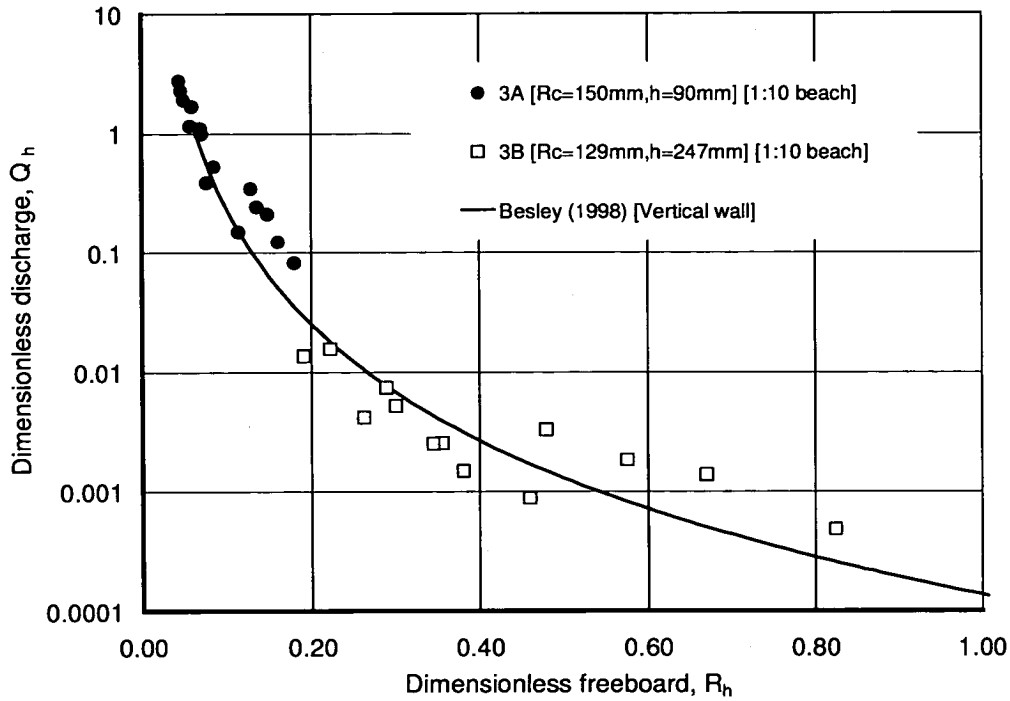

Figure 3: Overtopping discharge on a 10:1 battered wall, compared to the prediction (for vertical walls) of Besley *et al* (1998).

Careful analysis of the problem in defining N_{ow} precisely, reduces to a particular difficulty the exact definition of an "overtopping event". Clearly such events cannot constitute *all* occasions when some water passes over the wall, as that would increase with each improvement in measurement precision, but must there be a limit of only one overtopping event per incident wave? A method to overcome these difficulties by defining a consistent threshold level before an overtopping event is counted is therefore under development. Only then can a useful improvement of the N_{ow} prediction tool be made.

3.2 Near-Vertical Walls

The matrix of tests for a vertical wall was repeated for near-vertical walls with 10:1 and 5:1 batter for a 1:10 approach bathymetry. Measurements of Q_h for 10:1 and 5:1 walls (Figures 3 and 4 respectively) indicate discharges slightly in excess (by factors of up to 3 – 4 for certain conditions) of those measured for the vertical wall (Figure 1) and those predicted by Besley *et al* (1998) over a wide range of dimensionless freeboards. For the tested conditions, the 10:1 and 5:1 battered wall exhibit similar overtopping characteristics. Initial analysis suggests that an amplification factor based on the predicted mean dimensionless discharge for the vertical case should be applied. For the 10:1 battered wall, the average increase is by a factor of 1.3, and for the 5:1 battered wall, the factor is 1.4.

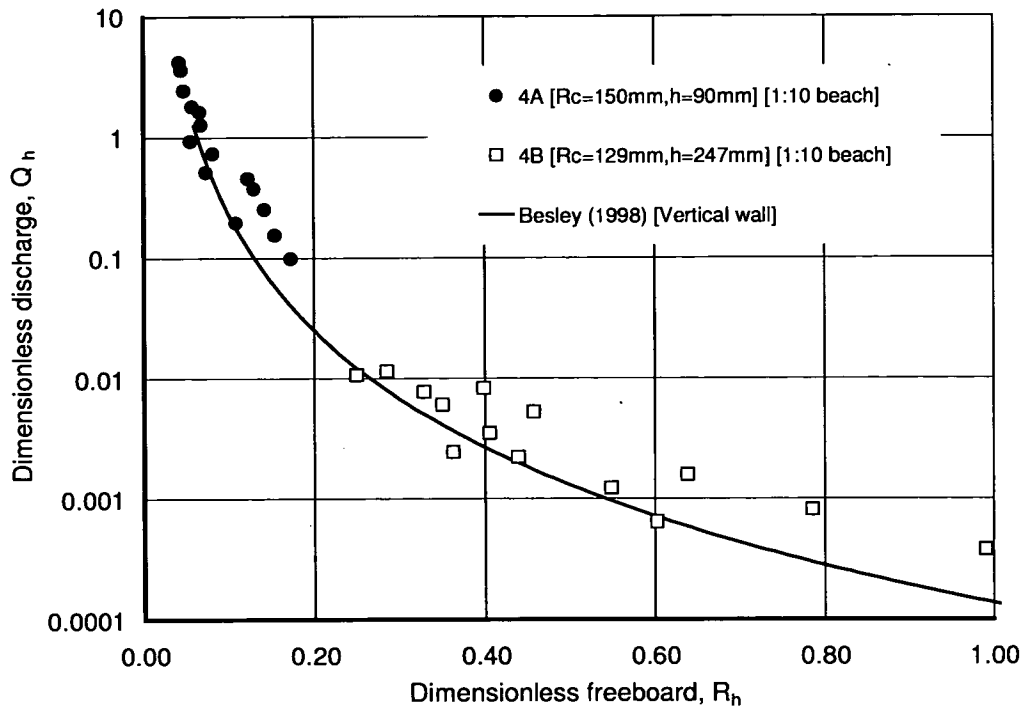

Figure 4: Overtopping discharge on a 5:1 battered wall, compared to the prediction (for vertical walls) of Besley *et al* (1998).

3.3 Composite Structures

Besley *et al* (1998) referred to the investigations of Allsop *et al* (1995) in which the overtopping characteristics of composite structures were investigated. In a similar analytical procedure to vertical structures, a wave breaking parameter d_* was defined by:

$$d_* = \frac{d}{H_s}\left(\frac{2\pi h}{gT^2}\right) \tag{4}$$

which classified whether the mound was large or small. If $d_* < 0.3$, the mound was classified as small and similar overtopping characteristics for vertical wall are predicted. However when $d_* > 0.3$, the mound was classified as large and the overtopping characteristics are corrected for the presence of the mound. Within the data available from limited previous studies, Besley *et al* (1998) suggested that it was not possible to distinguish different overtopping performance under impacting or reflecting conditions.

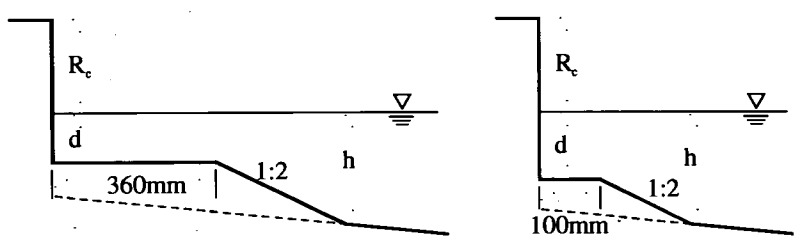

Figure 5: Layout of composite vertical wall for experimental investigation in present study

The present work has, to date studied two vertical-composite structures: one with a large mound (Berm A, Figure 5, left), and one with a small mound/toe berm (Berm B, Figure 5, right)

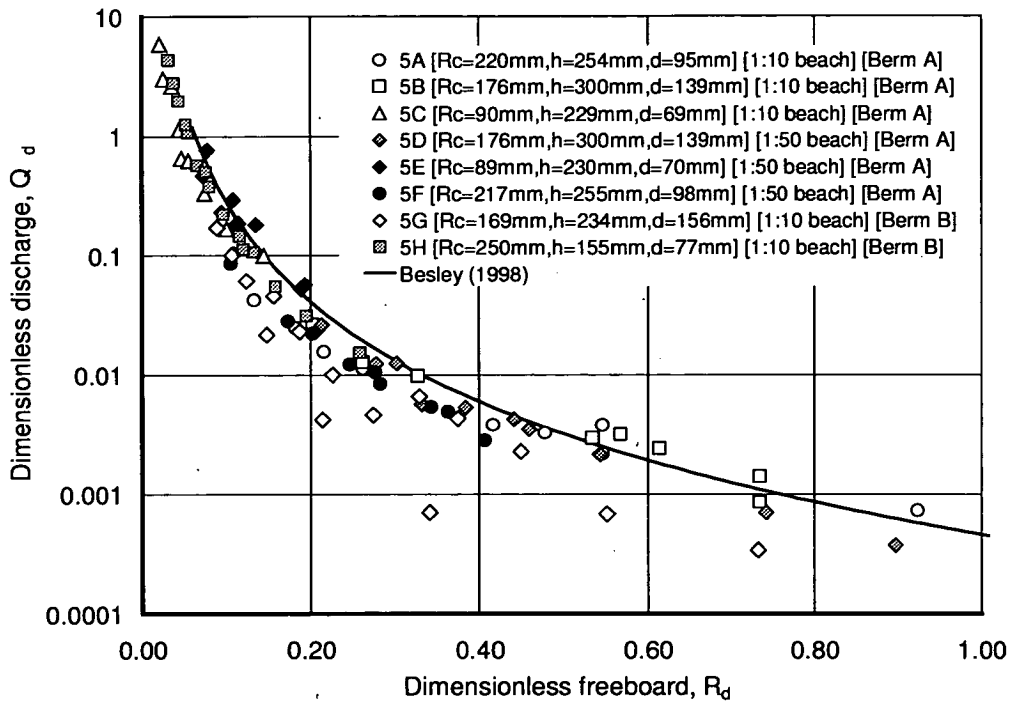

Figure 6: Overtopping discharge on a vertically composite structures with wide berm, compared to the prediction of Besley *et al* (1998).

Mean overtopping discharge (Q_d) measurements for the composite structures (Figure 6) show that the methods of Besley *et al* (1998) may be used as a conservative indicator of Q_d. It is noticeable that Q_d is significantly over-predicted (by factors of up to 10) for some of the small mound (Berm B) conditions. Further tools will be required to better quantify the effect of small and middle-sized mounds. Reflecting and impacting conditions were investigated within this present study but, as with vertical structures, the transition between reflecting and impacting conditions appears not to cause any clear deviation from the prediction method of Besley *et al* (1998).

4. THROW VELOCITY

Video records of the vertical wall tests (test sets 2A, 2B, 2C) were analysed manually and the velocity of the thrown discharge for the largest overtopping events determined. The largest 20 individual overtopping events were selected and, for each, the throw velocity (u_z) was inferred from the "time of flight" of the overtopping water. For each test, the mean of the highest 4% of values of u_z, $u_{z,\,1/25}$ was determined, and this average is plotted here against the wave breaking parameter, h_* (Figure 7).

It is noticeable in Figure 7 that, when $h_* > 0.15$, the non-dimensionalised throw velocity is roughly constant at a value ~2.5, but when $h_* < 0.15$ the non-dimensionalised throw velocity increases very significantly reaching values ~6 and above. This suggests that whilst the mean discharge values discussed in Section 3, above, seem relatively little influenced by changes of wave breaking characteristics, the hazard derived from those discharges may vary dramatically. It is interesting to note that the largest velocities measured here, suggest prototype velocities equivalent to 40 ms^{-1}. Large-scale testing at UPC, Barcelona will provide a much firmer basis for such scaling.

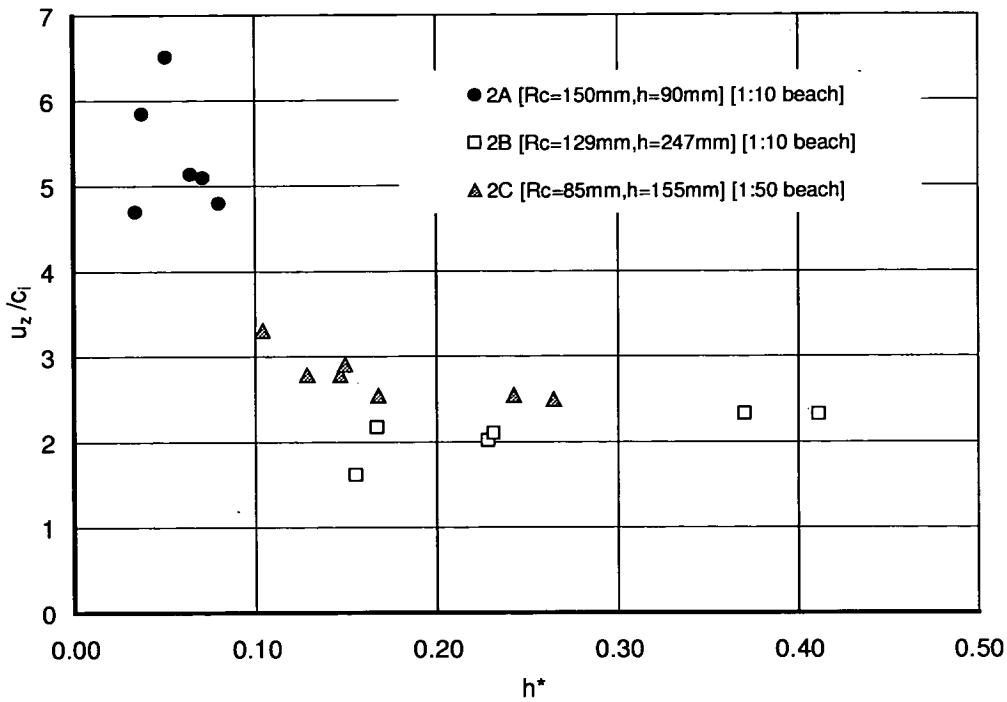

Figure 7: 1/25-level throw velocities $u_{z,\,1/25}$, plotted with h* parameter (vertical wall).

5. CONCLUSIONS

The prediction method of Besley *et al* (1998) for mean overtopping discharge may be used under conditions when impulsive wave action is significant or dominant, with mean discharges remaining well-predicted (typically within a factor of two). The mean overtopping discharge does not appear to be significantly affected by the transition from pulsating to impulsive conditions.

Near-vertical walls of steep batter (10:1 or 5:1) show discharges in excess of those predicted by Besley *et al* (1998). Initial analysis suggests that an amplification factor based on the predicted mean dimensionless discharge for the vertical case should be applied. For the 10:1 battered wall, the average increase is by a factor of 1.3, and for the 5:1 battered wall, the factor is 1.4.

The velocity at which overtopping discharge is thrown has been measured for a range of wave / structure combinations. For pulsating waves at a vertical wall, the velocities appear to be approximately constant at 2.5 times the inshore wave celerity. Throw velocities of up to 6.5 times the inshore wave celerity have been measured under highly impulsive wave / structure combinations. These potentially hazardous conditions occur when $h_* < 0.15$.

ACKNOWLEDGEMENTS

This work is funded by the UK EPSRC (GR/M42312), and supported by the VOWS Management Committee also including members from Manchester Metropolitan University (Derek Causon, David Ingram, Clive Mingham), Posford-Duvivier (Dick Thomas, Keming Hu), Bullen & Co (Mark Breen, Dominic Hames), HR Wallingford (Philip Besley), all of whose input and support is gratefully acknowledged. The VOWS project is also particularly pleased to acknowledge guidance and helpful supervision of their collaborative work of the EPSRC CEWE Project Manager, Michael Owen.

REFERENCES

Allsop, N.W.H., Besley, P. & Madurini, L.. (1995), "Overtopping performance of vertical and composite breakwaters, seawalls and low reflection alternatives", Paper to the final MCS Project Workshop, Alderney.

Allsop, N.W.H., McKenna, J.E., Vicinanza, D. & Whittaker, T.T.J. (1996), "New design methods for wave impact loadings on vertical breakwaters and seawalls", Proc 25th Int. Conf. Coastal Eng., Orlando, ASCE, New York.

Besley, P., Stewart, T. & Allsop, N.W.H. (1998), "Overtopping of vertical structures: new prediction methods to account for shallow water conditions", Proc. Conf. Coastlines, Structures and Breakwaters, Institution of Civil Engineers, Thomas Telford, London.

Causon, D. and Ingram, D. (2000), "Impulsive wave overtopping", abstract submitted to 27th Int. Conf. Coastal Eng., Sydney (ASCE).

De Waal, J.P. Tonjes, P. & van der Meer, J.W. (1996), "Overtopping of sea defences" Proc 25th Int. Conf. Coastal Eng. (ASCE), pp2216-2229, Orlando, ASCE.

Franco, L., de Gerloni, M. & van der Meer, J.W. (1994), "Wave overtopping on vertical and composite breakwaters", Proc 24th Int. Conf. Coastal Eng., Kobe, ASCE.

Goda Y. (1971) "Expected rate of irregular wave overtopping of seawalls" Coastal engineering in Japan, Vol 14, pp 45-51, JSCE, Tokyo.

Goda, Y, Kishira, Y, and Kamiyama, Y. (1975) 'Laboratory investigation on the overtopping rates of seawalls by irregular waves'. Ports and Harbour Research Institute, Vol 14, No. 4, pp 3-44, PHRI, Yokosuka.

Hedges, T.S. & Reis, M.T. (1998), "Random wave overtopping of simple sea walls: a new regression model", Proc. Instn. Civil Engrs. Water, Maritime & Energy, Volume 130, March 1998, Thomas Telford, London.

Owen, M.W. (1980), "Design of seawalls allowing for overtopping", HR Wallingford, Report EX924.

Owen, M.W. (1982), "Overtopping of Sea Defences", Proc. Intl. Conf. On Hydraulic Modelling of Civil Eng. Structures, Coventry, pp469-480, BHRA, Bedford.

Pearson, J., Bruce, T. & Allsop, N.W.H. (2001), "Prediction of wave overtopping at steep seawalls – variabilities and uncertainties", Proc "Waves '01", San Francisco (ASCE).

Simm, J.D. (Editor) (1991), "Manual on the use of rock in coastal and shoreline engineering", CIRIA special publication 83, CUR Report 154, 1991.

Van der Meer, J.W., Tonjes P. & de Waal J.P (1998) "A code for dike height design and examination" Proc. Conf. Coastlines, Structures and Breakwaters, Institution of Civil Engineers, March 1998, Thomas Telford, London.

APPENDIX 1: TEST CONDITIONS

Structure Configuration	Test Series	Configuration	Nominal wave period T_s [s]	Significant wave height H_{si} [mm]
Vertical	2A [1:10 beach]	R_c = 150mm h = 90mm	1.0	63, 67, 69, 70, 81
			1.33	63, 70, 76, 82
			1.6	62, 77, 82
	2B [1:10 beach]	R_c = 129mm h = 247mm	1.0	71, 79, 86, 92, 100
			1.33	81,93, 94, 100, 102
			1.6	71, 74, 89, 97, 105
	2C [1:50 beach]	R_c = 85mm h = 155mm	1.0	46, 55, 58, 61
			1.33	39, 58, 63, 64
			1.6	34, 44, 52, 62
	2D [1:50 beach]	R_c = 113mm h = 127mm	1.0	55, 57, 58
			1.33	53, 57, 58
			1.6	30, 40, 59, 62
10:1 batter	3A [1:10 beach]	R_c = 150mm h = 90mm	1.0	63, 66, 67, 69, 70
			1.33	63, 70, 76, 77, 82
			1.6	62, 71, 77, 79, 87
	3B [1:10 beach]	R_c = 129mm h = 247mm	1.0	71, 79, 86, 92, 100
			1.33	81,93, 94, 100, 102
			1.6	71, 74, 89, 97, 105
5:1 batter	4A [1:10 beach]	R_c = 150mm h = 90mm	1.0	63, 66, 67, 69, 70
			1.33	63, 70, 76, 77, 82
			1.6	62, 71, 77, 79, 87
	4B [1:10 beach]	R_c = 129mm h = 247mm	1.0	71, 79, 86, 92, 100
			1.33	81, 84, 90, 93, 100
			1.6	58, 71, 74, 89
Composite (Berm A)	5A [1:10 beach]	R_c = 220mm h = 254mm d = 95mm	1.0	64, 86, 92
			1.33	63, 63, 98
			1.6	63, 74, 88
	5B [1:10 beach]	R_c = 176mm h = 300mm d = 139mm	1.0	67, 89, 95
			1.33	63, 63, 95
			1.6	59, 87, 100
	5C [1:10 beach]	R_c = 90mm h = 229mm d = 69mm	1.0	46, 55, 63, 79
			1.33	63, 81
			1.6	45, 57, 74
	5D [1:50 beach]	R_c = 176mm h = 300mm d = 139mm	1.0	52, 66, 71, 77
			1.33	46, 59, 70, 82
			1.6	55, 60, 68, 91
	5E [1:50 beach]	R_c = 89mm h = 230mm d = 70mm	1.0	42, 53, 56
			1.33	34, 44, 53
			1.6	35, 39, 45
	5F [1:50 beach]	R_c = 217mm h = 255mm d = 98mm	1.0	60, 65, 70
			1.33	51, 61, 71
			1.6	49, 57, 76
Composite (Berm B)	5G [1:10 beach]	R_c = 169mm h = 234mm d = 156mm	1.0	63, 72, 79, 86, 91
			1.33	70, 79, 87, 96, 103
			1.6	73, 89, 96, 104, 114
	5H [1:10 beach]	R_c = 250mm h = 155mm d = 77mm	1.0	63, 72, 79, 86, 91
			1.33	70, 79, 87, 96, 103
			1.6	73, 89, 96, 104, 114

Appendix G: Allsop *et al.*, 2003

Allsop, N.W.H., Bruce, T., Pearson, J., Alderson, J. & Pullen, T. (2003), *Violent overtopping at the coast - when are we safe?* International Conf. on Coastal Management 2003, pp54–69, ICE London, Thomas Telford, ISBN 0-7277-3255-2

Appendix G
Allsop *et al.*, 2003

Allsop, N.W.H., Bruce, T., Pearson, J., Alderson, J. & Pullen, T. (2003), *Violent overtopping at the coast - when are we safe?* International Conf. on Coastal Management 2003, pp54–69, ICE London, Thomas Telford, ISBN 0-7277-3255-2

G.1 Declaration of contribution

This publication was the result of a genuine team effort between *VOWS* project physical modellers at Edinburgh and HR Wallingford. The author was involved in the design of the paper for the particular audience, and in the drafting and editing of the final text.

G.2 Published paper

overleaf

Violent wave overtopping at the coast, when are we safe?

WILLIAM ALLSOP [1], TOM BRUCE [2], JONATHAN PEARSON [2],
JOHN ALDERSON [3] & TIM PULLEN [3]
[1] University of Southampton, c/o HR Wallingford, Wallingford, OX10 8BA UK
[2] Division of Engineering, University of Edinburgh, Edinburgh, EH9 3JL
[3] HR Wallingford, Wallingford, OX10 8BA UK

SUMMARY

Every year, people drown being swept from UK coastal paths, breakwaters and seawalls (at least 12 deaths in 1999 – 2002). It is likely that the people concerned had little true idea of the hazard to which they were exposed, yet most overtopping hazards are easily predicted using results of recent research. This paper uses the results of recent and current UK and European research to: improve understanding of overtopping, including effects of different types of wave breaking; improve prediction methods for wave overtopping discharges and velocities; and extend / validate suggested limits to acceptable overtopping. The paper re-states and extends advice in the EA overtopping manual by Besley (1999) applying new information / advice where appropriate.

1. WAVE OVERTOPPING AT THE COAST

Many kilometres of urban infrastructure around coasts of UK and Europe are protected against wave overtopping and/or erosion by steep sea walls, often vertical or near vertical, sometimes with a toe berm. Such walls (Fig. 1) are also widely used to protect railway lines or roads along the coast, cliff protection as seen along lengths of the southern England and Italian coasts, and around ports world-wide.

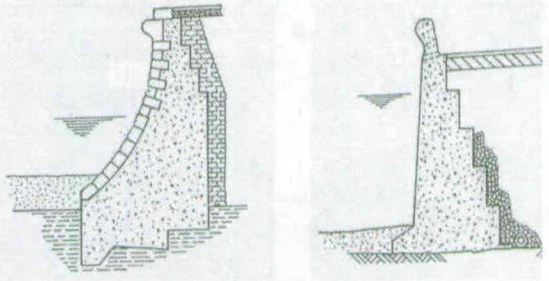

Fig. 1 Vertical or battered seawalls

Fig. 2 Overtopping watching at Oostende

It is generally appreciated that seawalls reduce wave overtopping, but a more sophisticated understanding is needed to be aware that seawalls cannot always stop overtopping. Under storm action, waves still overtop seawalls, sometimes frequently and sometimes violently. These processes may excite considerable public interest, see the example in Fig. 2 at Oostende where tourists gather during storms, and in Figs. 3 & 4 at Marine Drive, Scarborough, before the 2002 / 2003 improvements.

In winter storms, wave overtopping may cause local flooding, and/or potential hazards to people close behind the seawall. The most severe hazards to pedestrians are probably:

- direct impact causing direct injury;
- direct impact causing the person to fall backwards against a hard object;
- impact or flow velocities causing the person to lose their footing;
- backwash flows carrying a person off the wall into the sea.

Less severe hazards are getting wet and cold (itself a potential hazard); or being frightened by the threat of inundation.

Fig. 3 Overtopping on Marine Drive, Scarborough, 2002

Fig. 4 Public attitude to overtopping hazard!

Other hazards affect drivers and passengers in road vehicles or trains, see particularly the example in Fig. 5 of a driver swerving to avoid an overtopping wave, and the discussion by Kimura et al (2000) on road accidents on a coastal highway in Japan. In the UK, a number of coastal railway lines suffer significant overtopping, although the consequent dangers are not well-established.

Fig. 5 Driving hazard from overtopping

It is generally understood that climate change may cause sea-level rise and perhaps more severe storms, so many involved in coastal management are aware that there will be more locations where overtopping hazards will increase, although most analysis hitherto has concentrated on the contribution to flooding. Many of the public are also aware of climate change and flooding, but are generally much less aware of the hazards or frequency of seawall overtopping. Indeed few are aware that at least 12 people have been killed in the UK by wave overtopping or related processes during 1999-2002, and approximately 60 killed in Italy over the last 20 years. Any gaps in understanding common hazards on the shoreline are further aggravated by media references to occurrence of "freak waves", often phenomena that could be predicted by an informed person.

This paper uses results from VOWS, CLASH and SHADOW research projects to identify overtopping hazards; and to describe overtopping performance of steep and composite seawalls which frequently defend urban infrastrusture. The paper analyses hazards at a monitored coastal site, and draws in initial results from research in the UK and Europe.

2. OVERTOPPING PROCESSES AND PREDICTIONS

2.1 Wave processes

Any discusion on wave processes requires standard terms. Of these, the most critical processes for overtopping and wave forces are the form and severity of wave breaking. Historically these may have been divided into "breaking" and "non-breaking", but those terms convey erroneous messages and are imprecise. Whilst universal definitions are not yet available, two sets will be used in this paper.

For sloping structures like embankment seawalls, the surf similarity parameter $\xi_{op} = tan\ \alpha\ /\ \sqrt{s_{op}}$ (where α is the structure slope and $s_{op} = 2\pi\ H_s\ /\ g\ T_p^2$ is the wave steepness) is used to separate **"plunging"** ($\xi_{op} < 2$) and **"surging"** conditions ($\xi_{op} > 2$), see Fig. 6. These definitions are most commonly used in calculating armour stability for rubble mounds, see Meer (1984), also in the CIRIA / CUR Rock Manual (1991). The overtopping prediction method by Meer uses different relationships for "plunging" or "surging" waves, but the method by Owen does not apply such a distinction, see below.

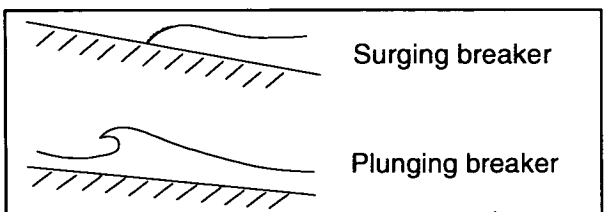

Fig. 6 Types of wave breaking

On steep walls (vertical, battered or composite), **"pulsating"** overtopping occurs when waves are relatively small in relation to the local water depth. These waves are not strongly influenced by the structure toe or approach slope. In contrast, **"impulsive"** breaking on steep walls occur when waves are larger in relation to local water depths, perhaps shoaling up over the approach bathymetry or structure toe itself. Under these conditions, some waves will break violently against the wall with (short-duration) forces reaching 10-40 times greater than for "pulsating" conditions, see McKenna (1995), Allsop et al (1996) and Allsop (2000).

2.2 Overtopping processes

Overtopping occurs when waves run up the beach, revetment, seawall or breakwater and pass over the crest of the defence. The frequencies, volumes and velocities of these overtopping events substantially influence the safety of the defence and of people living, working or travelling close behind the defence structure. Overtopping rates predicted by empirical formulae generally include "green water" discharges and splash, since both parameters were recorded during the scale model tests on which these prediction methods are based. Most laboratory studies on wave overtopping (research and site specific) have concentrated on measuring the mean overtopping discharge, Q_{bar}, usually derived from the total overtopping volume collected over 1000 waves, divided by the collection time. Those results have then been used to derive empirical prediction methods.

A second form of overtopping occurs when waves break on or seaward of the face of the structure and produce significant volumes of fine droplets. This "spray" can be carried over the wall under their own momentum and/or driven by wind. Spray overtopping may be

generated directly by wind acting on wave crests, most noticeable when waves reflected from steep walls interact with incoming waves to give severe local 'clapotii'. Effects of wind on spray overtopping are seldom modelled. Tests by de Waal et al (1992, 1996) suggest that onshore winds will have relatively little effect on green water overtopping, but may increase discharges under Q_{bar} = 1 l/s.m where much of the overtopping may take the form of spray. Studies by Ward et al (1994, 1996) explored wind effects on waves and overtopping processes at laboratory scale, and noted changes to shoaling, breaking and up-rush processes, but did not lead to any firm guidance on wind effects. Spray is not therefore presently believed to contribute significantly to overtopping volumes, and generally causes little hazard except reducing visibility and extending the spatial extent of salt spray effects. An important exception is the effect of spray in reducing visibility on coastal highways where the sudden loss of visibility may cause significant driving hazard, see the example for a Japanese coastal highway discussed by Kimura et al (2000).

2.3 Overtopping prediction methods

2.3.1 Empirical methods

For sea defence structures, the mean overtopping discharge may be predicted by empirical or numerical models. Overtopping varies with wall shape, crest level, water level and wave conditions. Generally design procedures are expected to calculate the crest freeboard (R_c = height of crest above water level) that would limit overtopping to below a chosen discharge limit, Q_{crit}, see Besley (1999) and section 3 below. Empirical models or formulae use relatively simple equations to describe mean overtopping discharges, Q_{bar}, in relation to defined wave and structure parameters. Empirical equations and coefficients based on use of dimensionless discharge parameters (e.g. Q^*, $Q\#$, Q_b, Q_n and Q_h) and freeboards (e.g. R^*, R_b, R_n, R_h or simply R_c/H_{si}) are, however, limited to a relatively small number of simplified structure configurations. Use out of range, or for other structure types, may require extrapolation or may not be valid.

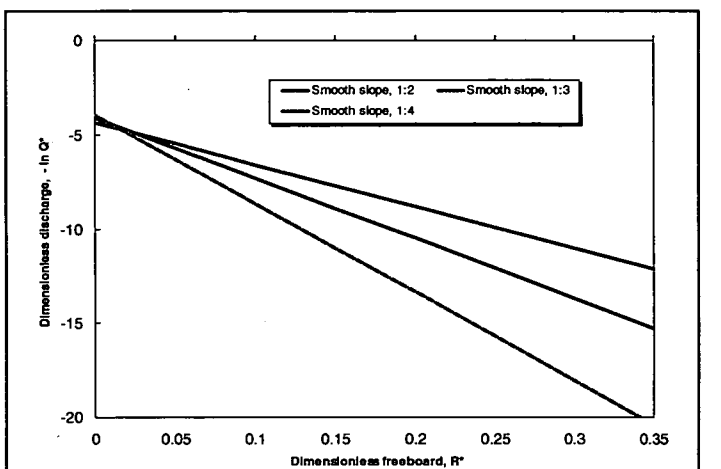

Fig. 7 Overtopping of simple slopes, after Owen

Simple slopes

Rural seawalls around UK are often of simple trapezoidal section, with slopes of 1:2 - 1:4. Overtopping of these slopes was related to freeboard R_c, and wave parameters H_s and T_m by Owen (1980, 1982). Dimensionless parameters Q^* and R^* are used in an exponential equation with roughness coefficient, r, and coefficients A and B for each slope:

$$Q^* = A \exp(-B R^*/r) \quad (2.1a)$$

where $$Q^* = q/(gT_mH_s) \quad (2.1b)$$

and $$R^* = R_c/T_m(gH_s)^{0.5} \quad (2.1c)$$

Coefficients A and B were initially given by Owen (1980) and revised by Besley (1999).

Owen's method is plotted as Q^* against R^* in Fig. 7. For embankments with small relative freeboards and/or large wave heights, the predictions come together, indicating that the slope

angle no longer has much influence in controlling overtopping. At this point, the slope is said to be "drowned out". Over the normal range of freeboards, the discharge characteristics for slopes 1:1, 1:1.15 and 1:2 are similar, but overtopping reduces significantly for slopes shallower than 1:2. Owen's method was developed for smooth slopes, but use of the roughness factor, r, allowed it to be extended to rough, and even armoured slopes.

Since 1980, alternative prediction methods for armoured slopes have been explored. In the Netherlands, methods for estimating overtopping on sea dikes have been developed by de Waal & Meer (1992) and Meer & Janssen (1994). Their method distinguishes between plunging and surging conditions as identified by the surf similarity or breaker parameter:

For **plunging waves**, $\xi_{op} < 2$, overtopping is calculated from:

$$Q_b = 0.06 \cdot e^{-4.7 \cdot R_b} \tag{2.2a}$$

$$Q_b = \frac{q}{\sqrt{gH_s^3}} \cdot \sqrt{\frac{s_{op}}{\tan\alpha}} \tag{2.2b}$$

$$R_b = \frac{R_c}{H_s} \cdot \frac{\sqrt{s_{op}}}{\tan\alpha} \cdot \frac{1}{\gamma_b \cdot \gamma_h \cdot \gamma_f \cdot \gamma_\beta} \tag{2.2c}$$

where Q_b = dimensionless overtopping discharge for breaking waves; R_b = dimensionless freeboard for breaking waves, and γ_b, γ_h, γ_f, and γ_β are reduction factors berm width, shallow depth, friction and angle of wave attack

Similar relationships are available for **surging waves**, $\xi_{op} > 2$, using different dimensionless parameters:

$$Q_n = 0.2 \cdot e^{-2.3 \cdot R_n} \tag{2.3a}$$

$$Q_n = \frac{q}{\sqrt{gH_s^3}} \tag{2.3b}$$

$$R_n = \frac{R_c}{H_s} \cdot \frac{1}{\gamma_b \cdot \gamma_h \cdot \gamma_f \cdot \gamma_\beta} \tag{2.3c}$$

where Q_n = dimensionless overtopping discharge for non-breaking waves, and R_n = dimensionless freeboard for non-breaking waves

Vertical walls

Historically, predictions of overtopping for vertical walls used a single formula, the method developed by Franco et al (1994) was applicable to deeper water relative to wave height. Allsop *et al* (1995), later refined by Besley et al (1998), demonstrated that overtopping processes at vertical and composite walls are also strongly influenced by the form of the incident waves, not just H_s and T_p. When waves are small compared to depth, waves impinging on a vertical / composite wall are generally reflected back. If the waves at the wall are large relative to depth, then they can break onto the structure, leading to significantly more abrupt overtopping characteristics. These observations led to formulation of a wave breaking parameter, h_*, given by:

$$h_* = \frac{h}{H_s}\left(\frac{2\pi h}{gT^2}\right) \tag{2.4}$$

Pulsating waves predominate when $h_* > 0.3$, for which the following is valid over $0.03 < R_c/H_s < 3.2$:

$$Q\# = 0.05 \exp(-2.78\, R_c/H_s) \quad (2.5a)$$
$$Q\# = Q/(gH_s^3)^{0.5} \quad (2.5b)$$

For **impulsive waves**, when $h_* \leq 0.3$, new dimensionless discharge, Q_h, and freeboard parameters, R_h, incorporated h_* to give a different prediction equation:

$$Q_h = 1.37 \times 10^{-4}\, R_h^{-3.24} \quad (2.6a)$$
$$Q_h = Q/(gh^3)^{0.5}/h_*^2 \quad (2.6b)$$
$$R_h = (R_c/H_s)\, h_* \quad (2.6d)$$

For composite structures, Besley *et al* (1998) re-defined the breaking parameter d_* based on h_*:

$$d_* = \frac{d}{H_s}\left(\frac{2\pi h}{gT^2}\right) \quad (2.7)$$

If $d_* \leq 0.3$, the mound was classified as small, and similar overtopping characteristics for vertical wall are predicted. When $d_* > 0.3$, the mound was classified as large and overtopping characteristics are corrected for the presence of the mound. These methods are described fully by Besley (1999).

Recently, Bruce *et al* (2001) extended the prediction method for impulsive waves to steep (nearly vertical) walls of 10:1 and 5:1 batter. Using the form of equation 2.5a, modifed coefficients were developed. For 10:1 batter:

$$Q_h = 1.78 \times 10^{-4}\, R_h^{-3.24} \quad (2.8a)$$

and for 5:1 batter:

$$Q_h = 1.92 \times 10^{-4}\, R_h^{-3.24} \quad (2.8b)$$

3. PERMISSIBLE OVERTOPPING LIMITS

In assessments of the effects of overtopping, most analysis has either evaluated flood volumes / areas, or has tried to estimate damage against suggested overtopping limits. Most advice on tolerable overtopping has used mean overtopping discharges, generally derived from total overtopping volumes collected over 500 to 1000 T_m. The mean discharge is then expressed as flow rate per metre run of seawall, typically $m^3/s.m$ or l/s.m. Mean overtopping discharges are the responsive measure of hydraulic performance, and are much more stable than any peak measures.

3.1 Mean discharges

Limits to identify onset of damage to seawalls, buildings or infrastructure, or danger to pedestrians and vehicles have been defined relative to mean overtopping discharges. Guidelance on tolerable limits were developed by Owen (1980) based on work in Japan by Fukuda et al (1974) were cited in the CIRIA Rock Manual edited by Simm (1991). Owen's suggested limits for safety of vehicles and pedestrians are summarised below and in Fig. 8.

Pedestrians :-					
Wet, but not unsafe			Q_{bar}	<	0.003 l/s.m
Uncomfortable	0.003 l/s.m	<	Q_{bar}	<	0.03 l/s.m
Dangerous	0.03 l/s.m	<	Q_{bar}		
Vehicles :-					
Safe at moderate / higher speeds			Q_{bar}	<	0.001 l/s.m
Unsafe at moderate / higher speeds	0.001 l/s.m	<	Q_{bar}	<	0.02 l/s.m
Dangerous	0.02 l/s.m	<	Q_{bar}		

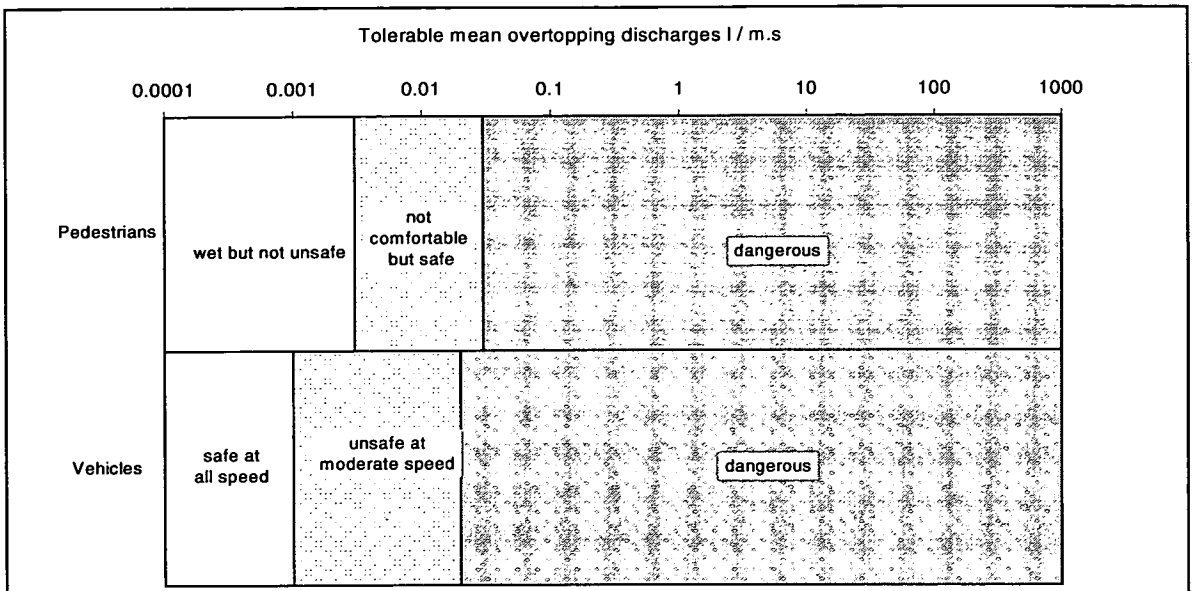

Fig. 8 Tolerable overtopping discharges, after Owen (1980) and Fukuda et al (1974)

Later revisions to these limits were suggested by Franco et al (1994), see Fig. 9. The changes were based on tests on vertical breakwaters with high walls, experiments with falling jets and studies in the Netherlands on the safety of "dyke masters" or inspectors on embankment seawalls. The limits suggested in Fig. 9 therefore apply to trained personnel, ready and equipped to get wet, but probably not to the general public!

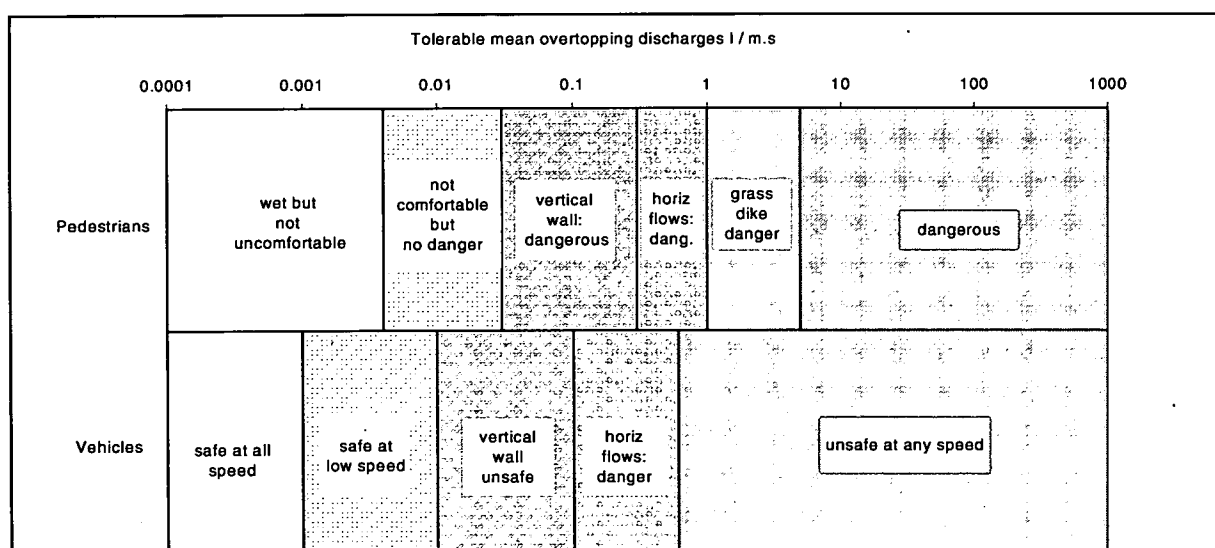

Figure 9 Tolerable mean discharges, after Franco et al

3.2 Peak overtopping volumes / discharges

Whilst common in practice, use of mean overtopping discharges in assessing safety levels without any other information is questionable. For many cases, it is probable that maximum individual volume (and velocity) are of much greater significance than mean discharge, both for damage to structures, and hazard to people. Franco et al (1994) and Besley (1999) have shown that, for a given level of mean discharge, the volume of the largest overtopping event

can vary significantly with wave condition and structural type. It may therefore become inconsistent to specify safety levels with reference to mean discharge levels alone. At present however, predictions of peak overtopping volumes or velocities remain subject to large uncertainties. This paper is intended to make some reduction in those uncertainties in advance of full results in early 2005 from the CLASH project (see: http://www.clash-eu.org).

Individual overtopping events have not yet been firmly linked with hazard levels, although some useful suggestions have been made. Franco *et al* (1994) demonstrated that danger to people or vehicles from individual overtopping events could be related to their volumes. Franco *et al* (1994) suggested a "safe" limit for an individual overtopping volume for people operating behind a vertical wall as V_{max} = 100 l/m, but for a horizontally composite structure (and a trained Dutch dyke inspector) it might be increased to V_{max} = 750 l/m. Franco *et al* (1994) however observed that a volume as low as V_{max} = 50 l/m could unbalance an individual when striking their upper body without warning. These experimenters were prepared to be hit by water and will therefore have tolerated more severe conditions than would be reasonable for workers or the public who are hit by water without warning.

Franco et al (1994) also noted that any "safe" limit would vary with structural type. Any given volume overtopping a vertical structure was more dangerous than the same volume following a more horizontal trajectory. Different velocities will influence the danger caused by any particular volume, and the elevation at which a person is hit will alter the degree of danger. These effects will be influenced by the form of wave breaking onto the structure, and by the geometry of the structure's crest detail, in particular the height of any parapet wall, if present. This is illustrated by Smith *et al* (1994) who report full-scale tests conducted on grass dykes, to determine safe overtopping limits for "dyke masters" carrying out inspection and repair work. These tests concluded that work on the dyke was unsafe for trained staff when the mean discharge exceeded Q_{bar} = 0.01 m^3/s.m or 10 l/s.m, probably corresponding to approximately $V_{max} \approx$ 1 m^3/m, or 1000 l/m. This is considerably higher than the limits determined by Franco *et al* (1994) for work behind a tall wall, but accords with their observation that safe limit of V_{max} varies with structural type. In Smith *et al*'s tests, most of the flow acted on the observer's lower legs only. Again, safety limits for trained personnel working on a structure and anticipating overtopping will be higher than those for other users.

Herbert (1996) monitored overtopping behind a vertical seawall at Colwyn Bay. During installation and operation of measurement equipment, Herbert observed that personnel could work safely on the crest of the wall up to Q_{bar} = 0.1 l/s.m. Individual overtopping volumes were not measured, but methods by Besley (1999) give V_{max} = 40 l/m for Q_{bar} = 0.1 l/s.m, in close agreement with Franco's limit of V_{max} = 50 l/m. Herbert (1996) also noted that overtopping became dangerous to vehicles when the mean discharge exceeded Q_{bar} = 0.2 l/s.m, suggesting a limit of V_{max} = 50 l/m should be applied as the upper safe limit for pedestrians and vehicles.

In summary, best present guidance for areas accessed by the public are to limit overtopping to:

For pedestrians (unaware) $Q_{bar} < 0.03$ l/s.m, V_{max} = 40 l/m
For trained staff (aware) $Q_{bar} < 0.1$ l/s.m, V_{max} = 100 l/m

These suggested discharges / volumes may probably be revised upwards where the overtopping discharges are not at high velocities, or only relate to flows at low level.

4. OVERTOPPING CHARACTERISTICS

4.1 Wave-by-wave volumes

The main wave overtopping characteristics (chiefly mean overtopping discharge, but also the proportion of overtopping waves and peak overtopping volumes) can be predicted for most simple structure types using methods described in the EA overtopping manual by Besley (1999) with additional methods and explanation by Allsop & Besley (2000), Besley *et al* (1998), Bruce *et al* (2001) and Pearson *et al* (2002).

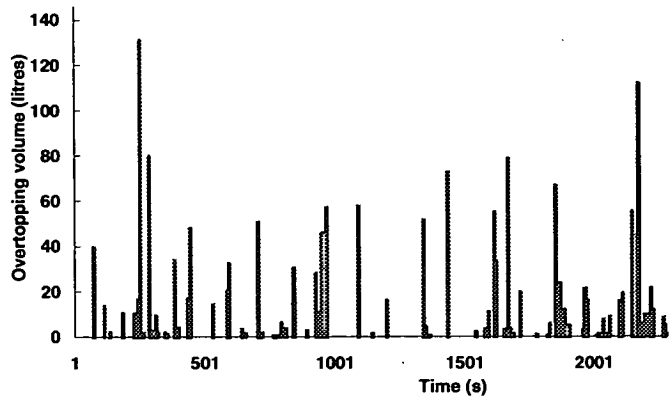

Figure 10 Wave-by-wave overtopping, pulsating conditions, h*=0.37, N_{ow} = 15%, from Big-VOWS

Relationships between peak and mean overtopping volumes can be illustrated in Figs. 10 and 11 by example results from Big-VOWS tests by Pearson *et al* (2002). Here the frequency of overtopping is quite high at $N_{ow\%}$ = 15%.

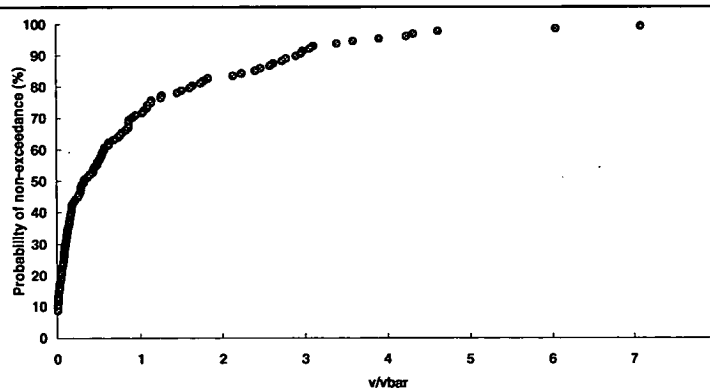

Figure 11 Distribution of wave-by-wave volumes, pulsating conditions, h*=0.37, N_{ow} = 15%, from Big-

The relationships between peak and mean overtopping volumes can be illustrated by considering the example results in Figs. 10 and 11. Here the frequency of overtopping is quite high at N_{ow}:N_w = 0.15 (= 15%). An average overtopping volume V_{bar} can be defined as

$$V_{bar} \equiv \frac{V_{total}}{N_{ow}} \qquad (4.1)$$

The distribution of individual overtopping volumes shown in Figure 11, typical of tests under impulsive conditions, suggested that the highest volume in the sequence, V_{max} is about 7 - 8 times the average overtopping volume, V_{bar}. Current guidance on admissible overtopping is based upon the mean discharge, Q_{bar} (in m^3/ s / m run). We can use our approximate relation between V_{bar} and V_{max} to arrive at a relation between Q_{bar} and V_{max}, and thus relate guidance based upon mean overtopping to the size of an individual, large event.

$$Q = \frac{\text{total volume}}{\text{total time}} \text{ per metre run} = \frac{N_{ow} \times V_{bar}}{\text{total time}} \qquad (4.2a)$$

$$\text{If} \quad V_{bar} \approx \frac{V_{max}}{8} \quad \text{then} \quad Q \approx \frac{N_{ow} \times V_{max}}{8 \times \text{total time}} \text{ per metre run} \qquad (4.2b)$$

$$\text{The total time} \approx N_w \times T_m \quad \Rightarrow Q \approx \frac{N_{ow}}{N_W} \frac{V_{max}}{8} \frac{1}{T_m} \quad \Rightarrow V_{max} \approx 8QT_m \frac{N_w}{N_{ow}} \qquad (4.2c)$$

For a seawall with design waves of T_m = 10s designed for minimal overtopping, *eg* Q_{bar} < 0.05 l/s.m, with (*eg*) 10% of waves overtopping, then peak overtopping volume, $V_{max} \approx 40$ l per m. As an individual volume, this may not seem very large in terms of flooding, but it is clearly more hazardous if projected at any significant speed, see below.

4.2 Overtopping velocities

Pearson et al (2002) and Bruce et al (2002) analysed velocities of waves overtopping vertical walls at both small and large scales. The largest 20 individual overtopping events were selected. For each of these overtopping events, the upward velocity (u_z) of the leading edge of the water was determined, and was non-dimensionalised by the inshore wave celerity c_i, given by $c_i = (gh)^{1/2}$. These relative velocities are plotted in Fig 12 against the wave breaking parameter, h_*.

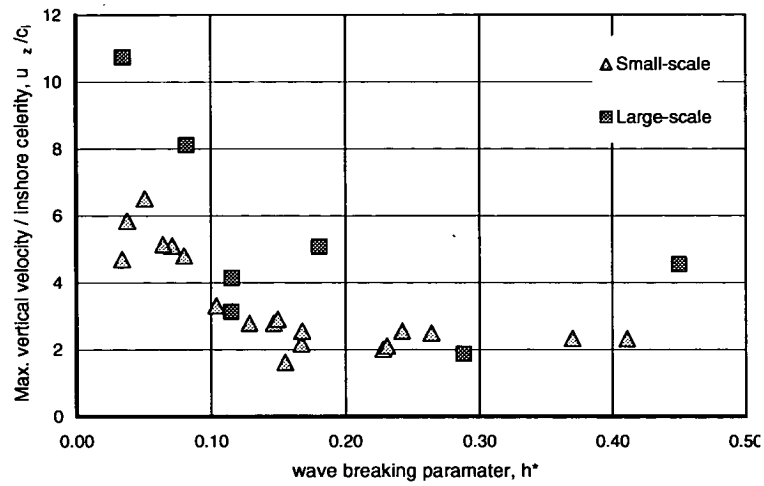

Figure 12 Overtopping velocities for vertical walls.

It is noticeable in Fig. 12 that, when $h_* > 0.15$, the non-dimensionalised throw velocity is roughly constant at $u_z/c_i \approx 2.5$, but these velocities increase very significantly when $h_* \leq 0.15$ reaching $u_z/c_i \approx 4$ - 10. This confirms that the hazard derived from overtopping discharges may vary dramatically with changes of wave breaking characteristics. The largest velocities measured here suggest prototype velocities equivalent to u_z = 40 m/s, at which speed an overtopping volume of v_{max} = 25 l per metre run becomes quite serious!

5. OVERTOPPING CASE STUDIES

Under the EC project CLASH (see: http://www.clash-eu.org) and de Rouck *et al* (2002), wave overtopping will be measured at full scale at 3 or 4 sites around Europe: the large breakwater at Zeebrugge; the rubble mound at Ostia; the vertical / composite wall at Samphire Hoe; and (possibly) part way up a shallow slope embankment dyke at Petten, see Pullen *et al* (2003). Those measurements will be presented at future conferences. At Samphire Hoe, as well as the current measurements, observations of overtopping hazards have also been made for the last seven years, and those observations are analysed here.

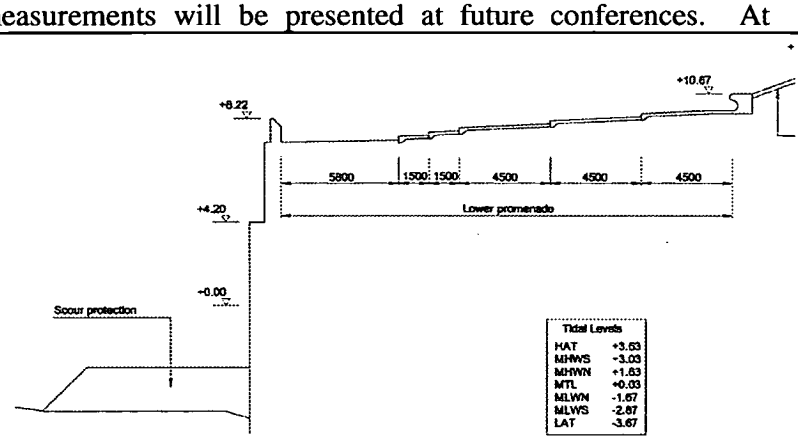

Figure 13 Cross-section of Samphire Hoe seawall

5.1 Samphire Hoe

Samphire Hoe reclamation (just west of Dover) was formed by 5 million m^3 of chalk spoil excavated from

the Channel Tunnel, and designated for public recreation. The seawall in Fig. 13 is exposed to waves from south and south west, but is popular with walkers and anglers. Eurotunnel was concerned to ensure that access to Samphire Hoe was safe, so commissioned HRW in October 1995 to devise a hazard warning system.

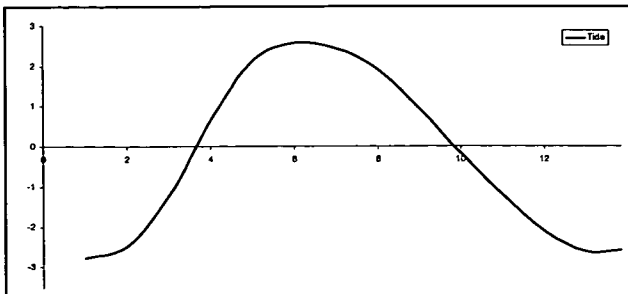

Figure 14 Example tide at Samphire Hoe

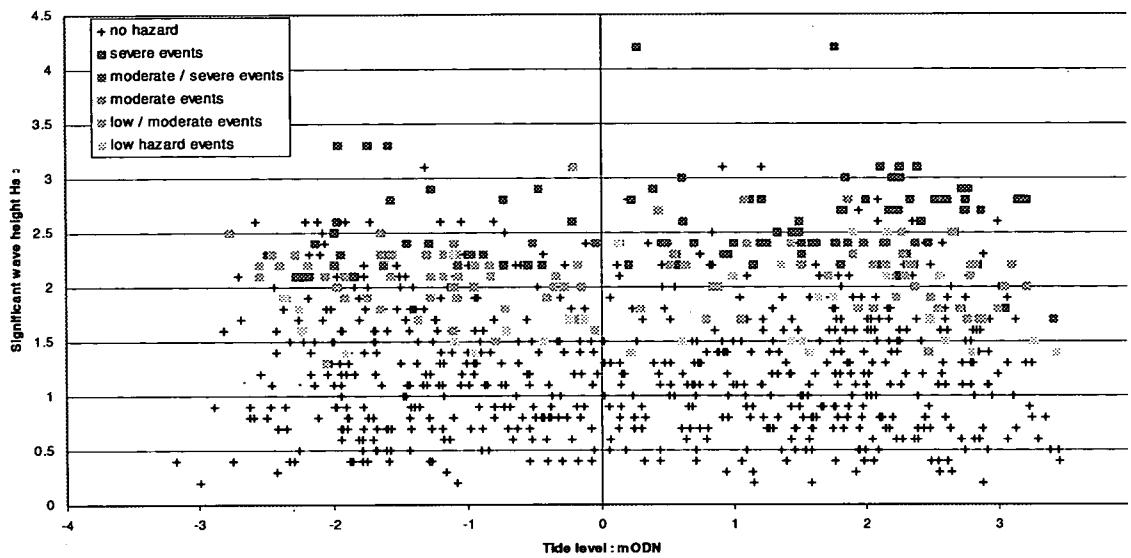

Figure 15 Occurrence of hazard events at Samphire Hoe

The project team argued then that guidance on acceptable levels of overtopping had not significantly improved since Owen's compilation of advice in 1980. Guidance on permissible overtopping was based on limited data, and was insufficient for estimation of safety limits for people. Herbert (1996) had conducted trial experiments for vertical walls with some success, but the range of comparison was very small and subject to uncertainties. Methods adopted by Sayers *et al* (1996) and Gouldby *et al* (1999) were therefore not related to overtopping discharges, but used direct observations to identify ranges of water level and wave conditions giving hazards. The UK Met Office's local area numerical weather model predicted hourly wind speeds 24 hrs in advance. Predicted winds, together with surge and tide levels, see example in Fig. 14, were then used to predict waves at Samphire Hoe using hindcasting and transformation models. On site four levels of hazard were used to record observations:

None	No observed overtopping.
Low	Occasional splash, white water (spray) only. A person may feel nervous, but no substantial danger.
Moderate	Occasional wave overtops the personnel barrier, momentary "green water" overtopping and some personal danger.
Severe	Consistent "green water" overtopping, causing substantial danger.

5.2 Overtopping hazard analysis, Samphire Hoe

Observations for October 2000 to March 2002 allow recorded overtopping hazards to be compared with predictions. At each observation time, the degree of hazard assessed locally, the tide level and the wave height are plotted as a point in Fig. 15. In general, the more severe hazards occur for higher wave heights, as expected. The surprise is that there is no similar correlation between hazards and high tide levels, despite a range of water levels over 6-7m. Hazardous effects occur at both high and low water levels. For simple monotonic overtopping responses, as in Fig. 7, high overtopping would be expected for high tide level and/or high waves, with low or no overtopping expected for low waves and/or low water levels. This can however be explained by careful use of overtopping prediction methods developed / improved by Defra / EA funded research at HRW and results from the VOWS project.

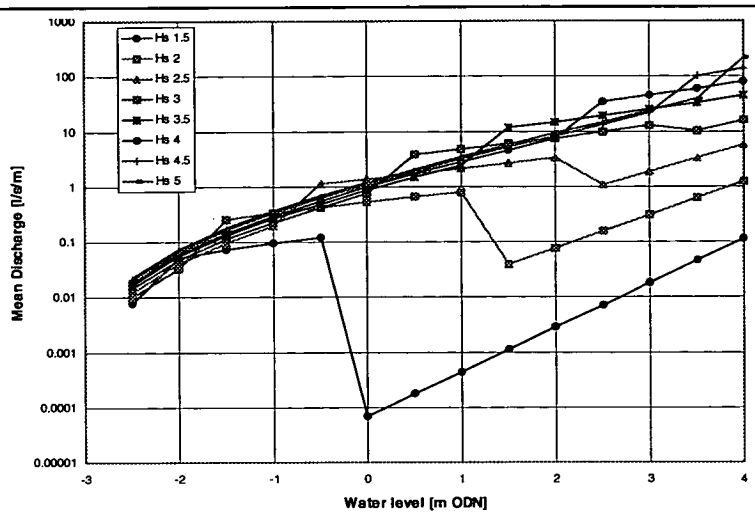

Fig. 16 Overtopping of composite wall at Samphire Hoe related to water level and nearshore wave height.

Three different methods have been used in the calculations in Fig. 16, corresponding to: **pulsating** conditions; **impulsive** breaking; and **broken** waves. The graph shows mean overtopping discharges against water level, for wave heights H_s = 1.5m to 5m. The mean wave steepness was taken as s_m = 0.05, typical of storms in the English Channel. The overtopping response functions are taken for composite walls under "pulsating" or "impacting" conditions after Bruce *et al* (2001), with a further part of the curves based on "broken" wave conditions, see Bruce *et al* (2003).

The straight lines towards bottom right of Fig. 16 predict overtopping disharges under "pulsating" wave conditions. Reducing water levels then lead to the onset of "impulsive" breaking onto the wall as waves shoal over the toe berm, at which point overtopping increases suddenly over a relatively small drop in water level, contrary to expectations given by any monotonic prediction method. At the lower water levels shown here, waves are broken before reaching the wall, but present guidance still suggests using the impulsive overtopping prediction method. The larger wave heights do not show the same behaviour as they are already too large to give "pulsating" conditions.

The methods illustrated above can then be applied to the data from Samphire Hoe shown previously in Fig. 15. The simple limit of $Q_{bar} < 0.03$ l/s.m is shown in Fig. 17 against observations from Samphire Hoe for October 2000 - March 2002 with tide levels and wave heights from the Met Office wave model. These comparisons reinforce the suggested upper limit for moderate hazard given by $Q_{bar} < 0.03$ l/s.m.

5.3 Overtopping hazard analysis, Colwyn Bay

Similar analysis for the A55 seawall at Colwyn Bay derived from observations made by Herbert (1996) are shown in Fig. 18. Here the transition zones between wave breaking types

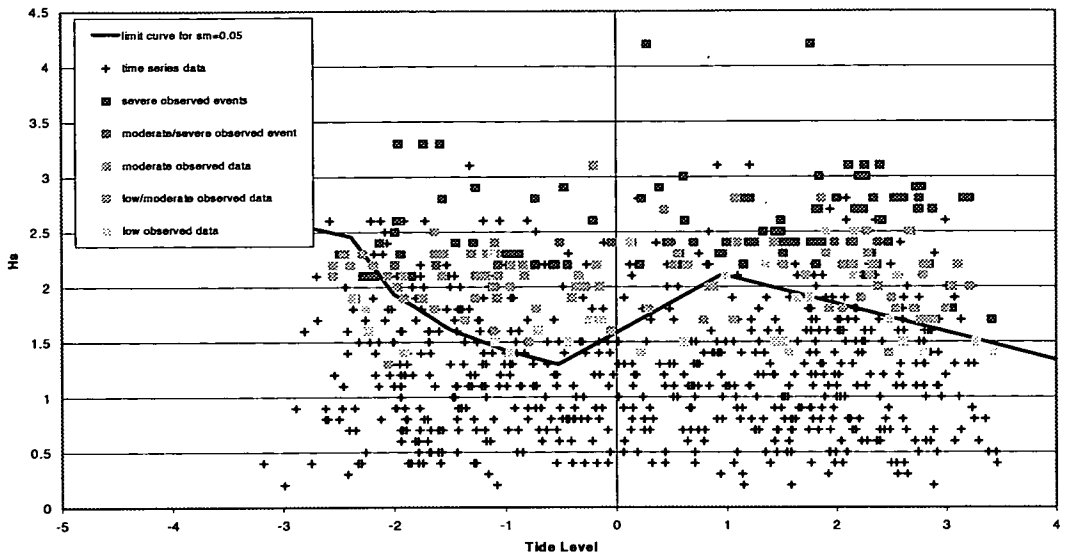

Fig. 17 Overtopping hazards at Samphire Hoe related to $Q_{bar} < 0.03$ l/s.m

are less extreme, and the limit given by $Q_{bar} < 0.03$ l/s.m. appears more conservative. The differences may however again relate to the observations at Colwyn Bay being made by trained personnel who were expecting to get wet.

5.4 Overtopping hazards elsewhere

During the second half of the CLASH project, July 2003-December 2004, observations of overtopping hazards at Oostende, Zeebrugge, Ostia, Samphire Hoe, and other sites will be used to generate a greater database from which to make firmer recommendations. In the meantime, it is worth noting occurrences of wave overtopping onto Japan national highway 336, Hokkaido discussed by Kimura *et al* (2000). A length of highway immediately after a tunnel is protected by a steep seawall (battered at 2.5:1) exposed to the Pacific. Analysis of video records of overtopping, together with waves measured up-coast and tides measured down-coast, were used to correlate damage to a passing vehicle with hind-cast calculations of overtopping. Kimura *et al* concluded that the car windscreen was damaged under overtopping of order $Q_{bar} = 10^{-5}$ m^3/s.m, despite being on the farther carriageway from the seawall. Overtopping was calculated using Goda's (1975) diagrams. This level of discharge is very low in relation to the hazard level in earlier guidance. It is possible that the simple method of deducing the overtopping discharge has missed impulsive breaking effects. This require further analysis.

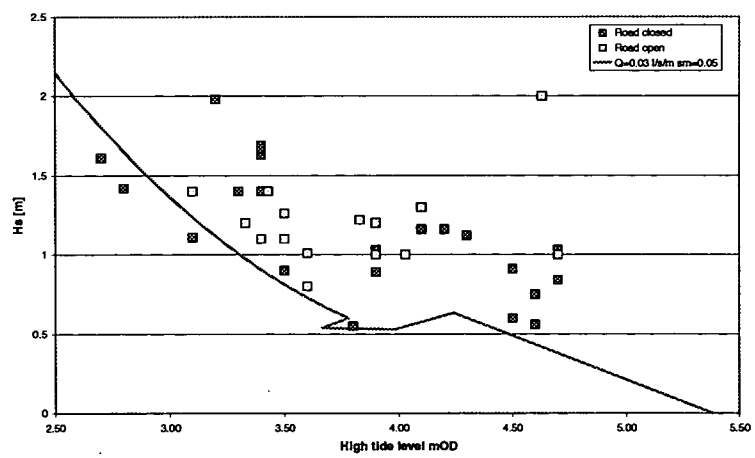

Fig. 18 Overtopping of wall at Colwyn Bay related to water level and nearshore wave height.

6. DISCUSSION AND RECOMMENDATIONS

Methods to predict wave overtopping at seawalls (primarily mean overtopping discharge, Q_{bar}) have improved in recent years, and will continue to do so under current research projects. Some recent extensions to empirical methods have been summarised here. New methods have been developed to predict overtopping characteristics for infrequent events, $N_{wo}\% < 5\%$, and to estimate overtopping velocities, u_z under impulsive conditions Further extensions and reductions in uncertainties are being developed in describing wave-by-wave and peak overtopping volumes, v_{max}, and overtopping behaviour under broken waves.

Guidance on overtopping hazards is still primarily based on mean overtopping discharge, although refinements to include peak volumes and velocities have been proposed. The best present guidance for areas accessed by the public is to limit overtopping to:

For pedestrians (unaware) $Q_{bar} < 0.03$ l/s.m, $V_{max} = 40$ l/m

For trained staff (aware) $Q_{bar} < 0.1$ l/s.m, $V_{max} = 100$ l/m

It is noted that these discharges / volumes may be revised upwards where overtopping velocities are low, or where flows only occur close to promenade / road level. It is anticipated that this guidance will be improved and extended when results from hazard measurements under the CLASH project become available.

Hazards from wave overtopping should be assessed using a staged approach. The stages will depend on the degree and probability of hazard, whether it is long-standing or is anticipated as a result of new-build, and the availability of site specific data. The key steps may be summarised:

1. Identify occurrence of overtopping hazards – For existing defences, local experience should be used to identify the occurrence of hazards (date/time and severity) and to relate each hazard event to key input parameters for the event: tide + surge; wave height, period and direction; beach level / slope, even if only be estimated within a range. Offshore wave conditions may be extracted for given dates / times from the most appropriate grid point on the UKMO wave model (archive copies held at HR Wallingford). Waves then need to be transformed inshore (shoaling, refraction, breaking) using suitable empirical methods. (Numerical models are probably not appropriate for this analysis). Data on hazards and input conditions might be presented in a form similar to that used here for Figs. 15, 17, 18, linking occurrence of hazard to key input parameters to identify the general trends of performance. For new defences, this step is taken after Stage 3 below.
2. Understand the overtopping characteristics of the defence – For any defence, new or existing, overtopping characteristics should be described against the likely range of the key input parameters including: tide + surge; wave height, period and direction; beach level / slope, to give Q_{bar}, and $N_{wo\%}$, u_z, and V_{max}, These characteristics might be presented in a form similar to Fig. 16 to identify sudden changes of performance.
3. Analyse experience to date – For an existing defence, incidents of overtopping hazards can be "back-analysed" using the data above to calculate overtopping characteristics, Q_{bar}, $N_{wo\%}$, u_z, and V_{max}, It may be worthwile to include "near miss" conditions when no hazard was observed despite the conditions, as long as this does not simply reflect the absence of any information. Each incident of hazard (or no hazard) can then be compared with calculations of overtopping characteristics, Q_{bar}, $N_{wo\%}$, u_z, and V_{max}. This process can be repeated covering the likely range for those parameters that can only be estimated. The result of this will be some "calibration" of the overtopping response characteristics, and design thresholds, for this defence.

4. Develop hazard warning system – The methods discussed above can be used to set up a simple warning system driven by wave conditions predicted by the UKMO wave model. This model computes at 1 hour intervals, and output can be configured to give tide + surge, wind and wave. Forecasts of waves / tide can be made up to 48 hours ahead, up-dated at, say, 4 hour intervals. Wave conditions for the offshore grid point can then be transformed to a nearshore point using empirical formulae set up for the chosen site and driven by the wave model output. The final stages are then to apply nearshore wave conditions / water levels to the overtopping model set-up and calibrated in Stages 2-3 above. This model can then calculate Q_{bar}, $N_{wo\%}$, u_z, and V_{max} to be contrasted with thresholds calibrated in Stage 3.

ACKNOWLEDGEMENTS

The VOWS research project was supported by EPSRC under GR/M42312 and GR/R42306, and built on earlier research at HR Wallingford supported by MAFF and EA. Work on hazard analysis from overtopping is being conducted under the CLASH project under EU contract EVK3-2001-0058 and supported by Defra / EA under FD2412. Further work by Universities of Edinburgh and Southampton is supported by an EPSRC project in Partnership in Public Awareness (GR/ S23827/01).

The White Cliffs Countryside Project and EuroTunnel are thanked for access to data from Samphire Hoe. Previous data and guidance from Phillip Besley at HR Wallingford is gratefully acknowledged, as is the helpful supervision of the collaborative VOWS work by the EPSRC CEWE Project Manager, Michael Owen.

REFERENCES

Allsop, N.W.H., Besley, P. & Madurini, L.. (1995), "Overtopping performance of vertical and composite breakwaters, seawalls and low reflection alternatives", Paper final MCS Project Workshop, Alderney.

Allsop, N.W.H., McKenna, J.E., Vicinanza, D. & Whittaker, T.T.J. (1996), "New design methods for wave impact loadings on vertical breakwaters and seawalls", Proc 25th Int. Conf. Coastal Eng., Orlando, ASCE, New York.

Besley P. (1999), "Overtopping of seawalls – design and assessment manual", R & D Technical Report W 178, ISBN 1 85705 069 X, Environment Agency, Bristol.

Besley, P., Stewart, T. & Allsop, N.W.H. (1998), "Overtopping of vertical structures: new prediction methods to account for shallow water conditions", Proc. ICE Conf. Coastlines, Structures and Breakwaters, Thomas Telford, London.

Bruce T., Allsop N.W.H. & Pearson J. (2001) "Violent overtopping of seawalls – extended prediction methods" Proc. ICE Conf. On Shorelines, Structures & Breakwaters, September 2001, pp 245-255, ICE, London

Bruce T., Allsop N.W.H. & Pearson J. (2002) "Hazards at coast and harbour seawalls - velocities and trajectories of violent overtopping jets" Proc. 28th Int. Conf. Coastal Eng. (ASCE), Cardiff

Bruce T, Pearson J & Allsop N.W.H. (2003) "Violent wave overtopping – extension of prediction method to broken waves" Proc. Conf. Coastal Structures '03, Portland, ASCE / COPRI, New York.

CIRIA / CUR (1991), "Manual on the use of rock in coastal and shoreline engineering", CIRIA special publication 83, Simm, J.D. (Editor), CIRIA, London.

Franco, L., de Gerloni, M. & van der Meer, J.W. (1994), "Wave overtopping on vertical and composite breakwaters", Proc 24th Int. Conf. Coastal Eng., Kobe, ASCE.

Fukuda N., Uno T. & Irie I (1974) "Field observations of wave overtopping of wave absorbing revetment" Coastal Engineering in Japan, Vol 17, pp 117-128, Japan Society of Civil Engineers, Tokyo.

Goda Y. (1971) "Expected rate of irregular wave overtopping of seawalls" Coastal engineering in Japan, Vol 14, pp 45-51, JSCE, Tokyo.

Goda, Y, Kishira, Y, & Kamiyama, Y. (1975) 'Laboratory investigation on the overtopping rates of seawalls by irregular waves'. Ports and Harbour Research Institute, Vol 14, No. 4, pp 3-44, PHRI, Yokosuka.

Gouldby B.P., Sayers P.B. & Johnson D (1999) "Real-time hazard forecasting: implementation and two years operation at Samphire Hoe, Dover" MAFF Conf. on River and Coastal Engineers, Keele.

Hedges, T.S. & Reis, M.T. (1998), "Random wave overtopping of simple sea walls: a new regression model", Proc. Instn. Civil Engrs. Water, Maritime & Energy, Volume 130, March 1998, Thomas Telford, London.

Herbert D.M. (1996) "Overtopping of Seawalls: a Comparison between Prototype and Physical Model Data" Report TR 22, HR Wallingford.

Kimura K, Fujiike T, Kamikubo K. Abe R & Ishimoto K (2000) "Damage to vehicles on a coastal highway by wave action" Proc. Conf. Coastal Structures '99, Santander, June 1999, publn. A.A. Balkema, Rotterdam.

Meer, J.W. van der, Tonjes P. & de Waal J.P (1998) "A code for dike height design and examination" Proc. ICE Conf. Coastlines, Structures & Breakwaters, T.Telford, London.

Owen, M.W. (1980), "Design of seawalls allowing for overtopping", Report EX924, Hydraulics Research, Wallingford.

Owen, M.W. (1982), "Overtopping of Sea Defences", Proc. Intl. Conf. On Hydraulic Modelling of Civil Eng. Structures, Coventry, pp469-480, BHRA, Bedford.

Pearson, J., Bruce, T. & Allsop, N.W.H. (2001), "Prediction of wave overtopping at steep seawalls – variabilities and uncertainties", Proc "Waves '01", San Francisco (ASCE).

Pearson, J., Bruce, T. & Allsop, N.W.H. (2002), "Violent wave overtopping – measurements at large and small scale", Proc. 28th Int. Conf. Coastal Eng. (ASCE) Cardiff.

Pullen T.A. Allsop, N.W.H. Bruce, T. & Geeraerts, J. (2003) "Violent wave overtopping: CLASH Field Measurements at Samphire Hoe" Proc. Coastal Structures 2003, ASCE.

Richardson, S. Pullen, T. & Clarke, S. (2002) "Jet Velocities of Overtopping Waves On Sloping Structures: Measurements and Computation" Paper 347 at ICCE 2002 Cardiff, July 2002 , publn ASCE, New York.

Rouck de J., Allsop N.W.H., Franco L. & van der Meer J.W. (2002) "Wave overtopping at coastal structures: development of a database towards up-graded prediction methods" Proc 28th Int. Conf. Coastal Engineering (ASCE), Cardiff, pp 2140-2152.

Waal, J.P. de Tonjes, P. & van der Meer, J.W. (1996), "Overtopping of sea defences" Proc 25th Int. Conf. Coastal Eng. (ASCE), pp2216-2229, Orlando, publn ASCE, New York.

Appendix H: Allsop *et al.*, 2005a

Allsop, N.W.H., Bruce, T., Pearson, J. & Besley, P. (2005a), *Wave overtopping at vertical and steep seawalls*, Proc. ICE, Maritime Engineering, 158, 3, pp103–114, ISSN 1741 7597

Appendix H
Allsop *et al.*, 2005a

Allsop, N.W.H., Bruce, T., Pearson, J. & Besley, P. (2005a), *Wave overtopping at vertical and steep seawalls*, Proc. ICE, Maritime Engineering, 158, 3, pp103–114, ISSN 1741 7597

H.1 Declaration of contribution

This paper was the culmination and synthesis of many years of work in physical modelling of wave overtopping led by the author and Allsop. The author was deeply involved at all stages from the drafting of the *VOWS* project proposal right through to writing and editing (through ¿40 versions!) large parts of the final text for this extended journal article. Bruce and Allsop led the writing of the paper, with some detailed input from Pearson and checking by Besley.

H.2 Published paper

overleaf.

Proceedings of the Institution of Civil Engineers
Maritime Engineering 158
September 2005 Issue MA3
Pages 103–114

Paper 13935
Received 10/10/2003
Accepted 04/08/2005

Keywords:
coastal engineering/ports & harbours/sea defences

William Allsop
Visiting Professor, University of Southampton; and Technical Director, HR Wallingford, UK

Tom Bruce
Lecturer, School of Engineering & Electronics, University of Edinburgh, UK

Jonathan Pearson
Research Fellow, School of Engineering & Electronics, University of Edinburgh (now at School of Engineering, University of Warwick), UK

Phillip Besley
Manager Engineering Hydraulics & Structures Group, HR Wallingford, UK

Wave overtopping at vertical and steep seawalls

W. Allsop BSc, MICE, CEng, T. Bruce MSc, J. Pearson BEng, PhD and P. Besley BSc, PhD

Wave overtopping is the critical response of most sea defence structures and one of the more important responses for many coast defences around the UK and other developed shorelines. Sea defences in rural areas are commonly provided by embankment seawalls. Steep or vertical seawalls are more commonly used in urban areas to protect against erosion, flooding and local overtopping hazards, and to protect the base of eroding cliffs in urban or rural areas. Vertically faced breakwaters have been common around many European countries, and caisson-type breakwaters are heavily used in Japan. For simple slopes or embankments, overtopping performance can be predicted by simple monotonic empirical formulae. Overtopping of vertical or slightly battered walls is however rather more complicated, with substantial differences in overtopping volumes and velocities depending on the form of wave interaction at or close to the wall. The present paper draws together results from a number of UK and European research projects over the last 10 years. Their results improve and validate prediction methods for wave overtopping discharges and velocities for steep battered, composite and vertical seawalls/breakwaters. The methods presented herein support, extend and qualify guidance given in the UK Environment Agency overtopping manual. The present paper shows how the use of these methods can now explain why overtopping of some seawalls/breakwaters can be greatest at mid-water level, rather than at the highest water levels.

NOTATION

A, B	empirical coefficients used in overtopping formulae
c_i	inshore celerity of incident waves at structure toe (m/s)
d	water depth over toe berm (m)
d_*	wave breaking parameter based on dimensionless depth over toe berm
g	acceleration due to gravity (=9·81 m/s^2)
h	water depth (m)
h_*	wave breaking parameter based on dimensionless depth
h_s	water depth at toe of structure (m)
$H_{1/3}$	average of highest 1/3 of wave heights (m)
H_{m0}	estimate of significant wave height from spectral analysis = 4·0$\sqrt{m_o}$ (m)
H_s	significant wave height [$H_{1/3}$ (m) or H_{m0} (m)]
H_{si}	inshore incident significant wave height (m)
m	slope of the foreshore : gradient = 1 : m
m ODN	elevation above Ordnance Datum at Newlyn (m)
N_z	number of zero-crossing incident waves
q	mean overtopping discharge per metre structure width (m^3/s per m or l/s per m)
q_{safe}	limiting mean overtopping discharge (m^3/s per m or l/s per m)
Q_*	Owen's dimensionless overtopping discharge = $q/(gT_mH_s)$
Q_b	plunging wave dimensionless discharge = $(q/\sqrt{(gh^3)})/\sqrt{(s_{op}/\tan\alpha)}$
Q_d	impulsive wave dimensionless discharge, composite walls = $q/\left[d_*^2\sqrt{gh_s^3}\right]$
Q_h	impulsive wave dimensionless discharge for vertical walls = $q/\left[h_*^2\sqrt{gh_s^3}\right]$
Q_n	surging wave dimensionless discharge = $q/\sqrt{(gH_s^3)}$
r	roughness coefficient for Owen formulae
R_*	Owen's dimensionless freeboard = $R_c/T_m\sqrt{(gH_s)}$
R_b	dimensionless freeboard for slopes, breaking waves = $(R_c/H_s)(\sqrt{s_{op}}/\tan\alpha)(1/\gamma_b\gamma_h\gamma_f\gamma_\beta)$
R_c	crest freeboard of structure, relative to still water level (m)
R_d	dimensionless crest freeboard, composite walls = $(R_c/H_s)d_*$
R_h	dimensionless crest freeboard, vertical walls = $(R_c/H_s)h_*$
R_n	dimensionless crest freeboard, surging waves = $(R_c/H_s)(1/\gamma_b\gamma_h\gamma_f\gamma_\beta)$
s_{op}	offshore wave steepness based on peak period = $2\pi H_{mo}/(gT_p^2)$
s_{om}	offshore wave steepness based on mean period = $2\pi H_{mo}/(gT_m^2)$
T_m	average wave period calculated from spectral moments, or zero-crossing analysis (s)
T_r	return period (1/years)
u_z	upward velocity of overtopping jet at wall crest (m/s)
V_{max}	maximum overtopping volume per wave per unit crest width (m^3/m or l/m)
α	angle between overall structure slope and horizontal (°)

ξ_{op}	breaker parameter (also known as *Iribarren number*) based on s_o (=tan $\alpha/\sqrt{s_{op}}$)
γ_b, γ_n, γ_f, γ_β	reduction factors for berm, shallow foreshore, roughness, and obliquity
γ_s	seaward face geometry reduction factors.[1]

1. WAVE OVERTOPPING AT THE COAST

Many kilometres of coastal infrastructure around the UK and Europe are protected against wave overtopping and/or erosion by steep sea walls, often vertical or near vertical (see Figs 1 and 2), sometimes with a toe berm or steep approach beach. Such seawalls will often have been constructed in stages with successive adaptations. Similar walls are also used to protect ports, or as protection to cliffs, railway lines or roads as seen along lengths of the UK and Italian coasts.

It is generally appreciated that seawalls can reduce, but will not wholly prevent wave overtopping. Overtopping is therefore implicit in UK and European practice. New or rehabilitated seawalls are now designed to provide levels of protection given by acceptable mean overtopping discharges at given return periods.

Recent practice in the UK implies that new developments in flood-prone areas should provide protection up to and including the $T_r = 1/100$ year return event for fluvial flooding, but up to $T_r = 1/200$ year return for coastal or estuarial flooding. More complete discussions on performance and funding are given by DTLR in PPG25[2] and the ICE design and practice guide on coastal defence edited by Brampton.[3] For urban areas on exposed coastlines, this requirement is quite onerous, and is usually only satisfied by using the promenade behind the seawall to accept much larger discharges, damping out and returning overtopping flows before they reach vulnerable infrastructure, buildings or people. Most alternative approaches require beach levels to be raised to reduce wave attack.

In rural areas, overtopping safety requirements may be met simply by limiting flood depths/volumes, but for residential or commercial developments in urban areas, the standard of protection may be set by mean overtopping discharge limits derived by reference to damage to buildings or hazard to people. It is generally agreed[4–6] that the safety of the public close behind a seawall may require that the mean overtopping discharge is limited to $q < 0{\cdot}03$ l/s per m. Achievement of this low level of overtopping requires significant confidence in the analysis of the overtopping characteristics of urban seawalls.

Along developed coasts, the safety of people using the coastline is of particular concern. In the UK, approximately two to four

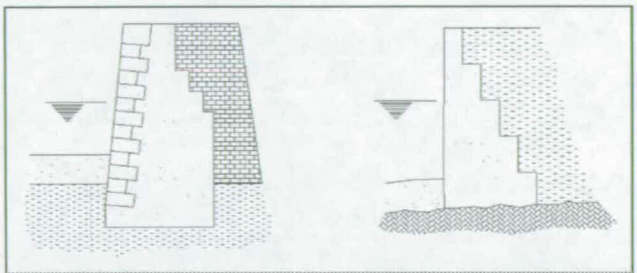

Fig. 1. Example seawalls, vertical and battered

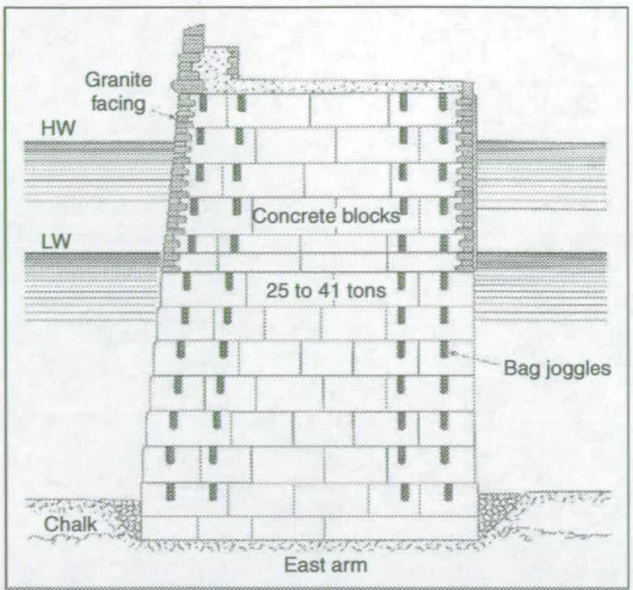

Fig. 2. Vertical breakwater wall (Dover)

people die every year being swept off, or falling from, seawalls, breakwaters, natural rock outcrops or beaches.[5] Evidence of wave impact damage to property was most graphically given by the trainload of pig iron washed off Dover East Breakwater in the 1940s and by the destruction of seafront shelters at Sidmouth in 1992. The economic case for improved accuracy/reliability of guidance is illustrated by considering that replacement costs of sea defences around England alone have been estimated as about £6 billion (c. US$9 billion). The UK government spends approximately £100 million (c. US$150 million) per annum on new or refurbished coastal defences, although damage from winter 1989/90 alone was estimated at £40 million (c. US$60 million). A substantial proportion of the cost of a sea defence scheme is related directly to the design crest height, with the volume of material in a defence often increasing in proportion to the overall height squared. The defence crest level is itself a direct consequence of the limiting overtopping discharge permitted. An uncertainty of 1·0 m in setting defence crest levels might cost £1500–2000 (c. US$2800) per metre length. Over a scheme of 2 km, such an uncertainty might be worth £3–4 million (c. US$5 million) out of a total budget of perhaps £10 million (c. US$15 million). With climate change projected to raise sea levels and increase wave heights, Sutherland and Gouldby[7] calculate that increasing design water levels by only 0·4 m would require typical defences to be raised by 0·6–0·8 m to maintain present overtopping performance, confirming the importance of identifying accurately overtopping performance of sea defences.

This paper uses overtopping measurements at small scale in UK and other European wave flumes (two-dimensional tests) from projects spanning 10 years to improve and validate predictions for overtopping discharges and velocities for steep battered, composite and vertical seawalls/breakwaters. Data are primarily derived from small-scale physical model tests under the European projects on vertical breakwaters MCS and PROVERBS, see Oumeraci *et al.*,[8] MAFF/DEFRA/Environment Agency sponsored research in UK on coastal defences and seawalls, and from the

EPSRC-funded project on *Violent Overtopping of Waves at Seawalls* (VOWS).

Data and methods presented in this paper support, extend and qualify guidance given previously in the UK Environment Agency overtopping manual by Besley[6] and data or methods described by Besley *et al.*,[9] Bruce *et al.*,[10,11] Pearson *et al.*[12] and Allsop *et al.*[5] This paper has been written to provide a reasonably complete summary of prediction methods so, rather than presenting only recent validations or extensions, the paper includes all key prediction methods for wave overtopping at vertical, battered, or composite seawalls/breakwaters, with new data or methods introduced where appropriate.

2. WAVE BREAKING AND OVERTOPPING PROCESSES

The frequency, volume and crest velocity/direction of overtopping events substantially influence safety of people living, working or travelling behind the defence, and of the structure itself. Overtopping rates predicted by empirical formulae generally include 'green water' discharges and splash, since both parameters were recorded during the scale model tests on which these prediction methods are primarily based. For vertical/steep walls fronted by steep slopes or toe berms, combinations of shoaling waves and steep slopes may lead to large waves plunging directly onto the wall, see example in Fig. 3. Here overtopping flows are sudden, and cannot be regarded as originating from normal wave up-rush processes.

Any discussion on wave interaction with defence structures requires that the key wave processes be categorised so that these different processes may be separated. In the past, terms such as 'breaking' and 'non-breaking' have been used, but these are both imprecise, and can convey erroneous messages. Although universal definitions are not yet agreed, key terms are defined below to describe breaking or overtopping processes in this paper.

For beaches and gently sloping structures, the physical form of the wave near maximum run-up can be predicted using the well-established surf similarity parameter (or *Iribarren number*) defined in terms of beach slope (α), and wave steepness (s_{op}, or sometimes s_{om}).

$$\xi_{op} = \tan\alpha/(s_{op})^{0.5} \quad (1)$$

Fig. 3. Example of violent overtopping at a vertical seawall

Conditions range from 'spilling' ($\xi_{op} < 0{\cdot}4$) through 'plunging' ($0{\cdot}4 < \xi_{op} < 2{\cdot}3$), and 'collapsing' $2{\cdot}3 < \xi_{op} < 3{\cdot}2$) conditions to 'surging' ($\xi_{op} > 3{\cdot}2$). There exists no sharp delineation from one regime to the next, although a useful distinction can be made more clearly between conditions where the wave actively breaks onto the slope (plunging), and those under which the wave simply runs up and back down without violence (surging), see Fig. 4. On sloping structures, these definitions are commonly used in calculating armour stability for rubble mounds, see the CIRIA/CUR Rock Manual,[13] or for overtopping see References 14 and 15.

On steep walls (vertical, battered or composite), 'pulsating' conditions occur when waves are relatively small in relation to the local water depth, and of lesser wave steepness. These waves are not critically influenced by the structure toe or approach slope. Waves run up and down the wall giving rise to (fairly) smoothly varying loads.

In contrast, 'impulsive' conditions occur on steep walls when waves are larger in relation to local water depths, perhaps shoaling up over the approach bathymetry or structure toe itself. Under these conditions, some waves will break violently against the wall with (short-duration) forces reaching 10 to 40 times greater than for 'pulsating' conditions.[16,17]

For steep/vertical walls, the onset of impulsive breaking is given primarily by the slope and/or width of the approach slope or toe berm, and by the incident wavelength. Methods to distinguish between breaking/response types for wave forces have been developed within the PROVERBS project.[8,18] A different approach was developed for overtopping by Besley *et al.*[9] using a wave breaking parameter, h_*, based on depth at the toe of the wall, h_s, and incident wave conditions inshore

$$h_* = \frac{h_s}{H_{si}}\left(\frac{2\pi h_s}{gT_m^2}\right) \quad (2)$$

Analysis by Allsop *et al.*,[16] reported by Besley *et al.*[9] suggest that pulsating conditions predominate at the wall when $h_* > 0{\cdot}3$, and impulsive conditions occur when $h_* \leq 0{\cdot}3$. This is discussed in Section 3 and illustrated further in Section 4 below.

Another helpful distinction describes the physical form of overtopping. Overtopping when waves break onto or over the seawall generally generates 'green water' where the overtopping volume is relatively continuous. For waves that break seaward of the face of the structure, or where the seawall is high in relation to the wave height, overtopping may be as a stream of fine droplets. This 'violent overtopping' or 'splash overtopping' can be carried over the wall under their own momentum, or may be driven by onshore wind. Violent overtopping may also be

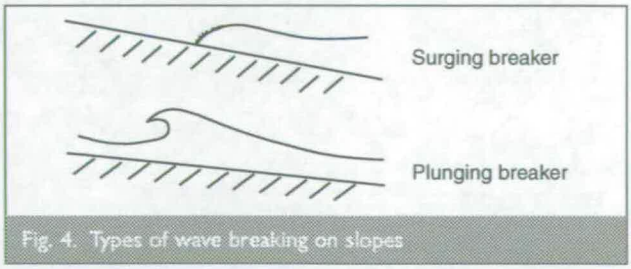

Fig. 4. Types of wave breaking on slopes

generated directly by wind acting on wave crests, most noticeably when waves reflected from steep walls interact with incoming waves to give severe local 'clapotii'. Effects of wind on spray overtopping are seldom modelled, largely due to inherent difficulties in scaling wind effects in laboratory tests, but also because the importance of wind effects has not yet been established. Tests by de Waal and van der Meer[19] and by de Waal *et al.*[20] suggest that onshore winds will have relatively little effect on green water overtopping, but that wind may increase overtopping of vertical walls by up to a factor of three for mean discharges under $q = 1$ l/s per m where much of the overtopping may take the form of spray. Pullen *et al.*[21] report experiments to measure the influence of wind on overtopping distributions for vertical walls, but generic advice beyond that of de Waal *et al.*[20] has yet to be developed.

3. OVERTOPPING PREDICTION METHODS

3.1. Introduction

The simplest and most robust method to predict wave overtopping is by use of a set of empirical equations relating overtopping discharges to seawall crest level, wall configuration and roughness, sea bed slope or toe berm size, local water depth and wave conditions. Such design methods are generally configured to calculate the crest freeboard (R_c) required to give an acceptable mean discharge. Empirical models or formulae use relatively simple equations to describe mean overtopping discharges, q, in relation to defined wave and structure parameters. As with any empirical method, these may be limited to relatively simple structure configurations. Use out of range, or for other structure types, may require uncertain and insecure extrapolation of the equations or coefficients.

This section gives guidance on overtopping prediction formulae for a variety of structures, together with new supporting data where appropriate. Section 3.2 reviews existing methods for the prediction of wave overtopping on simple slopes and Section 3.3 then examines plain vertical walls, making the case for the importance of distinguishing between pulsating and impulsive conditions. Section 3.4 gives new guidance for overtopping at the steeply sloping 'battered' walls that are found commonly. Section 3.5 examines prediction tools for composite structures and finally, Section 3.6 presented new guidance for overtopping of walls under conditions where very shallow water in front of the wall sees all waves reaching the wall already broken.

3.2. Overtopping on slopes

Rural seawalls on the coasts of Denmark, Germany, the Netherlands and the UK are often of simple trapezoidal section, formed by sandy and weaker clays requiring slopes of 1 : 4 to 1 : 8. In the UK the use of stiff clays allows relatively steep slopes of 1 : 2 to 1 : 4. Overtopping of these steeper slopes was related to freeboard R_c, and wave parameters H_s, T_m by Owen.[4,22] Owen defined dimensionless discharge and freeboard parameters Q_* and R_*

$$Q_* = \frac{q}{gT_m H_s} \quad (3)$$

$$R_* = \frac{R_c}{T_m\sqrt{gH_s}} \quad (4)$$

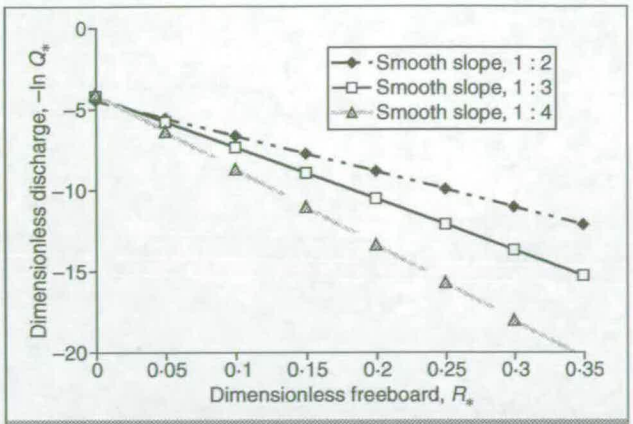

Fig. 5. Example monotonic prediction method for simple slopes, 1 : 2 to 1 : 4, after Owen[4]

Owen's equation was of exponential form (see Fig. 5) with roughness coefficient, r, and empirical coefficients A and B for each slope given in the Environment Agency overtopping manual by Besley[6]

$$Q_* = A\exp\left(-\frac{BR_*}{r}\right) \quad (5)$$

Equation (5) is valid for $0{\cdot}05 < R_* < 0{\cdot}3$. The form of Owen's equation is simple and monotonic. For embankments with small relative freeboards and/or large wave heights, predictions of overtopping discharge converge, indicating that the slope angle no longer has much influence in controlling overtopping. At this point, the slope is said to be 'drowned out'. Over the normal range of freeboards, the characteristics for slopes of 1 : 1, 1 : 1·15 and 1 : 2 are similar, but overtopping reduces significantly for slopes shallower than 1 : 2. Increasing wave height or period increases overtopping discharges, as does reducing the freeboard, either by lowering the crest or increasing the water level. Owen's method was developed for smooth slopes, but the roughness coefficient, r, allowed it to be extended to rough and even armoured slopes.

Alternative prediction methods for smooth and armoured slopes have been developed since 1980 for sea dykes by de Waal and van der Meer,[19] van der Meer and Janssen[14] and van der Meer *et al.*[15] The formulae that these references recommend distinguish between plunging and surging conditions on the structure slope as defined by the surf similarity parameter, ξ_{op}, and use different definitions of dimensionless discharge for breaking waves, Q_b, or dimensionless freeboard, R_b

$$Q_b = \frac{q}{\sqrt{gH_s^3}} \cdot \sqrt{\frac{s_{op}}{\tan\alpha}} \quad (6)$$

$$R_b = \frac{R_c}{H_s} \cdot \frac{\sqrt{s_{op}}}{\tan\alpha} \cdot \frac{1}{\gamma_b \cdot \gamma_h \cdot \gamma_f \cdot \gamma_\beta} \quad (7)$$

where γ_b, γ_h, γ_f and γ_β are reduction factors for berm width, shallow depth, roughness and wave obliquity.

In the method used by van der Meer *et al.*, overtopping for 'plunging' conditions, $\xi_{op} < 2$, is calculated from

$$Q_b = 0{\cdot}06\exp(-5{\cdot}2R_b) \quad (8)$$

The exponent of $-5{\cdot}2$ is quoted as a mean value with error bounds of $\pm 0{\cdot}55$. An exponent of $-4{\cdot}7$ may be used as a conservative predictor. Similar relationships are available for 'surging' conditions when $\xi_{op} > 2$, using different parameters, Q_n = dimensionless discharge for surging waves, and R_n = dimensionless freeboard

$$Q_n = \frac{q}{\sqrt{gH_s^3}} \quad (9)$$

$$R_n = \frac{R_c}{H_s} \cdot \frac{1}{\gamma_b \cdot \gamma_h \cdot \gamma_f \cdot \gamma_\beta} \quad (10)$$

where the prediction equation for overtopping under 'surging' conditions is given by

$$Q_n = 0{\cdot}2 \exp(-2{\cdot}6 R_n) \quad (11)$$

As for the exponent in equation (8), the exponent in equation (11) is a mean value through the data and is quoted $\pm 0{\cdot}35$. An exponent of $-2{\cdot}3$ is quoted as a conservative predictor. Equations (8) and (11) are given in the recent US *Coastal Engineering Manual* and Dutch *TAW* guidance manuals.[23,24]

3.3. Overtopping on vertical walls

The development of formulae to predict overtopping for vertical walls followed a similar path towards single or monotonic formulae. Graphical methods by Goda *et al.*[25] (see also Herbert and Owen[26]) showed that there could be two rather different processes, rather than a single monotonic process, but no formulae were developed to describe the overtopping predictions of those graphs, and the results obtained by Goda *et al.* were limited to relatively low wave steepnesses $s_{op} < 0{\cdot}036$, which excludes most storm wave conditions in the North Sea or Mediterranean.

For simple vertical breakwaters in deeper water, Franco *et al.*[1] developed a single empirical formula based on equation (11) using relative freeboard, R_c/H_s, reduction factors for specific front face geometries, γ_s (see Table 1), and dimensionless discharge, Q_n

$$Q_n = 0{\cdot}2 \exp\left(-\frac{4{\cdot}3}{\gamma_s}\frac{R_c}{H_s}\right) \quad (12)$$

which is valid for $0{\cdot}03 < R_c/H_s < 3{\cdot}2$.

Returning to intermediate and shallower water, Allsop *et al.*[16] refined by Besley *et al.*[9] demonstrated that overtopping processes at vertical and composite walls are strongly influenced by the form of incident wave breaking, not just by values of H_s and T_p alone. When waves are small in comparison with depth, the waves at vertical or composite walls are reflected. If the waves at the wall are large relative to depth, then they may break directly onto the structure, leading to significantly more abrupt overtopping.

Configuration	γ_s
Simple impermeable wall	1·0
Simple wall with bullnose	0·78
Perforated front chamber, closed deck	0·72–0·79
Perforated front chamber, open deck	0·58

Table 1. Seaward face geometry factors

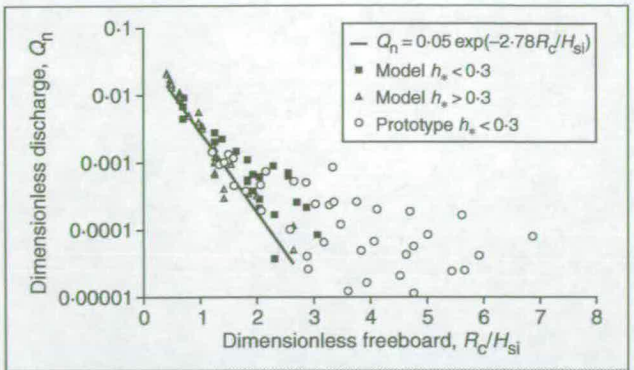

Fig. 6. Model and prototype overtopping discharges against equation of Franco *et al.*[1]

These observations, together with the development of the 'wave impact parameter map' in PROVERBS, see Allsop *et al.*,[27] led to development of a dimensionless depth parameter, h_* (equation (2)). The need to separate pulsating and impulsive breaking is illustrated in Fig. 6 in which unseparated data from model tests in the UK[9,28] and the Netherlands[19] are plotted together with a modified version of Franco's equation (equation (13), from Besley *et al.*[9])

$$Q_n = 0{\cdot}05 \exp\left(-2{\cdot}78 \frac{R_c}{H_s}\right) \quad (13)$$

which is valid over $0{\cdot}03 < R_c/H_s < 3{\cdot}2$. Much of the data for low values of R_c/H_s fit equation (13) well, but data at higher values of R_c/H_s fall very much higher than predicted by that method.

For 'impulsive' conditions given by $h_* \leq 0{\cdot}3$ and therefore excluding all pulsating conditions, Besley *et al.*[9] used the model test data from monolithic coastal structures (MCS) and other projects to derive a new equation for impulsive overtopping with new dimensionless discharge, Q_h, and freeboard parameters, R_h (Fig. 7). The new equation included h_* to give

$$Q_h = 1{\cdot}37 \times 10^{-4} R_h^{-3{\cdot}24} \quad (14)$$

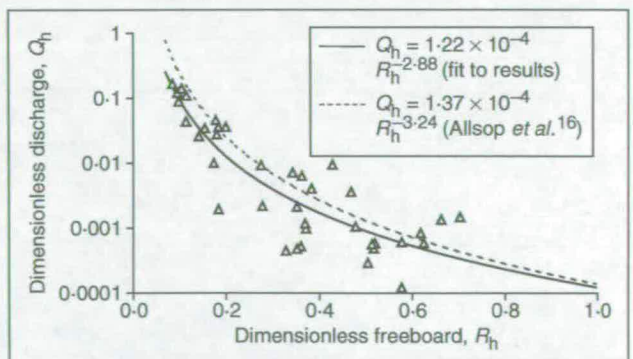

Fig. 7. Overtopping for impulsive conditions ($h_* < 0{\cdot}3$)

which is valid over $0{\cdot}05 < R_h < 1{\cdot}0$, where

$$Q_h = \frac{q}{h_*^2\sqrt{gh_s^3}} \quad (15)$$

$$R_h = h_* \frac{R_c}{H_{si}} \quad (16)$$

It is important to note that these equations were originally derived using small-scale model test data, but were later tested against full-scale data from field measurements obtained by Herbert[28] and showed relatively good agreement.

Measurements at small scale from the VOWS tests at Edinburgh were compared by Bruce *et al.*[10] with equation (14) (Fig. 8). In general, agreement between these data and the prediction is remarkably good, particularly given the wide range of dimensionless freeboards covered. There is a tendency for divergence from the original line of equation (14), so a slightly revised prediction line is suggested

$$Q_h = 1{\cdot}92 \times 10^{-4} R_h^{-2{\cdot}92} \quad (17)$$

which is valid over $0{\cdot}05 < R_h < 1{\cdot}0$.

3.4. Overtopping on battered/inclined walls

Within the VOWS study, the tests for vertical walls were repeated for near-vertical walls with 10 : 1 and 5 : 1 batter commonly found for older UK seawalls and breakwaters, as reviewed by Allsop and Bray.[29] A 1 : 10 approach slope was used, representative of shingle or steeper sand beaches. Measurements of Q_h for 10 : 1 and 5 : 1 walls (Figs 9 and 10, respectively) indicate discharges slightly in excess of those predicted by Besley *et al.*,[9] by factors of up to 3 to 4, over a wide range of dimensionless freeboards.

For conditions tested by Bruce *et al.*,[10] the 10 : 1 and 5 : 1 battered walls exhibit similar overtopping characteristics. Revised equations fitted to these data are given in equations (18) and (19), (valid over $0{\cdot}05 < R_h < 1{\cdot}0$).

$$Q_h = 1{\cdot}89 \times 10^{-4} R_h^{-3{\cdot}15} \quad (18)$$

for impulsive conditions on 10 : 1 battered walls and

$$Q_h = 2{\cdot}81 \times 10^{-4} R_h^{-3{\cdot}09} \quad (19)$$

for impulsive conditions on 5 : 1 battered walls.

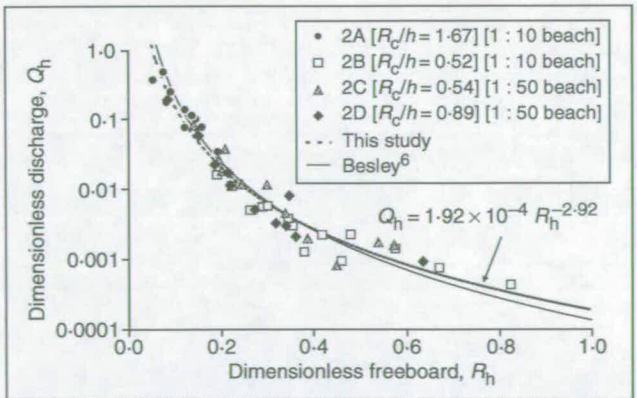

Fig. 8. Overtopping from VOWS tests compared with Besley[6] and revised prediction equation

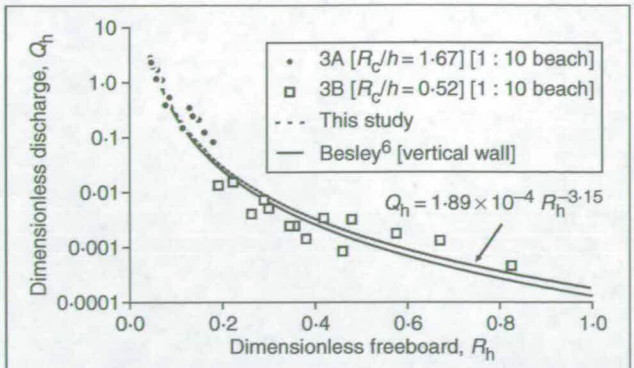

Fig. 9. Overtopping for a 10 : 1 battered wall

3.5. Overtopping on composite walls

Studies within the PROVERBS project on vertical breakwaters[8] have illustrated how a relatively small toe berm can change wave breaking characteristics, thus substantially altering the type and magnitude of wave loadings. Besley[6] notes that many vertical seawalls may be fronted by rock mounds with the intention of protecting the toe of the wall from scour (Fig. 11). The toe configuration can vary considerably, potentially modifying the overtopping behaviour of the structure. Three types of mound can be identified.

(*a*) Small toe mounds which have an insignificant effect on the waves approaching the wall; here the toe may be ignored and calculations proceed as for simple vertical (or battered) walls.
(*b*) Moderate mounds, which significantly affect wave breaking conditions, but are still below water level. Here a modified approach is required.
(*c*) Emergent mounds in which the crest of the armour protrudes above still water level. Prediction methods for these structures may be adapted from those for crown walls on a rubble mound, but are not discussed further here.

For overtopping of composite seawalls, Besley *et al.*[9] defined a modified breaking parameter d_* based on h_*

$$d_* = \frac{d}{H_{si}}\left(\frac{2\pi h_s}{gT_m^2}\right) \quad (20)$$

When $d_* > 0{\cdot}3$, the mound was classified as small and overtopping could be predicted by the standard method given previously for 'pulsating' conditions (equation (13)).

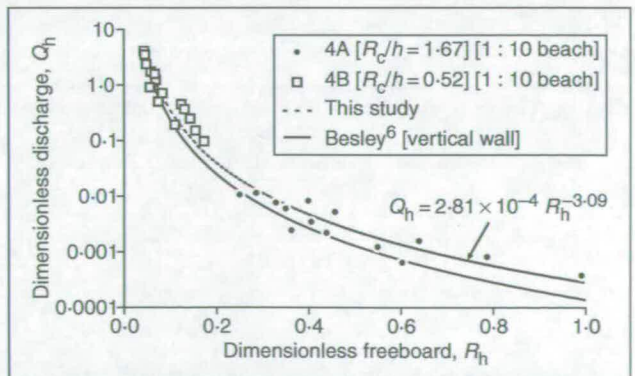

Fig. 10. Overtopping for a 5 : 1 battered wall

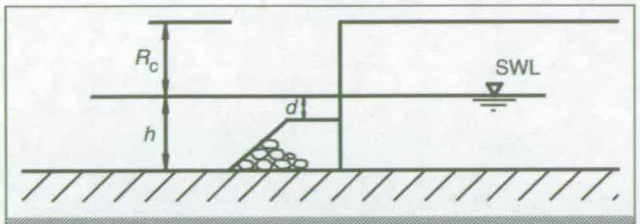

Fig. 11. Definition sketch for composite vertical structures

For larger mounds when $d_* \leq 0{\cdot}3$, Besley[6] recommends a modified version of the 'impulsive' prediction method, accounting for the presence of the mound by use of d and d_* (valid over $0{\cdot}05 < R_d < 1{\cdot}0$)

$$Q_d = 4{\cdot}63 \times 10^{-4} R_d^{-2{\cdot}79} \quad (21)$$

where

$$Q_d = \frac{q}{d_*^2 \sqrt{g h_s^3}} \quad (22)$$

$$R_d = d_* \frac{R_c}{H_{si}} \quad (23)$$

Results from the VOWS tests generally supported the use of this approach as a conservative prediction, but as presented by Bruce *et al.*[10] suggested that the prediction line of equation (21) might lie towards the upper bound of the data rather than representing any central estimate.

Re-examining the original data, it appears that the limit for 'impulsive' conditions on composite structures is better set at $d_* \leq 0{\cdot}2$ (rather than $d_* \leq 0{\cdot}3$), provided that this is only applied for conditions where $h_* \leq 0{\cdot}3$. This lower limit for the onset of impact conditions than recommended by Besley[6] is also partially supported by measurements of overtopping velocities described in Section 4. Measurements limited by $d_* \leq 0{\cdot}2$ are re-processed here in Fig. 12, and a more central estimate with less scatter is given by the revised prediction

$$Q_d = 5{\cdot}88 \times 10^{-4} R_d^{-2{\cdot}61} \quad (24)$$

which is valid for $h_* \leq 0{\cdot}3$ and $d_* \leq 0{\cdot}2$.

3.6. Overtopping of broken waves

Many seawalls are constructed at the back of a beach such that breaking waves never reach the seawall, at least not during frequent events where overtopping is of primary importance. For these conditions, particularly for typical shallow beach slopes, $m < 1/30$, design wave conditions may be given by waves which start breaking (possibly quite some distance) seaward of the wall. 'Broken' waves are inherently much less likely to re-form to give a plunging breaker, and so they are less likely to give 'impulsive' conditions at the wall.

In the region where the water depth at the toe is positive, $h > 0$, and 'broken' waves predominate (i.e. when dimensionless freeboard $R_h < \approx 0{\cdot}03$), tentative guidance is suggested by Bruce *et al.*[30] based on a modification and extrapolation of Besley's method (equation (14)). The modified equation below is plotted as the lower line in Fig. 13

$$Q_h = 0{\cdot}27 \times 10^{-4} R_h^{-3{\cdot}24} \quad (25)$$

which is valid for $R_h < 0{\cdot}03$.

For conditions falling in the range $0{\cdot}03 < R_h < 0{\cdot}05$, the data from Bruce *et al.*[30] suggest that it will probably be safe to extrapolate Besley's method (equation (14)) slightly outside of its recommended range, shown in the upper dotted line in Fig. 13.

For configurations where the toe of the wall is above water, $h < 0$, Bruce *et al.*[30] suggest an adaptation of the prediction equation for plunging waves by van der Meer and Janssen[14] using the sea bed slope of tan α in evaluating Q_b defined in equations (6)–(8), and an adjusted dimensionless freeboard R_{ba} defined in equation (27)

$$Q_b = 0{\cdot}06 \exp(-4{\cdot}7 R_{ba}) \quad (26)$$

which is valid over $1{\cdot}0 < R_{ba} < 4{\cdot}0$

$$R_{ba} \equiv R_b s_{op}^{-0{\cdot}17} \quad (27)$$

The results of this analysis are compared in Fig. 14 with predictions for sloping structures by van der Meer and Janssen.[14] Despite the differences between the structure in this study and those examined by van der Meer and Janssen, the overtopping characteristics are broadly similar. Equation (26) above is used to adjust the prediction of van der Meer and Janssen[14] in Fig. 14.

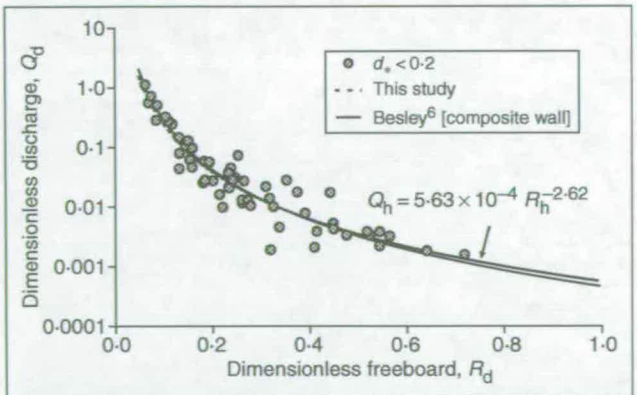

Fig. 12. Overtopping for composite walls

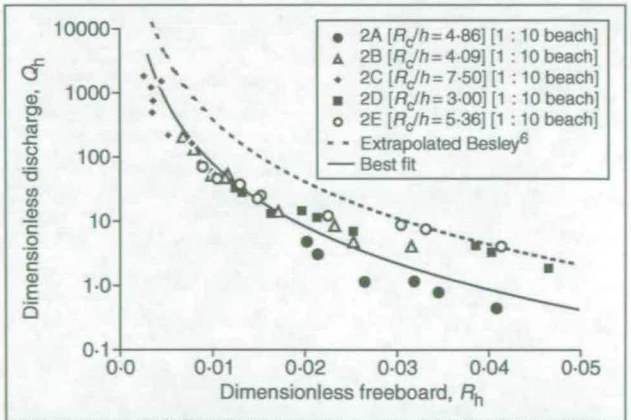

Fig. 13. Overtopping for broken waves on vertical walls, submerged toe

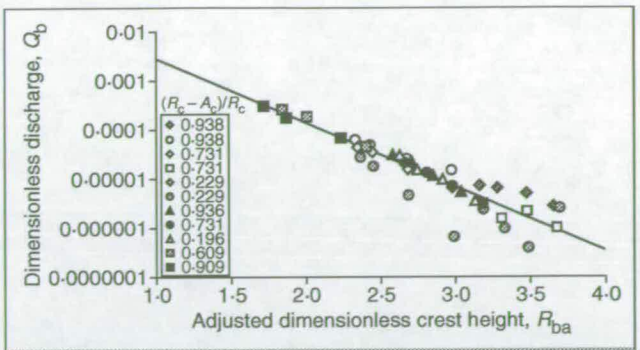

Fig. 14. Overtopping for broken waves on vertical walls, emergent toe

4. OVERTOPPING VELOCITIES

A key consequence of wave overtopping is the direct hazard presented to people or vehicles in the path of the discharge. Although the amount of water overtopping is of course linked to the level of this direct hazard, the velocity with which the water hits an object in its path must also be an important parameter in assessing hazard. The importance of the form of wave breaking onto vertical/battered walls demonstrated throughout Section 3 is further illustrated by the first measurements of overtopping velocities (peak vertical speeds) by Pearson *et al.*[12] and Bruce *et al.*[11] at both small and large scales. Video records were analysed of the largest 20 individual overtopping events (in $N_z = 1000$ waves). The upward velocity (u_z) of the leading edge of the water was estimated from frame-by-frame analysis, and u_z was non-dimensionalised by the inshore wave celerity c_i, given by $c_i = (gh)^{0.5}$. These relative velocities are plotted in Fig. 15 against the wave breaking parameter, h_*.

It is noticeable in Fig. 15 that, when $h_* > 0{\cdot}2$, the non-dimensionalised throw velocity is roughly constant at $u_z/c_i \approx 2{\cdot}5$, but these velocities increase very significantly when $h_* \leq 0{\cdot}2$ reaching $u_z/c_i \approx 3$–7. The only comparable data of which the authors are aware are the field observations of de Rouville *et al.*,[31] who describe uprushing (but not overtopping) jets of speeds between 23 and 77 m/s with maximum $u_z/c_i \approx 5{\cdot}5$, in excellent agreement with the new data.

By way of comparison with overtopping of sloping structures, Richardson *et al.*[32] measured overflow velocities of around $u_z/c_i \approx 2$ for 1 : 2 slopes under plunging conditions.

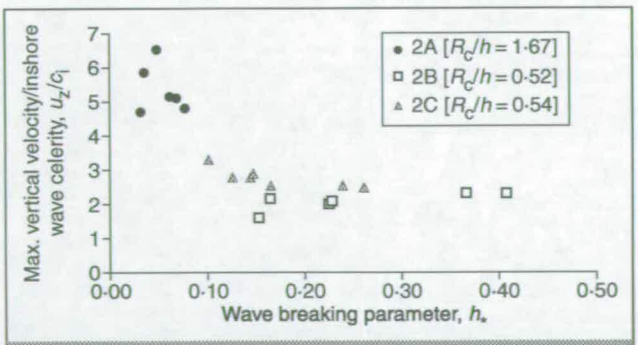

Fig. 15. Overtopping velocities for vertical walls

These measurements confirm that hazards derived from overtopping discharges may vary dramatically with changes of wave breaking characteristics. The largest velocities measured here for vertical/composite walls suggest prototype velocities equivalent to $u_z = 40$ m/s, at which speed an individual overtopping volume of even $V_{max} = 10$ litre per metre run may be imagined to pose a serious hazard.

5. OVERTOPPING CASE STUDIES

The use of prediction methods described above may be illustrated by examining overtopping at the forward vertical part of the composite seawall at the Samphire Hoe reclamation (just west of Dover). The reclaimed land was formed by 5 million m^3 of chalk spoil excavated from the Channel Tunnel. The vertical wall part of the composite sea defence in Fig. 16 is exposed to waves from south and south west, but is popular with walkers and anglers. Eurotunnel was concerned to ensure that access to Samphire Hoe was safe, so commissioned an overtopping hazard warning system, developed during the period 1996–2002. Methods by Sayers *et al.*[33] and Gouldby *et al.*[34] used direct observations to identify ranges of water level and wave conditions giving hazards. The UK Met Office's local area numerical weather model predicted hourly wind speeds 24 h in advance, and hence allowed the calculation of wave conditions at Samphire Hoe using forecasting and transformation models. On site, four levels of hazard were used to record observations.

(*a*) None: no observed overtopping.
(*b*) Low: occasional splash, white water (spray) only. A person may feel nervous, but no substantial danger.
(*c*) Moderate: occasional wave overtops the personnel barrier, momentary green water overtopping and some personal danger.
(*d*) Severe: consistent overtopping, green water and or violent splash, causing substantial danger.

Observations of overtopping hazards for October 2000 to March 2002 were compared with predictions by Allsop *et al.*[5] to support a safe overtopping limit for the public on a seawall promenade given by $q_{safe} \leq 0{\cdot}03$ l/s per m. As expected, the more severe hazards in that analysis occurred for higher wave heights, but there was no such correlation between hazards and tide levels, despite water levels ranging over 6–7 m. Experiments to measure wave overtopping at Samphire Hoe are described by Pullen *et al.*,[35] with a detailed comparison with laboratory measurements given by Pullen *et al.*[36]

Hazards at Samphire Hoe can occur at high and low water levels. This can be explained by careful use of the overtopping prediction methods described in Section 3 of this paper, although a few methods may need to be used out of their recommended ranges to cover the full range of likely water levels and wave conditions at Samphire Hoe.

Nominal wave conditions here of $H_s = 1{\cdot}5$ to 4 m and total water levels from −2·5 m ODN up to +4 m ODN are used to calculate overtopping for a composite wall. Three different methods from Section 3 above are used in the calculations in Fig. 17, corresponding to: 'pulsating' conditions; 'impulsive' breaking; and 'broken' waves. The structure is treated as a composite wall. For these calculations, the mean

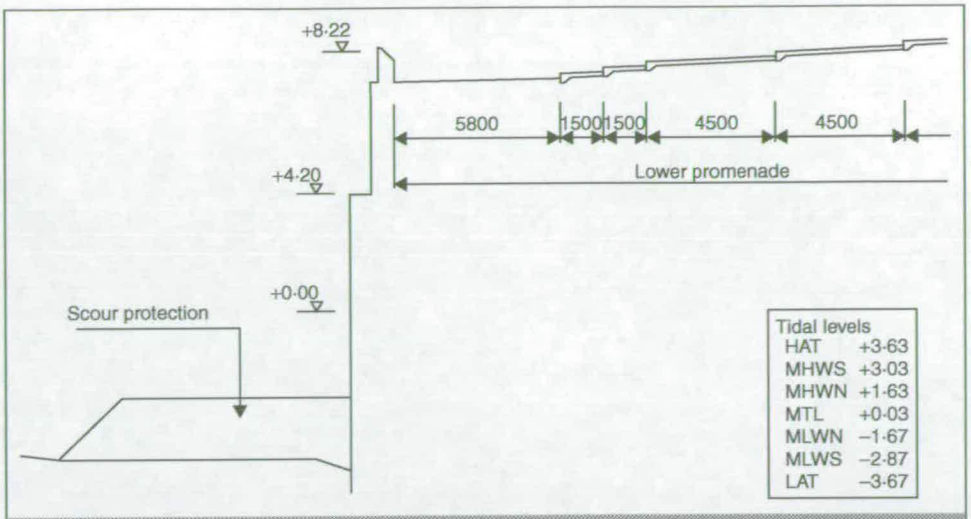

Fig. 16. Samphire Hoe sea defence

wave steepness was taken as $s_{om} = 0{\cdot}05$, typical of storms in the English Channel.

For the larger waves, the predictions follow an expected form, with overtopping reducing slowly with reducing water level (increasing freeboard). For smaller waves, the response is more complicated. The diagonal lines towards the bottom right of Fig. 17 predict overtopping discharges for smaller wave heights under 'pulsating' wave conditions. For these, however, reducing water levels can lead to the onset of 'impulsive' breaking as waves shoal over the toe berm. At this point, the overtopping equation changes suddenly, giving an abrupt increase in overtopping over a relatively small drop in water level. For the lowest wave conditions considered here, the dotted sections of line in Fig. 17 represent some extrapolation of the methods outside of their recommended range so it is possible that the 'step' change in overtopping will be less dramatic than shown. The same change, but to smaller degree, is however shown for larger wave conditions, and observations by the authors at sites such as Alderney and Scarborough confirm the general trend of relatively rapid change of overtopping behaviour.

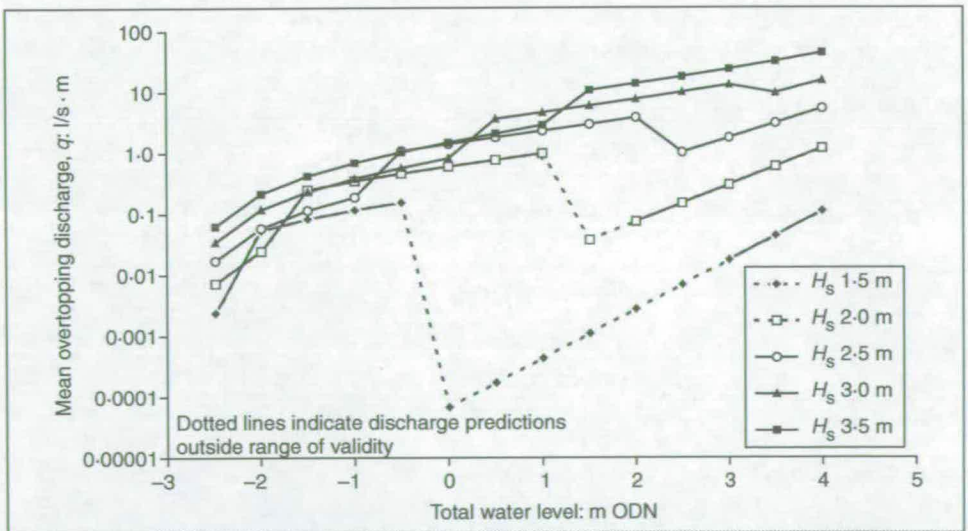

Fig. 17. Overtopping of composite wall at Samphire Hoe related to water level and nearshore wave height

6. DISCUSSION

Vertical, battered and composite walls may provide excellent defences against wave overtopping, but processes of overtopping are complex, and overtopping performance may depend critically on the type of wave breaking at the seawall. It is noted particularly that overtopping of vertical/composite walls may increase when water levels fall, and vice versa.

This paper has assembled data and guidance developed over the last 10 years to predict mean overtopping discharges for simple vertical walls; 5 : 1 and 10 : 1 battered walls; composite walls with toe berms. Guidance is given for 'pulsating', 'impulsive' and 'broken' wave conditions. These prediction methods are illustrated for a test case, showing some of the dramatic (and sometimes unexpected) effects on overtopping.

Additional data are presented to give an appreciation of upward jet velocities for 'impulsive' conditions at simple vertical walls.

The model tests discussed here did not include the effects of wind. It is possible that wind may alter wave overtopping discharges at vertical walls, but it is not certain that it will always increase overtopping. Studies that have tried to capture the 'upper limit' of wind-affected overtopping suggest that increases may be no more than three times.[20] Further data on overtopping with and without wind will be needed to test these initial views, and to quantify any spatial effects on overtopping.[21]

These methods are based primarily on small-scale data. Implicit in the use of these data to generate dimensionless empirical prediction equations is the assumption that small-scale results can be scaled to full scale without the need for any significant correction. It is important to test and to verify or qualify this assumption.

All empirical methods involve simplifications. Real structures

are complex in form, often variable in space and time, and are attacked by three-dimensional waves with potential for local concentrations and related effects. Where a sea defence structure must provide safety to people or valuable infrastructure, the design method must provide predictions to appropriate levels of reliability, so this still may require site specific physical model tests.

7. CONCLUSIONS

Current UK guidance as described by Besley[6] for overtopping of simple vertical walls distinguishes between 'pulsating' and 'impulsive' conditions on the basis of the parameter

$$h_* = \frac{h_s}{H_{si}}\left(\frac{2\pi h_s}{gT_m^2}\right)$$

with 'impulsive' conditions prevailing for $h_* < 0{\cdot}3$. For these conditions, mean overtopping is given by

$$Q_h = 1{\cdot}37 \times 10^{-4} R_h^{-3{\cdot}24}$$

valid over $0{\cdot}05 < R_h < 1{\cdot}0$, where

$$Q_h = \frac{q}{h_*^2\sqrt{gh_s^3}} \quad \text{and} \quad R_h = h_*\frac{R_c}{H_{si}}$$

Recent studies confirm this advice, but suggest that the predictor for 'impulsive' conditions should be applied only for $h_* < 0{\cdot}2$, and that some improvement in definition of mean overtopping is given by

$$Q_h = 1{\cdot}92 \times 10^{-4} R_h^{-2{\cdot}92}$$

which is valid over $0{\cdot}05 < R_h < 1{\cdot}0$.

For battered walls, the following adjusted equations may be applied under 'impulsive' conditions

$$Q_h = 1{\cdot}89 \times 10^{-4} R_h^{-3{\cdot}15}$$

on 10 : 1 battered walls and

$$Q_h = 2{\cdot}81 \times 10^{-4} R_h^{-3{\cdot}09}$$

on 5 : 1 battered walls.

For composite structures, a small modification to the predictor of Besley[6] is suggested. For $d_* < 0{\cdot}2$ (instead of 0·3)

$$Q_d = 5{\cdot}88 \times 10^{-4} R_d^{-2{\cdot}61}$$

which is valid for $h_* \leq 0{\cdot}3$ and $d_* \leq 0{\cdot}2$, where

$$Q_d = \frac{q}{d_*^2\sqrt{gh_s^3}} \quad \text{and} \quad R_d = d_*\frac{R_c}{H_{si}}$$

For conditions under which waves reaching the wall are all 'broken', two new formulae are suggested depending upon whether the toe of the wall is above or below the still water level.

For a water depth at the wall >0: switch to the adjusted form of Besley[6]

$$Q_b = 0{\cdot}27 \times 10^{-4} R_b^{-3{\cdot}24}$$

which is valid for $R_b \leq 0{\cdot}03$.

For a water depth at the wall <0: use adjusted form of van der Meer and Janssen[14]

$$Q_b = 0{\cdot}06 \exp(-4{\cdot}7 R_{ba})$$

which is valid over $1{\cdot}0 < R_{ba} < 4{\cdot}0$, where

$$R_{ba} \equiv R_b s_{op}^{-0{\cdot}17}$$

Velocities of overtopping jets on vertical walls may be estimated as six to 10 times the inshore wave celerity under 'impulsive' conditions, whereas a multiplier of 2·5 is typical for 'pulsating' conditions.

The importance of there being two very distinct physical overtopping regimes ('impulsive' and 'pulsating') is repeatedly emphasised. Not only must different prediction tools be employed, but the different conditions may give quite different hazards. A case study has illustrated that the switch between regimes with changes in water level through a tidal cycle can give rapid (and unexpected) changes in overtopping discharge and hazard.

8. ACKNOWLEDGEMENTS

The VOWS research project by Universities of Edinburgh and Sheffield was supported by EPSRC under GR/M42312 and GR/R42306, and built on earlier research at HR Wallingford supported by MAFF and Environment Agency. Further work by Universities of Edinburgh and Southampton is supported by an EPSRC project in Partnership in Public Awareness (GR/S23827/01). More recent work at Samphire Hoe has been supported by the CLASH project under contract EVK3-CT-2001-00058 and DEFRA/EA under FD2412, is gratefully acknowledged. The cooperation of Dave Johnson of Eurotunnel and Paul Holt of the White Cliffs Countryside Project, is also gratefully acknowledged.

The authors are grateful to EPSRC, DEFRA/Environment Agency and EC for funding these studies. They are also particularly grateful for previous data and guidance from the Environment Agency/EPSRC Project Manager for the CEWE programme, Michael Owen; and to Professor Yoshimi Goda, Professor Leo Franco and Dr Jentsje van der Meer whose positive comments assisted the VOWS team on a number of occasions.

The authors also thank colleagues in Edinburgh, Wallingford, Delft, Emmeloord, and Rome for their assistance and advice.

REFERENCES

1. Franco L., de Gerloni M. and van der Meer J. W. Wave overtopping on vertical and composite breakwaters. *Proceedings of the 24th International Conference on Coastal Engineering*, Kobe, 1994. ASCE, New York.
2. Department of Transport, Local Government and the Regions. *Planning Policy Guidance Note 25: Development and Flood Risk*. HMSO, London, 2001.
3. Brampton A. (ed.) *Coastal Defence–ICE Design and Practice Guide*. Thomas Telford, London, 2002.

4. OWEN M. W. *Design of Seawalls Allowing for Overtopping.* HR Wallingford, Wallingford, Report EX924, 1980.
5. ALLSOP N. W. H., BRUCE T., PEARSON J., ALDERSON J. S. and PULLEN T. Violent wave overtopping at the coast: when are we safe? *Proceedings of the International Conference on Coastal Management*, 2003. Thomas Telford, London, pp. 54–69.
6. BESLEY P. *Overtopping of Seawalls–Design and Assessment Manual.* R&D Technical Report W 178. Environment Agency, Bristol, 1999.
7. SUTHERLAND J. and GOULDBY B. Vulnerability of coastal defences to climate change. *Proceedings of the ICE, Water & Maritime Engineering*, 2003, **156**, No. WM2, 137–145.
8. OUMERACI H., KORTENHAUS A., ALLSOP N. W. H., DE GROOT M. B., CROUCH R. S., VRIJLING J. K. and VOORTMAN H. G. *Probabilistic Design Tools for Vertical Breakwaters.* Balkema, Rotterdam, 2001.
9. BESLEY P., STEWART T. and ALLSOP N. W. H. Overtopping of vertical structures: new prediction methods to account for shallow water conditions. *Proceedings of the ICE Conference on Coastlines, Structures and Breakwaters*, 1998. Thomas Telford, London.
10. BRUCE T., ALLSOP N. W. H. and PEARSON J. Violent overtopping of seawalls–extended prediction methods. *Proceedings of the ICE Conference on Shorelines, Structures and Breakwaters*, September 2001. Thomas Telford, London, pp. 245–255.
11. BRUCE T., ALLSOP N. W. H. and PEARSON J. Hazards at coast and harbour seawalls–velocities and trajectories of violent overtopping jets. *Proceedings of the 28th International Conference on Coastal Engineering*, Cardiff, 2002. ASCE, New York.
12. PEARSON J., BRUCE T., ALLSOP N. W. H. and GIRONELLA X. Violent wave overtopping–measurements at large and small scale. *Proceedings of the 28th International Conference on Coastal Engineering*, Cardiff, 2002. ASCE, New York.
13. CIRIA. *CIRIA/CUR Manual on the Use of Rock in Coastal and Shoreline Engineering*, CIRIA Special Publication 83 (SIMM J. D. (ed.)). CIRIA, London, 1991.
14. VAN DER MEER J. W. and JANSSEN J. P. F. M. Wave run-up and wave overtopping at dikes, in *Wave Forces on Inclined and Vertical Wall Structures*, (KOBAYASHI N. and DEMIRBILEK Z. (eds)). ASCE, New York, 1995, pp. 1–26.
15. VAN DER MEER J. W., TONJES P. and DE WAAL J. P. A code for dike height design and examination. *Proceedings of the ICE Conference on Coastlines, Structures and Breakwaters*, 1998. Thomas Telford, London.
16. ALLSOP N. W. H., BESLEY P. and MADURINI L. Overtopping performance of vertical and composite breakwaters, seawalls and low reflection alternatives. *Final MCS Project Workshop*, Alderney, 1995 (University of Hannover).
17. MCKENNA J. E. *Wave Forces on Caissons and Breakwater Crown Walls.* PhD thesis, Queen's University of Belfast, Belfast, September 1997.
18. ALLSOP N. W. H. and KORTENHAUS A. Hydraulic aspects, in *Probabilistic Design Tools for Vertical Breakwaters.* Balkema, Rotterdam, 2001, chapter 2, pp. 61–156.
19. DE WAAL J. P. and VAN DER MEER J. W. Wave run-up and overtopping on coastal structures. *Proceedings of the 23rd International Conference on Coastal Engineering*, 1992. ASCE, New York, pp. 1758–1771.
20. DE WAAL J. P., TONJES P. and VAN DER MEER J. W. Overtopping of sea defences. *Proceedings of the 25th International Conference on Coastal Engineering (ASCE)*, Orlando, 1996. ASCE, New York, pp. 2216–2229.
21. PULLEN T., ALLSOP N. W. H., PEARSON J. and BRUCE T. Violent wave overtopping discharges and the safe use of seawalls. *Proceedings of the 39th Flood and Coastal Management Conference*, York, June 2004. DEFRA, London.
22. OWEN M. W. Overtopping of sea defences. *Proceedings of the Conference on Hydraulic Modelling of Civil Engineering Structures*, Coventry, 1982. BHRA, Bedford, pp. 469–480.
23. BURCHARTH H. F. and HUGHES S. A. Fundamentals of design, in *2002 Coastal Engineering Manual, Part VI, Design of Coastal Project Elements*, (VINCENT L. and DEMIRBILEK Z. (eds)). US Army Corps of Engineers, Washington, DC, chapter VI-5-2, Engineer Manual 1110-2-1100.
24. TAW (VAN DER MEER J. W. (author)). *Technical Report on Wave Run-up and Wave Overtopping at Dikes.* Report of the TAW, Technical Advisory Committee on Flood Defence, Delft, The Netherlands, 2002.
25. GODA Y., KISHIRA Y. and KAMIYAMA Y. Laboratory investigation on the overtopping rates of seawalls by irregular waves. *Ports & Harbour Research Institute*, 1975, **14**, No. 4, 3–44.
26. HERBERT D. M. and OWEN M. W. Wave overtopping of sea walls–further research. *Proceedings of the ICE Conference on Coastal Structures and Breakwaters*, April 1995. Thomas Telford, London, pp. 81–92.
27. ALLSOP N. W. H., MCKENNA J. E., VICINANZA D. and WHITTAKER T. T. J. New design methods for wave impact loadings on vertical breakwaters and seawalls. *Proceedings of the 25th International Conference on Coastal Engineering*, Orlando, 1996. ASCE, New York.
28. HERBERT D. M. *Overtopping of Seawalls: a Comparison between Prototype and Physical Model Data.* HR Wallingford, Wallingford, Report TR22, 1996.
29. ALLSOP N. W. H. and BRAY R. N. Vertical breakwaters in the United Kingdom: historical and recent experience. *Proceedings of a Workshop on Wave Barriers in Deep Waters*, 1994. Port and Harbour Research Institute, Yokosuka, Japan, pp. 76–100.
30. BRUCE T., PEARSON J. and ALLSOP N. W. H. Violent wave overtopping–extension of prediction method to broken waves. *Proceedings of the Conference on Coastal Structures '03*, Portland, 2003. ASCE, New York.
31. DE ROUVILLE M. A., BRESSON M. M. P. and PETRY P. État actuel des Etudes internationales sur les Efforts dus aux Lames. *Annales des Ports et Chaussées*, 1938, **108**, No. VII, 5–113 (in French).
32. RICHARDSON S., PULLEN T. and CLARKE S. Jet velocities of overtopping waves on sloping structures: measurements and computation. *Proceedings of the 28th International Conference on Coastal Engineering*, Cardiff, 2002. ASCE, New York.
33. SAYERS P. B., BRAMPTON A. H., JONSON D. and ARAN B. Public access to the Samphire Hoe seawall: a site specific overtopping hazard warning system. *Proceedings of Tidal '96*, November 1996, Brighton.

34. GOULDBY B. P., SAYERS P. B. and JOHNSON D. Real-time hazard forecasting: implementation and two years operation at Samphire Hoe, Dover. *MAFF Conference of River & Coastal Engineers*, Keele, 1999. MAFF, London.
35. PULLEN T., ALLSOP N. W. H., BRUCE T. and GEERAERTS J. Violent wave overtopping: CLASH Field Measurements at Samphire Hoe. *Proceedings of the Conference on Coastal Structures '03*, Portland, 2003. ASCE, New York.
36. PULLEN T., ALLSOP N. W. H., BRUCE T., PEARSON J. and GEERAERTS J. Violent wave overtopping at Samphire Hoe: field and laboratory measurements. *Proceedings of the 29th International Conference on Coastal Engineering*, Lisbon, 2004. ASCE, New York.

What do you think?
To comment on this paper, please email up to 500 words to the editor at journals@ice.org.uk

Proceedings journals rely entirely on contributions sent in by civil engineers and related professionals, academics and students. Papers should be 2000–5000 words long, with adequate illustrations and references. Please visit www.thomastelford.com/journals for author guidelines and further details.

Appendix I: Pearson *et al.*, 2001

Pearson, J., Bruce, T. & Allsop, N.W.H. (2001), *Prediction of wave overtopping at steep seawalls – variabilities and uncertainties*, Proc. Ocean Wave Measurement and Analysis ('Waves 2001'), 2, pp1797–1808, ASCE, New York, ISBN 0-7844-0604-9

Appendix I
Pearson *et al.*, 2001

Pearson, J., Bruce, T. & Allsop, N.W.H. (2001), *Prediction of wave overtopping at steep seawalls – variabilities and uncertainties*, Proc. Ocean Wave Measurement and Analysis ('Waves 2001'), 2, pp1797–1808, ASCE, New York, ISBN 0-7844-0604-9

I.1 Declaration of contribution

The team of authors worked very closely in the specification of this test programme, the subsequent analysis of the data and in the editing of the paper text. The tests were carried out (principally) by Pearson, a post-doctoral Research Engineer working with the author at Edinburgh, with whom the author had long, almost daily discussions during the testing phase. Further data from HR Wallingford were brought into the paper by Allsop, who presented initial results at the conference. The final paper was subsequently written by Bruce and Pearson.

I.2 Published paper

overleaf

PREDICTION OF WAVE OVERTOPPING AT STEEP SEAWALLS – VARIABILITIES AND UNCERTAINTIES

Jonathan Pearson[1], Tom Bruce[2] and William Allsop[3]

Abstract: This paper presents results from collaborative research on Violent Overtopping of Waves at Seawalls (VOWS) describing overtopping performance and processes at steep seawalls. VOWS results have been used to develop / improve prediction methods for mean overtopping discharges, wave-by-wave overtopping volumes, and overtopping throw velocities. This paper discusses variabilities and uncertainties inherent in the overtopping processes, and presents example data on uncertainties to be used in probabilistic design or hazard evaluations. The dependency of these parameter uncertainties upon the proportion of wave overtopping waves is highlighted.

1. INTRODUCTION

In rural areas, coastal defences are often formed as simple embankments. In most instances where overtopping of an embankment seawall is being assessed, the responses of most interest are time-averaged ones, such as mean overtopping discharge over 500-1000 waves, or the total overtopping volume over (the upper part of) a tide.

The situation may be quite different for urban and harbour seawalls (and some breakwaters). In these cases, consideration of personal safety and potential damage to property drives the design and will require the proportion of overtopping waves (N_{ow} / N_w) within the design storms to be very low e.g. <1%. This places a much greater requirement on the accuracy of the design tool employed, not only for the number of overtopping waves (N_{ow}), but also for the prediction of individual maximum events. A further complication is that these structures

1 Research Fellow, Division of Engineering, University of Edinburgh, King's Buildings, Edinburgh, EH9 3JL, UK. J.Pearson@ed.ac.uk
2 Lecturer, Division of Engineering, University of Edinburgh, King's Buildings, Edinburgh, EH9 3JL, UK. Tom.Bruce@ed.ac.uk
3 Professor (associate), Civil Engineering, University of Sheffield, Technical Director, HR Wallingford, Wallingford, OX10 8BA UK. W.Allsop@shef.ac.uk

are often formed by steep or vertical walls, the description of whose overtopping is more complex than for sloping embankments, for example, wave breaking may occur at the structure.

Uncertainty is a general concept which refers to the condition of being unsure about something. In coastal engineering problems, uncertainty can be defined in a number of ways, such as statistical uncertainties may be defined as the estimated amount or percentage by which an observed or calculated value may differ from the true value, or knowledge uncertainty may occur due to a lack of knowledge of all the causes and effects in the physical processes.

Quantitative estimates of uncertainties in predicted overtopping parameters, eg Q_{bar}, N_{ow} are required as a component of probabilistic and hazard assessment. This paper examines the source of these variabilities and explains the way in which the level of variability / uncertainties varies with the structure type, eg high or low allowable N_{ow}.

2. PREVIOUS WORK

2.1 Mean overtopping discharges

Most design methods for seawalls hitherto have concentrated on predicting a crest level or other aspect of wall geometry to give a (tolerable) mean discharge or overtopping volume over a storm event. Tolerable discharges have been suggested by Owen (1980), Franco *et al* (1994) and Besley (1999). Prediction of mean overtopping discharge are generally based on empirical formulae fitted to laboratory measurements, see for example Goda *et al* (1975), Owen (1982), De Waal *et al* (1996), Hedges & Reis (1998), Van der Meer *et al* (1998). These formulae mainly assume non-breaking (or "pulsating") wave conditions, but studies by Besley *et al* (1998) and Van der Meer *et al* (1998) separate non-breaking and breaking (or "impulsive") processes. Besley *et al* (1998) indicate configurations of vertical / composite walls for which impulsive breaking may occur, and demonstrate that simple methods may under-estimate overtopping under impact conditions.

Allsop *et al* (1995) demonstrated that the overtopping processes were strongly influenced by the form of the incident waves. When waves are small compared to water depth, the waves impinging on a vertical / composite wall are generally reflected back. If the waves are large relative to water depth, then they can break onto the structure, leading to significantly more abrupt overtopping characteristics. These observations led to formulation of a wave breaking parameter, h*, given by:

$$h^* = \frac{h}{H_s}\left(\frac{2\pi h}{gT^2}\right) \qquad (1)$$

Allsop *et al* (1995) noted that reflecting or pulsating waves predominate when $h^* > 0.3$, and that impacting waves where more likely to occur when $h^* \leq 0.3$. Under impacting wave conditions, new dimensionless discharge (Q_h) and freeboard parameters (R_h), incorporating h* were established, and were given by:

$$Q_h = Q / (gh^3)^{0.5} / h^{*2} \quad (2)$$

$$R_h = (R_c / H_s)\, h^* \quad (3)$$

where Q is the mean overtopping discharge per metre run. Besley (1999) utilised the empirical studies of Allsop *et al* (1995) and de Waal *et al* (1992) for which $h^* \leq 0.3$ to derive the following relationship for vertical walls.

$$Q_h = 1.37 \times 10^{-4}\, R_h^{-3.24} \quad (4)$$

2.2 Peak overtopping discharges

In terms of tolerable safety limits, a much more useful parameter is the maximum individual volume. Allsop et al (1995) followed a similar analytical procedure to Franco et al (1994), and demonstrated that peak overtopping rates under impulsive conditions could be estimated. Allsop et al (1995) showed that for a number of experimental investigations on vertical seawalls, the statistical distributions of individual wave by wave overtopping were similar. Besley (1999) adopted these observations and suggested that by given the number of overtopping events for a particular storm duration, the peak individual overtopping discharge could be estimated.

For vertical structures under impulsive conditions ($h^* \leq 0.3$), Allsop et al (1995) demonstrated empirically that the that the proportion of overtopping waves could be given by:

$$N_{ow}/N_w = 0.031\, R_h^{-0.99} \quad (5)$$

where N_{ow} is the number of overtopping waves and N_w is the number of waves. Franco *et al* (1994) and subsequent analysis by Besley (1999) demonstrated that the wave by wave individual overtopping volumes could be described by a two parameter Weibull probability distribution. Besley (1999) suggested that the expected maximum individual overtopping volume, V_{max}, in a sequence of N_{ow} overtopping waves could be described by:

$$V_{max} = a\, (\ln(N_{ow}))^{1/b} \quad (6)$$

which for vertical seawalls subjected to impacting wave conditions, the Weibull scale parameter, $a = 0.92V_{bar}$, and the Weibull shape parameter, $b = 0.85$.

3. EXPERIMENTAL STUDY

Measurements have been carried out in the 2-dimensional wave flume in the Division of Engineering at the University of Edinburgh. The flume is 20m long, 0.4m wide and has an operating water depth of 0.7m. The flume is equipped with an absorbing flap-type wave maker. Experimental investigations have concentrated on a vertical seawall, in which a series of tests were undertaken to assess the repeatability, variabilities and uncertainties of the overtopping processes. For the vertical structure, a JONSWAP pseudo-random sea state spectra of varying length (128-4096 seconds, or roughly 100 – 4000 waves) was generated. For each of these conditions, approximately 10 repeat tests of different start phases have been performed. A summary of test conditions in shown in Table 1. Wave-by-wave overtopping discharge measurements have been obtained using a receiving container located behind the structure crest suspended from a load cell, the discharge measurement system was also tested to ensure consistent and repeatable results, therefore a number of preliminary experiments were performed in which known volumes of water were poured into the receiving container.

Table 1. Summary of repeatability tests *

	Seed modification factor		Total number
Sequence length	Mod=3	Mod=1,2....10	of tests
128	10	1	20
256	10	1	20
512	10	1	20
1024	10	1	20
4096	8	-	8

* Wave condition = H_s = 0.067m, T_m = 1.04s, R_c = 0.15m, h_s = 0.09m, h_* = 0.071

The objective of the 2-d tests was to extend existing prediction methods into regimes in which wave breaking at or onto the structure is significant. The matrix of conditions [significant wave height at the toe of the structure (H_s), peak period (T_p), water depth at structure (h) and crest freeboard (R_c)] is shown in Table 2. Further experimental studies were undertaken for a range of wave and water level configurations, a matrix of test conditions, together with more detailed results are presented in Bruce et al (2001).

Table 2. Summary of test conditions

Structure Configuration	Test Series	Configuration	Nominal wave period T_s [s]	Significant wave height H_{si} [mm]
Vertical	2A [1:10 beach]	R_c = 150mm h = 90mm	1.0	63, 67, 69, 70, 81
			1.33	63, 70, 76, 82
			1.6	62, 77, 82
	2B [1:10 beach]	R_c = 129mm h = 247mm	1.0	71, 79, 86, 92, 100
			1.33	81,93, 94, 100, 102
			1.6	71, 74, 89, 97, 105
	2C [1:50 beach]	R_c = 85mm h = 155mm	1.0	46, 55, 58, 61
			1.33	39, 58, 63, 64
			1.6	34, 44, 52, 62
	2D [1:50 beach]	R_c = 113mm h = 127mm	1.0	55, 57, 58
			1.33	53, 57, 58
			1.6	30, 40, 59, 62

* Sequence length = 1024seconds

4. RESULTS

4.1 System accuracy

Prior to undertaking any tests the accuracy of the overtopping measurement system was tested. Two tests, each of nine simulated overtopping events were performed in which known volumes of water were 'thrown' into the measurement container. The resulting data was then passed through an algorithm to identify and quantify individual overtopping events. Figure 1 shows sample output data, the lower trace is event detector, and the upper traces are raw and processed load cell data. Software finds events from lower trace (thresholded to, eg here, 2.5V). Load cell output between events divided into two, and discharge measurement based upon second half (allowing for settling after initial discharge into container).

Figure 1: Simulated series of pre-measured discharges. Lower trace is "event detector". Upper traces are raw and processed load cell output. Table shows corresponding results of 18 simulated events, with pre-measured volumes and volumes given by discharge measurement system / software.

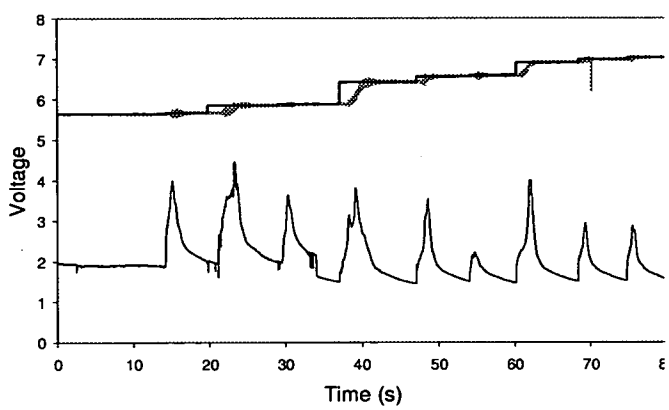

Actual volume (ml)	Measured volume (ml)	Relative error (%)	Actual error (ml)
300	273	9	- 27
50	47	6	- 3
100	93	7	- 7
1200	1201	0.1	+ 1
150	139	7	- 11
50	48	4	- 2
700	692	1	- 8
100	90	10	- 10
400	446	12	+ 46
100	61	39	- 39
400	402	0.5	+ 2
50	47	6	- 3
1200	1206	0.5	+ 6
300	299	0.3	- 1
50	48	4	- 2
700	704	0.6	+ 4
150	156	4	+ 6
100	106	6	+ 6
Totals	**6100**	**6057**	**0.7**	**- 43**

From the results, a difference of 43ml (=0.7%) in total volume between the measured and actual discharge is observed. This indicates there is no significant systematic error associated with the measurement system. During the design of the test matrix, the maximum individual overtopping volume for all the tests had a predicted value of 2000ml. It was therefore concluded that any errors in the measurement system were negligible.

4.2 Mean Overtopping Discharge

Measurements of mean overtopping discharge (described here by dimensionless discharge Q_h) for the simple vertical wall show agreement with Besley *et al*'s (1998) method over the full range of test conditions studied, typically to within a factor of two, see Figure 2. The largest proportion of impulsive events was recorded under test conditions "2A", see Table 2. Adopting the procedure of Allsop *et al.* (1995), the best-fit trend line from this study was found to be

$$Q_h = 1.55 \times 10^{-4} R_h^{-3.03} \quad (7)$$

with a corresponding least squares regression $R^2 = 0.92$. The results of this study when compared with the results from Besley *et al* (1998) show very similar characteristics, as shown by the two trend lines in Figure 2.

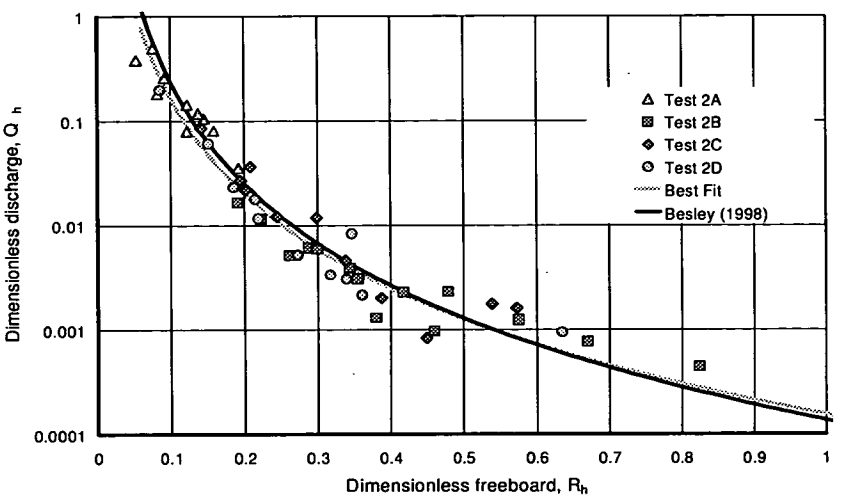

Figure 2: Overtopping discharge on a plain vertical wall, compared to the prediction of Besley *et al* (1998).

4.3 Number of overtopping waves/ Peak overtopping rates

A parameter which is vital in predicting peak overtopping volumes and statistics of wave-by-wave overtopping volumes is the number or proportion of overtopping waves (N_{ow}) – see Equation 5. The variation of N_{ow} with freeboard for vertical wall, as quantified from these tests, is shown in Figure 3. It is noticeable that the results of N_{ow} / N_w deviate significantly from the prediction by Equation 5, which leads to uncertainty in adopting previous prediction methods for individual maxima.

Careful analysis of the problem in defining N_{ow} precisely, reduces to a particular difficulty the exact definition of an "overtopping event". Clearly such events cannot constitute all occasions when some water passes over the wall, as that would increase with each improvement in measurement precision. Any definition must therefore generate a limit of only one overtopping event per incident wave. A method to overcome these difficulties by defining a consistent threshold level before an overtopping event is included is under development. Only then can a useful improvement be made in the prediction of N_{ow}.

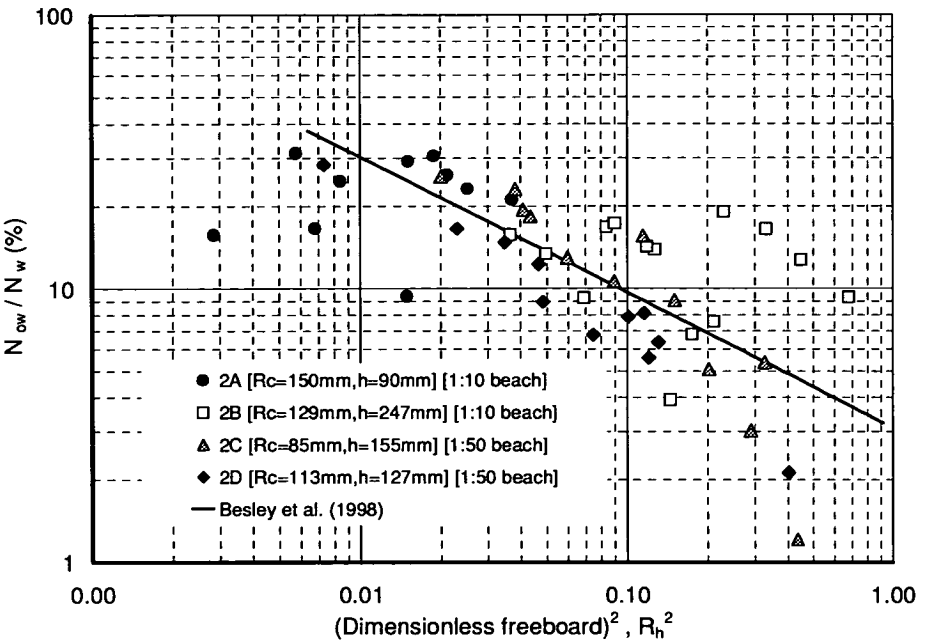

Figure 3: Percentage of waves overtopping a vertical wall, compared to Besley *et al* (1998).

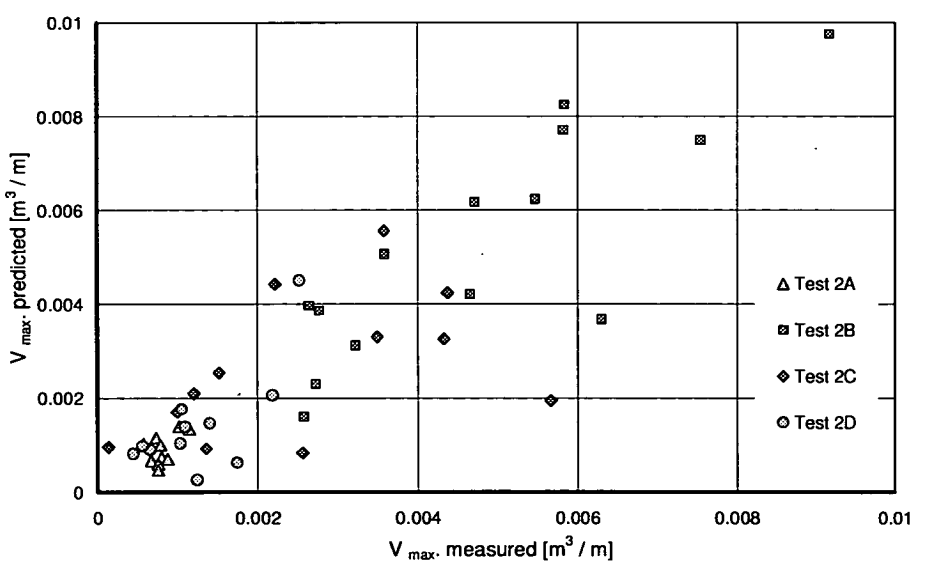

Figure 4: Comparison of measured and predicted maximum overtopping volumes

Maximum individual overtopping volumes predicted using methods by Besley (1998) are compared in Figure 4 with those measured. Despite the uncertainties in defining precisely what constitutes an overtopping event, it would appear that maxima may be slightly under-predicted. Nevertheless the results indicate a reasonable correlation between predicted and measured volumes.

4.4 Variabilities and repeatability

In order to asses the variabilities and repeatability on the overtopping characteristics, ten nominally identical repeats of each of 128s, 256s, 512s and 1024s were run. Eight nominally identical repeats of a 4096s test were also run, with equipment failure preventing the full set of ten repeats being completed. (ie, a total of 48 sequences). Figures 5 and 6 show the effect of the increase in sequence length upon four measures of overtopping: The error bars on Figures 5 & 6 represent ± one standard deviation

From Figure 5 it can be seen that, the mean discharge, Q is reasonably well settled from 512s tests and above, however it is noticeable that from the conditions tested that the mean overtopping volume varies with the selection of test sequence length, however similar characteristics were also observed in the measured wave heights, it can be therefore concluded that this variation is a function of the wave generating software rather then the overtopping characteristics. The maximum individual discharge increases slightly with the number of waves, which is as expected as the likelihood increases with sequence length.

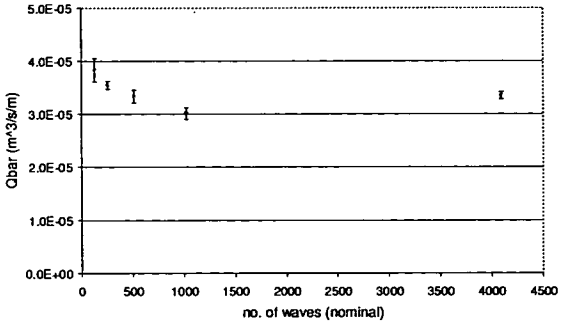

Figure 5: Q_{bar} with sequence length

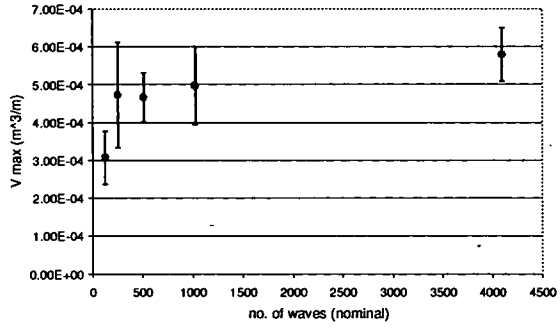

Figure 6: V_{max} with sequence length

4.5 Consistency between tests nominally identical except for JONSWAP seed

Additional experiments were performed whereby the tests reported in section 4.4, were repeated *except* that the JONSWAP seed is varied for each. Figure 7 characterises the effect upon the spread of data by looking at the way in which the standard deviation varies with sequence length for fixed and varying seeds.

From Figure 7, it can be seen that as expected the standard deviations of Q_{bar} have the lowest deviations: < 5% for same-seed, and ~ 8% for varying-seed, and the largest scatter is in V_{max} which is typically ~ 15 - 20%. For 1024s sequence (most stable data presented on this graph), there is an indication that the open symbols lie above the closed ones, ie, that scatter is increased with varying of seed. It can therefore be suggested that a typical scatter goes up from 5 - 8% for fixed seed to 10 - 15% for varying seed.

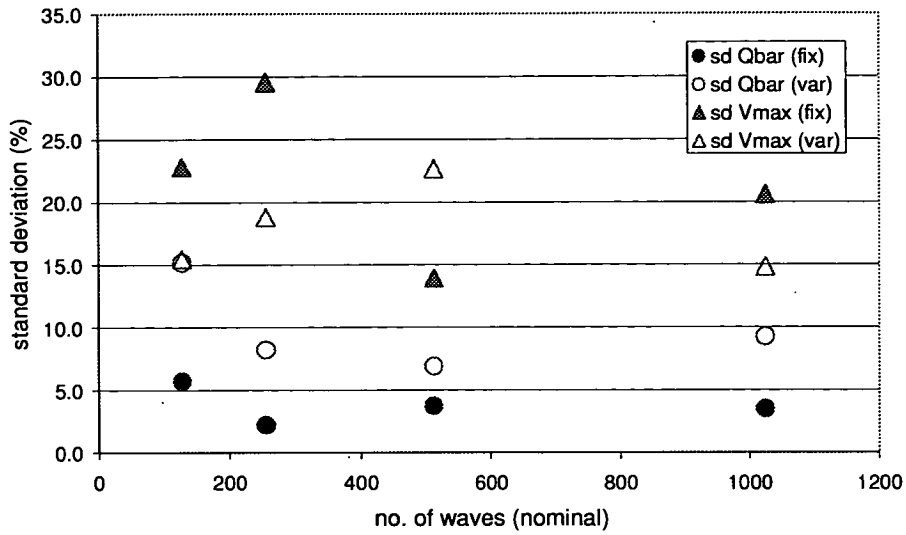

Figure 7: Standard deviations of overtopping measured for repeated tests. For each of four sequence lengths, std. Devs. are plotted for 10 same-seed and 10 varying-seed test groups. Filled symbols = fixed-seed, open symbols = varying-seed.

4.6 Variability and uncertainties due to definition of events of N_{ow}

Discussions on variability has so far concentrated on the variabilities due to a single wave / structure configuration, this section discusses the variabilities over the full range of tested conditions where N_{ow} varies. For each structure configuration [2A – 2D], 3 conditions have been further analysed whereby the 1000 wave test sequences have been split into ten (102s), five (204s) & two (512s) sections. The variabilities from one such test is shown in Figure 8 (2D-1).

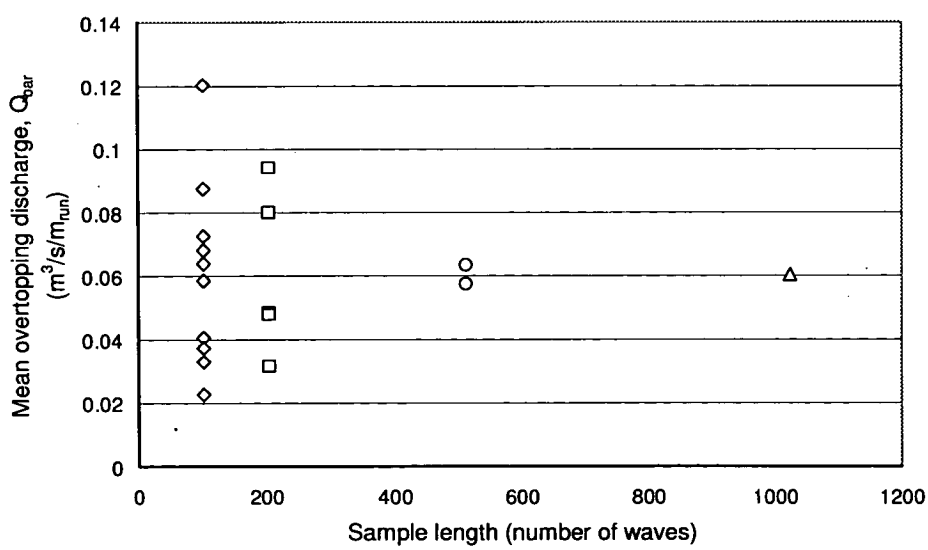

Figure 8: Variability of mean overtopping discharge of 1000 wave test split into various equal sections (Test shown 2D-1)

For a sub-set of core tests, the variability in overtopping with respect to sequence length has been determined. The variability in mean overtopping discharge rate for different test sequence lengths is shown in Figure 9, it is of note that for cases with lower overtopping events the variability in Q_{bar} is higher.

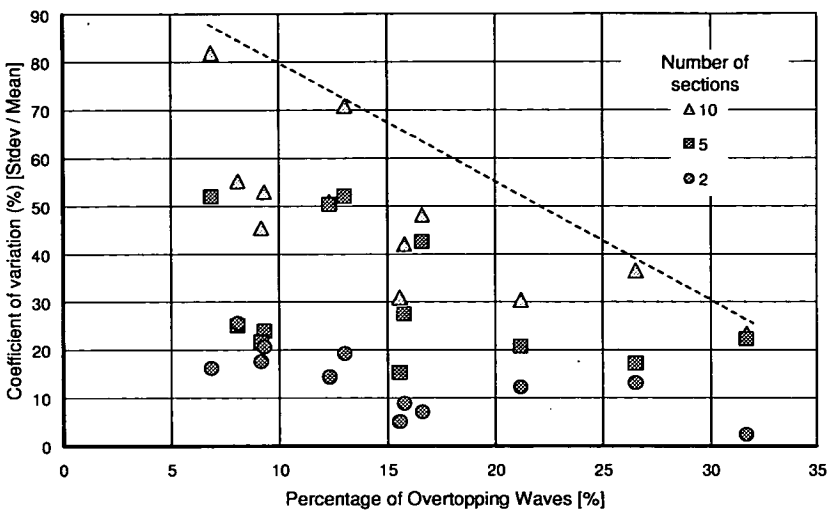

Figure 9: Standard deviation of mean overtopping discharge of 1000 wave test sequences split into various equal sections

Although showing some scatter, it is noticeable from Figure 9, that the variability for the lower overtopping cases (N_{ow} ~ 6%) are typically 3 times larger than those of the higher cases (N_{ow} ~ 30%), as indicated by the upper envelope (dotted line), further work is needed to quantify the variabilities when the test sequence length is significantly extended. Only then will it be possible to give qualitative confidence limits on overtopping measurements, such as those given in Figure 2.

5. CONCLUSIONS

The prediction method of Besley *et al* (1998) for mean overtopping discharge may be used under conditions when impulsive wave action is significant or dominant, with mean discharges remaining well-predicted (typically within a factor of two). From the tested conditions, it can be seen that the results of N_{ow} deviate from the prediction of Besley (1999), but nevertheless when these results are used to compare measured and predicted maximum overtopping volumes, the results show good agreement.

For mean overtopping discharge rates, when the same wave condition is run, standard deviations of Q_{bar} have the lowest deviations: < 5% for same-seed, and ~ 8% for varying-seed. For peak overtopping rates, the scatter in V_{max} is increased with varying of seed, with a typical scatter going up from 5 - 8% for fixed seed to 10 - 15% for varying seed.

The variability in mean overtopping discharge rates for different test sequence lengths increases as the number of overtopping events reduces. The coefficient of variation of Q_{bar} increases by a factor of approximately 3 with a reduction from 30% to 10% of overtopping waves.

ACKNOWLEDGEMENTS

This work is funded by the UK EPSRC (GR/M42312), and supported by the VOWS Management Committee also including members from Manchester Metropolitan University (Derek Causon, David Ingram, Clive Mingham), Posford-Haskoning (Dick Thomas, Keming Hu), Bullen & Co (Mark Breen, Dominic Hames), HR Wallingford (Philip Besley), all of whose input and support is gratefully acknowledged. The VOWS project is also particularly pleased to acknowledge guidance and helpful supervision of their collaborative work of the EPSRC CEWE Project Manager, Michael Owen.

REFERENCES

Allsop N.W.H., Besley P. & Madurini L. (1995). "Overtopping performance of vertical walls and composite breakwaters, seawalls and low reflection alternatives" Paper 4.7 in MCS Final Report, publn University of Hannover.

Besley P. (1999) "Overtopping of seawalls – design and assessment manual " R & D Technical Report W 178, ISBN 1 85705 069 X, Environment Agency, Bristol.

Besley P.B., Stewart T, & Allsop N.W.H. (1998) "Overtopping of vertical structures: new methods to account for shallow water conditions" Proceedings of Int. Conf. on Coastlines, Structures & Breakwaters '98, Institution of Civil Engineers, pp46-57, publn. Thomas Telford, London.

Bruce, T, Allsop, N.W.H. & Pearson, J. (2001) "Violent overtopping of seawalls – extended prediction methods" Proc. "Coastlines, Seawalls and Breakwaters '01" ICE, publn Thomas Telford, London.

Franco, L., de Gerloni, M. & van der Meer, J.W. (1994), "Wave overtopping on vertical and composite breakwaters", Proc 24th Int. Conf. Coastal Eng., Kobe, publn. ASCE, New York.

Goda, Y, Kishira, Y, and Kamiyama, Y. (1975) 'Laboratory investigation on the overtopping rates of seawalls by irregular waves'. Ports and Harbour Research Institute, Vol 14, No. 4, pp 3-44, PHRI, Yokosuka.

Hedges, T.S. & Reis, M.T. (1998), "Random wave overtopping of simple sea walls: a new regression model", Proc. Instn. Civil Engrs. Water, Maritime & Energy, Volume 130, March 1998, Thomas Telford, London.

Meer van der J.W., Tonjes P. & de Waal J.P. (1998) "A code for dike height design and examination " Proceedings of Coastlines, Structures & Breakwaters '98, Int. Conf. at Institution of Civil Engineers, March 1998, pp 5-21, publn. Thomas Telford, London

Owen, M.W. (1980), "Design of seawalls allowing for wave overtopping" HR Report EX 924, June 1980, Hydraulics Research, Wallingford.
Owen, M.W. (1982), "Overtopping of Sea Defences", Proc. Intl. Conf. On Hydraulic Modelling of Civil Eng. Structures, Coventry, pp469-480, BHRA, Bedford.

Waal, de J.P., & van der Meer, J.W. (1992), "Wave run-up and overtopping on coastal structures" Proc 23rd Int. Conf. Coastal Eng., pp1758-1771, publn. ASCE, New York.

Waal, de J.P., Tonjes, P. & van der Meer, J.W. (1996), "Overtopping of sea defences" Proc 25rd Int. Conf. Coastal Eng., pp2216-2229, Orlando, publn. ASCE, New York.

Appendix J: Bruce *et al.*, 2003

Bruce, T., Pearson, J. & Allsop, N.W.H. (2003), *Violent wave overtopping – extension of prediction method to broken waves*, Proc "Coastal Structures 2003", pp619–630, ASCE, Reston, Virginia, ISBN 0-7844-0733-9

Appendix J
Bruce *et al.*, 2003

Bruce, T., Pearson, J. & Allsop, N.W.H. (2003), *Violent wave overtopping – extension of prediction method to broken waves*, Proc "Coastal Structures 2003", pp619–630, ASCE, Reston, Virginia, ISBN 0-7844-0733-9

J.1 Declaration of contribution

Work for this paper was led by the author, who (after a helpful comment made by Prof. Goda after the presentation of Bruce *et al.* 2001 – see Section 3.4.2 – initiated investigation of this topic via his supervision of an honours undergraduate student project. The work was taken forward by the author together with Pearson, who was then a post-doctoral Research Engineer at Edinburgh working under the author's guidance. Pearson ably carried out the tests. The author and Pearson then spent quite some hours together pouring over the new data and possible analysis methods - discussion which eventually led to the synthesised tentative guidance Discussions with Allsop then led to final conclusions. The author took a leading role in the preparation and final editing of the text, and presented the paper at the conference.

J.2 Published paper

overleaf

Violent Wave Overtopping – Extension of Prediction Method to Broken Waves

Tom Bruce[1], Jonathan Pearson[2] & William Allsop[3]

Abstract

Well-verified guidance exists for the prediction of wave overtopping over vertical walls, including breaking / impulsive and non-breaking / pulsating wave attack. For broken waves, only Goda's (1975) design charts give guidance, and only for sea steepnesses $s_{op} < 0.036$.

This paper presents results of tests to quantify overtopping of vertical walls under predominantly broken wave attack. Tentative guidance is suggested. For cases where the toe of the wall is submerged, an adjustment to the method of Besley (1999) is suggested. For cases where the water level falls below the toe of the wall, adjustment to the method for sloping structures of van der Meer & Janssen (1995) is suggested.

Introduction

Coastlines are areas of high amenity value, and are under increasing pressure of use. Breakwaters, seawalls and related man-made structures provide shelter against waves for people working or travelling and are therefore under increasing scrutiny from public / regulatory bodies for performance and cost. Performance scrutiny will particularly increase if example structures are identified as increasing hazards in their vicinity.

Wave overtopping of seawalls are generally classified by empirical functions of wave and geometry, *eg* Goda (1975), Franco *et al* (1994), Besley (1999). Those descriptions have mainly covered non-breaking / pulsating wave conditions, yet many seawalls / breakwaters can suffer sudden and violent overtopping for those conditions where waves break impulsively against the wall (*eg* Figure 1).

1 Lecturer, School of Engineering & Electronics, University of Edinburgh, King's Buildings, Edinburgh, EH9 3JL, UK; Tom.Bruce@ed.ac.uk

2 Research Fellow, School of Engineering & Electronics, University of Edinburgh, King's Buildings, Edinburgh, EH9 3JL, UK. J.Pearson@ed.ac.uk

3 Visiting Professor, Civil Engineering, University of Southampton, and Technical Director Maritime Structures, HR Wallingford, Wallingford, OX10 8BA UK. W.Allsop@hrwallingford.co.uk

Figure 1: A broken wave overtopping the Admiralty Breakwater, Alderney (photo courtesy Gerald Müller / EPSRC BWIMCOST project).

Work under the EC MAST III MCS-project and "PROVERBS" indicated configurations of vertical and composite walls for which impulsive breaking events may occur, see e.g. Oumeraci *et al* (2001), Allsop et al (1996). Studies by Besley et al (1998), Bruce et al (2001) and Pearson et al. (2002) have suggested and verified predictive formulae for overtopping characteristics under these conditions. These studies are however limited in that little or no information is available on broken waves. (Indeed, it was a comment made by Prof. Goda to this effect after the presentation of Bruce et al., 2001, that was the seed for this work, see Allsop (2002).

Experiments presented in this paper aimed to quantify the mean overtopping processes of vertical seawalls under predominantly broken wave attack, and to advise on possible extensions of existing predictive formulae into the broken wave regime.

Current Design Guidance for Overtopping of Vertical Walls

Prediction of mean overtopping discharge are generally based on empirical formulae fitted to laboratory measurements, see for example Goda *et al* (1975), Owen (1982), De Waal *et al* (1996), Hedges & Reis (1998), Van der Meer *et al* (1998). These formulae mainly assume non-breaking (or "pulsating") wave conditions, but studies by Besley *et al* (1998) and Van der Meer *et al* (1998) separate non-breaking and breaking (or "impulsive") processes. Besley *et al* (1998) indicate configurations of vertical / composite walls for which impulsive breaking may occur, and demonstrate that simple methods may under-estimate overtopping under impact conditions.

Overtopping volumes and velocities are strongly influenced by the form of the incident waves (see Allsop et al, 1995, Besley et al, 1998, Bruce et al, 2002). When waves are small compared to the local depth, waves impinging on a vertical / composite wall are generally reflected. If waves are large relative to water depth, then they can break onto the structure, leading to significantly more abrupt overtopping characteristics. Besley, (1999) advises the use of a wave breaking parameter, h* , given by:

$$h_* \equiv \frac{h_s}{H_{si}} \frac{2\pi h_s}{T_m^2} \qquad (1)$$

When h* > 0.3 pulsating (non-breaking) waves predominate and the mean overtopping discharge, Q is given by:

$$\frac{Q}{\left(gH_{si}^3\right)^{0.5}} = 0.05\exp\left(-2.78\frac{R_c}{H_{si}}\right) \tag{2}$$

When h* < 0.3 impulsive (breaking) waves predominate and the mean overtopping discharge, Q is given by:

$$Q_h = 0.000137R_h^{-3.24} \tag{3}$$

where the dimensionless freeboard

$$R_h \equiv h_* \frac{R_c}{H_{si}} \tag{3b}$$

and the revised dimensionless discharge

$$Q_h \equiv \frac{1}{h_*^2}\frac{Q}{\left(gH_{si}^3\right)^{0.5}}. \tag{3c}$$

Besley (1999) gives no advice specific to broken waves when R_h extends beyond the stated range of validity. Only Goda et al. (1975) gives any significant advice for broken waves. Guidance for vertical walls with 1:10 and 1:30 beach slopes is available in the form of design charts (*eg* Figure 2) for offshore wave steepnesses, s_{op} = 0.012, 0.017 or 0.036, and relative water depths at the wall h_s / H_s' down to – 0.5. Comparisons will be made later between new data and these methods.

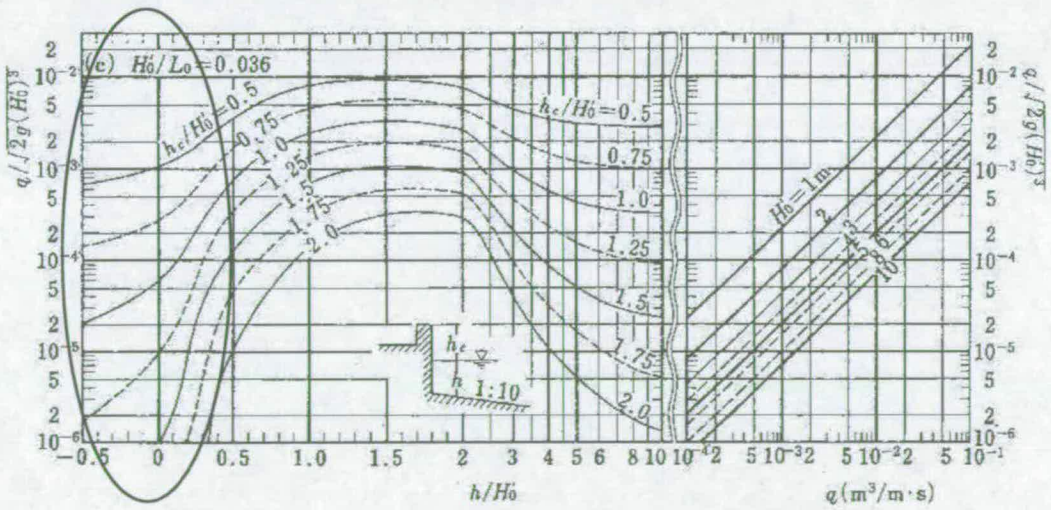

Figure 2: Mean wave overtopping prediction for s_{op} = 0.036 (adapted from Goda et al, 1975). Highlighted area represents approximate broken wave region. Note that Goda's h_c is equivalent to R_c in this paper, and Goda's $h \equiv h_s$.

New Laboratory Studies

A series of investigations were completed at small-scale in the wave channel in the School of Engineering at University of Edinburgh. The wave channel is 20 m long, 0.4 m wide and has an operating water depth of 0.7 m. The channel is equipped with an absorbing flap-type wavemaker. A 1:10 beach was installed, and the model structure was made out of perspex. Overtopping discharges were directed via a chute into a measuring container suspended from a load cell. Individual overtopping events were detected by two parallel strips of metal tape run along the structure crest which acted as a switch closed by the water. Wave-by-wave overtopping volumes (not reported here) were measured by determining the increment in the mass of water in the collection tank after each overtopping event. To reduce possible uncertainties in determining incident and reflected inshore wave conditions, all measurements of the inshore wave height, H_{si} were made by repeating the test sequence without the structure in place, and placing a wave gauge at the same location of the structure. Thus, H_s is based on measured inshore broken wave conditions. Each test consisted of a sequence of approximately 1000 irregular waves of a JONSWAP spectrum with γ=3.3. The experiments were separated into two distinct regimes of 'positive' and 'negative' water depths at the wall.

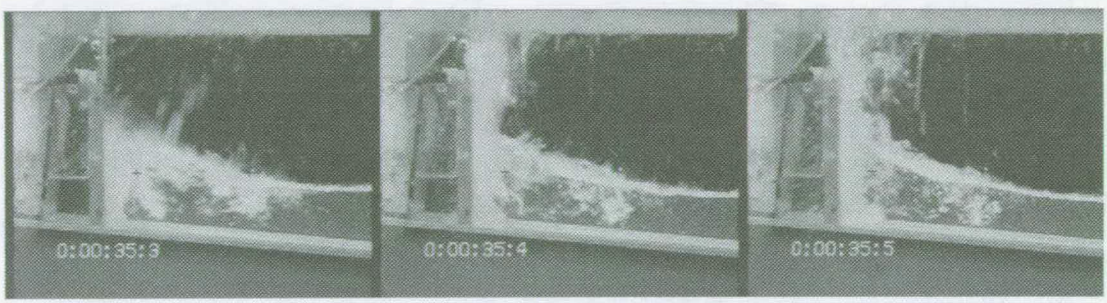

Figure 3: Experimental Testing : A broken wave impacting on the vertical wall

Results – Case 1: Still Water Level above Toe of Wall

The experiments were specifically designed to be outside Besley's stated range of validity, so the data are compared to an extrapolation of Besley's method.
It is clear from Figure 4 that although the broken wave data follows a similar functional form to the extrapolated breaking wave prediction curve, these data fall consistently below the present prediction line, with some indication of a crossover to/from Besley's line for $R_h > 0.03$. This reduction in overtopping discharge under broken wave conditions may be due to the "softening" of the interaction of the wave with the wall due to the entrainment of air in the wave.

Case 1: Positive water depth at toe of wall: For conditions where the still water level was above the toe of the wall (i.e. $h_s > 0$), a matrix of approximately 30 wave conditions gave:

wave height at structure	$(0.028 < H_{si} < 0.053$ m)
peak period	$(0.96 < T_p < 1.53$ s)
water depth at structure	$(0.012 < h_s < 0.035$ m)
crest freeboard	$(0.09 < R_c < 0.17$ m)

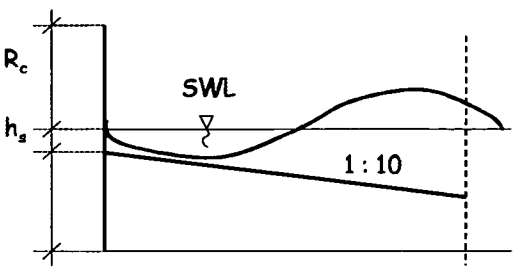

In the region where the water depth is positive, and ***broken*** waves predominate (i.e. when dimensionless freeboard $R_h <\approx 0.03$,), then tentative design guidance based on the predictive method of Besley can be adopted:

$$Q_h \text{ (broken)} \approx Q_h \text{ (breaking)} \times 0.2 \qquad (4)$$

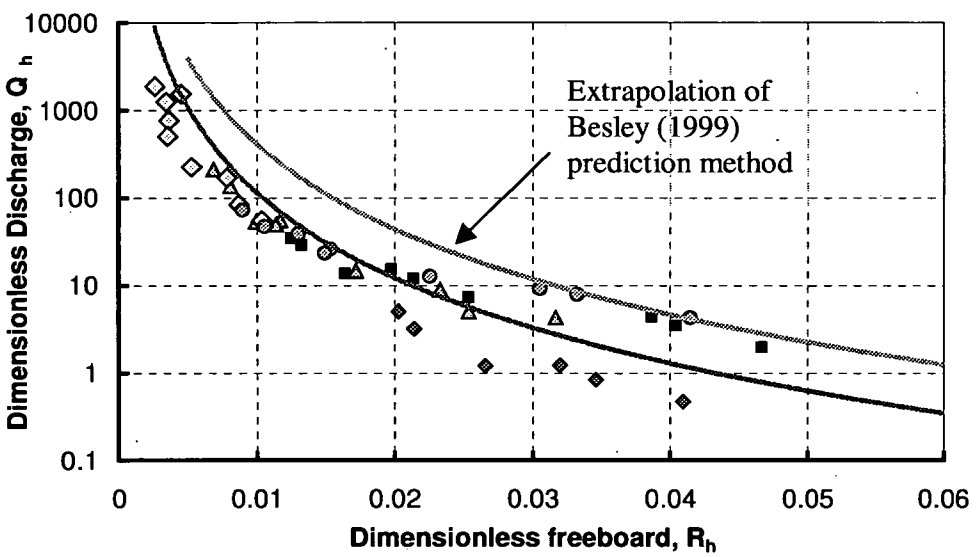

Figure 4: 'Positive' water depth: Mean overtopping data for broken wave conditions, compared with extrapolation of Besley (1998).

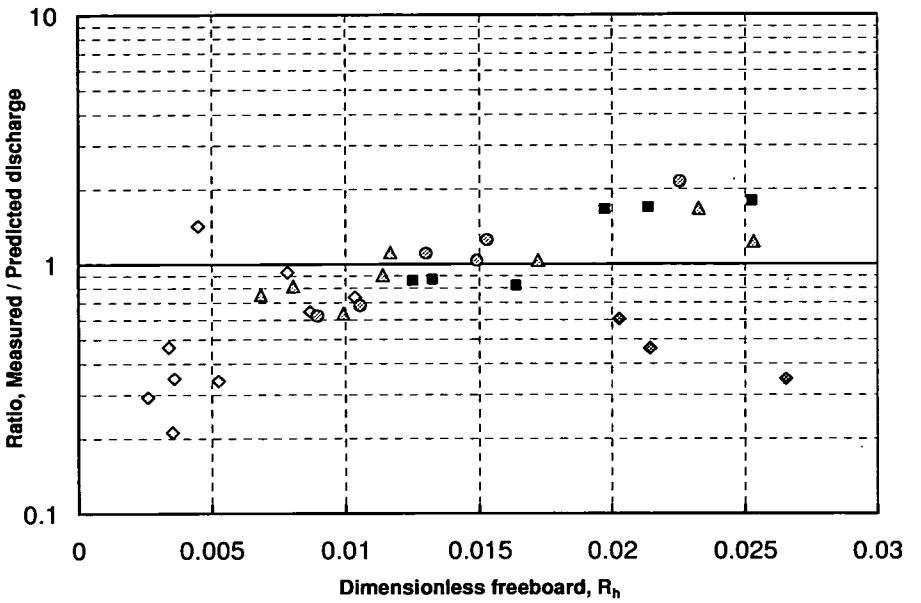

Figure 5: Comparison of the ratio of measured to predicted plotted with respect to dimensionless freeboard, R_h .

The effectiveness of the adjusted predictor may be gauged from Figure 5. The ratio of measured to predicted mean discharge is plotted against the dimensionless freeboard R_h. The ordinate is a log scale to show over- and under-predictions equally (*eg* a factor of 2 under-prediction lies the same distance above the line of perfect agreement as a factor of 2 over-prediction lies below). It can be seen that the majority of the data are predicted to within a factor of 2 (over or under), with the worst cases being conservative (*ie* safe) by a factor of 5.

Results – Case 2: Still Water Level below Toe of Wall

Case 2: Negative water depth at toe of wall: For this condition H_{so} is based on the offshore wave sea state. A matrix of 50 conditions gave:

wave height at structure	($0.067 < H_{so} < 0.113$ m)
peak period	($0.96 < T_p < 1.53$ s)
water depth at structure	($-0.037 < h_s < -0.005$ m)
crest freeboard	($R_c = 0.085$ m)
(measured from still water line as usual)	

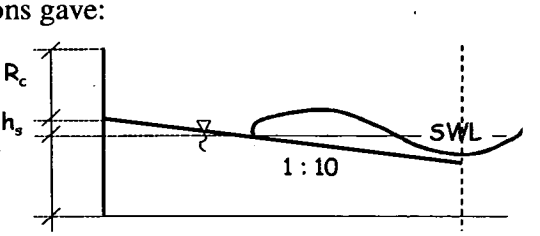

Conceptual model : A limitation of the overtopping prediction methods described by Besley (1999) is that the methodology collapses when $h_s <= 0$, i.e. the still water level is below the toe of the structure. In addition due to the nature of breaking waves, it is very difficult to define with any precision wave conditions within surf / swash zones. In view of these complications, it was decided to explore first a model based upon a simple slope as a basis for a method.

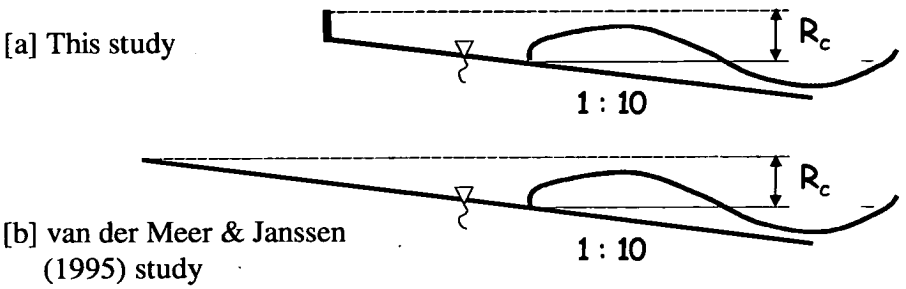

Figure 6: Conceptual model: Does a vertical wall on a plain slope (with negative water depth) have similar overtopping behaviour to a simple slope with same freeboard?

A method for estimating storm wave run-up and overtopping on sea dikes was developed by van der Meer & Janssen (1995), based on extensive laboratory testing of embankment seawalls. An analogy has been drawn here where it is assumed that the structure described in this present study [Fig 6(a)] exhibits similar overtopping characteristics to the sloping structures described by van der Meer & Janssen (1995) [Fig 6(b)]. The method of van der Meer & Janssen (1995) distinguishes between breaking and non-breaking wave conditions, as identified by the surf similarity / breaker parameter / Iribarren number (ξ_{op}), where

$$\xi_{op} = \frac{\tan\alpha}{\sqrt{s_{op}}} \tag{5}$$

where; α = nearshore slope, s_{op} = wave steepness = $2\pi / gT_p^2$, g = acceleration due to gravity, H_s = significant wave height near toe of the slope , T_p = peak period of the wave spectrum

When $\xi_{op} < 2$, waves plunge onto the slope, and the overtopping rate for breaking waves is calculated from an empirical relationship between the dimensionless overtopping rate, defined:

$$Q_b = \frac{q}{\sqrt{gH_s^3}} \cdot \sqrt{\frac{s_{op}}{\tan\alpha}} \tag{6}$$

and the dimensionless crest height defined:

$$R_b = \frac{R_c}{H_s} \cdot \frac{\sqrt{s_{op}}}{\tan\alpha} \cdot \frac{1}{\gamma_b \cdot \gamma_h \cdot \gamma_f \cdot \gamma_\beta} \tag{7}$$

where; Q_b = dimensionless overtopping rate for breaking waves, q = mean overtopping rate ($m^3s^{-1}m^{-1}$), R_b = dimensionless crest of beach profile with breaking waves, R_c = crest height of beach profile above still-water line (m), γ_b = reduction factor for influence of a berm, γ_h = reduction factor for influence of shallow foreshore, γ_f = reduction factor for influence of roughness and γ_β = reduction factor for influence of angle of wave attack. For tests reported here, $\gamma_b = \gamma_h = \gamma_f = \gamma_\beta = 1$.

The main overtopping prediction equation recommended by van der Meer & Janssen for plunging breaking waves is;

$$Q_b = 0.06 \cdot e^{-4.7 \cdot R_b} \tag{8}$$

Results from this study are compared in Figure 7 with predictions for sloping structures by van der Meer & Janssen (1995). It is noticeable that (despite the differences between the structure in this study and those examined by van der Meer & Janssen, 1995), the overtopping characteristics are broadly similar. In view of this "success", the prediction of van der Meer & Janssen (1995) has been adjusted, a best fit line through the data indicates that the dimensionless cress height, R_b can be adjusted to give:

$$R_b \rightarrow R_{ba} \equiv R_b \times s_{op}^{0.17} \tag{9}$$

Predictions using this adjustment factor are compared in Figure 8 to the data, demonstrating that the overtopping characteristics follow a similar trend over the full range of tested conditions. The ratio of measured to predicted discharges are then compared in Figure 9 in more detail.

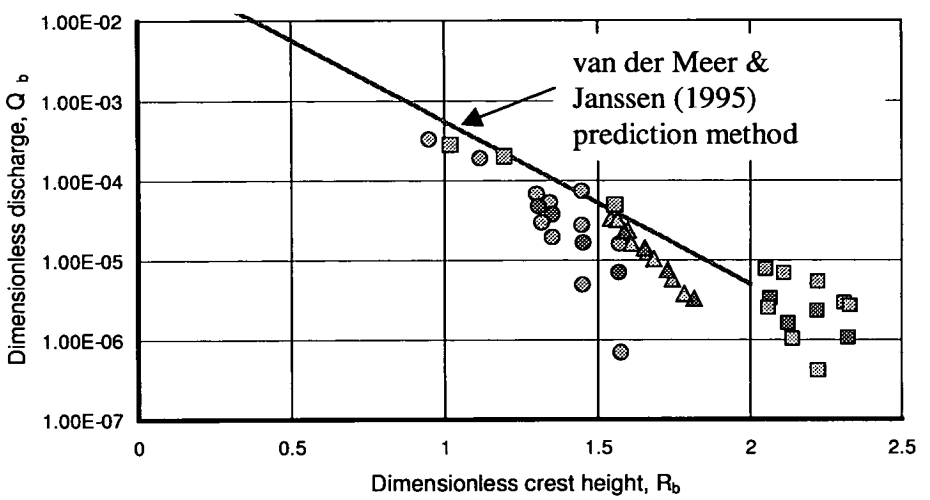

Figure 7: Negative water depth: Mean overtopping data for broken wave conditions, compared with conceptual model of van der Meer & Janssen (1995) for sloping structures

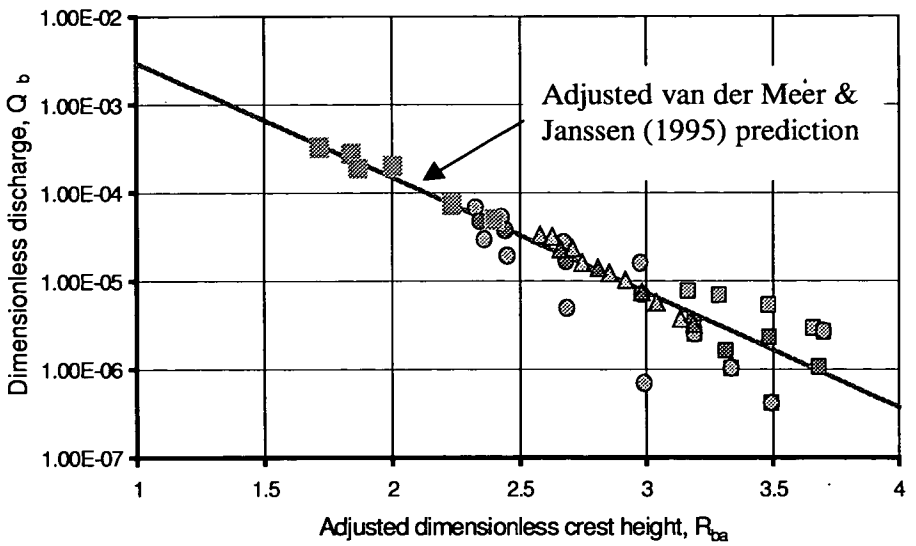

Figure 8: Negative water depth: Mean overtopping data for broken wave conditions, compared with adjusted van der Meer & Janssen (1995) sloping structure formulation.

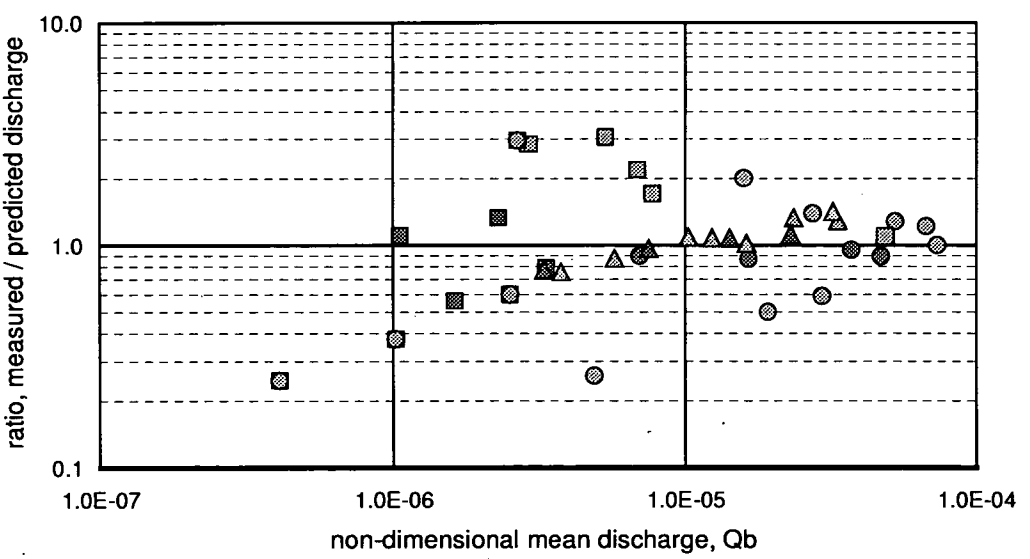

Figure 9: Comparison of the ratio of measured to predicted overtopping plotted with respect to non-dimensional mean discharge, Q_b.

Figure 9 adopts the design guidance given by Eq. (9) and compares the ratio of measured to predicted discharge, plotted here against the non-dimensional mean overtopping discharge Q_b. For $Q_b > 10^{-5}$ agreement is to within a factor of 2. As would be expected, for the smallest discharges ($Q_b < 10^{-5}$) the agreement is less good, but still to within a factor of 3 4.

Results (Cases 1 and 2) Comparison with Goda

The experimental results from this study have been compared with the design diagrams presented in Goda et al. (1975). As noted previously, graphical representations of mean overtopping discharges are reported for 3 offshore wave steepnesses, s_{op} = 0.012, 0.017 and 0.036. Thus for conditions of wave steepnesses between 0.017 and 0.036, predictions of discharges were interpolated, and extrapolated for steepnesses greater than 0.036. Due to the exponential variations inherent in most overtopping processes, interpolations and extrapolations were calculated linearly on the exponent of the discharges.

The ratio of measured to predicted mean discharge using Goda s charts is plotted against the measured mean discharge (Figure 10). It can be seen that for almost all the data, Goda's charts provide a safe upper bound. Measured overtopping discharges are typically lower than those interpolated / extrapolated from Goda et al (1975) by a factor of approximately 5 on the safe side. Due to the relatively small discharges that can be physically measured, the greatest deviations are at lower overtopping discharges, with variations of up to a factor 100.

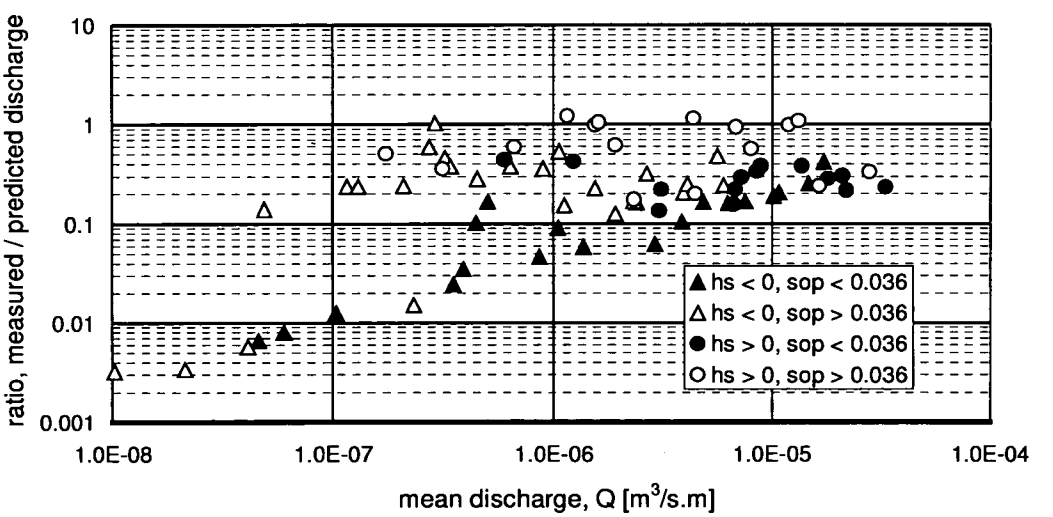

Figure 10: Mean overtopping discharges : Comparison of the ratio of measured to Goda s prediction plotted with respect to measured mean discharge, Q. Filled symbols imply interpolated estimates; hollow symbols imply extrapolations for $s_{op} > 0.036$.

Scaling

The aeration of broken waves (significantly greater in the sea, than in small scale laboratory tanks with fresh water) substantially complicates the interpretation of wave loads measured at small scale (*eg* Oumeraci *et al*, 2001). Whilst it is generally accepted that wave impact pressures measured at small scale will be too large, there is now strong evidence that overtopping characteristics for breaking waves at vertical walls scale robustly with no significant scale effect (see Pearson *et al*, 2002). Those studies also suggest that scaling of broken wave overtopping may be less problematic than for wave impact loads. Nevertheless, some calibration against large-scale and / or prototype measurements is now highly desirable.

Conclusions

For water depth at wall > 0: when dimensionless freeboard $R_h <= 0.03$, switch to adjusted form of Besley (1999);

$$Q_h\,(broken) \approx Q_h\,(breaking) \times 0.2$$

For water depth at wall < 0: use adjusted form of van der Meer & Janssen

$$R_b \rightarrow R_{ba} \equiv R_b \times s_{op}^{\,0.17}$$

The results from this study suggest that design guidance interpolated / extrapolated from Goda et al (1975) for broken wave regimes is safe, and indeed may be conservative by factors of approximately 5.

Acknowledgements

This work is part funded by the CLASH project under EU contract EVK3-CT-2001-00058. The second author was part-funded by UK EPSRC (GR/M42312, GR/R42306) whose support is gratefully acknowledged. The authors are grateful to Ahmed Nasr, Tim Watson and Benjamin Torrance for their assistance in data gathering, checking and analysis, and to Prof Yoshimi Goda and Dr Jentsje van der Meer whose comments stimulated the team to return to this problem.

References

Allsop, N.W.H. (Editor) (2002). *Breakwaters, coastal structures and coastlines* Proceedings of Conference at ICE, 26-28 September 2001, ISBN 0 7277 3042 8, Thomas Telford, (see pp506-516)

Allsop, N.W.H., Besley, P. & Madurini, L. (1995). "Overtopping performance of vertical walls and composite breakwaters, seawalls and low reflection alternatives." Paper 4.7 in *MCS Final Report*, publn University of Hannover.

Allsop, N.W.H., Vicinanza, D. & McKenna, J.E. (1996). "Wave forces on vertical and composite breakwaters.", *Research Report SR 443*, pp 1-94, HR Wallingford.

Besley, P. (1999). *Overtopping of seawalls – design and assessment manual.* R & D Technical Report W 178, ISBN 1 85705 069 X, Environment Agency, Bristol. (also from: http://www.environment-agency.gov.uk/commondata/105385/w178.pdf).

Besley, P.B., Stewart, T., & Allsop, N.W.H. (1998). "Overtopping of vertical structures: new methods to account for shallow water conditions." *Proceedings of Int. Conf. on Coastlines, Structures & Breakwaters '98*, Institution of Civil Engineers, pp46-57, publn. Thomas Telford, London.

Bruce, T., Allsop, N.W.H. & Pearson, J. (2001). "Violent overtopping of seawalls extended prediction methods." *Breakwaters, coastal structures and coastlines* Proceedings of Conference at ICE, 26-28 September 2001, pp 245 256, ISBN 0 7277 3042 8, Thomas Telford, London.

Bruce, T., Allsop, N.W.H. & Pearson, J. (2002). "Hazards at coast and harbour seawalls - velocities and trajectories of violent overtopping jets. " *Proc. 28th Int. Conf. Coastal Engineering*, 2, pp 2216 2226 (ASCE), ISBN 981 238 238 0

Franco, L., de Gerloni, M. & van der Meer, J.W. (1994). "Wave overtopping on vertical and composite breakwaters." *Proc 24th Int. Conf. Coastal Eng.*, Kobe, publn. ASCE, New York.

Goda, Y., Kishira, Y., & Kamiyama, Y. (1975). "Laboratory investigation on the overtopping rates of seawalls by irregular waves." *Ports and Harbour Research Institute*, 14, No. 4, pp 3 44, PHRI, Yokosuka.

Hedges, T.S. & Reis, M.T. (1998). "Random wave overtopping of simple sea walls: a new regression model." *Proc. Instn. Civil Engrs. Water, Maritime & Energy*, 130, March 1998, Thomas Telford.

van der Meer, J.W. & Janssen J.P.F.M. (1995). "Wave run-up and wave overtopping at dikes." Chapter 1 in *Wave Forces on Inclined and Vertical wall Structures*, pp 1-26, ed. Kobayashi N. & Demirbilek Z., ISBN 0-7844-0080-6, ASCE, New York.

van der Meer, J.W., Tonjes, P. & de Waal, J.P. (1998). "A code for dike height design and examination." *Proceedings of Coastlines, Structures & Breakwaters '98*, Int. Conf. at Institution of Civil Engineers, March 1998, pp 5 21, publn. Thomas Telford, London

Oumeraci, H., Kortenhaus, A., Allsop, N.W.H., de Groot, M., Crouch, R., Vrijling, H. & Voortman, H. (2001). *Probabilistic Design Tools for Vertical Breakwaters* A.A.Balkema.

Owen, M.W. (1982). "Overtopping of Sea Defences." *Proc. Intl. Conf. On Hydraulic Modelling of Civil Eng. Structures*, Coventry, pp469 480, BHRA, Bedford.

Pearson, J., Bruce, T., Allsop, N.W.H. & Gironella, X. (2002). "Violent wave overtopping - measurements at large and small scale." *Proc. 28th Int. Conf. Coastal Engineering*, 2, pp 2227 2238, (ASCE), ISBN 981 238 238 0

de Waal, J.P., Tonjes, P. & van der Meer, J.W. (1996). "Overtopping of sea defences." *Proc 25th Int. Conf. Coastal Eng.*, pp2216-2229, Orlando, publn. ASCE, New York.

Appendix K: Kortenhaus *et al.*, 2003

Kortenhaus, A., Pearson, J., Bruce, T., Allsop, N.W.H. & van der Meer, J.W. (2003), *Influence of parapets and recurves on wave overtopping and wave loading of complex vertical walls*, Proc "Coastal Structures 2003", pp 369–381, ASCE, Reston, Virginia, ISBN 0-7844-0733-9

Appendix K
Kortenhaus *et al.*, 2003

Kortenhaus, A., Pearson, J., Bruce, T., Allsop, N.W.H. & van der Meer, J.W. (2003), *Influence of parapets and recurves on wave overtopping and wave loading of complex vertical walls*, Proc "Coastal Structures 2003", pp 369–381, ASCE, Reston, Virginia, ISBN 0-7844-0733-9

K.1 Declaration of contribution

This paper emerged from informal discussion between the author and Kortenhaus when it emerged that both were (then) separately investigating similar problems.

Edinburgh contributed the data relating to overtopping at vertical walls with recurves / wave return walls. These data were taken variously by Pearson (then post-doctoral Research Engineer working under the author's guidance on *VOWS* and *CLASH* projects) and by a Masters student, Lamont. All of these tests were carried out under Bruce's supervision.

K.2 Published paper

overleaf

Influence of parapets and recurves on wave overtopping and wave loading of complex vertical walls

A. Kortenhaus[1], J. Pearson[2], T. Bruce[3], N.W.H. Allsop[4], J.W. van der Meer[5]

Abstract

Increasing sea water levels and storminess has intensified the need for structural measures to reduce wave overtopping without significantly raising the height of the wall. The use of recurves / wave return walls / parapets on vertical walls has been shown capable of significantly reducing wave overtopping, but may increase wave loading. Many parapet / recurve solutions have been used in practice, but no general guidance on their design are yet available. In this paper a significant amount of data have been gathered together under the EC CLASH project (EU project no. EVK3-CT-2001-00058) and studied more systematically for the first time. The paper discusses problems with systematic approaches to both overtopping and wave loading. It concludes with a simple reduction factor for wave overtopping depending on geometrical dimensions of the parapets and some guidance on wave loading for these cases.

1 Introduction

Coastal structures protecting against storm surges and wave attack are expected to become increasingly important due to the increased rate of storminess in recent decades. A rising awareness of people living along the coastlines requires increasing efforts to provide: i) reliable methods to design such structures; ii) constructional features to minimise hazards arising from overtopping water; iii) increased efficiency of overtopping reduction for vertical walls.

Parapets are seaward extensions to vertical or near-vertical walls which have an angle with the wall larger than zero. *Recurves* are either curved parapets or walls

[1] Senior research engineer, Leichtweiß-Institute for Hydraulics, Beethovenstr. 51a, 38106 Braunschweig, Germany; e-mail: a.kortenhaus@tu-bs.de

[2] Postdoctoral Fellow, School of Engineering and Electronics, University of Edinburgh, U.K.; J.Pearson@ed.ac.uk

[3] Lecturer, School of Engineering and Electronics, University of Edinburgh, U.K.

[4] Visiting Professor, University of Southampton; and Technical Director Maritime Structures, Coastal Structures Group, HR Wallingford, U.K.

[5] Head Coastal Structures, Infram, The Netherlands

with fully curved seaward faces. Both types are structural measures to reduce wave overtopping without increasing the crest height of the structure.

The paper aims to give guidance on the use and design of parapets both on simple vertical walls and structures with complex foreshores. The paper will propose simple design methods to: i) decrease the mean overtopping rate over the walls by using parapets; ii) consider the increase of forces and pressures at the wall.

2 Previous investigations

Studies on vertical (and sloping) seawalls have been performed for many case studies and systematic studies have investigated mean overtopping discharges (e.g. Besley (1999); Owen (1980)). Forces on vertical walls or breakwaters have been investigated extensively, with most studies referring back to Goda (1985) or its extension for more impulsive wave conditions (Takahashi (1996). Detailed analysis of impulsive loading was developed further under the EU PROVERBS project (Oumeraci et al. (2001)).

Seawalls and breakwaters with parapets / recurves have been less investigated with studies typically restricted to case studies rather than more generic investigations. Some early guidance for recurved parapet walls can be found in Owen and Steele (1991). Some special types of parapets for breakwaters have been investigated by Juhl (1992) with some reduction factors given.

An extreme seawall shape called Flaring Shaped Seawall (FSS), a deep circular cross-section with thin overhanging crest, has been investigated by Murakami et al. (1996); Kamikubo et al. (2000); Kamikubo et al. (2003). Tests suggest significant savings in crest level height with the reduction factor a function of dimensionless water depth, h/H_o. The efficiency of the recurve is greatest when $R_c/H_o > 1 - 1.5$, and an empirical formula was derived for critical crest freeboard. This shape would however be impossible to form in reinforced concrete as the projecting lip has insufficient depth.

Kortenhaus et al. (2001) studied the influence of a small deflector parapet attached to a simple vertical wall on top of a steep embankment. For $R_c/H_s > 1.5$, the parapet had considerable influence on the overtopping volume, as the relative freeboard was high enough for the recurve to function properly. For lower crest levels, $R_c/H_s < 1.2$, the parapet was overtopped by the incident wave and the wall shape had no significant effect. Variations in loading were also investigated for various relative angles of parapet to wall. For small freeboards or large waves given by $R_c/H_s < 1.2$, the load on the vertical wall below the parapet is significantly increased, by a factor of 2.0 in case of impulsive wave breaking and 1.7 for pulsating conditions. The loads on the parapet itself can be equal to those acting on the vertical wall.

During the *Violent Overtopping by Waves at Seawalls (VOWS)* project in UK, tests were run with a small recurve (or bullnose) on top of the vertical wall, under both impulsive and pulsating conditions. Impulsive wave conditions with high freeboard clearance (low water level) resulted in overtopping discharge for a recurve wall being reduced by a factor of 1/1000 compared to that of a vertical wall. Pulsating

wave conditions tested (with high water level and low clearance) showed a reduction in overtopping discharge by a factor of 1/10 when compared to a vertical wall.

Cornett et al. (1999) systematically investigated various overhanging and chamfered parapets at a vertical wall over a horizontal sea bottom with a small berm and three different water levels. Their measurements of overtopping showed reduced overtopping rates as compared to vertical walls for the range of relative freeboards investigated ($0.67 \leq R_c/H_s < 3.33$). The mean reduction for all cases is given as close to 0.6, but significant scatter in the results was reported.

In summary, there is no general method to bring various types of parapets / recurves together, schematise them and derive reduction factors depending on their geometry, size or form. For this purpose some data sets were brought together through the *CLASH* project, an analysis methodology was devised, and data sets were re-analysed to arrive at a possible *reduction factor* approach for recurves / parapets.

3 Methodology

To devise a consistent methodology, the mechanism of how wave overtopping is reduced needs to be understood. Videos and photos taken during the various tests at different institutions were therefore analysed to isolate the key physical process to reduce overtopping frequency or volumes, see Figure 1.

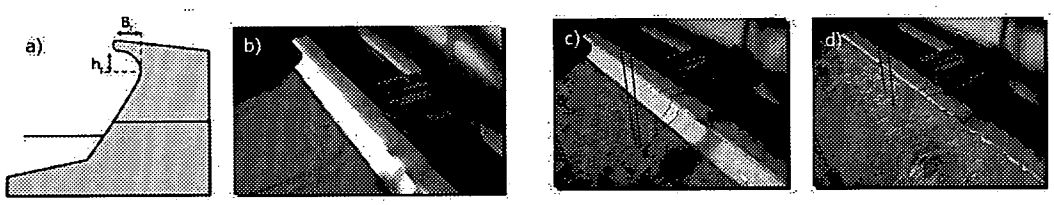

Figure 1: Physical process of a recurve wall to reduce wave overtopping

Figure 1a) shows the cross section tested where it can be seen that the relative freeboard was relatively high ($R_c/H_s \approx 1.5$). Figure 1b) shows the structure with just the still water level. Figure 1c) is a photo of the wave reaching the toe of the recurve whereas Figure 1d) shows how the wave is thrown seawards. The overall effect for larger relative freeboards is therefore that the wave energy is completely redirected. This contrasts with a vertical wall where the water mass is often thrown upwards and then falls behind the wall.

The analysis for lower crest freeboards or higher waves shows that this processes is no longer effective for large overtopping volumes as the wave is no longer "captured" below the overhanging part of the structure. In some cases, it is apparent that the volume under the parapet / recurve is filled during a wave event, with subsequent parts of the wave in some way riding over this filled volume. An analysis methodology was devised which considers the relative crest freeboard since it can be expected that any reduction factor for overtopping rates will vary over that factor (Figure 2).

First, test data have to be scanned for tests with parapets / recurves and similar tests (or well-verified prediction formulae) with similar parameters but with a vertical wall of the same overall crest level. From these matching pairs of tests the reduction factor k can be derived as a quotient of the corresponding wave overtopping rates. A similar approach is used to derive the amplification factor for wave loading. These factors need to be analysed and a relation to the various geometries of the parapets and recurves needs to be found.

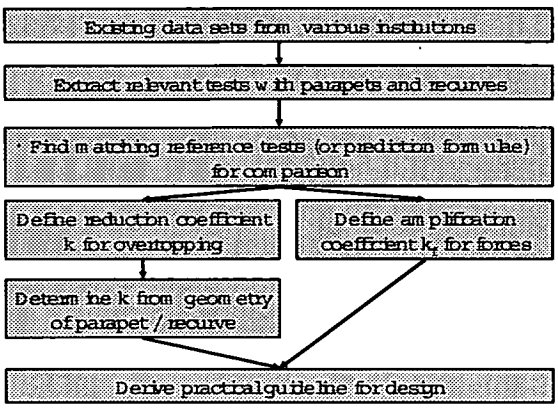

Figure 2: Methodology for possible reduction factors for overtopping

4 Overview of model tests

The main data base was provided by more than 300 hydraulic model tests in the wave flume of LWI (90 m length) summarised by Kortenhaus et al. (2001). Wall heights covered 2.0 - 3.6 m (prototype), six water levels 0.9 - 3.10 m, four wave heights H_s= 0.20 - 0.80 m and three wave periods T_p = 2.5 - 4.0 s, were varied for nine combinations of wall / parapet.

Over 80 small-scale investigations were carried out at the University of Edinburgh under the UK *VOWS* project. The Edinburgh channel is 20 m long, 0.4 m wide along its full length, has an operating water depth of 0.7 m and is equipped with an absorbing flap-type wavemaker. A 1:10 approach beach and model vertical wall with small recurve were used. Details of the testing set up and procedures (for the corresponding plain wall tests) are given by Bruce et al. (2001).

Model tests performed at Delft Hydraulics on combinations of slopes with (small) vertical walls and very shallow (flooded) quay areas with vertical walls are described by Van der Meer et al. (2002) and Den Heijer (1998).

The performance of recurved seawalls at Marina Rubicon in Lanzarote, and at the St Angelo harbour-side development in Malta measured at HR Wallingford were used to supplement the data above for idealised sections. Overtopping of the vertical breakwater for Marina Rubicon was reduced (slightly) by a bullnose applied to the simple vertical wall, but the main wall shape was not altered. This modification gave relatively small improvement. In devising the seawall for St Angelo, it was important to maximise overtopping reduction, and to minimise the probability of impulsive conditions. The seawall shape shown in the sequence in Figure 1 was therefore intended to smooth entry flows into the recurve, and maximise the wave return.

A summary of tests used for this paper is given in Table 1 using parameters defined in Figure 6.

Table 1: Test sets used for development of reduction factor approach (dimensions in model scale).

Model	fore-shore	type	no. of tests	h_c [m]*	B_r [m]*	h_r [m]*	Remarks
HWS3	horiz.	parapet	24	0.33-0.4	0.057	0.07	Berm
HWS5	horiz.	parapet	84	0.80	0.03-0.2	0.03-0.10	Vertical wall
HWS6	horiz.	parapet	197	0.33-0.4	0.01-0.07	0.01-0.07	Berm
VOWS	1:10	recurve	82	0.30	0.04	0.04	Vertical wall
Rubicon	shallow	bullnose	19	0.393	0.014	0.014	case study
harb. w.	horiz.	parapet	16	0.2-0.5	0.026	0.025	diff. Berms/quays

* h_c is the overall wall height, B_r and h_r are dimensions of the parapet (see Figure 6)

Mean overtopping discharges for all these model tests are plotted together in Figure 3 regardless of whether they have parapets, recurves or just simple vertical walls. For plotting these data the dimensionless overtopping rate $q/(g \cdot H_s^3)^{0.5}$ over a dimensionless freeboard R_c/H_s was used and the prediction formulae after Van der Meer and Janssen (1995) for sloping structures (non breaking waves) and Franco et al. (1995) for vertical breakwaters were plotted for comparison. At this stage, no distinction was made between impulsive breaking or pulsating conditions.

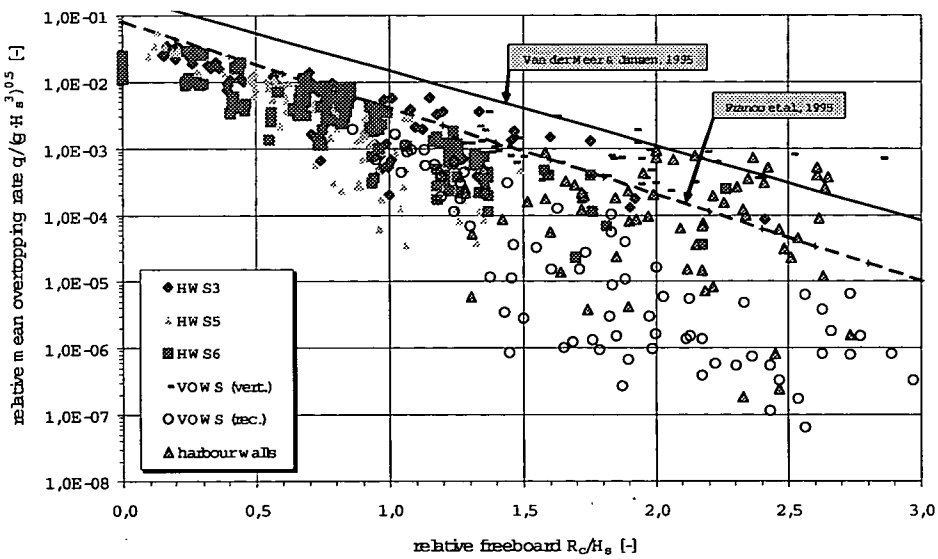

Figure 3: Dimensionless wave overtopping rate for available data sets plotted against dimensionless freeboard

The data in Figure 3 show considerable scatter, especially for higher relative crest freeboards and lower overtopping rates. This had been expected since video analysis has shown that parapets and recurves can lead to significant reductions for this range of parameters, so it can be assumed that lower relative overtopping rates

refer to tests with parapets or recurves. The following analysis of data will have to consider these differences.

5 Results – Wave Overtopping

Following the methodology described above, reduction factors for wave overtopping rates were defined, using pairs of tests where one test had a recurve or parapet installed and the reference test had not. The k-factor was then defined as:

$$k = \frac{q_{parapet}}{q_{no\ parapet}} \tag{1}$$

Only tests which had the same overall crest level were used for this comparison. In case of a simple vertical wall, the parapet was replaced by a simple vertical extension of the wall to ensure that a reduction of wave overtopping resulted only from the parapet and not from any increase in wall height. Plots in Figure 4 show examples for four different wall / parapet configurations (LWI sets *HWS5/6*) where the k-factor for wave overtopping is plotted against the relative freeboard R_c/H_s.

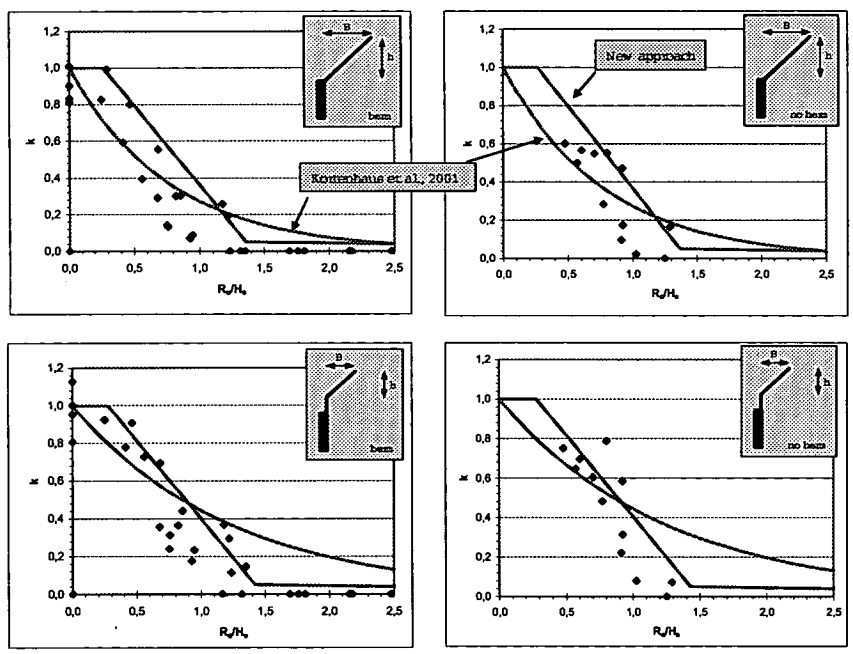

Figure 4: Typical reduction curves for wave overtopping rates as a function of relative crest freeboard R_c/H_s

Figure 4 shows typical decreases of k-factor with increasing relative crest freeboards. There is considerable scatter in these data, some from uncertainties in measuring overtopping, some because k itself results from dividing two measurements, and because many values of k are themselves derived from very low overtopping rates where considerable scatter can be expected. As a first step it was assumed that any method to predict reduction factors would be based upon a linear decrease in reduction factor with increasing freeboards. It was noted in Figure 4 that for some

parapets, the decrease only starts with a certain critical relative freeboard, which seems to be dependent on the height of the parapet used in relation to the overall wall height.

Figure 4 also shows two lines on each of the plots. The curved line represents the reduction method as proposed by Kortenhaus et al. (2001) which is actually a reduction factor as often used for different roughness of slopes in plots such as Figure 3. It shows that an exponential reduction underpredicts the k-factors for high overtopping rates and is too conservative for low overtopping. The straight lines give a first simple reduction factor approach described below.

In cases where reference tests with increased wall heights and no parapets were not available, vertical wall tests of the same geometry and foreshore but a different wall height were used to validate an appropriate formula to predict these overtopping rates. If good agreements were reached, the same formula was used to predict overtopping rates for walls having a crest level identical to the ones used for parapets. Figure 5 shows examples of how results were obtained for these cases.

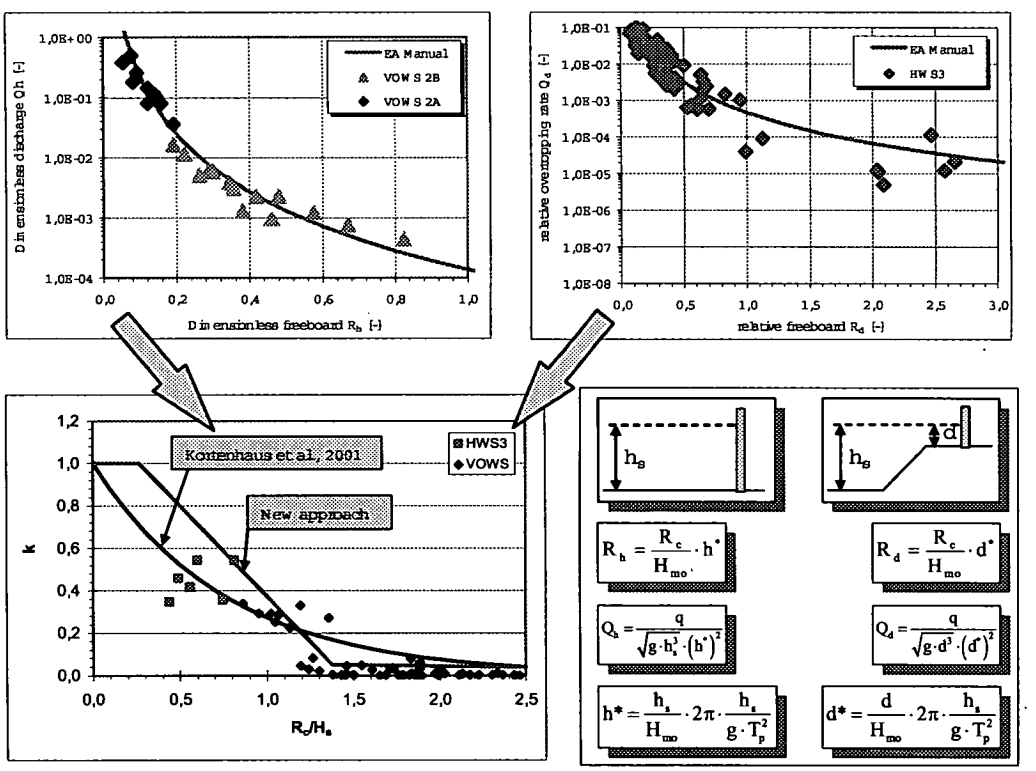

Figure 5: Reduction curves for wave overtopping rates as a function of relative crest freeboard R_c/H_s for predicted reference cases

The upper figures in Figure 5 shows the hindcast of the vertical wall tests with insufficient wall height for tests *VOWS* and *HWS3*. The model used for this data fitting was taken from Besley (1999) and data were plotted using the dimensionless overtopping rate Q_h and the dimensionless freeboard R_h (or if a bermed structure, R_d)

after Besley. The agreement between model and data points is seen to be sufficiently good to predict mean wave overtopping rates for higher walls without parapets as well. Reduction factors are then plotted against the relative freeboard in the lower part of Figure 5 showing that many of the data points lie in $R_c/H_s > 1$, suggesting very low values of k. The very low k-values for relative crest freeboards R_c/H_s larger than 1.5 have led to the third part of the proposed new approach where the k-factor is very small but non-zero.

In deriving a possible method to predict the reduction factor for wave overtopping, non-dimensional parameters were identified which seem to have strongest influence on the k-factor and its three components. These non-dimensional freeboard, parapet width and angle parameters are given in Figure 6 together with the principal form of the function to be derived for the new approach.

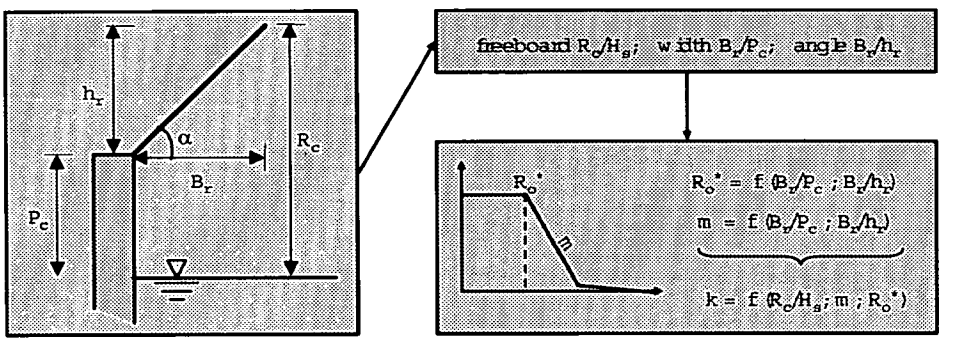

Figure 6: Definition of relative parameter to define a reduction factor for overtopping

Following the approach given in Figure 6, the key parameters R_0^* and m were obtained from detailed analysis of the data leading to the following equations:

$$R_0^* = 0.25 \cdot \frac{h_r}{B_r} + 0.05 \cdot \frac{P_c}{R_c} \tag{2}$$

$$m = 1.1 \cdot \sqrt{\frac{h_r}{B_r} + 0.2 \cdot \frac{P_c}{R_c}} \tag{3}$$

The final equation to determine the k-factor for wave overtopping due to parapets or recurves may then be written:

$$k = \begin{cases} 1.0 & \text{for } \dfrac{R_c}{H_s} \le R_0^* \\ 1 - \dfrac{1}{m}\left(\dfrac{R_c}{H_s} - R_0^*\right) & \text{for } R_0^* < \dfrac{R_c}{H_s} \le R_0^* + m^* \\ k_3 - 0.01 \times \left(\dfrac{R_c}{H_s} - R_0^* - m\right) & \text{for } \dfrac{R_c}{H_s} > R_0^* + m^* \end{cases} \tag{4}$$

In Eq. (4) k_3 is a factor to determine the last 'mild slope' part of determining the k-value. In the analysis of the available data for this paper it has been set to 0.05.

The value of m* is described as the intersection of the steep slope of the second part of the equation with the third part and is defined as follows:

$$m^* = m \cdot \left(1 - \frac{k_3}{1 - 0.01 \cdot m}\right) \tag{5}$$

When Eq. (4) is used to improve Figure 3 to include effects of parapets and recurves, the plot in Figure 7 results.

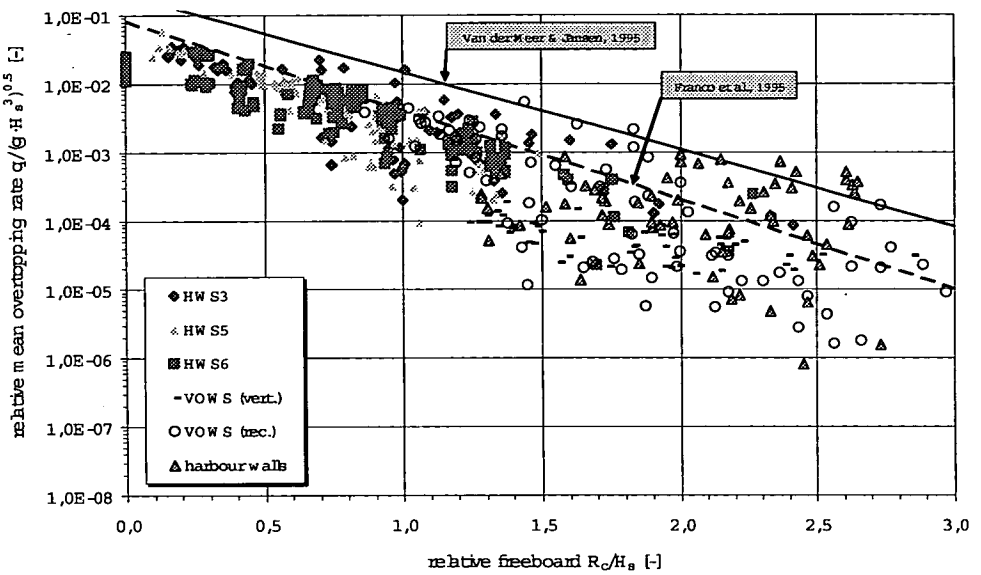

Figure 7: Dimensionless wave overtopping rate against dimensionless freeboard with correction for wave parapets and recurves

There is still a lot of scatter in Figure 7, but considering the significantly different geometries of the structures involved, some scatter had to be expected. Furthermore, the following points should be taken into account:

- the new approach is conservative for most cases so that predicted k-values are larger than measured ones, thus leading to some scatter in the 'corrected' data points in Figure 7;
- limited numbers of structures and data have been tested against the new procedure, so improvements with further data can still be expected
- a distinction between breaking and non-breaking waves at the structure has not yet been made (see Bruce et al. (2003))
- defining the k-factor as ratio of two overtopping rates may lead to dividing two small numbers by each other, especially for higher relative crest freeboards, thus leading to some additional scatter.

So additional analysis and more data are needed to confirm results obtained so far, but use of Eq. (4) for preliminary analysis is recommended until improved guidance becomes available.

6 Results – Wave Loading

Wave loads on a vertical wall are strongly dependent on the breaker type in front of the structure, see particularly Allsop et al. (1996). Kortenhaus et al. (2001) have investigated vertical harbour walls with steep foreshore slopes and have described the magnitude of loading and given some guidance on the type of pressure distributions. They showed that the principal increase of wave loading due to the parapet is different for impulsive wave breaking and non-breaking conditions, and calculated load increase factors of 1.7 or 2.0 respectively. These numbers do not however distinguish whether the increase of loading result from the increase of wall height or the shape of the parapet installed at the wall. The same comparison as used for reduction factors for wave overtopping (Figure 5) has therefore been used for the increase of wave loading at the wall by directly comparing the $F_{1/250}$ values of the horizontal wave force (Figure 8). All data points were used to draw a linear regression line to illustrate the tendency and the magnitude of factors for wave loading, k_F.

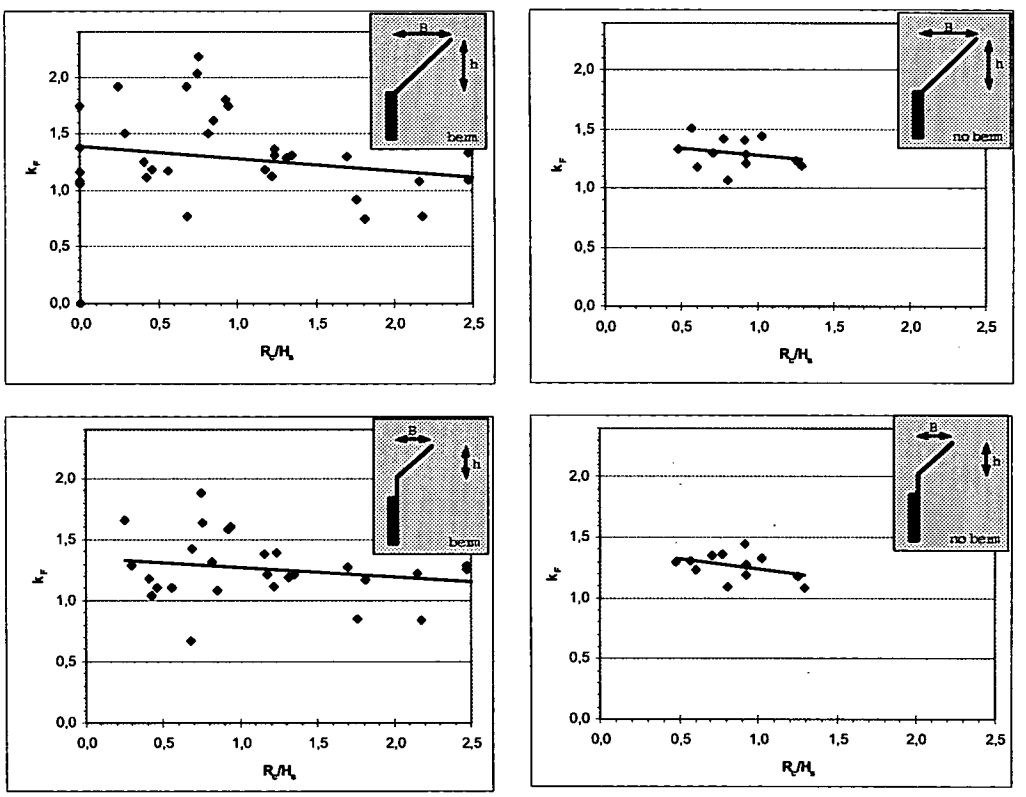

Figure 8: Relative increase of wave loading at various types of parapets induced by use of wave parapets

It can be seen from Figure 8 that there is a large scatter in the data, some of which results from uncertainties in measuring wave pressures on walls. Results for structures with berm (left side of Figure 8) and without berm (right side) are however comparable showing some tendency for k_F to decrease with increasing relative crest freeboard. More scatter can be seen in the left diagrams, perhaps due to breaking of

waves over the berm. The method of Besley (1999) derived from 2-d data however suggests impulsive conditions apply only for four data points on the left side and one data point on the right side. Most data in these diagrams can therefore be assumed to be quasi-static / *pulsating* conditions. Factors for relative freeboards R_c / H_s > 1.5 seem to be close to unity in average, average k_F-factors for the range smaller than 1.5 suggest a slightly higher factor (1.6) for the larger parapet in comparison to the smaller (1.3).

Differences to the higher factors of Kortenhaus et al. (2001) are due to ignoring the increase of wall height in the present analysis. Analysis of 60° angles have shown that the k_F-factor still increases (1.8) whereas almost no increase was found for 30° (1.1) and 15° (1.0).

This analysis is far from complete and currently only relates to measurements with limited geometries performed at LWI. Different breaking conditions need to be more fully included, and more data for recurved wave walls are needed. These results are however believed to give initial guidance on the shape-related increase of wave loading at walls with parapets for non-impulsive conditions. It should be noted that this is only the increase of wave loads on the plain vertical wall so that the wave loading on the parapet itself still has to be added.

7 Concluding remarks

A recurve or parapet at a vertical wall is capable of reducing wave overtopping discharges compared to that of a vertical wall, but the magnitude of the reduction factor itself depends on the amount of overtopping water.

A recurve wall will give most significant benefit when its shape and freeboard are together enough to prevent the wall from being overtopped by 'green water'. For (relatively) smaller walls, the influence of a recurve on 'green water' overtopping can be relatively small.

A simple approach is derived in this paper using data for recurves and parapets from different flume tests with different geometries of vertical and battered walls. The cross sections of the parapets vary significantly and were therefore simplified and categorised. Analysing these parapet walls in relation with their corresponding simple vertical wall tests of the same overall crest level reduction factors were obtained in Eq. (4) which mainly depend on the parapet geometries and dimensions.

Any addition of a recurve / sloping parapet may increase loadings on the vertical wall. Whereas earlier investigations suggested overall increases of 1.7-2.0 (depending on the type of wave attack experienced at the site) resulting from both the increase in wall height and the shape of the parapet, this analysis has found that the shape-related increase of wave loadings for non-impulsive conditions and simple angled parapets depends on the angle of the parapet and its length resulting in factors in between 1.1 and 1.8 for relative crest freeboards $R_c/H_s < 1.5$.

Both these results (for wave overtopping and loading) need to be confirmed by further model tests and ongoing analysis. The results are very promising for lower overtopping rates where overtopping reduces significantly and wave loading does not

significantly increase. These suggest that further investigations in this field could prove fruitful in delivering savings in crest level assessment.

8 Acknowledgements

Parts of this study have been performed in the framework of the European CLASH project (Crest level assessment of coastal structures) under EU contract no. EVK3-CT-2001-00058. The VOWS project work described in this paper has been supported by the UK EPSRC (GR/M42312, GR/R42306). The assistance of Arran Lamont is also gratefully recognised. Furthermore, some tests at LWI were performed for the Hamburg harbour authority ('Strom- und Hafenbau') and the 'Baubehörde' in Hamburg. The support by these authorities is gratefully acknowledged. Additional support for the first author to present this paper at the conference was provided by the German Research Council (DFG), whose support is also gratefully acknowledged.

References

Allsop, N. W. H., McKenna, J. E., Vicinanza, D. & Whittaker, T. J. T. (1996). "New design methods for wave impact loadings on vertical breakwaters and seawalls." *Proceedings International Conference Coastal Engineering (ICCE)*, Orlando, Florida, USA, pp. 2508-2521.

Besley, P. (1999). "Wave overtopping of seawalls: design and assessment manual." R&D Technical Report, HR Wallingford, Wallingford, U.K., no. W178, 37 pp., 5 tables (also from: http://www.environment-agency.gov.uk/commondata/105385/w178.pdf).

Bruce, T., Allsop, N. W. H. A. & Pearson, J. (2001). "Violent overtopping of seawalls - extended prediction methods." *Breakwaters, coastal structures and coastlines - Proceedings of the International Conference*, London, UK, pp. 245-256.

Bruce, T., Pearson, J. & Allsop, N. W. H. A. (2003). "Violent wave overtopping - extension of prediction methods to broken waves." *Proceedings Coastal Structures 2003*, Portland, Oregon, USA.

Cornett, A., Li, Y. & Budvietas, A. (1999). "Wave overtopping at chamfered and overhanging vertical structures." *Proceedings International Workshop on Natural Disasters by Storm Waves and Their Reproduction in Experimental Basins*, Kyoto, Japan, 14 pp.

Den Heijer, F. (1998). "Golfoverslag en krachten op verticale waterkeringsconstructies (Wave overtopping and forces on vertical structures)." Delft Hydraulics Report, De Voorst, The Netherlands, August 1998 (in Dutch).

Franco, L., De Gerloni, M. & Van Der Meer, J. W. (1995). "Wave overtopping on vertical and composite breakwaters." Final Proceedings, MAST II, MCS-Project: Monolithic (Vertical) Coastal Structures, 16 pp.

Goda, Y. (1985). "Random seas and design of maritime structures." University of Tokyo Press, Tokyo, 323 pp.

Juhl, J. (1992). "Investigations on the effect of structural measures on wave impact forces and overtopping." Proceedings 3rd Project Workshop, MAST I, G6-S/Project 2: Wave impact loading on vertical structures, Hannover, Germany, 18 pp.

Kamikubo, Y., Murakami, K., Irie, I. & Hamasaki, Y. (2000). "Study on practical application of a non-wave overtopping type seawall." *Proceedings International Conference Coastal Engineering (ICCE)*, Sydney, Australia, pp. 2215-2228.

Kamikubo, Y., Murakami, K., Irie, I., Kataoka, Y. & Takehana, N. (2003). "Reduction of wave overtopping and water spray with using flaring shaped seawall." *Proceedings of the International Offshore and Polar Engineering Conference (ISOPE)*, Honolulu, Hawaii, USA, pp. 671-676.

Kortenhaus, A., Haupt, R. & Oumeraci, H. (2001). "Design aspects of vertical walls with steep foreland slopes." *Breakwaters, coastal structures and coastlines - Proceedings of the International Conference*, London, U.K., pp. 221-232.

Murakami, K., Irie, I. & Kamikubo, Y. (1996). "Experiments on a non-wave overtopping type seawall." *Proceedings International Conference Coastal Engineering (ICCE)*, Orlando, Florida, USA, pp. 1840-1851.

Oumeraci, H., Kortenhaus, A., Allsop, N. W. H., De Groot, M. B., Crouch, R. S., Vrijling, J. K. & Voortman, H. G. (2001). "Probabilistic design tools for vertical breakwaters." Probabilistic Design Tools for Vertical Breakwaters, Balkema, Rotterdam, The Netherlands, 392 pp.

Owen, M. W. (1980). "Design of seawalls allowing for wave overtopping." Hydraulics Research, Wallingford, Wallingford, U.K., Report EX 924.

Owen, M. W. & Steele, A. A. J. (1991). "Effectiveness of re-curved wave return walls." HR Wallingford, Wallingford, U.K., Report SR 261.

Takahashi, S. (1996). "Design of vertical breakwaters." *Short Course International Conference Coastal Engineering (ICCE)*, Orlando, Florida, 85 pp.

Van der Meer, J. W. & Janssen, J. P. F. M. (1995). "Wave run-up and wave overtopping at dikes and revetments." Wave forces on inclined and vertical wall structures, New York, USA, pp. 1-27.

Van der Meer, J. W., Langenberg, J. W., Klein Breteler, M., Hurdle, D. P. & den Heijer, F. (2002). "Wave boundary conditions and overtopping in complex areas." *Proceedings International Conference Coastal Engineering (ICCE)*, Cardiff, UK, pp. 2092-2104.

Appendix L: Pearson *et al.*, 2004

Pearson, J., Bruce, T., Allsop, N.W.H., Kortenhaus, A. & van der Meer, J.W. (2004), *Effectiveness of recurve wave walls in reducing wave overtopping on sea-walls and breakwaters*, Proc. 29th Int. Conf. Coastal Engineering, 4, pp 4404–4416, ASCE / World Scientific, Singapore, ISBN 981-256-298-2

Appendix L
Pearson *et al.*, 2004

Pearson, J., Bruce, T., Allsop, N.W.H., Kortenhaus, A. & van der Meer, J.W. (2004), *Effectiveness of recurve wave walls in reducing wave overtopping on seawalls and breakwaters*, Proc. 29th Int. Conf. Coastal Engineering, 4, pp 4404–4416, ASCE / World Scientific, Singapore, ISBN 981-256-298-2

L.1 Declaration of contribution

Bruce was responsible for the reworking of the existing data set (gathered for Kortenhaus *et al*, 2003) for lowest k, and for the synthesis of the new recommendation. He also presented the paper to the conference and led the drafting and final editing of the paper.

L.2 Published paper

overleaf

EFFECTIVENESS OF RECURVE WALLS IN REDUCING WAVE OVERTOPPING ON SEAWALLS AND BREAKWATERS

JON PEARSON, TOM BRUCE

School of Engineering & Electronics, University of Edinburgh, The King's Buildings, Edinburgh, EH9 3JL, Scotland, UK

WILLIAM ALLSOP

Univ. Southampton & HR Wallingford, Howbery Park, Wallingford, Oxon, OX10 8BA

ANDREAS KORTENHAUS

Leichtweiss Institut, Technical University of Braunschweig, Beethoven Str 51A, 38106 Braunschweig, Germany

JENTSJE VAN DER MEER

INFRAM, P.O. Box 16, 8316 ZG Marknesse, The Netherlands

Designers of vertical seawalls and breakwaters have often included some form of seaward overhang (*recurve / parapet / wave return wall / bullnose*) as part of the structure with the design motivation of reducing wave overtopping by deflecting back seaward uprushing water. Despite a lengthy track record in the field and relevance to current design issues, very little generic guidance is available for their incorporation into seawall / breakwater design. This paper reports a study whose aim is the formulation of generic guidance for recurve structure design. Particular attention is given to high freeboard and / or wave breaking conditions under which the recurve / parapet gives very large reductions (recurve k-factor < 0.05). The paper presents tentative guidance in the form of a decision chart. Finally, overtopping and loading results from a case study into a wall of particularly complex geometry are presented and compared with earlier studies. Forces on the vertical wall are found to be highly impulsive in nature and approximately double the magnitude of those expected on a simple wall, with additional forces of a similar magnitude measured on the underside of the parapet.

1. Introduction

For well over a century, designers of seawalls and breakwaters have often included some form of seaward overhang as part of the structure. This design feature is referred to variously as a *recurve / parapet / wave return wall / bullnose*. While arguably there are some distinctions to be made between these, they all share the design motivation of reducing wave overtopping by deflecting back seaward uprushing water (Figure 1). This design feature (for simplicity hereafter referred to as a *recurve* if it is curved, otherwise *parapet*) has many

attractions, not least at a time when there is evidence of increased storm activity in many parts of the world placing increased pressure on the performance of existing coastal defence structures. For reasons of visual amenity, simply enhancing the performance of a wall against overtopping by increasing the crest level may not always be a satisfactory option – recurves offer an alternative.

With such a lengthy track record in the field and relevance to current design issues, it is surprising that very few systematic studies have been carried out and even less generic guidance offered for their incorporation into seawall / breakwater design.

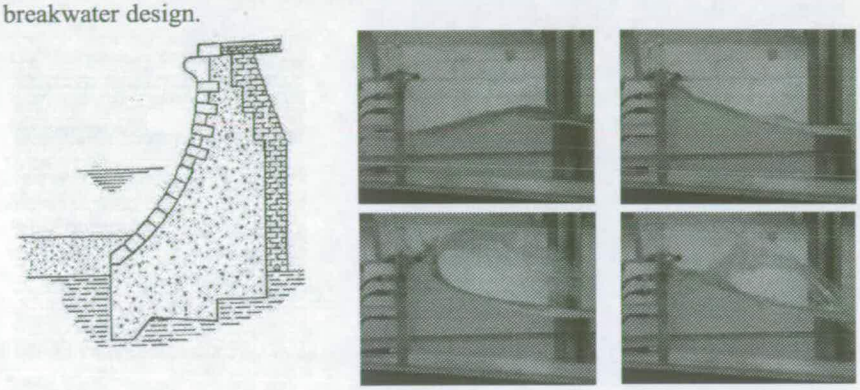

Figure 1. Left, a seawall with recurve. Right, a model recurve in the laboratory at Edinburgh.

This paper updates reporting of an on-going UK / German / Dutch collaborative study whose aim is the formulation of generic guidance for recurve / parapet structure design. It begins with a review of previous studies and a detailed reprise of initial project findings. Particular attention is then paid to modelling conditions (generally high freeboard and / or wave breaking) under which the recurve / parapet gives very large reductions (by greater than a factor of 20; *ie* recurve k-factor < 0.05). Finally, overtopping and loading results from a case study into a wall of particularly complex geometry are presented and compared with earlier studies.

2. Previous studies

Systematic hydraulic model studies of wave overtopping date back to the 1970s (*eg* Goda, 1971 & 1975). Most work focussed upon simple sloping structures (*eg* Owen, 1980), later extended / modified to rubble mound structures and to steep and vertical walls (*eg* Franco *et al*, 1994 & 1995; van der Meer & Janssen, 1995; van der Meer *et al* 1998). For vertical walls, early studies were carried out under wave / structure combinations which gave few or no breaking waves at the wall. In the mid-90s it was realised that a transition to breaking or *impulsive*

conditions at a wall caused a significant change in overtopping performance not predicted by existing methods. Recent investigations (*eg* Allsop *et al*, 1995; Bruce *et al*, 2001; Pearson *et al*, 2002; Napp *et al*, 2004) have focussed on these impulsive conditions and verified / expanded guidance on the subject. Current guidance includes the UK *Environment Agency Overtopping Manual* (Besley, 1999) and even more recently in The Netherlands, the *TAW Manual* (van der Meer, 2002).

Early studies of structures with some form of recurve include the work of Owen & Steele (1991) and Juhl (1992). These studies offer overtopping reduction factors but are not generic in nature.

In Japan, a detailed research programme has investigated a *non wave overtopping seawall* (also known as a *flaring shaped seawall, FSS*). This type of structure has a large radius curve starting well below still water level whose radius changes with elevation. Results of regular wave tests and numerical simulations are given in Kamikubo *et al* (2000), with new irregular wave data being presented elsewhere at this conference (Yamashiro *et al*, 2004). The investigators demonstrated a reduction in required crest level of up to *c.* 30%.

Cornett *et al* (1999) describe an extensive and systematic investigation of the influence of parapets on overtopping. The test programme included "chamfered" walls where the parapet was angled landward rather than overhanging seaward. For conventional seaward leaning parapets, reduction factors of ten or more are reported even for parapets inclined at angles as little as 30^0. Helpful summary charts are presented with comparisons to standard formulae, but it is admitted that the overtopping response was found to be "highly variable" resulting quite some unresolved scatter.

Kortenhaus *et al* (2001) report on a series of tests in which overtopping and wave loading are measured for vertical walls with and without parapet. They found that the parapet is effective in reducing overtopping only under conditions where the relative crest freeboard $R_c/H_s > 1.5$. Wave loading on the structure was found to be significantly increased by the presence of the parapet for lower freeboards, $R_c/H_s < 1.2$, with factors of 2.0 and 1.7 being quoted for impulsive and non-impulsive waves respectively. This study, together with work in the UK under the *Violent Overtopping by Waves at Seawalls (VOWS)* project formed the starting point for the current investigation. First results were reported at the *Coastal Structures '03* conference (Kortenhaus *et al*, 2003). These are summarised in the next section.

3. Review of tentative generic method (Kortenhaus *et al*, 2003)

Analysis was carried out of overtopping measurements from a number of datasets which included a wide range of recurve / parapet types, plain and composite walls and impulsive and non-impulsive conditions at small and large scale. It was seen that some "with recurve" data fell as much as three orders of magnitude below the discharges measured (or expected) for the plain structure. The effectiveness of the recurve / parapet in reducing overtopping was quantified by the *k-factor* defined as

$$k \equiv \frac{q_{\text{with\_recurve}}}{q_{\text{without\_recurve}}}$$

Plotting k against relative freeboard R_c/H_s for each structure / recurve combination (example in Figure 2) suggested a three-regime predictor going from "little or no effect" to "very large reduction" regimes via a transition regime. The first regime extends to $R_c/H_s = R_0^*$, with the transition to the third regime occurring at $R_c/H_s = m^*$. Equations for k, R_0^* and m^* are as follows.

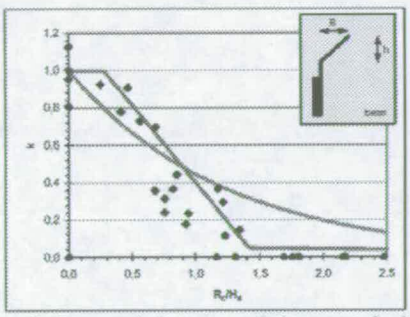

Figure 2. Recurve k-factor *vs* relative crest freeboard (from Kortenhaus *et al*, 2003). The curve shows an earlier predictor (from Kortenhaus *et al*, 2001).

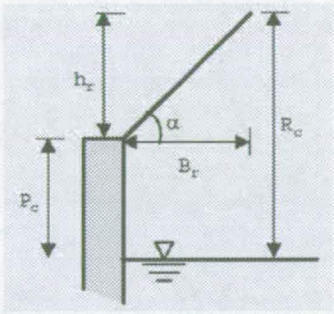

Figure 3. Parameter definition sketch.

$$k = \begin{cases} 1.0 & \text{for } \dfrac{R_c}{H_s} \le R_0^* \\ 1 - \dfrac{1}{m}\left(\dfrac{R_c}{H_s} - R_0^*\right) & \text{for } R_0^* < \dfrac{R_c}{H_s} \le R_0^* + m^* \\ k_{23} - 0.01\left(\dfrac{R_c}{H_s} - R_0^* - m^*\right) & \text{for } \dfrac{R_c}{H_s} \ge R_0^* + \mathrm{m}^* \end{cases} \qquad (1)$$

where k_{23} is the k-factor at which the lowest k regime begins[†] (set to 0.2[‡]) and

[†] k_{23} was referred to as k_3 in Kortenhaus *et al* (2003).

[‡] The value of 0.2 is preferred to 0.05 used in Kortenhaus *et al* (2003).

$$R_0^* \equiv 0.25.\frac{h_r}{B_r} + 0.05\frac{P_c}{R_c} \tag{2}$$

$$m \equiv 1.1\sqrt{\frac{h_r}{B_r}} + 0.2\frac{P_c}{R_c} \qquad m^* \equiv m(1 - k_{23}) \tag{3), (4)}$$

Applying this model for k to the available dataset and plotting the dimensionless mean discharge *adjusted by the k-factor* against relative crest freeboard gave the graph in Figure 4. This k-factor approach gave a useful reduction in the scatter in the data, and showed that the adjusted data generally lay on the conservative side of van der Meer and Janssen (1995). However, there was quite some data which lay very much below the line, by up to a factor of 100. This is in line with the scatter observed in the lowest k regime ($R_c/H_s \geq R_0^* + m^*$). The study has since been extended to focus on this regime of largest reduction factors – the topic of the next section.

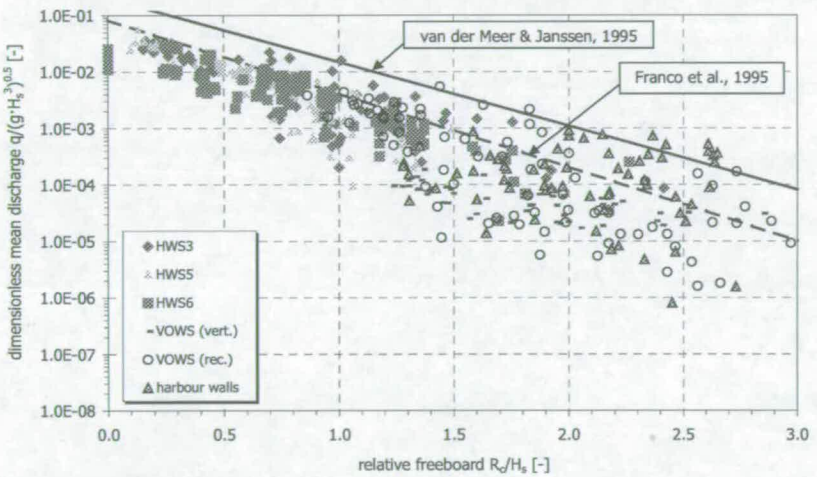

Figure 4. Non-dimensional mean overtopping discharge *vs* relative crest freeboard incorporating correction for reduction factor k (equation 1). From Kortenhaus *et al* (2003).

4. High freeboard / low k cases

The basis for this part of the study is a dataset consisting of 85 tests carried out at small-scale supplemented by five tests carried out under closely comparable conditions at large scale (at UPC Barcelona, see Pearson *et al*, 2002). That the lowest k (largest reduction) regime of Kortenhaus *et al* (2003) performs generally conservatively but not particularly well for these tests is shown in Figure 5, where the measured k-factor is plotted against the value predicted.

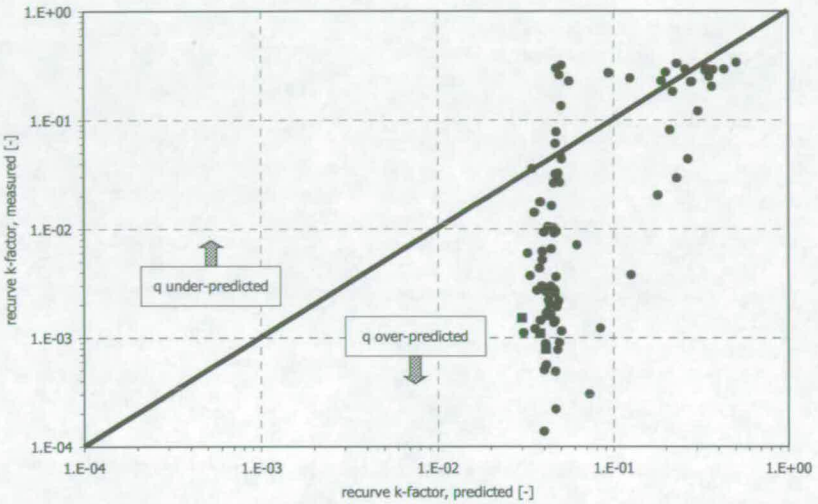

Figure 5. Measured k-factor *vs* predicted, VOWS data. Circles are small-scale data (85 tests); squares are large-scale data (five tests). Note logarithmic axes.

Exploration of the dependency of k upon key structural and wave parameters found some dependency upon both relative crest freeboard ($k \downarrow$ as $R_c/H_s \uparrow$ with quite some scatter) and upon the relative water depth at the base of the wall ($k \downarrow$ as $h_s/H_s \downarrow$ again with quite some scatter). The dependency upon relative freeboard is explained by the observation that the higher the relative freeboard, the more vertically upward any uprushing water travels, and the more effectively this is thrown entirely seaward by the recurve. The relative depth dependency seems to rest upon the fact that the incident waves are increasingly likely to be breaking (or even broken) at the wall as this parameter decreases. Again, such conditions favour vertically thrown uprush and improved recurve efficiency.

Combining these to give k as a function of $R_c/H_s \times H_s/h_s = R_c/h_s$ reduces scatter somewhat and reveals some organised behaviour. Plotting the ratio of measured to predicted k (Figure 6), it would appear that an approach similar to that taken for all cases (Section 3) should be taken, with the response falling into three regimes;

1. $R_c/h_s \leq 0.6$; k as per Kortenhaus *et al* (2003);
2. $0.6 < R_c/h_s \leq 1.1$; $k \rightarrow k \times 180 \exp(-8.5\, R_c/h_s)$;
3. $R_c/h_s > 1.1$; $k \rightarrow k \times 0.02$.

The effectiveness of this adjustment to k can be gauged from Figure 7, which plots the ratio of the measured to new predicted k-factors against dimensionless discharge. The data is now scattered around the ideal (ratio = 1) line and all predictions fall within one order of magnitude of measurements.

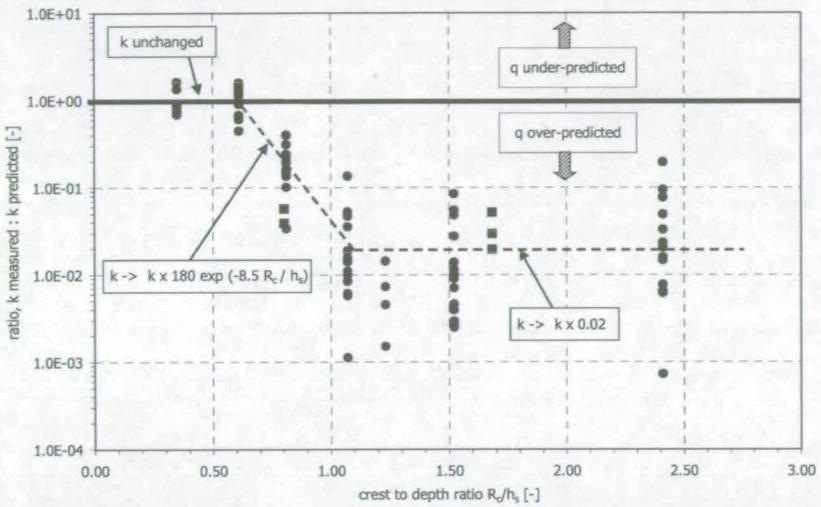

Figure 6. Ratio of k measured to k predicted by Kortenhaus *et al* (2003) plotted against crest to depth ratio. Lines show proposed three-regime adjustment.

It might be expected that scatter would be greatest for the very smallest discharges, and indeed this appears to be the case here (Figure 7). For non-dimensional mean discharges $q > 10^{-5}$, the scatter reduces to give agreement to with a factor of approximately two. The inherent scatter for the lowest discharges may mean that it is unlikely that k-factors of less than perhaps 0.05 could be safely realised in design, and certainly not without detailed physical model studies. The methodology is summarised in a decision chart (Figure 8).

5. Promenade wall case study

5.1. *Introduction*

This section reports results from a design study of an unusual seawall to defend against *very* long return period conditions. There are some important visual constraints on fixing the overtopping discharge by crest freeboard alone. Consideration instead is being given to a wall with parapet (Figure 9) whose crown deck will form a promenade. The purpose of the study was to determine a

suitable parapet extension B_r to limit overtopping to an admissible level under extreme conditions.

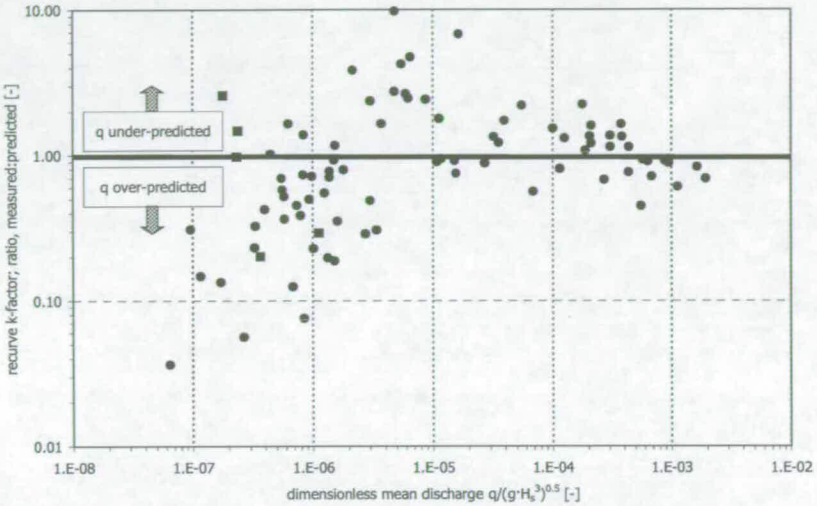

Figure 7. Ratio, measured:predicted *k*-factor plotted against non-dimensional overtopping rate.

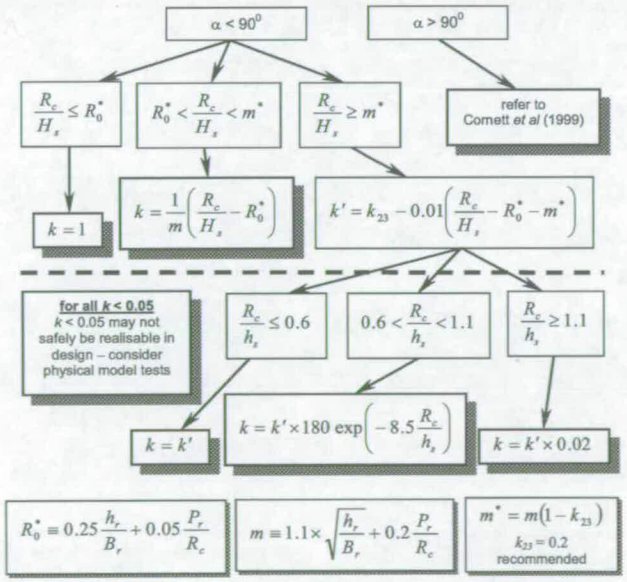

Figure 8. "Decision chart" summarising methodology for tentative guidance.

It can be seen from the cross-sections that this problem presents difficulties for application of the method described in Sections 3 and 4. Firstly, the recurve does not reach up to the crest of the structure, leaving a problem of what is h_r. The parapet section also begins at an unusually low relative elevation, P_c. It was decided that a physical model study should be carried out. Three cross-sections were tested with increasing parapet overhangs, B_r. Pressure measurements were made on the vertical wall and on the underside of the overhanging parapet.

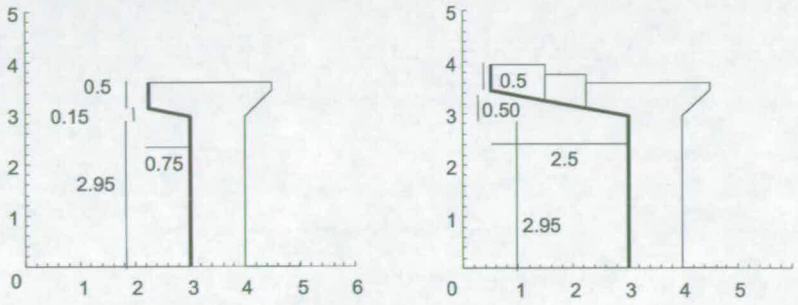

Figure 9. Left; the basic *"small recurve" structure*. Right; showing two added sections increasing parapet width B_r (*"medium recurve" and "large recurve"*). Dimensions in m at prototype scale.

5.2. *Overtopping observations and measurements*

Tests were carried out in the wave channel at the University of Edinburgh. The channel is 20m long by 0.4m wide with a working water depth of 0.7m. The channel is equipped with an absorbing flap-type wave paddle. Overtopping discharge was collected in a tank suspended from a load cell. Pressure measurements were taken using seven Druck PDCR 800 pressure transducers (natural frequency 28 kHz) sampled at 2 kHz. The test matrix included both uni- and bi-modal seas with nominal steepnesses around 0.04 and 0.02.

With a relatively small gap between still water level and the underside of the parapet, some particularly violent behaviour was observed, as incoming waves filled the gap under the parapet (Figure 10).

The overtopping results are shown in Figure 11. It is immediately striking that the mean discharge does not show as strong an influence from the parapet overhang B_r as the influence of steepness. Indeed, the overtopping response of these structures was seen to be very sensitive to wave period, with the shorter period waves generally more affected by the presence of the parapet than the longer waves. Observations show that these longer waves are more capable of filling the under-parapet gap and then overflowing this filled volume to overtop.

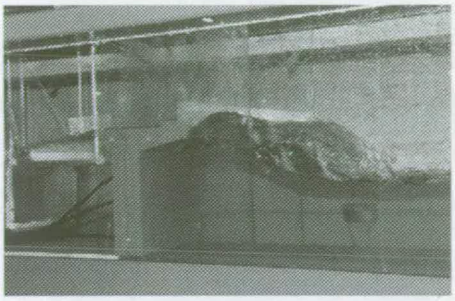

Figure 10. Example of a wave being deflected seaward in the promenade wall study

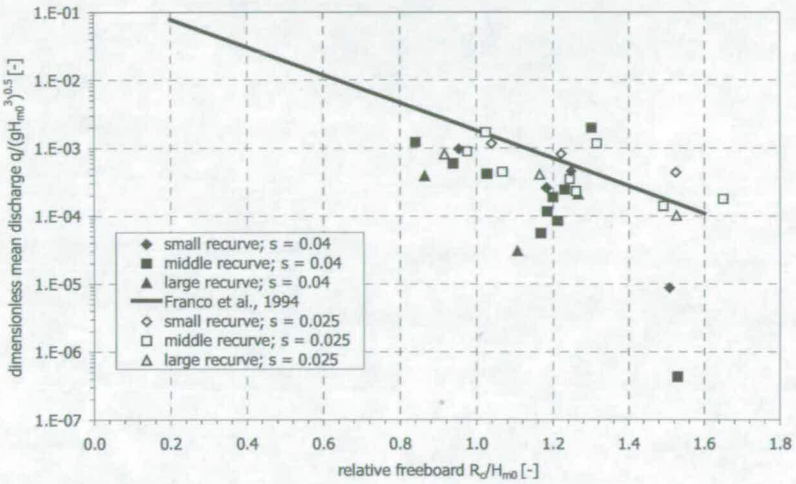

Figure 11. Graph of relative mean overtopping rate *vs* relative freeboard; all cross-sections. The only s=0.04 point lying above the line corresponds to a bi-modal sea for which the definition of steepness is less physically meaningful.

For completeness, a comparison of these measurements with the tentative generic method was made. Making the assumption that the parapet can be modelled as an average line from its base to the crest of the structure, overtopping was generally under-predicted by factors of up to ten. This reinforces the argument that this is a complex configuration with wave-structure interactions and resultant overtopping performance strongly affected by the parapet lying so close to still water level.

5.3. *Loadings on parapet*

It is clear from fundamental momentum considerations that a structure deflecting water through a greater angle must experience enhanced loadings, but how these are distributed (and thus the effect on overturning moments) is not well understood. Kortenhaus *et al* (2001) give horizontal load increase factors of 1.7 and 2.0 for non-impulsive and impulsive conditions respectively. The upward loads on the parapet are reported as being of a similar magnitude.

The results of the force measurements are summarised in Table 1, together with comparator forces from a Delft Hydraulics study. The forces have been non-dimensionalised in the conventional manner. The "upwards" force is the force acting normal to the underside of the parapet.

Table 1. Dimensionless forces measured on promenade wall, plain vertical wall comparison.

dimensionless force, $F / \rho g H_{m0}^2$	Horizontal [-]	Upwards, on parapet [-]
plain vertical wall (den Heijer, 1998)	9.3 – 11.4	
promenade wall, *small recurve*	17.2	16.3
promenade wall, *medium recurve*	20.5	21.1

Thus, for this parapet configuration structure, measured horizontal forces are higher than for a plain wall by factors $k_F \approx 2$, with further comparable (or even slightly larger) forces acting on the underside of the parapet. These factors are very much in line with those reported by Kortenhaus *et al* (2001).

Impulsive loads on a parapet are of some importance as the parapet structure is likely to have a higher natural frequency than the main part of the wall and thus may be able to "feel" and respond to the impulsive part of the loading to a greater extent. Observations of these tests suggested some highly impulsive loads, supported by very abrupt and loud slamming noises being heard repeatedly. Mean rise time measured at model scale was 2.0 ms (± 1.1 ms), with mean total impact duration 7.2 ms (± 2.7 ms).

6. Conclusions

Kortenhaus *et al* (2003) presented a generic method for the prediction of the reduction in overtopping due to recurves / parapets. Quite some scatter remained for the largest reductions (smallest k-factors). This paper has presented an extended method with focus on this regime. The method builds upon a dependency of recurve effectiveness upon the crest to depth ratio R_c / h_s. The combined prediction method is summarised in a "decision chart".

Results from a physical model study of a "promenade wall" with unusual parapet have been presented, illustrating the difficulty in applying a generic method to complex structures (in this case, one with parapet unusually close to

still water level). The model study showed that for this structure, overtopping reduction due to the parapet was more strongly influenced by wave period than by the parapet overhang, B_r.

Basic momentum considerations require that the presence of a recurve / parapet must increase the total load. Measurements of horizontal and upward loading on the "promenade wall" gave load horizontal increase factors (k_F) of around two as compared to loads on a simple vertical wall. Upward loads on the underside of the parapet were of a similar magnitude (indeed greater in some cases). These findings were in line with those of Kortenhaus *et al* (2001). Very short-duration impulsive (slamming) loads were measured as the gap under the parapet filled. Parapets may be particularly able to respond to (and be damaged by) such loads.

Acknowledgements

The authors gratefully acknowledge the work of Helge Holtorf who performed and analysed the model tests at LWI at an early stage of the project. The authors' international collaboration has been facilitated by the EC FP5 "CLASH" project (EVK3-2001-0058).

References

Allsop, N.W.H., Besley, P. and Madurini, L. 1995. Overtopping performance of vertical and composite breakwaters, seawalls and low reflection alternatives. Proc. final MCS project workshop, Alderney, pub. University of Hannover.

Besley, P. 1999. Overtopping of seawalls – design and assessment manual. R&D Technical Report W 178, Environment Agency, UK (ISBN 1 85705 069 X)

Bruce, T., Allsop, N.W.H. and Pearson, J. 2001. Violent overtopping of seawalls – extended prediction methods, Proc. "Breakwaters, coastal structures and coastlines", pp 245–256, Thomas Telford, London (ISBN 0 7277 3042 8)

Cornett, A., Li, Y. and Budvietas, A. 1999. Wave overtopping at chamfered and overhanging vertical structures. Proc. Intl. workshop on natural disasters by storm waves and their reproduction in experimental basins, Kyoto, Japan.

Den Heijer, F. 1998. Golfoverslag en krachten op verticale waterkerings-constructies. WL | delft hydraulics report H2014 (in Dutch)

Franco, L., de Gerloni, M. and van der Meer, J.W. 1994. Wave overtopping on vertical and composite breakwaters, Proc 24th Int. Conf. Coastal Eng., pp1030–1045 (ISBN 0-7844-0089-X)

Franco, L., de Gerloni, M. and van der Meer, J.W. 1995. Wave overtopping on vertical and composite breakwaters. Proc. final MCS project workshop, Alderney, pub. University of Hannover

Goda, Y. 1971. Expected rate of irregular wave overtopping of seawalls. Coastal Engineering in Japan, Vol 14, pp 45–51, JSCE, Tokyo.

Goda, Y., Kishira, Y. and Kamiyama, Y. 1975. Laboratory investigation on the overtopping rates of seawalls by irregular waves. Ports & Harbour Research Institute, vol 14, no. 4, pp 3–44, PHRI, Yokosuka.

Juhl, J. 1992. Investigations on the effect of structural measures on wave impact forces and overtopping. Proc. 3rd project workshop, MAST I G6-S, Hannover, Germany (pub. University of Hannover)

Kamikubo, Y., Murakami, K. Irie, I. and Hamasaki, Y. 2000. Study on practical application of a non-wave overtopping type seawall. Proc 27th Intl. Conf Coastal Eng, pp2215–2228 (ISBN 0-7844-0549-2)

Kortenhaus, A. Haupt, R. and Oumeraci, H. 2001. Design aspects of vertical walls with steep foreland slopes. Proc Breakwaters, coastal structures and coastlines, London (ICE), pp 221–232 (ISBN 0-7277-3042-8)

Kortenhaus, A., Pearson, J., Bruce, T., Allsop, N.W.H. and van der Meer, J.W. 2003. Influence of parapets and recurves on wave overtopping and wave loading of complex vertical walls. To appear in Proc "Coastal Structures '03" (ASCE)

Napp, N., Pearson, J., Bruce, T. and Allsop, N.W.H. 2004. Overtopping of seawalls under oblique wave attack and at corners. To appear in Proc. 29th Int. Conf. Coastal Engineering (ASCE)

Owen, M.W. 1980. Design of seawalls allowing for overtopping. Report EX924, Hydraulics Research, Wallingford, UK.

Owen, M.W. and Steele, A.A.J. 1991. Effectiveness of re-curved wave return walls. Report SR 261, HR Wallingford, Wallingford, UK.

Pearson, J., Bruce, T., Allsop, N.W.H. and Gironella, X. 2002. Violent wave overtopping – measurements at large and small scale. Proc. 28th Int. Conf. Coastal Engineering, pp 2227–2238, (ASCE) (ISBN 981 238 238 0)

Van der Meer, J.W. 2002. Technical report on wave run-up and wave overtopping at dikes. Report of the TAW, Technical Advisory Committee on Water Defences, The Netherlands

Van der Meer, J.W. and Janssen, J.P.F.M. 1995. Wave run-up and wave overtopping at dikes. Wave Forces on Inclined and Vertical wall Structures, pp 1–26, ed. Kobayashi N. & Demirbilek Z., ASCE (ISBN 0-7844-0080-6)

Van der Meer, J.W., Tonjes, P. & de Waal, J.P. 1998. A code for dike height design and examination. Proc. Coastlines, Structures & Breakwaters '98 (ICE), pp 5–21, pub. Thomas Telford, London

Yamashiro, M., Yoshida, A. and Irie, I. 2004. Development of non wave-overtopping type seawall in deepwater. To appear in Proc 29th Intl. Conf. Coastal Eng. (ASCE)

Appendix M: Napp *et al.*, 2002

Napp, N., Allsop, N.W.H., Bruce, T. & Pullen, T. (2002), *Overtopping of seawalls under oblique and 3-d wave conditions*, Proc. 28th Int. Conf. Coastal Engineering, 2, pp 2178–2190, ASCE / World Scientific, Singapore, ISBN 981 238 238 0

Appendix M
Napp *et al.*, 2002

Napp, N., Allsop, N.W.H., Bruce, T. & Pullen, T. (2002), *Overtopping of seawalls under oblique and 3-d wave conditions*, Proc. 28th Int. Conf. Coastal Engineering, 2, pp 2178–2190, ASCE / World Scientific, Singapore, ISBN 981 238 238 0

M.1 Declaration of contribution

The author was Napp's principal supervisor throughout Napp's PhD studies. The author's contribution has therefore been one of training and close supervision throughout. The author and Napp shared very many lengthy and interesting discussions during the data analysis and presentation phases.

This being Napp's first major presentation and publication, the author took an extended role in guiding Napp in the structuring and editing of both.

M.2 Published paper

overleaf

Overtopping of Seawalls under Oblique and 3-D Wave Conditions

Nicolas Napp[1], Jonathan Pearson[2], Stephen Richardson[3], Tom Bruce[4], William Allsop[5], and Tim Pullen[6]

Abstract: The majority of prediction methods for overtopping of seawalls are based on physical model tests under simple 2-dimensional conditions. There is some evidence (not unambiguous) that overtopping may increase at small degrees of obliquity, and that corners (in plan) may give local concentrations of overtopping. This paper, produced as part of the VOWS project on impulsive (violent) overtopping of vertical seawalls, describes experiments to measure mean and wave-by-wave overtopping discharge under conditions of oblique wave attack and at 3-d corners. Results analysed in the first phase of this 3-d study suggest that mean overtopping discharges reduce significantly with increasing angle of wave attack and that the occurrence of impulsive overtopping diminishes rapidly with obliquity of wave attack > 30°. It is also observed that overtopping may not increase in corners with an approach beach or berm.

1. INTRODUCTION

Seawalls and breakwaters seldom align perfectly with incoming waves, but many prediction methods for overtopping (particularly those developing new formulae for vertical walls) are only valid for shore-normal wave attack ($\beta = 0°$). Relatively few data are available from laboratory or field measurements where waves approach the wall obliquely (see section 2) and those few generally give data under conditions with little or no wave breaking at the structure. There are also few data on wave overtopping at corners and junctions, although there are evidence from sites around the world that there can be substantially enhanced overtopping in re-entrant corners (*eg* Margate, Figure 1).

1 PhD Researcher, Division of Engineering, University of Edinburgh, King's Buildings, Edinburgh, EH9 3JL UK; nicolas.napp@ed.ac.uk
2 Research Fellow, Division of Engineering, University of Edinburgh, King's Buildings, Edinburgh, EH9 3JL
3 PhD Researcher at Manchester Metropolitan University (now Coastal Structures Group, HR Wallingford)
4 Lecturer, Division of Engineering, University of Edinburgh, King's Buildings, Edinburgh, EH9 3JL UK
5 Professor Associate, University of Sheffield; Technical Director, Maritime Structures, HR Wallingford
6 Coastal Engineer, Coastal Structures Group, HR Wallingford, OX10 8BA

Figure 1: Overtopping event at a corner (Margate).

To help to clarify these effects, particularly for violent wave overtopping, a series of 3-d wave basin tests have been performed under the UK *Violent Overtopping by Waves at Seawalls (VOWS)* project. The VOWS project seeks to improve and extend guidance on prediction methods for wave overtopping events at vertical and steeply battered sea-walls, with particular emphasis upon wave / structure combinations for which impulsive wave breaking may occur. The project was run by two teams: a physical model team formed by researchers from Edinburgh and Sheffield Universities with support from HR Wallingford, and a numerical model team based in Manchester Metropolitan University. The VOWS physical model project included three main stages:

- small-scale 2-d wave flume tests (at Edinburgh)
- large-scale 2-d wave flume tests (at UPC Barcelona)
- small-scale 3-d wave basin tests (at HR Wallingford)

The small-scale 2-d wave flume tests focused on vertical and battered walls and included the investigation of wave return walls and recurves (Bruce *et al.*, 2001). The large-scale 2-d flume tests looked at scale effects (Pearson *et al.*, 2002). The small-scale wave basin tests reported here were intended to extend 2-d results to take account of 3-d effects, specifically:

- Obliquity of wave attack
- Different plan geometries including corners (concave)

2. EXISTING GUIDANCE

The VOWS 3-d physical model tests were undertaken to clarify the effects of oblique wave attack and different plan geometries on wave overtopping. In particular, the model tests were intended to investigate whether obliquity can enhance wave overtopping for small angles as has been suggested for sloping walls. If any such increase was detected, it was intended to quantify by how much and at what conditions the increase might be expected. It was also hoped to identify the degree of any reduction of discharge with obliquity, perhaps related to obliquities which influence the transition from impulsive to pulsating conditions.

Although substantial wave overtopping in corners and elbows has been reported on sites around the world, it has not been confirmed by experimental studies. Site specific studies at HR Wallingford on rubble mound slopes and for UK sloping seawalls have often suggested reductions of overtopping around convex and concave corners, although some junctions between seawall and/or breakwaters have shown clear evidence of increased overtopping. The VOWS 3-d studies were intended to address this problem and derive some guidance on the spatial variability of overtopping events around corners.

The technical literature gives contradictory advice as to whether oblique wave attack always reduces wave overtopping. Tautenhain *et al.* (1982) suggested that regular wave run-up could increase by 10% at small obliquities (β = 0° to 35°). Owen (1980) found increased overtopping for random (long-crested) waves at β = 0° to 30° for simple sloping and bermed structures, with maxima for $\beta \approx 15°$. Juhl *et al.* (1994) confirmed increased overtopping for small freeboards and small obliquities for simple rubble slopes (without superstructure) under long-crested waves, but found reduced overtopping for $20° < \beta < 30°$. At large freeboards most tests showed less overtopping for increased obliquity, but a few tests showed increased overtopping at β = 10°.

Tests by de Waal *et al.* (1992) on sloping structures confuse the issue by finding increased overtopping for a few tests at $10° < \beta < 30°$. Mean overtopping for long-crested waves remained almost constant for $\beta < 30°$ and then decreased for $30° < \beta \leq 60°$. For short-crested waves de Waal *et al.* (1992) predict less effect of obliquity, claiming that some large waves still arrive at small obliquities even for large mean approach angles, giving higher overtopping than for long-crested waves. Franco *et al.* (1995) looked at the effect of obliquity and "multi-directionality" with $\beta < 60°$ and spreading up to 30° for plain vertical walls, perforated fronts, wave return walls, and impermeable slopes and berms. In all cases they found reduced overtopping for increasing angle of wave obliquity. Daemrich *et al.* (1999) investigated obliquity on overtopping for a vertical wall with a 1:1.7 approach revetment and a short (1m) berm, performed with long-crested random waves and β = 0, 20 and 40°. These show reduced overtopping with increasing obliquity.

The numerical model by Moriya *et al.* (1996) calculated mean overtopping for vertical walls on the basis of wave energy flux. Dodd (1998) developed a non-linear shallow water wave model for overtopping of sloping structures. Both models predict decreased overtopping for increasing obliquity with no local increases. It should however be noted that neither model would be able to reproduce the processes of impulsive wave breaking, so their conclusions are probably only valid for pulsating conditions.

One aspect of considerable importance to overtopping of vertical / battered walls approached by a steep beach or berm, is the transition from pulsating (sometimes termed reflecting) conditions, to more violent breaking (or impulsive) conditions, and *vice versa.* These were studied at length during the EC PROVERBS project, see Allsop *et al.* (2000), within which guidance was developed on conditions leading to wave impacts under normal wave attack, see Allsop *et al.* (1996). For wave forces, that advice was later qualified for oblique and short-crested waves by Allsop & Calabrese (1999a,b) who found rapid reductions in impact pressures for relatively small obliquities or short-crestedness.

3. EXPERIMENTS

Test Conditions

The physical model tests at HR Wallingford on the vertical seawall used a wave basin 22m long by 19m wide, with a multi-crested absorbing wave maker. To assist design of the physical model, a numerical model using shallow water wave equations and Cartesian cut-cells was run to optimise test structure configurations. These simulations explored the influence of wave guide length on diffraction out of the modelled area and/or reflections within it.

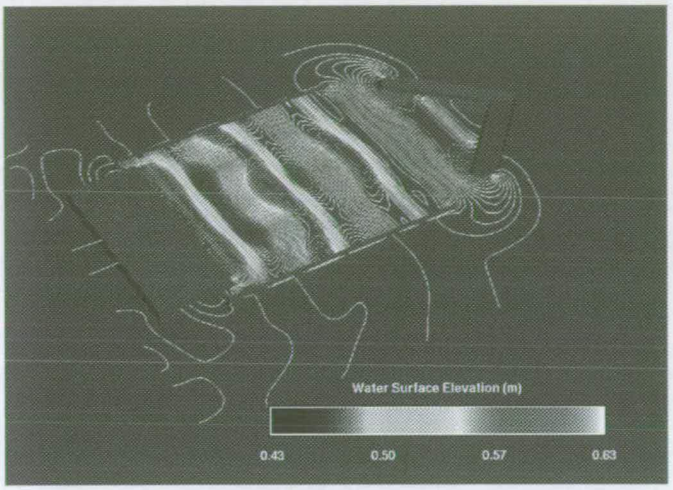

Figure 2: Numerical wave basin with a 90° corner; Mingham *et al.* (2002).

An example of a test run is shown in Figure 2 with the paddle on the left and a 90° re-entrant corner on the right. The numerical modelling also helped reduce testing for re-entrant corners, from five different approach angles to two representative ones. The numerical model results (once compared with physical model results) will be used to extend the range of different configurations for which predictions can be made. A more complete description of this modelling is given by Mingham *et al.* (2002).

In the case of plain obliquity, as in Figure 3, the approach angle β was varied through: $\beta = 0°, 15°, 30°$ and $60°$. Both approach beach and wall were moved in each change of direction. Two other plan geometries were investigated:

- 90° corner / elbow (Figure 4)
- 120° corner / elbow (Figure 5)

The vertical wall - including the approach bathymetry - and the tested wave conditions were designed for predominantly impulsive conditions where overtopping has been shown in 2-d tests to be significantly greater than for pulsating conditions. The criterion adopted to ensure significant breaking onto the wall was the h* parameter as defined by Besley *et al.* (1998):

$$h^* \equiv \left(\frac{h_s}{H_{si}}\right)\left(\frac{2\pi h_s}{gT_{mi}^{\ 2}}\right) \qquad (1)$$

where h_s = water depth at the toe (m); H_{si} local significant wave height (m); T_{mi} = local mean wave period (s).

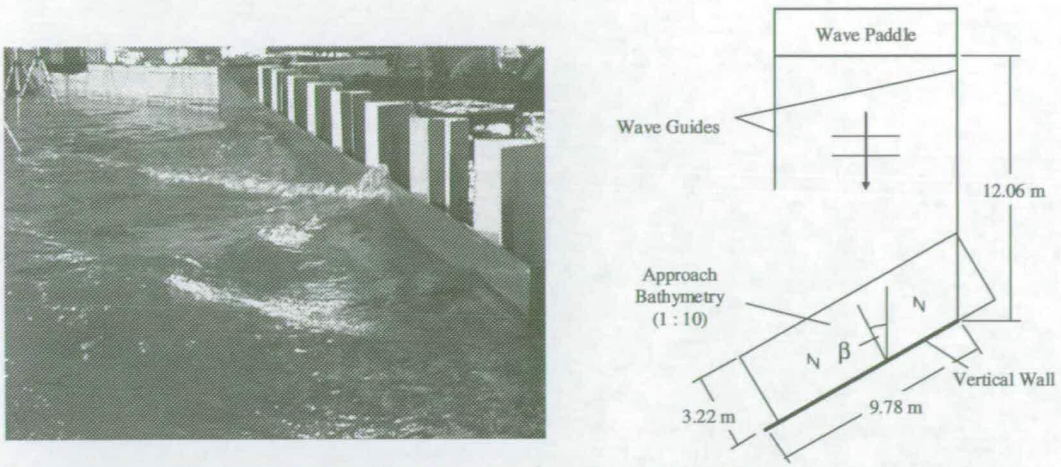

Figure 3: Basin set-up for plain obliquity.

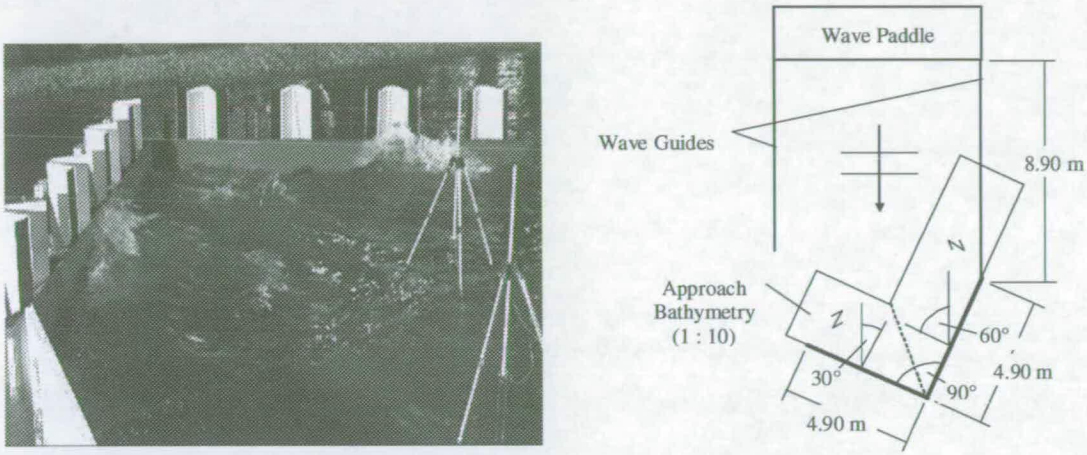

Figure 4: Basin set-up for 90° corner.

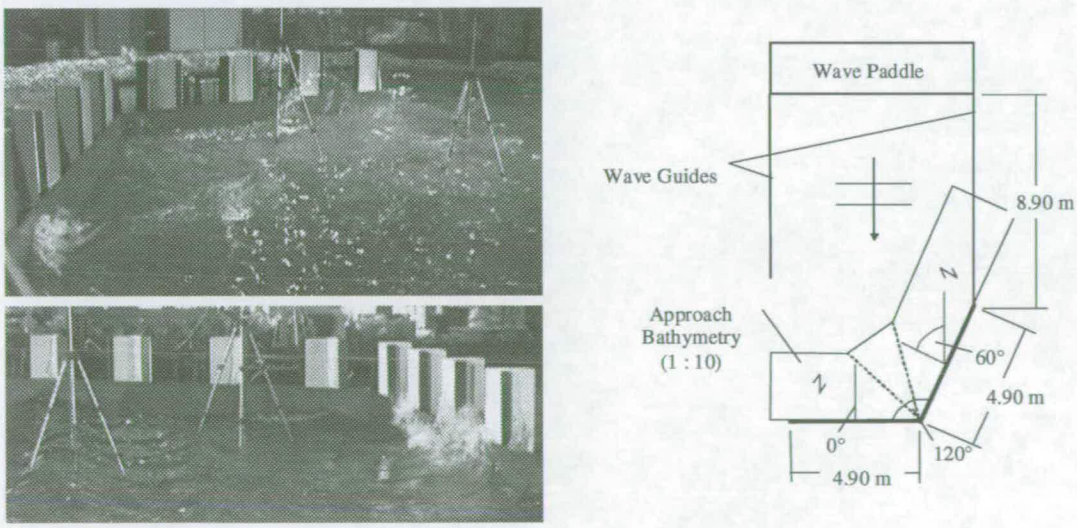

Figure 5: Basin set-up for 120° corner.

Besley (1999) suggests that pulsating / non-breaking waves predominate for h* > 0.3, and that impulsive breaking wave conditions become increasingly prevalent for h* < 0.3. The mean overtopping discharge for *pulsating conditions* ($h^* > 0.3$) can be described by:

$$\frac{Q}{\sqrt{gH_s^3}} = 0.05\exp\left(-2.78\frac{R_c}{H_s}\right) \tag{2}$$

where Q = mean discharge ($m^3/s.m$); R_c = freeboard (m). For *impacting conditions* ($h^* < 0.3$), the suggested relation is:

$$Q_h = 1.37\times10^{-4}\frac{1}{R_h^{3.24}} \tag{3}$$

It should be noted that this relation uses different non-dimensional discharge and freeboard, Q_h and R_h defined as

$$Q_h \equiv \frac{Q}{\sqrt{gh_s^3}\times h^{*2}} \qquad R_h \equiv \left(\frac{R_c}{H_s}\right)h^* \tag{4}$$

The cross-section of the structure is shown in Figure 6. The 1:10 approach beach led up to the structure toe 0.35m above the basin floor. The vertical wall had a total height from floor to crest of 0.725m. The cross-section remained the same for all test conditions. The structures were tested at two water depths shown in Table 1.

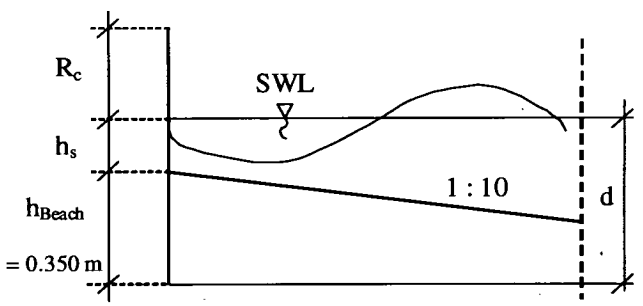

Figure 6: Cross-section of VOWS-3d vertical wall

Table 1: Tested Water Depths and Freeboards

Water depth d, m	Freeboard R_c , m	Depth at toe of structure h_s, , m
0.525	0.200	0.175
0.450	0.275	0.100

Each test-run consisted of approximately 1000 long-crested irregular waves with a JONSWAP spectrum ($\gamma = 3.3$). Waves at the structure were determined by calibration tests with the approach beach in place, but without the (reflecting) wall. Nominal wave conditions are summarised in Figure 7, and wave steepnesses (defined in deep water) fell in the range:

$$0.015 < s_{0P} < 0.065 \tag{5}$$

The h^*-parameter as an indicator of the impulsiveness of the interaction between structure and waves gave predictions from highly impulsive to almost entirely reflecting conditions:

$$0.02 < h^* < 0.30 \tag{6}$$

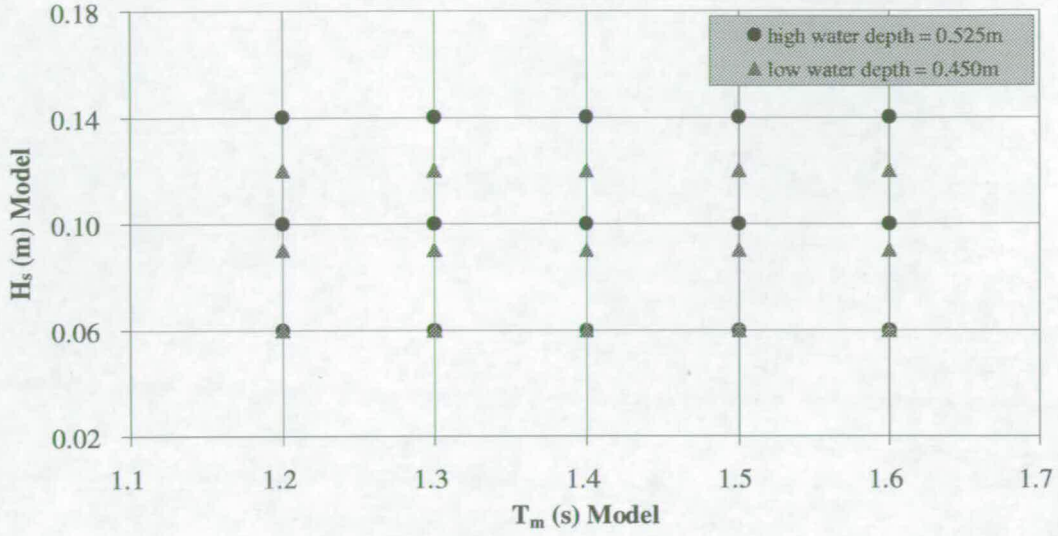

Figure 7: Matrix of test conditions

Overtopping Measurement Equipment

The main measurements in this study were of mean and wave-by-wave overtopping discharges. Spatial variations of these were given by six measurement points along the walls, each using a chute directing water into a container suspended from a load cell (Figure 8a). The load cell output was analysed to give individual overtopping volumes from "steps" in the mass of water. Two aluminium strips across the chute formed an "event detector" (see Figure 8b), giving a signal for each flow over it.

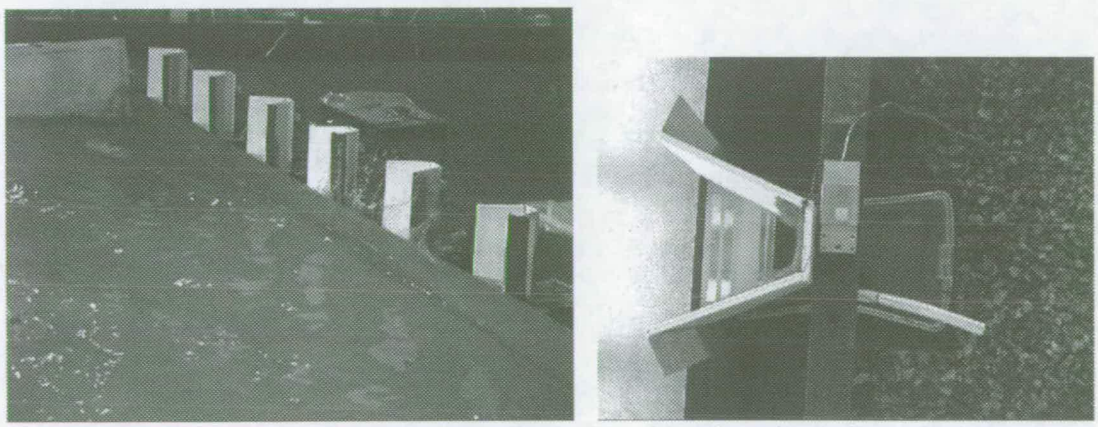

Figure 8: Collection stations: a) along the wall and b) plan view of one device (wave from the left).

4. RESULTS: EFFECT OF OBLIQUE WAVE ATTACK

Measurements of mean overtopping discharge for simple obliquity are summarised in Figure 9 to 12 as dimensionless mean discharge Q_h as defined in Equation (3) against dimensionless freeboard R_h. Tests without measurable overtopping discharge are shown as $Q_h = 0.00001$, corresponding to the lowest detectable volume for these tests.

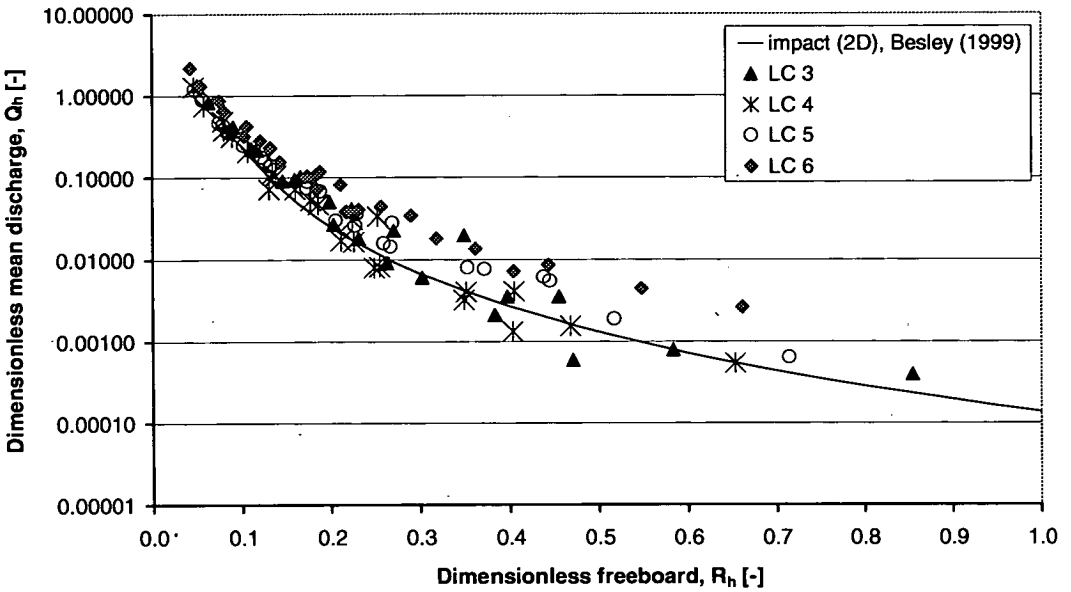

Figure 9: Obliquity $\beta = 0°$.

Results for $\beta = 0°$ in Figure 9 represent reference data against which tests under oblique attack will be compared. The data follow the trend of the $\beta = 0°$ prediction line, although some discharges exceed this. This predictor has been shown by Bruce *et al.* (2001) to be very reliable, so it appears likely that the main reason for these differences lie in variations of wave height H_s along the structure. Results in this paper have used simple analysis of the wave calibrations, but will need to be refined to confirm absolute values of the overtopping, but is not required in order to compare these results with data from the oblique wave tests, all calibrated by the same wave height values.

Results for oblique attack at $\beta = 15°$ on a plain wall are shown in Figure 10. It is clear that there is some reduction in overtopping discharges at this small obliquity in as compared to $\beta = 0°$. There is no evidence of the small increase observed in some previous studies (see section 2). Observations during testing and the data's adherence to the shape of the impulsive prediction line confirm that conditions are still predominantly violent / impulsive.

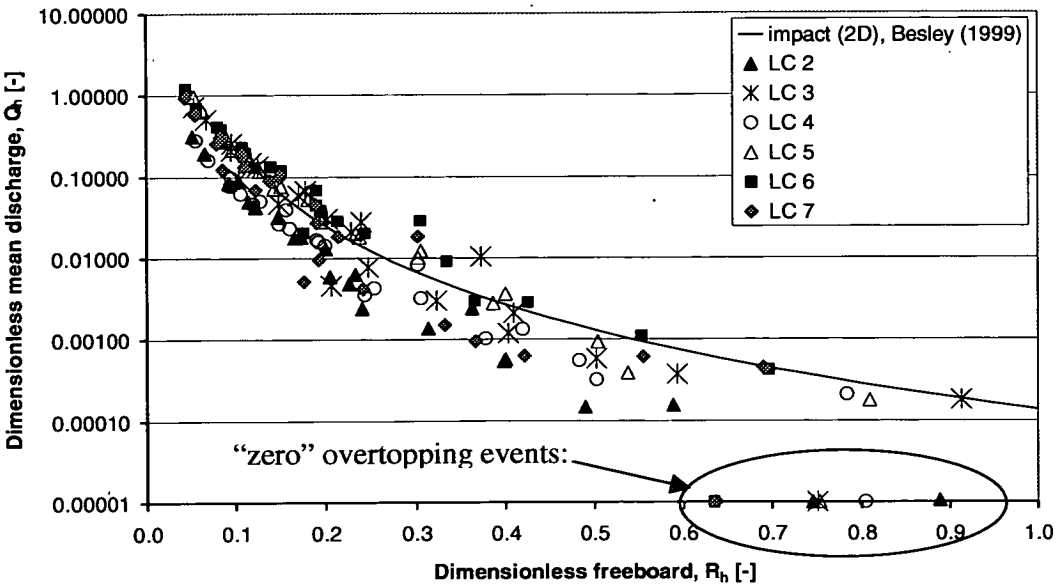

Figure 10: Obliquity $\beta = 15°$.

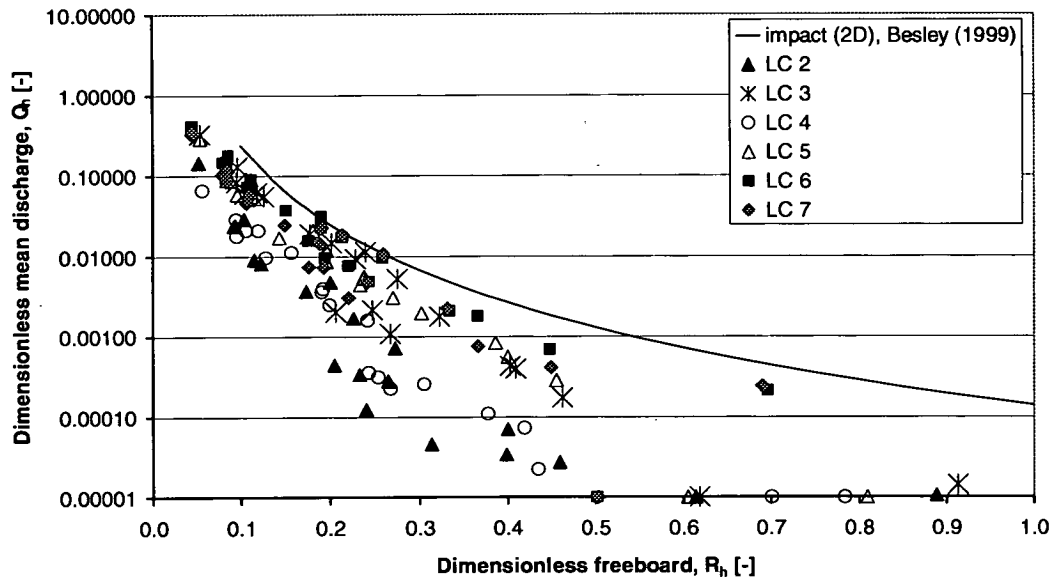

Figure 11: Obliquity $\beta = 30°$.

Data for $\beta = 30°$ are presented in Figure 11. Again, there is no evidence of any (even small) increase in overtopping. Rather, most conditions show notable reductions in overtopping, particularly when compared to $\beta = 0°$. A striking feature is that the reduction is not uniform, but some tests show much larger proportional reductions than others. This corresponds to the observation that some test conditions continue to give a high proportion of impulsive events, but that other conditions no longer show impulsive breaking. For such conditions, Besley's (1999) methods may no longer be appropriate, confirming effects observed for wave forces by Allsop & Calabrese (1999a, b), and suggesting that modified prediction methods may be needed.

Results for β = 60°, are shown in Figure 12. The effect of the additional 30° of obliquity is again striking, with further reductions in overtopping compared to β = 0°, 15° or 30°. The form of the relationship between Q_h and R_h no longer bears much resemblance to the prediction line for impulsive conditions under normal attack. At these large obliquities, methods to predict the form of wave breaking onto the wall have broken down, a conclusion supported by the observation of significantly less impulsive breaking in these tests. It is worth noting that these results show reductions of at least one order of magnitude relative to any prediction using β = 0°, and possible reductions of 2-3 orders of magnitude.

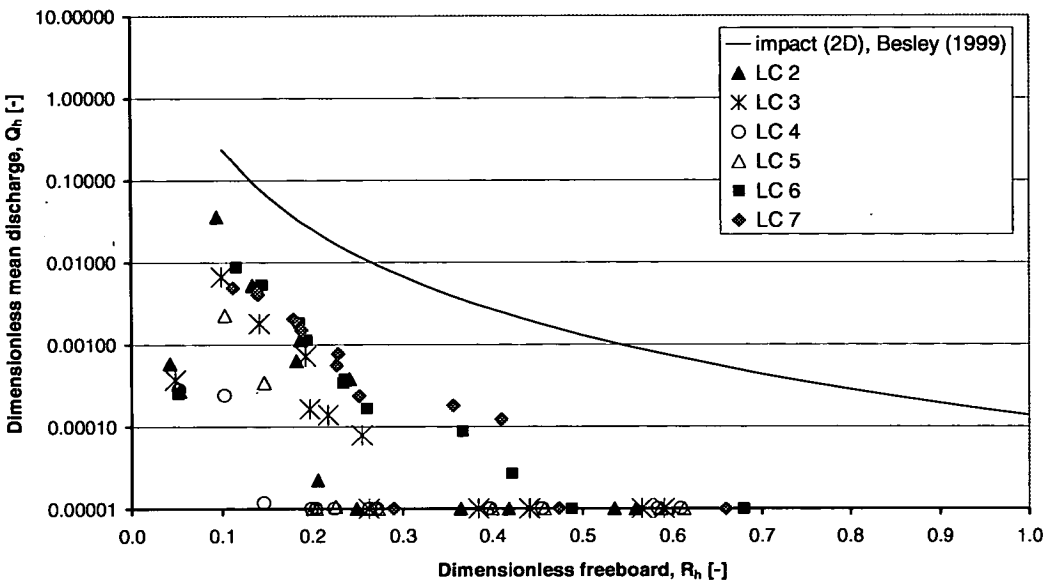

Figure 12: Obliquity β = 60°

5. RESULTS: EFFECT OF A CORNER / ELBOW

The overtopping discharge in 90° and 120° corners in Figure 13 and 14 respectively, are much less easily explained. Containers 4 and 5 ("LC 4", "LC5") were located next to the corner, although they do not capture all water in the corner. Despite their closeness to the corner, it can be seen the mean discharge for both containers is lower than for the predicted (no obliquity) condition.

There are however other measurement points showing some increases, but that is not unexpected where strong reflections from one length of wall can reach the other length of wall, and may interact strongly with incoming waves.

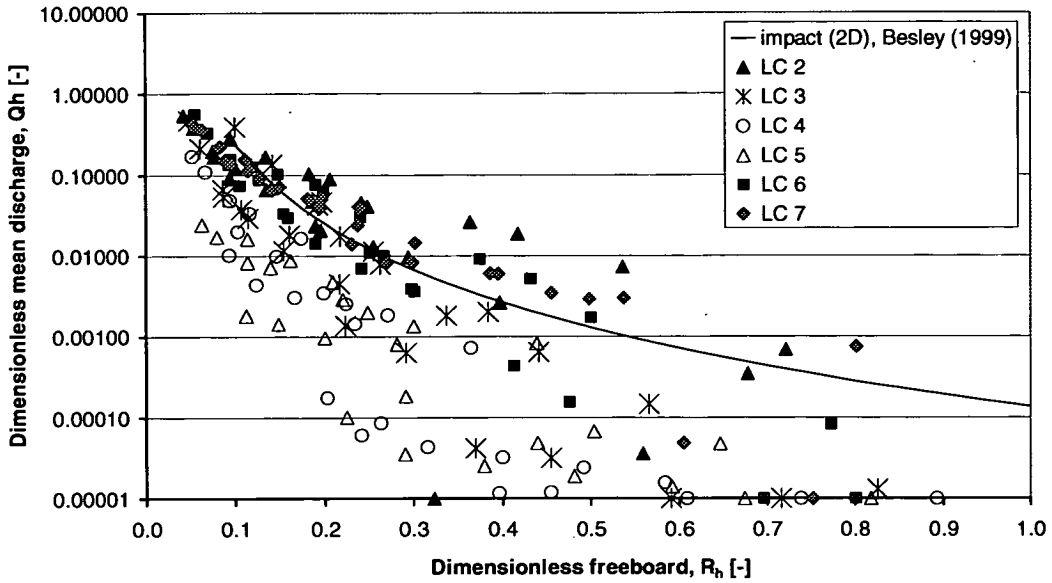

Figure 13: 90° corner / elbow.

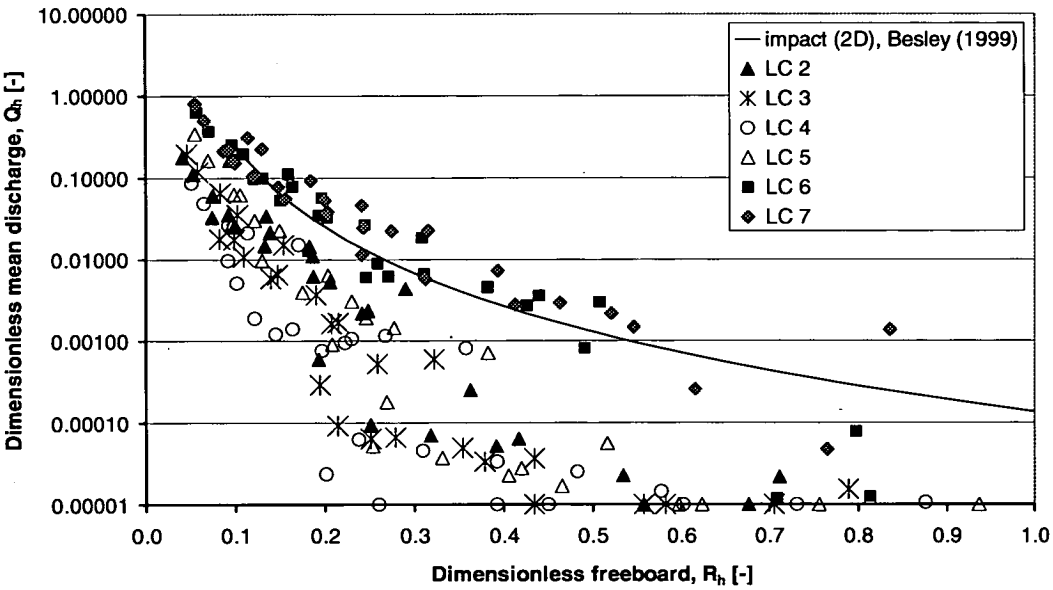

Figure 14: 120° corner / elbow.

Clearly, overtopping processes here are influenced by the changes to impulsive / pulsating breaking discussed earlier; to local refraction effects on the approach beach; effects of waves reflected from one side to the other, and local concentrations. It appears quite likely that the expected concentration of overtopping in these corners has been negated (in part) by some of these more complex effects.

6. CONCLUSIONS

Mean overtopping discharges for vertical walls under impulsive conditions reduce with increasing angle of wave attack. There is no evidence of the small increase in overtopping at small obliquities as reported in some earlier studies.

The occurrence of impulsive overtopping events diminishes rapidly with obliquity of wave attack. For large obliquities, it may therefore be inappropriate to use the h^* parameter on its own as an indicator of whether impulsive conditions will occur.

Under the conditions tested, no evidence of any significant increase in mean overtopping in the neighbourhood of corners was found, but this may be strongly influenced by the limited range of conditions tested. This conclusion might well be reversed if only pulsating conditions had been measured.

It is clearly important to distinguish between effects caused by the form of wave breaking, and those arising from plan and section geometry. Further work will be needed to clarify some of these effects, particularly to identify conditions under which the switch between impulsive and pulsating conditions occurs with varying angles of wave attack.

ACKNOWLEDGEMENTS

The work described in this paper has been supported by the UK EPSRC (GR/M42312, GR/R42306), and supported by the VOWS Management Committee including members from Manchester Metropolitan University (Derek Causon, David Ingram, Clive Mingham), HR Wallingford (Philip Besley), Posford-Haskoning (Dick Thomas), Bullen & Co, whose support is gratefully acknowledged. The VOWS project is particularly pleased to acknowledge guidance and helpful supervision to their collaborative work from the EPSRC CEWE Project Manager, Michael Owen.

The physical modelling was also substantially assisted by sharing test facilities, test structures, measurement devices and related respourses funded by the DEFRA / EA research projects FD 2410 & FD2412 Coastal Flooding Hazard by Wave Overtopping (SHADOW Phase I & II).

Further work on hazards arising from overtopping, including field measurements of overtopping at its effects, is being conducted under the European CLASH project under contract EVK3-2001-0058 in the EC 5th Framework programme.

REFERENCES

Allsop, N.W.H. & Calabrese, M. (1999a), "Impact loadings on vertical walls in directional seas", Proc. 26th Int. Conf. on Coastal Eng., pp 2056 - 2068, June 1998, Copenhagen, ISBN 0-7844-0411-9, ASCE.

Allsop, N.W.H. & Calabrese, M. (1999b), "Forces on vertical breakwaters: effects of oblique or short-crested waves", Research Report SR465, HR Wallingford.

Allsop, N.W.H., Vicinanza, D. & McKenna, J.E. (1996), "Wave forces on vertical and composite breakwaters", Research Report SR 443, pp 1-94, HR Wallingford, March 1996.

Allsop, N.W.H., Kortenhaus, A., Oumeraci, H. & McConnell, K.J. (2000), "New design methods for wave loadings on vertical breakwaters under pulsating and impact conditions", Proc. Coastal Structures '99, Santander, pp 595-602, ISBN 90 5809 092 2, publn. Balkema, Rotterdam.

Besley, P. (1999), "Overtopping of seawalls – design and assessment manual", R & D Technical Report W 178, ISBN 1 85705 069 X, Environment Agency, Bristol.

Besley, P., Stewart, T. & Allsop, N.W.H. (1998), "Overtopping of vertical structures: new methods to account for shallow water conditions", Proc. Int. Conf. on Coastlines, Structures & Breakwaters '98, Institution of Civil Engineers, pp46-57, publn. Thomas Telford, London.

Bruce, T., Allsop, N.W.H. & Pearson, J. (2001), "Violent overtopping of seawalls – extended prediction methods", Proc. Int. Conf. on "Coastlines, Seawalls and Breakwaters '01" ICE, publn Thomas Telford, London.

Daemrich, K. F. & Mathias, H. J. (1999), "Overtopping at vertical walls with oblique wave approach", Proc. Conf. COPEDEC V, Cape Town, pp 1294-1301, publn. COPEDEC, Sri Lanka.

Dodd, N. (1998), "A numerical model of wave run-up, overtopping and regeneration", Proc ASCE, Jo. Waterway, Port, Coast & Ocean Eng., Vol 124, No 2, pp 73-81, ASCE.

Franco, C., Franco, L., Restano, C. & van der Meer, J.W. (1995), "The effect of wave obliquity and short-crestedness on the overtopping rate and volume distribution on caisson breakwaters", MAST II-MCS Project Final Proceedings, University of Hannover.

Juhl, J. & Sloth, P. (1994), "Wave overtopping of breakwaters under oblique waves", Proc. 24th ICCE, Kobe, Japan, pp 1182-1196, ASCE.

Moriya, Y. & Mizuguchi, M. (1996), "Wave overtopping rate and reflection coefficient for obliquely incident waves", Proc. 25th ICCE, Orlando, pp 2598-2611, ASCE.

Mingham, C.G., Causon, D.M., Ingram, D.M. & Richardson, S.R. (2002), "Numerical simulation of wave-seawall interaction", Proc. Int. Conf. on Coastal Eng. 2002, Cardiff, July 2002, ASCE.

Owen, M.W. (1980), "Design of sea walls allowing for wave overtopping", Report EX 924, HR Wallingford.

Pearson, J., Bruce, T., Allsop, N.W.H. & Gironella, X. (2002), "Violent wave overtopping – measurements at large and small scale", Proc. Int. Conf. on Coastal Eng. 2002, Cardiff, July 2002, ASCE.

Tautenhain, E., Kohlhase, S. & Partenscky, H-W. (1982), "Wave run-up at sea dikes under oblique wave approach", Proc. 18th ICCE, Cape Town, pp. 804-810, ASCE.

de Waal J.P. & van der Meer J.W. (1992), "Wave Runup and Overtopping on Coastal Structures" Proc.23rd ICCE, Venice, pp 1758-1771, ASCE.

Appendix N: Napp *et al.*, 2003

Napp, N., Pearson, J., Bruce, T. & Allsop, N.W.H. (2003), *Overtopping of seawalls under oblique wave attack and at corners*, Proc. "Coastal Structures 2003", pp 528–541, ASCE, Reston, Virginia, ISBN 0-7844-0733-9

Appendix N
Napp *et al.*, 2003

Napp, N., Pearson, J., Bruce, T. & Allsop, N.W.H. (2003), *Overtopping of seawalls under oblique wave attack and at corners*, Proc. "Coastal Structures 2003", pp 528–541, ASCE, Reston, Virginia, ISBN 0-7844-0733-9

N.1 Declaration of contribution

The author was Napp's principal supervisor throughout Napp's PhD studies. The author's contribution has therefore been one of training and close supervision throughout. Bruce and Napp shared very many lengthy, detailed and interesting discussions during the data analysis and presentation phases. In particular, problems arising out of being the first users of new wave paddles during testing at HR Wallingford (discussed in Section 3.8) resulted in extended and difficult sessions (some including Allsop) to ensure a secure and supportable calibration of data.

N.2 Published paper

overleaf

Violent overtopping of vertical seawalls under oblique wave conditions

Nicolas Napp[1], Jonathan Pearson[2], Tom Bruce[3], and William Allsop[4]

Abstract

Most prediction methods for wave overtopping are based on physical model tests under simple 2-D conditions. This paper describes experiments to measure mean and wave-by-wave overtopping discharge under oblique wave attack. Results suggest that overtopping discharges reduce significantly only for angles of wave attack > 30°. With increasing obliquity, impulsive events transform to "impact-like" events ($0° < \beta \leq 30°$) and then eventually to reflecting waves (60°). Tentative guidance is given for appropriate formulae for each obliquity.

Introduction

Predicting wave overtopping is one of the most important steps in the design of any sea defence. Some prediction methods can distinguish between pulsating and impacting wave attack on a vertical seawall, but there is guidance only for pulsating waves on the effect of wave obliquity (see Franco et al, 1995). For impacts, which can give very much larger discharges than pulsating methods predict, there is no guidance on the effect of obliquity on overtopping. There are, however, indications by Allsop & Calabrese (1999b) that impacts reduce at increasing obliquity.

The key concern here is not the volume of water that may cause flooding, but the safety of people using the sea defence structures. Any safety analysis using methods for only pulsating waves could give entirely wrong guidance. Pulsating methods might not only under-predict the amount of overtopping water, but they also give no hint as to the suddenness of any event.

To clarify the effects of obliquity on mean and wave-by-wave discharges, and on the percentage of impacting waves, 3-d wave basin tests have been performed under the *Violent Overtopping by Waves at Seawalls (VOWS)* project. The VOWS

[1] PhD Researcher, School of Engineering & Electronics, University of Edinburgh, King's Buildings, Edinburgh, EH9 3JL UK; nicolas.napp@ed.ac.uk
[2] Research Fellow, School of Engineering & Electronics, University of Edinburgh, King's Buildings, Edinburgh, EH9 3JL
[3] Lecturer, School of Engineering & Electronics, University of Edinburgh, King's Buildings, Edinburgh, EH9 3JL UK
[4] Visiting Professor, University of Southampton; Technical Director, Maritime Structures, HR Wallingford

project seeks to improve and extend guidance on prediction methods for wave overtopping events at vertical and steeply battered sea-walls, with particular emphasis on wave / structure combinations for which impulsive wave breaking may occur. VOWS included a physical model team of researchers from Edinburgh and Sheffield Universities with support from HR Wallingford; and numerical modellers from Manchester Metropolitan University. Physical modelling included three stages:

- small-scale 2-d wave flume tests (at Edinburgh)
- large-scale 2-d wave flume tests (at UPC Barcelona)
- small-scale 3-d wave basin tests (at HR Wallingford)

The small-scale 2-d tests focused on vertical and battered walls and included the investigation of wave return walls and recurves (Bruce et al., 2001). The large-scale 2-d flume tests looked at scale effects (Pearson et al., 2002). The wave basin tests reported here were intended to extend 2-d results to 3-d, specifically effects of:

- Obliquity of wave attack
- Different plan geometries including corners (concave)

This paper focuses on effects of oblique wave attack on mean overtopping discharge.

Existing Guidance

The VOWS 3-d model tests were undertaken to clarify the effects of oblique wave attack and different plan geometries on wave overtopping. In particular, the model tests were intended to investigate when and by how much the proportion of impacts decreases as this may have substantial effect on overtopping volumes.

These tests also investigated whether obliquity can increase overtopping as suggested for sloping walls under small angles. The literature gives contradictory advice as to whether oblique attack reduces overtopping. Tautenhain *et al.* (1982) suggest that regular wave run-up can increase by 10% at small obliquities ($\beta = 0°$ to 35°). Owen (1980) found increased overtopping for random (long-crested) waves at $\beta = 15°$ to 30° for simple sloping structures, with maxima for $\beta \approx 15°$. Juhl *et al.* (1994) confirmed increased overtopping for small freeboards and small obliquities for simple rubble slopes under long-crested waves, but found reduced overtopping for $20° < \beta < 30°$. At large freeboards most tests showed less overtopping for increased obliquity, but a few tests showed increased overtopping at $\beta = 10°$.

Tests by de Waal *et al.* (1992) on sloping structures compound the problem by suggesting increased overtopping for a few tests at $10° < \beta < 30°$. Mean discharges for long-crested waves remained almost constant for $\beta < 30°$ and then decreased for $30° < \beta \leq 60°$. For short-crested waves de Waal *et al.* (1992) predict less effect, claiming that some large waves still arrive at small obliquities even for large mean approach angles, giving higher overtopping than for long-crested waves. Franco *et al.* (1994) looked at the effect of obliquity and "multi-directionality" with $\beta < 60°$ and spreading up to 30° for plain vertical walls, perforated fronts, wave return walls, and impermeable slopes and berms. In all cases they found reduced overtopping for increasing angle of wave obliquity. Daemrich *et al.* (1999) investigated obliquity on overtopping for a vertical wall with a 1:1.7 approach revetment and a short (1m) berm, performed with long-crested random waves and $\beta = 0$, 20 and 40°. These show reduced overtopping with increasing obliquity.

One aspect of considerable importance to overtopping of vertical / battered walls approached by a steep beach or berm, is the transition from pulsating (reflecting) conditions, to violent breaking (or impulsive) conditions, and *vice versa.* These were studied at length during the EC PROVERBS project, see Allsop *et al.* (2000), within which guidance was developed on conditions leading to wave impacts under normal wave attack, see Allsop *et al.* (1996). For wave forces, that advice was qualified for oblique and short-crested waves by Allsop & Calabrese (1999a, b) who found rapid reductions in loads for relatively small obliquities or short-crestedness.

The vertical wall – including immediate approach bathymetry – and the test wave conditions (see Chapter 3) were designed to give predominantly impulsive conditions where methods based on 2-d tests suggest that overtopping will be significantly greater than for pulsating conditions. The criterion adopted to ensure significant breaking was h*<0.3, as defined by Besley *et al.* (1998);

$$h^* \equiv \left(\frac{h_s}{H_{si}}\right)\left(\frac{2\pi h_s}{gT_{mi}^{\ 2}}\right) \tag{1}$$

where h_s = water depth at the toe (m); H_{si} local significant wave height (m); T_{mi} = local mean wave period (s). Besley (1999) suggests that pulsating / non-breaking waves predominate for h* > 0.3, and that impulsive breaking wave conditions become increasingly prevalent for h* < 0.3. The mean overtopping discharge for *pulsating conditions* ($h^* > 0.3$) can be described by:

$$\frac{Q}{\sqrt{gH_s^{\ 3}}} = 0.05\exp\left(-2.78\frac{R_c}{H_s}\right) \tag{2}$$

where Q = mean discharge (m^3/s.m); R_c = freeboard (m). For *impacting conditions* ($h^* < 0.3$), the suggested relation is:

$$Q_h = 1.37\times10^{-4}\frac{1}{R_h^{\ 3.24}} \tag{3}$$

It should be noted that this relation uses different non-dimensional discharge and freeboard, Q_h and R_h defined as

$$Q_h \equiv \frac{Q}{\sqrt{gh_s^{\ 3}\times h^{*2}}} \qquad R_h \equiv \left(\frac{R_c}{H_s}\right)h^* \tag{4}$$

Experimental Facilities, Techniques, and Analysis Methods

Test conditions Tests at Wallingford used a wave basin 22m long by 19m wide, with a multi-crested absorbing wave maker. Four different angles of wave attack were tested: β = 0°, 15°, 30° and 60° (Figures 1 and 2). Both approach beach and wall were moved in each change of direction. The cross-section of the structure is shown in Figure 3. The 1:10 approach beach led up to the structure toe 0.35m above the basin floor. The vertical wall had a total height from floor to crest of 0.725m. The same cross-section was tested for 30 conditions for each wave obliquity.

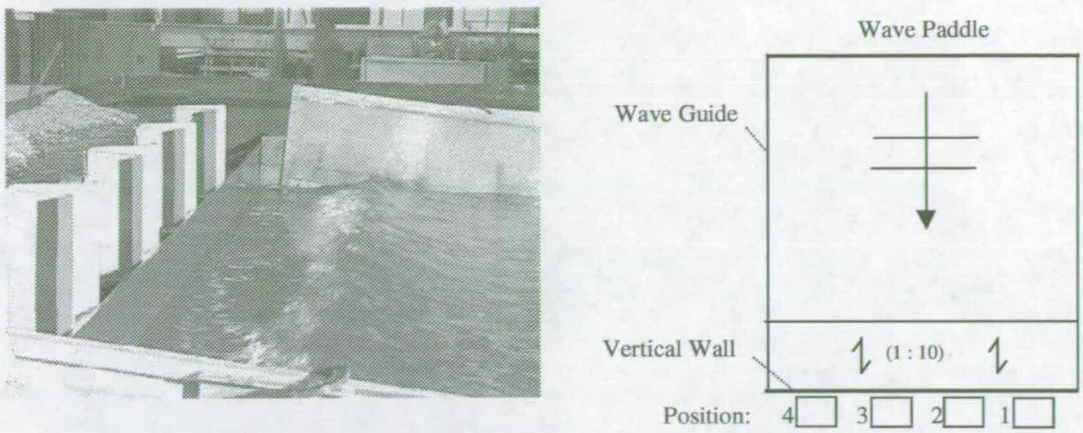

Figure 1: Basin set-up for 0° obliquity.

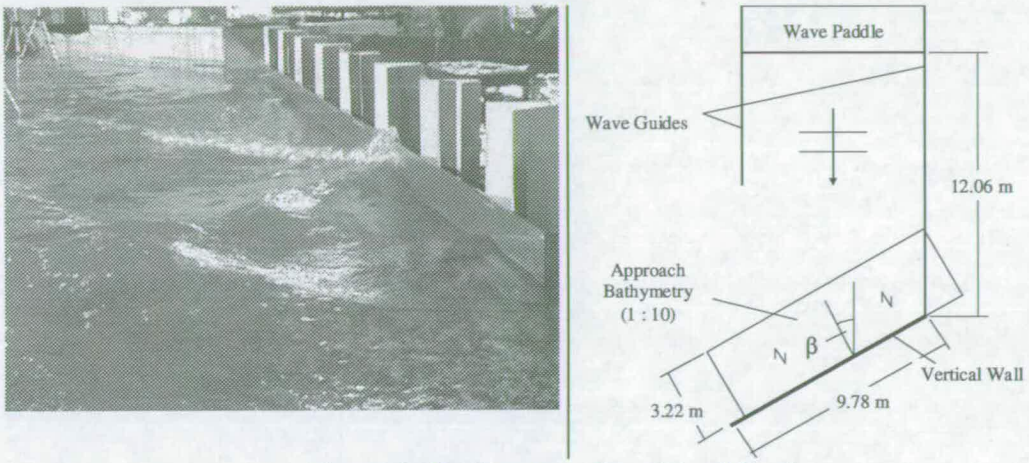

Figure 2: Basin set-up for plain obliquity

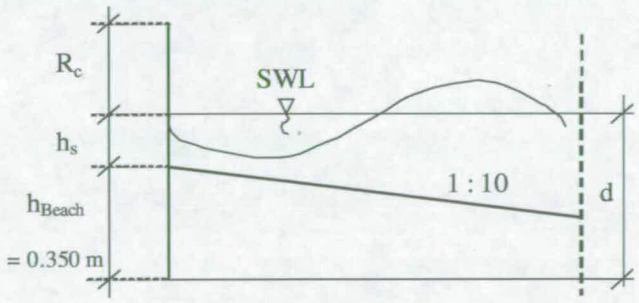

Figure 3: Cross-section of VOWS-3d vertical wall

Table 1: Structures tested

Water depth d (m)	Freeboard R_c (m)	Depth at toe of structure h_s (m)
0.525	0.200	0.175
0.450	0.275	0.100

Table 2: Nominal wave conditions tested

Water depth d (m)	Nominal wave periods T_n (s)	Nominal wave heights H_{si} (m)
0.525	1.2; 1.3; 1.4; 1.5; 1.6	0.06; 0.10; 0.14
0.450	1.2; 1.3; 1.4; 1.5; 1.6	0.06; 0.09; 0.12

Each test consisted of 1000 (approx.) long-crested irregular waves with a JONSWAP spectrum (γ=3.3). Waves at the structure (summarised in Table 2) were determined by calibration tests with the approach beach in place, but without the (reflecting) wall. Wave steepnesses (defined in deep water) fell in the range:

$$0.015 < s_{0P} < 0.065 \qquad (5)$$

The h^*-parameter as an indicator of impulsiveness of the waves gave predictions from highly impulsive to almost entirely reflecting conditions:

$$0.02 < h^* < 0.30 \qquad (6)$$

Overtopping Measurement Equipment

Mean and wave-by-wave overtopping volumes (and hence discharges) were measured at six positions along the test walls, each using a chute into a container hung from a load cell (Figure 4). The load cell output was analysed to give individual overtopping volumes from "steps" in the mass of water. Two metal strips across the chute formed an "event detector", giving a signal for each flow over it.

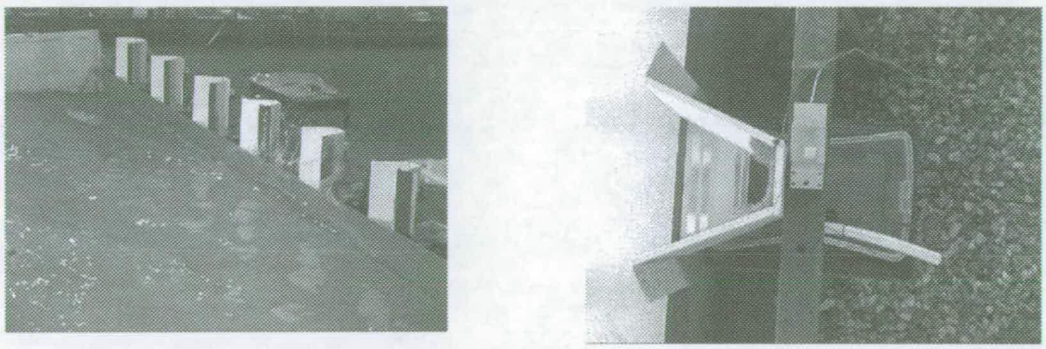

Figure 4: Collection stations: a) along wall and b) plan view (wave from left).

Results – Transition from pulsating to impulsive behaviour

The "mode" of a sea-state (i.e. predominantly reflecting / pulsating or impulsive) has a major influence on the overtopping. Predictions of mean overtopping for β=0° lie between almost "zero" and three orders of magnitude higher for "impacting" conditions than for "reflecting" conditions (Besley, 1999).

At larger obliquities, increasing proportions of waves which would have broken directly onto the wall (impacts) at β=0° start "sliding" along the wall. This behaviour does not give impact events as defined for the 2D case, but for overtopping it leads to similar results (i.e. a power law-type relation). This phenomenon will be called an "impact-like" event in this paper. The "impact-like" event is an intermediate step in the transition from impacting to reflecting events. At

β=0°, waves broke before the structure, impacted onto it, or reflected from it. With increasing obliquity (i.e. β=15° or 30°) impacts change to "impact-like" behaviour and then to reflecting. At β=60° no impacts nor "impact-like" events occurred and all previous impulsive conditions (i.e. at β=0°) gave reflecting / pulsating behaviour.

An example "impact-like" event at β=30° is shown in Figure 5. The same behaviour was observed at 15°. The wave reaches the wall at the far side of the structure (pictures "1" and "2") and at first simply starts reflecting back from the wall. As the wave travels on it builds up in height until the part of the crest, which is just about to reflect from the wall, begins to collapse (break, impact) against the wall covering the little space between wave front and structure (picture "3"). This forms an air pocket which is then compressed. When the forward momentum of the wave is used up the pressure is released suddenly and water is "thrown" upwards.

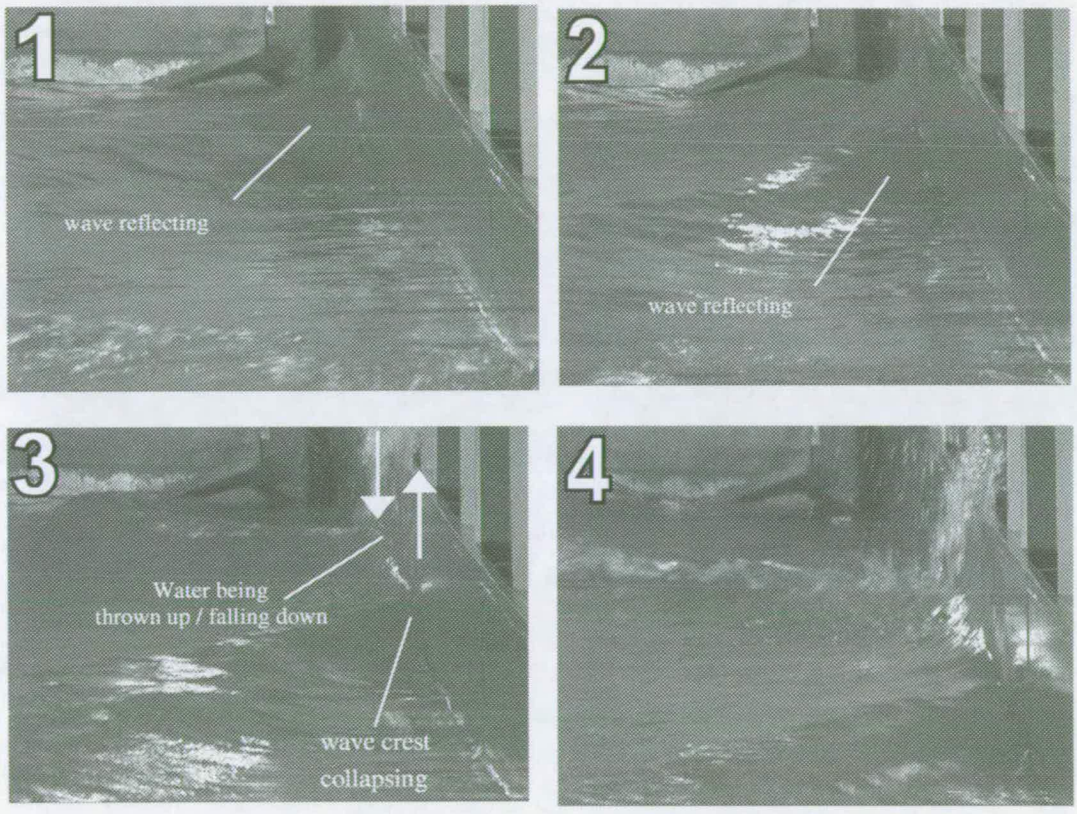

Figure 5: "Impact-like" event at β=30°

This phenomenon is called an "impact-like" event because it is only the crest of the wave that breaks onto the wall and not the whole wave. It is important to note that the wave first appears to be in reflecting mode and then the crest (only) collapses. The wave build-up along the wall triggering the "impact-like" event, however, may not be necessary. This depends on the properties of the incoming wave. The "violence" of an "impact-like" event varies from very low, i.e. only a few drops of water are thrown up, to practically impacting in the classical sense.

This example of an "impact-like" event also explains to some extent spatial variabiations for oblique wave attack (see below). Travelling along the wall, the wave first builds up increasing overtopping until it swaps from reflecting to "impact-like" behaviour. At this point the overtopping increases further. When the wave crest starts to break, however, then the wave loses some height and eventually tumbles down reducing the overtopping significantly. Once stabilised, it starts building anew.

Results – Mean overtopping discharge

Obliquity 0° (Reference Tests)

The reference configuration (β = 0°) is taken as well-tested and is used as an important benchmark for all other configurations. Figure 6 shows measurements of mean discharge for impacting conditions after Besley (1999). The dimensionless discharge Q_h is presented against the dimensionless freeboard R_h.

The solid line represents the prediction line for impacting conditions after Besley (1999) plotted fully over its valid range, whereas the dashed line is the trend-line fitted through the measured data. Only tests with predominantly impacting waves were taken into account ignoring the encircled cluster of points, which could be shown in a video analysis to be in reflecting mode. The dashed trend-line represents the combined trend of all four measurement points. As has been expected, no significant spatial variation along the wall can be seen and the overall trend is very much in line with Besley's prediction.

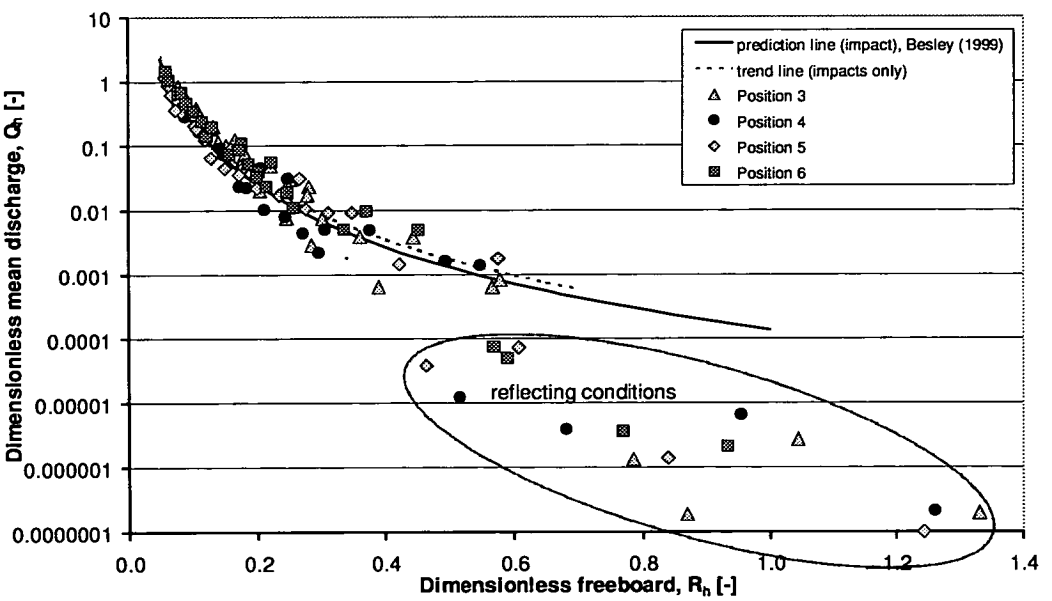

Figure 6: Mean discharge (β = 0°) for impacting conditions after Besley (1999)

Besley (1999) suggests the h* parameter to predict whether the waves of a particular sea-state are predominantly impacting or reflecting (see equation (1)). He draws the line at h* = 0.3: all sea-states with h* $\leq$ 0.3 are predominantly impacting otherwise reflecting. The cluster of points in Figure 6, however, were identified to be in reflecting mode yet giving h* values of 0.14 – 0.30. Other tests, on the other hand, with h* parameters in a similar range were in impacting mode, as shown in Figure 7.

Relative measured to predicted mean discharges are plotted in Figure 7 for the reference test ($\beta = 0°$) against h*. The predictions (based again on Besley, 1999) assumed impacting conditions for all sea-states. All impacting tests are within a factor of "3" of the ideal value ("1.0"), except for one test which is off by a factor of about "5". The reflecting tests are over predicted by 1 to 3 orders of magnitude, underlining the importance of a robust predictor for the breaking regime.

The results in Figure 7 show up limitations of h* as the only predictor for the impulsiveness. Within the range $0.14 \leq h^* \leq 0.21$ impulsive and reflecting tests apparently coexist. This parameter implies that an increase in wave period can compensate in impulsiveness for a reduction in wave height, but this is not confirmed in this study. Indeed, no influence of period on percentage of impacts could be found.

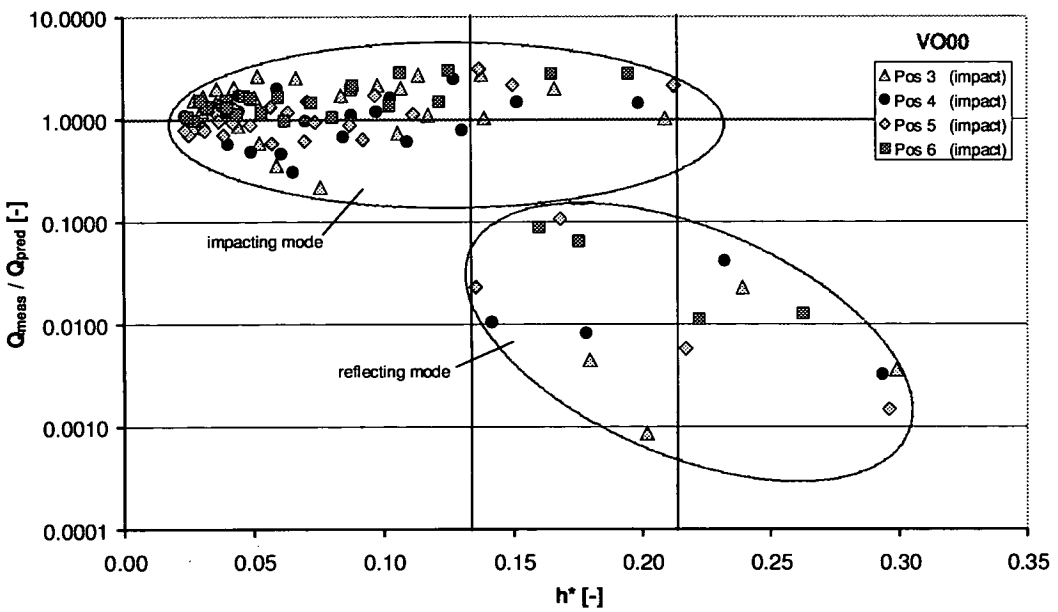

Figure 7: Ratio of measured to predicted mean discharge ($\beta = 0°$) against h*, prediction for impacting conditions after Besley (1999)

The test matrix was designed to study the effect of obliquity on violent wave overtopping and not to reinvestigate 2d prediction tools. The range of sea-states tested might have been too limited to show up the influence of the period ($0.014 < s_{om} < 0.052$). Future work might extend the test matrix towards longer periods (leaving wave heights, etc. constant) to investigate the effect on wave breaking.

The PROVERBS parameter map (Oumeraci et al, 2001) also provides an indicator for the occurrence of wave impacts at plain vertical walls. If the ratio of inshore significant wave height to water depth at the toe of the wall is $H_{si}/h_i < 0.35$ then waves are predicted to be in reflecting otherwise in impacting mode. Figure 8 shows again the ratio of measured to predicted mean discharge for the reference test ($\beta = 0°$) this time plotted against H_{si}/h_i. As before, the prediction assumed impacting conditions for all sea-states and was determined after Besley (1999).

The result is unambiguous: all reflecting tests lie to the left of the threshold ($H_{si}/h_i = 0.35$) and all impacting tests to the right. Thus, the PROVERBS parameter

map seems to give a robust indication whether waves are in impacting mode or not. Generally, it could be shown in this study that the percentage of impacts onto the structure increased with increasing relative wave height (H_{si}/h_i).

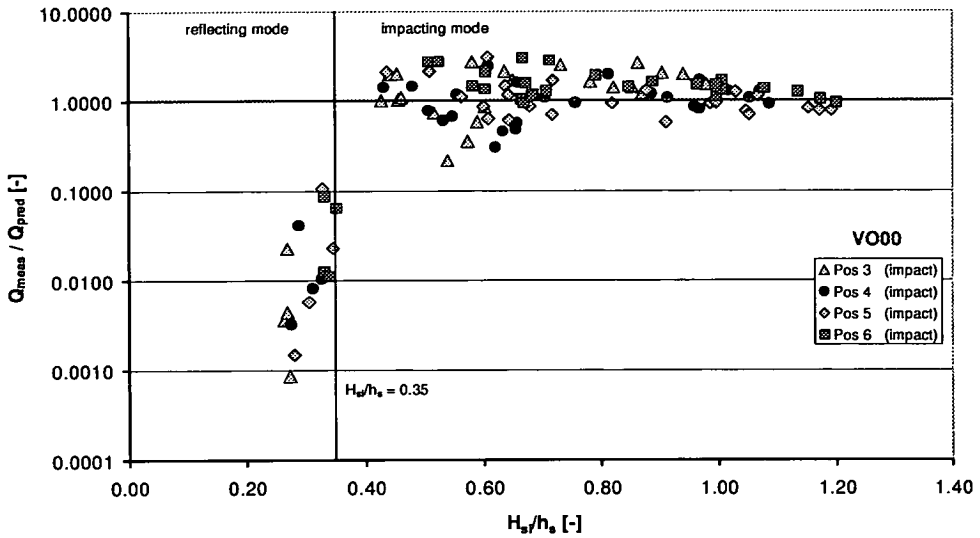

Figure 8: Ratio of measured to predicted mean discharge ($\beta = 0°$) against H_{si}/h_i, prediction for impacting conditions after Besley (1999)

Obliquity 15°

In Figure 9 dimensionless mean discharges for $\beta = 15°$ has been plotted against dimensionless freeboard after Besley (1999) for impacting conditions. The solid black line represents the prediction for normal (2D) wave attack. Three trend lines have been added. The solid line shows the overall trend for all measurement points. The dotted black line gives the trend for position 4 only and the lighter dotted one for position 6. All trend lines were derived with results for impacting conditions only. At 15° obliquity this includes "impact-like" behaviour, defined earlier.

All trend lines have a similar shape as the 2D prediction line (i.e. a power law relationship). There is, however, a noticeable spatial variation between individual positions: the highest dimensionless overtopping could be measured at position 6, the lowest at position 4 with the difference of about a factor of 3.

The spatial variation was very consistent for all tested wave conditions and could also be confirmed qualitatively at 30° obliquity (see next chapter). The exact location of reduced overtopping might vary with the actual length of the seawall and, hence, cannot be predicted with certainty based on this set of studies. Thus, for a conservative design the use of the trend line for position 6 – which is practically identical to the 2D prediction line – should be recommended.

Measured to predicted overtopping (Q_{meas}/Q_{pred}) are compared in Figure 10 against the relative wave height H_{si}/h_i (see also Figure 8). Predictions are based on Besley's (1999) method for impacting conditions and perpendicular (2D) wave attack. The spatial variability of overtopping volumes can be seen even more clearly in this Figure: Overtopping at position 6 appears to be slightly higher than the 2D

prediction, whereas position 4 lies noticeably lower. Position 3 and 5 both gave very similar results in the mid-range slightly lower than the 2D prediction.

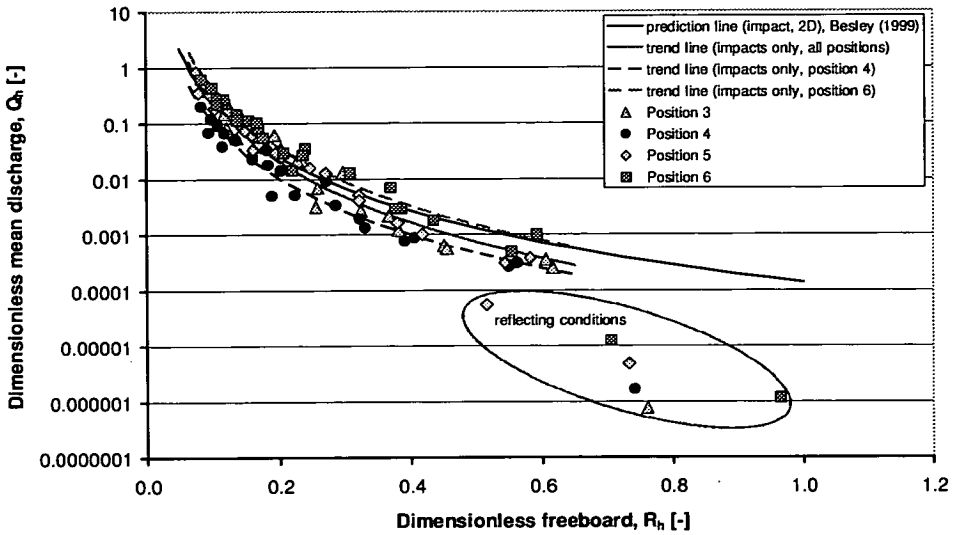

Figure 9: Mean discharge (β = 15°) for impacting conditions after Besley (1999)

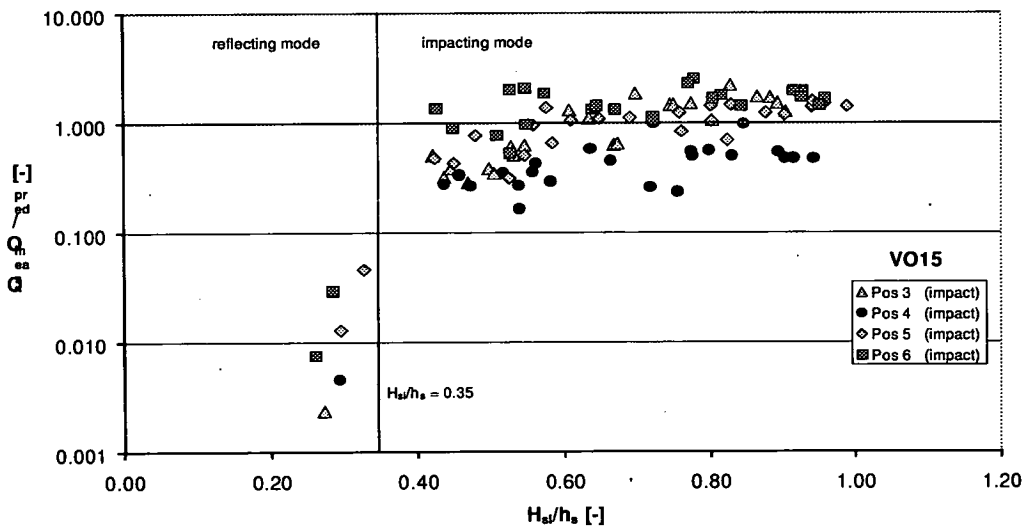

Figure 10: Ratio of measured (β = 15°) to predicted discharge (β = 0°) against H_{si}/h_i

For more impulsive tests with relative wave heights of $H_{si}/h_i > 0.60$ the ratio of Q_{meas}/Q_{pred} appears to be fairly constant for each individual measurement point. Less impulsive tests in the range of $0.35 < H_{si}/h_i < 0.60$, however, appeared to be more effected by the change in the angle of wave attack to 15°, as the ratio of Q_{meas}/Q_{pred} reduced slightly. In this range the percentage of impacts reduced faster and a greater number of tests have changed from impacting to "impact-like" behaviour, reducing also the amount of overtopping. This effect is much more pronounced at 30° obliquity (Figure 12).

Obliquity 30°

As for the other plan geometries the dimensionless mean discharge (β = 30°) has been plotted against the dimensionless freeboard after Besley (1999) for impacting conditions (Figure 11). Again, the solid black line represents the prediction line for perpendicular (2D) wave attack after Besley. Three trend lines have been added. The solid red line shows the overall trend for all measurement points. The dotted black line gives the trend for position 4 only and the dotted pink one for position 6. All trend lines were derived with the results for predominantly impacting test conditions only. The definition of "impacting tests" at an angle of 30° obliquity includes tests which display "impact-like" behaviour as defined in section 0.

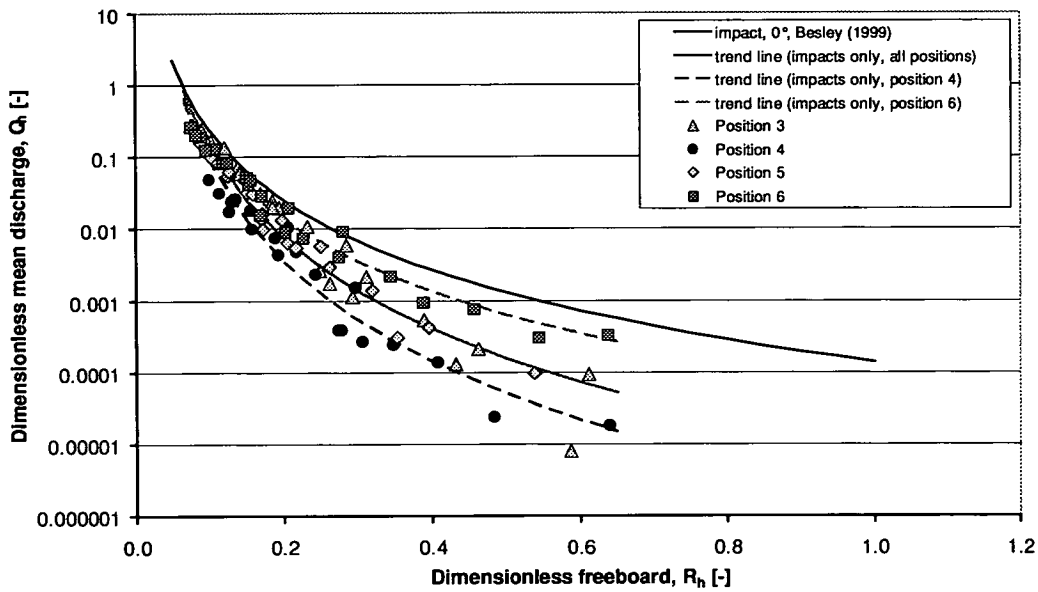

Figure 11: Mean discharge (β = 30°) for impacting conditions after Besley (1999)

All trend lines have again a similar shape as the 2D prediction line (i.e. a power law relationship). As for 15° obliquity there is a noticeable difference between individual positions with overtopping varying by factors of up to 4. The location of reduced overtopping might vary with the actual length of the seawall and, hence, cannot be predicted with certainty based upon these studies. In order to ensure a conservative design the use of the trend line for position 6 should be recommended.

In Figure 12 the ratio of measured to predicted overtopping (Q_{meas}/Q_{pred}) has been plotted against the relative wave height H_{si}/h_i. The prediction is based again on Besley's (1999) method for impacting conditions and normal wave attack. Again, spatial variability of overtopping volumes can be seen clearly.

As for 15° more impulsive tests with relative wave heights of $H_{si}/h_i > 0.60$ showed a fairly constant ratio of Q_{meas}/Q_{pred} for each individual measurement point. Less impulsive tests in the range of $0.35 < H_{si}/h_i < 0.60$, however, appeared to be much more effected by the change in the angle of wave attack to 30°, with greatly reduced ratios of Q_{meas}/Q_{pred}. In this range the percentage of impacts reduced much faster and a greater number of tests have changed from impacting to "impact-like" behaviour, reducing also the amount of overtopping.

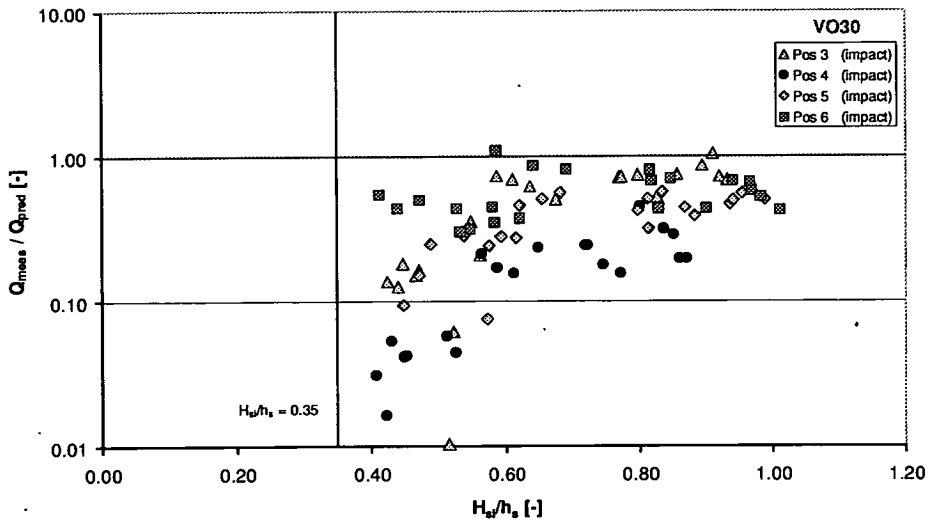

Figure 12: Ratio of measured ($\beta = 30°$) to predicted mean discharge ($\beta = 0°$) against H_{si}/h_i, prediction for impacting conditions after Besley (1999)

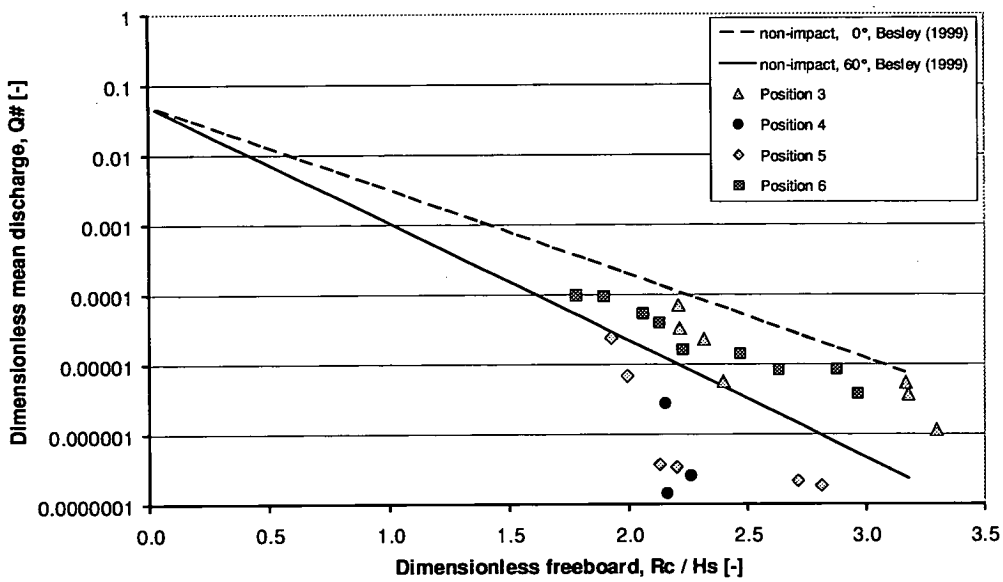

Figure 13: Mean discharge ($\beta = 60°$) for reflecting conditions after Besley (1999)

Obliquity 60°

Figure 13 shows the results for mean overtopping discharge for 60° compared with the non-impulsive method (Besley, 1999). The solid black line represents the prediction line for an angle of wave attack of 60°, whereas the dotted black line indicates the prediction line for the 2D case. Due to the spatial effect mentioned above, positions 4 and 5 give noticeably less overtopping than predicted. Positions 3 and 6, however, appear to lie between the predictions for $\beta = 60°$ and for $\beta = 0°$.

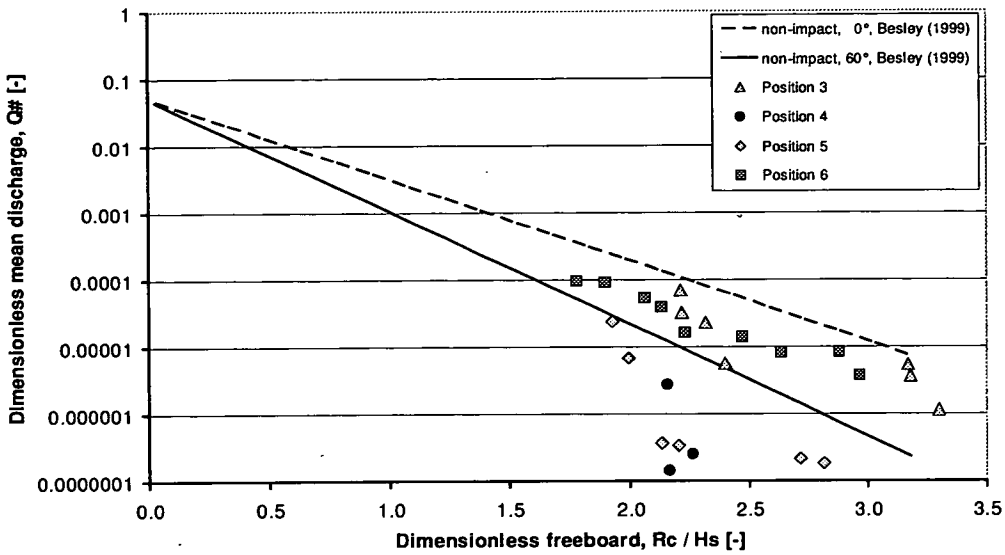

Figure 13: Mean discharge ($\beta = 60°$) for reflecting conditions after Besley (1999)

Conclusions

Impacting events changed first to "impact-like" and then eventually to reflecting events with increasing angel of wave attack. At 60° neither impacts nor "impact-like" events occurred, and all waves broke before, reflected from, or broke along / away from the structure.

A high degree of spatial variation could be measured for all obliquities. The mean overtopping rates varied by factors of up to 4 along the structure. The exact location of the maximum rates could not be determined. In order to ensure a conservative design, the use of the maximum rates is recommended below.

The mean overtopping discharge for the reference test ($\beta = 0°$) was almost identical to Besley's (1999) predictions and no spatial variation could be detected for this structure configuration.

At 15° the mean discharges along the wall were slightly reduced, but the maximum measured overtopping rates were again nearly identical to Besley's (1999) predictions. No reduction is recommended for this angle of wave attack.

At 30° the mean discharge was reduced significantly, but again the peak rates were much higher and allow only for a relatively small reduction for the recommended prediction to

$$Q_h = 0.61 \times 10^{-4} \frac{1}{R_h^{3.35}}$$

At 60° no wave impacts could be measured. Besley's (1999) prediction for reflecting conditions at 60° seems to slightly under predict the previously (at 0°) violent test conditions. Thus, the use of Besley's (1999) prediction for reflecting conditions at 0° is recommended.

Acknowledgements

This work was funded by EPSRC (GR/M42312, GR/R42306), and supported by the VOWS Management Committee including members from Manchester Metropolitan University (Derek Causon, David Ingram, Clive Mingham), HR Wallingford (Philip Besley), Posford-Haskoning (Dick Thomas), Bullen & Co, whose support is gratefully acknowledged. The VOWS project particularly acknowledges helpful supervision from the EPSRC CEWE Project Manager, Michael Owen.

The physical modelling was substantially assisted by sharing facilities, measurement devices and related resources funded by DEFRA / EA research projects FD 2410 & FD2412 (SHADOW Phase I & II). Further work on hazards arising from overtopping, including field measurements of overtopping at its effects, is conducted under the EU CLASH project (contract EVK3-2001-0058).

References

Allsop, N.W.H. & Calabrese, M. (1999a). "Impact loadings on vertical walls in directional seas." *Proc. 26th Int. Conf. on Coastal Eng.*, pp 2056 - 2068, ISBN 0-7844-0411-9, ASCE.

Allsop, N.W.H. & Calabrese, M. (1999b). "Forces on vertical breakwaters: effects of oblique or short-crested waves.", *Research Report SR465*, HR Wallingford.

Allsop, N.W.H., Vicinanza, D. & McKenna, J.E. (1996). "Wave forces on vertical and composite breakwaters." *Research Report SR 443*, pp 1-94, HR Wallingford.

Allsop, N.W.H., Kortenhaus, A., Oumeraci, H. & McConnell, K.J. (2000). "New design methods for wave loadings on vertical breakwaters under pulsating and impact conditions." *Proc. Coastal Structures '99*, Santander, pp 595-602, ISBN 90 5809 092 2, publn. Balkema, Rotterdam.

Besley, P. (1999). *Overtopping of seawalls – design and assessment manual.* R & D Technical Report W 178, ISBN 1 85705 069 X, Environment Agency, Bristol.

Besley, P., Stewart, T. & Allsop, N.W.H. (1998). "Overtopping of vertical structures: new methods to account for shallow water conditions." *Proc. Int. Conf. on Coastlines, Structures & Breakwaters '98*, ICE, pp46-57, publn. Thomas Telford, London.

Bruce, T., Allsop, N.W.H. & Pearson, J. (2001). "Violent overtopping of seawalls – extended prediction methods." *Proc. Int. Conf. on "Coastlines, Seawalls and Breakwaters '01"* ICE, publn Thomas Telford, London.

Daemrich, K. F. & Mathias, H. J. (1999). "Overtopping at vertical walls with oblique wave approach." *Proc. Conf. COPEDEC V*, Cape Town, pp 1294-1301, publn. COPEDEC, Sri Lanka.

de Waal J.P. & van der Meer J.W. (1992). "Wave runup and overtopping on coastal structures." *Proc.23rd ICCE*, Venice, pp 1758-1771, ASCE.

Franco, C., Franco, L., Restano, C. & van der Meer, J.W. (1995). "The effect of wave obliquity and short-crestedness on the overtopping rate and volume distribution on caisson breakwaters." *MAST II-MCS Project Final Proceedings*, University of Hannover.

Juhl, J. & Sloth, P. (1994). "Wave overtopping of breakwaters under oblique waves." *Proc. 24th ICCE*, Kobe, Japan, pp 1182-1196, ASCE.

Owen, M.W. (1980). *Design of sea walls allowing for wave overtopping.* Report EX 924, HR Wallingford.

Pearson, J., Bruce, T., Allsop, N.W.H. & Gironella, X. (2002). "Violent wave overtopping – measurements at large and small scale." *Proc. Int. Conf. on Coastal Eng. 2002*, ASCE.

Tautenhain, E., Kohlhase, S. & Partenscky, H-W. (1982). "Wave run-up at sea dikes under oblique wave approach." *Proc. 18th ICCE*, Cape Town, pp. 804-810, ASCE.

Appendix O: Napp *et al.*, 2004

Napp, N., Bruce, T., Pearson, J. & Allsop, N.W.H. (2004), *Violent overtopping of vertical seawalls under oblique wave conditions*, Proc. 29th Int. Conf. Coastal Engineering, 4, pp 4482–4493, ASCE / World Scientific, Singapore, ISBN 981-256-298-2

Appendix O: Napp *et al.*, 2004

Napp, N., Bruce, T., Pearson, J. & Allsop, N.W.H. (2004), *Violent overtopping of vertical seawalls under oblique wave conditions*, Proc. 29th Int. Conf. Coastal Engineering, 4, pp 4482–4493, ASCE / World Scientific, Singapore, ISBN 981-256-298-2

Appendix O
Napp *et al.*, 2004

Napp, N., Bruce, T., Pearson, J. & Allsop, N.W.H. (2004), *Violent overtopping of vertical seawalls under oblique wave conditions*, Proc. 29th Int. Conf. Coastal Engineering, 4, pp 4482–4493, ASCE / World Scientific, Singapore, ISBN 981-256-298-2

O.1 Declaration of contribution

The author was Napp's principal supervisor throughout Napp's PhD studies. The author's contribution has therefore been one of training and close supervision throughout. In particular, it was in these discussions, cross-referencing data and video records, that the author and Napp began to gain the understanding of the changing nature of overtopping processes with increasing wave obliquities - the basis of the synthesised guidance offered in the conclusions.

O.2 Published paper

overleaf

VIOLENT OVERTOPPING OF VERTICAL SEAWALLS UNDER OBLIQUE WAVE CONDITIONS

NICOLAS NAPP, TOM BRUCE AND JONATHAN PEARSON

School of Engineering & Electronics, University of Edinburgh, King's Buildings, Edinburgh, EH9 3JL, UK, e-mail: nicolas.napp@ed.ac.uk

WILLIAM ALLSOP

Visiting Professor, University of Southampton;
Technical Director, Maritime Structures, HR Wallingford

Most prediction methods for wave overtopping are based on physical model tests under simple 2-D conditions. This paper describes final results of a physical model study measuring mean and wave-by-wave overtopping discharges over a vertical seawall under impulsive and oblique long-crested wave attack. The design guidance offered for these conditions shows that a significant reduction in overtopping can only be expected for obliquities > 30°. With increasing obliquity, impulsive events transform to "impact-like" events ($0° < \beta \leq 30°$) and then eventually to reflecting (non-breaking) waves (60°). Spatial variability of overtopping volumes along the seawall could be measured and was considered in the design guidance.

1. Introduction

Seawalls and breakwaters seldom align perfectly with incoming waves, but many prediction methods for wave overtopping are only valid for shore-normal wave attack. In particular, there is limited guidance available for either mean or wave-by-wave overtopping discharges over vertical seawalls subject to oblique and impulsive wave attack. Impulsive wave attack (i.e. waves break onto the structure) may lead to substantially higher overtopping volumes than pulsating (reflecting) wave attack and can arise at relatively low water levels.

Mean and wave-by-wave overtopping discharges represent important quantities in the design of coastal structures. They not only affect the structural safety and determine the capacity of the drainage system behind the structure, but also pose a hazard to communications, buildings, and members of the public.

This paper describes experiments and analysis to provide design guidance in wave overtopping of vertical seawalls under oblique and impulsive wave attack. The guidance extends existing design tools for wave overtopping which cover both wave conditions (reflecting and impulsive) under shore-normal wave attack, but only reflecting conditions under oblique wave attack.

Special attention is given to the transition from impulsive to reflecting wave conditions, which give significant reductions in overtopping towards higher obliquities. For moderate obliquities (15° and 30°) a new intermediate wave condition is defined as the "impact-like" condition, which – in terms of overtopping – has still to be treated as impulsive. Contrary to a few previous investigations on sloping walls, no increase in overtopping could be found at small obliquities (15°). Spatial variability, however, could be measured along the seawall and has been considered in the design guidance offered in this paper.

2. Existing Guidance

This physical model study was undertaken to derive design guidance for impulsive mean and wave-by-wave overtopping of a vertical seawall under oblique wave conditions. This includes the investigation of any possible increase in overtopping at small obliquities and the existence of any spatial variability, about which no reports and guidance on spatial variability along vertical seawalls could be found in literature.

The few studies in literature investigating vertical seawalls and sloped structures under long and short crested, regular and irregular wave attack give contradictory advice as to whether oblique attack may increase overtopping at small obliquities. Tautenhain et al. (1982), Owen (1980), Juhl and Sloth (1994) and de Waal and van der Meer (1992) found a small increase of up to 10% in overtopping for few test conditions, whereas Franco et al. (1994) and Daemrich and Mathias (1999) only found reductions.

Design guidance for mean overtopping of vertical seawalls has been offered by Goda (1971) in the form of design diagrams. Although these diagrams cover impulsive overtopping the range of wave steepnesses and relative freeboards does not cover all typical situations along the North Sea coastline. Other studies focused either solely on deepwater wave attack (Ahrens and Heimbaugh, 1988; and Franco et al., 1994) or on regular waves (Mizuguchi, 1993).

The UK Environment Agency manual (EA manual, 1999) summarises results which include investigations by Allsop et al. (1995) and Besley *et al.* (1998), who investigated the overtopping characteristics on vertical walls. It gives guidance on mean and wave-by-wave overtopping of seawalls under perpendicular (2D) wave attack. An important feature is the distinction between waves in reflecting or impacting mode using a so-called "h*" parameter. The EA manual then offers two different sets of formulae for each wave mode, thus covering impacting waves in relatively shallow water. Guidance for oblique wave attack, however, is only offered if the waves are in deeper water and thus in reflecting mode.

3. Experimental Facilities, Techniques, and Analysis Methods

3.1. *Test conditions*

Tests at HR Wallingford used a wave basin 22m long by 19m wide, with a multi-crested absorbing wave maker. Four different angles of wave attack were tested: $\beta = 0°$, 15°, 30° and 60° (Figure 1). Both approach beach and wall were moved in each change of direction. The 1:10 approach beach led up to the structure toe 0.35m above the basin floor. The vertical wall had a total height from floor to crest of 0.725m. The same cross-section was tested for 30 conditions for each wave obliquity.

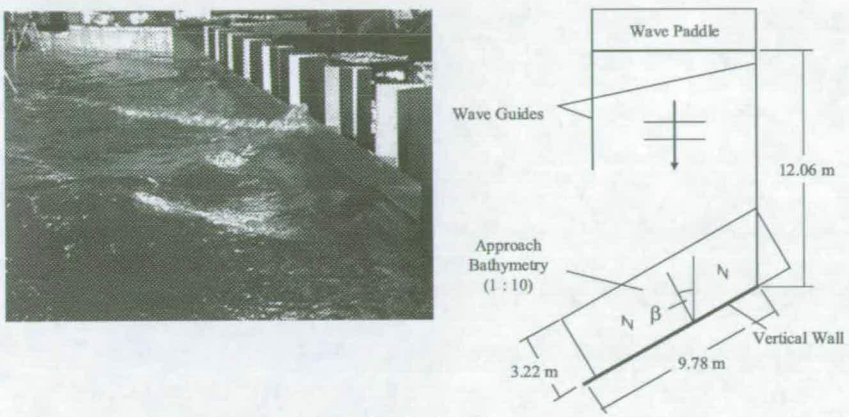

Figure 1: Example basin set-up for plain obliquity, $\beta = 30°$.

Table 1 gives an overview of the water depths and freeboards tested and Table 2 shows the nominal wave conditions.

Table 1. Structures tested.

Water depth d (m)	Freeboard Rc (m)	Depth at toe of structure
0.525	0.200	0.175
0.450	0.275	0.100

Table 2. Nominal wave conditions tested.

Water depth d (m)	Nominal wave periods T_p (s)	Nominal wave heights H_{si} (m)
0.525	1.2; 1.3; 1.4; 1.5; 1.6	0.06; 0.10; 0.14
0.450	1.2; 1.3; 1.4; 1.5; 1.6	0.06; 0.09; 0.12

Each test consisted of 1000 (approx.) long-crested irregular waves with a JONSWAP spectrum (γ=3.3). Waves at the structure (summarised in Table 2)

were determined by calibration tests with the approach beach in place, but without the (reflecting) wall. Wave steepnesses (defined in deep water) fell in the range:

$$0.015 < s_{0P} < 0.065 \tag{1}$$

The h^*-parameter as an indicator of impulsiveness of the waves gave predictions from highly impulsive to almost entirely reflecting conditions:

$$0.02 < h^* < 0.30 \tag{2}$$

3.2. *Overtopping Measurement Equipment*

Mean and wave-by-wave overtopping volumes (and hence discharges) were measured at four positions along the test walls, each using a chute into a container hung from a load cell (see also Figure 1). The load cell output was analysed to give individual overtopping volumes from "steps" in the mass of water. Two metal strips across the chute formed an "event detector", giving a signal for each flow over it.

4. Impulsive Wave – Structure Interactions

The "mode" of a sea-state (i.e. predominantly reflecting / pulsating or impulsive / impacting) has a major influence on the overtopping. Predictions of mean overtopping for $\beta=0°$ lie between almost "zero" and three orders of magnitude higher for "impacting" conditions than for "reflecting" conditions (EA manual, 1999).

At larger obliquities, increasing proportions of waves which would have broken directly onto the wall (impacts) at $\beta=0°$ start "sliding" along the wall. A closer look at this "sliding" reveals that it is actually the wave crest that collapses (breaks, impacts) against the wall covering the little space between wave front and structure. As for classical 2D wave impacts this forms an air pocket which is then compressed. When the forward momentum of the wave is used up the pressure is released suddenly and water is thrown upwards.

These events are less violent than classical impacts as defined for the 2D case, but for overtopping they lead to similar results (i.e. a power law-type relation as opposed to the exponential relation for reflecting conditions). This phenomenon has been named an "impact-like" event by the authors. The "impact-like" event is an intermediate step in the transition from impacting to reflecting events. At $\beta=0°$, waves broke before the structure, impacted onto it, or reflected from it. With increasing obliquity (i.e. $\beta=15°$ or $30°$) impacts change to "impact-like" behaviour and then to reflecting. At $\beta=60°$ neither impacts nor

"impact-like" events occurred. Waves broke either clear of the structure or broke along the wall neither entrapping nor compressing pockets of air.

Due to the length restriction of this paper a more detailed discussion of the "impact-like" event and its differentiation from a classical 2D impact has to be deferred but will be offered in the next publication. This will include series of pictures taken from the physical model studies. As will then also be discussed the "impact-like" behaviour can to some extent explain the spatial variability of overtopping volumes measured along the wall (see next sections).

5. Mean Overtopping Discharge

The reference configuration ($\beta = 0°$) is taken as well-validated and is used as an important benchmark for all other configurations. Figure 2 shows measurements of mean discharge for impacting conditions after the EA manual (1999). The dimensionless discharge Q_h is presented against the dimensionless freeboard R_h (see section 7 for explanation of non-dimensional freeboard R_h and discharge Q_h).

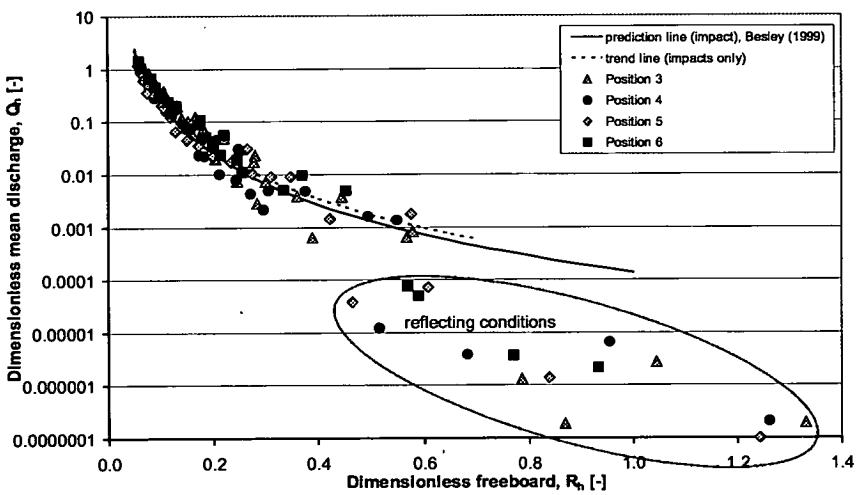

Figure 2. Mean discharge ($\beta = 0°$) for impacting conditions after the EA manual (1999)

The solid line represents the prediction line for impacting conditions after the EA manual (1999) plotted fully over its valid range, whereas the dashed line is the trend-line fitted through the measured data. Only tests with predominantly impacting waves were taken into account ignoring the encircled cluster of points, which could be shown in a video analysis to be in reflecting mode. The dashed trend-line represents the combined trend of all four measurement points.

As expected, no significant spatial variation along the wall can be seen and the overall trend is very much in line with the EA manual's prediction.

The results for the tests of $\beta = 15°$ and 30° are very similar qualitatively. In Figure 3 the dimensionless mean discharge measured at $\beta = 30°$ has been plotted against the dimensionless freeboard after the EA manual (1999) for impacting conditions. Again, the solid black line represents the prediction line for perpendicular (2D) wave attack after the EA manual. Three trend lines have been added. The solid line between the two dotted lines shows the overall trend for all measurement points. The lower dotted black line gives the trend for position 4 only and the upper dotted line for position 6. All trend lines were derived with the results for predominantly impacting test conditions only. This includes tests in "impact-like" mode as defined in the previous chapter.

All trend lines have again a similar shape as the 2D prediction line (i.e. a power law relationship). For 15° and 30° obliquity, however, there is a noticeable difference between individual positions with overtopping varying by factors of up to 4. The location of reduced overtopping might vary with the actual length of the seawall and, hence, cannot be predicted with any degree of certainty in this study. In order to ensure a conservative design, two design formulae are suggested: one giving the mean value over all measurement positions and the other giving the conservative results for the highest measured discharges.

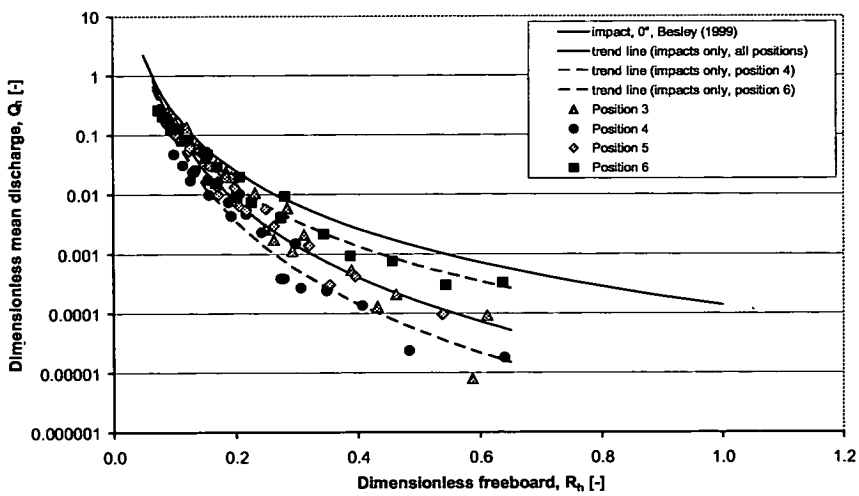

Figure 3. Mean discharge ($\beta = 30°$) for impacting conditions after the EA manual (1999)

No wave impact could be observed for 60° obliquity, thus no plot for impulsive conditions is presented.

Design guidance for oblique wave attack under impulsive conditions is given in chapter 7. The recommendations also take account of the spatial variability measured along the seawall.

6. Individual Overtopping Discharge

The EA manual (1999) offers design guidance for V_{max} based on the Weibull distribution of individual overtopping events. Figure 4 shows the result of this prediction method for the measurements taken for the reference configuration (0° obliquity). The ratio of measured to predicted maximum overtopping events has been plotted against the relative wave height H_{si}/h_s separating reflecting from impacting conditions. Tests with $H_{si}/h_s < 0.35$ could be shown to be in reflecting mode, whereas all tests with $H_{si}/h_s > 035$ were in impacting mode (PROVERBS parameter map, Oumeraci et al., 2001). As can be seen the design guidance after the EA manual (1999) gives a robust prediction of maximum individual overtopping events and the scatter involved is not significantly larger than for the prediction of the mean discharge Q.

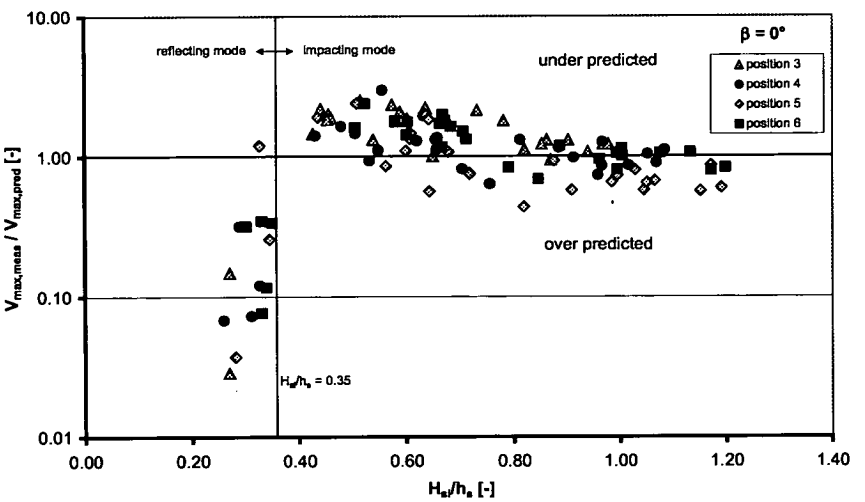

Figure 4. Ratio of measured to predicted maximum discharges (β = 0°) after EA manual (1999)

In the case of oblique wave attack (i.e. 15° and 30° obliquity) new Weibull "a" and "b" parameters have been derived. Furthermore, the spatial distribution of overtopping events also affects peak discharges and must be accounted for.

As the exact location of high and low discharges along the seawall cannot be predicted a "worst case" approach using the highest measured discharges is recommended (see section 7). Figure 5 shows good agreement for position 6 which gave the highest discharges and all other positions were predicted on the safe side.

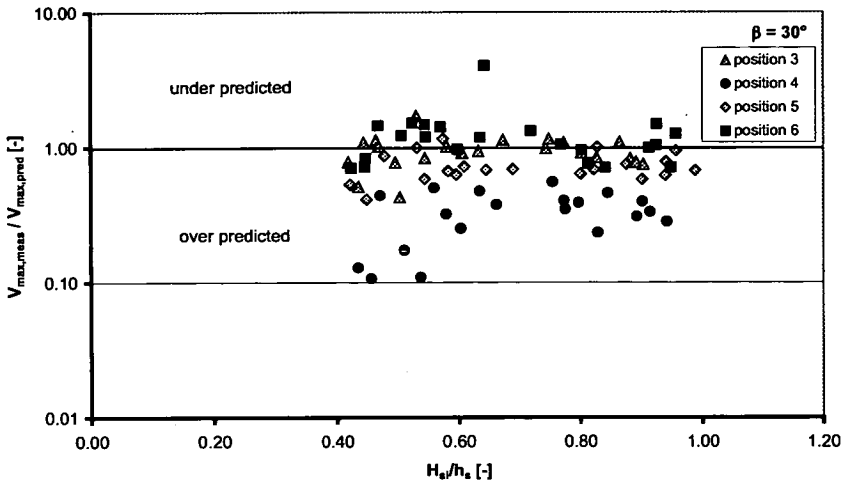

Figure 5: Ratio of measured to predicted maximum discharges (β = 30°) after EA manual (1999)

7. Implications for design

7.1. *Mode of the Waves*

The design guidance for oblique wave attack under impulsive conditions offered in this paper is essentially an extension to the EA manual (1999). The first step in a design of a plain vertical seawall is to establish whether the waves at the toe of the structure are predominantly in reflecting or impacting mode. At this point the angle of wave attack has no influence, unless it is 60° or larger (see below). The EA manual (1999) suggests here the h* parameter:

$$h^* \equiv \left(\frac{h}{H_s}\right)\left(\frac{2\pi h}{gT_m^2}\right) \tag{3}$$

The notations and symbols are used in the usual way. If $h^* > 0.3$ then reflecting waves predominate, otherwise if $h^* \leq 0.3$ then impacting waves predominate. Some test conditions in this study were not correctly classified by

the h* parameter. As the distinction between reflecting and impacting conditions is vital to the design, another criterion offered by the PROVERBS project (Oumeraci et al., 2001) is introduced. Reflecting waves predominate if $H_{si}/h_s <$ 0.35, otherwise it is impacting waves. In this study this criterion led to a clear distinction between modes.

It should be noted that these criteria are guidelines only and it is recommended to test wave conditions against both. In order to ensure a conservative design it is suggested to assume impacting conditions if either criterion indicates that such conditions could exist.

The h* and the H_{si}/h_s criteria were strictly speaking derived for perpendicular wave attack. In the case of wave overtopping the increasing number of "impact-like" events at larger obliquities of up to 30° must be treated as wave impacts. Thus, once waves are established to be in impacting mode for perpendicular wave attack, they must be treated as impacting up to 30° obliquity.

If waves are in reflecting condition then the appropriate formulae presented in the EA manual (1999) are recommended. Guidelines for impulsive conditions are given below. In the case of perpendicular wave attack they are identical to the EA manual (1999).

7.2. *Mean Overtopping Discharge*

The design guidance for mean overtopping of vertical seawalls under impulsive perpendicular (2D) wave attack as offered by the EA manual (1999) has been validated in this study. This guidance is now extended to oblique wave attack. In order to take account of the spatial variability of overtopping volumes along the wall two sets of formulae are offered:

The first one does not consider spatial variations and the best fit formulae for all measurement positions are given. In practical designs this can be useful if the evaluation of flood risk is the driving force. The second one considers the spatial variations as a worst case. As the position of maximum overtopping cannot be predicted, the formulae for the second approach have been derived from the measurement point with the highest overtopping. This can be useful for a conservative design or for the evaluation of overtopping hazards if the methods are based on mean rather than individual peak discharges.

Once the mode of the waves has been established as impulsive, the following formulae are suggested:

The dimensionless discharge Q_h and freeboard R_h are given by:

$$Q_h = \frac{Q}{(gh^3)^{0.5}\ h^{*2}} \qquad R_h = \frac{R_c}{H_s}\ h^* \qquad (4), (5)$$

The final results are summarised in Table 3.

Table 3. Summary of prediction formulae for mean discharge.

	0°	15°	30°	60°
1. mean	$Q_h = 0.000137\ R_h^{-3.24}$	$Q_h = 0.000058\ R_h^{-3.66}$	$Q_h = 0.000008\ R_h^{-4.22}$	EA manual(1999) refl. cond. 60°
2. worst case	as per 1st approach and 0° obliquity	as per 1st approach and 0° obliquity	as per 1st approach and 15° obliquity	EA manual(1999) refl. cond. 0°

7.3. *Individual Overtopping Discharge*

As for the mean discharge the design guidance offered by the EA manual (1999) has been validated for the 2D case and is now extended to oblique wave attack.

The spatial variability of overtopping volumes also affects the peak individual overtopping discharges. There are no tools available to determine the exact location of peak discharges and, in order to ensure a conservative prediction of maximum discharges, the worst case approach is recommended. Thus, the tools presented in this section are based on the highest measurements along the seawall.

The basic formulae for V_{max} and V_{bar} are given as follows:

$$V_{max} = a\left(\ln(N_{ow})\right)^{1/b} \qquad V_{bar} = Q_h\ T_m\ N_w / N_{ow} \qquad (6), (7)$$

The dimensionless discharge Q_h and freeboard R_h are given in equation (2). Table 4 summarises the input parameters:

Table 4. Input parameters for V_{max}.

	Q_h	N_{ow}/N_w	a	b
0°	$0.000137\ R_h^{-3.24}$	$0.031\ R_h^{-0.99}$	$0.92\ V_{bar}$	0.85
15°	$0.000137\ R_h^{-3.24}$	$0.010\ R_h^{-1.58}$	$1.06\ V_{bar}$	1.18
30°	$0.000058\ R_h^{-3.66}$	$0.010\ R_h^{-1.40}$	$1.04\ V_{bar}$	1.27
60°	all tests in reflecting mode – use EA manual (1999)			

8. Conclusions

The design guidance for mean overtopping of vertical seawalls under impulsive perpendicular (2D) wave attack as offered by the EA manual (1999) could be validated in this study.

This guidance has been extended to oblique wave attack in this paper with formulae offered for mean and wave-by-wave discharges.

A new form of impulsive wave-structure interaction called "impact-like" behaviour has been introduced for oblique wave attack of up to 30°.

Neither wave impacts nor "impact-like" events could be observed at 60° obliquity.

Spatial variability of overtopping volumes along the seawall could be measured for all obliquities and has been accounted for in the extended design guidance.

No increase in overtopping could be found for small angles of wave attack

Acknowledgments

This work was funded by EPSRC (GR/M42312, GR/R42306), and supported by the VOWS Management Committee including members from Manchester Metropolitan University (Derek Causon, David Ingram, Clive Mingham), HR Wallingford (Philip Besley), Posford-Haskoning (Dick Thomas), Bullen & Co, whose support is gratefully acknowledged. The VOWS project particularly acknowledges helpful supervision from the EPSRC CEWE Project Manager, Michael Owen. The support of Tim Pullen (HR Wallingford) and Ibrahim Bay (University of Liverpool) during the testing phase at HR Wallingford is greatly acknowledged.

References

Ahrens, J.P., and M.S. Heimbaugh. 1988. Seawall Overtopping Model, Proc. 21st Int. Conf. on Coastal Eng., Malaga, pp.795-806.

Allsop, N.W.H., P. Besley, and L. Madurini. 1995. Overtopping performance of vertical and composite breakwaters, seawalls and low reflection alternatives, Paper 4.7 in MCS Final Report, publn University of Hannover.

Besley, P., T. Stewart, and W. Allsop. 1998. Overtopping of vertical structures: new methods to account for shallow water conditions, Proc. Int. Conf. on Coastlines, Structures & Breakwaters '98, ICE, pp46-57, publn. Thomas Telford, London.

Daemrich, K. F. and H.J. Mathias. 1999. Overtopping at vertical walls with oblique wave approach, Proc. Conf. COPEDEC V, Cape Town, pp 1294-1301, publn. COPEDEC, Sri Lanka.

De Waal J.P. and J.W. van der Meer. 1992. Wave Runup and Overtopping on Coastal Structures, Proc.23rd ICCE, Venice, pp 1758-1771, ASCE.

EA manual. 1999. Overtopping of seawalls – design and assessment manual, R & D Technical Report W 178, ISBN 1 85705 069 X, Environment Agency, Bristol.

Franco L., M. de Gerloni, and J.W. van der Meer. 1994. Wave overtopping on vertical and composite breakwaters, Proceedings 24th ICCE, Kobe, pp 1030-1045, ASCE, New York.

Goda Y. 1971. Expected rate of irregular wave overtopping of seawalls, Coastal Engineering in Japan, Vol 14, pp 45-51, JSCE, Tokyo.

Juhl J. and P. Sloth. 1994. Wave Overtopping of Breakwaters under Oblique Waves, Proc. 24th Int. Conf. Coastal Eng., 1994, Kobe, Japan, pp 1182-1196, publn. ASCE, New York.

Mizuguchi M. 1993. Wave overtopping rate over a vertical wall and reflection coefficient, Coastal Eng. in Japan, Vol. 36, No.1, pp.37-47.

Oumeraci H., A. Kortenhaus, W. Allsop, M. de Groot, R. Crouch, H. Vrijling, and H. Voortman. 2001. Probabilistic design tools for vertical breakwaters, Proverbs workshop, ISBN 90 5809 249 6.

Owen, M.W. 1980. Design of sea walls allowing for wave overtopping, Report EX 924, HR Wallingford.

Tautenhain E., S. Kohlhase, and H.W. Partenscky. 1982, Wave runup at sea dikes under oblique wave approach, Proc. 18th ICCE, ASCE, Cape Town, South Africa, no. 18, Volume I, pp. 804-810, publn. ASCE, New York.

Tsuruta S. and Y. Goda. 1968. Expected Discharge of Irregular Wave Overtopping, Proc. Int. Conf. Coastal Eng., 1968, pp 833-852, publn. ASCE, New York.

Appendix P: Pearson *et al.*, 2002

Pearson, J., Bruce, T., Allsop, N.W.H. & Gironella, X. (2002), *Violent wave overtopping – measurements at large and small scale*, Proc. 28th Int. Conf. Coastal Engineering, 2, pp 2227–2238, ASCE / World Scientific, Singapore, ISBN 981 238 238 0

Appendix P
Pearson *et al.*, 2002

Pearson, J., Bruce, T., Allsop, N.W.H. & Gironella, X. (2002), *Violent wave overtopping – measurements at large and small scale*, Proc. 28th Int. Conf. Coastal Engineering, 2, pp 2227–2238, ASCE / World Scientific, Singapore, ISBN 981 238 238 0

P.1 Declaration of contribution

The author was very closely involved with the *Big-VOWS* project right from the submission of the initial Expression of Interest, through project scoping meetings, to detailed specification of structure and wave conditions on site. The "throw trajectory detector" was developed from an idea of the author's. The author was in Barcelona for the first two weeks of the experimental programme there. During this time he spend very many hours working on detailed design of test conditions, both with Pearson and with the local support team. The tests and raw data analysis were carried out by Pearson (the project's post-doctoral Research Engineer), ably supported by the local team. The paper was drafted by Pearson with detailed support, input and editing from the author.

P.2 Published paper

overleaf

VIOLENT WAVE OVERTOPPING – MEASUREMENTS AT LARGE AND SMALL SCALE

Jonathan Pearson[1], Tom Bruce[2], William Allsop[3] and Xavier Gironella[4]

Abstract: It has often been suggested that wave overtopping processes measured in physical models may include scale effects which could influence the reliability of any predictions to full scale. This paper describes studies at small- and large-scale under the VOWS (Violent Overtopping of Waves at Seawalls) collaborative research project, and presents detailed results on overtopping performance of 10:1 battered seawalls, at small- and large-scale. These results can be used to predict mean overtopping discharges and wave-by-wave overtopping volumes. Overtopping measurements are compared with predictions for vertical walls. Results quantify mean overtopping rates and characterise the uncertainties of scale effects in overtopping measurements. Within experimental limitations, the results show no significant difference in small and large scale overtopping, demonstrating that guidance from small-scale studies can be used with confidence to predict overtopping in prototype situations.

1. INTRODUCTION

In most developed coastal areas, seawalls protect towns, road, rail and rural infrastructure against wave overtopping. Similar structures protect port installations worldwide, and may be used for cliff protection. Design methods for seawalls primarily focus on predicting (and limiting) the volume of overtopping over a sample period, and methods for breakwaters focus on reducing waves in the harbour. Those prediction methods are however substantially based on the results of small-scale physical model tests which have been scaled directly up to prototype without correction for possible scale effects.

1 Research Fellow, School of Engineering and Electronics, University of Edinburgh, King's Buildings, Edinburgh, EH9 3JL, UK. J.Pearson@ed.ac.uk
2 Lecturer, School of Engineering and Electronics, University of Edinburgh, King's Buildings, Edinburgh, EH9 3JL, UK. Tom.Bruce@ed.ac.uk
3 Professor (associate), Civil Engineering, University of Sheffield, Technical Director, HR Wallingford, Wallingford, OX10 8BA UK. W.Allsop@shef.ac.uk
4 Lecturer, Universitat Politècnica de Catalunya, Jordi Girona, 1-3, Campus Nord. 08034 Barcelona, Spain. xavi.gironella@upc.es

It is generally assumed, although there is relatively little explicit validation, that overtopping (primarily mean overtopping discharges) under pulsating / non-breaking wave action will scale correctly from small-scale tests. The scaling of two other processes are however less well supported. Despite early work by Franco *et al.* (1994) and Besley (1999), there are few data on the distribution of wave-by-wave overtopping volumes, and particularly maximum individual volumes, and these may be influenced by small-scale processes.

The second area of concern relates to impulsive wave processes at structures. In relatively deep water, waves are generally reflected back from vertical / steep walls without much breaking. Most established design methods were developed for these pulsating conditions. If however waves are large relative to the local depth, as when a submerged berm or slope is formed in front of the wall, then waves may shoal on the slope and can break directly onto the wall, known as "impacting" conditions. Processes of pulsating wave overtopping are generally well-understood and predictable, but for impulsive breaking on steep walls, the processes are much more violent. Significant scale effects on wave impact pressures measured at small scale in laboratory flumes have long been known, and simple correction factors have been suggested for those pressures by Howarth *et al.* (1996). It might therefore be expected that overtopping under impact conditions might similarly be affected by scale effects.

The importance of violent overtopping processes has been studied within a UK collaborative research project on Violent Overtopping of Waves at Seawalls (VOWS) by a team from Edinburgh, Sheffield and Manchester Metropolitan Universities.

Within the VOWS project, Bruce *et al.* (2001) has reported a series of 2-dimensional laboratory tests on overtopping processes at vertical / battered walls under impulsive conditions, and Napp *et al.* (2002) report similar small-scale tests to explore 3-dimensional effects. Those results gave good agreement with previous prediction methods for the tested configurations, confirming that the VOWS tests were consistent with previous research. But those VOWS tests, and all previous investigations have been conducted at relatively small-scale ($H_{s(model)} < 0.25$m). Application of test results (or the prediction methods derived from them) to prototype requires that all potential scale effects are identified, where possible, quantified and that appropriate correction factors are applied.

This paper describes new research under the VOWS project, presenting data on overtopping performance of 10:1 battered seawalls from 2-dimensional tests at both small- and large-scale. The paper compares results with previous prediction methods on plain vertical configurations. These new results have been used to revise prediction methods for mean overtopping discharges, wave-by-wave and peak overtopping volumes.

2. PREVIOUS WORK

2.1 Mean overtopping discharges

Many urban seawalls and harbour breakwaters are formed by vertical, or near vertical walls. In any design analysis, the overtopping characteristics of these structures are generally tested against a (tolerable) mean discharge over a particular storm event. Prediction of mean overtopping discharges are primarily based on empirical formulae developed from laboratory measurements, although early results of Goda (1975) were presented graphically. Goda's results show both pulsating and impulsive behaviour, but most formulae cover predominantly pulsating wave conditions. Studies by Franco *et al.* (1994), Allsop *et al.* (1995) generated new data on mean and peak overtopping under pulsating and impulsive conditions, showing how overtopping is strongly influenced by the form of wave breaking. Prediction methods by Besley *et al.* (1998) identify configurations of vertical or composite walls for which impulsive breaking may occur, and demonstrate that methods based only upon pulsating conditions will under-estimate overtopping under impacting conditions.

When waves incident at a vertical / composite wall are small compared to water depth, they are generally reflected back without breaking. If the waves are however large relative to water depth, then they may shoal on any approach slope or berm, and may break directly onto the structure, leading to significantly more abrupt overtopping. These observations led to formulation of a wave breaking parameter, h*, given by:

$$h^* = \frac{h}{H_s}\left(\frac{2\pi h}{gT^2}\right) \qquad (1)$$

Allsop *et al.* (1995) observed that pulsating conditions predominate when $h^* > 0.3$, and that impacting conditions were more likely to occur when $h^* \leq 0.3$. Bruce *et al.* (2002) also note particularly violent breaking effects for $h^* < 0.15$. Under pulsating conditions when $h_* > 0.3$, overtopping can be predicted by:

$$Q\# = 0.05 \exp(-2.78\, R_c/H_s) \qquad (2)$$

where Q# is the dimensionless discharge, given by $Q/(gH_s^3)^{0.5}$. Under impacting conditions, new dimensionless discharge (Q_h) and freeboard parameters (R_h) incorporating h* were established, and were given by:

$$Q_h \equiv Q / (gh^3)^{0.5} / h^{*2} \qquad (3a)$$

and

$$R_h \equiv (R_c / H_s)\, h^* \qquad (3b)$$

where Q is the mean overtopping discharge per metre run. Besley (1999) used results from studies by Allsop *et al.* (1995) and de Waal *et al.* (1992) for $h^* \leq 0.3$ to suggest the following prediction formula for overtopping of vertical walls:

$$Q_h = 1.37 \times 10^{-4}\, R_h^{-3.24} \qquad (4)$$

2.2 Peak overtopping discharges

In terms of tolerable safety limits, a potentially more useful parameter is the maximum individual overtopping volume. Franco *et al.* (1994) measured wave-by-wave overtopping volumes, and Allsop *et al.* (1995) showed that statistical distributions of these volumes were similar for a number of studies on vertical seawalls. For vertical structures under

impulsive conditions ($h^* \leq 0.3$), Allsop *et al.* (1995) demonstrated empirically that the proportion of overtopping waves could be given by:

$$N_{ow}/N_w = 0.031\ R_h^{-0.99} \quad (5)$$

where N_{ow} is the number of overtopping waves and N_w is the number of waves.

Franco *et al.* (1994) and Besley (1999) demonstrated that wave by wave individual overtopping volumes could be described by two parameter Weibull probability distributions. Besley (1999) suggested that the expected maximum individual overtopping volume, V_{max}, in a sequence of N_{ow} overtopping waves could be described by:

$$V_{max} = a\ (\ln(N_{ow}))^{1/b} \quad (6)$$

where for vertical seawalls subjected to impacting wave conditions, the Weibull scale parameter, $a = 0.92V_{bar}$, and the Weibull shape parameter, $b = 0.85$.

3. EXPERIMENTAL STUDIES

The small-scale investigations were completed in the wave channel in the School of Engineering at University of Edinburgh. The channel is 20m long, 0.4m wide along its full length, has an operating water depth of 0.7m and is equipped with an absorbing flap-type wavemaker. A 1:10 beach and the perspex model wall were installed, see Figure 1.

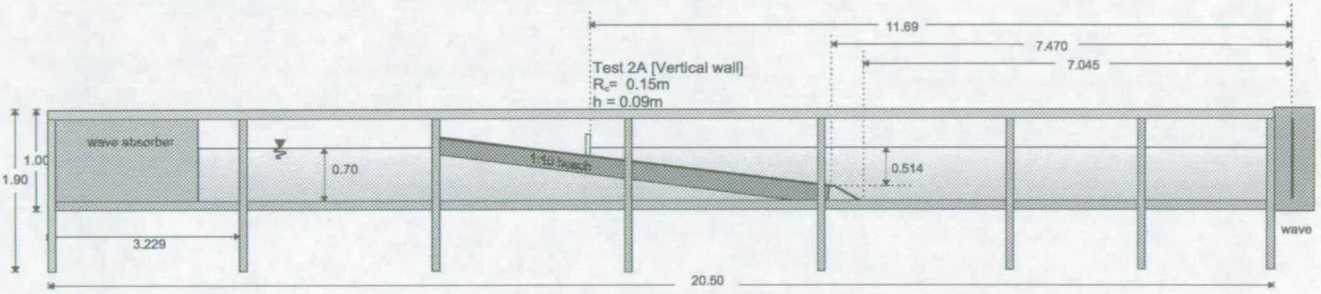

Figure 1: Schematic of test configuration in Edinburgh wave flume

Overtopping discharges were directed via a chute into a measuring container suspended from a load cell. Individual overtopping events were detected by two parallel strips of metal tape run along the structure crest which acted as a switch closed by the water. Wave-by-wave overtopping volumes were measured by determining the increment in mass of water in the collection tank after each overtopping event.

A matrix of 30 test conditions [significant wave height at the toe of the structure (H_s), statistical period (T_s), water depth at structure (h) and crest freeboard (R_c)] covered configurations where impulsive conditions were expected to occur. Each test consisted of a sequence of approximately 1000 irregular waves of a JONSWAP spectrum with $\gamma = 3.3$.

The large-scale experiments were all completed in the CIEM / LIM wave flume at Universitat Politècnica de Catalunya, Spain. This flume is 100m long, 3m wide along its full length, and has an operating depth of up to 4m at the absorbing-wedge paddle. For these experiments, a 1:13 concrete approach beach was constructed up to the test structure.

As with the small-scale tests, overtopping discharges were directed via a chute into a measuring container suspended from the measurement load cell. Each overtopping event was detected by two parallel strips of metal tape in the collection chute. As for the small-scale tests, each test consisted of a sequence of approximately 1000 irregular waves of a JONSWAP spectrum with $\gamma = 3.3$, and a matrix of about 30 different conditions was selected to match (where possible) the small-scale tests.

The objective of these large-scale tests was to determine (and if necessary quantify) scale effects in existing prediction methods in regimes in which wave breaking at or onto the structure is significant. The matrices of conditions for both small- and large-scale tests are shown in Table 1.

Table 1: Summary of test conditions

Structure Configuration	Test Series	Configuration	Nominal wave period T_s [s]	Significant wave height H_{si} [mm]
10:1 batter Small-scale	3A [1:10 beach]	R_c = 150mm h = 90mm	1.0	63, 66, 67, 69, 70
			1.33	63, 70, 76, 77, 82
			1.6	62, 71, 77, 79, 87
	3B [1:10 beach]	R_c = 129mm h = 247mm	1.0	71, 79, 86, 92, 100
			1.33	81,93, 94, 100, 102
			1.6	71, 74, 89, 97, 105

Structure Configuration	Test Series	Configuration	Nominal wave period T_s [s]	Significant wave height H_{si} [m]
10:1 batter Large-scale	1A [1:13 beach]	R_c = 1.16m h = 0.83m	2.56	0.48, 0.45, 0.37
			3.12	0.60, 0.56, 0.39
			3.29	0.67
			3.64	0.60
	1B [1:13 beach]	R_c = 1.40m h = 0.83m	1.98	0.25
			2.56	0.48, 0.45, 0.37
			3.12	0.63, 0.60, 0.56, 0.39
			3.64	0.60
	1C [1:13 beach]	R_c = 1.46m h = 0.53m	1.98	0.25, 0.22
			2.56	0.48, 0.45, 0.37, 0.23
			3.12	0.63, 0.60, 0.56, 0.39
			3.29	0.67
			3.64	0.60

4. RESULTS

4.1 System accuracy

Prior to undertaking any tests, the accuracy of the overtopping measurement system was checked. A series of simulated overtopping events were performed in which known volumes of water were 'thrown' into the measurement container. The resulting data from the load cell were then passed through an algorithm to identify and quantify individual overtopping events. These results indicated that derived and actual total volumes differed by no more than 0.7%, suggesting that any errors in the measurement system were negligible. More detailed descriptions on quality control and variabilities were given by Pearson *et al.* (2001).

4.2 Measurement of inshore wave conditions

To reduce possible uncertainties in determining incident and reflected inshore wave conditions, all measurements of the inshore wave height, H_s were made by repeating the test sequence without the structure in place, and placing a wave gauge at the same location of the structure. The procedure was undertaken at both small- and large-scale. Both wave flumes were equipped with active wave absorption systems to remove reflected waves from the structure during overtopping tests.

4.3 Mean Overtopping Discharge

Mean overtopping discharge (described here by dimensionless discharge Q_h, Equation 3) are plotted in Figures 2 and 3 for the 10:1 battered wall at small- and large-scales respectively. Results are compared with the prediction method for impulsive conditions by Besley (1999) for a simple vertical wall. For the small-scale tests, Fig. 2 shows Q_h for 10:1 walls slightly in excess (by factors of up to 3 – 4) of those predicted by Besley (1999) over a wide range of R_h. Adopting the procedure of Allsop *et al.* (1995), the best-fit trend line for 10:1 walls at small-scale was found to be

$$Q_h = 1.89 \times 10^{-4} R_h^{-3.15} \quad (7)$$

with a corresponding least squares regression $R^2 = 0.95$.

When compared to the predictive method of Besley (1999) for vertical walls (Equation 4), it can be seen that the overtopping increases by an average factor of 1.3.

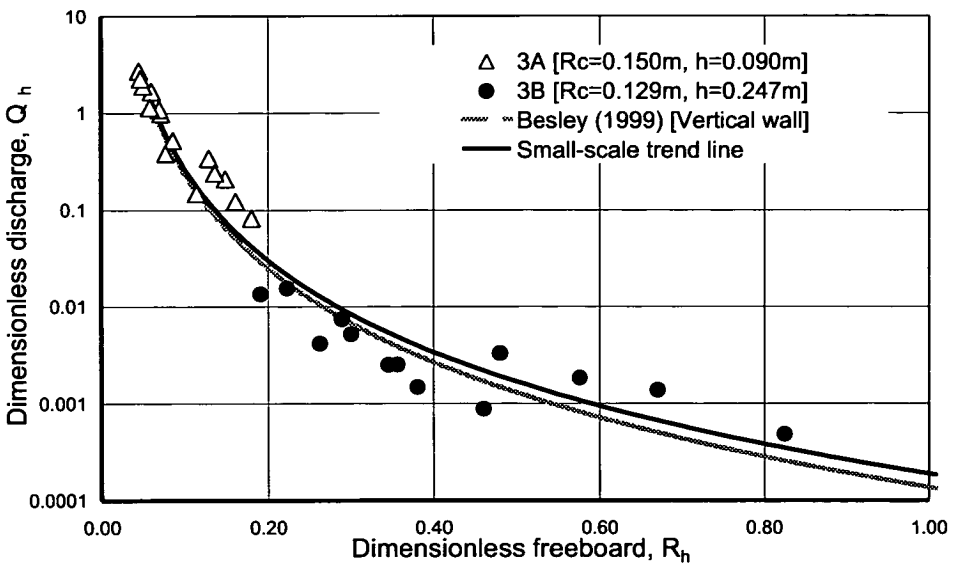

Figure 2: Overtopping on a 10:1 battered wall at small-scale, compared to the prediction for vertical walls (Equation 7)

For large-scale tests on the 10:1 wall in Figure 3, Q_h exhibits very similar characteristics as the small-scale results in Figure 2. When compared to the vertical wall prediction line of Besley *et al.* (1998), it is noticeable that scatter in the data are rather less for the large-scale tests. The best-fit trend line for large-scale tests on the 10:1 wall was

$$Q_h = 1.34 \times 10^{-4} R_h^{-3.20} \quad (8)$$

with a corresponding least squares regression $R^2 = 0.95$.

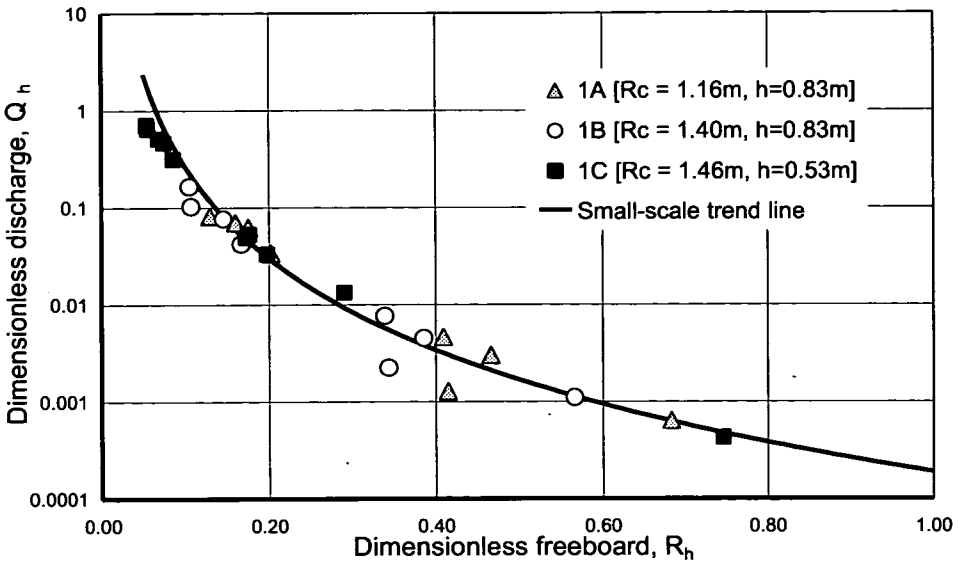

Figure 3: Overtopping on a 10:1 battered wall at large-scale, compared with the small-scale prediction for battered walls.

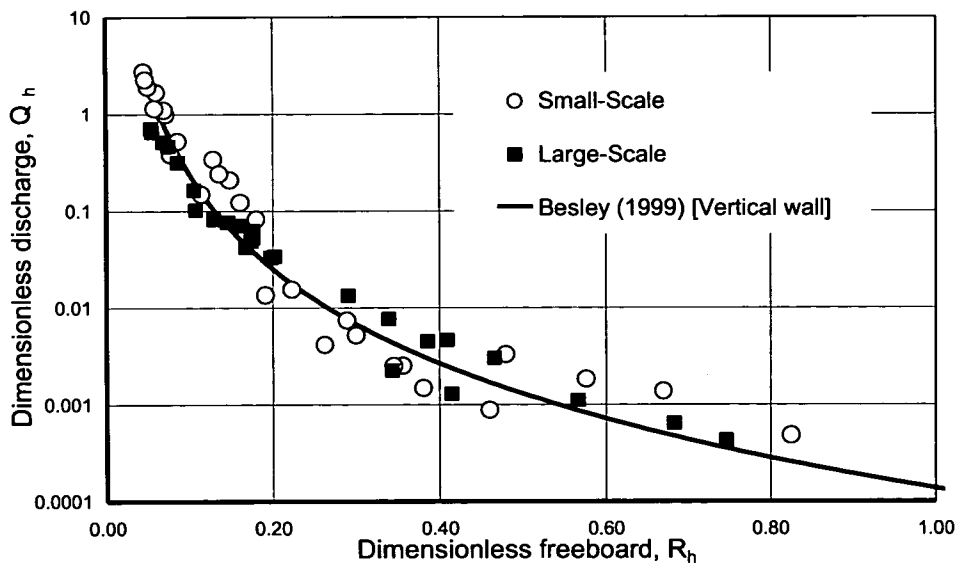

Figure 4: Overtopping on 10:1 battered walls, compared to the prediction (for vertical walls) of Besley (1999).

All small- and large-scale measurements are compared with the vertical prediction method of Besley (1999) in Figure 4. The results demonstrate good agreement exists between large- and small-scale results, indicating that for this case, scale effects are not significant.

4.4 Number of overtopping waves

A parameter which is vital in predicting peak overtopping volumes and statistics of wave-by-wave overtopping volumes, and is supported by very few data, is the number or proportion of overtopping waves (N_{ow}). The variation of N_{ow} with freeboard for vertical

wall, as quantified from the small-scale tests is shown in Figure 5. It is noticeable that the results of N_{ow} / N_w deviate significantly from the prediction by Equation 5, which leads to uncertainty in adopting previous prediction methods for individual maxima.

Careful analysis of the problem in defining N_{ow} reduces to a particular difficulty of the exact definition of an "overtopping event". Clearly such events cannot constitute all occasions when any water passes over the wall, as that would increase without limit with each improvement in measurement precision. Any definition must therefore generate a limit of only one overtopping event per incident wave. Two alternatives have been explored. In initial considerations, a minimum overtopping volume was based on an idealisation of the volume of water in a "typical" wave (H_s and T_m). This had the disadvantage that this threshold then changed for each test condition. The alternative method to overcome these difficulties would be to define a minimum significant measurement volume of order 1/1000 of the total collection volume. In designing any experiments focussed on hazards to people, it is important that this minimum fall well below any tolerable discharge limit.

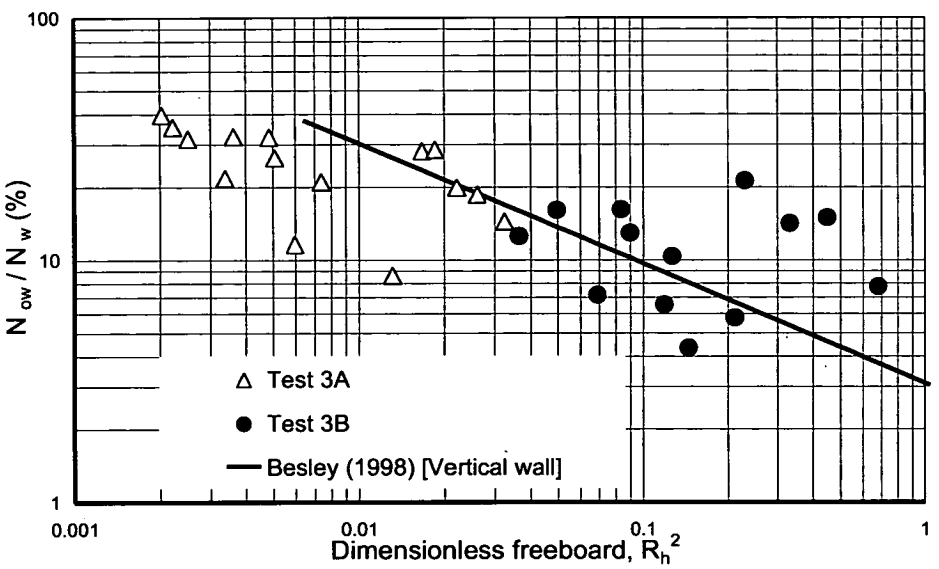

Figure 5: Percentage of waves overtopping a vertical wall at small-scale, compared to Besley (1999).

The percentage of overtopping waves for the large-scale tests are shown in Figure 6, compared with predictions by Besley (1999). The data follow the general trend of the prediction line well and if one neglects the two outlier points, then the scatter in the data is much less.

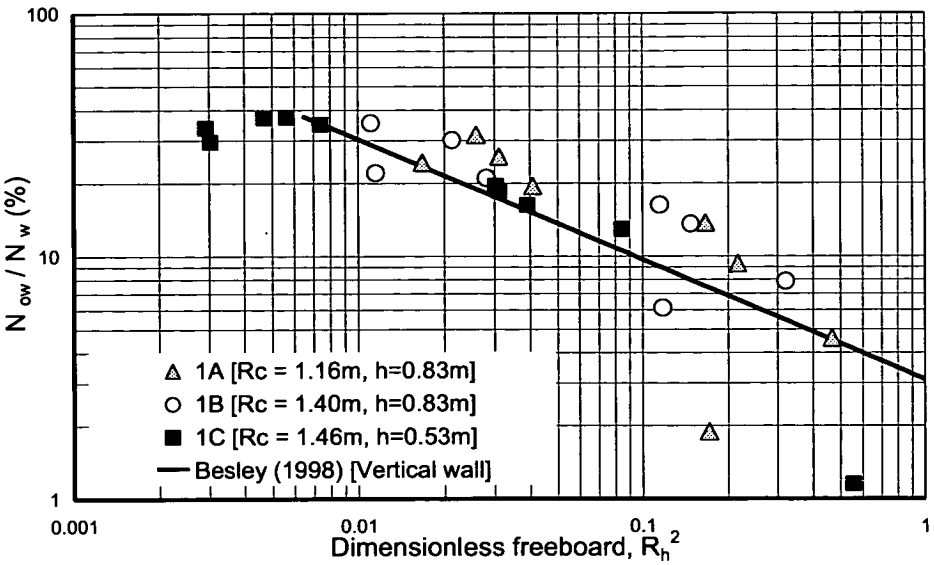

Figure 6: Percentage of waves overtopping a vertical wall at large-scale, compared to Besley (1999).

4.5 Peak overtopping rates

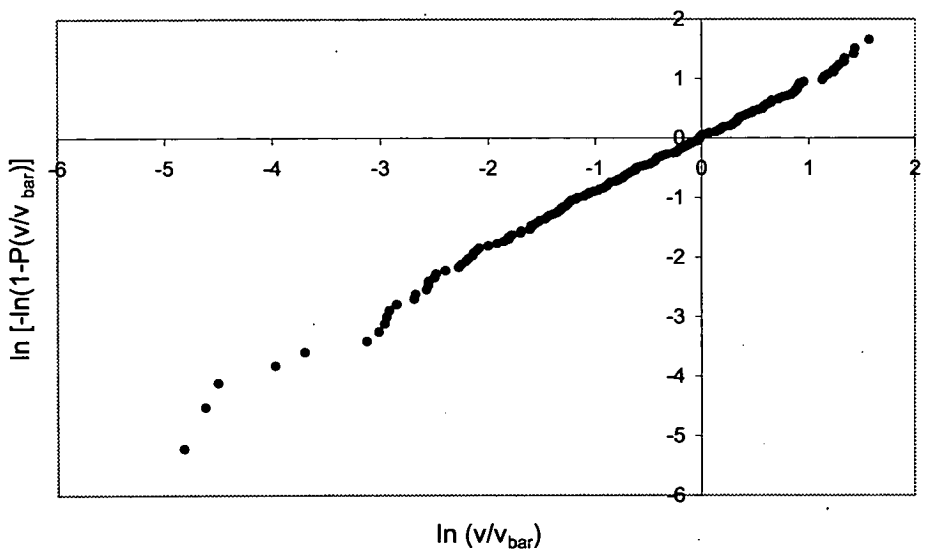

Figure 7: Typical distribution of wave-by-wave volumes
(Test: BigVows 1C, H_s=0.45m,T_s=2.56s)

To determine peak discharge rates, the analytical prediction method of Besley (1999) assumes that the wave by wave individual overtopping volumes follow a Weibull distribution. Figure 7 shows the individual overtopping volumes for one typical test case plotted on a Weibull scale. It is noticeable that the results are linear, indicating a good goodness of fit, which gives confidence in Besley's (1999) analytical method for predicting peak overtopping rates.

Maximum individual overtopping volumes predicted using the appropriate method for vertical walls by Besley (1999) are compared in Figure 8 with those measured at small-scale. Despite the uncertainties discussed above in defining precisely what constitutes an overtopping event, it would appear that measured maxima values correlate reasonably with the predicted values, particularly given the inherent scatter in these parameters.

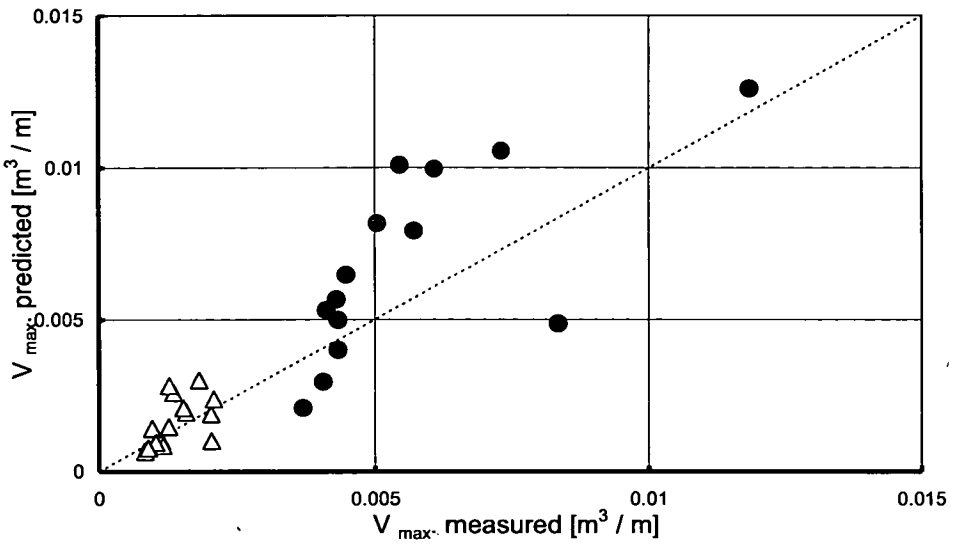

Figure 8: Comparison of measured and predicted peak overtopping volumes, small-scale.

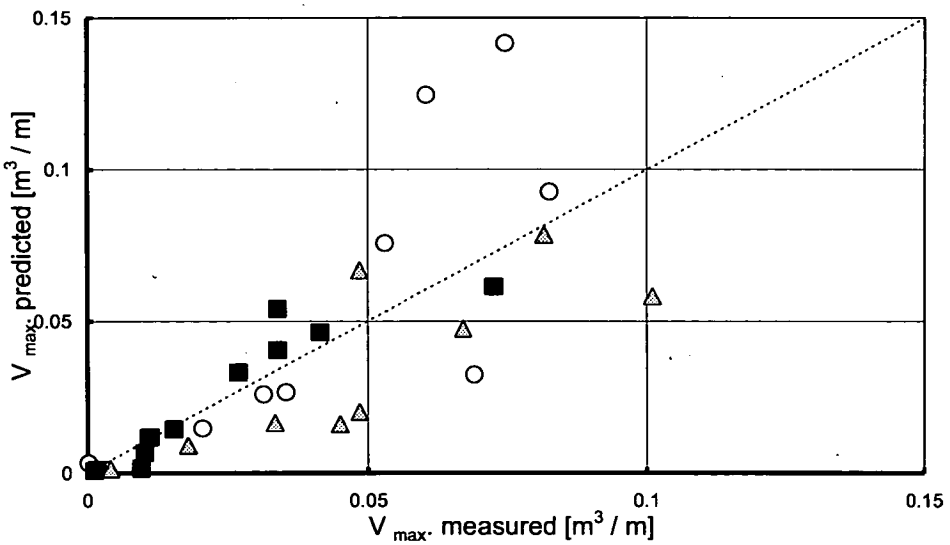

Figure 9: Comparison of measured and predicted peak overtopping volumes, large-scale

Maximum individual overtopping volumes predicted using methods for vertical walls by Besley (1999) are compared in Figure 9 with those measured at large-scale. As for the small-scale results, the measured maximum values correlate well with the predicted values, typically within a factor of two.

5. DISCUSSION

The purpose of small-scale hydraulic model testing is to provide data / methods that can be used to predict processes at full-scale. It is therefore important to be able to quantify any "scale" effects, those that emanate simply from the scale of the modelling. Example possible scale effects arise from distortions to viscous flow, or by surface tension effects on bubbles and droplets. The general trend of the results presented above lead to the encouraging conclusion that "scale" effects are not significant for mean or peak overtopping volumes for these types of coastal structure under impulsive wave conditions. These results also suggest that scale effects are likely to be minimal for pulsating wave conditions, as the test conditions described here were specifically chosen as more likely to be influenced by any scale effects than pulsating overtopping processes.

It is however apparent that there can sometimes be "model" effects which arise because a particular process is not reproduced, or is reproduced with some distortion. The most obvious of these "model" effects are the absence of wind, and use of fresh water rather than sea water. The useful and well argued tests by de Waal *et al.* (1992, 1996) suggest that heavy overtopping is very little influenced by wind, but it is probable that wind effects will be important for small discharges, particularly when accompanied by severe breaking processes. The use of fresh water rather than sea water alters the inclusion and persistence of air bubbles in the water. It is known that this will influence wave impact pressures, but there is no evidence for this "model" effect to alter overtopping processes.

This paper has not discussed data variabilities, but those aspects were previously described by Pearson *et al.* (2001).

6. CONCLUSIONS

The prediction methods of Besley *et al.* (1998), Besley (1999), for mean overtopping discharge may be used under conditions when impulsive wave action is significant or dominant, with mean discharges remaining well-predicted (typically within a factor of two) without any significant scale effect.

Measurements of the number of overtopping waves, N_{ow} are generally consistent from small- to large-scale, and fit well with predictions of Besley *et al.* (1998), Besley (1999).

There is good agreement between measured and predicted maximum overtopping volumes at both small- and large-scales, well inside the inherent scatter in this parameter.

ACKNOWLEDGEMENTS

This work is funded by the UK EPSRC (GR/M42312), and supported by the VOWS Management Committee also including members from Manchester Metropolitan University (Derek Causon, David Ingram, Clive Mingham), Posford-Haskoning (Dick Thomas), Bullen & Co., HR Wallingford (Philip Besley, Tim Pullen), all of whose input and support is gratefully acknowledged. The VOWS project is also particularly pleased to acknowledge guidance and helpful supervision of their collaborative work of the EPSRC CEWE Project Manager, Michael Owen.

The VOWS team are most grateful to the UPC Barcelona team for excellent support during the Big-VOWS tests under the EC TAMRI "HYDRALAB" project - Xavi Gironella (our co-author), Quim Sospedra, Javier Pineda and Agustin Sanchez-Arcilla.

REFERENCES

Allsop, N.W.H., Besley, P. & Madurini L. (1995), "Overtopping performance of vertical walls and composite breakwaters, seawalls and low reflection alternatives", Paper 4.7 in MCS Final Report, publn University of Hannover.

Besley, P. (1999), "Overtopping of seawalls – design and assessment manual", R & D Technical Report W 178, ISBN 1 85705 069 X, Environment Agency, Bristol.

Besley, P., Stewart, T, & Allsop, N.W.H. (1998), "Overtopping of vertical structures: new methods to account for shallow water conditions", Proc. Int. Conf. on Coastlines, Structures & Breakwaters '98, Institution of Civil Engineers, pp46-57, publn. Thomas Telford, London.

Bruce, T, Allsop, N.W.H. & Pearson, J. (2001), "Violent overtopping of seawalls – extended prediction methods", Proc. Int. Conf. on "Coastlines, Seawalls and Breakwaters '01" ICE, publn Thomas Telford, London.

Franco, L., de Gerloni, M. & van der Meer, J.W. (1994), "Wave overtopping on vertical and composite breakwaters", Proc 24th Int. Conf. Coastal Eng., Kobe, publn. ASCE.

Goda, Y, Kishira, Y, & Kamiyama, Y. (1975), "Laboratory investigation on the overtopping rates of seawalls by irregular waves", Ports and Harbour Research Institute, Vol 14, No. 4, pp 3-44, PHRI, Yokosuka.

Howarth, M.W., Vann, A.M., Davis, J.P., Allsop, N.W.H. & Jones, R.J. (1996), "Comparison of wave impact pressures on armour units at propototype and model scale", 25th Intl. Conf. on Coastal Eng., Orlando, ASCE.

Napp, N., Pearson, J., Richardson, S., Bruce, T., Allsop, N.W.H. & Pullen, T. (2002), "Overtopping of seawalls under oblique and 3-d wave conditions", Proc 28th Intl. Conf. on Coastal Eng.,Cardiff, ASCE.

Pearson, J., Bruce, T. & Allsop, N.W.H. (2001), "Prediction of wave overtopping at steep seawalls – variabilities and uncertainties", Proc. Conf. Waves '01, San Francisco, pp 1797 – 1808, ASCE.

de Waal, J.P. & van der Meer, J.W. (1992), "Wave run-up and overtopping on coastal structures", Proc 23rd Int. Conf. Coastal Eng., pp1758-1771, ASCE.

de Waal, J.P., Tonjes, P. & van der Meer, J.W. (1996), "Overtopping of sea defences", Proc 25rd Int. Conf. Coastal Eng., pp2216-2229, Orlando, ASCE.

Appendix Q: Pullen *et al.*, 2003

Pullen, T., Allsop, N.W.H., Bruce, T. & Geeraerts, J. (2003), *Violent wave overtopping: CLASH field measurements at Samphire Hoe*, Proc "Coastal Structures 2003", pp 469–480, ASCE, Reston, Virginia, ISBN 0-7844-0733-9

Appendix Q
Pullen *et al.*, 2003

Pullen, T., Allsop, N.W.H., Bruce, T. & Geeraerts, J. (2003), *Violent wave overtopping: CLASH field measurements at Samphire Hoe*, Proc "Coastal Structures 2003", pp 469–480, ASCE, Reston, Virginia, ISBN 0-7844-0733-9

Q.1 Declaration of contribution

The author was one of a closely-knit Edinburgh / HR Wallingford team on the Samphire Hoe field / laboratory comparisons, being involved at all stages of the planning, testing and reporting of the work. The Edinburgh flume tests were carried out by the project's post-doctoral Research Engineer, Pearson, working under the guidance of the author. The author took a detailed interest in the synthesis of the conclusions and in the editing of the paper.

Q.2 Published paper

overleaf

Violent wave overtopping: CLASH field measurements at Samphire Hoe

Tim Pullen[1], William Allsop[2], Tom Bruce[3] & Jimmy Geeraerts[4]

Abstract

As part of a major European research project into wave overtopping at coastal structures, overtopping discharges have been measured at full-scale on a vertical seawall in Southeast England. The measurement site, Samphire Hoe, is an area of reclaimed land just west of Dover on the English channel coast, and is an ideal location for monitoring overtopping. The site is described in detail, and the design and operation of the measurement equipment are also outlined. Overtopping was measured on three occasions and the storms and their results are discussed. It is shown that the field measurements compare well with empirical prediction methods by Besley (1999) and Bruce et al (2001). Additional discussion interprets the hazardous nature of each of the storms.

Introduction

The processes of wave overtopping of seawalls are not yet understood fully, particularly those that may cause risks to people close behind seawalls. There remain important gaps in knowledge, despite significant improvements in recent years. To help reduce uncertainties in the prediction of coastal flooding, HR Wallingford (HRW) were commissioned under the CLASH research project to help develop improved prediction methods for use by coastal engineers . CLASH ("Crest level assessment of coastal structures by full scale monitoring, neural network

[1] Coastal Structures Group, HR Wallingford, Howbery Park, Wallingford, OXON, OX10 8BA, UK. Tel: 0 (044) 1491 822231, t.pullen@hrwallingford.co.uk
[2] Technical Director, HR Wallingford; Senior Research Fellow, University of Southampton, c/o HR Wallingford, w.allsop@hrwallingford.co.uk
[3] Division of Engineering, Edinburgh University, King's Buildings, Sanderson Building, Edinburgh EH9 3JL, Scotland. tom.bruce@ed.ac.uk
[4] Ghent University, Dept of Civil Engineering, Technologiepark 904, 9052 Ghent, Belgium. jimmy.geeraerts@ugent.be

prediction and hazard analysis on permissible wave overtopping") comprises 13 European partners at universities and research institutions, and a substantial amount of this work involves the collection of field data on overtopping and subsequent testing in the laboratory (see http://www.clash-eu.org). A particular motivation for this research was the suggestion by earlier research in another EC project, OPTICREST, that there might be unexpected scale effects in some hydraulic modelling in which small-scale tests might under-predict overtopping at full scale. While these suggestions were not subsequently supported by large scale tests on vertical and battered seawalls by the VOWS ("Violent overtopping by waves at seawalls") team in the large flume at Barcelona, see Pearson *et al.* (2002), it is clear that this uncertainty could have substantial impacts.

The results of the CLASH project are intended to benefit citizens in low lying and populated coastal regions, who depend critically on the performance of coastal structures for defence against storm surges, wave attack, flooding and erosion. Continuing sea level rise and climate change emphasis the need for reliable and robust predictions of overtopping hazards as higher storm surges and more severe storms may lead to flooding. The CLASH project will produce generally applicable prediction methods on the required crest height of most coastal structure types, based on permissible wave overtopping and hazard analysis. Within CLASH, HRW were committed to a programme of full scale measurements of wave overtopping at the seawall protecting the Samphire Hoe reclamation, Kent, England. Other CLASH field measurements have been carried out at Zeebrugge in Belgium on a breakwater armoured with Antifer cubes (De Rouck *et al.,* 2003), and a rock armoured breakwater at Ostia in Italy (Franco *et al.*, 2003). The work involved in the design of the overtopping equipment, the methodology, and the first winter's field measurements and analysis at Samphire Hoe are described in this paper. A fuller report is given by Pullen & Allsop (2003).

Samphire Hoe

Samphire Hoe, shown in Figure 1 where the study area has been boxed, is located in the Southeast corner of England immediately to the west of Dover, and is an area of reclaimed land comprising 4.9Mm^3 of chalk marl excavated from the Channel Tunnel. The area of approximately 300,000m^2 is enclosed by a vertical seawall with a crest level at +8.22(mODN) and a toe level at –2.42(mODN). To the top of the seawall is a 1.25m parapet wall fronting a 25m stepped promenade where the field monitoring equipment is deployed (see Figure 2). Samphire Hoe, which is owned by Eurotunnel, has been landscaped and is operated by the White Cliffs Countryside Project as a public recreational area. The reclamation is exposed to waves from the southwest and southeast, and is subject to overtopping by spray (often termed white water overtopping) on approximately 30 days per year as a result of waves breaking over the rubble toe berm and impacting on the seawall face (see Figure 3). Whole wave overtopping (usually termed "green water overtopping") is also observed regularly.

HRW has a long standing relationship with the management of the Samphire Hoe site, and has designed and implemented over six years an overtopping hazard

warning system using tailored input data from the UK Met Office, see Gouldby *et al.* (1999). These systems use forecasts of wind speed and direction with predicted tide and surge levels, to predict potential occurrences of hazards from wave overtopping. This system does not use direct calculations of overtopping discharges, but has been steadily refined over 5 years of operation, using hourly observations of hazard from overtopping, categorised as low, medium or severe, and recorded by on-site personnel who are responsible for the safety of the public. The site is, therefore, an ideal location to set up a programme of field measurements. In particular, the existing hazard warning system facilitated the identification of potential storms prior to the deployment of the field monitoring equipment.

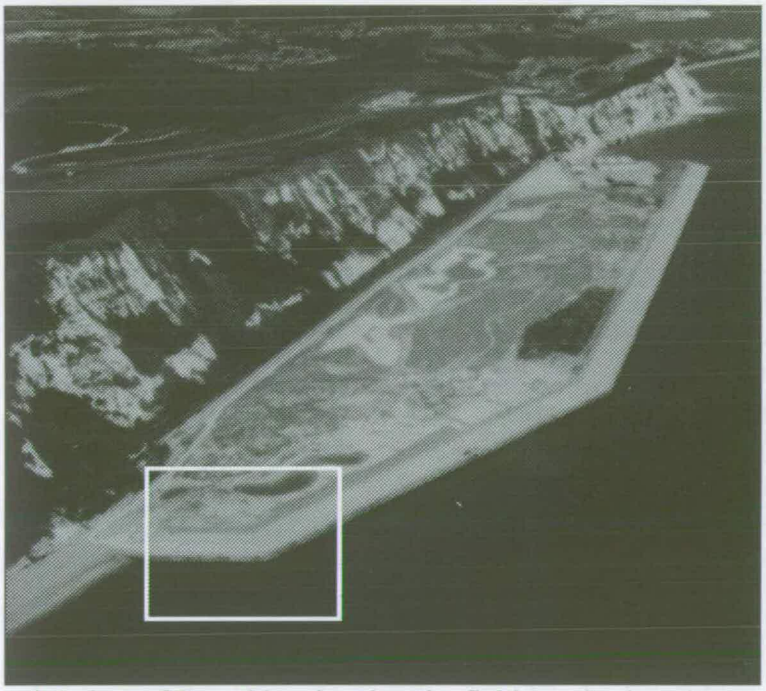

Figure 1: Aerial view of Samphire showing the field monitoring site

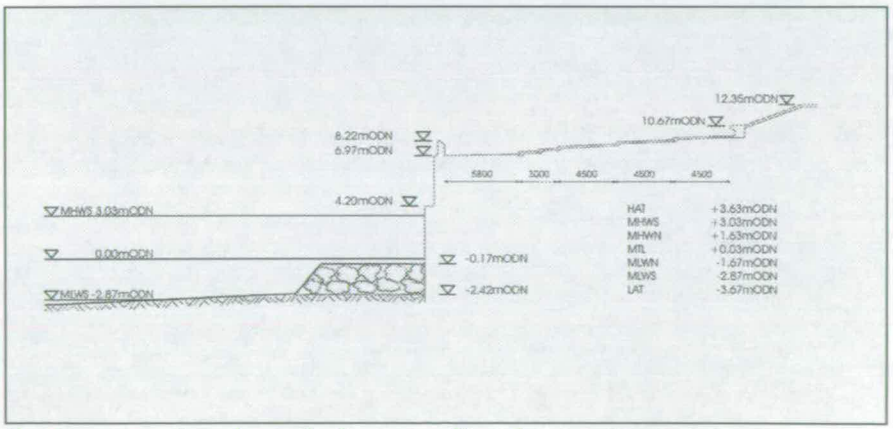

Figure 2: Cross section through the seawall at the monitoring site

Field Monitoring Equipment

The principal objective in the design of the field monitoring equipment, was to be able to capture sufficient overtopping discharges across the promenade to determine with sufficient accuracy both the total volume and the spatial distribution. As can be seen from Figure 3, the overtopping discharge is distributed over a wide area and it would clearly have been impracticable to attempt to capture all of this discharge. Moreover, certain constraints were imposed on HRW by the site owner that prevented the placement of tanks in certain areas. Also, the equipment had to be transported to the site and installed on each visit, and so it had to be handled easily, constructed quickly and be easily transportable.

The main pieces of equipment for measuring the overtopping, were three volumetric tanks placed across the promenade of the seawall. The first tank was placed directly behind the parapet wall, and the others were placed inline with the first on the first and second steps of the promenade. This arrangement, along with the control box attached to the rear of the parapet wall, can be seen in Figure 4. Each of the three tanks are divided into two compartments, each with a nominal capacity of 240 litres, and equipped with 350mbar Druck PTX1830 pressure transducers for measuring the head of water in each compartment. The collected data were recorded at 4Hz on a dataTaker DT800 logger housed in the control box. This was equipped with a 64Mb Compact Flash memory card, and controlled from a laptop via an RS232 radio modem link. The whole arrangement was battery powered, and a total of 36 hours total recording time was possible.

Figure 3: Violent wave overtopping at Samphire Hoe (Photograph courtesy of Eurotunnel and the White Cliffs Countryside Project)

The overtopping discharges captured in the tank compartments were allowed to drain freely, and so it was necessary only to capture the instantaneous head in each compartment following each individual overtopping event. This was necessary because the compartments would fill in a very short period during extreme conditions, but more particularly, it enabled the individual wave-by-wave discharges

to be determined. This required that two principal criteria were met. Firstly, that none of the overtopping compartments should ever overfill, and secondly, that the compartments should have sufficient capacity to accommodate the maximum anticipated discharges. To facilitate the requirements for these criteria, it was necessary to estimate the likely overtopping discharges and distribution of the overtopping in advance. Once this had been established it was possible to determine the size and the number of discharge holes in each tank compartment and then calibrate them.

The hazard warning system, described above, devised by HRW provided details of storms where overtopping had taken place, giving wave height, period, wave direction and water levels. An example scatter plot of wave heights and tide levels where overtopping has occurred at Samphire Hoe between October 2000 and March 2002, is shown in Figure 5. These data, and the data for the wave period, were fitted to an approximate normal distribution and the values with the highest probability of occurrence were used to establish a design wave condition. Overtopping discharge varies considerably with the water level in front of the structure, both the type of overtopping (pulsating or impacting) and the rate of discharge. Besley's (1999) method for a composite vertical wall was used to calculate maximum and peak overtopping discharges for a range of water levels from the top of the berm up to Mean High Water Springs (MHWS, refer to Figure 2) using the design wave condition. With a design overtopping discharge rate and associated peak volume the next stage was to determine how this might be distributed across the promenade.

Figure 4: The tanks in position, with the control box to the right of the front tank

There is very little guidance currently available that describes how overtopping is distributed spatially, as most research has focussed on predicting mean overtopping rates for simple structures. Jensen & Sorensen (1979) presented

some results for the distribution behind a rubble mound structure, and linear and exponential distributions had been anticipated from photographic and video images of waves overtopping vertical seawalls. Knowing what distributions might be expected is important for two reasons. It was necessary to have a good approximation during the design of the tanks, but it is especially useful when estimates of the discharges falling between the tanks during the analysis of the data are required. The logarithmic spatial distribution of the overtopping discharge, according to Jensen & Sorensen, for the maximum predicted discharge, is shown in Figure 6. This shows overtopping volumes in 0.25m sections across the promenade, where the darker sections are those captured by the tanks and the lighter those not captured. This distribution, in principal, provides a means of estimating the total volume of overtopping.

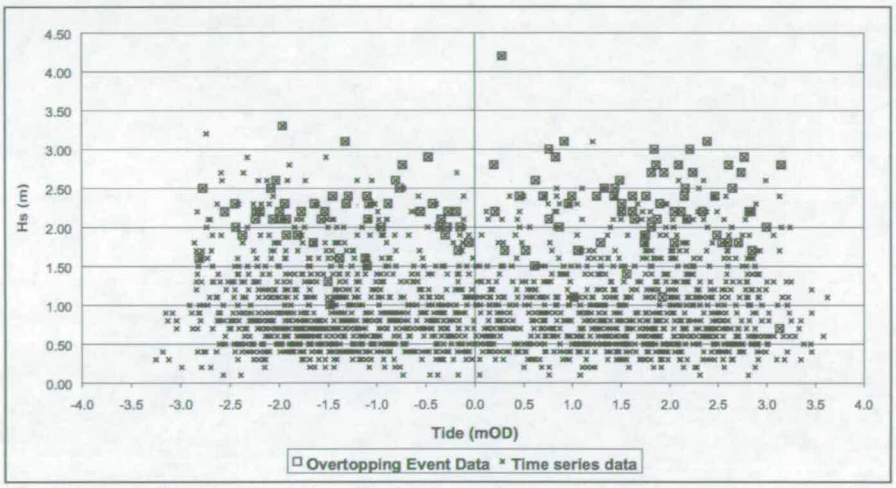

Figure 5: Recorded wave heights during overtopping storms at Samphire Hoe

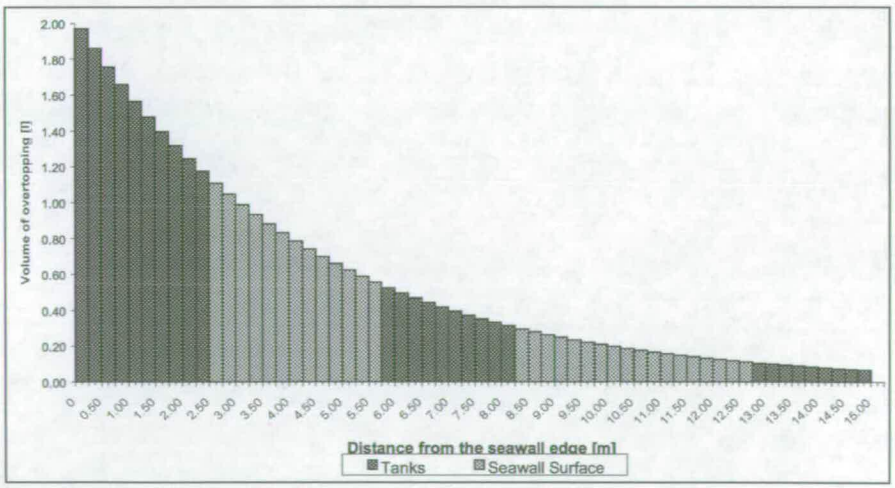

Figure 6: Spatial distribution of overtopping across the promenade

Field measurements at Samphire Hoe

The assessment of the occurrence of potential overtopping storms began with a close examination of the weather forecast during the preceding week, and a more detailed study of the hazard warning system at Samphire Hoe during the final 48 hours before the anticipated storm. The general criteria for suitable storms (for these measurements) at Samphire Hoe are a low pressure system travelling across the Atlantic with a steep pressure gradient arriving over the English channel. This will generally ensure that minimum wind speeds of 8~10m/s can be expected with wind directions between 150° and 240°. These conditions will generally produce wave heights of $H_s > 2m$, which is sufficient to cause overtopping at the monitoring site. During the winter and spring of 2003 there were few storms during this season that caused overtopping at Samphire Hoe, but weather forecasts suggested two occasions when it was useful to deploy the monitoring equipment at Samphire Hoe. The first visit was during March '03 where one storm was monitored on the 10th, and the second visit was during May '03 when storms were monitored on the 1st & 2nd. A range of conditions were encountered during these visits, and overtopping varied from light spray to high discharges from waves impacting violently on the seawall. For simplicity the three monitored storms will be referred to simply as Storm 01 (10 March), Storm 02 (1 May)& Storm 03 (2 May).

During Storm 01 overtopping water was seen to appear regularly over the top of the parapet wall, but this was in general sporadic and was spread along the length of the western splay wall. Those discharges that did pass over the top of the parapet wall were blown widely across the promenade as spray by high wind velocities, but no measurable quantities of overtopping discharge entered into the tanks. A conservative estimate of the mean overtopping discharge rate for this storm would be of the order of say 0.05l/s.m. As discussed by Franco *et al.* (1994) and Allsop *et al.* (2003), this overtopping rate should normally be considered as hazardous, where a tolerable discharge rate of around 0.03l/s.m is considered an upper limit for public safety. On this occasion the presence of the high wind velocities meant that the discharges were more unpleasant than they were hazardous, distributed as they were over a large area.

During the early stages of Storm 02 the wind speeds were at force 7, resulting in similar plumes of spray witnessed during the earlier storm. Predicted overtopping discharge rates are shown in Figure 7 against the water level for this storm. From Figure 7 it can be seen that a maximum overtopping discharge of approximately 1.4l/s.m was predicted at 12:00, but a peak discharge of 0.28l/s.m was recorded during the storm. This discrepancy is partially explained by the presence of the high winds, as most of the overtopping discharges were being blown across the seawall promenade and not falling into the overtopping tanks. Nevertheless, the conditions in the area immediately behind the parapet wall were considerably more hazardous than during the previous storm.

As can be appreciated from Figure 1, Samphire Hoe is a large area, and depths of water in front of the seawall vary considerably along its 2km length. As a consequence, the depth of the berm in front of the seawall also varies, with different sections being exposed as the water level changes. Generally, the ratio between the

depth of water in front of the berm and that over it, will affect how and when a wave overtops. At the corner of the seawall, to the right of the white box in Figure 1, the berm is deeper than at the measurement site. For Storm 03 there were very high winds during the early stages of the storm, and observations were made in this area when plumes of overtopping water were being blown over distances in excess of 100m. Considerable quantities of this discharges were falling directly behind the parapet wall, where individual discharge volumes of between approximately 300l/m and 500l/m were estimated. If it is assumed that this represents about half the water in each overtopping event, then the remaining half was being blown across areas of the order of 3000m^2. Clearly the conditions were hazardous, and it was possible to determine a qualitative description of the hazards.

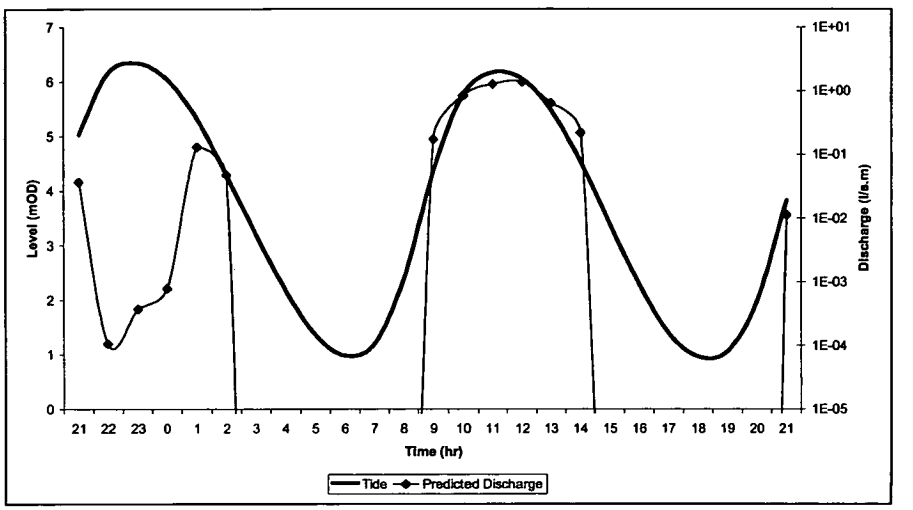

Figure 7: The predicted overtopping discharges shown varying with the water level

The volumes of water landing across the promenade became less severe on each tier, with the least landing on the top tier. It was decided that the only way to gain an improved scientific understanding of the potential hazards involved, was to stand directly in the path of the overtopping plume. It was agreed that standing on the top tier was equivalent to standing in a very heavy rain shower. Towards the lower tier, where it was still considered to be reasonably safe, the experience was similar to that which might be expected during a heavy hailstorm accompanied by a firm push on the back. Under these conditions, any unprepared people would be at high probability of being knocked over. Conditions directly behind the parapet wall were too hazardous to be approached closely. Later, when the water level had risen far enough to bring the overtopping to the measurement site, the wind speeds had become insignificant. Without the winds the overtopping discharges were being directed vertically upwards and coming down in the area directly behind the parapet wall. The peak discharges measured during the storm were in excess of 3.0l/s.m, which is two orders of magnitude greater that the tolerable limit for public safety at 0.03l/s.m, but the presence of the wind changed the nature of this hazard significantly.

Analysis and discussion

A brief description of pertinent methods and results will be given here and a more comprehensive account is given by Pullen & Allsop (2003).

Each of the storms, specifically Storms 01 & 02, lasted several hours, and the water levels and wave conditions changed throughout this time. To allow for this, the measurements have been divided up into ½ hour periods. Each ½ hour period was assessed separately, and the recorded mean discharges were compared with Besley's (1999) predictions for mean overtopping discharges for a composite vertical wall. Strictly speaking, this techniques is not wholly correct, as the Samphire Hoe seawall is actually slightly battered, stepping back as it does in three distinct sections. Nonetheless, they do provide an adequate means of comparing the results to known methods for these types of structures. Increased factors of 1.3 & 1.4 for walls battered to 10:1 & 5:1, respectively, are given by Bruce *et al.* (2001), and it is probable that these could be applied to composite structures, too.

Having established the individual overtopping discharges in each of the tank compartments, it was first necessary to approximate the discharges that had fallen outside of the tanks. Only then could a realistic comparison be made. It will be recalled from above, that the anticipated spatial distribution of the discharges might be similar to that described by Jensen & Sorensen (1979). Whilst this serves as a useful description, more often the actual behaviour was very different. For example, from the account of Storm 03 given above, it is noted that the overtopping discharges were often directed vertically upwards and came down directly behind the parapet wall, with the result that discharges were only captured in the front two tank compartments. For other events there was little difference among the volumes collected in the front four compartments

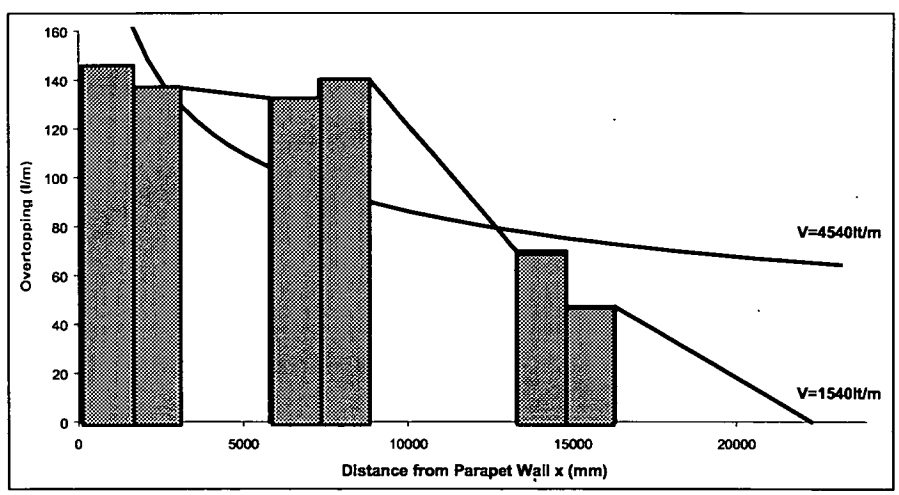

Figure 8: Trapezoidal distribution of overtopping discharges

For the analysis of the data a trapezoidal distribution of the individual volumes was assumed between the recorded data points and the back of the promenade 23.2 m from the seawall crest. The trapezoidal distribution of a large

discharge is shown in Figure 8, which shows overtopping distributed across all 6 tank compartments. Different distributions were assumed depending on how many tanks received a discharge, but each assumed this basic approach. In effect, the missing water was calculated between compartments 2 & 3, 4 & 5 and from the end of 6 to the point at 23,200mm in front of the recurve as appropriate. When the last discharge was in compartments 1, 3 or 5 then the distribution would stop at that point. The total discharge is therefore the sum of the discharges in the tanks and the interpolated discharges between the tanks. A comparison of the difference between a trapezoidal (1540l/m) and a logarithmic discharge (4540l/m) is also shown in Figure 8 for the same captured volumes, and it is clear from this example that the trapezoidal distribution is a more realistic approximation.

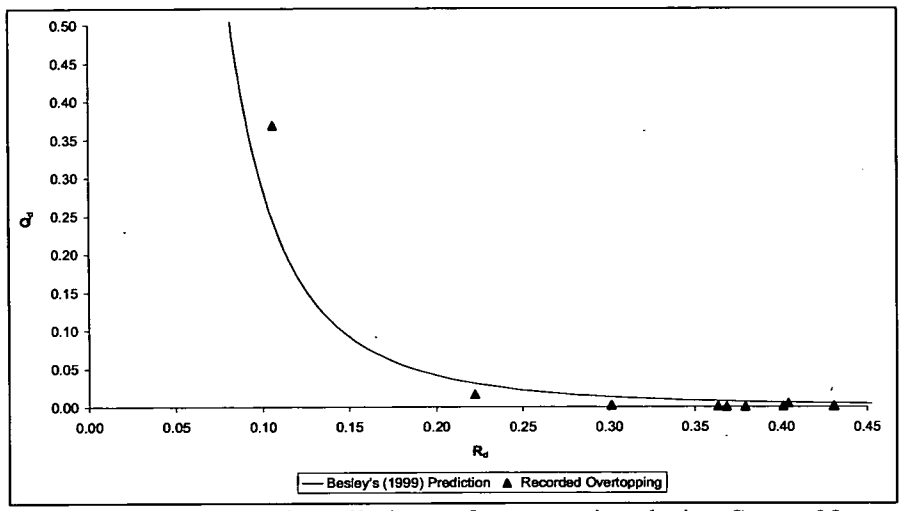

Figure 9: Measurements and predictions of overtopping during Storm 02

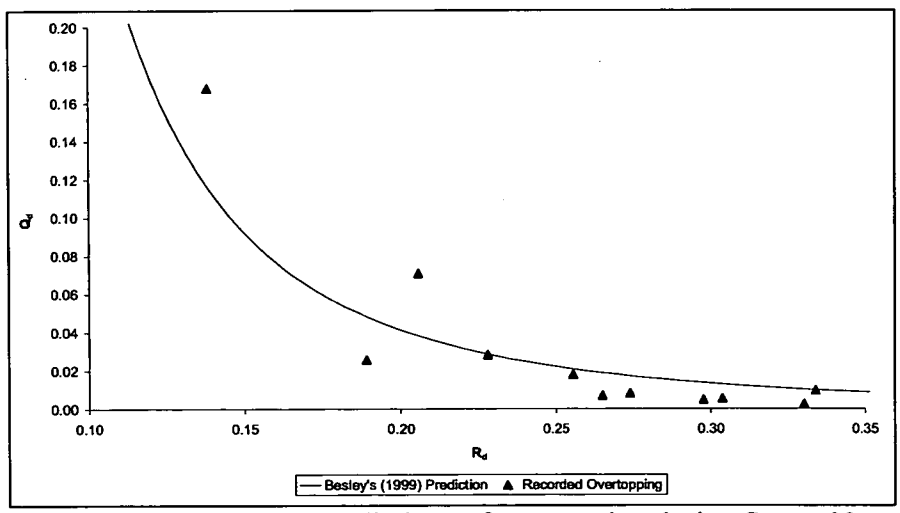

Figure 10: Measurements and predictions of overtopping during Storm 03

The analysed results of Storm 02 are shown in Figure 9, and those for Storm 03 are shown in Figure 10. These figures compare the field measurements with Besley's (1999) empirical overtopping prediction method for a composite vertical seawall. It is clear that they show that the general behaviour over the valid range is in agreement with the predictions. The most significant observation that can be made is that the data are slightly below the prediction line in Figure 9 but more or less on the prediction line in Figure 10. This should be expected as much of the overtopping water was being blown across the promenade during Storm 02, and so therefore the captured overtopping will be below that predicted. However, for Storm 03 the wind had little or no affect on the overtopping plumes, and so we see a good agreement with the prediction.

Conclusions

The methods for capturing overtopping discharges and recording the individual wave-by-wave volumes during field measurements have been described. The monitoring equipment at this site was deployed during three storms that yielded wave overtopping. Measurements from these storms identify mean and peak overtopping discharges.

During the storms qualitative descriptions of the hazards posed by the discharges were made. It was noted how the presence of the wind affects the way that hazard might be assessed. In particular, when wind velocities are high the falling discharges are much less hazardous than when wind velocities are low.

The data processing used a trapezoidal method of approximating the missing data between the tank compartments. This trapezoidal method is a first calculation of the total overtopping discharge, and more sophisticated techniques may improve the calculation of the total volumes. Nonetheless, there is an excellent agreement between Besley's (1999) prediction and the recorded data, which supports the conclusions of Pearson *et al.* (2001), that there are little or no scale affects between laboratory and field measurements.

Acknowledgements

The support of the European Community Fifth Framework for CLASH under contract EVK3-CT-2001-00058 and Defra / EA under FD2412, is gratefully acknowledged. The cooperation of Dave Johnson of Eurotunnel and Paul Holt of the White Cliffs Countryside Project, is also gratefully acknowledged. Many thanks, too, to Dr. Stephen Richardson and John Alderson of HRW who assisted during the field measurements.

References

Allsop, W., Bruce, T., Pearson, J., Alderson, J & Pullen, T.A. 2003 Violent overtopping at the coast, when are we safe? Int. Conf. on Coastal Management, Brighton, pp 54-69, ISBN 0 7277 3255 2, publn. Thomas Telford, London

Besley P. 1999 Overtopping of seawalls – design and assessment manual. R & D Technical Report W 178, ISBN 1 85705 069 X, Environment Agency, Bristol. Also from: http://www.environment-agency.gov.uk/commondata/105385/w178.pdf

Bruce, T, Allsop, N.W.H. & Pearson, J. 2001 Violent overtopping of seawalls – extended prediction methods Proc. Coastlines, Seawalls and Breakwaters 2001 ICE, publn Thomas Telford, London

De Rouck, J., Van de Walle, B., Geeraerts, J., Troch, P. & Van Damme, L. 2003 Full Scale Wave Overtopping Measurements. Proceedings of Conf. Coastal Structures '03, Portland, USA.

Franco, L., de Gerloni, M. & van der Meer, J.W. 1994 Wave overtopping on vertical and composite breakwaters. Proc 24th Int Conf Coastal End., Kobe, ASCE

Franco, L., Bellotti, G., Briganti, R., De Rouck, J. & Geeraerts, J. 2003 Field measurement of wave overtopping at Ostia yacht harbour breakwater. Proceedings of Conf. Coastal Structures '03, Portland, USA.

Gouldby B.P., Sayers P.B. & Johnson D 1999 Real-time hazard forecasting: Review of implementation and two years operation at Samphire Hoe, Dover. Paper to MAFF Conference on River and Coastal Engineers, Keele.

Jensen, O.J. & Sorensen, T. 1979 Overspilling / overtopping of rubble mound breakwaters. Results of studies, useful in design procedures. Coastal Engineering Vol. 3 1979 pp. 51-65

Pearson J., Bruce T., Allsop W. & Gironella X 2002 Violent wave overtopping – measurements at large and small scale. Proceedings of 28th Int. Conf. Coastal Engineering (ASCE), Cardiff

Pullen, T.A. & Allsop, N.W.H. 2003 CLASH Workpackage 3.3: Samphire Hoe field measurements. Technical Report TR133, HR Wallingford.

Appendix R: Pullen *et al.*, 2004

Pullen, T., Allsop, N.W.H., Bruce, T., Pearson, J. & Geeraerts, J. (2004), *Violent wave overtopping at Samphire Hoe: field and laboratory measurements*, Proc. 29th Int. Conf. Coastal Engineering, 4, pp 4379–4390, ASCE / World Scientific, Singapore, ISBN 981-256-298-2

Appendix R
Pullen *et al.*, 2004

Pullen, T., Allsop, N.W.H., Bruce, T., Pearson, J. & Geeraerts, J. (2004), *Violent wave overtopping at Samphire Hoe: field and laboratory measurements*, Proc. 29th Int. Conf. Coastal Engineering, 4, pp 4379–4390, ASCE / World Scientific, Singapore, ISBN 981-256-298-2.

R.1 Declaration of contribution

The author was one of a closely-knit Edinburgh / HR Wallingford team on the Samphire Hoe field / laboratory comparisons, being involved at all stages of the planning, testing and reporting of the work. The Edinburgh flume tests were carried out by the project's post-doctoral Research Engineer, Pearson, working under the guidance of the author. The author took a detailed interest in the synthesis of the conclusions (including extended discussions with Pullen) and in the editing of the paper.

R.2 Published paper

overleaf

VIOLENT WAVE OVERTOPPING AT SAMPHIRE HOE: FIELD AND LABORATORY MEASUREMENTS

TIM PULLEN & WILLIAM ALLSOP
Engineering Hydraulics and Structures Group, HR Wallingford
Howbery Park, Wallingford, OXON, OX10 8BA, UK

TOM BRUCE & JONATHAN PEARSON
School of Engineering and Electronics, University of Edinburgh
Kings Building, Mayfield Road, Edinburgh, EH9 3JL, UK

JIMMY GEERAERTS
Dept of Civil Engineering, Ghent University
Technologiepark 904, 9052 Ghent, Belgium.

As part of a major European research project into wave overtopping at coastal structures, overtopping discharges have been measured at full-scale on a composite vertical seawall in Southeast England. The measurement site, Samphire Hoe, is an area of reclaimed land just west of Dover on the English channel coast, and is an ideal location for monitoring overtopping. The site is described, and the design and operation of the measurement equipment are also outlined. Overtopping was measured on three occasions and the storms and their results are discussed. Laboratory simulations of these storms in a 2d flume and a 3d basin are also described, and the results are compared to field measurements. It is shown that the field measurements compare well with the laboratory simulations and the empirical prediction method of Besley (1999).

1. Introduction

The processes of wave overtopping of seawalls are not yet understood fully, particularly those that may cause risks to people close behind seawalls (Allsop *et al.*, 2003). There remain important gaps in knowledge, despite significant improvements in recent years. To help reduce uncertainties in the prediction of coastal flooding, HR Wallingford (HRW) and the University of Edinburgh (UEDIN) were commissioned under the CLASH research project to help develop improved prediction methods for use by coastal engineers. CLASH ("Crest level assessment of coastal structures by full scale monitoring, neural network prediction and hazard analysis on permissible wave overtopping") comprises 13 European partners at universities and research institutions, and a substantial amount of this work involves the collection of field data on overtopping and subsequent testing in the laboratory (also see Geeraerts *et al.*, 2004).

The results of the CLASH project are intended to benefit citizens in low lying and populated coastal regions, who depend critically on the performance of coastal structures for defence against storm surges, wave attack, flooding and erosion. Continuing sea level rise and climate change emphasise the need for reliable and robust predictions of overtopping hazards as higher storm surges and more severe storms may lead to flooding. The CLASH project will produce generally applicable prediction methods on the required crest height of most coastal structure types, based on permissible wave overtopping and hazard analysis.

Within CLASH, HRW were committed to a programme of full scale measurements of wave overtopping at the seawall protecting the Samphire Hoe reclamation, Kent, England, shown in Figure 1. These field measurements were completed during the Spring of 2003 and laboratory simulations of these storms were undertaken at UEDIN during Autumn 2003 and at HRW during Summer 2004. In this paper a description of the field and laboratory measurements will be presented and the results compared.

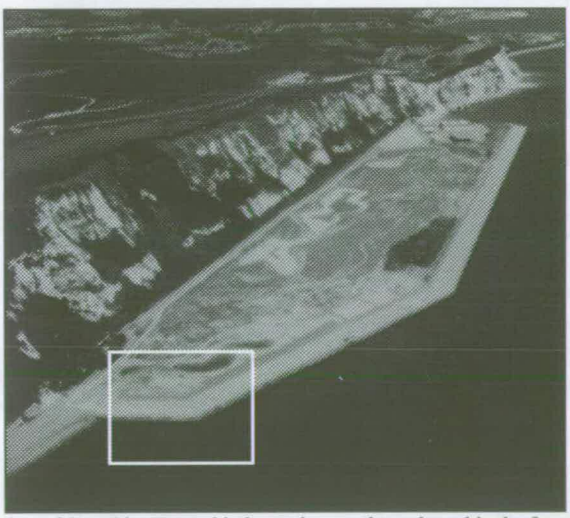

Figure 1: Arial view of Samphire How with the study area shown boxed in the foreground

2. Samphire Hoe

Samphire Hoe is located in the Southeast corner of England immediately to the west of Dover, and is an area of reclaimed land comprising 4.9Mm^3 of chalk marl excavated from the Channel Tunnel. The area of approximately 300,000m^2 is enclosed by a vertical seawall (see Figure 2) with a crest level at +8.22 mODN

and a toe level at –2.42 mODN. To the top of the seawall is a 1.25m parapet wall fronting a 25m stepped promenade where the field monitoring equipment was deployed. Samphire Hoe, which is owned by Eurotunnel, has been landscaped and is operated by the White Cliffs Countryside Project as a public recreational area. The reclamation is exposed to waves from the southwest and southeast, and is subjected to overtopping on approximately 30 days per year.

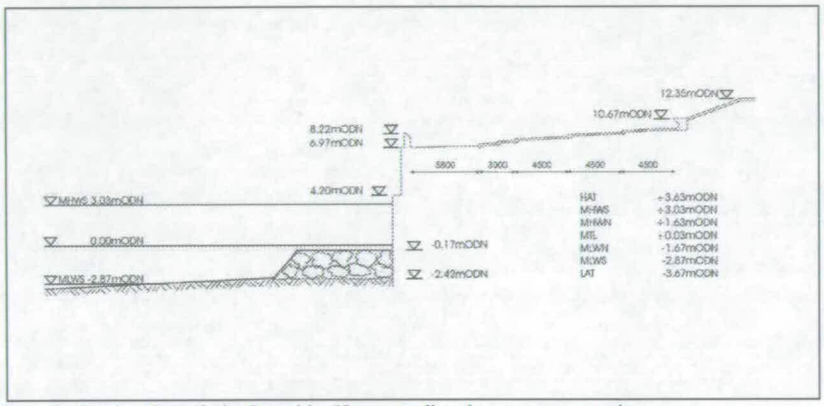

Figure 2: Section through the Samphire Hoe seawall at the measurement site

3. Field Monitoring Equipment

The principal objective in the design of the field monitoring equipment, was to be able to capture sufficient overtopping discharges across the promenade to determine with sufficient accuracy both the total volume and the spatial distribution. As can be seen from Figure 3, the overtopping discharge is distributed over a wide area and it would clearly have been impracticable to attempt to capture all of this discharge. The equipment had to be transported to the site and installed on each visit, and so it had to be handled easily, constructed quickly and be easily transportable.

The main pieces of equipment for measuring the overtopping were three volumetric tanks placed across the promenade of the seawall. The first tank was placed directly behind the parapet wall, and the others were placed inline with the first on the first and second steps of the promenade. This arrangement, along with the control box attached to the rear of the parapet wall, can be seen in Figure 4. Each of the three tanks are divided into two compartments, each with a nominal capacity of 240 litres, and equipped with 350 mbar Druck PTX1830 pressure transducers for measuring the head of water in each compartment. The collected data were recorded at 4Hz on a dataTaker DT800 logger housed in the control box. This was equipped with a 64Mb Compact Flash memory card, and

controlled from a laptop via an RS232 radio modem link. The whole arrangement was battery powered, and a total of 36 hours total recording time was possible.

Figure 3: Violent wave overtopping at Samphire Hoe (Photograph courtesy of Eurotunnel and the White Cliffs Countryside Project)

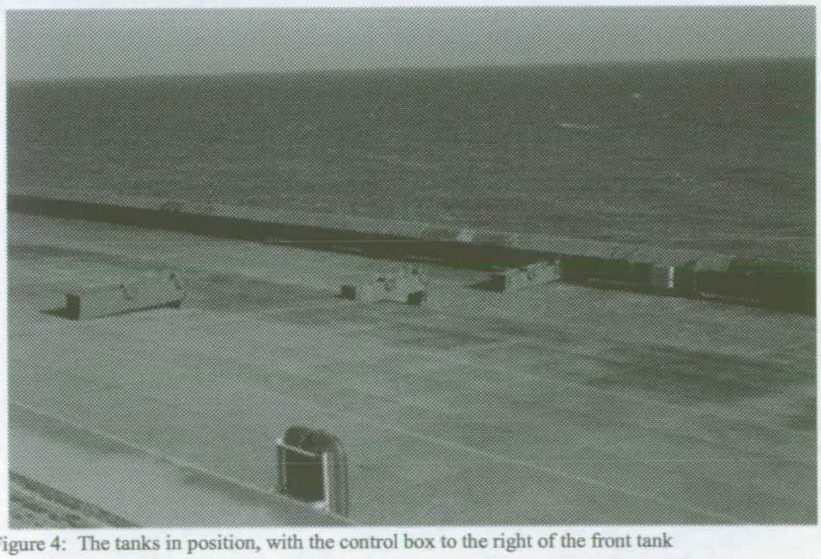

Figure 4: The tanks in position, with the control box to the right of the front tank

The overtopping discharges captured in the tank compartments were allowed to drain freely, and it was only necessary to capture the instantaneous head in each compartment, following each individual overtopping event, to

establish the volume of the discharge. This was necessary because the compartments would fill in a very short period during extreme conditions, but more particularly, it enabled the individual wave-by-wave discharges to be determined. This required that two principal criteria were met. Firstly, that none of the overtopping compartments should ever overfill, and secondly, that the compartments should have sufficient capacity to accommodate the maximum anticipated discharges. Knowledge of the expected wave and water level conditions, and application of Besley's (1999) empirical prediction method for composite vertical walls, allowed the size and number of the drainage holes to be determine for each storm. Overtopping volumes falling between the tanks were estimated from the recorded volumes in the adjacent tanks, and the sum of these were used to establish the total volume for each individual event. Analysis of the volumes in each of the tank compartments also allowed the spatial distribution of the overtopping to be described.

4. Field Measurements at Samphire Hoe

The general criteria for suitable storms causing overtopping at Samphire Hoe are a low pressure system travelling across the Atlantic with a steep pressure gradient arriving over the English channel. This will generally ensure that minimum wind speeds of $8 \sim 10$ m/s can be expected with wind directions between 150° and 240°. These conditions will generally produce wave heights of $H_s > 2$ m, which are sufficient to cause overtopping at the monitoring site. During the winter and spring of 2003 the monitoring equipment was deployed on 10 March, 1 May & 2 May. A range of conditions were encountered during these deployments, and overtopping varied from light spray to high discharges from waves impacting violently on the seawall.

During 10 March storm, overtopping water was seen to appear regularly over the top of the parapet wall, but this was in general sporadic and was spread along the length of the seawall. Those discharges that did pass over the top of the parapet wall were blown widely across the promenade as spray by high wind velocities, but no measurable quantities of overtopping discharge entered into the tanks. A conservative estimate of the mean overtopping discharge rate for this storm would be of the order of say 0.05 l/s/m. On 1 May the wind speeds were at force 7 causing a significant proportion of the overtopping discharges to be distributed as plumes of spray. Nevertheless, with higher discharges than the previous storm, sufficient overtopping was captured to enable an accurate discharge rate to be determined, and where a maximum discharge rate of 0.94 l/s/m was recorded. For the 2 May storm there were no winds and the overtopping discharges were being directed vertically upwards and coming down

in the area directly behind the parapet wall. The maximum discharge measured during the storm was 3.30 l/s/m and peak volumes in excess of 1.5 m^3/m were recorded. The discharges recorded during the storms of 1 & 2 May 2003 have been compared to the empirical prediction method of Besley (1999) for a composite vertical wall, and are shown in Figure 5. A more detailed discussion on the field measurements has been given by Pullen *et al.* (2003)

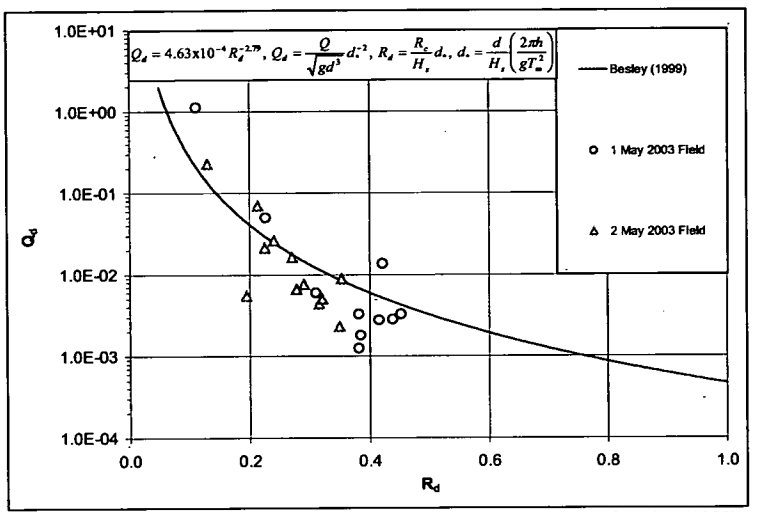

Figure 5: Field measurements compared to the empirical prediction method of Besley (1999)

5. Laboratory Measurements

The Samphire Hoe model was constructed in a 2d laboratory flume at a scale of 1:40 in the School of Engineering at University of Edinburgh, UK. This wave flume is 20 m long, 0.4 m wide and has an operating water depth of 0.7 m. The side walls and the bottom of the flume are made of glass, and the facility is equipped with a moveable impermeable beach that allows a range of slopes from approximately 1:5 to 1:50. Waves were generated by a flap type wave paddle with active absorption. For the 3d basin study at HRW, the model was constructed in a deep water basin at a scale of 1:20. The seawall was modelled over approximately 120 m, which allowed for the direction of the waves and any hydraulic affect that may be expected from waves diffracting around the corner of the walls. The bathymetry was taken down to an offshore depth of h = 18.42 m. Waves were generated by a multi-element wave paddle with active absorption.

Measurements were made of the offshore waves, the waves at the toe of the structure and the wave overtopping characteristics (discharges, individual volumes and spatial distribution). Different equipment was used in each of the two laboratory studies, but the fundamental measurement techniques were the same for both. To determine the wave characteristics, resistance type wave gauges were used with a precision of ±2%. The resistance from the gauge is converted to a voltage, and the relationship between water level and voltage is linear.

Overtopping discharges were directed via a chute into a measuring container suspended from a load cell, which was capable of determining individual volumes to within an accuracy of 2 l/m. Individual overtopping events were detected by high gain resistance gauges that acted as a switch when closed by the water. Wave-by-wave overtopping volumes were measured by determining the increment in the mass of water in the collection tank after each overtopping event following the general approach first used by Franco *et al.* (1994), and subsequently applied at other laboratories in the UK and Europe. The mean spatial overtopping discharges were determined in a series of individual compartments inline and set normal to the seawall. These tanks are calibrated 1 litre containers that can be read to within an accuracy of ±2.5 ml. By expressing the volumes in each of the individual chambers as a proportion of the total collected volume, a model of the spatial distribution can be established (refer to Pullen *et al.* (2004) & Bruce *et al.* (2005) for further details).

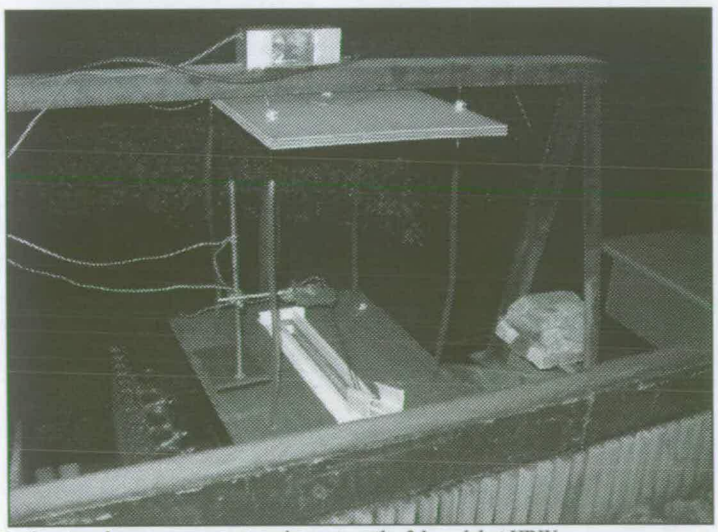

Figure 6: Overtopping measurement equipment on the 3d model at HRW

Figure 6 shows the arrangement of the principal equipment for the 3d laboratory study at HRW. The loadcell is at the top from which is suspended the main overtopping tank suspended freely inside an outer container to separate it from the water in the wave basin. Above the tank the chute is shown, and this simulates the extent and absolute position of the overtopping tanks used for the field measurements (refer to Figure 4). To the front of the chute is the main overtopping detector, and the time-stamped signal from this is compared to the signal from the main overtopping tank so that the individual wave-by-wave volumes can be determined. To the left of the main tank assembly, the spatial distribution tanks can be seen.

6. Analysis

Figure 7 and Figure 8 show the results for the field and both the two laboratory test programmes plotted against Besley's (1999) empirical prediction for the 1 & 2 May 2003 storms, respectively. Generally, the results are in excellent agreement with the prediction, and there are very few exceptions.

In Figure 7 there are a number of results where the values of Q_d are below the prediction line, and this is particularly the case for the field and the 3d simulation results. The wave conditions and water levels for these measurements are very close to the transition between pulsating and impacting conditions (refer to Allsop *et al.* (1995) and Besley (1999)). Pulsating waves will have large vertical run-up values but will not necessarily overtop the crest. Those that are more impacting will send large plumes directly into the air but are less likely to travel over the crest in the absence of any significant wind. During the tests it was observed that when potential overtopping discharges did occur they fell back into the sea as a result of the absence of wind, whereas for the field results, much of the overtopping was blown away from the tanks by the wind. An allowance for the loss of discharges, that not falling into the tanks, was considered during the analysis of the field data, however, in this case it is clear that considerably more water than was originally estimated was lost due to wind blown effects. Moreover, it should be recalled that there were gaps between the overtopping tanks at Samphire Hoe, and that the discharges landing between the tanks have been estimated. It is therefore not possible to be certain what those discharges were, only that they are the best that can be determined. Any differences between the field and laboratory results for certain cases may be entirely due to the difference between the methods used for measuring them. The Edinburgh results show a generally better agreement with Besley (1999) because there was no obliquity ($\beta = 0°$) for these tests, whereas the field and the 3d tests had $\beta = 10°$.

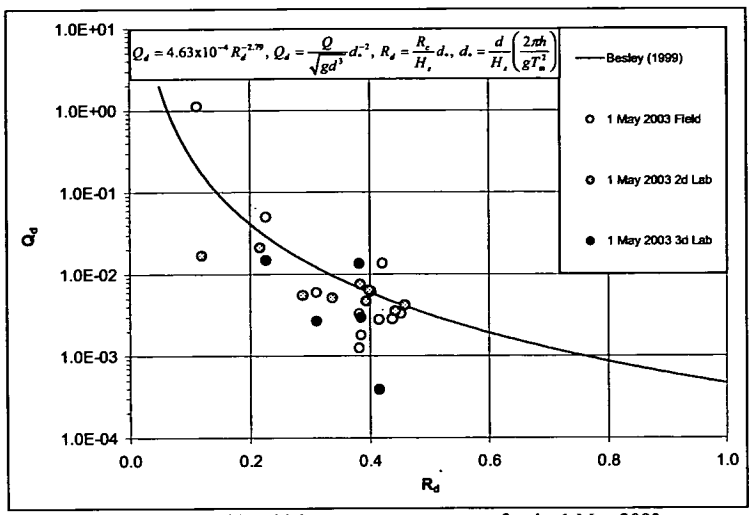

Figure 7: Comparison of the field and laboratory measurements for the 1 May 2003 storm

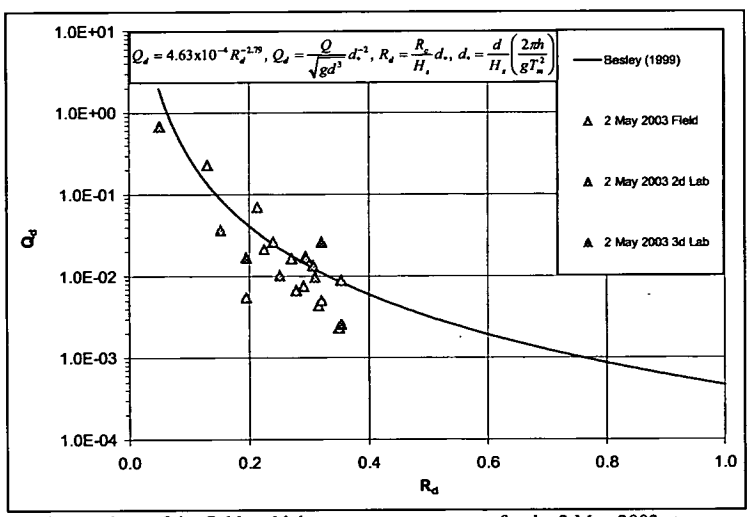

Figure 8: Comparison of the field and laboratory measurements for the 2 May 2003 storm

The 2 May results, shown in Figure 8, are much less scattered than the 1 May results and this may be attributed to two significant factors. There was no wind associated with this storm and the impacting wave and water level conditions were generally more severe than for the previous storm. These results are in excellent agreement with Besley's (1999) prediction, with many lying directly on the prediction curve.

The data from the field and laboratory tests have been compared here and found to be in excellent agreement with Besley's (1999) empirical prediction for composite vertical walls. However, the principal investigation here is how the field measurements and the direct laboratory simulations compare. Figure 9 shows the direct comparisons between the dimensional discharges for the field measurements and the 2d & 3d laboratory test programmes. It is clear that the results are in agreement, with two being directly on the one-to-one comparison line, and the others being mainly clustered around these. There is one significant outlying point, and an explanation for this has been given above. There is a general indication from the cluster of data above the line, that the laboratory measurements may record slightly higher discharges than the field, but these are generally balanced by those below the line. To summarise, these comparisons show that there are no scale effects when the field and laboratory measurements are compared directly.

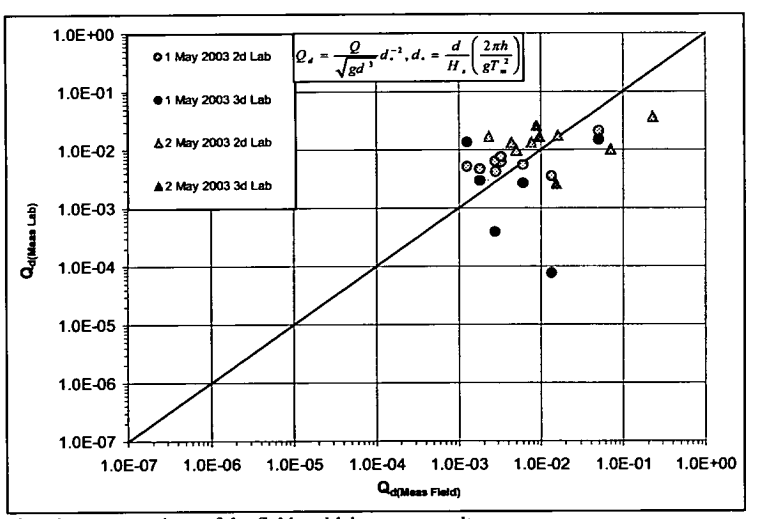

Figure 9: Direct comparison of the field and laboratory results

7. Conclusions

The methods for capturing overtopping discharges and recording the individual wave-by-wave volumes during field and laboratory measurements of overtopping at composite vertical seawalls have been described. The monitoring equipment at the site was deployed during three storms that yielded wave overtopping. Measurements from these storms provided mean overtopping discharges, and these have been simulated in two separate laboratory models at two different scales.

The results from the field and the 2d & 3d laboratory measurements of mean overtopping discharges have been compared. These results have also been compared with the empirical prediction method of Besley (1999) for a composite vertical wall. There are differences among the results, and these can generally be ascribed to modelling effects. These are due to differences between the overtopping tanks in the field and the laboratory, and the presence of wind. It has been shown that there are no scale effects when the field and laboratory measurements are compared, and that generally the results are in agreement with Besley (1999). Moreover, the analysis supports the conclusions of Pearson *et al.* (2001), that there are little or no scale affects between laboratory and field measurements for vertical and composite vertical seawalls.

Acknowledgements

The support of the European Community Fifth Framework for CLASH (http://www.clash-eu.org) under contract EVK3-CT-2001-00058 and defra / EA under FD2412, is acknowledged. The cooperation of Dave Johnson of Eurotunnel and Paul Holt of the White Cliffs Countryside Project, is also gratefully acknowledged. Many thanks, too, to Dr. Stephen Richardson & John Alderson of HRW who assisted during the field measurements, and Coline Romestaing & Jo Wright of HRW for their assistance during the 3d laboratory measurements.

References

Allsop, N.W.H., Besley, P. & Madurini, L. 1995 Overtopping performance of vertical and composite breakwaters, seawalls and low reflection alternatives. Paper to the final MCS Project Workshop, Alderney

Allsop, W., Bruce, T., Pearson, J., Alderson, J & Pullen, T.A. 2003 Violent overtopping at the coast, when are we safe? Int. Conf. on Coastal Management, Brighton, pp 54-69, ISBN 0 7277 3255 2, publn. Thomas Telford, London

Besley P. 1999 Overtopping of seawalls – design and assessment manual. R & D Technical Report W 178, ISBN 1 85705 069 X. Download from the link at www.hrwallingford.co.uk/projects/overtopping/index.html

Bruce, T. Pullen, T. Allsop, W. & Pearson, J. 2005 How far back is safe? Spatial distributions of wave overtopping. Proc. Coastlines, Seawalls and Breakwaters, ICE, Thomas Telford, London

Franco, L., de Gerloni, M. & van der Meer, J.W. 1994 Wave overtopping on vertical and composite breakwaters. Proc 24th Int. Conf. Coastal. Engng., Kobe, ASCE

Geeraerts, J. Troch, P., de Rouck, J. Williems, M. Franco, L., Bellotti, G., & Briganti, R. 2004 Wave overtopping at Ostai yacht harbour breakwater compariosn between prototype and model tests in 2d and 3d. Proc 29th Int. Conf. on Coastal Engng. Lisbon, Portugal.

Pearson J., Bruce T., Allsop W. & Gironella X 2002 Violent wave overtopping – measurements at large and small scale. Proceedings of 28th Int. Conf. Coastal Engineering (ASCE), Cardiff

Pullen T., Allsop, N.W.H. Bruce, T. & Geeraerts, J. 2003 Violent wave overtopping: CLASH Field Measurements at Samphire Hoe. Proc. Coastal Structures 2003, ASCE.

Pullen T, Allsop W., Pearson J. & Bruce T. 2004 Violent wave overtopping discharges and the safe use of seawalls defra Flood & Coastal Management Conference, York, June.

Appendix S: Bruce *et al.*, 2001b

Bruce, T., Franco, L., Alberti, P., Pearson, J. & Allsop, N.W.H. (2001b), *Violent wave overtopping: discharge throw velocities, trajectories and resulting crown deck loading*, Proc. Ocean Wave Measurement and Analysis ('Waves 2001'), 2, pp 1783–1796, ASCE, New York, ISBN 0-7844-0604-9

Appendix S
Bruce *et al.*, 2001b

Bruce, T., Franco, L., Alberti, P., Pearson, J. & Allsop, N.W.H. (2001b), *Violent wave overtopping: discharge throw velocities, trajectories and resulting crown deck loading*, Proc. Ocean Wave Measurement and Analysis ('Waves 2001'), 2, pp 1783–1796, ASCE, New York, ISBN 0-7844-0604-9

S.1 Declaration of contribution

Alberti was a student at University of Roma Tre, working under the guidance of Prof. Franco. Alberti visited Edinburgh for four months, where he carried out the tests reported here under the day-to-day guidance of the author. The paper was presented to the conference by the author, and was involved further in detailed preparation and editing of the paper text.

S.2 Published paper

overleaf

VIOLENT WAVE OVERTOPPING: DISCHARGE THROW VELOCITIES, TRAJECTORIES AND RESULTING CROWN DECK LOADING

Tom Bruce[1], Leopoldo Franco[2], Paolo Alberti[3], Jonathan Pearson[4] and William Allsop[5]

Abstract: This paper discusses wave processes that happen *after* a wave has impacted on a coastal structure. The paper gives, for the first time, measurements of the throw of overtopping waves at vertical seawalls / breakwaters, including their velocity / trajectory, and the loadings that result when overtopping water lands back onto the deck of the structure.

1. INTRODUCTION

Pressures generated by overtopping waves on the crown deck of a vertical breakwater or seawall have a direct effect upon the serviceability of the structure, on durability of the crown pavement, and on the safety of infrastructure or equipment placed behind the crown wall. Impact of overtopping on people, vehicles (road or rail) constitute significant potential hazards, see Figure 1 which shows overtopping at a major commuter railway line at Saltcoats, on the Scottish coast south of Glasgow. Despite these dangers, and significant investigations on wave impacts on vertical / steep walls, these (post-overtopping) processes and loadings have seen almost no detailed study. One of the few references dates back to Shield (1895), who made a qualitative description of the phenomenon, and linked crown deck loadings with damage to breakwaters at Alderney and Wick.

Recent anecdotal evidence indicates the magnitude of the phenomenon. A steel plate covering an enclosure on the crown deck of the South Breakwater at Peterhead, Scotland was observed to have been "dished" during a storm which gave rise to violent overtopping events. The plate measured ~ 0.7 m x 0.7 m x 12 mm, and was dished by ~ 20 mm, suggesting pressures ~800 kN/m^2. (This example will be re-visited later in the paper.)

1 Lecturer, Division of Engineering, University of Edinburgh, King's Buildings, Edinburgh, EH9 3JL, Scotland, UK; Tom.Bruce@ed.ac.uk
2 Professor, Dept Civil Engineering, University of Rome III, via V. Volterra 62, 00146 Rome, Italy
3 Research Engineer, Dept Civil Engineering, University of Rome III, via V. Volterra 62, 00146 Rome, Italy
4 Research Fellow, Division of Engineering, University of Edinburgh, Scotland, UK.
5 Professor (associate), Civil Engineering, University of Sheffield, UK / Technical Director, HR Wallingford.

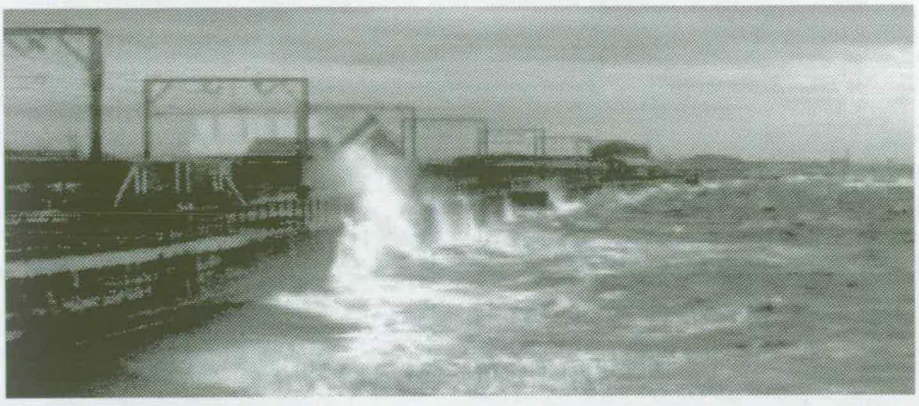

Figure 1: Overtopping of seawall at Saltcoats, Scotland (photo: HR Wallingford)

This paper reports results from physical model studies on impact pressures which, although at small scale, provides a first source of information for the estimation of wave impact pressures on the crown deck of a breakwater or seawall by overtopping waves (Sections 2 - 3). Also reported for the first time are measurements of velocity of throw discharge as it leaves the crest of the structure (Sections 4 - 5).

2. WAVE ACTION AT VERTICAL SEAWALLS / BREAKWATERS

2.1 Physical description of problem

The form of interaction of a wave with a vertical or near-vertical seawall or breakwater may be seen to fall into two broad categories: "impacting / impulsive" or "pulsating / reflecting" (Figure 2). The physics of the two cases are quite distinct and, as a result, different prediction models are required. A key outcome of the EC project PROVERBS, see Oumeraci *et al* (2001), was the development of a "parameter map" or "decision diagram" identifying wave / structure geometry combinations particularly susceptible to breaking wave events. Thus, it has become possible to characterise a wave / structure combination as "impacting" or "pulsating". In terms of wave overtopping phenomena, this distinction relates to *green water* versus *violent / impulsive* overtopping events.

Figure 2: Pulsating (left) and impulsive (right) wave action at a wall.

- *Green water* overtopping results from a pulsating wave running up and over the crest
- *Impulsive* or *violent* overtopping results when a wave breaks at or close to the structure, throwing the discharge in a near-vertical direction with some violence.

"Spray" overtopping, wind action on the overtopping discharge and upon the incident waves are, for reason of difficulty in scaling, not included in most laboratory studies. Studies by Ward et al (1994, 1996) suggest that very strong winds may influence run-up and

overtopping, but experiments by de Waal et al (1996) indicate that the contribution by spray overtopping is small in relation to realistic design cases.

The magnitude and characteristics of the loadings on the front face of a structure under impacting conditions have been the subject of extensive research under PROVERBS resulting in prediction formulae, see Allsop & Vicinanza (1996), Allsop (2000). Similar categorisation for overtopping events is discussed by Besley et al (1998) and Besley (1999) who applied a parameter h* (Section 4).

2.2 Overtopping discharge throw and resulting forces

A wave colliding with a vertical wall is reflected both horizontally and vertically. If the wave run-up is higher than the crest, the water impinging the vertical wall is projected into the air with a vertical velocity u_{0z} and a horizontal velocity u_{0x} due to the original motion direction. Gravity and air resistance govern the flying jet's subsequent trajectory.

Considering water density ρ to be constant during the impact, and assuming dissipating phenomena and inertial forces to be negligible, the pressure generated by a jet with a velocity v impacting on a flat horizontal surface in stationary conditions would be given by $p = \rho v^2$. Thus if we knew the velocity of the landing water, we could infer a value of the generated pressure. In reality however, this phenomenon is rather more complex and is non-stationary, so cannot be described fully theoretically.

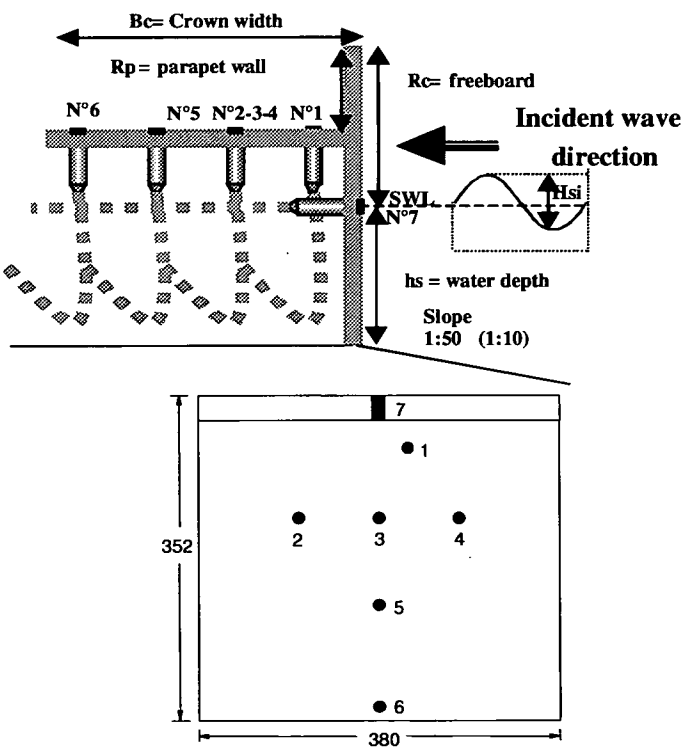

Figure 3: Model seawall and locations of pressure transducers - elevation (upper) and plan view (lower). Dimensions in mm.

3. CROWN DECK LOADING

3.1 Experimental Setup

Model tests at the Engineering Fluids Mechanics laboratory of the University of Edinburgh used a 20m long, 0.4m wide wave flume with an operating water depth of 0.7 m. The absorbing wave maker is controlled by a PC and generated waves to a JONSWAP spectrum. Each test used approximately 1000 waves. An artificial seabed with a changeable slope modelled different water depths at the structure toe. The sidewalls and the base of the tank are glass, allowing good visualisation of the flows. The model seawall shown in Figure 3 was constructed from clear acrylic (Perspex) and mounted on the impermeable beach. It consisted of a vertical board 27 mm thick and of a horizontal board that can be set at two different heights from the toe, thus reproducing conditions with and without a parapet wall. Pressures were measured with seven transducers connected to a signal-conditioning unit that is itself connected to a PC. This system provides a time history of the pressure and allows sampling at rates up to 2 kHz with little distortion in order to capture the shape of the pressure impulse. The crown slab has six slots designed to hold the pressure transducers, placed with the sensor facing up to measure the pressure generated by the falling water.

3.2 Test Matrix

The experimental programme was intended to cover the widest possible range of conditions and study both low and high crested structures. From visual observation during preliminary tests, it was noticed that a low crested structure allows large green overtopping which presumably produces small impacting pressures but high total loads. Conversely, a high crested structure allows smaller overtopping rates but projects the overtopping jets up to large heights with consequent large falling impacts. It was difficult then to establish which of the two conditions was the most dangerous and also whether the presence of a parapet wall could influence the phenomenon. A total of 80 tests were performed; two front wall heights were employed and, by changing the water depth (h_s), eight different freeboards (R_c) were tested. Table 1 shows the range of structure geometries and random sea conditions tested. Measurements of wave transmission by overtopping are reported separately by Alberti *et al* (2001).

Table 1: Test conditions for crown deck loading experiments

R_c = 0; 50; 85; 98; 140; 150;155;198 mm	
h_s = 85; 142; 155; 190; 240 mm	$60 \le H_{si} \le 113$mm
$0 \le R_c/H_{si} \le 2.51$	$1.06 \le d/H_{si} \le 3.36$
$0.02 \le s_p \le 0.06$	T_p= 1.0, 1.3, 1.7 s
B_c= 350 mm	R_p= 0; 100 mm

As these processes are highly dynamic, rapid data sampling is essential for accurate measurements. Sampling at f_{samp} = 2 kHz was adopted to detect short duration peak pressures, noting that Schmidt (1992) measured peak pressure generated by waves on a vertical wall at f_{samp} = 2 kHz with only 2% reduction over those measured at f_{samp} = 11 kHz.

3.3 Results

Example pressure histories for two transducers are shown in Figure 4. Transducer 1 is immediately behind the crest of the structure; transducer 2 is a further 70 mm behind the crest. Two quite distinct forms are observed. At transducer 1, a very sudden rise to a high peak pressure is observed, consistent with a highly impulsive event – here, the direct impact of the falling overtopping discharge jet. The event looks somewhat different at transducer 3, where a quasi-static load is observed as the overtopping volume which landed at / near transducer 1 flows out over the surface of the deck. This form of trace would also be consistent with a *green water* overtopping event.

The pressure rise time at transducer 1 is exceedingly rapid, with the maximum reached in about 2 ms. Pressure oscillations and multiple peaks are observed after the first maximum, due to the compression of air pockets. This indicates that entrapped air has a role in the phenomenon for low crested structures, although it should be noted that this role may be exaggerated in 2-d wave channel tests such as these. The expansion of entrapped air can generate suction (negative force) which may be significant in, *eg*, dislodging elements in a blockwork wall.

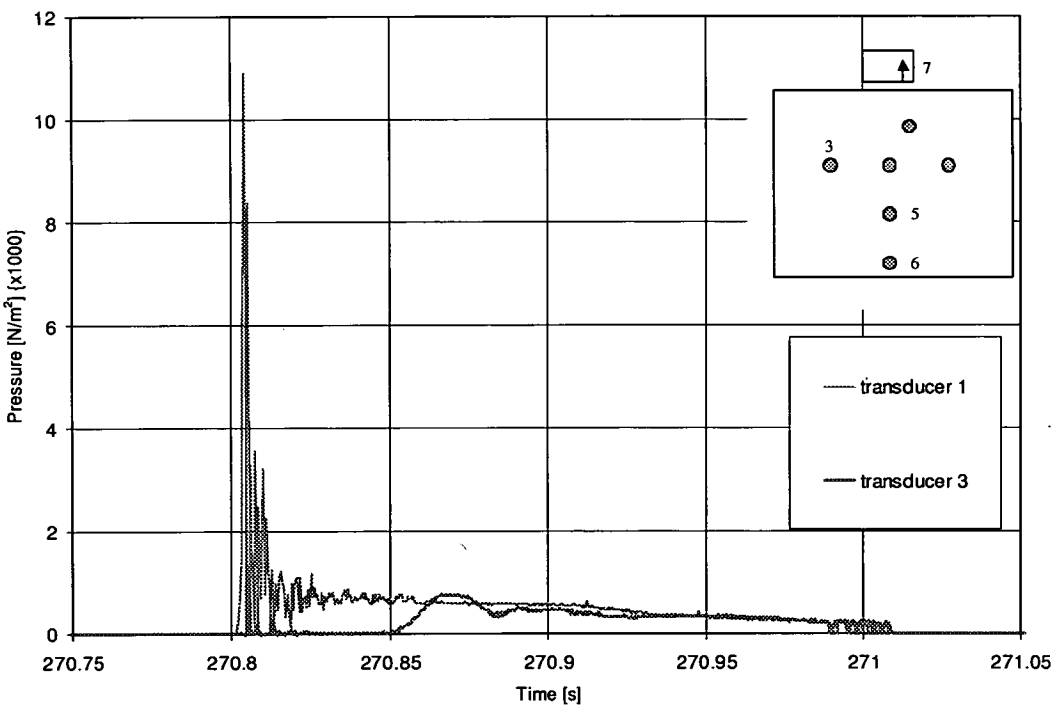

Figure 4: Example pressure histories on the crown deck.

The pressure peaks are evidently highly localised so the exact position of the transducer is of great importance to the measurements. The area of the slab where maximum pressures were measured is within a distance of 1.5 H_{si} from the seaward wall. The higher the crest elevation the closer is this distance to the front wall. For low crested structures (R_c/H_{si} < 0.5), the distance of maximum peak pressures location increases up to 2 H_{si}. Behind this area the pressure is due to the quasi-static load of the water that, after landing, is

transformed in a horizontal landward flow, see Takahashi (1994). These observations are again consistent with the distinction between green water and impulsive overtopping events.

To assess their significance, the highest peak pressures measured during each test (one per test) over the crown slab are plotted in Figure 5 against the highest peak pressures measured on the front wall for that test. The two measurements do not necessarily arise from the same tests as no clear relation was found between them. The two populations have a similar order of magnitude, with pressures on the front wall reaching higher values.

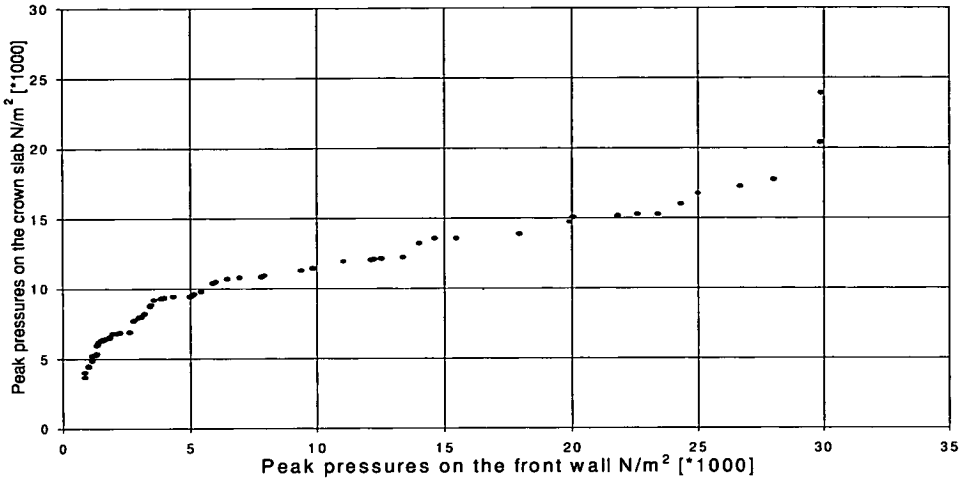

Figure 5: Maximum pressures on the crown deck plotted against (for each test) front face pressure maximum.

As expected, plunging breakers generally generate the highest pressures, at least under high-freeboard conditions. All attempts to correlate pressure maxima with crest elevations or sea state parameters (wave period and steepness) gave little insight, confirming that the process is highly stochastic, as might be expected from the complex overtopping dynamics. However, this should not to be seen as a failure in the investigation: it is well-known that pressure measurements are deeply influenced by boundary conditions and the transient and localised nature of them is frequently test specific. Even pressures generated by nominally identical conditions are only predictable in a statistical sense, see Walkden (1997).

Within the 71 tests on the 1/50 sloped beach the dimensionless pressure $P^* = P_{1/250}/\rho g H_{si}$, has a maximum value of $P^*=17$ and a mean value of $P^*=8$. The highest value was obtained with the highest freeboard without the parapet wall, but there is no general trend with variable freeboard. Comparison of Weibull non-exceedance probabilities for pressure on the front wall (based on the number of waves) and on the crown slab (based on the number of overtopping events) in Figure 6 show broadly similar distributions.

Moving from the distribution of pressure events for a single test to seek a more general result, an equation was fitted to the Weibull distributions for the 20 largest events (at any transducer location) from each of the 71 tests. The resulting equation with correlation coefficient of 0.84 is:

$$Ln\left(-Ln\left(1-prob\left(\frac{P}{\rho g H_{si}}\right)\right)\right)=0.21+0.6\,Ln\left(\frac{P}{\rho g H_{si}}\right)-0.14\frac{R_c}{H_{si}} \qquad (1)$$

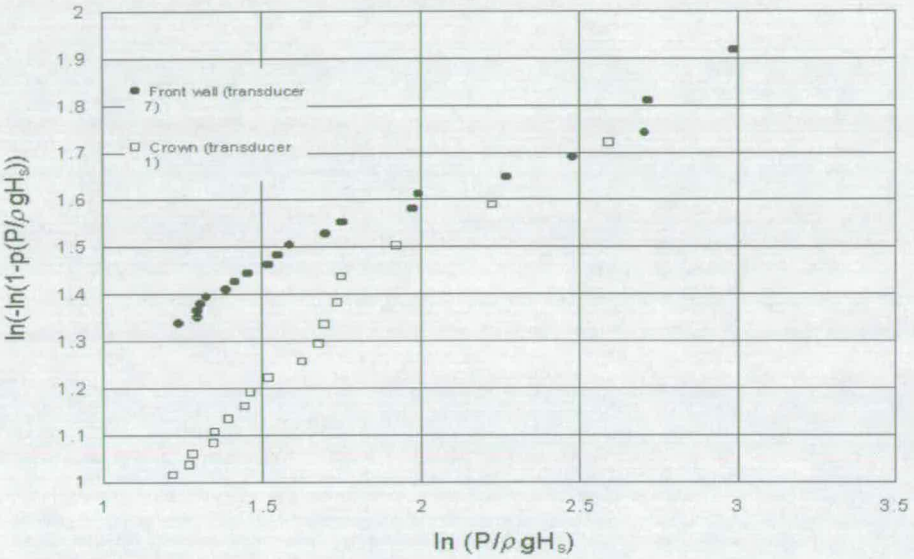

Figure 6: Weibull probability for pressures on front wall and crown deck.

Returning to the example of the dished deck plate; representative figures for the key parameters; $H_s \sim 5$m, $T_p \sim 8$s, two-hour storm peak giving ~ 1000 waves; used in equation (1) give $p_{max} \sim 850$ kN/m^2 – in broad agreement with the order of magnitude inferred from the damage observation.

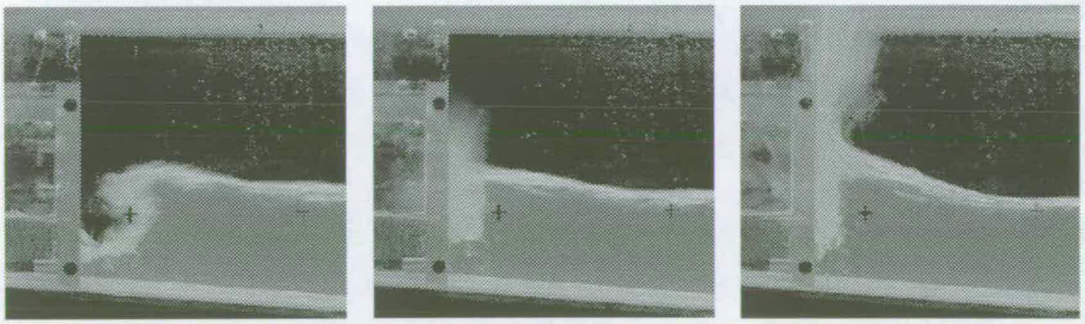

Figure 7: Frames from video used in measurement of throw velocities.

4. OVERTOPPING DISCHARGE THROW VELOCITY

As noted in Section 2.2, if the velocity and trajectory of the overtopping discharge "jet" was known, it could give an estimator for the magnitude and location of the pressures. The uncertainties in this process make direct measurements, as reported above, more reliable. There is however another strong motivation for the direct measurement of velocities and trajectories – the assessment of immediate hazard to pedestrians and vehicles in the path of an overtopping event.

The vertical velocity of the thrown discharge was measured directly from video records, see Figure 7, for each of the largest 20 discharge events recorded from a 1000-wave sequence. This was done for 14 1000-wave tests over a range of wave and structure parameters, from which Weibull distributions of throw velocities were plotted (Figure 7).

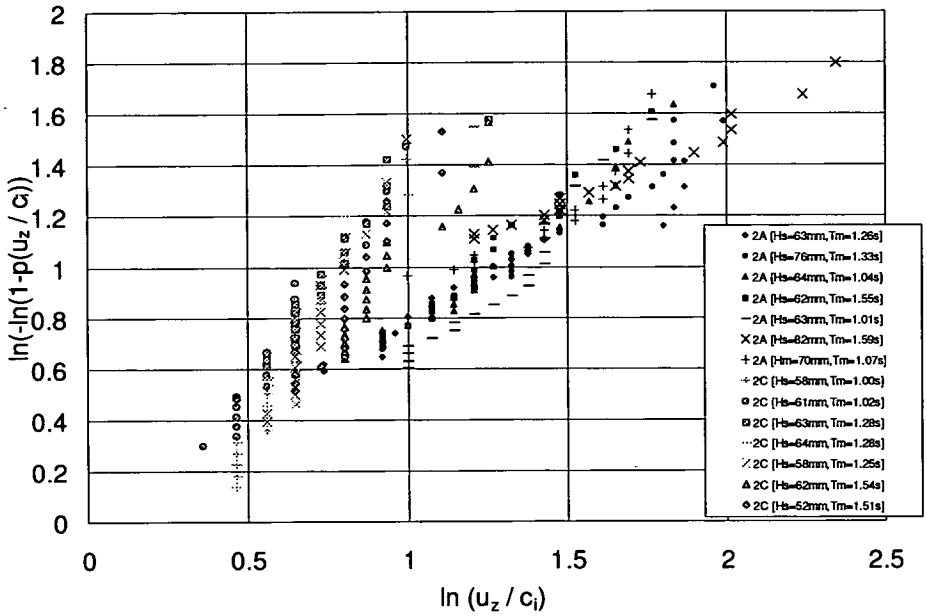

Figure 8: Weibull distribution of throw velocities associated with 20 largest discharge events; 14 tests.

It is clear that the throw velocity distributions form two distinct "populations". For the largest events (upper points on the chart), the group to the right reach a given non-exceedance probability level at velocities significantly greater than those in the left group. This observation is consistent with the qualitative distinction drawn between *green water* and *impulsive* overtopping events.

The dependence of the throw velocity upon wave parameters was investigated. For this purpose, a single measure of vertical throw velocity, u_z, was adopted to characterise each test condition. This measure was chosen as $u_{z,\,1/25}$ – the mean of the largest 4% of throw velocities for that 1000-wave sequence, based upon the recorded number of overtopping events, $N_{OW,\,actual}$. The 1/25 level was chosen in the expectation that it would provide a more stable (arbitrary) measure than a higher non-exceedance level, *eg* 1% or 1/100. Comparison of $u_{z,\,1/25}$ with the usual inshore wave parameters (zero-crossing period, significant wave height and wave steepness) gave little indicator of a possible throw velocity predictor.

Physically, what is required is a predictor which characterises the violence of wave action at the wall for a particular sea state / structure combination. Besley (1999), after Allsop *et al* (1995) presents the "h*" parameter for such a purpose:

$$h^* \equiv \left(\frac{h_s}{H_{si}}\right)\left(\frac{2\pi h_s}{g T_{mi}^2}\right) \qquad (2)$$

where h_s is the water depth at the structure. Besley suggests that *impulsive* wave action is significant for $h^* < 0.3$; *pulsating* conditions dominating for $h^* > 0.3$.

Then throw velocity $u_{z\ 1/25}$, can be non-dimensionalised by inshore wave celerity, $c_I = (gh_s)^{0.5}$ plotted in Figure 9 against h^* . The result is striking: for $h^* > \sim 0.15$, the dimensionless throw velocity is fairly constant at ~ 2 – 2.5 times the inshore wave celerity, but as h^* drops below 0.15, the dimensionless throw velocity is observed to increase quite dramatically to 5 or 6 times the inshore wave celerity. This observation is in line with the qualitative distinction between *green water* and *impulsive* overtopping regimes. For $h^* >$ 0.15, the wave is running up and over the structure at a velocity of the same order as that of the wave crest. For $h^* < 0.15$, the overtopping discharge is thrown violently up at speeds greatly in excess of even the wave crest velocity.

The findings here suggest that whilst transition from *impulsive* to *green water* overtopping may start at h^* around 0.3, as suggested by Besley (1999), the process becomes significantly more violent as h^* reduces to 0.15 or less.

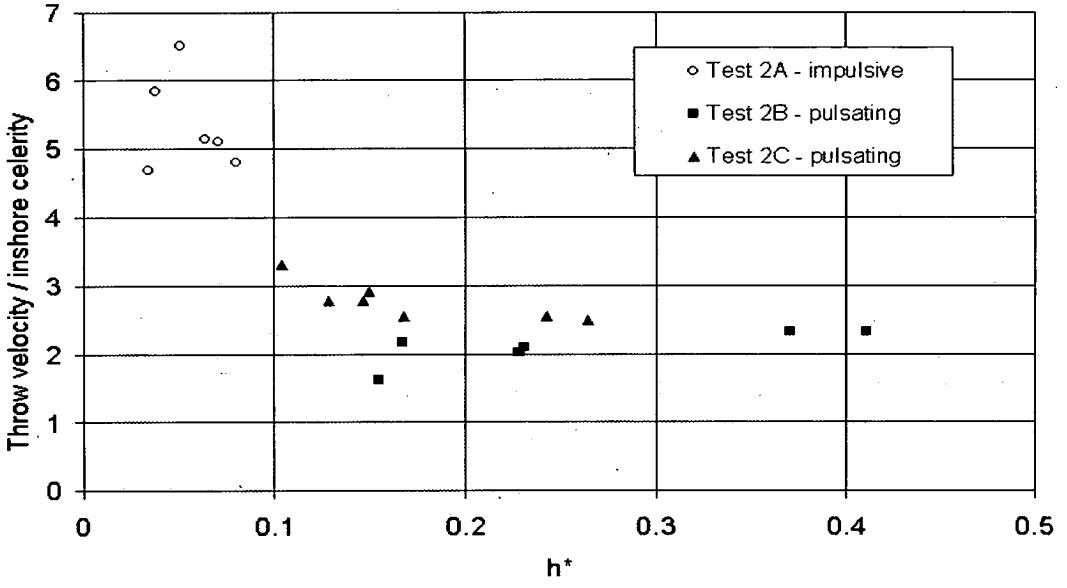

Figure 9: Dimensionless throw velocity plotted against h*.

5. THROW TRAJECTORY

The further key element in relating overtopping discharge to actual hazards is the prediction of the loaction of the hazard. The crown deck loading measurements reported in Section 3 give some indication. Equally, knowledge of the initial throw velocity (speed *and* direction), combined with a model of the subsequent travel could give useful insights. However, a direct approach has some merit, at least as a means of calibrating a model, which could subsequently be developed to quantify *eg* wind effects. Here, we report a first attempt at automated measurement of the trajectory of the thrown discharge, at the large wave flume at Universitat Polytechnica Catalunya, Barcelona, Spain.

The "throw board" (Figure 10, left, and visible above the left-hand end of the wall's crest in Figure 14, right) consisted of a 64 individual detector elements arranged in an 8 x 8 array at 350mm pitch. Each detector consists simply of a pair of conductors, making a switch which is closed by the presence of water. The state of all 64 switches is converted to 64 digital (on/off) signals and these signals sampled by a PC at 300 Hz. The board itself is mounted with its top and rear tilted very slightly in, in order to minimise interference to the flow of the discharge as it moves over the board.

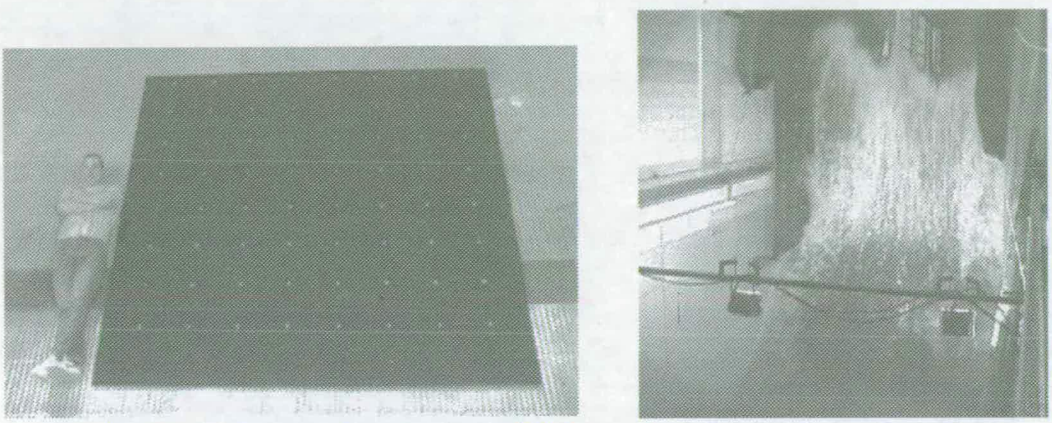

Figure 10: The trajectory detector board (left) and (right) in place above the test structure in the large flume at UPC, Barcleona.

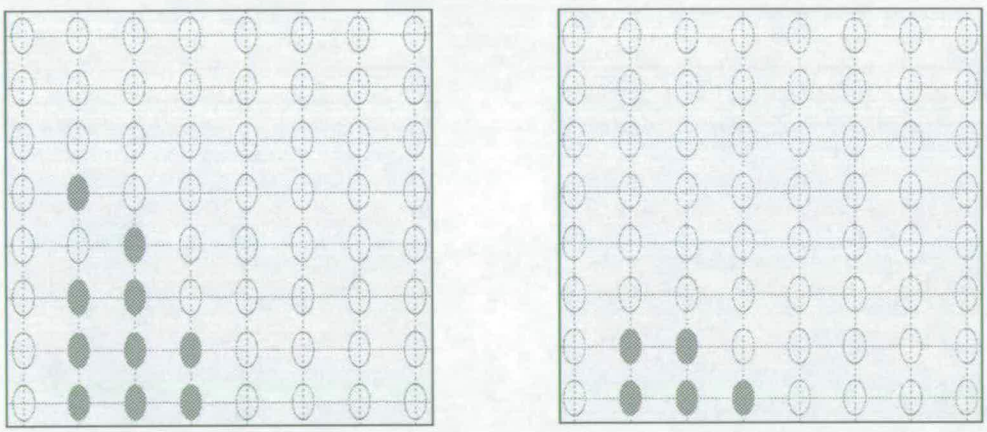

Figure 11: "Snapshot" examples of output from overtopping trajectory device.

A real-time display of the status of the detectors was implemented to enable qualitative assessment of the operation of the devise. A macro written in "Excel" enables a visual "playback" of events from the stored data file. Visualised data during an impulsive overtopping event (left) and green water event (right) are shown in Figure 11. Trajectory data have been obatined from 30 tests at UPC, Barcelona, each test of 1000 irregular (JONSWAP) waves. Systematic analysis of these data is in progress at the time of writing.

6. CONCLUSIONS

Wave impact pressures have been measured on the crown deck of a small-scale breakwater model for 71 test conditions, with each test consisting of 1000 waves of a JONSWAP spectrum. Over all tests, the pressure at 1/250 level may be described by:

$$2 < \frac{p_{1/250}}{\rho g H_{si}} < 17 \quad \text{with a mean value of 8.}$$

For high-crested structures ($R_c / H_{si} > 0.5$) the pressure maxima were observed typically to fall within a distance of 1.5 H_{si} behind the structure crest. For lower-crested structures ($R_c / H_{si} < 0.5$), this distance was observed to increase to ~ 2 H_{si} .

An approximate Weibull distribution has been fitted to all data on crown deck pressures.

It has been observed that, for a given sea state / structure geometry condition. crown deck pressure maxima are smaller than *but of the same order of magnitude as* the pressure maxima recorded on the front face of the structure.

For wave / structure conditions giving a large number of impulsive events ($h^* < 0.15$), it has been observed that the velocity of the thrown overtopping discharge is 5 - 7 times the inshore wave celerity. For less impulsive regimes ($h^* > 0.15$), throw velocities ~ 2 - 2.5 times the inshore wave celerity are observed.

Measurements of the trajectories followed by overtopping discharge have been carried out at large scale. Full analysis and identification to actual hazard are underway. Tests at prototype sites may be required if scale and wind effects are to be fully investigated.

ACKNOWLEDGEMENTS

Paolo Alberti's work in Edinburgh was supported by the "Blockwork Coastal Structures Network" funded by the UK EPSRC (under GR/M00893). Work on throw velocities was carried out under the UK "Violent Overtopping by Waves at Seawalls (VOWS)" project, funded by the EPSRC (GR/M42312). Access to the large wave channel at UPC Barcelona was made possible by the EC-funded "Hydralab" project under the Transnational Access to Major Research Infrastructure (TAMRI) scheme. These tests were further supported by the UK EPSRC under GR/R42306. The support of the UPC team under Prof Sanchex Arcilla and Javier Pineda is gratefully acknowledged, with special thanks for the efforts of Xavi Gironella, Quim Sospedra and Oscar Galego.

REFERENCES

Alberti P., Bruce, T. and Franco L. 2001. Wave transmission behind vertical walls due to overtopping, *Proc Coastlines, structures and breakwaters 2001*, Institution of Civil Engineers, London.

Allsop N.W.H. 2000. Wave forces on vertical and composite walls. Chapter 4 in *Handbook of Coastal Engineering*, pages 4.1-4.47, Editor J. Herbich, ISBN 0-07-134402-0, publn. McGraw-Hill, New York.

Allsop N.W.H., Besley P. and Madurini L. 1995. Overtopping performance of vertical walls and composite breakwaters, seawalls and low reflection alternatives. Paper 4.7 in MAST II *MCS Project Final Report*, publn University of Hannover.

Allsop N.W.H. and Vicinanza D. 1996. Wave impact loadings on vertical breakwaters: development of new prediction formulae. *Proc. 11th International Harbour Congress*, Antwerpen, Belgium.

Besley P. 1999. Overtopping of seawalls – design and assessment manual. R & D Technical Report W 178, ISBN 1 85705 069 X, *Environment Agency*, Bristol.

Besley P.B., Stewart T, and Allsop N.W.H. 1998. Overtopping of vertical structures: new methods to account for shallow water conditions. *Proc. Int. Conf. on Coastlines, Structures & Breakwaters '98*, pp46-57, ICE / Thomas Telford, London.

Oumeraci, H., Kortenhaus, A., Allsop, N.W.H., de Groot, M., Crouch, R., Vrijling, H. and Voortman, H. (2001) "*Probabilistic Design Tools for Vertical Breakwaters*" publn. A.A.Balkema, ISBN 90 5809 248 8.

Schmidt R., Oumeraci H. and Partenscky H-W. 1992. Impact loads induced by plunging breakers on vertical structures. *Proc. 23rd Int. Conf. on Coastal Eng,* 2, pp1545-1558 (ASCE)

Shield, W., 1885: *Principle and Practice of Harbour Construction* Longmans' *Civil Engineering Series.* London.

Takahashi S., 1994: An Investigation of the Wave Forces Acting on Breakwater Handrails. *Proc. 23rd Int. Conf. on Coastal Eng,* 1, pp1046-1060 (ASCE)

De Waal, J.P. Tonjes, P. and van der Meer, J.W. 1996. Overtopping of sea defences. *Proc 25th Int. Conf. Coastal Eng*. pp2216-2229 (ASCE)

Walkden, M.J., Crawford, A.R., Hewson, P.J. and Bullock, G.N. 1997. Scaling, *Proc. Task 1 Edinburgh technical workshop of PROVERBS project* , EC DG XII MAS3-CT95-0041

Ward, D.L., Wibner, C.G., Zhang, J. and Edge, B. 1994. Wind effects on runup and overtopping. *Proc 24th Int. Conf. Coastal Eng.*, pp1687-1699, (ASCE)

Ward, D.L., Zhang, J., Wibner, C.G. and Cinotto, C.M. 1996. Wind effects on runup and overtopping of coastal structures. *Proc 25th Int. Conf. Coastal Eng.* pp2206-2216 (ASCE)

Appendix T: Bruce *et al.*, 2002

Bruce, T., Allsop, N.W.H., & Pearson, J. (2002), *Hazards at coast and harbour seawalls – velocities and trajectories of violent overtopping jets*, Proc. 28th Int. Conf. Coastal Engineering, 2, pp 2216–2226, ASCE, World Scientific, Singapore, ISBN 981 238 238 0

Appendix T
Bruce *et al.*, 2002

Bruce, T., Allsop, N.W.H., & Pearson, J. (2002), *Hazards at coast and harbour seawalls – velocities and trajectories of violent overtopping jets*, Proc. 28th Int. Conf. Coastal Engineering, 2, pp 2216–2226, ASCE, World Scientific, Singapore, ISBN 981 238 238 0

T.1 Declaration of contribution

For this paper, the author drew together data and evidence from a number of sources, particularly from laboratory data and footage taken by Pearson under *VOWS* and *Big-VOWS* projects (Sections 3.3 and 3.9) – work carried out under the author's detailed guidance. The author presented the paper to the conference, and led the drafting and editing of the final paper.

T.2 Published paper

overleaf

HAZARDS AT COAST AND HARBOUR SEAWALLS –VELOCITIES AND TRAJECTORIES OF VIOLENT OVERTOPPING JETS

Tom Bruce[1], Jonathan Pearson[2] and William Allsop[3]

Abstract: This paper describes new research under the VOWS (Violent Overtopping of Waves at Seawalls) project. Established guidance on admissible overtopping volumes is based upon values of mean discharge. In cases where hazard to pedestrians / vehicles are concerned, it is clear that an admissible level of overtopping would be more appropriately based upon the volume of an individual overtopping event. Further, the hazard presented is not only a function of the volume of that overtopping wave, but also of the speed and trajectory of the jet. Methods exist to predict maximum individual overtopping volumes. This paper presents new data and a first predictive tool for overtopping "throw velocities", and first data from a device designed to measure directly the trajectories of overtopping jets.

1. INTRODUCTION

One of the main purposes of seawalls and related structures around harbours and along coastlines is to provide shelter against wave action for people, working, travelling, recreating, (see examples, Figure 1). For the last 20 years, most useful design methods to dimension such seawalls against effects of wave overtopping have concentrated on the mean overtopping discharge averaged over 500 or 1000 random waves. Some recent research has given more emphasis on wave-by-wave overtopping volumes, but even the most recent work has only just started to identify key aspects of performance which affect the safety of people working or travelling behind such seawalls. It is clear that improved

1 Lecturer, School of Engineering and Electronics, University of Edinburgh, King's Buildings, Edinburgh, EH9 3JL, UK. Tom.Bruce@ed.ac.uk
2 Research Fellow, School of Engineering and Electronics, University of Edinburgh, King's Buildings, Edinburgh, EH9 3JL, UK. J.Pearson@ed.ac.uk
3 Professor (associate), Civil Engineering, University of Sheffield, Technical Director, HR Wallingford, Wallingford, OX10 8BA UK. W.Allsop@shef.ac.uk

guidance will require not only reliable tools for the prediction mean overtopping; volumes of individual, overtopping volumes; but must also include the speed and trajectory of these peak discharges (Figure 2).

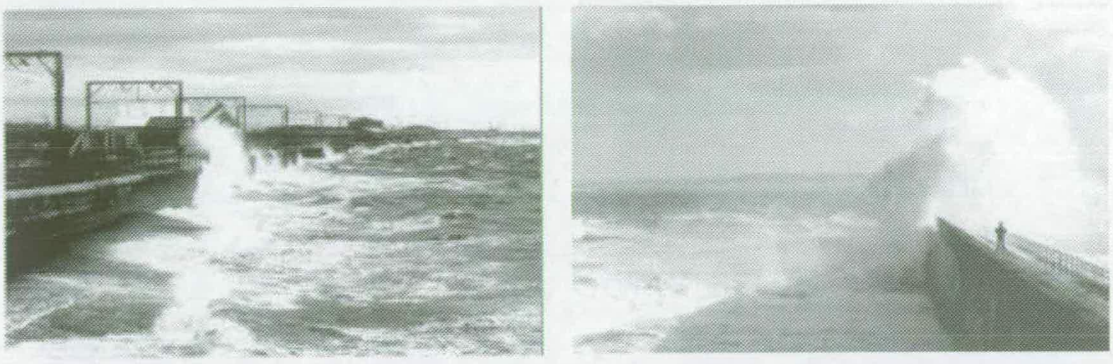

Figure 1: Hazards at the coastline; left, to communications – a major commuter railway line into Glasgow, Scotland – and right, to people – Hartlepool, England.

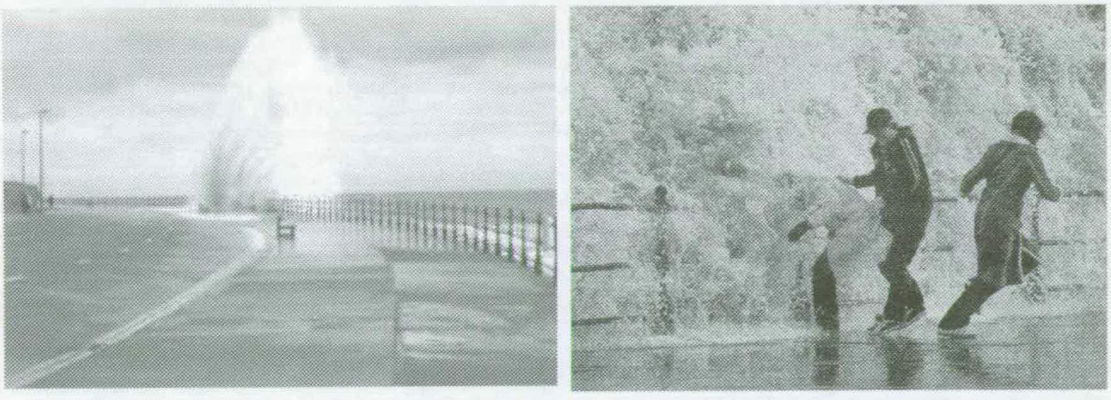

Figure 2: Public attitudes to overtopping hazards at Scarborough, England.

In the UK, a major research programme supported by the Engineering and Physical Sciences Research Council (EPSRC) has studied occurrence and behaviour of violent overtopping events. The VOWS project (Violent Overtopping of Waves at Seawalls) has included experimental work in wave flumes and basins by Universities of Edinburgh and Sheffield, with support from industry partners. Advances in numerical modelling of these processes are being developed at Manchester Metropolitan University.

One of the ambitions of this research is to understand and quantify the processes of violent overtopping jets. Tests at small scale at Edinburgh gave initial results, but it was felt important to explore, and perhaps quantify, any scale effects. A major series of large scale tests have therefore been completed in the large wave flume at Universitat Politècnica de Catalunya (UPC), Barcelona, and details are given in these proceedings by Pearson *et al.* (2002).

This paper presents new data on overtopping throw velocities at both small and large scale. Also presented are initial analysed data from a device designed to track the trajectory of overtopping jets.

2. PREVIOUS WORK

Established guidance upon appropriate design levels for admissible overtopping is based primarily on work by Fukuda *et al.* (1974), Goda (1971), Goda *et al.* (1975). A unified set of thresholds based on these mean overtopping discharges were tabled by Owen (1980), see Figure 3a, and modifications were then suggested by Franco *et al.* (1994) (Figure 3b). Design advice by Besley (1999) suggested that Franco's modifications may have been biased towards users aware of possible overtopping hazards rather than members of the public.

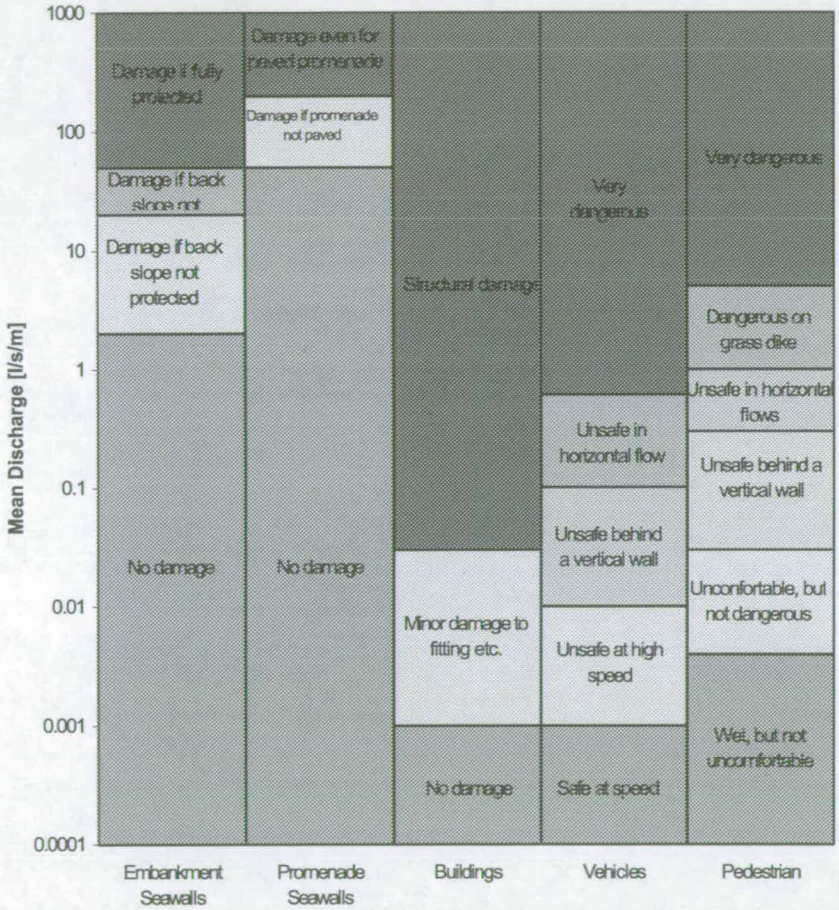

Figure 3: Threshold discharges by Franco *et al.* (1994), developed from Owen (1980), Fukuda *et al.* (1974) and Goda (1975).

Franco *et al.* (1994) and Besley (1999) have shown that, for a given mean discharge, the volume of the largest overtopping event varies significantly with wave condition and structural type. Franco *et al.* (1994) used model tests and experiments on volunteers (see Figure 4) to suggest that a "safe" limit for an individual overtopping volume for people operating behind a vertical wall was $V_{max} < 0.1 m^3/m$. The authors also acknowledge that a volume as low as $V_{max} = 0.05 m^3/m$ could unbalance an individual when striking their upper body without warning. For a structure with more horizontal flows, the limiting peak volume might be increased to $V_{max} = 0.75 m^3/m$.

Figure 4: "Assessing the first author's stability under water jets", Franco *et al.* (1994)

Franco *et al.* (1994) also noted that a given volume overtopping a vertical structure was more dangerous than the same volume overtopping a horizontally composite structure. Two effects will be important here for personal safety. Different velocities influence the danger caused by any particular overtopping volume, and the elevation at which a person is hit will alter the degree of danger. These effects are influenced by the form of wave breaking on the structure, and by the geometry of the structure crest, in particular the height / shape of any crown wall. Smith *et al.* (1994) reported full-scale tests on grass dykes where an observer stood on the dyke crest. Analysis of Smith's data suggests that work on the dyke was unsafe when $Q_{bar} > 0.01$ m^3/s.m, corresponding to $V_{max} \approx 1$ to 2 m^3/m.

The use of mean overtopping discharges alone therefore represent significant simplification of complex processes, and Franco and Besley agree that well-supported thresholds should be based on information on individual overtopping volumes, and on the velocity and trajectories of their jets. There is however little or no quantitative guidance for the estimation of the velocity and trajectory of overtopping jets except some observations by Jensen (1983, 1984) on the distribution of overtopping with distance.

Bruce *et al.* (2001) measured overtopping induced loads on the crown deck of a vertical breakwater at small-scale. Pressure transducers were arranged in a line running back from the wall crest. Results indicated that the region subject to the largest loading from overtopping flow / jets varied according to whether the overtopping was impulsive or more "green water" in character, but for a vertical wall with no wind effect, the main area of impact was limited to 2 H_s from the seaward edge of the wall.

The aforementioned laboratory studies neglect any effect of wind upon the discharge quantity and velocity / trajectory. Studies by Ward *et al.* (1994, 1996) suggest that very strong winds influence overtopping, the study of de Waal *et al.* (1996) suggests that the influence of wind upon mean discharge is not dramatic. It is clear, however, from any observation of overtopping under very windy conditions that the level of hazard and its spatial location / extent may be strongly influenced by wind, *eg* Kimura *et al.* (1999). Small-scale laboratory studies cannot reliably model wind influence due to scaling barriers (water mass break up scales by Weber; wind drag on discharge scales by Reynolds). The solution will lie in combined physical and numerical modelling. Data on throw velocities in this and related studies will provide essential input conditions to such modelling.

3. EXPERIMENTAL STUDIES: THROW VELOCITIES

The first stages of the VOWS physical modelling comprised a programme of parametric testing at small scale in the wave flume at University of Edinburgh. The flume measures 20m x 0.4m, with a water depth of 0.7m, and is equipped with an absorbing flap-type wavemaker, see Bruce *et al.* (2001) and Pearson *et al.* (2002). Structures tested were a plain vertical wall, near-vertical walls (10:1 and 5:1 batter), composite vertical structures, and a vertical wall with return wall. Tests were of 1000 random waves to a JONSWAP spectrum with $\gamma = 3.3$. Wave conditions were selected to include conditions under which a significant proportion of waves were breaking or broken at the structure. Mean and wave-by-wave overtopping discharges were measured. Results relating to the overtopping discharges are reported in Bruce *et al.* (2001). Scale effect studies are presented by Pearson *et al.* (2002).

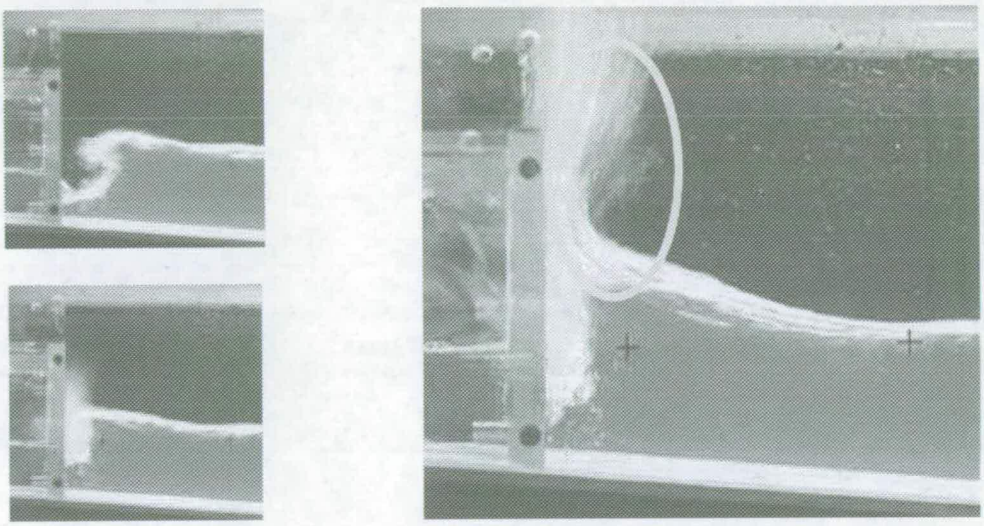

Figure 5: Video measurement of throw velocity in small-scale tests.

All tests were video-taped. From these video records, the velocity at which the overtopping discharge was thrown upwards past the crest of the structure (the "throw velocity") was derived (Figure 5). The largest 20 individual overtopping events were selected and the throw velocities for each were inferred from the "time of flight" of the overtopping water. The distributions of these individual velocity magnitudes are shown in Figure 6 where throw velocity values have been non-dimensionalised by the inshore wave celerity. As per convention, the Weibull plot shows larger values of the (non-dimensional) velocity along the x-axis and larger non-exceedance probabilities up the y-axis.

The striking feature of the distributions in Figure 6 is that they fall broadly into two populations, suggesting that two distinct physical mechanisms are being observed. For a given non-exceedance probability, the upper/left group show smaller throw velocities that the lower/right group. The interpretation is that the lower/right population are sequences in which violent / impulsive overtopping is taking place and dominating the largest throw velocities measured.

Because the throw velocities appear to depend critically upon whether the overtopping is "green water" / "non-impulsive" or "violent" / "impulsive", a means of determining to which group a particular wave / structure configuration belongs is required. Helpful guidance for plain vertical walls and vertically composite structures is given by the "parameter map" developed under the PROVERBS project (Oumeraci *et al.*, 2001). This distinguishes between impulsive and non-impulsive conditions, but no indication of the "intensity" of impulsive events, *ie* how violent are breaking events?

For plain vertical structures, a possible indicator of the violence of breaking is the h^* wave breaking parameter (Besley, 1999, after Allsop *et al.*, 1995):

$$h^* \equiv \frac{h}{H_s}\left(\frac{2\pi h}{gT^2}\right)$$

Allsop *et al.* (1995) and Besley (1999) suggest that values of $h^* > 0.3$ correspond to non-breaking (termed pulsating or reflecting) conditions, with breaking conditions (termed impulsive) becoming ever more prevalent as h^* reduces below 0.3.

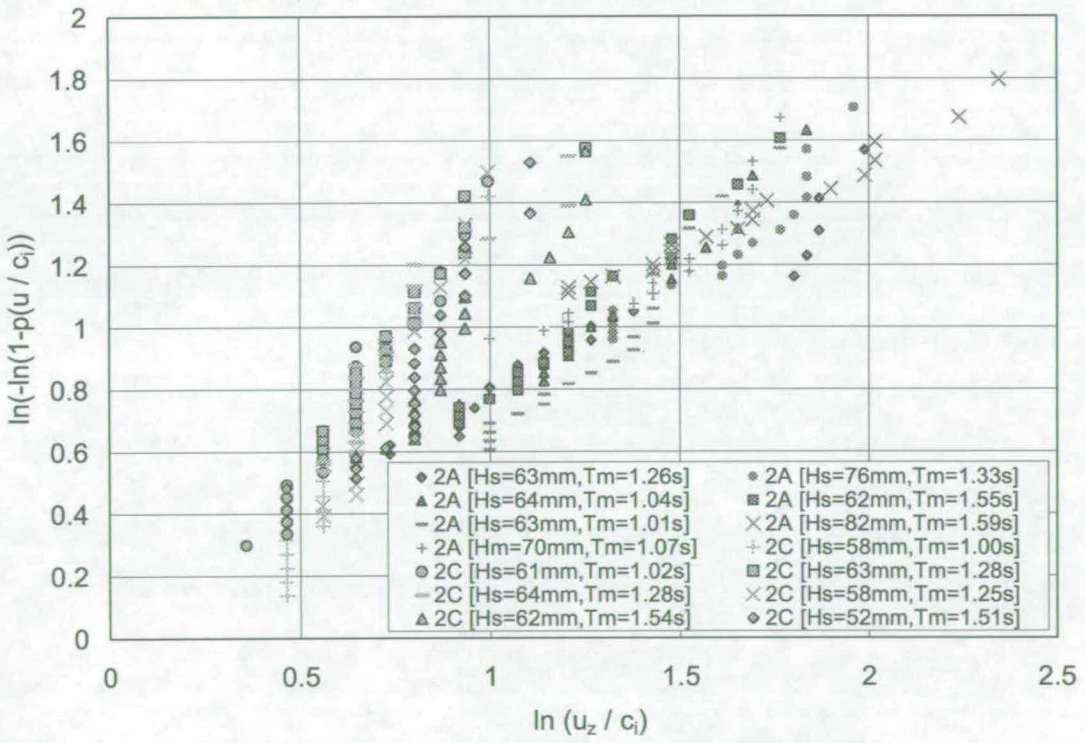

Figure 6: Distribution of throw velocities of individual overtopping events plotted on Weibull axes; 14 test conditions; c. 1000 waves per test.

In order to establish whether h^* was a useful parameter, a measure of the characteristic throw velocity for a given wave / structure combination was required. Rather than look at the variation of the maximum throw velocity itself with h^*, a more stable (and dimensionless) measure of characteristic throw velocity was preferred. For each test, the mean of the highest 4% of values of u_z, $u_{z,\ 1/25}$ was determined, and this average (non-dimensionalised by the inshore wave celerity) is plotted against the wave breaking parameter, $h*$, in Figure 7.

The results in Figure 7 are striking. For pulsating conditions, and through the initial onset of impulsive effects, $h^* > \sim 0.2$ the dimensionless throw velocity is roughly constant at a value ~2.5. As the degree of impulsive breaking increases, $h^* < \sim 0.2$, the dimensionless throw velocity increases very significantly, reaching values ~6 and above.

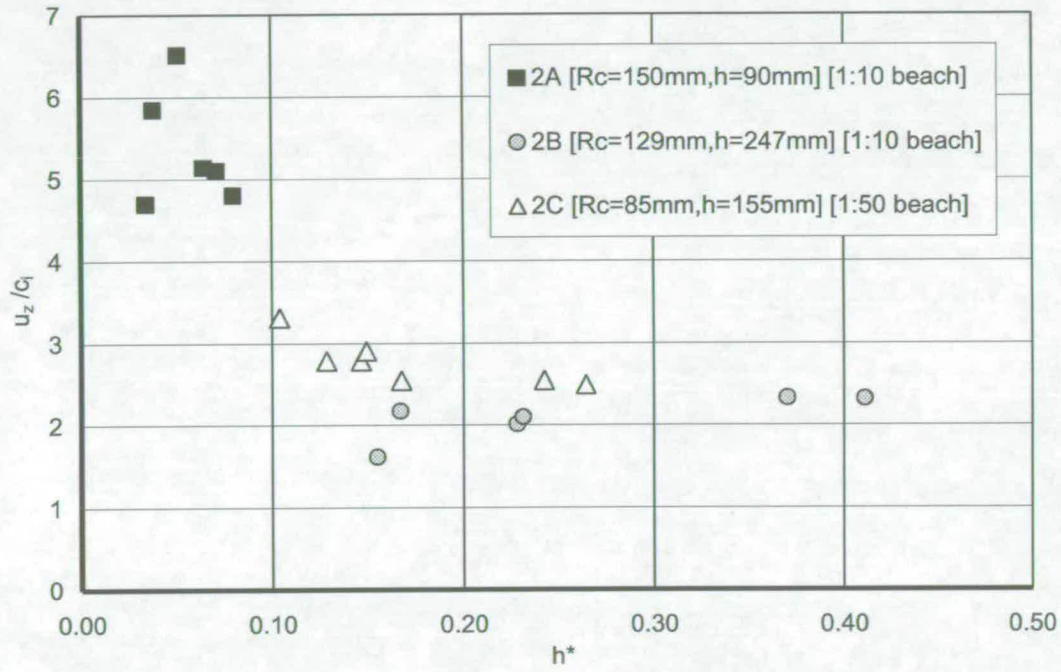

Figure 7: Dimensionless throw velocities $u_{z,\ 1/25}/c_I$, for a simple vertical wall from small scale tests.

Similar throw velocity data have also been extracted from video records of the large-scale tests at UPC Barcelona (tests described by Pearson *et al.*, 2002). These results have been plotted in comparison to the small-scale data in Figure 8. It is clear that the largest measured (non-dimensional) velocities are somewhat greater than those measured at small-scale, although the form of the relationship with the h^* parameter is comparable. Further study suggests that the cross-flume variation in velocities is greater in the large-scale tests, and that taking a cross-flume average throw velocity yields closer agreement.

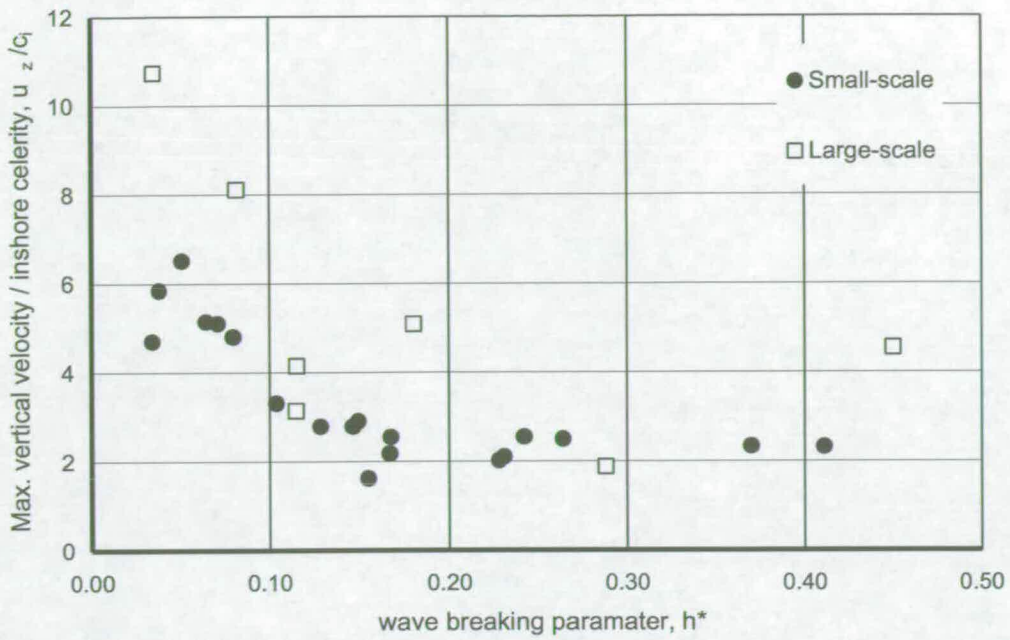

Figure 8: Dimensionless throw velocities $u_{z,\,1/25}/c_I$, for a 10:1 battered wall from large-scale tests

4. EXPERIMENTAL STUDIES: THROW TRAJECTORIES

The measurements presented in section 3 were derived from analysis of video recordings, a slow and laborious task, and gave only velocities in one direction. For the large-scale tests in the flume at UPC, Barcelona (see Pearson *et al.*, 2002) the Big-VOWS team developed a device to automate measurement of velocities / trajectories of thrown discharges. This device (shown in Figure 9a) consisted of an array of 64 individual detector elements mounted on a plane above the wall crest in line with the length of the flume. Each detector element is an electrical switch which is "closed" in the presence of water. The status of all the switches was monitored at 400Hz. Software then allows the reconstruction of the trajectory of individual throw events. The detector is visible in Figure 9b as the dark board immediately to the left of the up-rushing discharge.

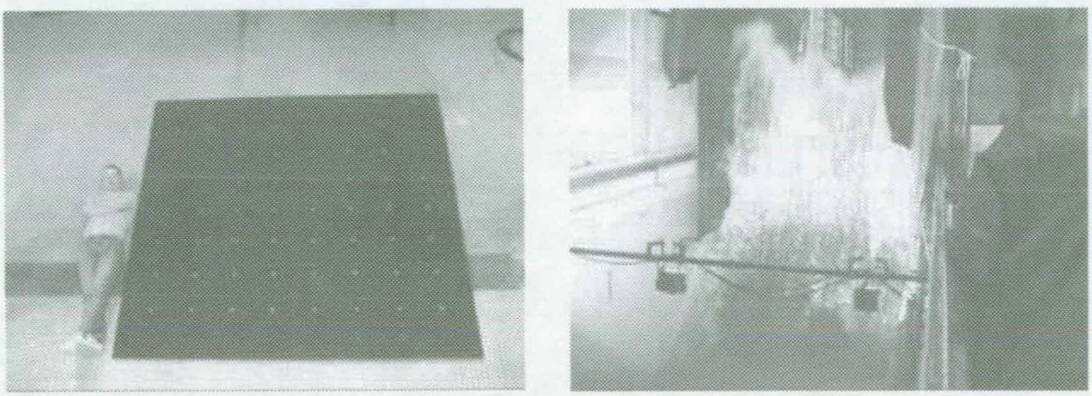

Figure 9: (a, left) Throw trajectory measurement device showing the 8 x 8 array of water detectors; (b, right) the device *in situ* above the crest of the test wall at UPC, Barcelona.

Use of this measurement device is illustrated in Figure 10 where (simulated) contacts at each of the nodes are illustrated by a grey block.

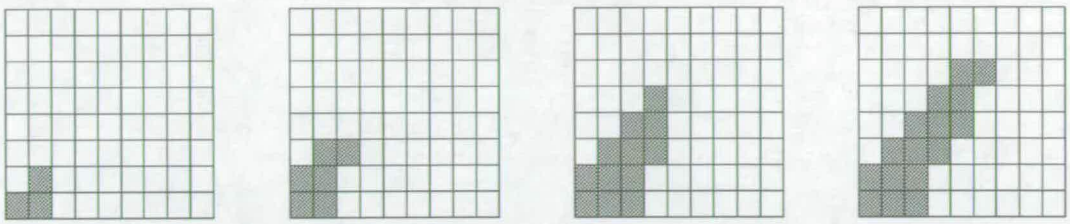

Figure 10: Schematic of the throw measurement device showing successive contacts as the overtopping jet passes the device.

Figure 11: Synchronised video and throw detection at 0.17s intervals (Test series Big-VOWS C11 : H_s=0.67m, T_s=3.29s).

Figure 11 shows a sequence of images at 0.17s intervals of synchronised video and throw detection. The white circles on the vertical throw board indicate the presence of water. Early results show that the visual observations from the video and the signals from the throw system correlate well, although further processing may be necessary as under certain conditions the signal from the throw system stays 'on' for up to 1 second after the water has receded. It was observed visually during the tests that water ran down the board, thereby tripping the detection system.

5. DISCUSSION

Small-scale hydraulic model tests are used to provide data to predict processes at prototype scale. In using those methods in analysis / design, it is vital to quantify both "scale" and "model" effects. Scale effects emanate simply from the scale of the modelling, and include effects from distortions to viscous flow, or by surface tension effects on bubbles and droplets. The results from scale effect tests (showing no significant scale errors on mean and peak overtopping) are discussed in these proceedings by Pearson *et al.* (2002).

Model effects may arise because a particular process is not reproduced, or is distorted. The most obvious such effects on overtopping processes are due to wind (or to its absence in the model) and effects of fresh water *vs.* sea water. Use of fresh water rather than sea water alters percentage and persistence of air bubbles in the water, thus changing its compressibility during impacts. It is known that these effects influence wave impact pressures, but there is no evidence for this "model" effect to alter overtopping processes.

The useful and well argued tests by de Waal *et al.* (1992, 1996) suggest that heavy overtopping is very little influenced by wind, but it is probable that wind effects will be important for small discharges, particularly when accompanied by severe breaking processes.

6. CONCLUSIONS

The transition from largely reflecting wave conditions at a vertical seawall / breakwater to conditions under which breaking or broken waves occur gives rise to an increase in the velocity at which the overtopping discharge is thrown past the structure crest. There is clearly a commensurate increase in the hazard to pedestrians or vehicles in the vicinity.

Some throw velocity have been measured at 6-10 times the inshore wave celerity, whereas a multiplier of 2.5 is typical for non-breaking conditions.

Measurements of wave throw trajectories have been carried out at large-scale; full analysis and linking to hazard assessment is beginning

ACKNOWLEDGEMENTS

The work described in this paper has been supported by the UK EPSRC (GR/M42312, GR/R42306), and by the VOWS Management Committee including members from Manchester Metropolitan University (Derek Causon, David Ingram, Clive Mingham), HR Wallingford (Philip Besley), Posford-Haskoning (Dick Thomas), Bullen & Co. The VOWS project is particularly pleased to acknowledge guidance and helpful supervision to their collaborative work from the EPSRC CEWE Project Manager, Michael Owen. The VOWS team are also most grateful to the UPC Barcelona team for excellent support during the Big-VOWS tests under the EC TAMRI "HYDRALAB" project - Xavi Gironella, Quim Sospedra, Javier Pineda, Agustin Sanchez-Arcilla. The assistance of Nikolas Forde in the video analysis of the large scale tests is gratefully acknowledged.

Further work on hazards arising from overtopping, including field measurements of overtopping at its effects, is being conducted under the European CLASH project under contract EVK3-2001-0058 in the EC 5th Framework programme.

REFERENCES

Allsop, N.W.H., Besley, P. & Madurini, L. (1995), "Overtopping performance of vertical walls and composite breakwaters, seawalls and low reflection alternatives", Paper 4.7 in MCS Final Report, publn University of Hannover.

Besley, P. (1999), "Overtopping of seawalls – design and assessment manual", R & D Technical Report W 178, ISBN 1 85705 069 X, Environment Agency, Bristol.

Bruce, T., Allsop, N.W.H. & Pearson, J. (2001), "Violent overtopping of seawalls – extended prediction methods", Proc. "Coastlines, Seawalls and Breakwaters '01" ICE, publn Thomas Telford, London.

Franco, L., de Gerloni, M. & van der Meer, J.W. (1994), "Wave overtopping on vertical and composite breakwaters", Proc 24th Int. Conf. Coastal Eng., Kobe, publn. ASCE.

Fukuda, N., Uno, T. & Irie, I. (1974), "Field observations of wave overtopping of wave absorbing revetment", Coastal Engineering in Japan, Vol 17, pp 117-128, Japan Soc. of Civil Engs, Tokyo.

Goda Y. (1971), "Expected rate of irregular wave overtopping of seawalls", Coastal Engineering in Japan, Vol 14, pp 45-51, JSCE, Tokyo.

Goda, Y., Kishira, Y. & Kamiyama, Y. (1975), "Laboratory investigation on the overtopping rates of seawalls by irregular waves", Ports and Harbour Research Institute, Vol 14, No. 4, pp 3-44, PHRI, Yokosuka.

Jensen, O.J. (1983), "Breakwater superstructures", Proc. Conf. Coastal Structures '83, Arlington, pp272-285, ASCE.

Jensen, O.J. (1984), "A monograph on rubble mound breakwaters" Danish Hydraulic Institute, Horsholm.

Kimura, K., Fujiike, T., Kamikubo, K., Abe, R. & Ishimoto, K. (1999), "Damage to vehicles on a coastal highway by wave action", Proc. Conf. Coastal Structures '99, Santander, June 1999, publn. A.A. Balkema, Rotterdam.

Oumeraci, H., Kortenhaus, A., Allsop, N.W.H., de Groot, M.B., Crouch, R.S., Vrijling, J.K. & Voortman, H.G. (2001), "Probabilistic design tools for vertical breakwaters", ISBN 90 580 248 8, publn. Balkema, Rotterdam.

Owen, M.W. (1980), "Design of seawalls allowing for wave overtopping", HR Report EX 924, June 1980, Hydraulics Research, Wallingford.

Pearson, J., Bruce, T. & Allsop, N.W.H. (2002), "Violent wave overtopping – measurements at large and small scale", Proc. 28th Int. Conf. Coastal Eng, Cardiff, ASCE.

Smith, G.M., Seijffert, J.W.W. & van der Meer, J.W. (1994), "Erosion and overtopping of a grass dike: large scale model tests", Proc 24th Int. Conf. Coastal Eng., pp2639-2652, Kobe, ASCE.

de Waal, J.P. & van der Meer, J.W. (1992), "Wave run-up and overtopping on coastal structures", Proc 23rd Int. Conf. Coastal Eng., pp1758-1771, ASCE.

de Waal, J.P., Tonjes, P. & van der Meer, J.W. (1996), "Overtopping of sea defences", Proc 25th Int. Conf. Coastal Eng., pp2216-2229, Orlando, ASCE.

Ward, D.L., Wibner, C.G., Zhang, J. & Edge, B. (1994), "Wind effects on runup and overtopping", Proc. 24th Intl. Conf. On Coastal Eng., pp1687-1699, ASCE.

Ward, D.L., Zhang, J., Wibner, C.G. & Cinotto, C.M. (1996), "Wind effects on runup and overtopping of coastal structures", Proc. 25th Intl. Conf. On Coastal Eng., pp2206-2216, ASCE.

Appendix U: Bruce *et al.*, 2005

Bruce, T., Pullen, T., Allsop, N.W.H. & Pearson, J. (2005), *How far back from a seawall is safe? Spatial distributions of wave overtopping*, Proc. Coastlines, Structures & Breakwaters 2005, pp166–176, ICE London, Thomas Telford, ISBN 0 7277 3455 5

Appendix U
Bruce *et al.*, 2005

Bruce, T., Pullen, T., Allsop, N.W.H. & Pearson, J. (2005), *How far back from a seawall is safe? Spatial distributions of wave overtopping*, Proc. Coastlines, Structures & Breakwaters 2005, pp166–176, ICE London, Thomas Telford, ISBN 0 7277 3455 5

U.1 Declaration of contribution

This paper resulted from a close cooperation with colleagues at HR Wallingford (Pullen and Allsop). The initial small-scale work on spatial distribution was led by the author via a Masters student project (carried out by Masterton under the author's day-to-day supervision). The author also led some earlier investigations into the effect of wind on overtopping discharge which, although not directly included in this paper, laid a most useful foundation for the work at HR Wallingford reported in this paper. The author presented the paper to the conference and led the drafting and editing of the subsequent paper.

U.2 Published paper

overleaf

HOW FAR BACK FROM A SEAWALL IS SAFE? SPATIAL DISTRIBUTIONS OF WAVE OVERTOPPING

Tom Bruce, School of Engineering and Electronics, University of Edinburgh, King's Buildings, Edinburgh, EH9 3JL, UK. Tom.Bruce@ed.ac.uk, Tel: +44 131 650 8701
Tim Pullen, HR Wallingford, Howbery Park, Wallingford, OX10 8BA, UK
William Allsop, University of Southampton & HR Wallingford
Jonathan Pearson, School of Engineering and Electronics, University of Edinburgh,

Abstract

Many methods have been developed to describe the mean overtopping discharge over seawalls, but there are very few data on how those discharges are distributed spatially landward. Studies under the CLASH project included field measurements of overtopping of a (nearly) vertical seawall at Samphire Hoe, Kent. Field measurements of overtopping, including measurements of the spatial distribution of overtopping volumes, were then compared with physical model tests in 2-dimensions in a wave flume study at the University of Edinburgh and in 3-dimensions in a wave basin study at HR Wallingford.

This paper gives new information on the spatial distribution (backward) of water volumes from overtopping on vertical or steeply battered walls. The results are derived from studies in UK under EPSRC, EC FP5 and defra / EA funded research. It is found that, for the worst cases studies, mean discharge is reduced to 10% of its value at the crest by a distance of 0.25 × (wavelength of incident waves) landward of the structure crest. Local conditions will be an important consideration in translation of this reduction in mean discharge to a commensurate reduction in hazard.

Introduction

Hazards to pedestrians, vehicles and infrastructure are closely related to the spatial distributions of overtopping volumes, as well as their velocities. Better understanding of areas affected by overtopping will improve analysis of: hazard zones; loads on buildings; and effects of wind; thus allowing engineers to identify vulnerable infrastructure and hazardous areas. This paper presents information from three sources on overtopping velocities, spatial distribution and overtopping loadings, significantly improving tools to define overtopping hazard areas.

Figure 1. Samphire Hoe reclamation, port of Dover in background.

Many urban seawalls or breakwaters are formed by vertical, near-vertical or recurved walls. These are often more effective than embankment slopes in reducing overtopping and in use of space. The main performance criteria

used to judge the adequacy of these structures are limits on mean overtopping discharge, see Besley (1999) and Allsop *et al.* (2003). Some data are available on peak overtopping volumes, but experience and data on distributions of peak volumes are very sparse. Wave overtopping hazards are influenced by overtopping volumes; velocities of overtopping waves; their spatial distribution; and loads on people or structures in their path. To date, there have been few data on the effects of overtopping, either above or below present discharge limits. New data however suggest that forces from overtopping waves may substantially exceed those for which most buildings are designed, even 15-20 m back from the seawall.

Jensen & Sorensen (1979) suggest an exponential distribution of overtopping volumes given by: $q_x = q_0 \exp(-0.1x)$ where q_x is the overtopping rate per landward distance from the wall (x). q_0 is an initial value at x = 0m (immediately behind the wall), -0.1 describes how rapidly the exponent decays. This method is not generic in nature and has not however been tested for vertical walls, particularly under impulsive breaking when overtopping throw velocities can be very much greater, see Bruce *et al.* (2002).

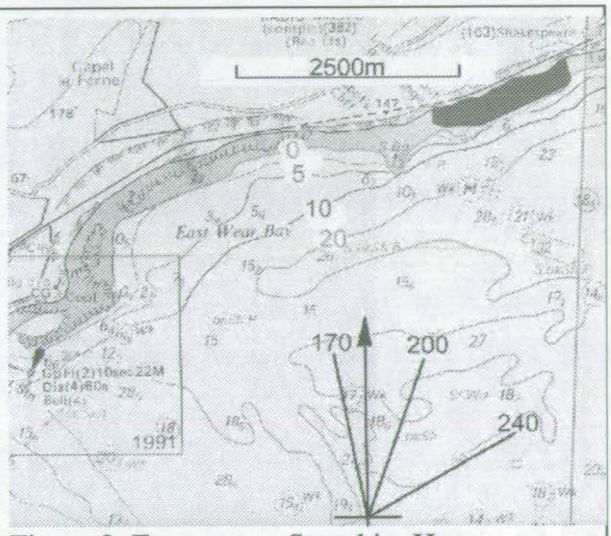

Figure 2. Exposure at Samphire Hoe.

Field measurements

Samphire Hoe is an area of reclaimed land formed by 4.9 Mm^3 of chalk marl excavated from the Channel Tunnel. The area of approximately 300,000m^2 is enclosed by a vertical (slightly stepped) seawall with a crest level at +8.22mODN and a rubble berm at –2.42mODN. The Samphire Hoe reclamation (Figure 1) is owned by Eurotunnel, and is run on their behalf by the White Cliffs Countryside Project (WCCP) as a public recreational area. It is exposed to waves from southwest to southeast (Figure 2) and is subject to overtopping on approximately 30 days / year with waves breaking over the rubble berm and impacting on the seawall face.

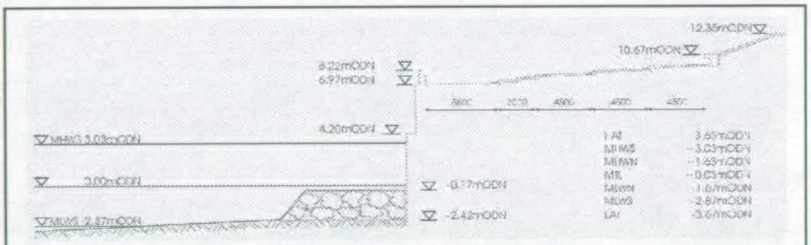

Figure 3. Section of Samphire Hoe Seawall.

At Samphire Hoe, wave overtopping was measured close to the southwest corner, about 40m from the corner. The seawall (Figure 3) fronts a wide promenade onto which were bolted a series of

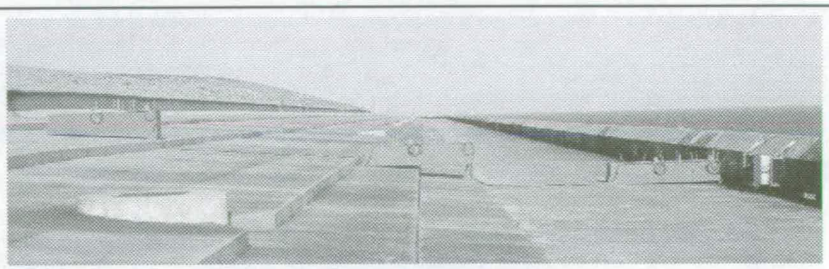
Figure 4. Overtopping tanks at Samphire Hoe.

continuously draining tanks (Figure 4), equipped to measure instantaneous volumes for individual overtopping events. These gave mean overtopping discharge rates and peak volumes. The tanks spaced across the promenade measured the spatial distribution of the overtopping. Details of these field measurements have been given by Pullen *et al.* (2003 & 2004).

Overtopping at Samphire Hoe was measured during three storms on 10th March 2003, 1st May 2003 and 2nd May 2003. Overtopping was very low during the first storm, so it is not discussed here, but successful measurements in the other two storms are described below.

1st May 2003 Storm

Measurements were made in wind speeds of 15~20m/s (force 6–7). The maximum overtopping discharge was approximately $q = 1.0$ l/s/m and the maximum predicted discharge was $q = 1.4$ l/s/m. During this event overtopping was blown over a wide area by the strong wind. From observations during the storm and subsequent video analysis, it was estimated that approximately two-thirds of the overtopping discharges were not collected in the overtopping tanks. Discharges for this storm were therefore multiplied by 3 to represent the true discharges.

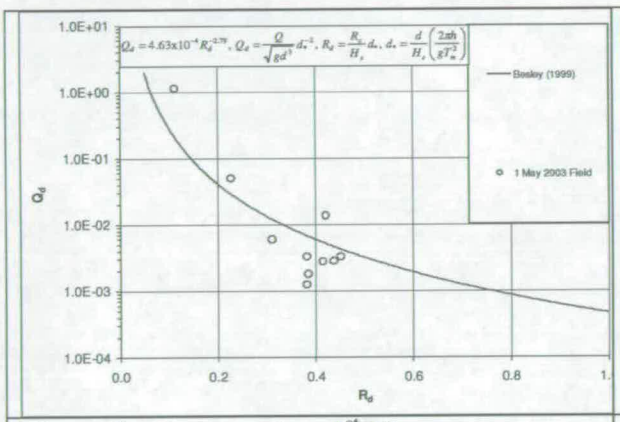

Figure 5a. Overtopping, 1st May.

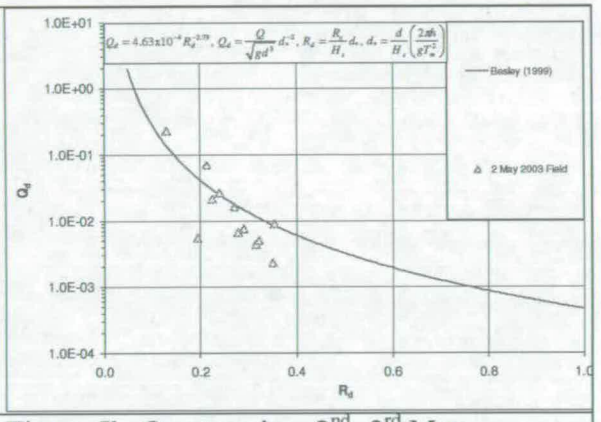

Figure 5b. Overtopping, 2nd -3rd May .

2nd/3rd May 2003 Storm

Measurements in the storm of 2nd – 3rd May 2003 lasted from 2145 until 0415 the following morning. Before overtopping was recorded, wind speeds had been at gale force, but dropped substantially by the time that overtopping was recorded. Overtopping trajectories were generally upwards, coming down mainly in the area directly behind the parapet wall. Little or no overtopping was blown by the wind. In this case no "wind" factor was applied to the data summarised in Figure 5b. The highest recorded mean overtopping discharge during the storm was $q = 3.3$ l/s/m in excellent agreement with the prediction according to Besley (1999) of $q = 3.1$ l/s/m.

Laboratory Tests

Within the CLASH project, two physical model studies of overtopping at Samphire Hoe were carried out – a 2d model at 1:40 in the flume at Edinburgh and a 3d model at 1:20 in a deep water basin at HRW. The principal objective of the tests was to simulate field conditions to test the

Figure 6. 2-d wave flume at Edinburgh.

overtopping behaviour of this seawall. Further parametric tests were added to give a wider dataset. For each wave condition and water level combination, mean and wave-by-wave overtopping discharges were recorded. Data on the spatial distribution were recorded for selected conditions in the Edinburgh tests and on all of the HRW tests, which included tests with wind.

2-d tests at Edinburgh

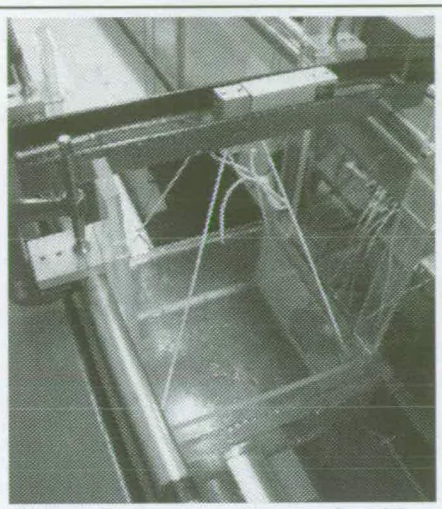

Figure 7. Overtopping tank with load cell

The 2-d tests at small-scale were completed in the 20 m long, 0.4 m wide wave channel in Edinburgh, with an operating water depth of 0.7 m (Figure 6). The flume is equipped with a moveable impermeable beach that allows a range of slopes from approximately 1:5 to 1:50. Waves are generated by an absorbing flap type wave paddle giving seas with H_s up to 0.11m and T_p up to 2.0s.

Overtopping discharges were directed into a measuring container suspended from a load cell, Figure 7. Individual overtopping events were detected on the seawall crest, with event volumes measured by the mass increment in the tank after each overtopping event. For selected conditions, the spatial distribution of overtopping volumes was determined in each compartment of a divided collection chamber, shown schematically in Figure 8. The spatial distribution was given by expressing volumes in each individual chamber as a proportion of the total volume.

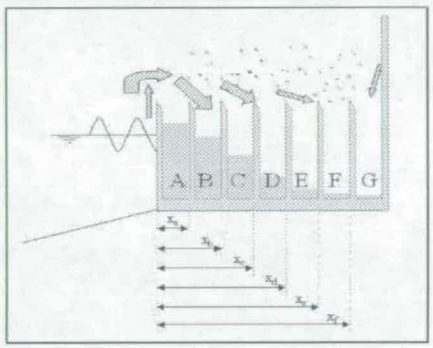

Figure 8. Spatial distribution tank

3-d tests at Wallingford

The 3-d model was constructed in a deep wave basin at 1:20 (Figure 9). Approach slopes started at 1:20 from –14.75mCD up to the final approach at 1:30. Horizontal bathymetry modelled the plateau in the foreshore area. The seawall was constructed in timber including the Larsen piles and the set back parapet wall.

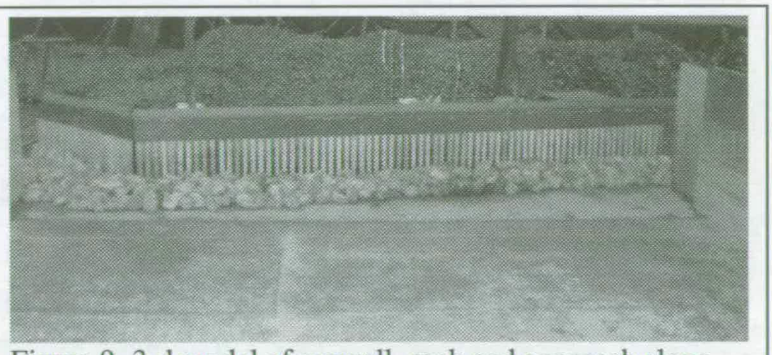

Figure 9. 3-d model of seawall, rock and approach slope.

Toe berm rock was scaled to a porosity $n = 35\%$ and $D_{n50} = 1.5$m. Waves were generated by a multi-element wave paddle with active absorption capable of producing irregular sea states, and wave guides were used to contain the waves within the modelled area.

Wave conditions and water levels from the storms of 1st -3rd May 2003 were calibrated with a set of parametric wave / water level combinations to examine the general overtopping

behaviour of the structure. Model test runs each consisted of c. 1000 irregular waves generated by a JONSWAP spectra for $\gamma = 3.3$. Each test part was run for a single water level, wave height (H_s, specified at the wave maker) and peak period T_p. Wave conditions at the toe of the berm covered $H_{m0} = 1.1$~2.4m, all from 180°N, approximately 10° oblique to the seawall.

Overtopping measuring equipment determined total and wave-by-wave volumes. Discharges flowed into the 60 litre overtopping tank via a chute from the parapet wall at +8.22mODN. This tank was suspended by a load-cell measuring up to 100 kg. Individual volumes (Figure 10) were determined with accuracy equivalent to 2 l/m at prototype scale. Overtopping detectors were placed at the rear of the chute, and inside the entrance to the tank.

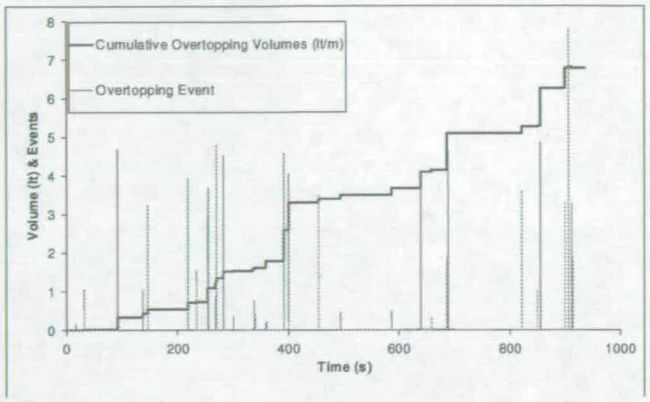

Figure 10. Example wave-by-wave overtopping record.

Landward distributions were recorded in a separate set of six 1 litre tanks along a line normal to the seawall adjacent to the main tank. The tanks were placed as closely as possible, shown schematically in Figure 11. An adjusted width compensated for the missing areas.

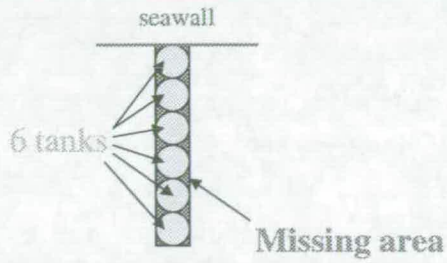

Figure 11. Spatial distribution tanks.

Wind measurements and overtopping

Wave overtopping usually takes place under windy conditions. The effects that wind has on overtopping have been discussed by Ward *et al.* (1996) and de Waal *et al.* (1996). Though wind may cause overtopping of part of the uprushing jet that would otherwise have fallen back into the sea, physical models seldom include wind largely due to difficulties in scaling model wind effect to prototype scale. Tests by de Waal *et al.* (1996) suggested that overtopping at relatively low discharges may be particularly affected by wind, with increases of a factor of up to three reported.

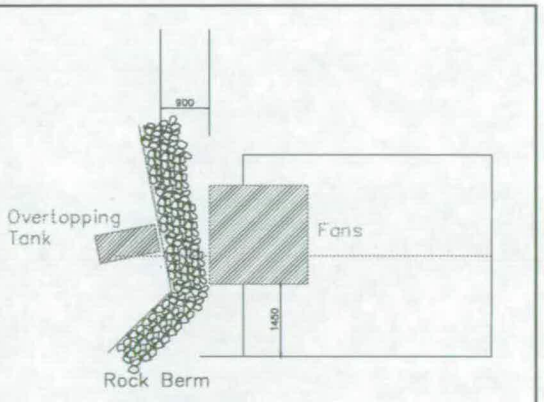

Figure 12. Addition of wind fans.

For these tests four large fans (Figure 12) were placed directly in front of the seawall in the area in front of the measuring equipment. Wind speeds were measured across the test position, averaged to give the basic wind speeds. The fans were placed close to the seawall to ensure that the wind did not change incident waves, but simply assisted the overtopping discharge over the parapet wall in a manner analogous to the paddle wheel used by de Waal *et al.* (1996).

Overtopping at composite Vertical Seawalls

Overtopping performance of vertical walls is dependent upon the type of incident wave at the wall. In deep water, waves hit the structure and reflect back seawards (reflected / non-breaking / pulsating waves). As waves become limited by water depth, they tend to break over the seawall (so-called impacting waves), causing a significant change in overtopping performance. For composite vertical structures including toe berms, as at Samphire Hoe, a modified breaking parameter by Besley (1999) takes account of the relative berm height:

$$d_* = \frac{2\pi dh}{H_s g T_m^2}$$

where d is the water depth over the berm. Besley (1999) suggested that the berm is classified as large when $d^* \leq 0.3$, whereas the mound is classified as small when $d^* > 0.3$ and the wave behaves as with plain vertical walls.

Besley (1999) derived empirical formulae predicting dimensionless discharge on a composite vertical seawall for impacting waves valid for $0.05 < R_d < 1.0$, where:

$$Q_d = 4.63 \text{x} 10^{-4} R_d^{-2.79}$$

Q_d is the dimensionless discharge, and R_d, the dimensionless crest freeboard given by:

$$R_d = \frac{R_c d_*}{H_s}$$

Mean overtopping discharges q (m^3/s/m) can be obtained from Q_d:

$$q = Q_d d_*^2 \left(g d^3\right)^{0.5}$$

To establish a conceptual model for the spatial distribution of the overtopping discharges, the parameter q^* is defined as a dimensionless discharge as follows:

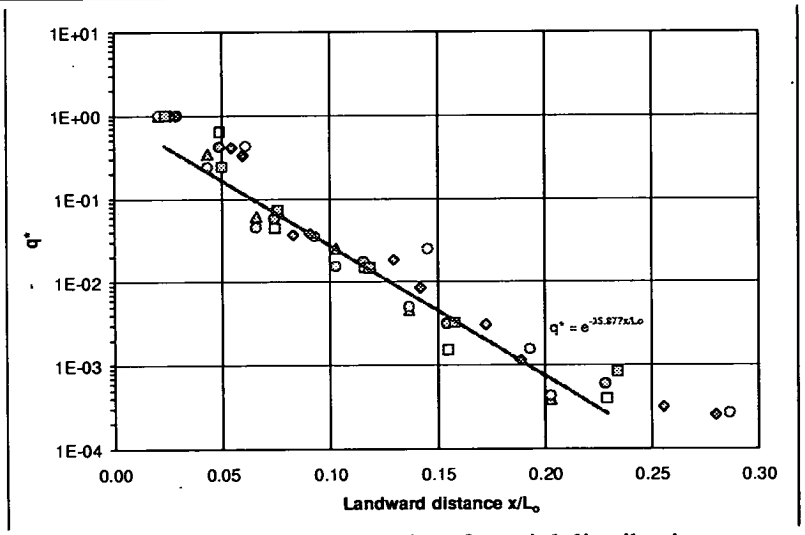

Figure 13. Example results of spatial distribution

$$q^* = \frac{Q_{Bar_i}\left(x/L_o\right)}{Q_{Bar_{Total}}\left(x/L_o\right)} \quad (1)$$

where the $Q_{Bar\ I}$ are the discharges at landward distances of x/L_o from the crest, and where L_o is the offshore wavelength. By plotting the q^* as a function of x/L_o it is possible to establish a general relationship in the form of an exponential decay,

$$q^* = \exp\left[-k\left(\frac{x}{L_0}\right)\right] \tag{2}$$

where k determines the spatial distribution. k is derived from the gradient of the best fit line as shown in Figure 13. It is possible to plot the results as a function of the dimensionless landward distance to show the percentage of the discharge that has landed after a distance of x/L_o. Figures 14 & 15 show these cumulative distributions for collected volumes V_I and V_{Total}, the ratio of $Q_{Bar\ I}$ to $Q_{Bar\ Total}$ being the same. The individual lines represent distributions measured for different wave conditions for a given wind speed. The bold line shows the limiting (*ie* most landward spread) trend.

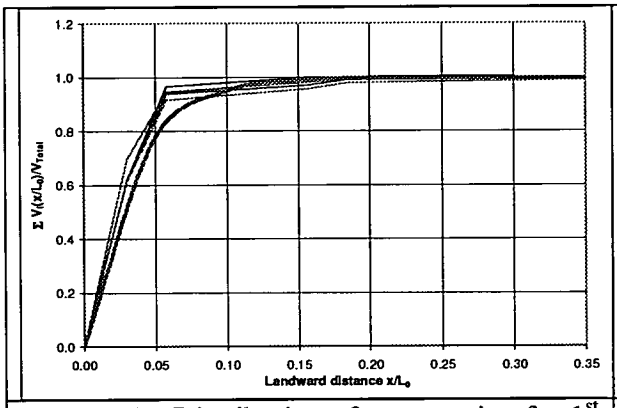

Figure 14a. Distribution of overtopping for 1st May storm from HRW wave basin tests

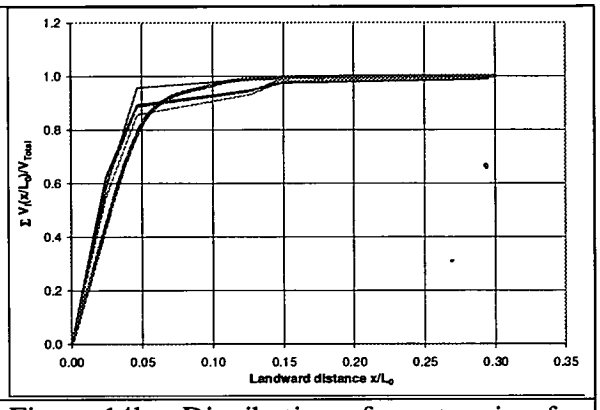

Figure 14b. Distribution of overtopping for 2nd May storm from HRW wave basin tests

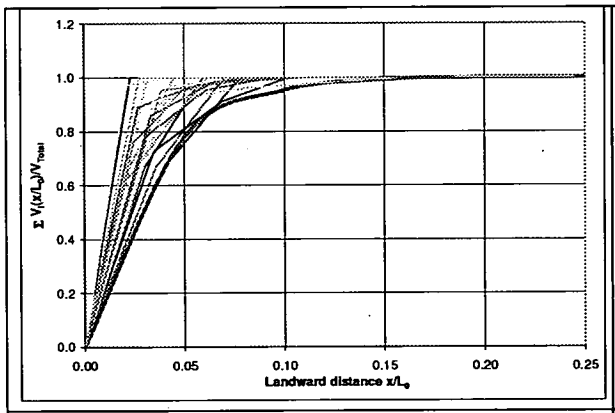

Figure 15a. HRW parametric tests: spatial distributions. Limiting k = 30.

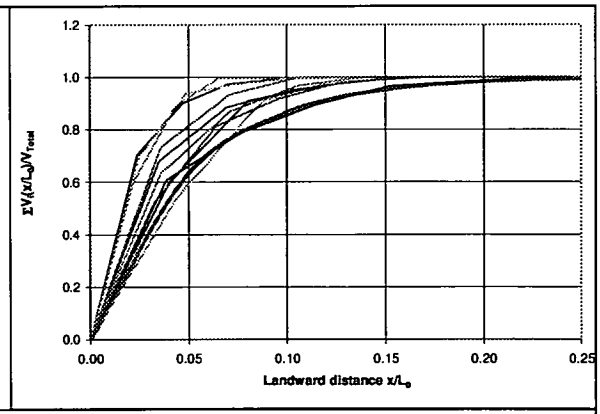

Figure 15b. HRW tests with a model wind speed of 15m/s. Spatial distributions show a limiting k = 20.

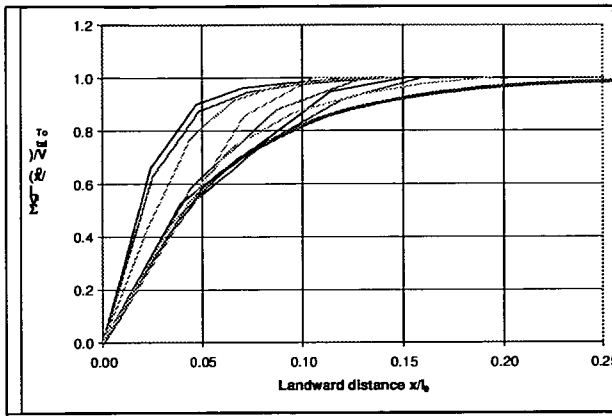

Figure 15c. HRW tests with a model wind speed of 26m/s. Spatial distributions show a limiting k = 17.

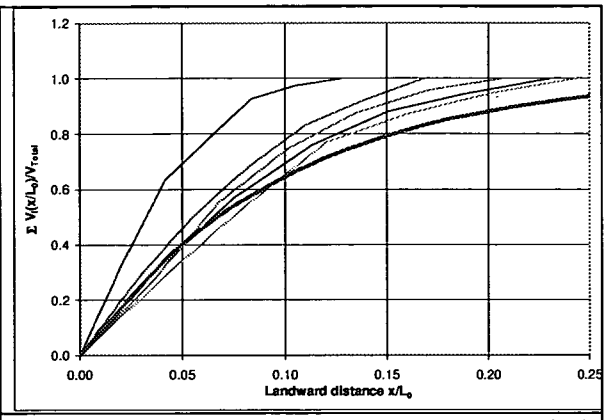

Figure 15d. HRW tests with a model wind speed of 28m/s. Spatial distributions show a limiting k = 10.

Discussion

The generic spatial distributions from the field measurements and selected laboratory measurements with no wind are summarised in Figure 15a.[1] The Edinburgh values are not shown separately as they have the same value of $k = 30$ as the 3D parametric tests. The general trend shown in Figures 15b, c and d shows that the distribution increases with increasing wind speed.

As discussed earlier, each of the spatial distributions can be approximated by:

$$q^* = \exp\left[-k\left(\frac{x}{L_0}\right)\right]$$

where the value of k is dependent on the wind speed. By exploring the relationship between the laboratory wind speed (v_w) and k, it is found that with a correlation of approximately $R^2=0.85$, that values of k are given by the following expression;

$$k = 29\exp(-0.03v_w) \qquad (3)$$

This distribution has been plotted for a range of wind speeds and is shown in Figure 16. Each of the curves represent the limiting value, or widest spatial distribution, for the various wind speeds shown. Despite no straightforward way to scale wind speeds from lab to prototype scale, it would appear that the above expression for k for the HRW laboratory tests gives a conservative predictor when compared to the field measurements.

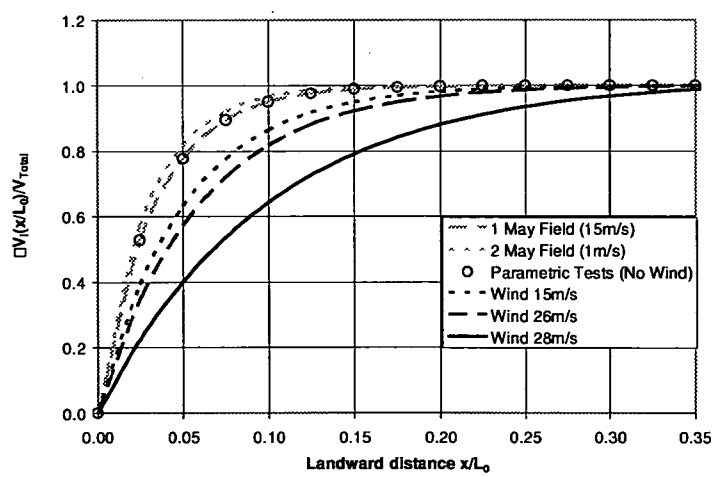

Figure 16. Generic spatial distributions from the field and laboratory measurements

Figure 17 shows that when discharges are low, the addition of wind increases the discharge by up to an order of magnitude. There are some scatter among the data for the central group for increased discharge, and virtually no difference when the discharges are much higher. The straightforward summary being that, the increase due to wind is large when the discharge is small and its effect decreases as the discharge increases, which is in agreement with de Waal *et al.* (1996) and Ward *et al.* (1996).

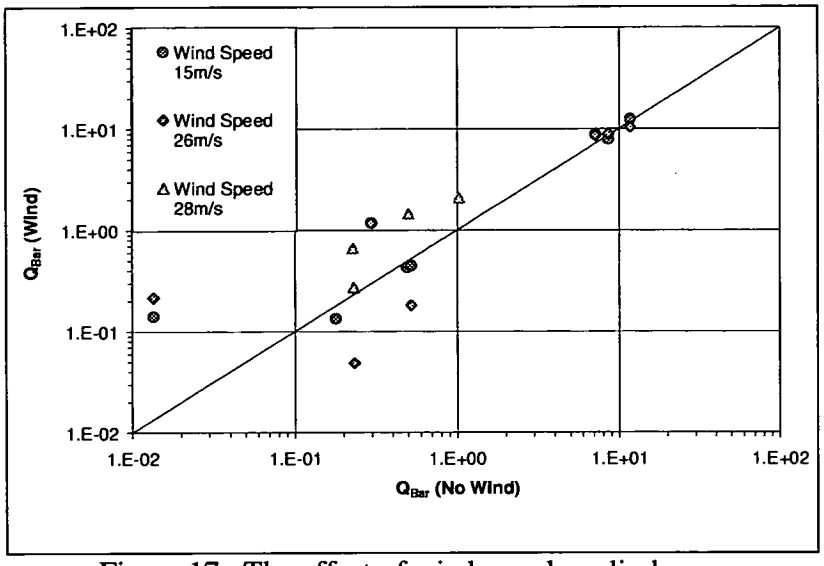

Figure 17. The effect of wind speed on discharge.

The results may also be compared with observations made during the early period of the 2nd May 2003 storm described by Pullen & Allsop (2003), and before overtopping occurred at the monitoring site. Wave-by-wave overtopping volumes of $0.5m^3/m$ were observed regularly with some volumes being in excess of this, and storm force winds were blowing diagonally across the promenade. It was noted at the time that most of the discharge was landing in the area directly behind the parapet wall, and that spray was being blown over distances in excess of 100m. With the discharge landing mainly on the bottom four tiers of the promenade (13.3m) and with a peak period of approximately $T_p = 6.5s$ at the time, then this gives a value $x/L_o = 0.2$. That is, approximately 90% of the discharge for a wind speed of 20~30m/s was landing within $x/L_o = 0.25$, and this is in agreement with Figure 16.

In terms of hazard, data suggests that the mean discharge at a distance of $x/L_o = 0.25$ behind the structure crest will have reduced by a factor of 10. Recent analysis under the EC CLASH project has further supported the existing guidance for safety of pedestrians at a mean discharge of 0.03 litres/s/m. By way of example, the analysis presented here would suggest that a **vertical wall** giving a discharge of 0.3 litres/s/m under a particular storm condition (one not designed for pedestrian access to crest area) would see discharge reduced to 0.03 litres/s/m at a distance of 0.25 × the wavelength behind the crest. Caution and local knowledge and conditions however must be considered, *eg* whether the heaviest overtopping discharge immediately behind the crest will subsequently flow landward over the structure, an effect which in itself could cause a hazardous condition shoreward.

Conclusions

The landward distribution of overtopping discharge is of particular interest in considerations of the location of hazard to people and structures in the vicinity. Previous studies have suggested an exponentially decaying distribution but have offered no generic guidance.

Measurements of the landward distribution of overtopping discharge behind a (near-) vertical wall have been carried out as part of a field measurement campaign at Samphire Hoe and as part of small scale 2d and 3d laboratory studies (at Edinburgh and HR Wallingford).

Observations and measurements at the field site confirmed that wind has a huge influence upon the landward distribution of overtopping discharge. In the absence of wind, field, small-scale model and predicted overtopping discharges were all in excellent agreement.

Small-scale tests at HR Wallingford with wind effect included demonstrated a relationship between wind speed and the rate of exponential decay in overtopping discharge with landward distance. For a given wind speed, the predictor based upon laboratory wind gives a conservative prediction of landward distribution (*ie* gives a greater landward extent than that measured at the Samphire Hoe field site).

Acknowledgements

Part of this work has been conducted under CLASH (EC contract EVK3-2001-0058) with support from defra / EA under FD2412. Some data have been derived from specialist consultancy studies at HR Wallingford. The authors are grateful Stephen Masterton (now IC, London) for work at Edinburgh on landward distributions, Dr Steve Richardson and John Alderson (HRW) for assistance in the CLASH field measurements, Coline Romestaing and Jo Wright for assistance in the 3-d tests at HRW, and Dave Johnson of Eurotunneal & Paul Holt of the White Cliffs Countryside Project.

References

Allsop, N.W.H., Bruce, T., Pearson, J., Alderson, J.S. & Pullen, T. (2003) *Violent wave overtopping at the coast, when are we safe? Proc.* Int. Conf. on Coastal Management 2003, pp 54–69, ISBN 0 7277 3255 2, publn. Thomas Telford, London.

Besley, P. (1999) *Overtopping of seawalls – design and assessment manual* R & D Technical Report W 178, ISBN 1 85705 069 X, Environment Agency, Bristol; Download from: www.hrwallingford.co.uk/projects/overtopping/index.html

Bruce, T., Pearson, J. & Allsop, N.W.H. (2002) *Hazards at coast and harbour seawalls - velocities and trajectories of violent overtopping jets* Proc. 28th Int. Conf. Coastal Eng., Cardiff, July 2002, pp 2216–2226, ISBN 981 238 238 0, publn. World Scientific Publishing, Singapore.

Jensen, O.J. & Sorensen, T. (1979) *Overspilling / overtopping of rubble mound breakwaters. results of studies, useful in design procedures*, Coastal Engineering 3, pp51–65 (Elsevier)

Pullen, T, Allsop, N.W.H., Bruce, T. & Geeraerts, J. (2003) *Violent wave overtopping: CLASH field measurements at Samphire Hoe*, Proc. Coastal Structures 2003, pp469–480, ASCE, New York.

Pullen, T., Allsop, N.W.H., Bruce, T., Pearson, J. & Geeraerts, J. (2004). *Violent wave overtopping at Samphire Hoe: field and laboratory measurements*, to appear in Proc. 29th Intl. Conf. On Coastal Eng (ASCE)

De Waal, J.P., Tonjes, P. & van der Meer, J.W. (1996), *Overtopping of sea defences*, Proc 25rd Int. Conf. Coastal Eng., pp2216–2229, Orlando, ASCE, New York.

Ward, D.L., Zhang, J., Wibner, C.G., & Cinotto, C.M. (1996). *Wind effects on runup and overtopping of coastal structures*. Proc 25rd Int. Conf. Coastal Eng., pp2206–2216, Orlando, ASCE, New York.

Appendix V: Wolters *et al.*, 2005

Wolters, G., Müller, G., Bruce, T. & Obhrai, C. (2005), *Large scale experiments on wave downfall pressures on vertical and steep coastal structures*, Proc. ICE, Maritime Engineering, 158, pp137–145

Appendix V
Wolters *et al.*, 2005

Wolters, G., Müller, G., Bruce, T. & Obhrai, C. (2005), *Large scale experiments on wave downfall pressures on vertical and steep coastal structures*, Proc. ICE, Maritime Engineering, 158, pp137–145

V.1 Declaration of contribution

The author was invited to join the author team for this paper because of his previous work (at small-scale) on the subject (Bruce *et al.*, 2001b).– prior to this publication, the only publication dealing with the topic of wave downfall pressures. The author contributed the comparison with the small-scale predictor. He was also involved in synthesis of conclusions and in detailed editing of the whole paper.

V.2 Published paper

overleaf

Proceedings of the Institution of Civil Engineers
Maritime Engineering 158
December 2005 Issue MA4
Pages 137–145

Paper 13682
Received 05/02/2004
Accepted 21/10/2005

Keywords:
coastal engineering/models (physical)/sea defences

Guido Wolters
Researcher/Advisor, WL| Delft Hydraulics, Marine, Coastal & Industrial Infrastructure, Delft, the Netherlands

Gerald Müller
Senior Lecturer, School of Civil Engineering and The Environment, University of Southampton, UK

Tom Bruce
Lecturer, School of Engineering and Electronics, University of Edinburgh, UK

Charlotte Obhrai
Researcher/Advisor, HR Wallingford, Wallingford, UK

Large-scale experiments on wave downfall pressures

G. Wolters Dipl-Ing (TH), PhD, G. Müller MSc, Dipl-Ing, PhD, T. Bruce MSc and C. Obhrai PhD

Many exposed vertical or steep-fronted coastal structures experience large horizontal impact pressures generated by breaking waves. Breaking and non-breaking waves can however also generate a large uprush of water at the structure, in some cases reaching heights of 70 m and more. This uprush is often carried over the structure, leading to overtopping. It has only recently been shown in small-scale model tests that the downfalling water mass can also generate significant vertical impact loadings on the deck of a breakwater. Within an ongoing research project, large-scale measurements of wave impact and downfall generated pressures on vertical and steeply-faced seawalls and breakwaters were conducted in the Large Wave Channel (GWK) at the Coastal Research Centre (FZK) in Hanover, Germany. The downfall pressures were found to consist of very short pressure peaks (durations down to 0·5 ms) of up to 220 kPa magnitude (corresponding to 12 $\rho g H_i$). The highest downfall pressures occurred for near-breaking waves; non-breaking and breaking waves generated smaller pressures of 20–70 kPa (corresponding to 2–6 $\rho g H_i$). The magnitude of the observed downfall pressures is in the range of horizontal wave impact pressures and suggests that this type of loading, for which no guidance exists, should be considered in the design of coastal structures.

1. INTRODUCTION

When slamming against a vertical or steep-fronted coastal structure, breaking waves create horizontal wave impact pressures. These pressures are very short, but can be extremely high with measured pressures ranging from 746 kPa (field measurements) to 3·9 MPa (large-scale model tests).[1] Breaking waves can also create high overtopping volumes (Fig. 1(a) centre). Depending on the nature of the wave arriving at the wall, either a large sheet of water, termed green water (generated by non-breaking waves), or a violent uprushing spray (generated by the impact of breaking or broken waves) are produced, resulting in a very wide range of discharge volumes and frequency of occurrence.[2] In this context the form of the structure's front face, which is exposed to wave action, is of extreme importance, with backward inclinations generating higher overtopping volumes.[3] The downfalling water mass can inflict damage on the deck of coastal structures, including the bending ('dishing') of manhole covers,[4,5] damage to infrastructure and the harbour wall, and even the breaking of the roadway, hollowing of the core and subsequent breaching of the breakwater[6] (Fig. 1(b)).

The Admiralty Breakwater as shown in Figs 1(b) and 2, which was the model for the large-scale tests conducted in this study, is a blockwork structure, 870 m in length, with a front face inclined at approximately 27° to the vertical but with a vertical parapet wall. It consists of a rubble mound with a vertical superstructure with an average seabed depth of 20 m below low water. The maximum tidal range is 7 m. Mean high water springs (MHWS) is 6·2 m above chart datum (i.e. above the stone mound). During storms, immense volumes of water are projected to a height of fully 75 m. The falling water mass has damaged the roadway of the breakwater frequently, and the rubble mound in front of the structure has been scooped out on occasions as stated by Shield[6]

> 'The high parapet at Alderney caused the whole force of the waves to be thrown against the superstructure, and immense volumes of water were projected, during storms, to a height of fully 200 feet, by the falling of which the roadway of the breakwater was frequently damaged, and the rubble mound scooped out.'

Another example of damage induced by wave downfall was documented at the east pier at Helgoland, where roadway stones facing the harbour side were plucked out by the falling water mass.[7] The downfall in front of the structure was also regarded as responsible for the undermining of the toe of the structure and subsequent settlement.

Figure 1(c) and (d) show the breakwater in Rapallo, Italy during a storm. The water is thrown over the parapet wall and impacts onto the breakwater behind the wall. Fig. 1(c) shows the situation during overtopping and downfall; note the ragged lines in the bottom right corner which indicate that the block road cover of the breakwater has been removed by the downfall. In Fig. 1(d) the lamp-posts along the far side of the breakwater have disappeared.[8]

Despite this evidence, there exists little guidance for the assessment and quantification of the effect of downfalling overtopping discharge, and what exists is based solely on small-scale model tests. In naval engineering on the other hand, pressures generated by overtopping waves are well known, and therein referred to as green water slam.[5] This paper reports the results from the first series of large-scale measurements of this phenomenon on vertical and steeply-faced seawalls and breakwaters. The measurements

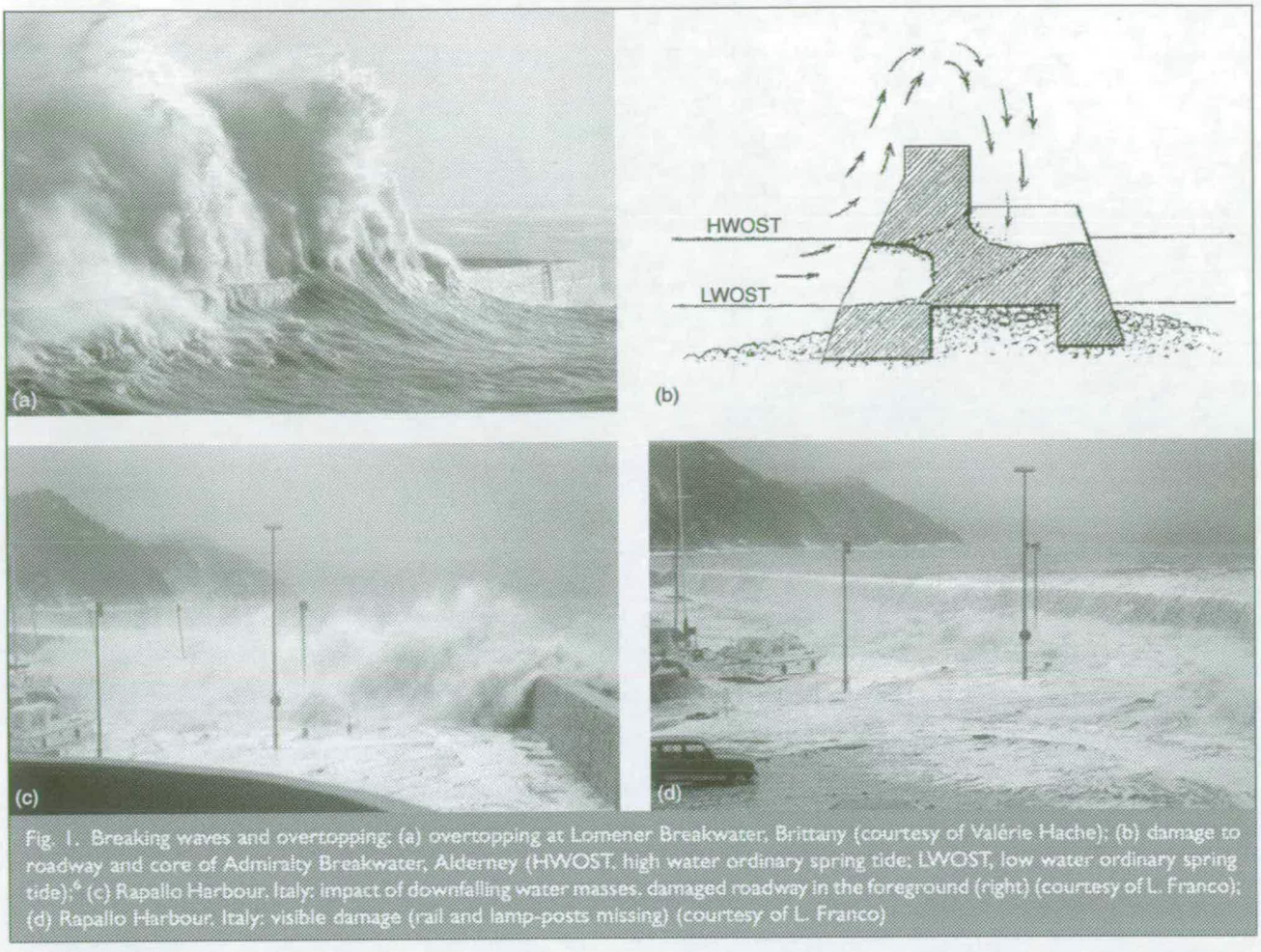

Fig. 1. Breaking waves and overtopping: (a) overtopping at Lomener Breakwater, Brittany (courtesy of Valérie Hache); (b) damage to roadway and core of Admiralty Breakwater, Alderney (HWOST, high water ordinary spring tide; LWOST, low water ordinary spring tide);[4] (c) Rapallo Harbour, Italy: impact of downfalling water masses, damaged roadway in the foreground (right) (courtesy of L. Franco); (d) Rapallo Harbour, Italy: visible damage (rail and lamp-posts missing) (courtesy of L. Franco)

indicate that downfall pressures should be considered for the design of coastal structures exposed to breaking waves.

2. PREVIOUS WORK

2.1. Downfall pressures

Although damage to decks of breakwaters have been reported in the literature, the downfall pressures together with the wave uprush velocities were measured only recently for the first time in a series of small-scale model tests.[5] Recorded downfall pressures in these experiments had magnitudes of up to 25 kPa (approximately 15 $\rho g H_s$) for significant wave heights, H_s, of 0·06–0·113 m and water depths at the structure (a composite breakwater model) of $h = 0{\cdot}085$–$0{\cdot}240$ m. The measured downfall pressures had very short rise times of less than 2 ms and were very localised, with the largest pressures occurring directly behind the crest of the structure. The magnitude of the downfall pressures was found not to be directly related to the wave impact pressure (i.e. high impacts did not coincide with high downfall pressures and vice versa), but no further information was given. The maximum downfall pressures however were in the range 60–70% of the highest impact pressures recorded over a series of 1000 irregular waves.

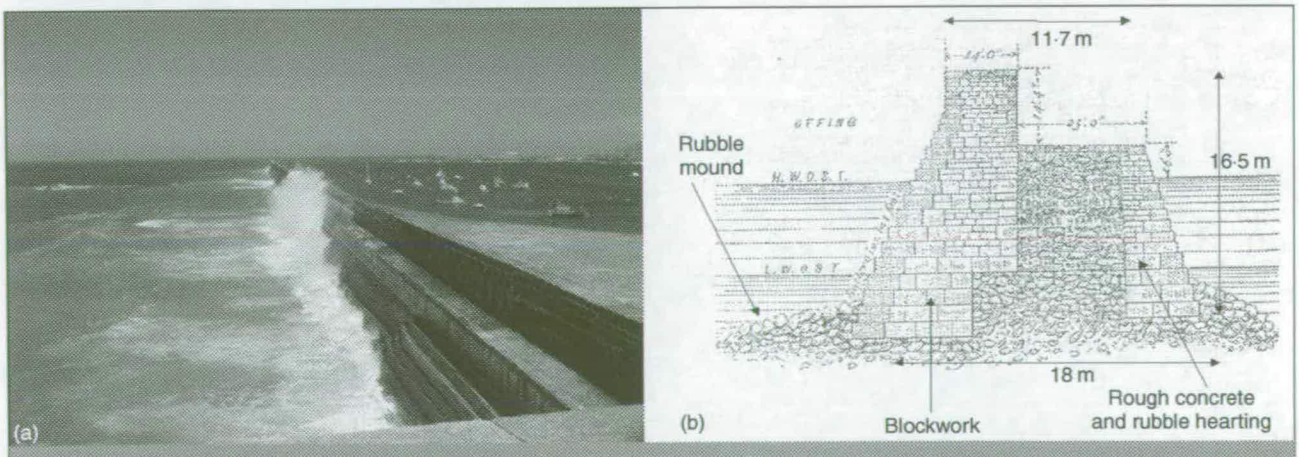

Fig. 2. Admiralty Breakwater, Alderney: (a) view of Admiralty Breakwater; (b) cross-section

From these tests, a tentative prediction tool was developed in the form of a Weibull distribution, derived as an average of the Weibull distributions of the 20 largest downfall pressures (measured at any of their upward-pointing transducers) from each of their 71 small-scale tests (equation (1)).

$$\ln\left\{-\ln\left[1-\text{prob}\left(\frac{P}{\rho g H_{si}}\right)\right]\right\} = 0{\cdot}21 + 0{\cdot}6\ln\left(\frac{P}{\rho g H_{si}}\right) - 0{\cdot}14\frac{R_c}{H_{si}} \quad (1)$$

where H_{si} is the incident significant wave height at the toe of the structure (m); R_c is the freeboard (i.e. crest height of the structure–mean water level) (m); P is the downfall pressure (Pa); g is the acceleration due to gravity (m/s^2); and ρ is the water density (kg/m^3).

The nature of wave downfall suggests that downfall pressure magnitudes are related to uprush height (and subsequently the vertical uprush velocity of the wave). In large- and small-scale overtopping experiments it was found that the throw velocity can be up to seven times the inshore wave celerity for breaking waves, whereas a factor of 2·5 is typical for non-breaking waves.[9]

In a different set of small-scale tests, the effect of downfalling water, caused by wave impact-induced uprush, on pressures on the seabed in front of a seawall was investigated.[10] The pressures inflicted by breaking waves on a vertical wall model and the seabed in front of it were measured simultaneously, and video-imaging techniques used to relate the impact of the downfalling water mass to the pressure time trace recorded on the seabed. The results showed that significant downfall-related pressures of up to 10% of the impact pressure magnitude can be expected to occur on the seabed. This mechanism still warrants further investigation.

2.2. Wave overtopping

The mechanism of wave downfall implies that the pressures generated depend on the volume and the velocity of the downfalling water. This suggests a close relationship to wave overtopping. In the following, a brief review of overtopping will be given in order that key physical mechanisms can be identified and discussed.

Overtopping volumes have been measured by many researchers for varying forms of seawalls, including vertical and sloped walls, plain or composite structures, much of which is summarised in the current EA Overtopping Manual.[2] The overtopping performance of vertical walls is dependent upon the incident wave conditions: as wave heights become limited by the water depth, waves begin to break onto/over the seawall (impacting waves), causing a (sometimes sudden) change in the overtopping performance.[11] This led to the introduction of a parameter h_*, which determined whether overtopping performance was dominated by reflected non-breaking or impacting conditions and which was defined as

$$h_* = \left(\frac{h}{H_s}\right)\left(\frac{2\pi h}{gT_m^2}\right) \quad (2)$$

where h is the water depth at the toe of the structure (m), H_s is the significant wave height at the toe of the structure (m), and T_m is the mean wave period at the toe of the structure (s).

Non-breaking waves predominate when $h_* > 0{\cdot}3$; impacting waves or impulsive wave regimes when $h_* \leq 0{\cdot}3$. Overtopping equations were derived for both types of wave action. The fit of the data was superior to all previously derived equations and for this reason this method is now recommended for use with vertical walls.

The guidance also indicates that the previously used mean overtopping discharges do not directly relate to the observed damage to coastal structures, demonstrating the significance of individual large overtopping events. Such single wave events are often held responsible for serious damage to parapets, breakwater crowns and roadways.[6]

3. LARGE-SCALE TESTS

3.1. Introduction

Within an ongoing research project on breaking wave impact pressures on coastal structures (*BWIMCOST*), the authors conducted large-scale measurements of wave downfall pressures in the Large Wave Channel (GWK) in Hanover, Germany. These model tests were designed as a 1 : 4 model of the Admiralty Breakwater on Alderney, where currently field measurements of impact pressures and pressure propagation into cracks are conducted.[12] In the first stage of the model tests, a vertical structure was employed which is assumed to simulate the overtopping regime on Alderney more accurately than an inclined wall.

3.2. Experimental set-up

The tests were conducted in the GWK, located at the Coastal Research Centre (FZK) in Hanover, Germany. The GWK has a length of 324 m, a width of 5 m and an operating water depth of 7 m. The model employed in the large-scale tests consisted of a 5 m × 2·5 m × 2·5 m sand-filled concrete caisson with a mass of 30 t, which was located on top of a rubble mound (Figs 3 and 4).

The rubble mound started 20 m in front of the structure with a slope of 1 : 4·7 for the first 10 m and then changing to 1 : 10·7. The overall height of the rubble mound at the base of the structure is 3 m. The rubble mound was constructed of sand, topped by a geotextile mat and a 0·45 m layer of stones (~0·2 m diameter) on the surface. The caisson was mounted on a 0·3 m thick concrete base-plate with tensile stress anchors and held in position by a 0·53 m wide and 0·30 m high steel joist at the back end which was anchored within the tank walls and a line of L-shaped concrete sections at the front. Another joist similar to the one at the bottom was fitted at the top end of the caisson to prevent it from tilting. The caisson was fronted by a concrete panel of 0·15 m thickness which held all the measuring equipment. It was attached to the caisson by tensile stress anchors. The caisson walls had a thickness of 0·15 m.

Three downfall pressure transducers were mounted behind each other on the top of the caisson with distances from the front

face of 90, 190 and 600 mm and a distance of 2·21 m from the right tank wall. The caisson was subjected to regular breaking waves of 1·2–1·7 m incident wave height and 4–10 s period. Irregular wave tests were also carried out. The focus of this paper is however on the regular wave tests since the results from irregular waves could not be used for reasons explained later. The uprush reached heights of at least 20 m, giving an estimate of vertical velocities of approximately 20 m/s. 0·5 MPa pressure transducers from Druck Messtechnik (PDCR 831) were employed in the GWK tests, using a sampling frequency of 10 kHz. The uprush velocity was determined using the PDCR 831 pressure sensors and the pressure aeration units (PAUs) which were specially designed by the University of Plymouth.
A full description of the set-up and all sensors is given in Bullock *et al.*[12]

The GWK tests were set up primarily to investigate the characteristics of breaking wave impact loads and therefore do not constitute a complete wave parameter study, but rather focus on a certain range of wave conditions which caused wave breaking at the structure. The results presented for the GWK tests are therefore only valid for the following wave conditions with incident wave height H_i and period T_i

3	$H_i/h = 0{\cdot}3 - 1{\cdot}8$, $T_i = 5{-}9$ s

Only overtopping in the impulsive wave regime is addressed in this study; green water effects and very fine spray are only included as a side-effect.

Due to the particular aim of the investigations (i.e. the determination of physical characteristics of breaking wave impact loads), the study employed mainly regular waves, which allowed for a relatively high dynamic similarity between individual breakers. The investigations with irregular wave spectra produced generally far fewer impulsive overtopping events and overall did not allow the study of extreme wave heights and wave steepness (due to restrictions in the wave paddle motion) to the extent that the regular tests did. Furthermore, in the initial test period where downfall pressures were recorded, irregular wave tests did not produce much overtopping. A general probability assessment of downfall pressures at large scale for various sea states was therefore not possible.
At the present stage, the results obtained therefore only give an indication of the upper limit of the downfall pressure range.

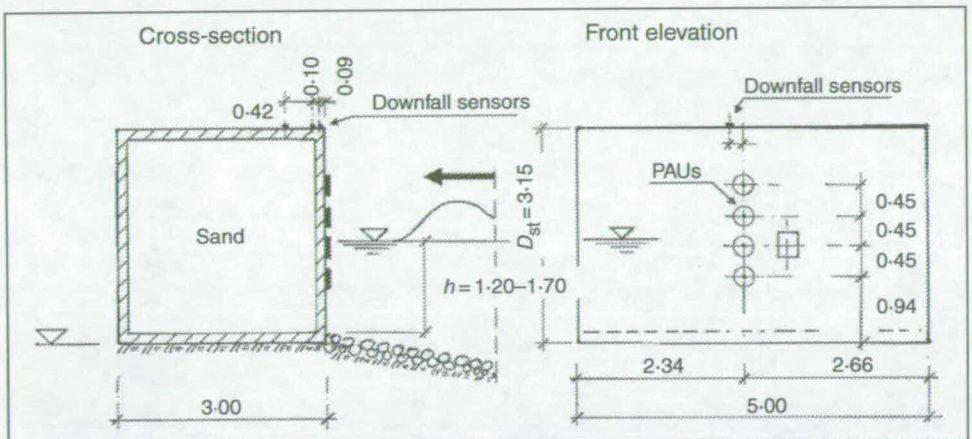

Fig. 3. Test set-up at the GWK (Hanover, Germany; dimensions in m)

4. RESULTS

4.1. Pressure–time traces

The maximum downfall pressure peaks were found not to coincide with high horizontal impact events, and they occurred typically 3 s after the horizontal wave

Fig. 4. Pictures of the GWK set-up (Hanover, Germany): (a) front view; (b) panel with the three downfall pressure transducers mounted on top of the caisson at the seaward edge

impact pressure. This time separation corresponds well with the uprush velocities of 15–20 m/s recorded and indicates that the maximum downfall pressures are caused by those small fluid 'packets' which reached the highest point of the uprush. This is depicted in Fig. 5(a) where the pressures measured at the front face of the structure and at the downfall pressure sensor nearest to the seaward edge of the structure are shown for the event which generated the highest downfall pressure. The footprint of the downfall pressures illustrates the highly localised nature of these pressures (Fig. 5(b)) (transducer locations are given as distance from the front edge of the breakwater). Furthermore the relatively large 'green water' mass which does not take part in the uprush, namely that which more or less flows up and over the structure crest as a compact water mass, is clearly identifiable, see Fig. 5(c) (downfall pressure peak at $t = 1{\cdot}9$ s).

The pressure–time traces of the wave downfall measured in the GWK have a distinct shape, resembling wave impact pressures. The lower, green-water-induced downfall pressures are characterised by rise times of up to 2 ms (Fig. 5(c)). The shape of the highest downfall pressure peaks, as seen in Fig. 5(d), is a sharp almost triangular impact with a rise time of 0·2 ms and a typical duration of around 0·5 ms. Downfall pressures of up to 220 kPa were recorded in the GWK tests corresponding to 12 $\rho g H_i$.

4.2. Pressure maxima

From observations and previous small-scale experiments it appeared that downfall pressures might be linked directly to either wave impact pressures or uprush velocities. The new GWK data indicate no direct correlation between wave impact pressures or uprush velocities and downfall pressures (Fig. 6(a), P_{down} plotted against P_{impact} and Fig. 6(b) P_{down} plotted against v_{up}).

In order to understand the mechanism giving the largest downfall pressures, a closer look at Figs 6 and 7 is required. Fig. 6(a) shows that the largest downfall pressures have corresponding impact pressure magnitudes of 30–50 kPa or 2–3 $\rho g H_i$. It is also notable that higher horizontal impact pressures result in significantly smaller downfall pressures. The highest downfall pressures occurred for uprush velocities of approximately 12 m/s (Fig. 6(b)). Looking now at Fig. 7(a), it can be seen that an uprush velocity of 12 m/s corresponds to horizontal impact pressures of 30–50 kPa. It can therefore be inferred that a certain wave condition, namely 'near breaking' waves, generates the highest downfall pressures.

By way of explanation it can be assumed that smaller waves generate a more compact water mass but for a lower uprush

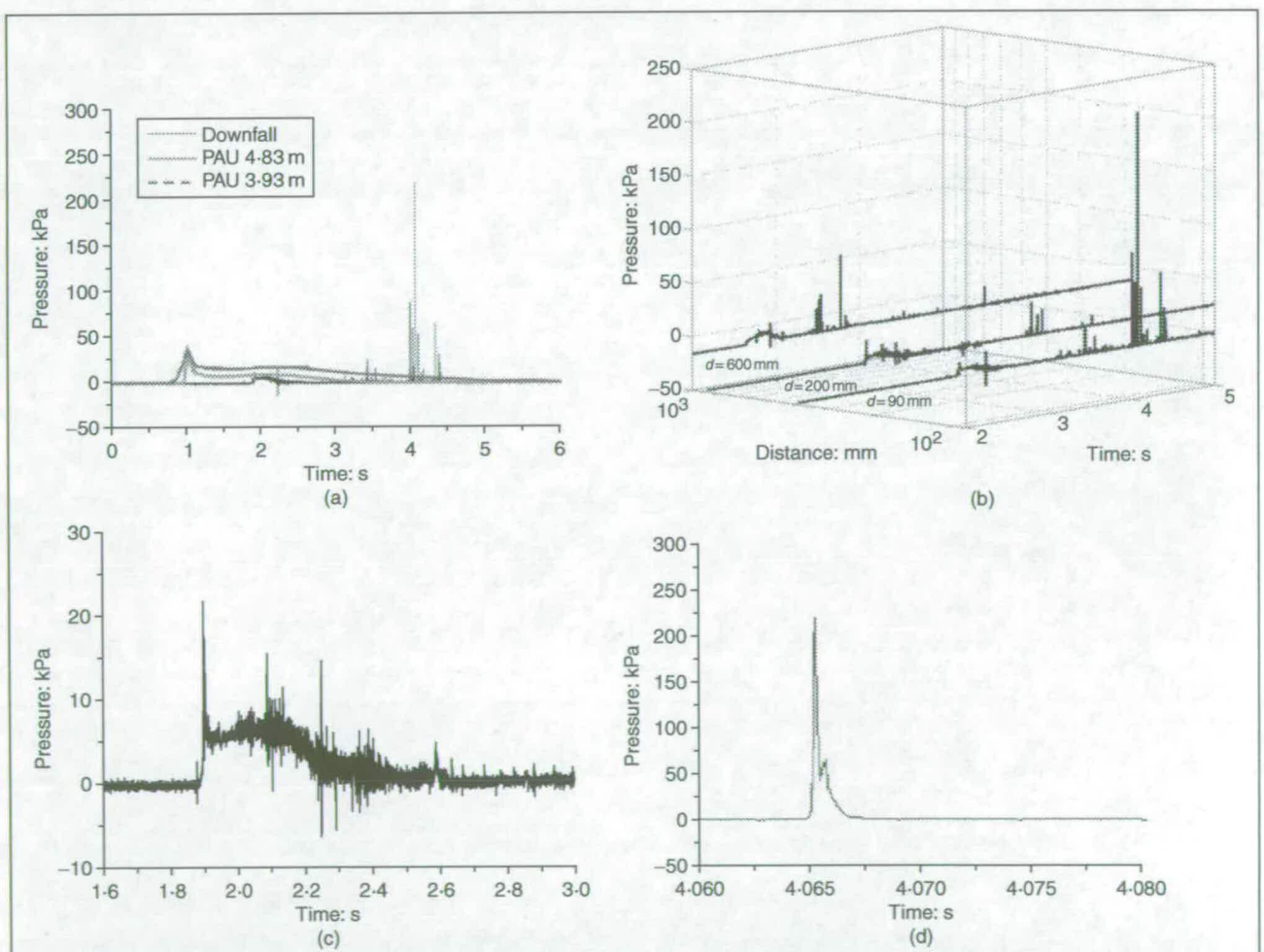

Fig. 5. Horizontal and vertical pressures for highest downfall pressure, $P_{max} = 220$ kPa: (a) impact pressures at front face and deck; (b) footprint on top, $P_{max} = 220$ kPa; (c) low downfall pressure at $t = 1{\cdot}85$ s; (d) high downfall pressure at $t = 4{\cdot}065$ s

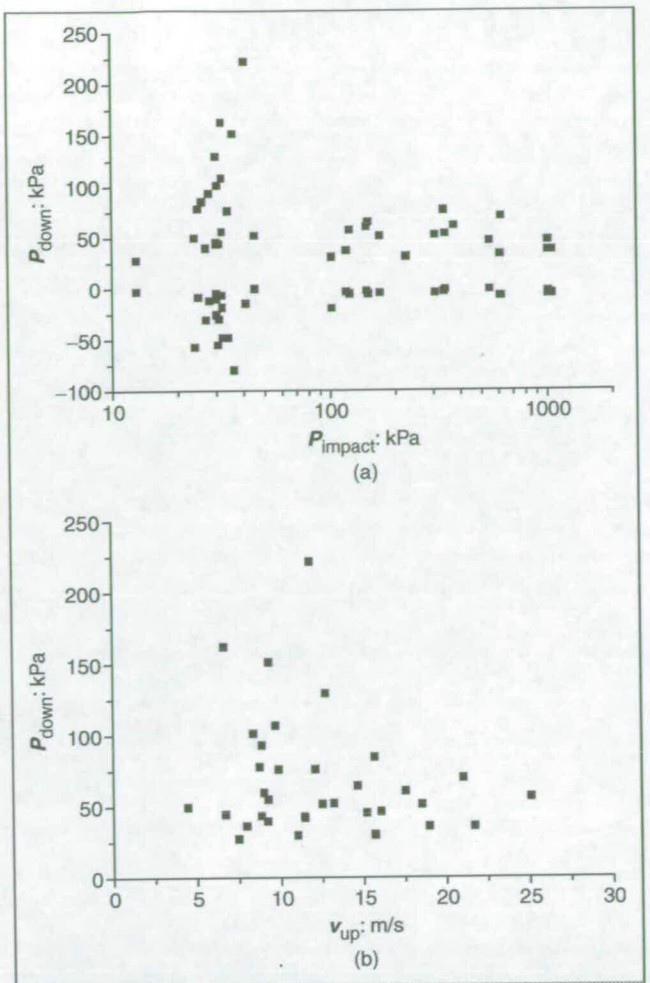

Fig. 6. Downfall pressures P_{down} as functions of impact pressure P_{impact} and uprush velocity v_{up}: (a) downfall and impact pressures; (b) downfall pressure and uprush velocity

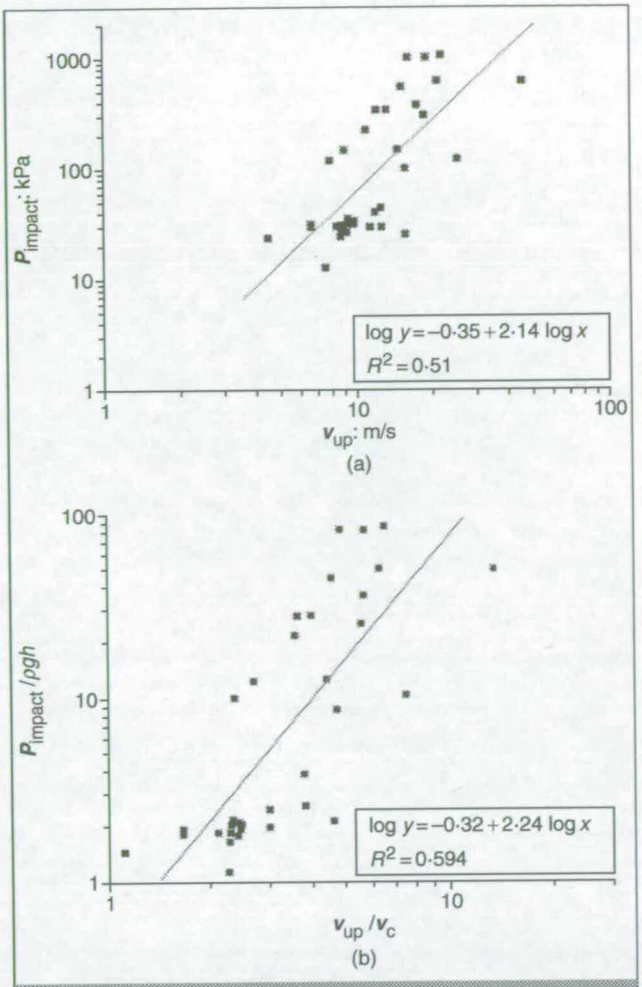

Fig. 7. Horizontal impact pressures and uprush velocities: (a) impact pressure and uprush velocity; (b) non-dimensionalised graph

velocity or downfall height, larger waves create higher uprush velocities but this causes the water mass to disintegrate to a greater extent. The magnitude of wave downfall pressures therefore does not necessarily depend directly on the impacting wave but also significantly on the properties of the downfalling water mass, namely the compactness of the water mass and its impact velocity. The downfall pressures reach a maximum for uprush velocities of 8–12 m/s, corresponding to a ratio of uprush velocity to shallow water wave celerity of $v_{up}/v_c = 2{\cdot}0–3{\cdot}5$ at water depths of 1·2–1·7 m at the structure.

A clear relationship between impact pressure magnitude and uprush velocity was found (Fig. 7) with velocities increasing for increasing pressures. The downfall pressure therefore appears to be more closely related to the overtopping process than to horizontal wave impact pressures. The impact velocity of the downfalling water mass, as the missing relationship between P_{down} and v_{up} seems to indicate, might not be as important as previously assumed, with the physical form of the jet and the break-up process playing a key role.

For design purposes, the uprush velocity g_{up}, as given in Fig. 7(b), was non-dimensionalised using the inshore wave celerity $v_c = \sqrt{gh}$. The results are very much in line with previous large- and small-scale measurements, where dimensionless uprush velocities of up to seven times the inshore wave celerity under impulsive conditions were reported.[5,9]

Negative (suction) downfall pressures of down to −85 kPa were also recorded on the top of the structure in the GWK experiments. They could be caused either by a high velocity flow on the top of the structure or by the elastic response of the compressed water mass during impact (decompression). Considering the short duration of the negative pressures (typically approximately 1 ms) the former reason however seems unlikely. Compressibility effects seem to be therefore of primary importance in the downfalling water impact phenomenon.

4.3. Influence of freeboard

The data analysis showed that the maximum downfall pressures occurred for the highest water levels within the wave tank; that is, for a minimum freeboard. The higher water level tests were usually connected to lower impact pressures because the waves did not become steep enough to break. The tests were conducted for a very narrow range of wave heights at the structure. The use of the conventional relative freeboard parameter R_c/H_i was therefore not considered meaningful.

A simple freeboard parameter, the ratio of water depth h to the height of the structure D_{st}, $h_{cl} = h/D_{st}$, was introduced based on the observations and the interpretation of the test results.

The relationship between downfall pressures and the freeboard parameter shows that downfall pressures increase for increasing h/D_{st} values (Fig. 8). A comparison with the h_* value was considered not meaningful since the h_* value is based on random wave data, whereas in the current investigation only regular waves were employed.

5. DISCUSSION

5.1. Effects of downfall pressures

The effects of downfall pressures on coastal structures have so far not been considered in design recommendations. The experiments showed that breaking and 'near breaking' waves not only generate horizontal loads, but also vertically acting loads on the structure. Wave downfall will not (at least initially) affect the stability of the structure, but it can damage individual elements such as manhole covers or pavements (as seen for example at the Admiralty Breakwater, Alderney) and could lead to the initiation of wider damage and even failure.[13] Although downfall pressures are highly localised, their effect on coastal structures can be significant due to another mechanism, namely pressure propagation. Similar to wave impact pressures, it can be expected that the downfall pressures can enter water- or air-filled joints and cracks of the structure generating splitting pressures inside the structure which can last significantly longer than the impact pressures on the front wall or crest of the structure.[14,15] This can lead for example to the removal of corner blocks at the harbour side of the structure, pavement plates, etc. and subsequent further damage (Fig. 1(c) and (d)).

5.2. Design pressures and affected area

The prediction of downfall pressures is at present still connected with large uncertainties. In the absence of any other information on this topic, the information derived from the GWK tests has to be used for a preliminary estimation of pressure magnitudes. The maximum downfall pressures occur for near breaking waves, so it must be established whether wave breaking (or impulsive) conditions exist at the structure. As the maximum wave downfall pressures are a function of the ratio of uprush speed v_{up} to celerity of the incoming wave v_c, both of which are subject to Froude scaling, and since the incident wave height H_i is limited by the water depth at the structure, a simplified estimate of downfall pressures can be made, in the absence of any scaling law, also using Froude scaling (equation (4))

$$\max P_{down} = 12\rho g H_i [\mathrm{N/m^2}] \quad (4)$$

The footprint of the downfall pressure is difficult to determine; test results point to the fact that the full-scale pressure for breaking wave-induced downfall on a vertical structure may only act over a landward extent of approximately 1·5 m. The highest downfall pressures occurred close to the seaward corner of the structure (90 mm from the seaward face). In reality, however, the slope of the front face, wave conditions varying from plunging breakers and wind will have an influence on the location, footprint and magnitude of downfall events, so that the downfall pressures can be expected to act further landwards and/or have larger footprints—possibly over the full width of the structure. For simplicity, the authors suggest a triangular pressure distribution for the near impact conditions on the vertical wall investigated in this study. Pressures increase from zero to maximum within 0·75 m and reducing to zero within the same distance; whereby the point of maximum pressure can occur at a distance of more than 0·75 m away from the seaward corner in order to take account of wind effects.

These findings are consistent with recent research by Bruce *et al.*[16] on overtopping discharge and landward overtopping distribution for vertical structures. Their study is the first that includes wind effects on spatial overtopping distribution. Furthermore, Bruce *et al.*[16] have shown that an exponentially decaying distribution of overtopping discharge with distance from the seaward edge of the structure provides a reasonable approximation of the footprint. Even in the presence of very strong on-shore wind effects, Bruce *et al.*[16] conclude that 90% of the overtopping discharge lands within one-quarter of a wavelength of the structure's seaward crest.

In a second series of experiments with an inclined front face of 26° to the vertical, as described in Bullock *et al.*,[1] the overtopping water mass was frequently projected more than 5 m landward from the front face, so that the entire structure was overtopped. However, no downfall pressure records exist for these tests.

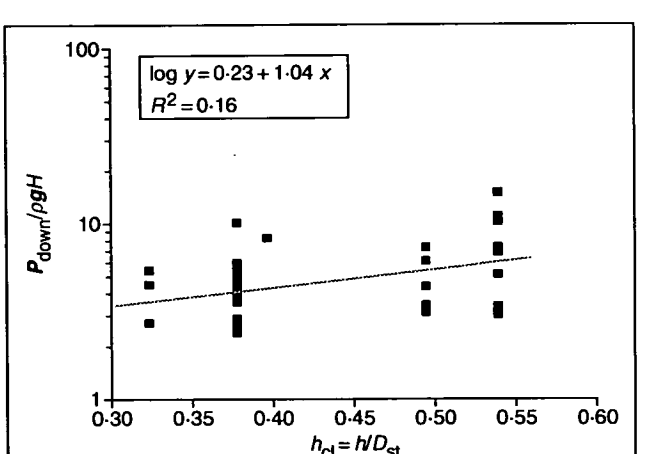

Fig. 8. Downfall pressures as a function of wave and freeboard parameter influence

5.3. Scale effects

So far, very little is known about scale effects on downward pressures, as no comparative field measurements are available. However, it can be assumed that tests with fresh water give conservative results since the downfall pressures appear to be related to the velocity of the uprush and the compactness of the falling mass of water. The velocity of fluid particles in a wave obeys Froude scaling, so that full-scale velocities should be modelled in the tests. Only one full-scale measurement of uprush

velocities, Rouville *et al.*'s measurements,[17] is known to the authors. It was found that vertical velocities can reach 77 m/s or six to seven times the horizontal velocity of the wave. This compares well with the test results reported here (Fig. 7(b)) and with those reported by Bruce *et al.*[9]

The compactness of the water mass will however depend on the kinetic energy and the surface tension which, respectively, try to break up and hold together the water mass. At full scale, the tendency of a water mass to break up will probably be higher since the kinetic energy of particles is higher, whereas the surface tension will be even slightly less since seawater contains salt and organic detergents that reduce surface tension. Reports of damage to breakwaters do however suggest downfall pressures of up to 800 kPa,[5] so that Froude scaling of the large-scale results does not seem unrealistic.

Some comparison with the prediction of Bruce *et al.*[5] is illuminating, although a definitive statement is not possible due to the fact that regular waves were used in the GWK tests reported here. On inspection of equation (1), it is clear that the maximum dimensionless downfall pressure is a function of relative freeboard (R_c/H_s) only, and therefore this predictor does not make the discrimination between near-breaking and breaking waves that the results reported in this paper suggest is important. Nevertheless, an order-of-magnitude comparison could be arrived at via the questionable substitution of H_s with $H_i/1{\cdot}8$ (taking $H_{max} \approx 1{\cdot}8 \times H_s$ for a 1000-wave sequence). Over all the GWK tests, downfall pressure maxima are generally overpredicted by this rather crude approach, although the largest measured pressure is actually predicted to within 3%. Over the range of conditions studied, the prediction is conservative, overpredicting by factors of up to 2·5. Thus, if it can be established that waves are in a breaking or near-breaking regime at the structure, it appears that equation (1) gives an order-of-magnitude indication of likely downfall pressure maxima.

5.4. Implications for design

For the design of a coastal structure, wave downfall pressures cannot be seen as an isolated loading mechanism but need to be considered within the overall framework of the effect of waves on a structure's stability, structural strength and integrity (Fig. 9). Whereas horizontal wave loads can affect the local load resistance (structural strength) and the stability of a structure, wave downfall can damage the structure from the top, at some stage magnifying the effect of horizontal wave loads. Both horizontal and vertical pressures can be transmitted through cracks and fissures inside the structure, leading to the removal of blocks and thereby disturbing the integrity of the structure.[18] Further blocks can then be removed more readily by the wave, leading to greater damage or a breach of the structure.

5.5. Limitations

The current state of knowledge about downfall pressures is limited mostly because results from recent field measurements are not yet available and scale effects are not yet fully quantified. The formulae given are based on maximum downfall pressures because sufficient data for a statistical analysis are not available; the character of the measurements does however point to the fact that downfall pressures are of a random character since the downfall pressures generated by waves of equal height can vary by an order of magnitude. More data are therefore required both from full- and model-scale experiments. However, for design purposes the exact knowledge of downfall pressures is, at the current state of knowledge, possibly not of overriding value. Rather, it appears more important for the designer to be aware of the possibility of such loadings, their effects, their order of magnitude and likely areas of action. The design of structural elements for approximate loads in order to give them sufficient and consistent strength appears to be more appropriate than the current practice of designing for random loads or neglecting downfall pressures completely in the absence of any information or recommendation.

6. CONCLUSIONS

As part of an ongoing field and large-scale investigation on the effect of wave impact pressures on coastal structures, downfall pressures on breakwater crowns and decks were measured in large-scale tests on a 1 : 4 model of the Admiralty Breakwater. The highest downfall pressure recorded so far was 220 kPa with a duration of 0·5 ms. It was found that the highest downfall pressures occur for near-breaking waves and a low freeboard—the wave-induced vertical pressures are therefore not directly correlated to horizontal wave impact pressures. Downfall pressures exceed the hydrostatic head of the

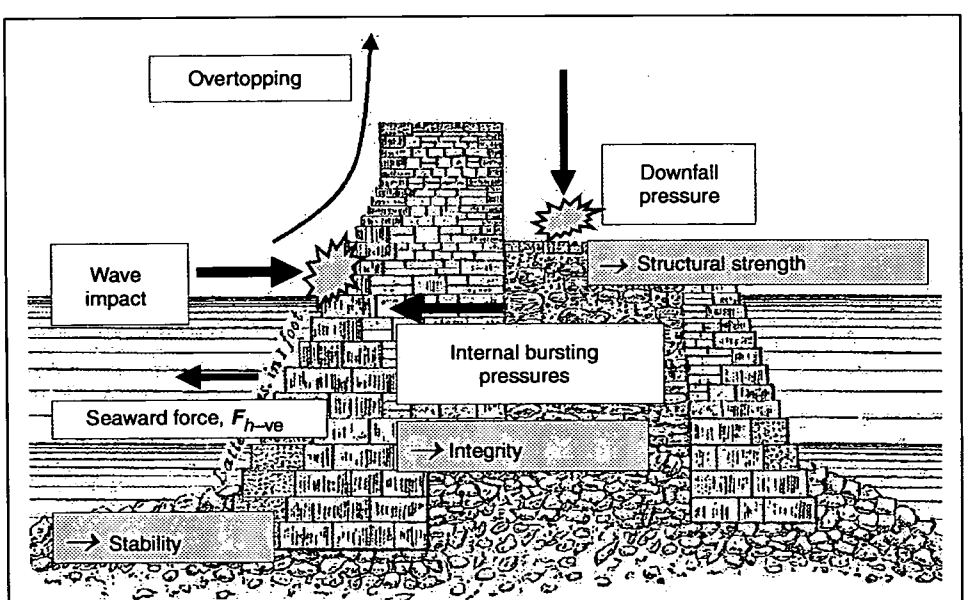

Fig. 9. Effect of wave impacts on a coastal structure (Figure based on an idea by W. Allsop, HR Wallingford)

impacting wave by a factor of 5–12 and often have very short pressure rise times of 0·06–2 ms.

To date, downfall pressures are not mentioned in design recommendations. The magnitude of the downfall pressures determined in the tests, as well as reported damage, suggest that these loadings should be considered for the design of coastal structures. Some preliminary recommendations for the determination of downfall pressures and their effect on coastal structures are therefore given, whereby the downfall pressures are determined as a function of the incident wave height, the uprush velocity and the freeboard ratio. The vertical downfall pressures are subsequently integrated into the wider concept of design considerations for wave effects on coastal structures.

7. ACKNOWLEDGEMENTS

The authors gratefully acknowledge the help of Professor G. N. Bullock, Professor H. Peregrine and Dr H. Bredmose as partners in the BWIMCOST project. The support of EPSRC under Grant No. GR/R30600 is also acknowledged. The large-scale tests in the Large Wave Channel (GWK) of the Coastal Research Centre (FZK) were supported by the European Community under the Access to Research Infrastructures action of the Human Potential Programme (contract HPRI-CT-1999-00101). The cooperation of Joachim Grüne (FZK) is recognised. Professor Leopoldo Franco and Paolo Alberti (both University of Rome 3) supported the project and provided additional material.

REFERENCES

1. Bullock G., Obhrai C., Müller G., Wolters G., Peregrine H. and Bredmose H. Advances in the understanding of wave impact forces. *Proceedings of the ICE Conference on Coastlines, Structures and Breakwaters.* Thomas Telford, London, 2005 (in press).
2. Besley P. *Overtopping of Seawalls–Design and Assessment Manual.* Environment Agency, Bristol, 1999, R & D Technical Report W 178.
3. Oumeraci H., Kortenhaus A., Allsop N. W. H., De Groot M. B., Crouch R. S., Vrijling J. K. and Voortman H. G. *Probabilistic Design Tools for Vertical Breakwaters.* Balkema, Rotterdam, 2001.
4. Bruce T., Franco L., Alberti P., Pearson J. and Allsop N. W. H. Violent wave overtopping: discharge throw velocities, trajectories and resulting crown deck loading. *Proceedings of the 4th International Conference on Ocean Wave Measurement and Analysis ('Waves 2001').* ASCE, Reston, VA, USA, 2001, pp. 1783–1796.
5. Health and Safety Executive (HSE). *Review of Greenwater Waveslam Design & Specification Requirements for FPSO/FSU's.* Health and Safety Executive, London, 2000, Offshore Technology Report–OTO 2000 004.
6. Shield W. *Principles and Practice of Harbour Construction.* Longmans, London, 1895.
7. Eckhardt A. Erfahrungen über Wellenwirkung beim Bau des Hafens in Helogoland (Experiences with wave action during the construction of Heligoland Harbour, in German). *Jahrbuch der Hafenbautechnischen Gesellschaft Hamburg,* 1932, 12, 92–102.
8. Alberti P., Bruce T. and Franco L. Wave pressures on the crown deck of upright breakwaters. *Proceedings of the 4th International Conference on Coasts, Ports and Marine Structures, ICOPMAS 2000, Bandar Abbas, Iran,* 2000.
9. Bruce T., Pearson J. and Allsop N. W. H. Hazards at coast and harbour seawalls–velocities and trajectories of violent overtopping jets. *Proceedings of the 28th International Conference on Coastal Engineering, Cardiff.* World Scientific, Hackensack, NJ, USA, 2002, 2216–2226.
10. Müller G. and Wolters G. Impact forces on the sea bed created by wave uprush. *Proceedings of the 4th International Conference on Coasts, Ports and Marine Structures, ICOPMAS 2000, Bandar Abbas, Iran,* 2000. Paper 605 (available for download at http://www.csg.soton.ac.uk/Index.htm).
11. Allsop N. W. H., Besley P. and Madurini L. Overtopping performance of vertical walls and composite breakwaters, seawalls and low reflection alternatives. In *MAST II.* University of Hanover, 1995, Paper 4.7 in MCS Project Final Report.
12. Bullock G., Obhrai C., Müller G., Wolters G., Peregrine D. H. and Bredmose H. Field and laboratory measurement of wave impacts. *Proceedings of the 3rd International Conference on Coastal Structures.* ASCE, Reston, VA, USA, 2003, pp. 343–355.
13. Wolters G. *Characteristics of Wave Impact-induced Pressure Pulse Propagation into Cracks of Coastal Structures.* PhD thesis, Department of Civil Engineering, Queen's University, Belfast, UK, 2004.
14. Müller G., Hull P., Allsop N. W. H., Bruce T. and Franco L. Wave effects on blockwork structures: model tests. *Journal of Hydraulic Research,* 2002, 40, No. 2, 117–124.
15. Wolters G., Müller G., Bullock G., Obhrai C., Peregrine D. H. and Bredmose H. Field and large scale model tests of wave impact pressure propagation into cracks. *Proceedings of the 29th International Conference on Coastal Engineering, Lisbon.* World Scientific, Hackensack, NJ, USA, 2004, 4027–4039.
16. Bruce T., Pullen T., Allsop N. W. H. and Pearson J. How far back from a seawall is safe? Spatial distributions of wave overtopping. *Proceedings of the ICE Conference on Coastlines, Structures and Breakwaters.* Thomas Telford, London, 2005 (in press).
17. Rouville M. A., Besson M. M. P. and Petry P. Etudes Internationales sur les effort dus aux lames. *Annales des Ponts et Chaussées,* 1938, 108, No. VII, 5–113 (in French).
18. Bezujien A., Wolters G. and Müller G. Failure mechanisms for blockwork breakwaters. *Proceedings of the ICE Conference on Coastlines, Structures and Breakwaters.* Thomas Telford, London, 2005 (in press).

What do you think?
To comment on this paper, please email up to 500 words to the editor at journals@ice.org.uk

Proceedings journals rely entirely on contributions sent in by civil engineers and related professionals, academics and students. Papers should be 2000–5000 words long, with adequate illustrations and references. Please visit www.thomastelford.com/journals for author guidelines and further details.

Appendix W: Allsop *et al.*, 2004

Allsop, N.W.H, Bruce, T., Pearson, J., Franco, L., Burgon, J. & Ecob, C., (2004), *Safety under wave overtopping: how overtopping processes and hazards are viewed by the public*, Proc. 29th Int. Conf. Coastal Engineering, 4, pp 4263–4274, ASCE / World Scientific, Singapore, ISBN 981-256-298-2

Appendix W
Allsop *et al.*, 2004

Allsop, N.W.H, Bruce, T., Pearson, J., Franco, L., Burgon, J. & Ecob, C., (2004), *Safety under wave overtopping: how overtopping processes and hazards are viewed by the public*, Proc. 29th Int. Conf. Coastal Engineering, 4, pp 4263–4274, ASCE / World Scientific, Singapore, ISBN 981-256-298-2

W.1 Declaration of contribution

This paper emerged from the "Safe at the Seaside" project, led by the author (see Section 4.3.1). Preparation of this paper constituted a genuine team effort, with contributions from Edinburgh and Roma Tre (Franco). Later, the author played a significant role in editing the final paper.

W.2 Published paper

overleaf

SAFETY UNDER WAVE OVERTOPPING – HOW OVERTOPPING PROCESSES AND HAZARDS ARE VIEWED BY THE PUBLIC

WILLIAM ALLSOP

University of Southampton, & Technical Director, HR Wallingford, Howbery Park, Wallingford OX10 8BA UK (e-mail: w.allsop@hrwallingford.co.uk)

TOM BRUCE [1], JON PEARSON [2]

[1] Lecturer & [2] Research Fellow, School of Engineering & Electronics, University of Edinburgh, UK

LEOPOLDO FRANCO

Modimar s.r.l.; Professor, University of Rome 3, Italy

JO BURGON [3], CHRISTINE ECOB [4]

[3] Head, Access & Recreation, National Trust, Cirencester, UK;
[4] Communications Manager, National Flood Warning Centre, Environment Agency, Frimley, UK

Whilst researchers have substantially improved methods to predict wave overtopping, the public often seem to be unaware of the dangers of wave action at the coastline, as indicated by the 2-4 deaths each year in UK and Italy. This is compounded by ignorance by some engineers and managers of key aspects of overtopping, including the wide range of overtopping responses, effects of wave breaking on occurrence of violent overtopping, overtopping velocities or spatial distribution. This paper describes the strategy and initial findings of a "Partnership for Public Awareness" project to explore and improve understanding of these hazards, and thus to reduce deaths and injuries caused by wave overtopping. Updated guidance on overtopping hazards and tolerable limits on overtopping responses is also presented.

1. Introduction

Worldwide, people choose to live close to the coast with waterfront properties commanding 50–100% premium on price. Use of the coast, including recreation, is increasingly all-season, even under storm and post-storm conditions. Yet surge tides and heavy waves may cause substantial hazards along shorelines as demonstrated by 2–4 deaths each year in each of Italy and UK.

Figure 1. Overtopping hazard.

Recent coastal engineering research has sought to improve understanding of wave and overtopping processes at seawalls; to provide better laboratory and field data; to extend prediction tools; and to identify safe limits for overtopping for use by engineers and managers. To prevent or reduce deaths or hazards from wave overtopping, however, other improvements are also needed in public awareness and understanding of wave and coastal processes, and hence of wave overtopping. This paper presents some findings from a "Partnership in Public Awareness (PPA)" project run in the UK which is intended to bring to public understanding results of recent research. The academic team within the PPA had recently completed research on processes and severity of violent overtopping of waves at seawalls under the VOWS project funded by EPSRC, see Bruce *et al* (2001). This work had been expanded by research by others supported by other UK Government departments or agencies. Further advances are being developed within the EC funded CLASH research project (see: http://www.clash-eu.org/).

Figure 2. Public watching / dodging overtopping at Oostende, Belgium.

Rather than engage direct with the public on a complex subject requiring a multi-disciplinary approach and commensurate resources, the PPA team of coastal engineers and scientists opted to work with and through national agencies which already take responsibility for public safety on the coastline, and who already have procedures and campaigns to engage with the public on these themes. The PPA team offered to support those engagements by developing new graphical and interpretative material explaining wave and overtopping hazards along the shoreline. In doing so, the PPA team initially expected that some basic understanding of coastal and wave processes could be assumed. At an early stage in the project, however, the "user team" identified that conventional engineering descriptions of wave overtopping would need to

be presented within a rather broader framework with explanations of waves, tides, and basic coastal processes. That required a wider effort in technical communication.

2. Wave overtopping hazards

Low-lying coastal areas are often protected by seawalls against flooding or erosion. Hazards from wave overtopping arise under three categories:

Figure 3. One public response to an overtopping hazard! The spray may contain shingle.

- **Direct hazard** of disruption, injury or death to people living, working or travelling in the area defended;
- **Damage to property** and / or infrastructure, including loss of economic resource, or disruption to a process;
- **Damage to defence** structure(s), short- or long-term.

The main societal response to these hazards is commonly to construct new defences, but responses should now always consider three options:

- **Move or modify human activities** in the area subject to flooding hazard, modifying land use category;
- **Accept occasional hazard** at acceptable risk by providing for temporary use with warning and evacuation systems, and/or use temporary or demountable flood defence systems to reduce direct hazards;
- **Increase defence standard** to reduce risk to acceptable levels by enhancing the defence and / or reducing loadings.

Figure 4. Example thrill-seeking behaviour?

For seawalls to protect against wave overtopping, the crest level must be dimensioned to give acceptable levels of overtopping under specified extreme conditions (water level and waves). Setting safe levels of overtopping is difficult, as the key processes of hazard generation by overtopping of seawalls are not yet fully understood. For example, recent research has shown that some seawall types may overtop more violently at mean water than at high water. This apparently contradictory finding arises when waves at lower water levels are tripped by the approach beach or wall toe to give impulsive breaking conditions, see Allsop *et al* (2003). Sea level rise and changes to storm patterns emphasise the need for reliable and robust predictions of overtopping hazards, yet population pressures on land use have sometimes led to planning decisions that increase rather than reduce coastal hazards.

Analysis within the PPA and CLASH suggest that approximately 2–4 people are killed each year in each of UK and Italy through direct effects of waves on the shoreline, chiefly on seawalls and similar structures. Some of those may be primarily caused or enhanced by "thrill-seeking" behaviour, or may happen under the effects of alcohol or drugs. Given the number of such occurrences that may have been substantially influenced by ignorance of these hazards, it seemed possible that increased public awareness of wave and coastal processes could assist reduce this waste of life. This impression is forcibly reinforced by the example in Figure 4 where a parent has taken their child "wave dodging". In this instance, the child slipped off the wall, but was simply bruised, soaked and probably very frightened. Others have drowned.

3. Public perception of overtopping

It is generally appreciated by engineers and coastal managers that seawalls reduce wave overtopping, but it requires a sophisticated understanding to be aware that seawalls do not always stop, but simply reduce overtopping. Under storm action, waves still overtop seawalls, sometimes frequently and sometimes violently. These processes may excite considerable public interest, see the

example in Figure 2 at Oostende where tourists gather during storms, in Figure 3 at Scarborough (before the recent improvements), or at Dover, Figure 4. The key problem identified during the PPA project is that most messages to tell the public about the seaside and coastal activities (particularly those marketing a vision) present only the "sunny" view of coastal processes. There is no motivation for the developer / architect / advertiser to show "stormy" or winter views where hazards might be more easily perceived. This imbalance is compounded by tools that communicate messages of hazard well to engineers and scientists, but do not carry the same message to members of the public.

Figure 5a. Beach, seawall and promenade at San Sebastian (Spain).

Figure 5b. Artificial beach, breakwaters and resort at Lanzarote (Canary Islands)

Examples of this problem are illustrated in Figures 5 and 6. The first of these show example of coastal structures as experienced by most members of the public. The sun is shining, the waves are small. There are no obvious hazards. Contrasting views of substantially greater hazard are shown in Figure 6 showing severe waves at two small harbours. The first photo (Figure 6a)

shows waves of H_s = 3–3.5m at the Italian harbour of Salivoli (Tuscany) in November 2001. The second shows waves equivalent to H_s = 4m at the harbour of Hartlepool, UK, as modelled at a scale of about 1:40. All coastal engineers will be able to perceive equivalent levels of hazard to either situation, experienced as she / he is in scaling the process in Figure 6b to full scale. The problem identified by the non-engineer members of the PPA project is that members of the public cannot easily make the same mental jump. To them, there is no obvious hazard from waves of 50–100mm height! It was clear, therefore, that any graphic or photograph seeking to explain wave / coastal / overtopping processes would have to take account of this perception "blind-spot".

Figure 6a. Yacht harbour of Salivoli (Tuscany, Italy) during storm in November 2001.

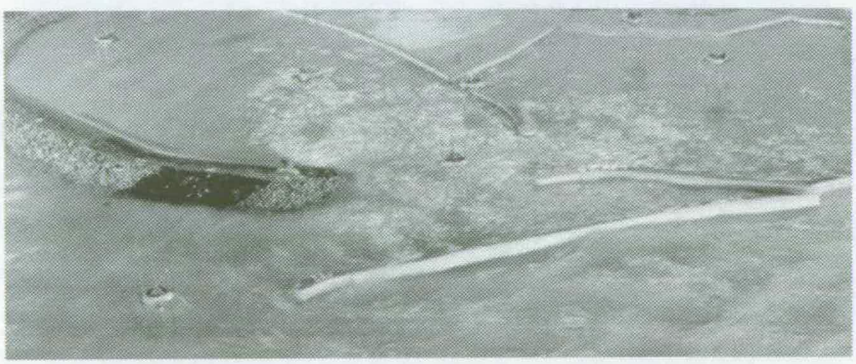

Figure 6b. West Harbour, Hartlepool (UK) under 1:50 year storm, physical model.

4. Changing public perceptions

Changes to public behaviour will partially be driven by changes to direct management practices at coastal sites, but will also require improvements in awareness of potential hazards, and some understanding of the key drivers. This will require changes on a number of fronts: increasing general awareness of sea and coastal processes; greater awareness of hazards posed by wave overtopping and related processes; and use of site specific warnings.

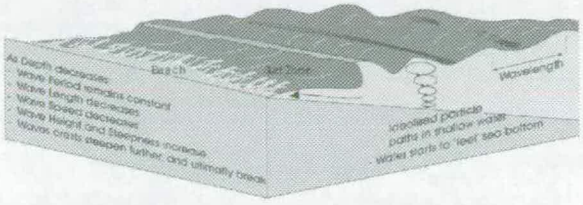

Figure 7. An example of clear graphic showing coastal wave process, but note that there is no scale.

4.1. *Background awareness of coastal processes*

At the most general level, work is needed by coastal engineers in general to engage with the public media to explain coastal engineering processes in general. Most such work is most obviously focussed on teaching, where each learning increment builds on previous understanding. The example in Figure 7 shows wave processes in cartoon fashion, but does not need to be correct in terms of scale.

A major danger in producing simplifying explanations are the consequences of media tendencies to sensationalise the issue, submerging reality in hyperbole. Use of the term "freak waves" for any large wave (however predictable by modelling of wave statistics or processes of wave-wave interactions) is the prime example of such distortions. The use of such "tabloid" expressions debases the public view of the probability of encountering large waves. A particular area of weakness is the widespread lack of understanding of shoaling of swell waves, likely to give inshore waves many times greater than offshore where waves of low steepness (say $s_{op} < 0.5\%$) shoal up over steep slopes. Given that this is exactly the process by which surfing waves are generated, it is perhaps surprising that so few professionals and public appreciate the process which was probably the prime cause of the incident at Giant's Causeway (Northern Island) shown in Figure 8, in which a

number of children and a "responsible adult" were swept into the sea. Happily, all were rescued on this occasion.

Figure 8. Pictures from video of overtopping incident at Giant's Causeway, 16th August 2002.

4.2. *Specific warnings*

The most immediate action of any owner or responsible authority aware of a potential hazard is to ensure that the public are made aware of the hazard. The general issue of hazards on coastal structures has been discussed by Halcrow (1997) and Heald (2002) who show examples of poor signage. Better examples of warnings from National Trust sites are shown in Figures 9a and 9b.

A more complete approach to raising awareness is illustrated in Figure 10 where the full range of hazards at Giant's Causeway are identified. It may be noted that the sign in Figure 10 specifically identifies the inherent danger of large waves on the more exposed end of the Causeway.

Figure 9a. Example warning notice, tidal threat.

Figure 9b. Example notice, overtopping threat

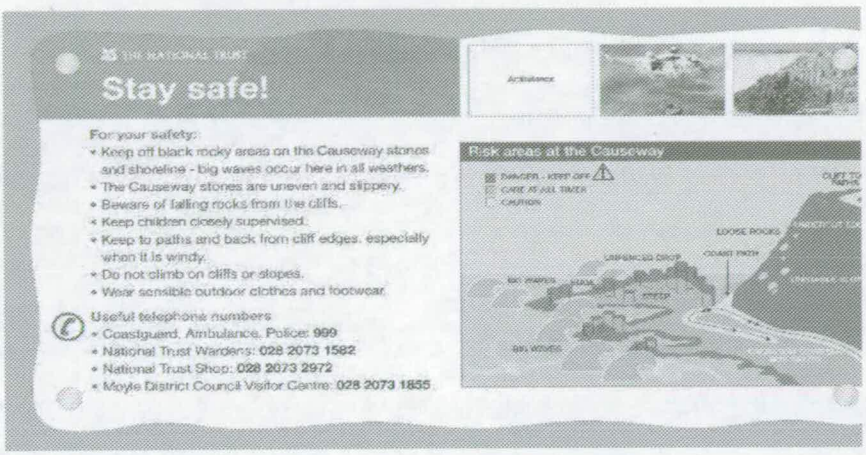

Figure 10. Example information board, Giant's Causeway (Northern Ireland).

4.3. *Improving general awareness of overtopping hazards*

As illustrated earlier, some tools that can be used to train coastal engineers, scientists, and perhaps managers, may not be so useful in informing the public. Example cartoons developed by HRW and the PPA project for the UK Environment Agency are shown in Figure 11 to illustrate the development of overtopping and possible damage under extreme storms.

5. Overtopping safety levels and concluding remarks

Guidance on tolerable limits were developed by Owen (1980) based on work in Japan by Fukuda *et al* (1974). Later revisions to these limits were suggested by Franco *et al* (1994). Under the CLASH project, analysis of data from sites that experience overtopping, (eg. Herbert, 1996; Gouldby *et al.,* 1999; Allsop *et al,* 2003; Pullen *et al,* 2003) is being used to refine advice on overtopping limits for different structure types and users. The revised analysis suggests that limits on both mean discharge and peak volume should be used, with distinctions being made for the seawall type, the form of the overtopping flow, and whether the people involved are expecting to be hit by water.

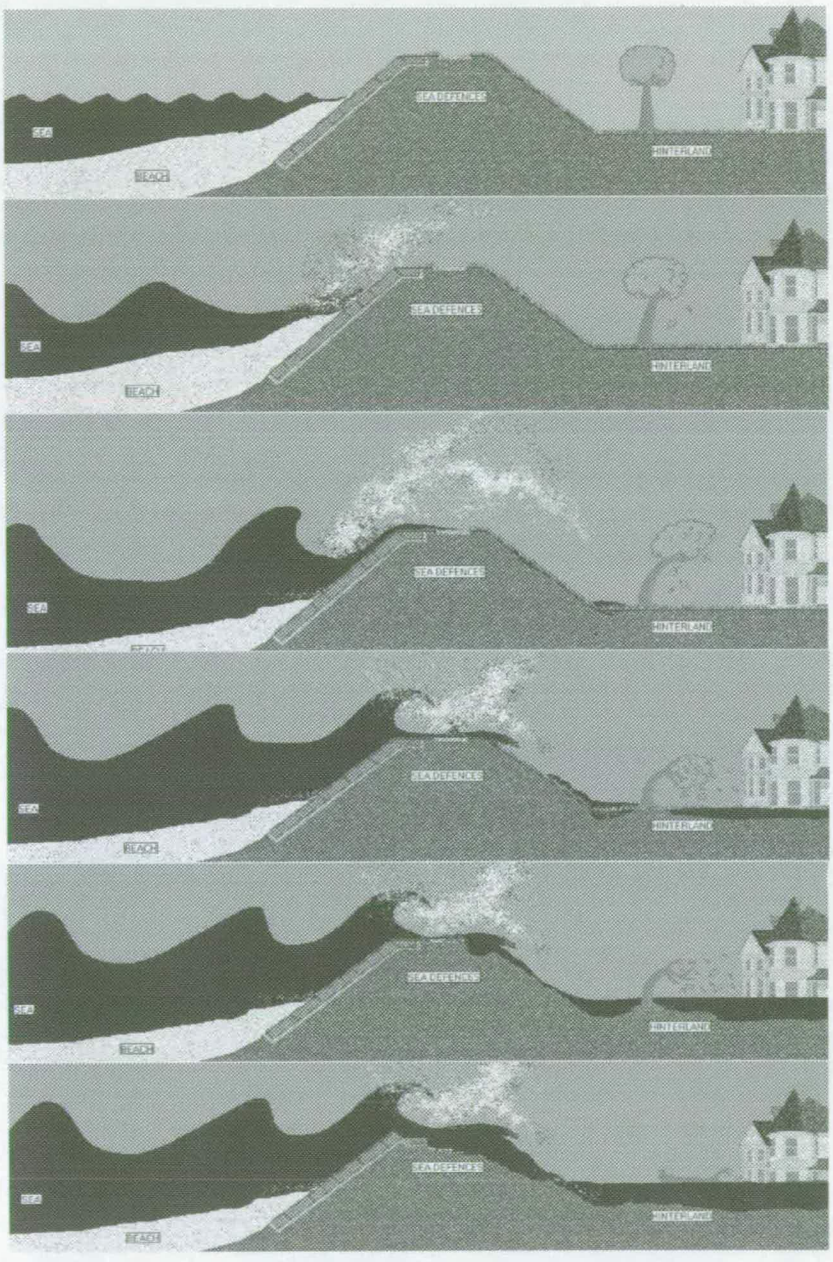

Figure 11. Example cartoons to illustrate possible damage to sea defences.

Table 1. Suggested limits for (mean) wave overtopping discharges and peak (individual wave event) volumes

Hazard type / reason	**Mean discharge, q**	**Peak volume, V_{max}**
Pedestrians		
Unaware pedestrian, no clear view of the sea, relatively easily upset or frightened, narrow walkway or close proximity to edge	0.03 l/s.m	2-5 l/m at high level or velocity
Aware pedestrian, clear view of the sea, not easily upset or frightened, able to tolerate getting wet, wider walkway.	0.1 l/s.m	20-50 l/m at high level or velocity
Trained staff, well shod and protected, expecting to get wet, overtopping flows at lower levels only, no falling jet, low danger of fall from walkway	1-10 l/s.m	500 l/m at low level,
Vehicles		
Driving at moderate or high speed, impulsive overtopping giving falling or high velocity jets	0.01-0.05 l/s.m	5 l/m at high level or velocity
Driving at low speed, overtopping by pulsating flows at low levels only, no falling jets	10-50 l/s.m	1 m^3/m

The lower limits for members of the public sheltered from a clear view of incoming waves is still as currently recommended in UK. These limits can however be relaxed upwards for trained personnel, and for pulsating wave flows over the crest of embankment seawalls. More dangerous overtopping flows typically occur behind vertical seawalls and breakwaters (Franco *et al*, 1994).

Under the PPA, new graphical materials are being developed to explain coastal and overtopping processes, and their practical significance, to much wider audiences, see examples in Figure 11. Considerable further effort will be needed to remind many citizens that coastal flooding is particularly hazardous, and to translate the results of recent research to persuade the girls in Figure 2 to understand why putting your head in water travelling at up to 40 m/s may be unwise!

Acknowledgments

VOWS research was supported by EPSRC under GR/M42312 and GR/R42306, following research at HR Wallingford supported by MAFF (now Defra) and EA. Work on hazard analysis is being conducted under the CLASH project under EU contract EVK3-2001-0058 and supported by Defra / EA under FD2412. Further work by Edinburgh and Southampton is supported by an EPSRC Partnership in Public Awareness project (GR/ S23827/01).

References

Allsop, N.W.H., Bruce, T., Pearson, J., Alderson, J.S. and Pullen, T. 2003. Violent wave overtopping at the coast – when are we safe?, Proc. ICE Conf. Coastal Management '03, Thomas Telford.

Bruce, T., Allsop, N.W.H. and Pearson, J. 2001. Violent overtopping of seawalls – extended prediction methods, Proc. Breakwaters, coastal structures and coastlines, pp 245-256, Thomas Telford, London, ISBN 0 7277 3042 8

Franco, L., de Gerloni, M. and van der Meer, J.W. 1994. Wave overtopping on vertical and composite breakwaters, Proc 24th Intl. Conf. Coastal Engineering, 1, pp1030-1045, ASCE.

Fukuda, N., Uno, T. and Irie, I. 1974. Field observations of wave overtopping of wave absorbing revetment, Coastal Engineering in Japan, Vol 17, pp 117-128, Japan Society of Civil Engineers, Tokyo.

Gouldby, B.P., Sayers, P.B. and Johnson, D. 1999. Real-time hazard forecasting: implementation and two years operation at Samphire Hoe, Dover, MAFF Conf. on River and Coastal Engineers, Keele.

Halcrow. 1997. Public safety of access to coastal structures, Report to Environment Agency, EA report 522

Heald, G. 2002. Design on the Rocks?, Proc. Breakwaters, coastal structures & coastlines, pp 471-481, (ICE) ISBN 0 7277 3042 8, Thomas Telford, London.

Herbert, D.M. 1996. Overtopping of Seawalls: a Comparison between Prototype and Physical Model Data, Report TR 22, HR Wallingford.

Owen, M.W. 1980. Design of seawalls allowing for overtopping, Report EX924, Hydraulics Research, Wallingford.

Pullen, T.A., Allsop, N.W.H., Bruce, T. and Geeraerts, J. 2003. Violent wave overtopping: CLASH Field Measurements at Samphire Hoe. Proc. Coastal Structures 2003, ASCE, Portland.

Appendix X: Allsop *et al.*, 2005b

Allsop, N.W.H, Franco, L., Bellotti, G., Bruce, T. & Geeraerts, J. (2005b), *Hazards to people and property from wave overtopping at coastal structures*, Proc. Coastlines, Structures & Breakwaters 2005, pp153–165, ICE London, Thomas Telford, ISBN 0 7277 3455 5

Appendix X
Allsop *et al.*, 2005b

Allsop, N.W.H, Franco, L., Bellotti, G., Bruce, T. & Geeraerts, J. (2005b), *Hazards to people and property from wave overtopping at coastal structures*, Proc. Coastlines, Structures & Breakwaters 2005, pp153–165, ICE London, Thomas Telford, ISBN 0 7277 3455 5

X.1 Declaration of contribution

This paper arose directly from cooperative research under the *CLASH* project (Section 3.10.1) involving partners from Edinburgh, HR Wallingford (Allsop) Roma Tre (led by Franco) and University of Gent (Geeraerts). It was a genuine team effort, with all authors contributing significantly to the gathering of the data and evidence, its synthesis, and to the preparation of the final text.

X.2 Published paper

overleaf

HAZARDS TO PEOPLE AND PROPERTY FROM WAVE OVERTOPPING AT COASTAL STRUCTURES

William Allsop, Technical Director, HR Wallingford; Visiting Professor, University of Southampton, UK
Leopoldo Franco, Professor, University of Rome Tre & Modimar Srl., Rome, Italy
Giorgio Bellotti, Researcher, Dipartimento di Scienze, dell'Ingegneria Civile (DSIC), University of Rome Tre Rome, Italy
Tom Bruce, Lecturer, School of Engineering, University of Edinburgh, , UK
Jimmy Geeraerts, Researcher, Ghent University, Ghent, Belgium,

SYNOPSIS

Processes of wave overtopping that cause hazards to people or property close behind seawalls are not well understood. There remain important gaps in knowledge on overtopping and post-overtopping processes, on the limits to overtopping volumes, discharges or velocities that might be accepted, despite significant improvements in recent years. To help reduce uncertainties in analysis and management of wave overtopping, recent research has developed improved prediction methods for use by coastal engineers. This paper reports the principal conclusions on hazards arising from wave overtopping developed within the European CLASH project, supplemented by UK research studies SHADOW, VOWS and "Safe at the Seaside".

1. WAVE OVERTOPPING

The main requirements of sea or coast protection structures are to stop / reduce coastal erosion, and to reduce risks of flooding. In doing so, they will not stop wave overtopping, simply limit its frequency of occurrence and effects.

Figure 1 Overtopping hazards at Oostende

On urbanised frontages, seawalls or breakwaters must allow people to live, work and enjoy themselves safely behind the defence structure. Designers / owners of such structures must therefore be able to identify key hazards from overtopping , predict their occurrence (at least statistically) and prepare action plans to deal with the risks. The main hazards, particularly on or close to coast defence structures, are of death, injury, property damage or disruption.

On average, approximately 3 people are killed each year in each of UK and Italy through direct effects of waves, chiefly on seawalls and similar structures (see appendices to CLASH WP6 report by Allsop, 2005). That tourists gather during storms at Ostend (Fig 1) / Dawlish /

Brighton / Scarborough or elsewhere (see examples in Allsop *et al*, 2003) illustrates that they are seldom fully aware of the seriousness of some wave overtopping hazards.

Within Europe, the CLASH research project has been developing new design tools to predict wave overtopping for a very wide range of coastal structures using results from laboratory and field measurements, and including analysis of hazards from overtopping. This paper will discuss results from CLASH and other projects on such hazards, and will give guidance on damage / disruption from wave overtopping. In doing so, it will use results of direct measurements and indirect analysis to extend / refine guidance by Owen (1980), Besley (1999), Franco *et al* (1994) and Allsop *et al* (2003).

Figure 2 Overtopping measurements at Samphire Hoe

2. CLASH RESEARCH PROJECT

2.1 Outline of CLASH

The CLASH project supported under EC contract EVK3-2001-0058, led by University of Ghent, is intended improve analysis and design methods for coastal structures against storm surges, wave attack, flooding, and erosion see web site: http://www.clash-eu.org/. Results are intended to produce generic prediction methods for crest height of most coastal structures based on permissible wave overtopping supported by hazard analysis. Activities by 13 partner universities / research institutes are divided into ten Work Packages: of which the most interesting for this paper were WP 3. Full scale measurements (see examples in Figs 2 & 3); WP 4. Laboratory tests; and WP 6. Hazard analysis.

Figure 3 Overtopping tank at Ostia

A particular motivation for the CLASH research was the suggestion in the OPTICREST project, see De Rouck *et al* (2002), that there might be unexpected scale (and model) effects in which small-scale tests on armoured slopes might under-predict overtopping at full scale. Large scale tests on vertical and steeply battered walls within Big-VOWS in the large flume at Barcelona, see Pearson *et al* (2002), suggested that scale effects might be negligible for impermeable and smooth structures, but further analysis suggests that some scale effects may derive from scaling of roughnesss and/or permeability and the absence of wind effects in scale models, see de Rouck *et al* (2005).

As part of the overall study, CLASH partners have therefore measured wave overtopping events at full scale at three coastal sites in Europe (WP 3). Those processes have been simulated by laboratory tests (WP 4) and compared with full scale measurements (WP 7).

This paper summarises the analysis of direct hazards of overtopping conducted under WP6 of CLASH, supported by data from WP3 and WP4.

2.2 Activities in CLASH Work Package 6

The overall aim of WP6 was to derive and/or refine guidance on hazards presented by overtopping. The specific objectives are to:

- Compare measured events and hindcast events with records of observed hazard in order to derive / refine limits for safety of pedestrians, car users, travellers in other vehicles;
- Derive / refine limits of overtopping for hazard to buildings and related items;
- Evaluate the risks of economic loss.

Observations of overtopping hazard have been made at selected field sites. Hazard events had already been recorded over 4 years at Samphire Hoe by personnel responsible for public safety. Similar observations were made at Zeebrugge and Ostia under CLASH, supplemented by video records and/or direct observations during field measurements. At Zeebrugge, "instrumented" persons (dummies) have been used to give indicators of overtopping violence.

Separately, Bouma *et al.* (2005) developed / refined methods to evaluate risks of economic losses, (occurrence probability x damage per event) for all relevant overtopping events. This task included Economic Assessment Approach for direct and indirect economic impacts.

3. Wave overtopping processes and hazards

3.1 Direct hazards

Around the coastlines of Europe and elsewhere, low-land lying areas, towns, transport infrastructure (including ports) are often protected by seawalls or related structures against flooding or erosion by waves and/or extreme surges. The hazards from direct wave and overtopping effects may cause consequences under three general categories:

a) **Direct hazard** of injury or death to people living, working or travelling in the area defended;
b) **Damage to property, operation and / or infrastructure** in the area defended, including loss of economic (environmental or other) resource, or disruption / delay to an economic activity / process;
c) **Damage to defence** structure(s), either short-term or longer-term.

Hazards driven by overtopping can be categorised by a number of simple direct responses:

- mean overtopping discharge, q;
- individual and peak overtopping volumes, V_i and V_{max};
- overtopping velocities over the crest or promenade, horizontally and vertically, v_{xc} and v_{zc} or v_{xp} and v_{zp} ;
- overtopping flow depth, again measured on crest or promenade, d_{xc} *or* d_{xp}.

Less direct responses, or similar responses, but further back, may be needed in assessing the effects of overtopping, perhaps categorised by:

- overtopping falling distances, x_c;
- post-overtopping wave pressures (pulsating or impulsive), p_{qs} or p_{imp};
- post-overtopping flow depths, and horizontal velocities.

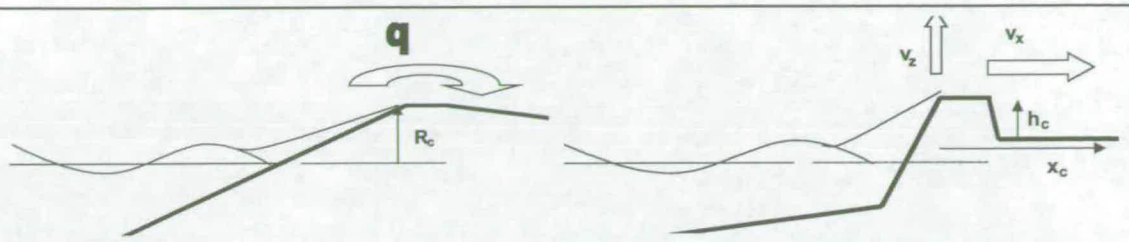

Figure 4a and b Overtopping at embankment and vertical / battered seawalls

3.2 *Responses to overtopping*

The main response to these hazards has most commonly been the construction of new defences, but any logical response should now always consider three options, in increasing order of intervention:

a) **Move human activities** away from the area subject to overtopping and/or flooding hazard, thus modifying the land use category and/or habitat status;

b) **Accept occassional hazard** at acceptable probability (acceptable risk) by providing for temporary use and/or short-term evacuation with reliable warning and evacuation systems, and/or use of temporary / demountable defence systems;

c) **Increase defence standard** to reduce risk to (permanently) acceptable levels probably by enhancing the defence and / or reducing loadings.

The results of the CLASH project are primarily associated with response c), although results of this work may inform either of responses a) or b).

For any structure expected to ameliorate wave overtopping, the crest level and/or the front face configuration will be dimensioned to give acceptable levels of wave overtopping under specified extreme conditions or combined conditions (e.g. water level and waves). Setting acceptable levels of overtopping depends on the use of the defence structure itself, the land behind, national or local standards, and the economic and social basis for funding the defence. Bouma *et al* (2005) describes methods to value the hazards (and therefore the value of their avoidance), and analysis described here suggests levels of overtopping that have been judged appropriate for various activities. Neither of these will however supecede national / local standards and administrative practice which will guide any final decision on protection standard. For instance, practice on sea defence funding in UK is outlined by Brampton (2002) and Department of Transport, Local Government & the Regions (2001).

3.3 *Defence types*

Where the option is taken to increase defence standards, a seawall or related structure may be required, often formed as sloping embankments or dykes with revetment protection, or (perhaps more common in UK, France and Italy) as a steep or vertical retaining wall with promenade (see Figs. 1 & 2). Coastal structures may include seawalls or breakwaters formed from blockwork or mass concrete, with vertical, near vertical,

Figure 5 Overtopping flows on a sloping revetment

or sloping faces. Under wave attack, sloping embankments tend to break waves onto the slope with overtopping being a relatively gentle process (see Fig. 5).

Steeper / vertical or compound structures are more likely to experience intense local wave impact pressures, may overtop severely or with greater velocities (see Figs 6 & 7), but may also reflect much of the incident wave energy. Reflected waves cause additional wave disturbance and/or may initiate or accelerate local bed scour / erosion with consequent effects on increasing any depth-limited wave heights.

4. Evidence of overtopping hazards

4.1 Types of overtopping

Overtopping when waves run up the face of the seawall over the crest is termed 'green water'. Different overtopping occurs when waves break seaward of the defence structure or onto its seaward face, producing significant volumes of spray. Overtopping spray may be carried over the wall either under its own momentum or driven by an onshore wind. Spray may also be generated by wind acting directly on wave crests, particularly noticeable when reflected waves from steep walls interact with incoming waves to give severe local 'clapotii'.

Figure 6 Overtopping at vertical wall, Chania, Crete

Figure 7 Wave overtopping at vertical breakwater and seawall, Margate

Without a strong onshore wind, spray probably does not contribute significantly to overtopping volumes, but may cause some direct hazards. The overtopping in Fig. 6 would certainly surprise a less-aware pedestrian, and could cause him / her to lose their footing and fall. The overtopping in Fig. 7 could be severe enough to knock over even an aware person.

Light spray may contribute little to direct hazard except reducing visibility and extending the spatial extent of salt spray effects. An exception is the effect of spray in reducing visibility on coastal highways where sudden loss of visibility may cause significant driving hazard. An example on Japan National Highway 336 is discussed by Kimura *et al.* (2000).

Effects of wind and generation of spray are seldom modelled. Tests by de Waal *et al.* (1992, 1996) suggested that onshore winds have relatively little effect on large green water events, but may increase discharges under q = 1 l/s.m where much of the overtopping may take the form of spray. Such discharges are however already substantially greater than discharge limits suggested for pedestrians or vehicles. Substantial advances have been made on this issue within CLASH, on field measurements and laboratory tests, see e.g. Pullen *et al.* (2003), and De Rouck *et al.* (2005).

4.2 Guidance on limiting overtopping discharges / volumes

In assessments of flooding by wave overtopping, most analysis evaluates flood areas using total overtopping volumes. This aspect is not covered by this paper which focusses on direct and local effects of wave overtopping discharges / volumes. Most descriptions of overtopping have been in terms of mean discharges averaged over 250 to 1000 T_m. The mean discharge q is then expressed as flow rate per metre run of seawall, typically m^3/s.m or l/s.m.

Limits to identify onset of damage to seawalls, buildings or infrastructure, or danger to pedestrians and vehicles have been defined relative to mean discharges or peak volumes. Guidelines quoted in the CIRIA / CUR Rock Manual and EA Overtopping Manual were derived by Owen (1980) using work in Japan by Goda *et al* (1975) and Fukuda *et al.* (1974). Significantly different limits were given for embankment seawalls (with back slopes) and promenade seawalls (without back slopes), and for pedestrians or vehicles.

Table 1 Previous guidance on tolerable mean overtopping discharges (l/s.m)

Embankment seawalls :-					
Damage if crest not protected	2	<	q	<	20
Damage if back slope not protected	20	<	q	<	50
Promenade Seawalls :-					
Damage if promenade not paved	50	<	q	<	200
Buildings :-					
Minor damage to fittings etc	0.001	<	q	<	0.03
Structural damage			q	>	0.03
Vehicles :-					
Safe at moderate / higher speeds			q	<	0.001
Unsafe at moderate / higher speeds	0.001	<	q	<	0.02
Dangerous			q	>	0.02
Pedestrians :-					
Wet, but not unsafe			q	<	0.003
Uncomfortable, but not unsafe	0.003	<	q	<	0.03
Dangerous			q	>	0.03

De Gerloni *et al* (1991), Franco *et al.* (1994) and Besley (1999) argued that use of mean discharges only in assessment of safety levels is unsafe, suggesting that maximum individual volumes are often of much greater significance than average discharges. These researchers have shown that, for given mean discharge, the volume of the largest overtopping event can vary significantly with wave condition and structural type. There remain however two difficulties in specifying safety levels with reference to peak volumes and not to mean discharges. Methods to predict peak volumes are less well-validated. Secondly, data relating individual overtopping events to hazard levels are still rare.

Franco *et al* (1994) used model tests and volunteers to demonstrate that danger to people or vehicles could be related to peak overtopping volumes, suggesting a "safe" limit for people working behind a vertical wall might be V_{max} = 100 l/m, but that this could be increased to V_{max} = 750 l/m where flows were horizontal and could be seen. The researchers also noted that a volume as low as V_{max} = 50 l/m could unbalance an individual when striking their upper body without warning.

Smith *et al* (1994) reported full scale tests on embankments where an observer on the dyke judged safe overtopping limits for personnel carrying out inspection and repair work. They concluded that work on the dyke was unsafe when overtopping exceeded q = 10 l/s.m, probably corresponding to V_{max} = 1000 to 2000 l/m. This is considerably higher than limits by Franco *et al* (1994) for work behind a crown wall, but matches the observation that the safe limit of V_{max} varies with structure type and the different ways in which water strikes the individual. For Smith *et al*'s tests, most of the overtopping acted on the observer's legs only. Safety limits for trained personnel aware of overtopping will be higher than for other users.

Further guidance on safety was derived by Herbert (1996) during measurements of overtopping behind a vertical seawall. During installation and operation of the equipment, Herbert observed that personnel could work safely on the crest of the wall up to q = 0.1 l/s.m, perhaps giving peak volumes of V_{max} = 40 l/m, in close agreement with Franco *et al*'s estimate of V_{max} = 50 l/m to cause someone to lose their balance.

Herbert (1996) also suggested that overtopping became dangerous to vehicles when above q = 0.2 l/s.m, corresponding to V_{max} = 60 l/m. This suggests that V_{max} = 50 l/m should be applied as a safe upper limit for both pedestrians and vehicles driven at any speed.

4.3 New evidence on personnel hazards

Every year, about 3 people drown in each of UK and Italy being swept from breakwaters, seawalls and rocky coasts. [Incidents for UK for 1999-2002 and for Italy between 1983-2002 were assessed within CLASH WP6.] To the individual, the waves responsible for such incidents may appear to be sudden and surprising, so it is probable that the people concerned had relatively little idea of the hazard to which they exposed themselves. It is however likely that many of these events could be predicted by informed analysts using weather or wave forecasting and applying results of recent research.

Figure 8 Categorisation of hazards at Samphire Hoe: low; moderate; and high

An early overtopping warning system was described by Gouldby *et al.* (1999) for Samphire Hoe near Dover. This artificial reclamation was formed by chalk spoil from the Channel Tunnel retained by a vertical sheet pile wall. The promenade is used for leisure, but may be overtopped during storms (see Figs 2 & 8), so careful management of access is important to ensure visitor safety. A warning system was therefore developed in which hazards at three levels were predicted by output from an appropriate wave model. Wave conditions were correlated with incidents of known overtopping hazard, categorised as low, moderate or high, (see Fig. 8). These warning levels were then communicated by the use of warning flags, and ultimately by closing access to the seawall. Use of this system was analysed by Allsop *et al.* (2003) to support the continuing use of $q \leq$ 0.03 l/s.m as a safe limit for (unaware) pedestrians when subject to impulsive jets.

4.4 Perceptions of overtopping

It is appreciated by engineers and coastal managers that seawalls reduce wave overtopping, but it requires a sophisticated understanding to be aware that seawalls do not stop, but simply reduce overtopping. Under storm action, waves still overtop seawalls, sometimes frequently and perhaps violently, and may excite considerable public interest.

Figure 9 Artificial beach, breakwaters and resort at Lanzarote

A key communication problem is that most messages about the seaside and coastal activities (particularly for marketing) present only the "sunny" view of coastal processes. The developer / architect / advertiser will never show "stormy" or winter views where hazards might be more easily perceived. This imbalance is compounded where tools that communicate messages of hazard to engineers and scientists do not carry the same message to the public.

Figure 10 Yacht harbour of Salivoli (Tuscany), November 2001

Examples of this problem are illustrated in Figs 9-10. The first of these show coastal structures as experienced by most members of the public. The sun is shining, the waves are small. There are no obvious hazards. Substantially greater hazard is shown in Fig 10 showing waves of H_s = 3.0-3.5m overtopping the marina breakwater of Salivoli (Tuscany) during a severe storm. The problems of perception are described further at this conference by Bellotti *et al* (2005) who recorded hazard perceptions by viewers of video from the field measurements at Ostia.

5. Post- overtopping velocities and loads

5.1 Overtopping velocities

Few data have been available on overtopping velocities. Pearson *et al* (2002) and Bruce *et al* (2002) present measurements of upward velocities (v_z) for vertical / battered walls under impulsive and pulsating conditions. Measured upward velocity v_z is related to the inshore wave celerity given by $c_i = (gh)^{1/2}$. Relative velocities, v_z/c_i, were plotted against the breaking parameter, $h_* = (h/H_s).(2\pi h/gT_m^2)$. Non-dimensional velocities were roughly constant at $v_z/c_i \approx 2.5$ for pulsating / slightly impulsive conditions $h_* > 0.2$, but overtopping velocities increase significantly for impulsive conditions when $h_* \leq 0.2$ reaching $v_z/c_i \approx 3$ - 7.

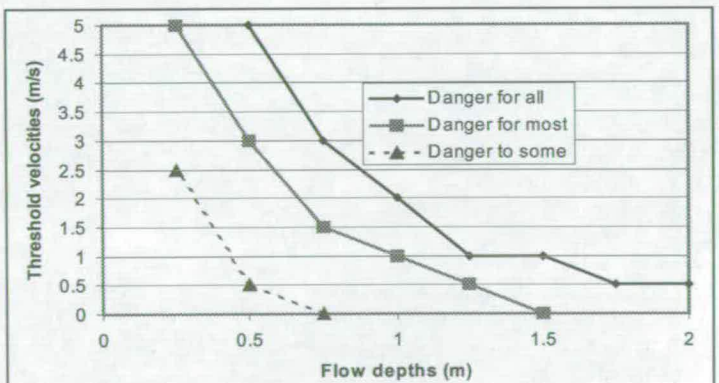

Figure 11 Suggested velocity / depth limits (steady flows) after Ramsbottom et al. (2004)

For simply sloping embankments, Richardson *et al* (2002) measured crest velocities of around $v_z/c_i \approx 2$ behind a 1:2 slope under plunging conditions. Simulations for 1:1-1:5 slopes discussed by Allsop (2005) showed overtopping bore velocities in the range v_c = 2-5 m/s. Measurements of overtopping velocities in the Samphire Hoe 3-d model gave peak velocities of v_z = 1-9m/s, corresponding to $v_z/c_i \approx 0.2 - 1.2$, much lower than found by the VOWS tests. Analysis of video recordings from a 3-d seawall model, gave horizontal velocities behind the recurve seawall of v_x = 3.5 to 5.5m/s.

These levels of velocity may be put into context by findings from UK studies on flood risks to people, see Ramsbottom *et al.* (2004) who present hazard classification tables based on steady flow velocities. Their suggested limits are re-represented here in Fig. 11. As these velocity / depth limits were originally derived for relatively steady flows, it would be wise to take a precautionary view of these limits in the derivation of any suggested limits. The middle threshold in Fig. 11 suggests that flow velocities above $v_z \geq 2.5$m/s will be difficult to resist for depths greater than d > 0.5m, and $v_z \geq$ 5m/s will be difficult to resist for depths greater than d > 0.25m. For wave overtopping, it is probable that impulsive flows will be safe only at lower velocities than shown here.

5.2 *Post overtopping wave loads on structures*

Wave loads have seldom been measured on defence structures, buildings behind sea defences, or on people. Under CLASH, post overtopping loads on person-sized dummies and a length of pipeline have been measured at full scale at Zeebrugge, see Geeraerts *et al* (2003), and at small scale at LWI. Post-overtopping load tests described by Allsop (2005) on a promenade seawall with overtopping velocities of v_x = 3.5 to 5.5m/s, gave pressures on the 1m high secondary wall set 7m back from a recurved seawall shown in Fig 12. These pressures are plotted against q measured just behind the primary seawall.

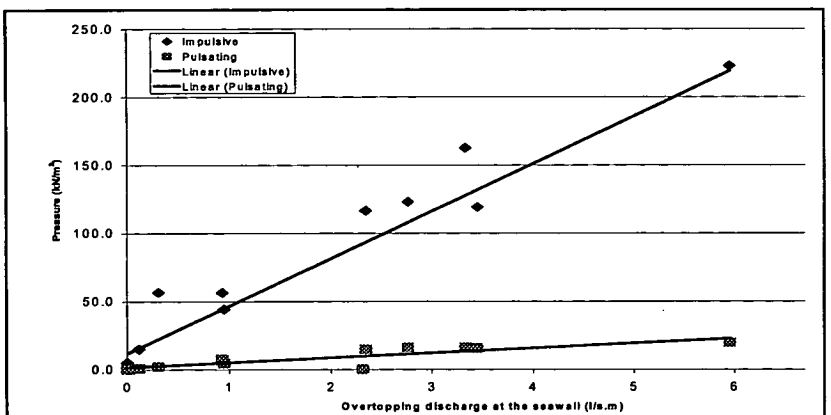

Figure 12 Wave loads on 1m high secondary wall set 7m behind seawall (tests at HRW, see Allsop, 2005)

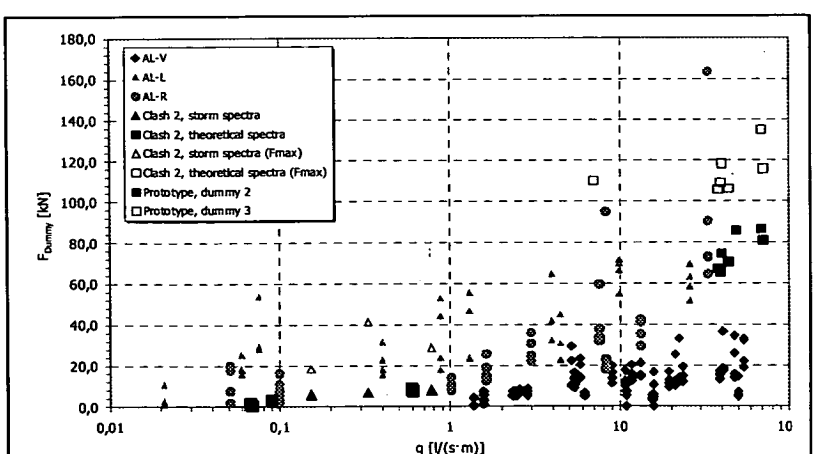

Figure 13 Wave loads on dummies (tests at LWI)

The impulsive pressures were approximately 11 x greater than the quasi-static loads. Extrapolating the

trend lines in Fig. 12 down to an overtopping condition of q=0.03 l/s.m suggest that the quasi-static pressures might reduce to $p_{q\text{-}s} \approx 2$ kN/m^2, but that impulsive pressures might not fall below $p_{imp} \approx 20$ kN/m^2 . These may be put into context by noting that few windows in buildings are designed for horizontal wind loads above $p_{av} \approx 0.5$ kN/m^2.

Measurements on the person dummies at Zeebrugge are discussed by Kleidon & Geeraerts in Allsop (2005). Summary results are shown in Fig. 13.

These measurements suggest that wave loads on a person increase rapidly for increasing overtopping discharges. Endoh & Takahashi (1994) suggests force limits on individuals up to F_h = 140 kN. Given other data collected for this and related studies, this force limit however appears much too high.

5.3 Damage to vessels in Italian marinas

In Italy, many coastal harbours and marinas provide berths along a quaywall at the rear side of the main breakwater. The parapet wall of these breakwaters is however often set lower than might otherwise be expected, chiefly to comply with visual impact constraints. Wave overtopping is therefore often too high, with fairly frequent damage to berthing structures, equipment (eg. electric plant) and vessels. Storms on 6 November 2000 and 11 November 2001 caused significant damage at four marinas on the Italian NW coast: Porto Sole (Sanremo), Marina degli Aregai (Imperia), Carlo Riva (Rapallo) and Salivoli (Piombino), all protected by rock armoured breakwaters in relatively shallow water (7-10 m MSL).

At Sanremo, overtopping damage to the breakwater was limited to kerb displacement (200 m), cracking of pavement, some removal of flagstones, but some 22 concrete pedestals for water and electric supply were destroyed. One floating pier (110 m long) sunk in the inner mooring basin for a total estimated structural damage of €500,000. Eight small yachts, four cars and one van were washed into the harbour with a loss for their owners estimated as €600,000. The quaywall at + 1.3m MSL was flooded due to set-up and wave penetration with additional damage to harbour facilities. The total loss was estimated at €2,000,000.

Figure 14 Overtopping damage at Rapallo marina

Table 2	**Damage incidents in Italian Marinas**				
Marina	Date	Water level (m)	H_s (m)	T_p (s)	$q_{measured}$ (l/s.m)
Salivoli	11 Nov 2001	+0.5	4.3	8-11	5-20
Rapallo	6 Nov 2000	+0.7	5.2	9.3	35
Sanremo	6 Nov 2000	+0.5	5.5	11	25

At the old Rapallo marina, apart from the damage to breakwater armour, overtopping caused collapse of 120 m of gravity type quaywall (Fig. 14). Reconstruction cost about €1,000,000, with damage to fittings estimated as €700,000, and a total cost of €2,500,000. At the newer

marinas at Aregai and Salivoli, structural damage due to overtopping was less (around €200,000) with less vessel damage.

Overtopping events at these harbours analysed within CLASH suggest damage levels. In each case, the storm waves were depth-limited at the breakwater. Overtopping was measured in 2-d model tests at University of Florence by Aminti et al. (2001), see Table 2, while individual volumes were estimated from video records. Severe damage was estimated to occur with peak volumes of around 40-50m^3/m and mean discharges of $q \approx$ 25-50 l/s.m, with minor damage occurring with volumes up to 10m^3/m and mean discharges of $q \approx$ 10 l/s.m.

6. Guidance on overtopping limits

Methods to predict wave overtopping at seawalls (primarily mean overtopping discharge, Q_{bar}) have improved in recent years, and will continue to do so under current and future research projects. The limits suggested by CLASH WP 6 in Table 3 derive from a generally precautionary principle informed by previous guidance and by the various observations and measurements made by the CLASH partners and research colleagues.

Table 3 Revised limits for overtopping mean discharges or peak volumes		
Hazard type / reason	Mean discharge, q	Peak volume, V_{max}
Pedestrians		
Unaware pedestrian, no clear view of the sea, relatively easily upset or frightened, narrow walkway or close proximity to edge	0.03 l/s.m	2-5 l/m at high level or velocity
Aware pedestrian, clear view of the sea, not easily upset or frightened, able to tolerate getting wet, wider walkway.	0.1 l/s.m	20-50 l/m at high level or velocity
Trained staff, well shod and protected, expecting to get wet, overtopping flows at lower levels only, no falling jet, low danger of fall from walkway	1-10 l/s.m	500 l/m at low level,
Vehicles		
Driving at moderate or high speed, impulsive overtopping giving falling or high velocity jets	0.01-0.05 l/s.m	5 l/m at high level or velocity
Driving at low speed, overtopping by pulsating flows at low levels only, no falling jets	10-50 l/s.m	1 m^3/m
Property		
Damage to windows / cladding / fittings set back 5-10m		
Structural elements set back 5-10m		
Sinking small boats set 5-10m from wall. Damage to larger yachts	q = 10 l/s.m	1 - 10 m^3/m
Significant damage or sinking of larger yachts	q = 50 l/s.m	5 - 50 m^3/m

ACKNOWLEDGEMENTS

The CLASH WP6 report was edited by William Allsop with contributions by Tom Bruce and Jon Pearson (Edinburgh); Leopoldo Franco and Giorgio Bellotti (Rome Tre), Jimmy Geeraerts (Ghent), Andreas Kortenhaus and Peggy Kleidon (LWI, Braunschweig), and John Alderson, Tim Pullen and Coline Romestang at HRW. Funding from EC under EVK3-CT-. 2001-00058 and Defra / EA under. FD2412, is gratefully acknowledged. VOWS was

supported by EPSRC under GR/M42312 and GR/R42306, and built on earlier research by HRW supported by MAFF and EA. Additional input was given by the EPSRC project on Participation in Public Awareness "Safe at the Seaside" under GR/S23827/01.

REFERENCES

Allsop N.W.H., Bruce T., Pearson J. Alderson J.S. & Pullen T. (2003) *Violent wave overtopping at the coast, when are we safe?* Proc. Int. Conf. on Coastal Management 2003, pp 54-69, ISBN 0 7277 3255 2, publn. Thomas Telford, London.

Allsop N.W.H., Bruce T., Pearson J., Franco L., Burgon J. & Ecob C. (2004) *Safety under wave overtopping – how overtopping processes and hazards are viewed by the public* Proc. 29th ICCE, Lisbon, publn. ASCE

Allsop N.W.H. (2005) *CLASH Work Package 6: Analysis of overtopping hazards*, Report D38, publn. HR Wallingford and University of Ghent, see: http://www.clash-eu.org/

Aminti, P.L. & Franco, L. (2001) *Hydraulic performance of overspill channel on top of rubble mound breakwaters.* Proc. Int. Conf. Of Ocean Engineering, Chennai, India, Dec.2001

Bellotti G., Briganti R., & Franco L. (2005) *Analysis of perceived hazard from wave overtopping at the Ostia harbour rubble mound breakwater: a pilot test* Paper 92 to Conf. Breakwaters '05, ICE, London.

Besley P. (1999) *Overtopping of seawalls – design and assessment manual* R & D Technical Report W 178, ISBN 1 85705 069 X, Environment Agency, Bristol.

Bouma J.J, Francois D., Schram A. (2005) *CLASH Workpackage 6: Hazard Analysis, including socio-economic impacts - Task 4: Assessment of socio-economic impacts*, CLASH report D39, University of Ghent, see: http://www.clash-eu.org/

Bruce T., Allsop N.W.H. & Pearson J. (2001) *Violent overtopping of seawalls – extended prediction methods* Proc. ICE Conf. On Shorelines, Structures & Breakwaters, pp 245-255, Thomas Telford.

Bruce T., Allsop N.W.H. & Pearson J. (2002) *Hazards at coast and harbour seawalls - velocities and trajectories of violent overtopping jets* Proc. 28th ICCE, Cardiff, publn. ASCE

Brampton A. (Editor) (2002) *Coastal defence – ICE design and practice guide* ISBN 0 7277 3005 3, Thomas Telford, London

CIRIA / CUR (1991) *Manual on the use of rock in coastal and shoreline engineering* CIRIA special publication 83, Simm, J.D. (Editor), CIRIA, London.

Department of Transport, Local Government & the Regions (2001) *Planning Policy Guidance Note 25: Development and Flood Risk.* HMSO, London.

De Gerloni M., Franco L., & Passoni G. (1991) *The safety of breakwaters against wave overtopping*, Proc. ICE Conf. on Coastal Structures and Breakwaters '91, pp. 335-342, Thomas Telford.

De Rouck J., van der Meer J.W., Allsop N.W.H., Franco L. & Verhaeghe H (2002) *Wave overtopping at coastal structures – a database towards up-graded prediction methods* Proc. 28th ICCE, Cardiff, pp 2140-2152, ISBN 981 238 238 0, publn. World Scientific Publishing.

De Rouck, J., Van de Walle, B., Geeraerts, J., Troch, P., Van Damme, L., Kortenhaus, A., Medina, J.R. (2003) *Full Scale Wave Overtopping.* Proc. Conf. Coastal Structures '03, pp 494-506, ASCE.

De Rouck J., Geeraerts, J., Troch, P., Kortenhaus, A., Pullen, T., Franco, L., (2005) *New results on scale effects for wave overtopping at coastal structures* Proc. Int. Conf. on Coastlines, Structures and Breakwaters 2005, ICE, London, UK.

Endoh K & Takahashi S (1994) *Numerically modelling personnel danager on promenade breakwater due to overtopping waves* Proc. 24th ICCE, Kobe, pp 1016-1029, publn. ASCE.

Franco, L., de Gerloni, M. & van der Meer, J.W. (1994) *Wave overtopping on vertical and composite breakwaters* Proc 24th ICCE, pp 1030-1045, Kobe, ASCE.

Franco, L., Bellotti, G., Briganti, R., De Rouck, J., Geeraerts, J. (2003) *Full scale measurements of wave overtopping at Ostia yacht harbour breakwater.* Proc. Conf. Coastal Structures '03, Portland, USA.

Fukuda N., Uno T. & Irie I (1974) *Field observations of wave overtopping of wave absorbing revetment* Coastal Engineering in Japan, Vol 17, pp 117-128, JSCE, Tokyo.

Geeraerts, J., Troch, P., De Rouck, J., Van Damme, L., Pullen, T. (2003) *Hazards resulting from wave overtopping – Full Scale Measurements.* Proc. Conf. Coastal Structures '03, pp 481-493, ASCE.

Goda, Y, Kishira, Y, & Kamiyama, Y. (1975) *Laboratory investigation on overtopping rates of seawalls by irregular waves* Ports & Harbour Research Institute, Vol 14, No. 4, Yokosuka.

Gouldby B.P., Sayers P.B. & Johnson D (1999) *Real-time hazard forecasting: implementation and two years operation at Samphire Hoe, Dover* MAFF Conf. on River and Coastal Engineers, Keele.

Herbert D.M. (1996) *Overtopping of seawalls: a comparison between prototype and physical model data* Report TR 22, HR Wallingford.

Kimura K, Fujiike T, Kamikubo K. Abe R & Ishimoto K (2000) *Damage to vehicles on a coastal highway by wave action* Proc. Conf. Coastal Structures '99, Santander, June 1999, publn. A.A. Balkema, Rotterdam.

Owen, M.W. (1980) *Design of seawalls allowing for overtopping* Report EX924, Hydraulics Research, Wallingford.

Pearson, J., Bruce, T. & Allsop, N.W.H. (2002) *Violent wave overtopping – measurements at large and small scale* Proc. 28th Int. Conf. Coastal Eng. (ASCE) Cardiff.

Pullen T.A. Allsop, N.W.H. Bruce, T. & Geeraerts, J. (2003) *Violent wave overtopping: CLASH Field Measurements at Samphire Hoe* Proc. Coastal Structures 2003, ASCE.

Ramsbottom D, Wade S, Bain V, Floyd P, Penning-Rowsell E, Wilson T & Fernandez A (2004) *Flood Risks to People, Phase 2 Interim Report 1,* R & D Report FD 2321/IR1, DEFRA Flood Management Division, London.

Richardson, S. Pullen, T. & Clarke, S. (2002) *Jet velocities of overtopping waves on sloping structures: measurements and computation* Paper 347 at ICCE 2002 Cardiff, July 2002 , publn ASCE, New York.

Smith G.M., Seijffert J.W.W. & Meer J.W. van der (1994) *Erosion and overtopping of a grass dike: large scale model tests* Proc 24th ICCE, pp 2639-2652, Kobe, publn. ASCE.

Waal, J.P. de Tonjes, P. & van der Meer, J.W. (1996) *Overtopping of sea defences* Proc 25th Int. Conf. Coastal Eng. (ASCE), pp2216-2229, Orlando, publn ASCE, New York.